

*Strategies
and Tactics
in Organic
Synthesis*

Volume 8

Edited by
MICHAEL HARMATA



Academic Press is an imprint of Elsevier
Radarweg 29, PO Box 211, 1000 AE Amsterdam, The Netherlands
525 B Street, Suite 1900, San Diego, CA 92101-4495, USA

First edition **2012**

© **2012** Elsevier Ltd. All rights reserved.

No part of this publication may be reproduced, stored in a retrieval system or transmitted in any form or by any means electronic, mechanical, photocopying, recording or otherwise without the prior written permission of the publisher

Permissions may be sought directly from Elsevier's Science & Technology Rights Department in Oxford, UK: phone (+44) (0) 1865 843830; fax (+44) (0) 1865 853333; email: permissions@elsevier.com. Alternatively you can submit your request online by visiting the Elsevier web site at <http://elsevier.com/locate/permissions>, and selecting Obtaining permission to use Elsevier material

Notice

No responsibility is assumed by the publisher or editor for any injury and/or damage to persons or property as a matter of products liability, negligence or otherwise, or from any use or operation of any methods, products, instructions or ideas contained in the material herein. Because of rapid advances in the medical sciences, in particular, independent verification of diagnoses and drug dosages should be made

British Library Cataloguing in Publication Data

A catalogue record for this book is available from the British Library

Library of Congress Cataloging-in-Publication Data

A catalog record for this book is available from the Library of Congress

ISBN: 978-0-12-386540-3

For information on all **Elsevier** Publications
visit our Web site: www.elsevierdirect.com

Printed and bound in Great Britain

12 13 14 15 10 9 8 7 6 5 4 3 2 1

Working together to grow
libraries in developing countries

www.elsevier.com | www.bookaid.org | www.sabre.org

ELSEVIER

BOOK AID
International

Sabre Foundation

Dedication

This book is dedicated to all of the people, from family and friends to anonymous reviewers and referees, who have saved me from myself at crucial moments. Thanks very much!

Contributors

Numbers in Parentheses indicate the pages on which the author's contributions begin.

- Varinder K. Aggarwal** (1), School of Chemistry, University of Bristol, Cantock's Close, Bristol, B58 1TS, UK; E-mail: V.Aggarwal@bristol.ac.uk
- Naval Bajwa** (153), Department of Chemistry, The University of Alabama, Tuscaloosa, Alabama, USA; E-mail: naval.bajwa@yahoo.com
- Eric Ashley** (351), Global Process Chemistry, Merck Research Laboratories, Rahway, USA; E-mail: eric_ashley@merck.com
- Matthew A. Boone** (225), Eastman Chemical Company, Research Laboratories, P.O. Box 1972, Kingsport, Tennessee, USA; E-mail: mboone@eastman.com
- Stephen T. Chau** (375), Department of Chemistry, Vanderbilt University, Nashville, Tennessee, USA
- Pauline Chiu** (55), Department of Chemistry, The University of Hong Kong, Hong Kong, P. R. China; E-mail: pchiu@hku.hk
- Derrick L.J. Clive** (25), Chemistry Department, University of Alberta, Edmonton, Alberta, Canada; E-mail: derrick.clive@ualberta.ca
- Scott E. Denmark** (79), Department of Chemistry, University of Illinois at Urbana-Champaign, Urbana, Illinois, USA; E-mail: sdenmark@illinois.edu
- Catherine J. Fletcher** (1), School of Chemistry, University of Bristol, Cantock's Close, Bristol, B58 1TS, UK; E-mail: catherine.j.fletcher@gmail.com
- Andrey A. Fokin** (317), Department of Organic Chemistry, Kiev Polytechnic Institute, Kiev, Ukraine; E-mail: Andrey.Fokin@org.Chemie.uni-giessen.de
- Karl J. Hale** (127), The School of Chemistry and Chemical Engineering, Queen's University Belfast, Belfast, Northern Ireland, United Kingdom; E-mail: k.j.hale@qub.ac.uk
- Michael P. Jennings** (153), Department of Chemistry, The University of Alabama, Tuscaloosa, Alabama, USA; E-mail: jenningsm@bama.ua.edu
- Tetsuya Kobayashi** (79), Gilead Sciences, Inc., Foster City, California, USA; E-mail: Tetsuya.Kobayashi@gilead.com
- Daesung Lee** (171), Department of Chemistry, University of Illinois, Chicago, Illinois, USA; E-mail: dsunglee@uic.edu
- Yi Li** (127), The School of Chemistry and Chemical Engineering, Queen's University Belfast, Belfast, Northern Ireland, United Kingdom
- Carl J. Lovely** (199), Department of Chemistry and Biochemistry, The University of Texas at Arlington, Arlington, Texas, USA; E-mail: lovely@uta.edu

- Thomas Magauer** (261), Institute of Organic Chemistry, University of Vienna, Vienna, Austria; Department of Chemistry and Chemical Biology, Harvard University, Cambridge, Massachusetts, USA; E-mail: tmagauer@fas.harvard.edu
- Harry J. Martin** (261), Institute of Organic Chemistry, University of Vienna, Vienna, Austria; E-mail: harry.martin@univie.ac.at
- Frank E. McDonald** (225), Department of Chemistry, Emory University, Atlanta, Georgia, USA; E-mail: fmc dona@emory.edu
- Johann Mulzer** (261), Institute of Organic Chemistry, University of Vienna, Vienna, Austria; E-mail: johann.mulzer@univie.ac.at
- Christopher S. Regens** (79), Bristol-Meyers Squibb, New Brunswick, New Jersey, USA; E-mail: Christopher.Regens@bms.com
- Anna Robinson** (1), School of Chemistry, University of Bristol, Cantock's Close, Bristol, B58 1TS, UK; E-mail: aannarobinson@googlemail.com
- Richmond Sarpong** (291), Department of Chemistry, University of California, Berkeley, California, USA; E-mail: rsarpong@calmail.berkeley.edu
- Peter R. Schreiner** (317), Institute of Organic Chemistry, Justus-Liebig University, Giessen, Germany; E-mail: prs@org.chemie.uni-giessen.de
- Brian Stoltz** (351), Division of Chemistry and Chemical Engineering, California Institute of Technology, Pasadena, California, USA; E-mail: stoltz@caltech.edu
- Gary A. Sulikowski** (375), Department of Chemistry, Vanderbilt University, Nashville, Tennessee, USA; E-mail: gary.a.sulikowski@vanderbilt.edu
- Rongbiao Tong** (225), The Hong Kong University of Science and Technology, Department of Chemistry, Clear Water Bay, Kowloon, Hong Kong; E-mail: rtong@ust.hk
- Jason C. Valentine** (225), Kenyon & Kenyon LLP, NW, Washington, DC, USA; E-mail: JValentine@kenyon.com
- Ivan Volchkov** (171), Department of Chemistry, University of Illinois, Chicago, Illinois, USA; E-mail: ivolch2@uic.edu
- Craig M. Williams** (395), School of Chemistry and Molecular Biosciences, University of Queensland, Brisbane, Queensland, Australia; E-mail: c.williams3@mailbox.uq.edu.au
- Bin Wu** (375), Department of Chemistry, Texas A&M University, College Station, Texas, USA

Over the past two centuries, organic synthesis has become a powerful tool for supplying many of Nature's compounds—a vast, diverse, and functionally rich library, representing 3.8 billion years of chemical evolution and holding answers to many of the pressing problems of our time. Increasingly now the challenge in synthesis is to make such molecules in a step economical and green if not ideal fashion, one that impacts supply and enables scientific research. Of increasing importance is the special emerging opportunity to harness the power of synthesis for the design and preparation of nonnatural molecules, especially those with functions superior or complementary to what is found in Nature. While using only a part of the periodic table and only biosynthetic reactions, Nature provides uniquely inspiring examples of the remarkable structures and activities that can be achieved through function-oriented [bio]synthesis. Unconstrained in these ways, synthetic chemists, through design and synthesis, can open doors to new structures and activities never seen before, creating new fields of opportunities in chemistry, energy, materials research, chemical biology, medicine, and the many scientific disciplines that rely on new molecules and molecular insights for future innovation.

In this latest volume of *Strategy and Tactics*, we find a treasure trove of synthesis problems, strategies, insights, and perspectives provided by leading scholars in the field: Aggarwal (solandelactones); Clive (halichlorine); Chiu (pseudolaric acid); Denmark (papulacandin); Hale (eremantholide); Jennings (aigialomycin); Lee (dactylolide); Lovely (leucetta alkaloids); McDonald (abudinol); Martin, Magauer, and Mulzer (kendomycin); Sarpong (lyconadin alkaloids); Schreiner (diamondoids); Stoltz (lemonomycin); Sulikowski (apoptolidins); and Williams (vibsanin). From the first line of Chapter 1 “Nature has provided us with a bounty of complex molecules . . .” to the last line of Chapter 15 “to me, [the scholarship, friendships, and chemistry] are worth more than gold,” one finds the richness of experiences, ideas, and opportunities that draw so many to this field and why this field in turn is a key to advances in the whole of science. Reading in between the first and last lines, one finds examples of the personal perspectives and diversity of experiences that so enhance this series and elevate the reading experience: “I had not planned on being a chemist,” “Saved by Selenium,” “something had gone terribly wrong,” “The First Surprise,” “It is an exciting life,” “of great importance to human health,” “hopefully, this work will lead to exciting new anti-tumor chemical biology discoveries,” “being fairly desperate at this point,”

“this synthetic process highlights several new synthetic methodologies,” “approaches . . . guided by . . . biomimetic strategies,” “fascinated by the concept of cascade cyclizations,” “we take the liberty here of sharing a few ideas,” “an abundant source of drugs and drug leads,” “if one is to pursue a total synthesis, the process of target selection should be very important and deliberate,” “the function of the target must address important problems that have not been solved,” “natural diamond is the ultimate semiconductor,” “we were unsure at first whether it could be done,” “our goal to synthesize molecules that could positively impact human medicine,” “leading to a library of antineoplastic agents and antibiotics,” “over 60% of new anticancer agents approved by regulatory agencies since 1981 are of natural origin,” “opens avenues to the ready production of natural product analogs by means of chemobiosynthesis,” “I was running out of ring expansion ideas,” and “I was immediately captivated by the elegance of the complex caged bicyclic structures.” These comments are but a few of the wonderful and enriching experiences that await the reader. Knowing many of the contributors well and some being former coworkers, I found reading this tome to be equivalent to attending a private symposium as each contributor figuratively enters one’s reading room and shares their science in the didactic fashion of a live lecture. Not only did these contributions provide an enriching “read” and no doubt a source of continuing inspiration in the future, but they also stimulate recall of the many important contributions that these individuals have made over the years. Congratulations to them and their coworkers for this special narrative on their wonderful science!

In this 8th volume of *Strategy and Tactics in Organic Synthesis*, Professor Michael Harmata has again impressively captured a cross section of contemporary synthesis that informs, educates, and inspires. We are fortunate to have an educator and research scientist of his caliber so willing to invest such effort in advancing our science and our community. I had the pleasure of working with Professor Harmata when he was a postdoctoral fellow in my group. His fascination with reaction science and synthesis then and now is evident in this effort and the superb selection of scientists and the science they share. Our world is awash in major problems that cry out for expertise from those who see the world through a molecular lens and who can design and make molecules with function. It is hoped that this volume and those that preceded it will serve to inspire all to use the special skills possessed by synthetic chemists to address the growing list of challenges of our time.

Paul A. Wender
Stanford University, CA
April 2012

Preface

The state of organic synthesis has been in question for quite some time. Many thoughts about its dubious future have been expressed: “It is a mature field. There are no new reactions to be discovered. Engineered microbes can do the job better. The needs of life and material sciences can be more than met by present-day synthetic technology.” I have heard other more or less pessimistic statements about where the state of organic synthesis is and, by implication, where it is going. Is it just a tool that enables more important science to be done? No.

In a time when we can generally state that, given enough resources, we can prepare anything, why do we need to do more? Who needs new syntheses? Who needs little tweaks on reactions that have been done once and are only being rediscovered? One answer that is commonly given is that we in fact do not really have enough resources and if we are going to continue with life as we know it in a shrinking petroleum economy and a growing renewable resource economy, chemistry is going to have to change. Synthesis will have to change. Research will have to be done to initiate the change. Students will have to be trained to sustain the change. Is it in the process of changing? Yes.

Certainly, there have been many calls to do synthesis in an economic way, minimizing reagent use, protecting groups, chromatography, and waste generation. We are far from meeting goals with respect to the economy and sustainability, but progress is being made. Sustainability is key.

In a world of limited resources, there must be a limit to everything, even research. What should be done? What methodologies should be developed? What targets should be made? What should be done with them when they are made? These decisions will be made by funding agencies and the people they recruit to evaluate proposals. None of them, including me, can offer definitive answers to these questions. What are the scientific, professional, and personal consequences to guessing answers and being wrong? Good science is ignored; colleagues are put prematurely out of business; too many fight for too little. Population scientists and psychologists would no doubt predict outcomes to such a situation that would not be pleasant. Balance is needed.

We cannot expand forever, but we cannot shrink rapidly either. The scientific community must make decisions about scientific sustainability not only in the area of organic synthesis but also across the board so that good scientists have the opportunity for the dignity that comes with pursuing research and those who we might call genius can flourish unencumbered by needless barriers.

This book contains examples of outstanding efforts in organic synthesis, demonstrating that the process is by no means easy and that it takes the best of human beings in terms of creativity and fortitude to prepare even small molecules in a productive way. New chemistry and principles are discovered in the process, and people are educated, that they might provide the shoulders on which future generations stand to meet the needs of science and the public some years hence. The science and art of organic synthesis is an absolute necessity for the present and the future of both science and society. The outlook is bright, but only we who are knowledgeable and committed can keep it that way.

Being allowed to share in the science of colleagues I both respect and enjoy is a rare pleasure. Having a funded research program is invaluable as I pursue “broader impacts” such as this. I thank the National Science Foundation for their continued support of our efforts in the development of new areas of organic synthesis.

Finally, my thanks go out to Elsevier for having faith in this series and to Derek Coleman and Susan Dennis, in particular.

Michael Harmata

Total Syntheses of Solandelactones E and F

Anna Robinson, Catherine J. Fletcher and Varinder K. Aggarwal

School of Chemistry, University of Bristol, Bristol, B58 ITS, UK

Chapter Outline

1. Introductions and Background	1	3.1. Preparation of Aldehyde	37
1.1. Solandelactone and Related Natural Products	1	3.2. Preparation of Enantioenriched Lithiated Carbamate	13
1.2. Previous Syntheses	3	3.3. Completion of Solandelactone E	16
1.3. Aggarwal Methodology for the Synthesis of 2-ene-1,4-diols	4	4. Synthesis of Solandelactone F	19
2. Retrosynthetic Analysis	6	5. Conclusions	21
3. Synthesis of Solandelactone E	7		

1. INTRODUCTIONS AND BACKGROUND

1.1 Solandelactone and Related Natural Products

Nature has provided us with a bounty of complex molecules that synthetic organic chemists use to create new strategies and methodologies of general utility for synthesis. The family of solandelactones represents one such class of natural products. They are complex fatty acids that were isolated in 1996, from a species of small marine predators *Solanderia secunda* off the Asian coast [1]. They belong to a larger group of cyclopropyl lactones that are all members of the oxylipin family, including halicholactone and the constanolactones (Figure 1).

There are several interesting and prominent structural features within this group of compounds that present an attractive challenge, including medium-sized lactone rings and *trans*-cyclopropanes, which are linked in a series of four contiguous stereocenters. However, the feature that particularly attracted us was the *trans* double bond flanked by two hydroxyls known as a 2-ene-1,4-diol. We sought to specifically address the stereocontrolled synthesis of this

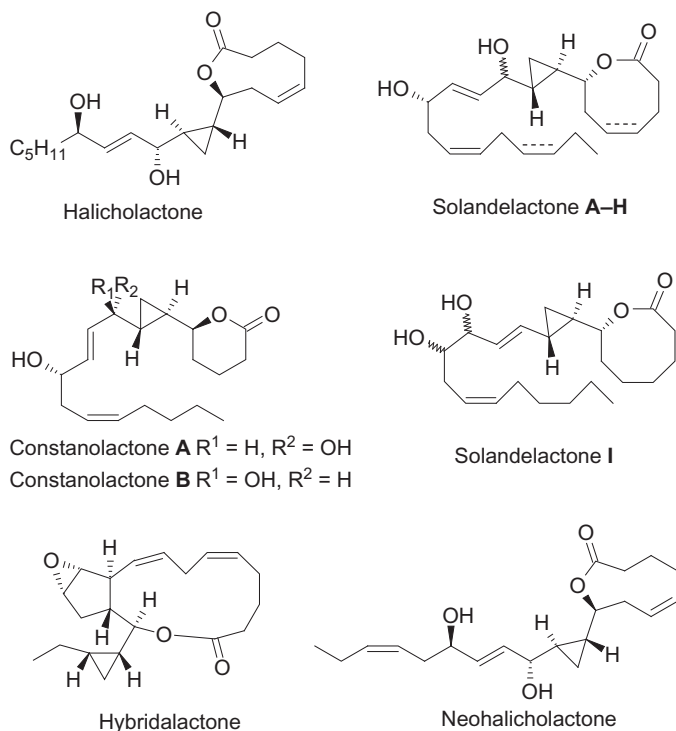


FIGURE 1 Cyclopropane containing marine oxylipins.

structural feature (*syn*- and *anti*-diols) as most previous syntheses had accepted low selectivity. Therefore, if we could establish methodology for the stereocontrolled synthesis of *syn*- or *anti*-2-ene-1,4-diols, then we could potentially access the entire family of solandelactones, as the remaining differences relate to the varying degrees of unsaturation in the molecule.

In total, nine members of the solandelactone family have been isolated, of which **A–H** contain the 2-ene-1,4-diol. These have been split into two groups depending on whether they have an *S* or *R* configuration at C11, with solandelactones **A**, **C**, **E**, and **G** being assigned as the *anti*-1,4-diols (C11*S*) and **B**, **D**, **F**, and **H** as the *syn*-1,4-diols (C11*R*). The C11 epimers have then been grouped into pairs related to the degree of unsaturation along the carbon chain (**A** and **B**, **C** and **D**, **E** and **F**, and **G** and **H**) (Figure 2).

It is important to note that initially Shin assigned the solandelactones (based on NMR and derivative studies) **A**, **C**, **E**, and **G** as the *syn*-diols (C11*R*) and **B**, **D**, **F**, and **H** as the *anti*-diols (C11*S*) [1]. However, Martin discovered upon completion of the intended first synthesis of solandelactone **F** that the spectral data matched instead with solandelactone **E** [2]. Upon correspondence with Shin, it was established that, rather than a scientific error, there had been a typographic mistake when correlating the names of the epimeric solandelactones with their structures in the original paper, and it was

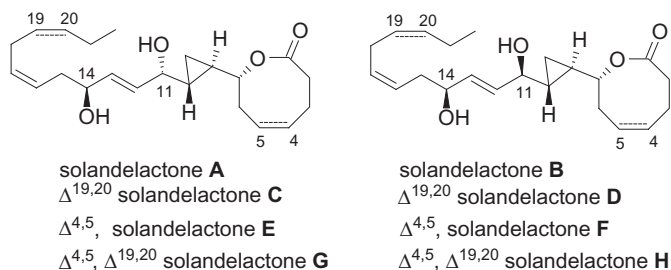
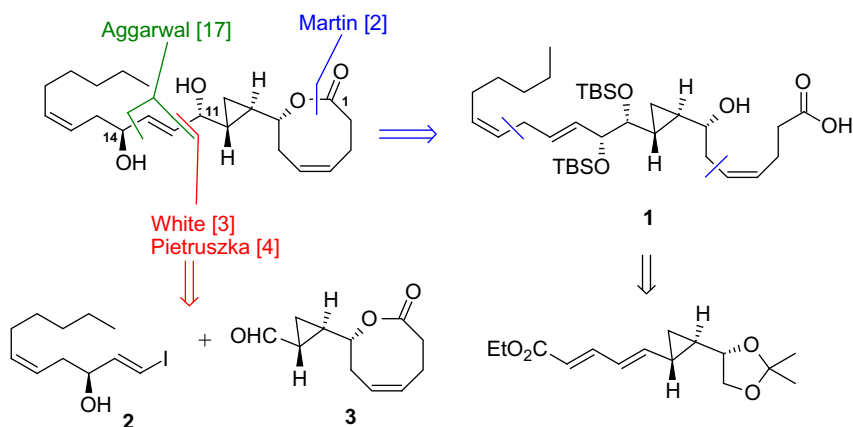


FIGURE 2 Assignments of solandelactones A–H.



SCHEME 1 Overview of retrosyntheses of solandelactone E.

agreed that the stereochemistry at C11 of all the solandelactones should be reassigned, as is now used (see Figure 2) [1,2].

1.2 Previous Syntheses

The structures of the solandelactones have recently been confirmed through syntheses by Martin [2] (solandelactone E), White [3] (solandelactones A, B, E, and F), and Pietruszka [4] (solandelactones A–H). Before a total synthesis was completed, both Datta [5] and Mohapatra [6] had completed partial syntheses (the cyclopropyl lactone fragment C1–C11), and Pale [7] had described the synthesis of fragment C12–C22. Taking solandelactone E as a primary example, the key disconnections employed by previous syntheses are summarized in Scheme 1. Martin chose to disconnect the lactone, leading back to precursor 1. The *syn*-E-1,4-diol was introduced in the final step with excellent stereocontrol by a 1,3-allylic transposition of the C11–C12 1,2-diol. However, the overall route is rather linear, with a total of 23 steps (longest linear sequence). Both White and Pietruszka, on the other hand, opted

for a more convergent synthesis, splitting the molecule into two halves, vinyl iodide **2** and aldehyde **3**, using the Nozaki–Hiyama–Kishi (NHK) reaction [8,9] to couple at a late stage. The stereocontrol in this reaction derives from a directing effect of the remote C14 stereocenter, rather than the cyclopropyl moiety, and only low diastereomeric ratios were observed [10a,11]. An evaluation of the NHK reaction, as used by White and Pietruszka, showed that it proceeded with poor stereocontrol at the newly formed stereocenter, leading to a roughly 2:1 mixture of epimers at C11, in favor of the *anti*-diol [3,4]. Therefore, each of these syntheses of solandelactones **A**, **C**, **E**, and **G** has resulted in the formation of the desired product in a moderate yield (maximum 66%) along with the corresponding C11 epimer, respectively, as the minor product **B**, **D**, **F**, or **H** (up to 33%). Fortunately, the diastereoisomers were separable by column chromatography, but for a synthesis that requires any of the solandelactones **B**, **D**, **F**, or **H**, this route is less than ideal.

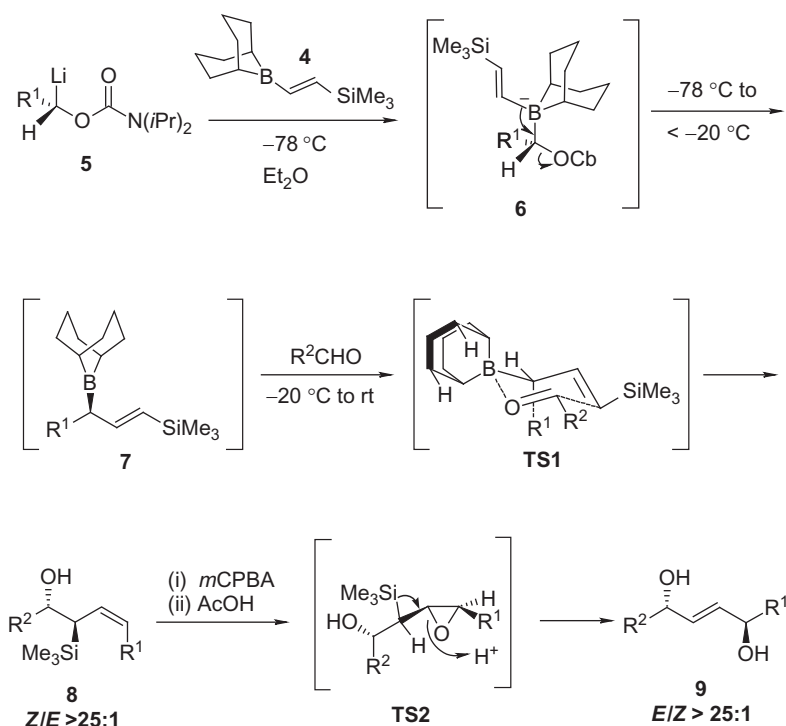
A similar situation is found with the syntheses of halicholactone, of which there are currently five published. Four of these form the C11–C12 bond using a poorly selective coupling reaction [11], whereas the fifth synthesis, Takemoto's route, avoids this strategy, but is also the longest synthesis to date [12]. Three of the four syntheses of constanolactones **A–D** also involve a poorly selective NHK reaction as the key step [13].

Thus far, the syntheses of these oxylipins all seem to suffer the same limitations, namely, that the synthesis is either concise but poorly stereoselective or highly stereocontrolled but lengthy. A synthesis that combined the best features of each would be the most desirable.

1.3 Aggarwal Methodology for the Synthesis of 2-ene-1,4-diols

In 2010, we published a novel method for the synthesis of *anti*-*E*-2-ene-1,4-diols (Scheme 2) [14]. The methodology involved the coupling of a lithiated carbamate, β -silyl vinyl borane **4**, and an aldehyde to give an allylsilane in high yield with high enantio- and diastereoselectivity. Subsequent epoxidation and acid-catalyzed elimination gave the corresponding 2-ene-1,4-diols with high enantio- and diastereoselectivity [15]. Lithiated carbamate **5** can be derived either from an enantioenriched stannane upon treatment with *n*-BuLi or via selective deprotonation of a carbamate with *s*-BuLi/(–)-sparteine [16]. Addition of β -silylvinyl borane gives boronate complex **6**, which undergoes 1,2-metallate rearrangement upon warming to give allylboronate **7**. This allylboronation reagent may undergo reaction with an aldehyde via a six-membered transition state (**TS1**), where R¹ is forced into an axial position by steric repulsion of the bulky borane group, leading to β -hydroxy-*Z*-allylsilane **8**. Subsequent epoxidation and acid-catalyzed elimination via **TS2** gave 2-ene-1,4-diol **9** with high enantio- and diastereoselectivity.

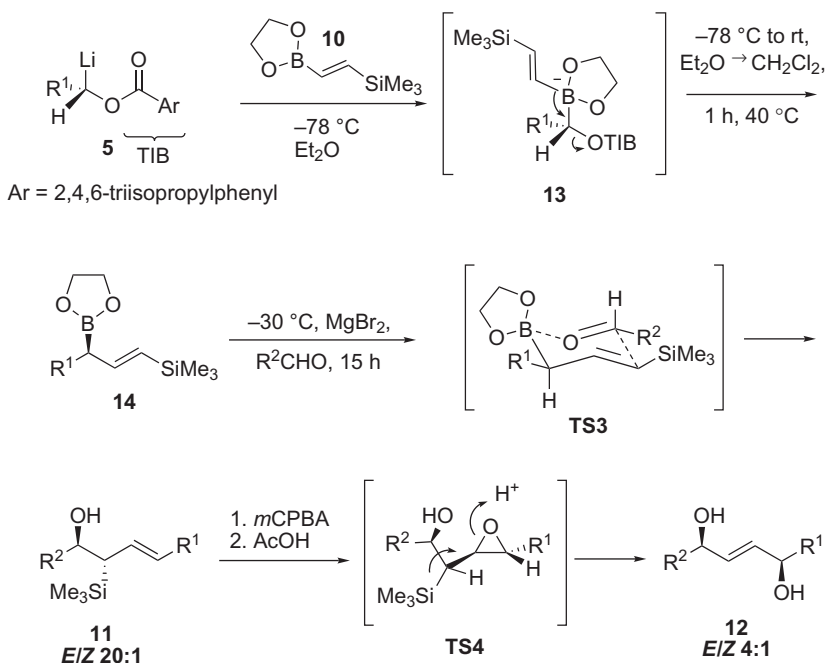
By using the same β -silylvinyl borane **4**, but changing the respective R groups on the carbamate and the aldehyde, this methodology could be

SCHEME 2 Methodology for the synthesis of *anti*-*E*-2-ene-1,4-diols.

applied to the synthesis of solandelactone **E**. Indeed, this would be an ideal strategy, as this would lead to a highly convergent synthesis with excellent stereocontrol, thus accomplishing the challenge laid before us at the beginning of this project.

In order to facilitate the synthesis of solandelactone **F**, an extension of this methodology was developed that allowed access to *syn*-*E*-2-ene-1,4-diols (Scheme 3). Changing the nature of the boron species to unhindered ethylene glycol boronic ester **10** alters the preferred transition state of allylboration to **TS3**, thus allowing the synthesis of β -hydroxy-*E*-allylsilane **11** [17]. Epoxidation and acid-catalyzed elimination via **TS4** gave *syn*-*E*-2-ene-1,4-diol **12**. From a mechanistic standpoint, the synthesis of *anti*- and *syn*-2-ene-1,4-diols is very similar; however, significant changes in the procedure were necessary to obtain similar results, due to the following challenges:

- (i) The 1,2-metallate rearrangement is much slower with boronic esters compared to boranes [15b,18] and requires either high temperature and long reaction times or addition of a Lewis acid, both of which, in this case, were detrimental to the yield. However, the carbamate-leaving group was replaced with the 2,4,6-triisopropyl benzoyl group [19], which allowed rearrangement of boronate complex **13–14** at 40°C without a Lewis acid.



SCHEME 3 Methodology for the synthesis of *syn-E*-2-ene-1,4-diols.

- (ii) The allylic boronic ester **14** is also much slower at allylboration compared to the allylborane **7** [20,15d], and thus solvent exchange was required together with addition of a Lewis acid [21].
- (iii) The diastereoselectivity in epoxidation of *E*-allylsilanes is considerably lower than for *Z*-allylsilanes [22,23].

Aside from the synthesis of 2-ene-1,4-diols, this methodology is of particular importance for the synthesis of the intermediate β -hydroxy allylsilanes, as this methodology has considerable advantages over those previously described. For example, both Roush [24,25] and Barrett [26] have described the synthesis of β -hydroxy allylsilanes using asymmetric allylboration of aldehydes; however, the scope is limited to the synthesis of terminal alkenes. Panek has developed a route via an Ireland–Claisen reaction [27]; however, although the method allowed for the synthesis of all isomers (*E/Z* and *anti/syn*), routes to some isomers were somewhat lengthy [28].

This chapter describes the synthesis of solandelactones **E** and **F** utilizing novel methodology developed within the Aggarwal group that markedly improved upon the selectivity of previous syntheses while maintaining a concise route.

2. RETROSYNTHETIC ANALYSIS

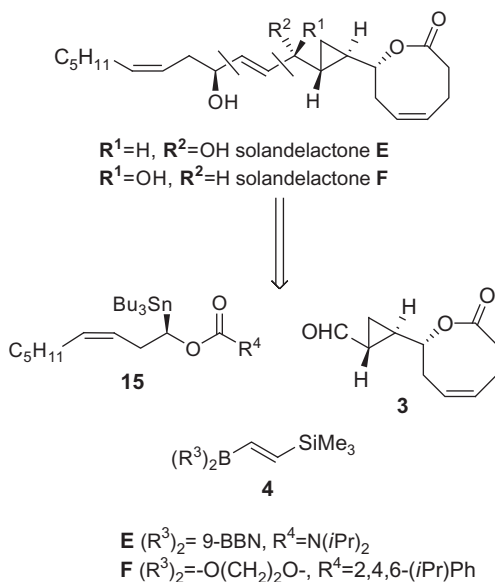
The 2-ene-1,4-diol subunit in both solandelactone **E** and **F** can be retrosynthetically disconnected using the methodology described above to yield a vinyl

boron species, an α -lithiated carbamate, and an aldehyde. Disconnection of solandelactones **E** and **F** in this way led to the three key components, aldehyde **3**, vinyl boron species **4**, and stannane **15** (Scheme 4).

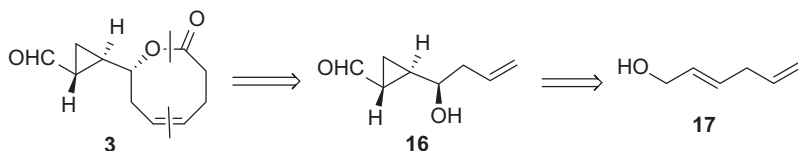
3. SYNTHESIS OF SOLANDELACTONE E

3.1 Preparation of Aldehyde 3

The first component we focused on was aldehyde **3**, which was already known in the literature, being an intermediate in both White's [3] and Pietruszka's [4] syntheses. However, we felt that these routes could be improved upon and we were keen to examine this theory. While White's synthesis implemented an impressive use of Claisen rearrangement to install the eight-membered lactone (first described by Holmes) [29] and Pietruszka's demonstrated his methodology for synthesis of enantioenriched cyclopropanes via kinetic enzymatic resolution [30], both required several protection and deprotection steps. Disconnection of lactone **3** led to cyclopropyl aldehyde **16**, which in turn would be derived from known diene **17** (Scheme 5). In the forward sense, **16** could be



SCHEME 4 Retrosynthesis of solandelactone **E** and **F**.

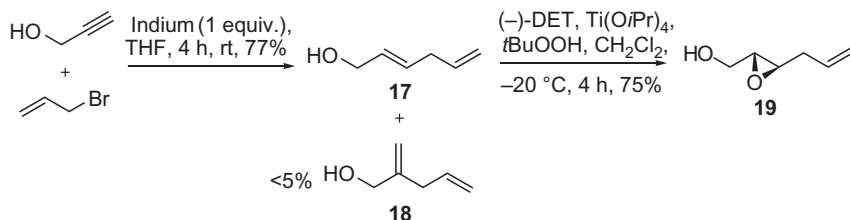


SCHEME 5 Retrosynthesis of aldehyde **3**.

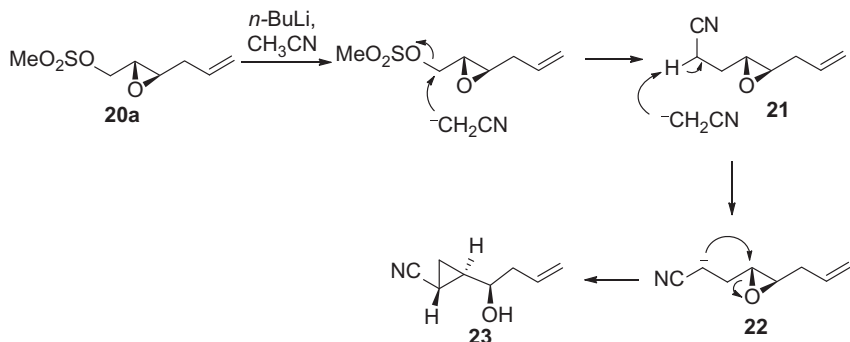
obtained from **17** through a sequence of Sharpless epoxidation, Taber cyclopropanation, and DIBAL reduction. Esterification and ring-closing metathesis (RCM) would complete lactone **3**. This route would give **3** in only seven steps from commercially available starting materials, effectively halving the length of previous efforts, while maintaining the high selectivity.

We began with the synthesis of diene **17** by following the procedure described by Ranu for the single-step indium-mediated coupling of allyl bromide and 2-propyn-1-ol [31]. The reaction gives an impressive 77% yield of linear product **17** with less than 5% of the branched product **18**, formed by intermolecular reaction between the allyl indium species and 2-propyn-1-ol, rather than intramolecular. Diene **17** was converted to epoxide **19** with high yield and excellent enantioselectivity, according to the Sharpless procedure [32] (Scheme 6). Epoxy alcohol **19** was an important intermediate to us as its stereochemistry dictated that of the final cyclopropyl lactone fragment **3**. Therefore, being able to incorporate the highly enantioselective and reliable Sharpless epoxidation to control stereochemistry was particularly pleasing.

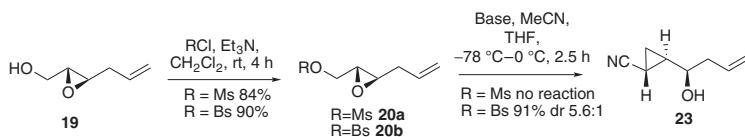
The cyclopropanation could be performed using deprotonated acetonitrile as used by Taber in his synthesis of (–)-delobanone [33]. Acetonitrile was deprotonated by addition of *n*-BuLi at -78°C , followed by addition of the dielectrophile substrate **20a**. Attack of lithiated acetonitrile is thought to occur first at the mesylate, with expulsion of the leaving group to give **21**. A second deprotonation α to the nitrile group gives **22**, which may undergo ring closure to form the cyclopropane while opening the epoxide to give **23** (Scheme 7).



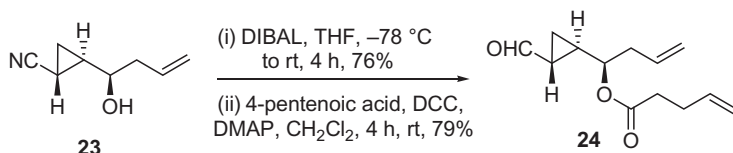
SCHEME 6 Synthesis of epoxy alcohol **19**.



SCHEME 7 Proposed mechanism for Taber cyclopropanation reaction.



SCHEME 8 Unproductive route to cyclopropane and alternative route.

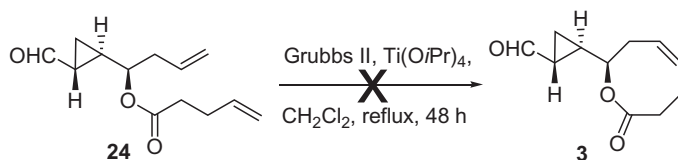
SCHEME 9 Synthesis of bis-olefin **24**.

Initially, methanesulfonate **20a** was chosen as the dielectrophile substrate, which was formed in good yield by reaction of alcohol **19** with methanesulfonyl chloride (MsCl). When cyclopropanation was attempted, complete consumption of the starting material was observed but no cyclopropanation product was detected (Scheme 8). It was postulated that the major problem was that the acetonitrile anion was deprotonating the acidic methyl on the methanesulfonate, preventing the desired reaction and leading to unwanted side products. Switching to benzenesulfonate **20b** gave cyclopropane **23** as the major product, and after investigation of conditions, NaHMDS was identified as the optimal base to give *trans* cyclopropane **23** in 77% yield (91% overall yield, 5.6:1 *trans:cis* ratio [separable]).

Reduction of the nitrile of **23** to the aldehyde was carried out using DIBAL in THF (Scheme 9). Following this, esterification with 4-pentenoic acid in the presence of DCC and DMAP afforded bis-olefin **24** in good yield (Scheme 9).

Before planning this route, we were aware that the synthesis of medium rings from linear precursors using RCM can be difficult, and in particular, eight-membered rings are often considered the hardest to form using this approach [34]. It has been suggested that RCM to form eight-membered rings is effective only with cyclic [35] or conformational [36] constraints. However, there had been some precedent for forming medium-ring lactones without these constraints using RCM. Of particular relevance was Mohapatra's synthesis of intermediates for halicholactone [37] and solandelactone [6] and Kitahara's total synthesis of halicholactone [11c]. Learning from these previous syntheses, it seemed that RCM was possible at low concentration (1 mM or lower). $\text{Ti}(\text{O}i\text{Pr})_4$ had also been shown to be beneficial in certain circumstances, as it inhibits complexation of the carbonyl with the intermediate Ru carbene, enabling the carbene to react with the remaining alkene.

The first attempt to form the eight-membered ring from bis-olefin **24** followed Mohapatra's conditions [6]. However, although all the starting material was consumed, no product was obtained (Scheme 10).



SCHEME 10 Unsuccessful ring-closing metathesis to form eight-membered ring.

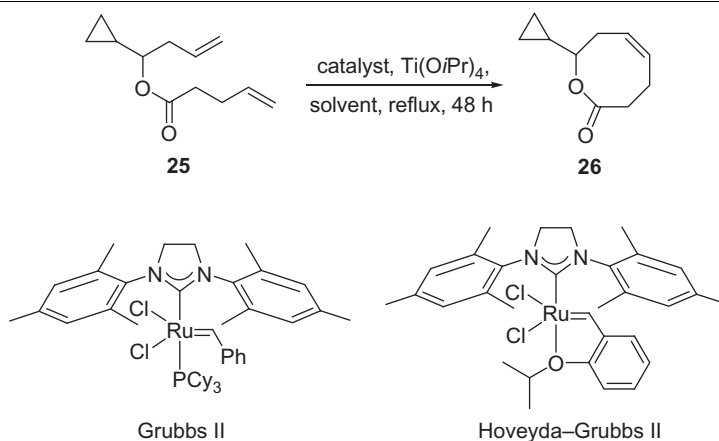


TABLE 1 Attempts at Ring-Closing Metathesis to Form an Eight-Membered Lactone

Entry	Solvent	Concentration	Catalyst	Result
1	CH_2Cl_2	1 mM	Grubbs II	42% 1:1 mixture monomer: dimer
2	CH_2Cl_2	2 mM	Grubbs II	No products recovered
3	Toluene	1 mM	Grubbs II	Complex mixture
4	Toluene	2 mM	Grubbs II	Low recovery, product observed by LCMS, complex mixture by NMR
5	CH_2Cl_2	1 mM	Hoveyda-Grubbs II	Complex mixture of large number of products
6	H_2O	0.3 M	Grubbs II	1:1 SM:product
7	CH_2Cl_2	1 mM	Grubbs II	No $\text{Ti}(\text{O}i\text{Pr})_4$, mixture of oligomers
8	CH_2Cl_2	1 mM	Grubbs II	Slow addition of SM, no reaction

Grela's review of ruthenium olefin metathesis catalysts highlighted the difficulty in predicting the efficiency of catalysts in a given metathesis reaction [38]. He concluded that, where possible, reactions should be carried out at 70°C in toluene with a second-generation catalyst; however, a thorough investigation of conditions is often required. With this in mind, solvent, concentration, and catalyst were screened on a model substrate **25** to form lactone **26** (Table 1).

Regrettably, all reactions on the substrate **25** with toluene, CH₂Cl₂, or water as a solvent, at various concentrations, with or without Ti(OiPr)₄, led to complex mixtures of starting material and oligomer products.

Previous literature demonstrates that the number and nature of substituents on a ring decide whether a ring will close or form oligomers under RCM reaction conditions. Successful examples of eight-membered ring formation by RCM generally rely on a conformational bias to position the olefins within close proximity [39]. While completing his synthesis of solandelactone **E** and **F**, White suggested that the significant difference in energy between the *s-cis* and *s-trans* esters (7.9 kcal/mol by a Hartree-Fock/6–31G** calculation) was responsible for the difficulties encountered when attempting RCM to form eight-membered lactones. The preferred *s-cis* conformation holds the reacting olefins apart and therefore could explain the difficulties with a RCM route to this substrate (Figure 3).

Both White (lactone **27**) and Pietruszka failed on substrates very similar to ours, whereas Mohapatra succeeded in forming lactone **28**. However, RCM does appear to be very substrate dependent, as lactam **29** was successfully closed but **30** gave no reaction (Figure 4) [40].

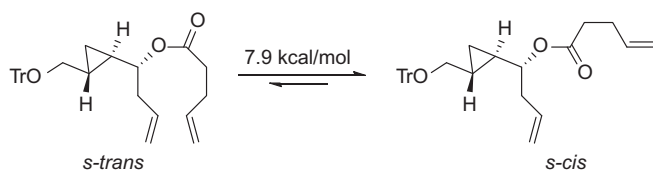


FIGURE 3 Difference in energy between *s-cis* and *s-trans* conformations of esters.

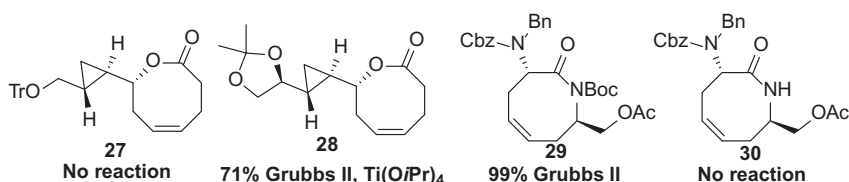
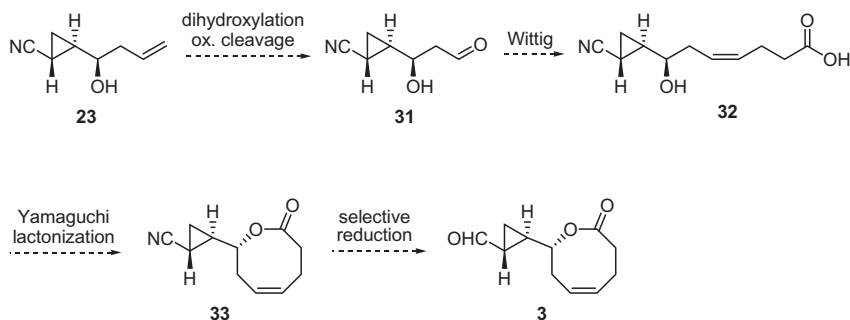


FIGURE 4 Recent literature examples of attempts to form eight-membered lactones and lactams by RCM.



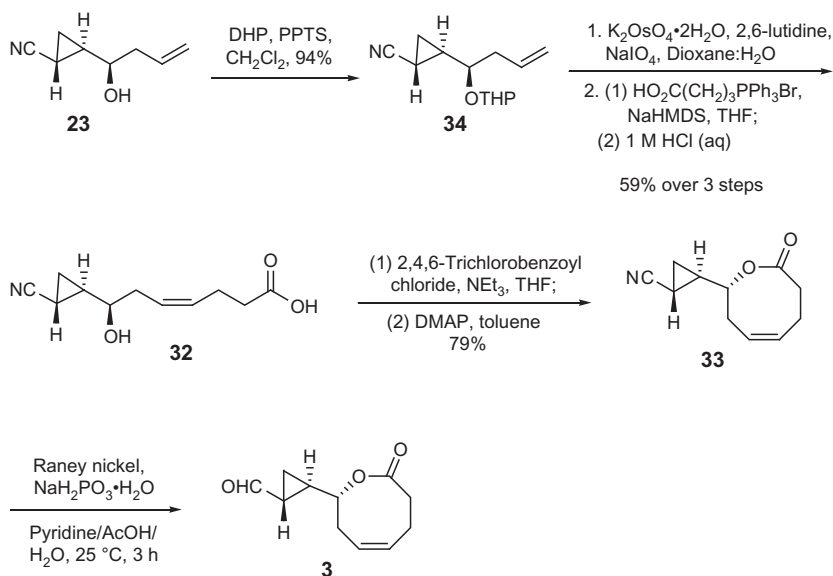
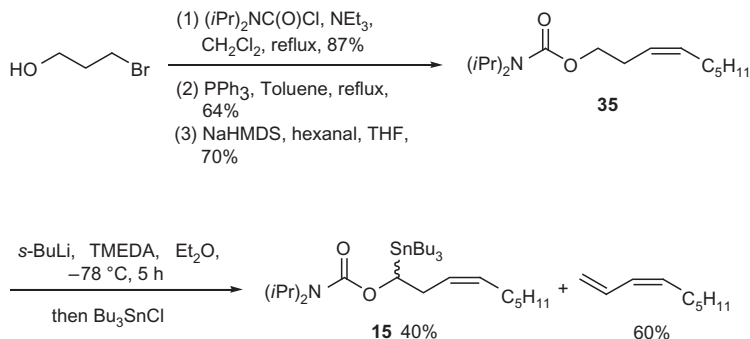
SCHEME 11 New route to lactone core in solandelactone **E**.

In fact, there are very few examples of RCM to form eight-membered ring lactones, with macrolactonization being far more common practice [40]. As we had encountered significant problems with RCM, we decided to focus on macrolactonization to close the ring.

There have been numerous literature precedents of macrolactonization to form eight-membered rings, including previous solandelactone syntheses [2,4,5]. Taking existing intermediate homoallylic alcohol **23** and subjecting it to dihydroxylation and oxidative cleavage would give aldehyde **31**, which can undergo Wittig reaction to give the acid **32**. Yamaguchi lactonization should give the lactone **33** and selective reduction would give the key aldehyde **3** for the lithiation–borylation–allylation chemistry (Scheme 11).

Alcohol **23** underwent protection to the THP ether **34**, which was then subjected to a three-step sequence of dihydroxylation/oxidative cleavage [41], Wittig reaction, and deprotection to give **32**. A protecting group was found to be necessary, as otherwise a substantial amount of *retro*-aldol of β-hydroxy aldehyde **31** was observed. THP was the chosen protecting group as it could withstand the reaction conditions and was quick and easy to install and remove. Macrolactonization was required to complete the synthesis of the solandelactone core of lactone **3**. Yamaguchi's method was chosen because previously reported syntheses of solandelactone have used this reaction with success [2,4,5]. Pleasingly, this was also true for substrate **32** and the lactone **33** was isolated in good yield. Employment of Raney nickel [42] on substrate **33** led to clean reduction of the nitrile to the aldehyde, whereas reduction with DIBAL [43] gave a mixture of products (Scheme 12).

This completed a novel route to the lactone core of solandelactones **E** and **F**, in 10 steps and 16% overall yield. Key steps included Sharpless epoxidation, modified Taber cyclopropanation, and Yamaguchi lactonization. This route represents a significant reduction in the number of steps as compared to previous syntheses, and despite having to modify the original strategy, only a single protecting group was required.

SCHEME 12 Synthesis of key cyclopropyl lactone **3**.SCHEME 13 Synthesis of carbamate **35** and initial lithiation experiments.

3.2 Preparation of Enantioenriched Lithiated Carbamate

Carbamate **35** was accessed in three steps from 3-bromopropan-1-ol in good yields. 3-Bromopropan-1-ol was carbamoylated and the bromide converted into the phosphonium salt. This underwent Wittig reaction with hexanal to give the desired carbamate **35** (Scheme 13).

Initially, the deprotonation of **35** was investigated by generating the lithiated species racemically (using TMEDA as the diamine instead of (–)-sparteine) and trapping with Bu₃SnCl to give stannane **15**. However, this only gave 40% of the desired product, stannane **15**. The remaining 60% was found

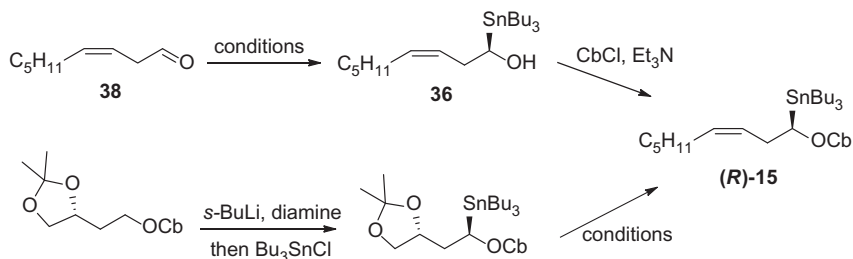
to be (*Z*)-nona-1,3-diene, which is derived from deprotonation at the allylic position followed by elimination of the carbamate group (Scheme 13).

Lithiation–deuteration experiments on carbamate **35** demonstrated that deprotonation was occurring mainly at the allylic position (which is more acidic than α to the carbamate) and elimination of the carbamate takes place at -78°C before the electrophile is added. Deprotonation at lower temperature was unsuccessful in improving selectivity. However, lithiation–deuteration experiments on stannane **15** showed that, once the lithiated species was generated, there was no transfer to the allylic position. This demonstrated that stannane **15** was a suitable intermediate toward solandelactone **E** and so an alternate route was investigated.

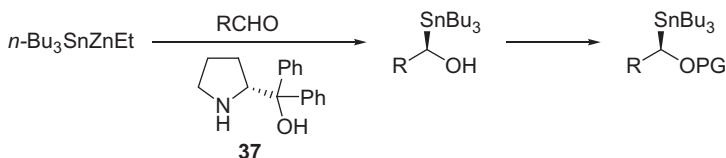
Two possible approaches to the synthesis of enantioenriched stannane (*R*)-**15** could be envisaged: by preparation of hydroxystannane **36**, followed by carbamoylation, or from lithiation–stannylation of an alternate carbamate, which does not contain acidic allylic protons, followed by conversion to the desired product (*R*)-**15** (Scheme 14). Our initial efforts turned to the synthesis of enantioenriched hydroxystannanes.

In 2008, Falck and coworkers published a novel method for the synthesis of hydroxystannanes from the corresponding aldehydes in high yields and enantioselectivities [44]. Addition of ethyl(tri-*n*-butylstannyl)zinc, generated *in situ* by transmetallation of tributyltin hydride with diethylzinc, to aldehydes in the presence of a pyrrolidine catalyst **37** gave the hydroxystannane with excellent stereocontrol. The reaction worked well on a number of aromatic and aliphatic aldehydes, which were either protected *in situ* as the acetate or immediately subjected to either thiocarbamoylation or *p*-nitrobenzoate protection (Table 2).

When *cis*-non-3-enal (**38**) was subjected to the Falck conditions, all the starting material was consumed though no product was formed (by TLC analysis), indicating degradation of starting material (Entry 1). Given this disappointing result, an example from the paper was replicated exactly, using benzaldehyde as the aldehyde, and we found that the yield was reproducible (60%) (Entry 2). However, attempts to reproduce the results for aliphatic aldehyde dihydrocinnamaldehyde were less successful. In our hands, all attempts with aliphatic aldehydes led to complete consumption of starting material, but low yields of products (Entries 3–5) and another method of synthesizing hydroxystannanes was investigated.



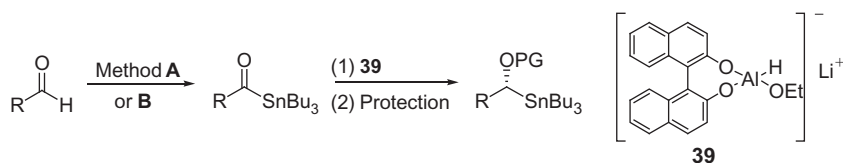
SCHEME 14 Alternative routes to stannane (*R*)-**15**.

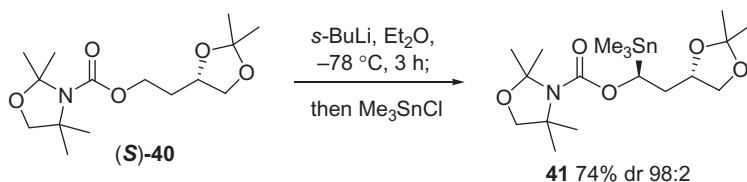
**TABLE 2** Attempts at Hydroxystannane Synthesis Using Falck Methodology

Entry	Aldehyde	PG	Yield	comments
1	<i>cis</i> -non-3-enal	–	–	No products found
2	Benzaldehyde	Acetate	60%	Acetate added <i>in situ</i>
3	Hexanal	Acetate	10%	Acetate added <i>in situ</i>
4	<i>cis</i> -non-3-enal	Acetate	10%	NMR yield
5	Dihydrocinnamaldehyde	Acetate	28%	NMR yield

The asymmetric reduction of acylstannanes to prepare enantiomerically enriched alkoxytannanes was first described by Chong in 1988 [45]. Extremely air sensitive acylstannanes were synthesized from nonselective addition of tri-*n*-butyltin magnesium chloride to an aldehyde followed by oxidation using a second equivalent of the aldehyde. These acyl stannanes were then reduced using BINAL-H reagents (**39**) to give hydroxystannanes in high yield and enantioselectivity. This methodology worked on a range of aliphatic acylstannanes, although selectivity dropped when more bulky substrates were used. Further studies by Marshall [46] used azodicarboxyldipiperidine (ADDP) as the oxidizing agent to prevent a second equivalent of aldehyde being necessary. This method of oxidizing alcohols was first reported by Mukaiyama in 1977 [47].

Several attempts were made to reproduce these results on *cis*-non-3-enal (**38**), but no evidence of the formation of an acylstannane was ever observed. Only small amounts of the racemic-protected hydroxystannane were isolated thus indicating no oxidation to the acylstannane. Using the test substrate crotonaldehyde as described by Marshall [46] gave complete conversion of the hydroxystannane to the acyl stannane, and therefore, it is possible to conclude that *cis*-non-3-enal (**38**) is simply not stable to these conditions (Table 3).





SCHEME 15 Hoppe trapping of lithiated chiral acetonides.

TABLE 3 Attempts at Synthesis of Acylstannanes

Entry	Aldehyde	Method	PG	Yield	Comments
1	<i>cis</i> -non-3-enal	A ^a	<i>p</i> -NO ₂ benzyl chloroformate	10%	Racemic
2	<i>cis</i> -non-3-enal	B ^b	MOM-Cl	17%	Complex mixture

^aA: 2 equiv. aldehyde, Bu₃SnMgCl, Et₂O, reflux.^bB: 1 equiv. aldehyde, Bu₃SnLi, ADDP, THF.

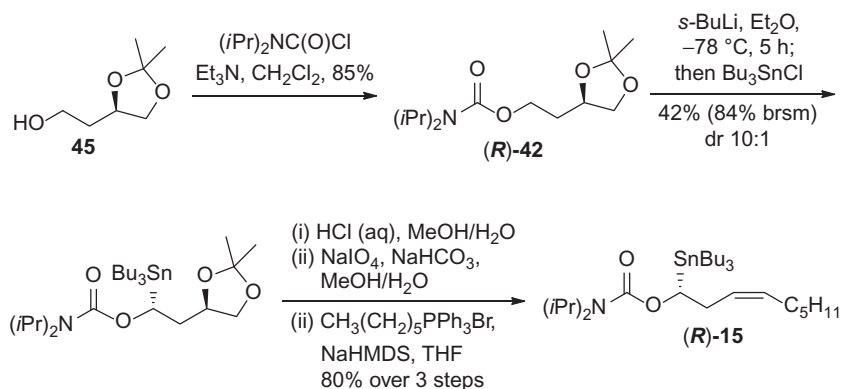
Having investigated two methods of synthesizing the hydroxystannane **36**, without success, it seemed prudent to investigate an alternate route to (**R**)-**15**.

In 1995, Hoppe showed that the 4-*O*-(2,2,4,4-tetramethyl-1-3-oxazolidine-3-carboxylate) of (*S*)-1,2-*O*-isopropylidene (*S*)-**40** can be deprotonated with *s*-BuLi at -78°C with high diastereoselectivity [48]. The lithiated carbamates can be trapped with various electrophiles in high yields and diastereoselectivities. Of particular interest to us was the trapping with Me₃SnCl, giving 74% yield of the stannane **41** in a 98:2 ratio of diastereomers (Scheme 15).

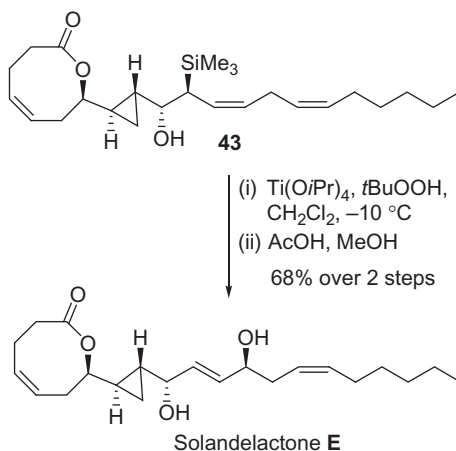
Carbamate (**R**)-**42** was prepared by carbamoylation of the corresponding commercially available alcohol **45**. Lithiation–stannylation of (**R**)-**42** proved to be somewhat variable in yield, with large amounts of starting material being recovered. Thorough investigation of temperature, time, solvent, reagent quality, and equivalents did not result in any improvement in the yield or diastereoselectivity. However, a one-pot deprotection–oxidative cleavage, followed by immediate Wittig reaction on the crude material, gave the desired stannane (**R**)-**15** in 80% yield over three steps (Scheme 16).

3.3 Completion of Solandelactone E

With all the components in hand, the key lithiation–borylation–allylation sequence was attempted with aldehyde **3** and enantioenriched stannane **15**. Pleasingly, allyl-silane **43** was obtained on the first attempt, albeit in low yield (Table 4, entry 1). A milder work-up was introduced (NaHCO₃) that improved the yield considerably, as presumably the NaOH/H₂O₂ was destroying the product over long reaction



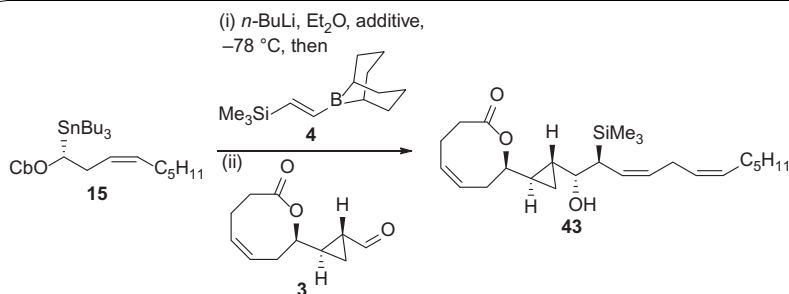
SCHEME 16 Synthesis of stannane carbamate side chain.



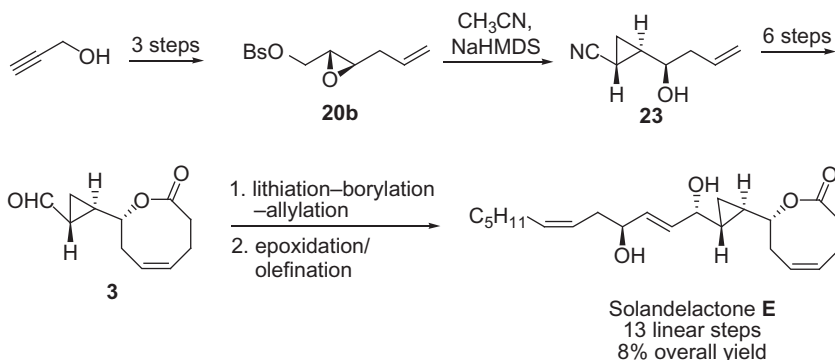
SCHEME 17 Completion of solandelactone E.

times. However, the major side product in this reaction was direct attack of the lithiated carbamate onto aldehyde **3**. This indicated that there was incomplete boronate complex formation, which is usually very fast. A visual inspection of the lithiated species showed a viscous mixture, indicating that the poor ate complex formation was simply due to poor mixing of the borane with the lithiated carbamate. This problem was easily solved by addition of TMEDA or THF to solubilize the lithiated carbamate, which allowed good stirring, leading to complete boronate complex formation and higher yields. Reducing the time of the NaOH/H₂O₂ work-up to 2 h gave the optimized yield of 73% (Table 4, entry 4). The dr of the product was 10:1, indicating there had been complete transfer of stereochemical information from the lithiated carbamate (enantiomeric ratio, er 10:1).

As the allylsilanes are not stable over long periods of time, this material was put directly into the epoxidation–olefination reaction (Scheme 17).

**TABLE 4** Optimization of the Key Lithiation–Borylation–Allylation Step

Entry	Additive	Work-up	Yield (%)
1	None	NaOH/H ₂ O ₂ (o/n)	15
2	None	NaHCO ₃	45
3	THF	NaOH/H ₂ O ₂ (2 h)	56
4	TMEDA	NaOH/H ₂ O ₂ (2 h)	73

**SCHEME 18** Summary of the total synthesis of solandelactone **E**.

However, using *m*CPBA as the epoxidation reagent (as used in our original methodology), poor chemoselectivity over the three double bonds in the molecule was observed. Ti(O*i*Pr)₄/*t*BuOOH was investigated as an alternative, as we postulated that a hydroxy-directed epoxidation could give high chemoselectivity for the *Z*-homoallylic alcohol.

Pleasingly, the epoxidation proceeded with total chemoselectivity and high stereoselectivity at the desired double bond. The acid-catalyzed elimination went smoothly to give a good yield of solandelactone **E**. The analytical data matched exactly with the reported data for both synthetic and natural solandelactone **E** [1–4]. This completed a short (13 steps, longest linear sequence) and highly selective synthesis of solandelactone **E** (Scheme 18).

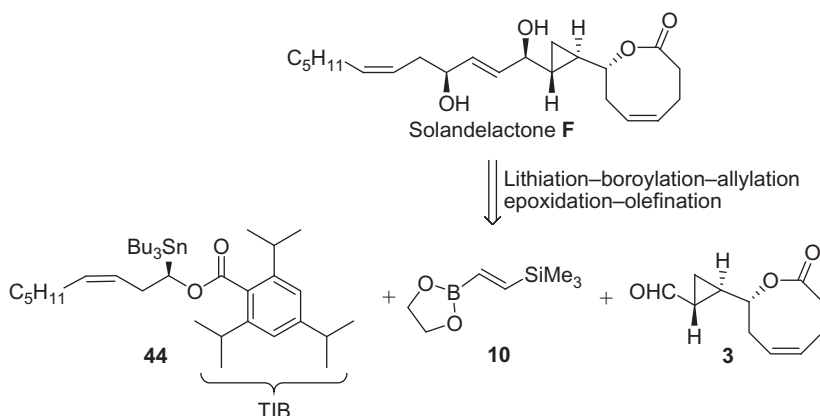
Not only is this synthesis the shortest to date, but more importantly, it is also highly selective. By utilizing the lithiation–borylation–allylation methodology developed in the group, previous selectivity issues when synthesizing the 2-ene-1,4-diol core have been avoided, while maintaining a concise route. The overall yield is slightly lower than other syntheses of a similar length (8% compared with 16% [3] or 19% [4]); however, it was felt that the novel disconnection and greater stereocontrol more than make up for this small drawback.

4. SYNTHESIS OF SOLANDELACTONE F

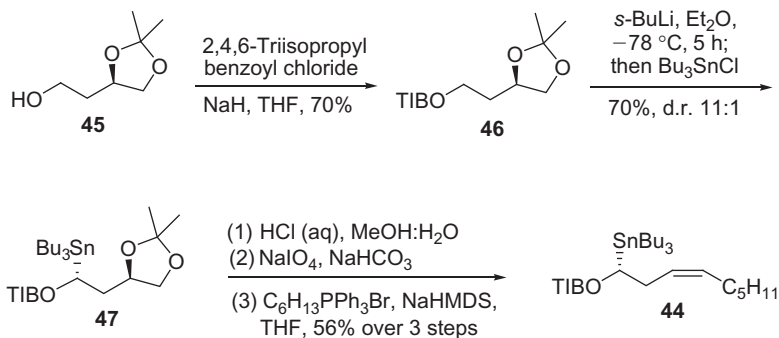
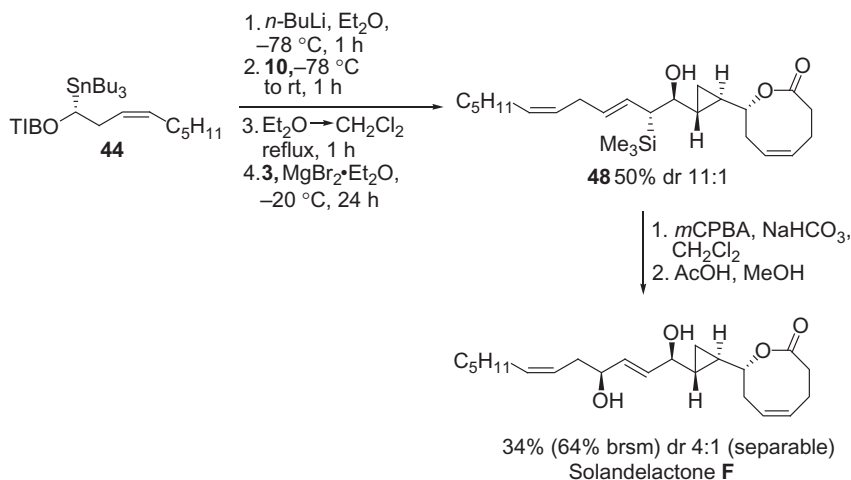
Pleased with our success in achieving the goals set for ourselves with the synthesis of solandelactone **E**, we turned our attention to the synthesis of solandelactone **F**. Disconnection of the *syn-E*-2-ene-1,4-diol according to the methodology described above gives aldehyde **3** (as used in the synthesis of solandelactone **E**), vinyl silyl boronic ester **10**, and stannane **44** (Scheme 19).

Synthesis of stannane **44** followed an analogous route to that previously described for the synthesis of the carbamate fragment **15** of solandelactone **E** (Scheme 20). Following conversion of the commercially available alcohol **45** into benzoate **46**, substrate-directed lithiation and trapping with Bu_3SnCl (as described by Hoppe) [48] furnished **47** with 11:1 dr (inseparable). Installation of the required aliphatic chain was achieved by a sequence of acetal deprotection, oxidative cleavage, and Wittig olefination to give stannane **44**.

Application of the optimized conditions for lithiation–borylation–allylation on stannane **44**, aldehyde **3**, and vinylsilyl boronic ester **10** gave the desired *E*-allylsilane **48** in 50% yield with the same dr as the er of the starting stannane **44** (11:1) (Scheme 21). Epoxidation with 1 equiv. of *m*CPBA



SCHEME 19 Retrosynthesis of solandelactone **F**.

SCHEME 20 Synthesis of stannane **44** for the synthesis of solandelactone **F**.SCHEME 21 Completion of solandelactone **F**.

resulted in chemoselective epoxidation of the *E*-homoallylic alcohol. Acid-catalyzed elimination gave solandelactone **F** as the major stereoisomer (4:1 dr in epoxidation). In this case, $\text{Ti}(\text{OiPr})_4/t\text{BuOOH}$ could not be used to assist with chemoselectivity as it gave poor stereoselectivity in favor of the undesired diastereomer (1:2). Epoxidation of β -hydroxy-*E*-allylsilanes using Yamamoto's method for homoallylic alcohols employing $\text{VO}(\text{acac})_2$ and bishydroxamic acid ligands gave very high stereoselectivity, but again in favor of the undesired diastereomer ($< 1:20$), leading to *syn*-*Z*-2-ene-1,4-diols as the major product [24].

This completed the synthesis of solandelactone **F** in 13 steps (longest linear sequence) from propargylic alcohol and is the first synthesis in which solandelactone **F** has been isolated as the major product in the final step [49].

All data matched with that reported for both the synthetic and natural solandelactone **F** [1,3,4]. It is incredibly satisfying that the key step, synthesis of the *E*-allylsilane **48**, a reaction with so many alternative pathways, worked so well on such a complex substrate. The overall yield was 4%, comparable to that obtained by White [3] and Pietruszka [4]. The lower yield here compared to the overall yield for solandelactone **E** is attributed to the complex nature of the final two steps in this synthesis.

5. CONCLUSIONS

The concise and highly selective syntheses of solandelactones **E** and **F** have been completed, using an efficient combination of both novel methodology, for the synthesis of 2-ene-1,4-diols [14, 49] and well-established protocols such as Sharpless epoxidation and Wittig olefination. The completion of these syntheses demonstrates the power of the lithiation–borylation–allylation sequence developed within the Aggarwal group.

Within the syntheses, a novel route to the lactone core **3** of solandelactones **E** and **F** has been developed, in 10 steps and 16% overall yield. The key steps included Sharpless epoxidation, modified Taber cyclopropanation, and Yamaguchi lactonization. Application of the lithiation–borylation–allylation methodology to this complex fragment demonstrates the robustness and synthetic utility of this methodology. Further, the lithiation–borylation–allylation step showed complete stereocontrol from the lithiated carbamate. Chemoselective epoxidation and olefination was achieved using $\text{Ti}(\text{O}i\text{Pr})_4/t\text{BuOOH}$, yielding solandelactone **E** in 13 steps.

Solandelactone **F** was completed using the complementary methodology for *syn*-2-ene-1,4-diols (Scheme 21). Again, complete control of stereochemistry was shown in the lithiation–borylation–allylation step to form the enantioenriched *E*-allylsilane (Table 4). Chemoselective epoxidation and olefination were achieved using *m*CPBA, yielding solandelactone **F** in 13 steps.

Having developed a route to both *syn* and *anti*-2-ene-1,4-diols and a concise route to aldehyde **3**, it is clear that the synthesis of all solandelactones **A–H** could be easily completed. Simple hydrogenation of the C4–C5 alkene in **3** would give the aldehyde required for solandelactones **A–D** and an alternative stannane benzoate (with an additional double bond) could be utilized in the synthesis of solandelactones **C**, **D**, **G**, and **H**.

REFERENCES

- [1] Y. Seo, K.W. Cho, J.-R. Rho, J. Shin, *Tetrahedron* 52 (1996) 10583–10596.
- [2] (a) J.E. Davoren, S.F. Martin, *J. Am. Chem. Soc.* 129 (2007) 510–511; (b) J.E. Davoren, C. Harcken, S.F. Martin, *J. Org. Chem.* 73 (2008) 391–402.
- [3] (a) J.D. White, W.H.C. Martin, C.M. Lincoln, J. Yang, *Org. Lett.* 9 (2007) 3481–3483; (b) J. D. White, C.M. Lincoln, J. Yang, W.H.C. Martin, D.B. Chan, *J. Org. Chem.* 73 (2008) 4139–4150.

- [4] J. Pietruszka, A.C. Rieche, *Adv. Synth. Catal.* 350 (2008) 1407–1412.
- [5] S. Varadarajan, D.K. Mohapatra, A. Datta, *Tetrahedron Lett.* 39 (1998) 1075–1078.
- [6] D.K. Mohapatra, G.S. Yellol, *Arkivoc* (2003) 21–33.
- [7] Da Silva, C. Barloy, P. Pale, *Tetrahedron Asymmetry* 9 (1998) 3951–3954.
- [8] K. Takai, K. Kimura, T. Kuroda, T. Hiyama, H. Nozaki, *Tetrahedron Lett.* 24 (1983) 5281–5284.
- [9] H. Jin, J. Uenishi, W.J. Christ, Y. Kishi, *J. Am. Chem. Soc.* 108 (1986) 5644.
- [10] For syntheses of halicholactone featuring a NHK coupling, see: (a) D.J. Critcher, S. Connolly, M. Wills, *J. Org. Chem.* 62 (1997) 6638–6657; (b) D.J. Critcher, S. Connolly, M. Wills, *Tetrahedron Lett.* 36 (1995) 3763–3766; (c) T. Takahashi, H. Watanabe, T. Kitahara, *Heterocycles* 58 (2002) 99–104; (d) C.-Y. Zhu, X.-Y. Cao, B.-H. Zhu, C. Deng, X.-L. Sun, B.-Q. Wang, Q. Shen, Y. Tang, *Chem. Eur. J.* 15 (2009) 11465–11468; (e) M. Bischof, V. Doum, A.C. M. Nordschild (née Rieche), J. Pietruszka, D. Sandkuhl, *Synthesis* (2010) 527–537.
- [11] J.D. White, M.S. Jensen, *J. Am. Chem. Soc.* 115 (1993) 2970–2971.
- [12] (a) Y. Takemoto, Y. Baba, G. Saha, S. Nakao, C. Iwata, T. Tanaka, T. Ibuka, *Tetrahedron Lett.* 41 (2000) 3653–3656; (b) Y. Baba, G. Saha, S. Nakao, C. Iwata, T. Tanaka, T. Ibuka, H. Ohishi, Y. Takemoto, *J. Org. Chem.* 66 (2001) 81–88.
- [13] For syntheses of constanolactone featuring a NHK coupling, see: (a) J. Pietruszka, A.C. M. Rieche, N. Schoene, *Synlett* (2007) 2525–2528; (b) C.B.-D. Silva, A. Benkouider, P. Pale, *Tetrahedron Lett.* 41 (2000) 3077–3081; (c) J.D. White, M.S. Jensen, *J. Am. Chem. Soc.* 117 (1995) 6224–6233.
- [14] (a) M. Binanzer, G.Y. Fang, V.K. Aggarwal, *Angew. Chem. Int. Ed.* 49 (2010) 4264–4268; For other related work on lithiated carbamates, see: (b) J.L. Stymiest, G. Dutheil, A. Mahmood, V.K. Aggarwal, *Angew. Chem. Int. Ed.* 46 (2007) 7491–7494; (c) G. Dutheil, M.P. Webster, P.A. Worthington, V.K. Aggarwal, *Angew. Chem. Int. Ed.* 48 (2009) 6317–6319; (d) M. Althaus, A. Mahmood, J. Ramón Suárez, S.P. Thomas, V.K. Aggarwal, *J. Am. Chem. Soc.* 132 (2010) 4025–4028.
- [15] W.R. Roush, P.T. Grover, *Tetrahedron Lett.* 31 (1990) 7567–7570.
- [16] (a) D. Hoppe, F. Hintze, P. Tebben, *Angew. Chem. Int. Ed.* 29 (1990) 1422–1424; (a) For reviews, see: D. Hoppe, T. Hense, *Angew. Chem. Int. Ed.* 109 (1997) 2376–2420 *Angew. Chem. Int. Ed.* 36 (1997) 2282–2316; (b) E. Beckmann, V. Desai, D. Hoppe, *Synlett* 15 (2004) 2275–2280; (c) E. Beckmann, D. Hoppe, *Synthesis* 37 (2005) 217–220.
- [17] A. Robinson, V.K. Aggarwal, *Angew. Chem. Int. Ed.* 49 (2010) 6673–6675.
- [18] (a) For examples, see: J.M. Stoddard, K.J. Shea, *Chem. Commun.* 40 (2004) 830–831; (b) A. Bottoni, M. Lombardo, A. Neri, C. Trombini, *J. Org. Chem.* 68 (2003) 3397.
- [19] (a) P. Beak, M. Baillargeon, L.G. Carter, *J. Org. Chem.* 43 (1978) 4255–4256; (b) F. Hammond-Schmidt, A. Hanninger, B.P. Simov, H. Völlenkle, A. Werner, *Eur. J. Org. Chem.* 64 (1999) 3511–3518; (c) R. Larouche-Gauthier, C.J. Fletcher, I. Couto, V. K. Aggarwal, *Chem. Commun.* 47 (2011) 12592–12594.
- [20] Allylboranes react readily with aldehydes at -78°C (a), whereas allylboronic esters require room temperature or above (b). For examples, see: (a) H.C. Brown, P.K. Jadhav, *J. Am. Chem. Soc.* 105 (1983) 2092–2093; (b) R.W. Hoffmann, B. Landmann, *Angew. Chem. Int. Ed. Engl.* 23 (1984) 437–438.
- [21] (a) J.W.J. Kennedy, D.G. Hall, *J. Am. Chem. Soc.*, 124 (2002) 11586; (b) For reviews, see: D. G. Hall, *Synlett* (2007) 1644; (c) J.W.J. Kennedy, D.G. Hall, D.G. Hall (Ed.), *Boronic Acids*, Wiley-VCH, Weinheim, Germany, 2005; p. 241, Chapter 6.
- [22] Y. Landais, L. Parra-Rapado, *Tetrahedron Lett.* 37 (1996) 1205–1208.

- [23] (a) I. Fleming, A.K. Sarkar, A.P. Thomas, *J. Chem. Soc. Chem. Commun.* (1987) 157–159; (b) I. Fleming, N.J. Lawrence, A.K. Sarkar, A.P. Thomas, *J. Chem. Soc. Perkin. Trans. 1* (1992) 3303–3308.
- [24] (a) W.R. Roush, P.T. Grover, *Tetrahedron Lett.* 52 (1990) 7567–7570; (b) W.R. Roush, P. T. Grover, *Tetrahedron* 48 (1992) 1981–1998.
- [25] W.R. Roush, A.N. Pinchuk, G.C. Micalizio, *Tetrahedron Lett.* 41 (2000) 9413–9417.
- [26] A.G.M. Barrett, J.W. Malecha, *J. Org. Chem.* 56 (1991) 5243–5254.
- [27] M.A. Sparks, J.S. Panek, *J. Org. Chem.* 56 (1991) 3431–3438.
- [28] I.E. Wrona, J.T. Lowe, T.J. Turbyville, T.R. Johnson, J. Beignet, J.A. Beutler, J.S. Panek, *J. Org. Chem.* 74 (2009) 1897–1916.
- [29] R.W. Carling, A.B. Holmes, *J. Chem. Soc. Chem. Commun.* (1986) 325–326.
- [30] J. Pietruszka, A.C.M. Rieche, T. Wilhelm, A. Witt, *Adv. Synth. Catal.* 345 (2003) 1273–1286.
- [31] B.C. Ranu, A. Majee, *Chem. Commun.* (1997) 1225–1226.
- [32] (a) For Sharpless epoxidation of this substrate, see: Y.E. Raifeld, A.A. Nikitenko, B. M. Arshava, I.E. Mikerin, L.L. Zilberg, G.Y. Vid, S.A. Lang Jr., V.J. Lee, *Tetrahedron* 50 (1994) 8613–8616; (b) X. Ginesta, M.A. Pericas, A. Riera, *Tetrahedron Lett.* 43 (2002) 779–782; (c) For Sharpless' seminal work on catalytic asymmetric epoxidation, see: Y. Gao, J.M. Klunder, R.M. Hanson, H. Masamune, S.Y. Ko, K.B. Sharpless, *J. Am. Chem. Soc.* 109 (1987) 5765–5780; (d) H.C. Kolb, M.S. Van Nieuwenhze, K.B. Sharpless, *Chem. Rev.* 94 (1994) 2483–2547.
- [33] D.F. Taber, G. Bui, B. Chen, *J. Org. Chem.* 66 (2001) 3423–3426.
- [34] G. Illuminati, L. Mandoli, *Acc. Chem. Res.* 14 (1981) 95–102.
- [35] S.J. Miller, S.-H. Kim, Z.-R. Chen, R.H. Grubbs, *J. Am. Chem. Soc.* 117 (1995) 2108–2109.
- [36] C.A. Tarling, A.B. Holmes, R.E. Markwell, N.D. Pearson, *J. Chem. Soc. Perkin. Trans. 1* (1999) 1695–1701.
- [37] D.K. Mohapatra, K.A. Durugkar, *Arkivoc* (2004) 146–155.
- [38] L. Gulajski, P. Sledz, A. Lupa, K. Grela, *Green Chem.* 10 (2008) 271–274.
- [39] J.R.D. Valle, M. Goodman, *J. Org. Chem.* 69 (2004) 8946–8948.
- [40] I. Shiina, *Chem. Rev.* 107 (2007) 239–273.
- [41] W. Yu, Y. Mei, Y. Kang, Z. Hua, Z. Jin, *Org. Lett.* 6 (2004) 3217–3219.
- [42] O.G. Backenberg, B. Staskun, *J. Chem. Soc.* (1962) 3961–3963.
- [43] For an example of the use of DIBAL reduction in this situation in synthesis, see: Hong, J. Yang, S.M. Weinreb, *J. Org. Chem.* 71 (2006) 2078–2089.
- [44] A. He, J.R. Falck, *Angew. Chem. Int. Ed.* 47 (2008) 6586–6589.
- [45] P.C.M. Chan, J.M. Chong, *J. Org. Chem.* 53 (1988) 5584–5586.
- [46] (a) J.A. Marshall, G.S. Welmaker, B.W. Gung, *J. Am. Chem. Soc.* 113 (1991) 647–656; (b) J.A. Marshall, A.W. Garofalo, K.W. Hinkle, *Org. Synth.* 77 (2000) 98–106.
- [47] K. Narasaka, A. Morokawa, K. Saigo, Y. Mukaiyama, *Bull. Chem. Soc. Jpn.* 50 (1977) 2773–2776.
- [48] H. Helmke, D. Hoppe, *Synlett* (1995) 978–980.
- [49] A. Robinson, V.K. Aggarwal, *Org. Biomol. Chem.* 10 (2012) 1795–1801.

The Marine Alkaloid Halichlorine: Its Defenses and Its Defeat

Derrick L.J. Clive

Chemistry Department, University of Alberta, Edmonton, Alberta, Canada

Chapter Outline

1. Introduction	25	7. The Ring A Problem and the Development of a General Annulation Method	38
2. The First Approach	27	8. The Continuing Saga of Ring A	43
3. The First Surprise	30	9. Formation of the Macrolactone	43
4. The Second Approach	32	10. The Optical Purity Problem	47
5. Saved by Selenium	34	11. Conclusion	50
6. A Stereochemical Disaster—But a Blessing in Disguise	38		

Two thirds of our planet are covered by water. Two thirds of our planet are unexplored.

1. INTRODUCTION

The quotation above comes from the start of a weekly television series about marine life. The programs first aired about half a century ago and referred to the teeming life beneath the surface of the sea. This was well before the era of marine natural products chemistry, but the quotation is still very apt in a chemical context. The pioneers of marine natural products [1] have amply shown us glimpses of the unimagined riches of bizarre structures and

associated biological activities to be found in marine organisms, and it is no wonder that such natural products provide a significant proportion of irresistible targets to synthetic chemists.

My own interest was directed to this area as a result of the Ph.D. program regulations in my Department: one of the hurdles, which is approached with some trepidation by graduate students, is the presentation of a review lecture in front of the whole Organic Chemistry Division. In satisfying this requirement, one member of my group gave a lecture on a marine alkaloid, and in consequence, he gained some familiarity with the area. He drew my attention to halichlorine (**1**) [2] (Figure 1) at a time when he had just completed his first research project—on the frog alkaloid epibatidine—and wanted to start a new one. The compound seemed to have all the characteristics to qualify as a worthwhile synthetic target: it had not been synthesized before, it represented a new and challenging structural type, it possessed potentially important biological properties, and it was not so large as to obviously require huge resources. As the structural type was new and did not seem to be accessible by analogy with prior synthetic work, it represented what is best described as a *complex* synthetic target, as distinct from a *complicated* target. By the latter term, I mean a compound that is not structurally simple but which can be made totally or mainly along lines already available in the literature, whereas the route to a *complex* target is largely not predictable on the basis of existing knowledge. Complex targets invariably place the experimentalist in positions that have not been faced before and so the chances of discovering something new are maximized.

The relevant prior literature comprised a route to the Weinreb amide **2** [3], a precursor of the 1,4-diene substructure of halichlorine, and a route to the spirocyclic amine **3** [4] (Figure 2). That spiro compound was to be one of the many [5,6] azabicyclic models to appear in the literature during the course of our work, but fortunately, none of the approaches resembled our own. This situation illustrates some of the pros and cons of choosing a complex target with notable biological properties: one rarely has the field to oneself, but that hazard is offset by the availability of a very large number of synthetic

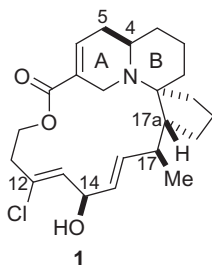


FIGURE 1 Structure of halichlorine.

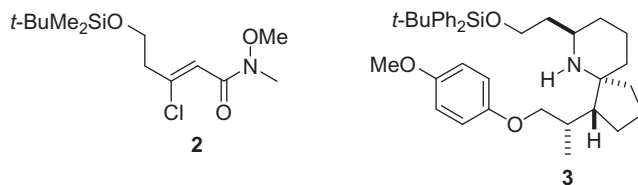


FIGURE 2 Reagent **2** and an early model compound.

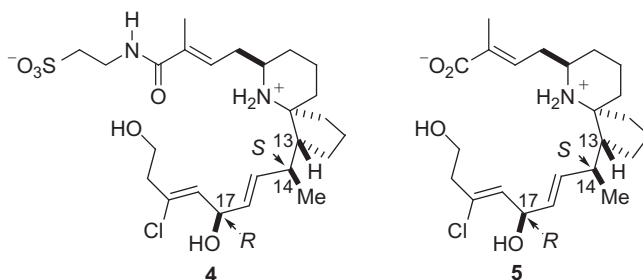


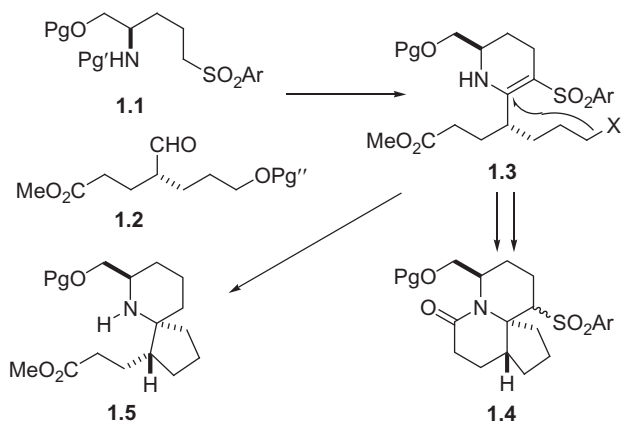
FIGURE 3 Taupinnaic acid and pinnaic acid.

approaches so that the chances are high that each research group will follow a different route; in the event, this was indeed the case with halichlorine.

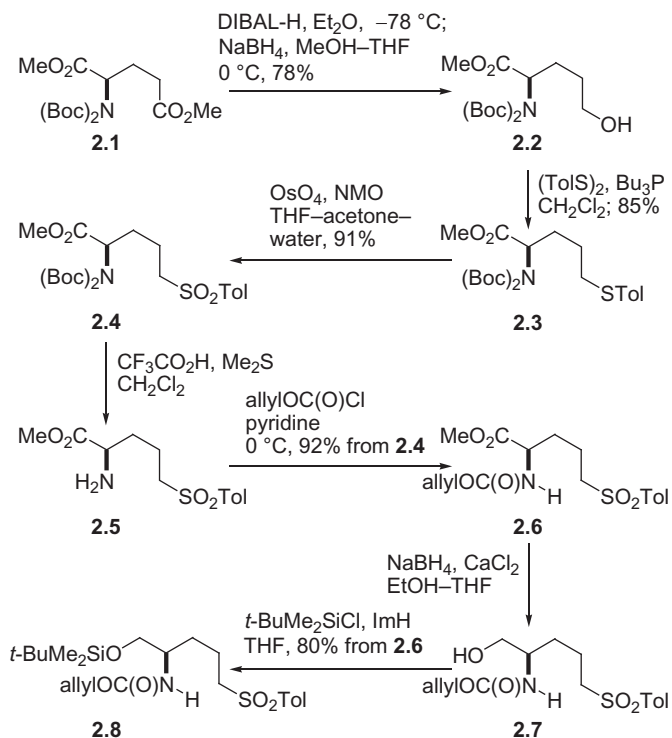
The compound owes its discovery [2] to an extensive research program [7] directed at the isolation of biologically active compounds from marine organisms. During this endeavor, a black marine sponge *Halichondria okadai* Kadota was collected in Japanese waters. Examination of the sponge extracts showed the presence of a substance—halichlorine (**1**)—which is a selective inhibitor of the induction of vascular cell adhesion molecule-1 [8] (VCAM-1), a property that renders it relevant to the study and/or treatment of inflammatory diseases [9] as well as the spread [8,10] of cancer cells. Two structurally related compounds, (**4**) and (**5**) (Figure 3), were later isolated [11] from a different organism and also found to have a significant biological property, in this case, inhibition of a cytosolic phospholipase, cPLA₂, again a property of potential value in connection with inflammatory diseases.

2. THE FIRST APPROACH

With a compelling combination of factors advocating the choice of halichlorine as a synthetic target, we began the difficult task of its synthesis. Our approach [12] was strongly influenced by the concepts of radical cyclization, a main area of research in my laboratory, and the initial plan was to link structures of types **1.1** and **1.2** so as to set the stage for radical cyclization along the lines **1.3**→**1.4** or **1.5** (Scheme 1). Of course, this approach obviously implies that an amino acid would serve as one of the starting materials, and to this end,



SCHEME 1 Initial plan.

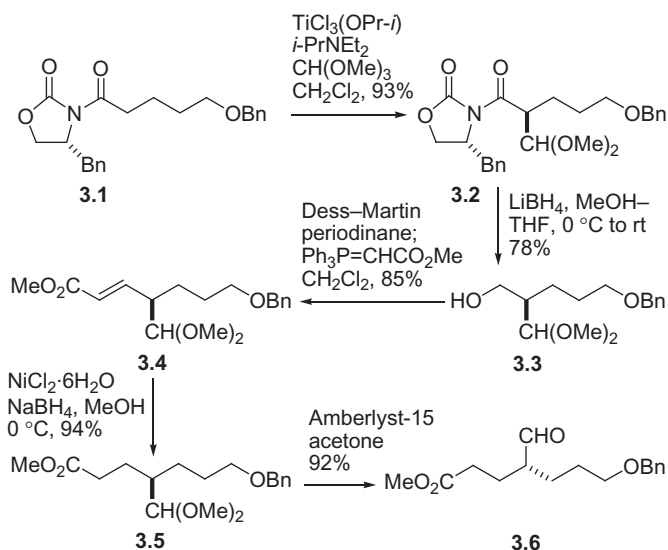
SCHEME 2 The upper segment. Tol=C₆H₄Me-*p*.

D-glutamic acid was converted (Scheme 2) into the diester **2.1** [13], which was selectively reduced in two steps (DIBAL-H and then NaBH₄) to alcohol **2.2**. Replacement of the hydroxyl by a (4-methylphenyl)thio group, using Tol₂S₂/Bu₃P, and oxidation with catalytic OsO₄ in the presence of

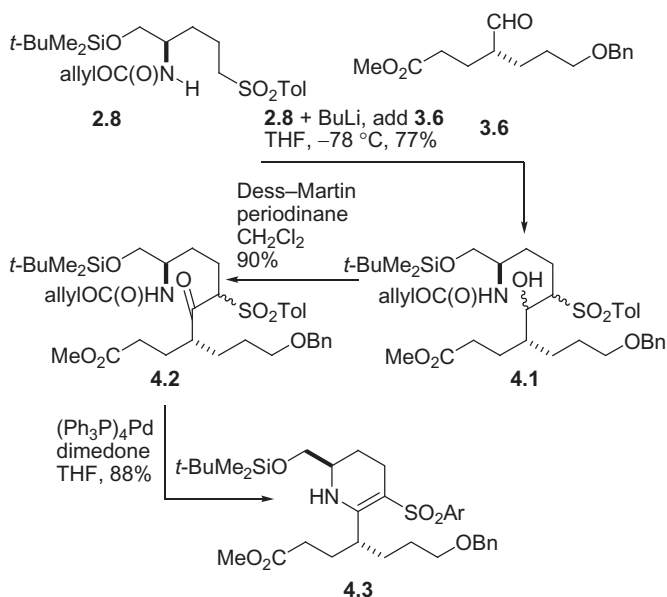
N-methylmorpholine-*N*-oxide gave **2.4**. Removal of the *N*-Boc groups in the normal way ($\text{CF}_3\text{CO}_2\text{H}$, Me_2S) and reprotection as an allyl carbamate took the route as far as **2.6**. Finally, ester reduction (NaBH_4 , CaCl_2) and silylation of the resulting alcohol furnished the first subunit for our needs.

The other component, also optically pure, was assembled by Evans asymmetric alkylation: The oxazolidinone **3.1** gave an excellent yield of **3.2** on reaction with $\text{CH}(\text{OMe})_3$ in the presence of $\text{TiCl}_3(\text{OPr-}i)$ and Hünig's base (Scheme 3). Removal of the chiral auxiliary (**3.2** \rightarrow **3.3**), oxidation of the resulting alcohol, and Wittig homologation yielded the olefinic ester **3.4**. The double bond was then saturated by treatment with NaBH_4 – NiCl_2 [14], and the dimethyl acetal group was hydrolyzed, yielding the required subunit **3.6**, all these transformations being achieved without racemization.

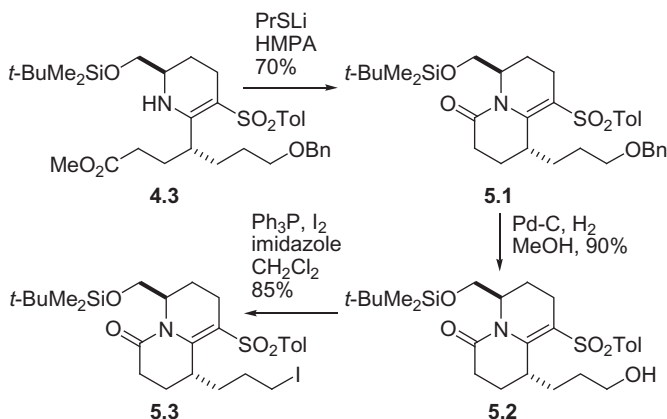
The two subunits were joined by deprotonation of **2.8** and reaction with **3.6** (Scheme 4). The resulting hydroxy sulfones **4.1** were easily oxidized (**4.1** \rightarrow **4.2**), and removal of the allyloxy group under standard conditions [$(\text{Ph}_3\text{P})_4\text{Pd}$, dimedone] afforded the desired enamine **4.3**. When this substance was treated with PrSLi in HMPA at room temperature, the lactam **5.1** could be isolated in 70% yield (Scheme 5). This was an unexpected result, as simple conversion of the ester to the acid would have been the normal outcome. In any event, with the lactam in hand it was then a simple matter to remove the *O*-benzyl group by hydrogenolysis (**5.1** \rightarrow **5.2**). Finally, replacement of the hydroxyl in **5.2** by iodine gave **5.3**, the substrate for the intended radical cyclization.



SCHEME 3 The lower segment.



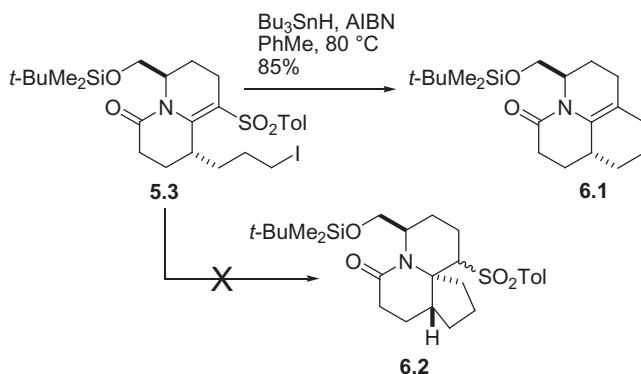
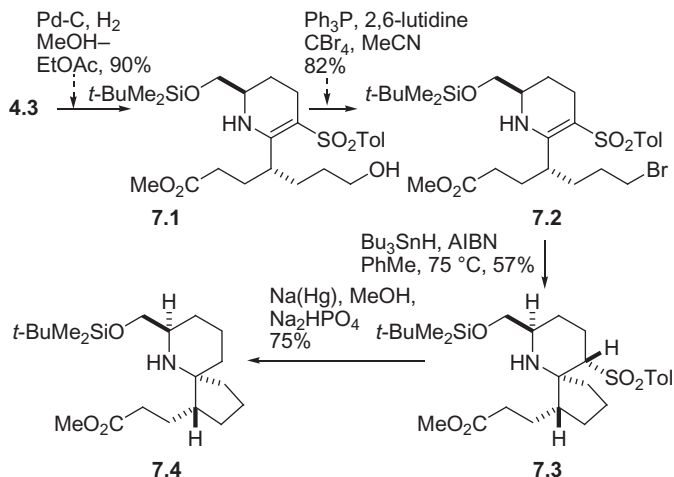
SCHEME 4 Linking of the subunits.



SCHEME 5 Formation of the radical cyclization precursor.

3. THE FIRST SURPRISE

Slow addition of Bu_3SnH and AIBN to a hot toluene solution of **5.3** gave a good yield (85%) of a cyclization product, but the material was **6.1** instead of the desired **6.2** [12]. The exclusive preference for 6-*endo* closure was surprising (Scheme 6). We wondered if steric factors, possibly subtle ones, were responsible, and so we decided to try cyclization of a related but more

SCHEME 6 6-*Endo-trig* cyclization.SCHEME 7 5-*Exo-trig* cyclization.

flexible system. With this in mind, the enamine **4.3** was subjected to hydrogenolysis conditions (Scheme 7) to release the alcohol **7.1**, which was converted into its bromide **7.2**. When the bromide was subjected to standard conditions for radical cyclization, it was converted into two products, the desired spirocycle **7.3** (57%) and the simple reduction product (replacement of Br by H, 30%).

Spirocycle **7.3** was obtained as a single isomer; the stereochemistry shown is based on TROESY NMR measurements. Desulfurization, using a large excess of 10% Na(Hg), afforded **7.4**. This represents the spirocyclic core segment of halichlorine but is not an advance over the prior synthetic work. The modest yield in the radical cyclization step dampened our enthusiasm for this route, and we decided on a different approach which, in the event, ultimately

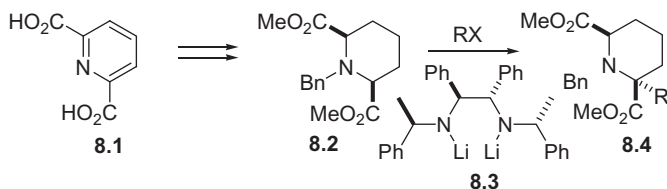
led to the target and also opened up a pathway to two very useful reactions—one for making rings and the other for making optically pure α -substituted piperidines.

However, before leaving our first approach, we examined a minor problem that had arisen. The desulfonylation step **7.3**→**7.4** was initially found to be very slow so that even after 24 h there was only 30% conversion, and a large excess of Na(Hg) was needed to raise the yield to an acceptable level. The majority of desulfonylations reported in the literature have been carried out with phenyl sulfones; our observations could imply that electron-donating substituents retard the process appreciably, and it was easy enough to establish that this is indeed the case [15]. We compared the desulfonylation of compounds containing 4-fluorophenyl-, 4-methylphenyl-, and 2-naphthyl sulfone units and found that the 4-fluorophenyl- and 2-naphthyl sulfones are desulfonylated rapidly (30 min) at $-10\text{ }^{\circ}\text{C}$, while the phenyl sulfone requires twice as long and the 4-methylphenyl sulfone reacted only partially under the same conditions.

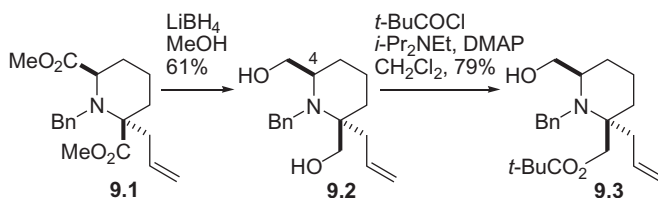
4. THE SECOND APPROACH

By the time we had taken our second approach to a promising stage, from which a successful outcome seemed likely, the Danishefsky group had completed the synthesis of both halichlorine and pinnaic acid [16,17], and there was already a large number of model studies on the azaspiro system [5], but fortunately, none of the other groups were following a similar route to ours.

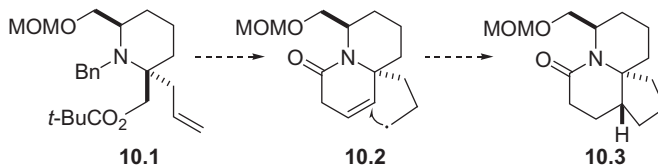
Our second route involved setting up the quaternary stereogenic center at a very early stage, and we planned to do this by using a method for asymmetric alkylation that had been reported [18] in the literature. The commercially available diacid **8.1** was esterified, hydrogenated, and N-benzylated, all by literature methods, to give **8.2** (Scheme 8). Deprotonation of this compound with the optically pure base **8.3**, followed by treatment with an alkyl halide, had been shown [18] to afford compounds of type **8.4** with very high ee. Six alkylating agents were used and three of the products were examined by chiral HPLC; the ee in each case was at the impressive level of $\geq 98\%$. Among the three experiments that were not examined in such detail was the use of allyl bromide, but it seemed reasonable to assume that the ee would also be high. It later turned out that our faith in this respect was misplaced, although with ultimately fortunate consequences, because it prompted us to



SCHEME 8 Asymmetric alkylation.



SCHEME 9 Asymmetric allylation.



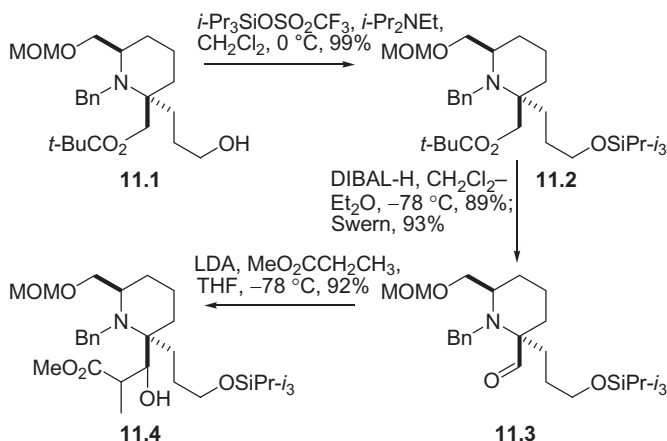
SCHEME 10 Plan for the spiro system.

develop a new route to optically pure piperidines to rectify the problem, as I shall describe later. At this stage, we repeated the asymmetric alkylation of **8.2**, using allyl bromide, to obtain **9.1**; only later would we discover that its ee was a mere 69% (Scheme 9). Both ester groups were reduced with LiBH_4 and we planned to then selectively protect the less hindered hydroxyl by pivaloylation. However, treatment of **9.2** with pivaloyl chloride unexpectedly gave **9.3**. In a later experiment, we monosilylated **9.2** and obtained the expected product [19] of silylation at the less hindered C(4)¹ hydroxymethyl group.

The fact that the pivaloylation of **9.2** had an unexpected outcome was of no consequence as the only requirement was that the hydroxyls of **9.2** be differently protected. Alcohol **9.3** was then protected as its MOM (methoxymethyl) ether **10.1**. Having reached this point, our plan was to construct a new ring, either five-membered or, as shown in Scheme 10, six-membered (**10.1**→**10.2**), in order to impart rigidity and then to carry out a radical cyclization (**10.2**→**10.3**); such an approach would allow us to form the spiro subunit and to set the stage for introduction of the C(17) methyl group, all in the correct stereochemical sense.

These plans were implemented by hydroboration of the pendant olefin in **10.1** and the resulting alcohol (**11.1**) was protected as a triisopropylsilyl ether (Scheme 11). The pivaloyl group was then removed in the standard way (DIBAL-H) and the hydroxymethyl group thus released was oxidized to the corresponding aldehyde (**11.3**). Condensation of the enolate derived from methyl propionate then gave a 92% yield of two isomers (**11.4**) in a 2:3 ratio. This result came as a great relief, as the aldehyde group of **11.3** is hindered

1. Atoms in intermediates are assigned the number they would have in halichlorine.



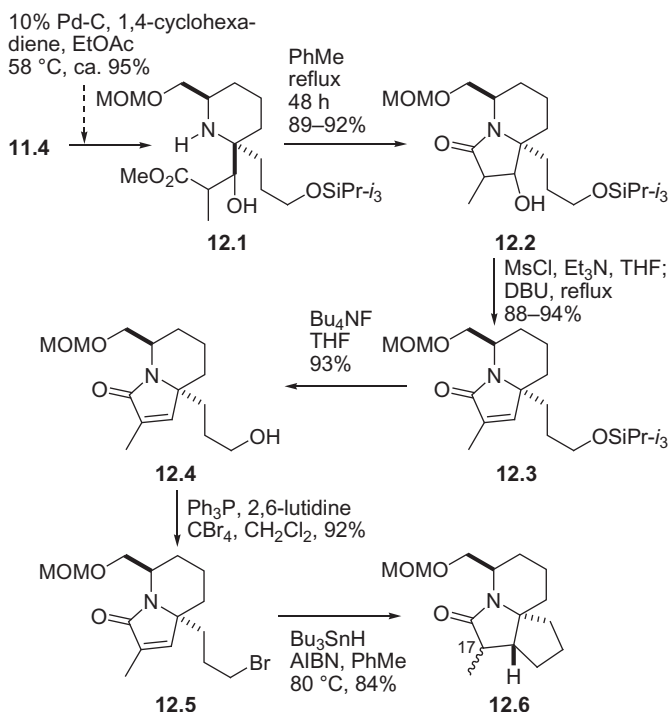
SCHEME 11 Chain elongation for making the spiro system.

and few of the condensations we tried with other carbanions or enolates were successful. Initially, we separated the isomers and processed them individually, but this is unnecessary, as both are equally suitable for our purposes.

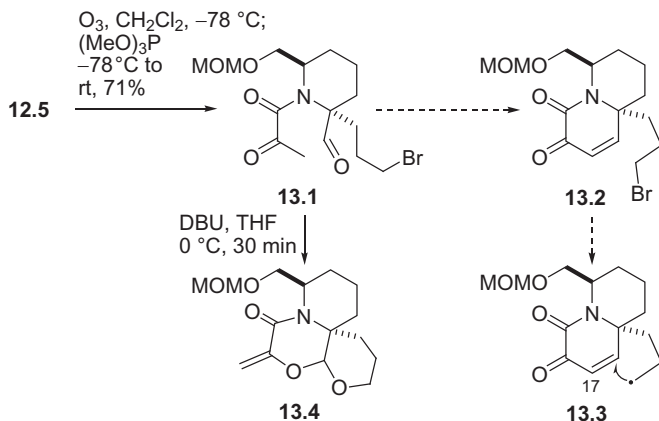
Removal of the *N*-benzyl group (Scheme 12) by brief heating with 10% Pd/C in the presence of 1,4-cyclohexadiene released the parent amines **12.1** (ca. 95% for each isomer). When these were heated for 2 days in boiling toluene, the isomeric lactams **12.2** were formed in good yield (89–92%). Mesylation and prolonged heating with DBU in THF then converted both lactams into the same compound (**12.3**) in about 90% yield for each isomer. At this point, removal of the silyl group and reaction with $\text{Ph}_3\text{P/CBr}_4$ installed a homolyzable substituent—the bromine atom—at the end of the pendant chain, and radical cyclization produced the tricyclic lactams **12.6**. The yield was very satisfactory (84%) but our ability to control the stereochemical outcome was not: lactams **12.6** were obtained as a 1:4 mixture of C(17) isomers with the desired β -isomer being the minor component, exactly as expected on steric grounds. However, although the ratio could be almost reversed by equilibration with *t*-BuOK/*t*-BuOH, the epimers were too difficult to separate for this route to be practical, and so we were forced to make some alterations in order to expand the opportunities for stereochemical control at C(17), while preserving as much of our previous work as possible.

5. SAVED BY SELENIUM

We retraced our steps only back to bromide **12.5** and then cleaved the double bond by ozonolysis (Scheme 13) so as to produce the tricarbonyl system **13.1**. Our hope was that treatment of the tricarbonyl compound with base would effect aldol condensation to give **13.2** so that radical cyclization (see **13.3**, arrow) would serve to generate the spiro system and form a structure whose



SCHEME 12 Radical cyclization of the bromide.



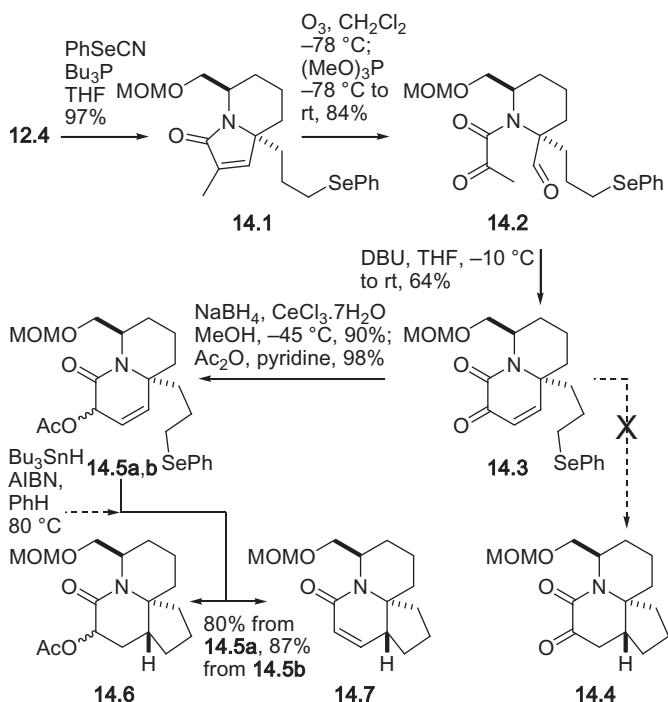
SCHEME 13 Plans for the bromide.

shape would allow easy control of the stereochemistry at C(17) when a methyl group was introduced. However, base treatment of **13.1** gave **13.4**, due to the sensitivity of the bromine to displacement. Fortunately, this problem was easily solved by taking advantage of the fact that selenides are much more stable

than bromides to bases and to displacement, while still providing an easily homolyzed bond (C—SePh).

Based on these considerations, alcohol **12.4** was converted in the standard way into selenide **14.1** (Scheme 14). Ozonolysis and reductive workup, both at low temperature, gave **14.2**, and intramolecular aldol condensation led to **14.3**, ready for radical cyclization to **14.4**. Both of the last two steps (**14.1**→**14.2**→**14.3**) deserve some comment: During the ozonolysis, the phenylseleno group in **14.1** is undoubtedly converted into a selenoxide, but fragmentation to an alkene does not occur at the low temperature of the ozonolysis so that addition of a reducing agent converts the selenoxide back to the selenide. The successful outcome of the intramolecular aldol condensation illustrates the role of a PhSe-group as a base-stable but homolyzable substituent that is also inert to nucleophilic displacement.

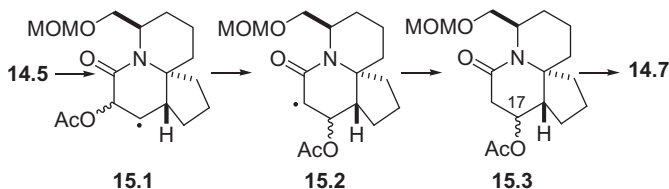
Although **14.3** was in hand, we still had to clear away one minor obstacle, because treatment of **14.3** with a stannane did not produce **14.4**, and we suspected that the enone system of **14.3** reacted in preference to the phenylseleno group. Accordingly, **14.3** was reduced under Luche conditions and the resulting alcohols were acetylated (**14.3**→**14.5a,b**). These epimeric acetates did undergo the desired radical cyclization in a perfectly satisfactory but



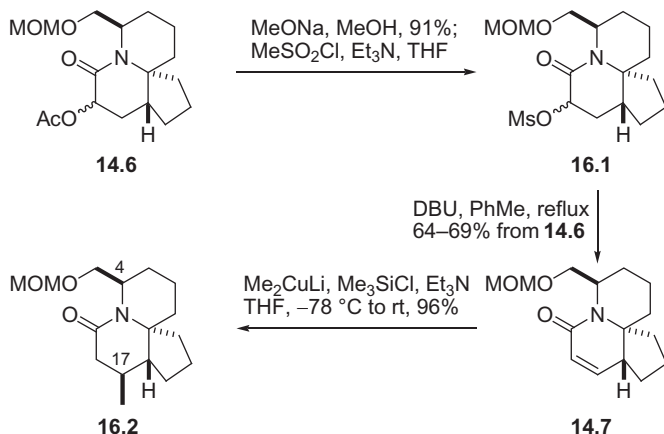
SCHEME 14 Radical cyclization of the selenide.

unanticipated way—unanticipated because we had not thoroughly considered the possible outcomes, an omission that is understandable in view of the very large number of uneventful radical cyclizations done in my group. What we isolated in the present case was a mixture (80% from **14.5a** and 87% from **14.5b**) of the desired acetates **14.6** and the unsaturated lactam **14.7**. This was of no consequence because **14.7** was intended to be the next intermediate in our route and is easily accessible from **14.6**. Its likely mode of formation is interesting. We assume that the intermediate radical **15.1** undergoes a 1,2-shift of the acetoxy group [20] to produce **15.2**, which is then reduced (**Scheme 15**). Elimination from the C(17) acetates **15.3** affords the observed unsaturated lactam **14.7**.

The acetates **14.6** were deacetylated (**Scheme 16**) by treatment with MeONa/MeOH and then mesylation and treatment with DBU in refluxing toluene served to convert all the radical cyclization products to the unsaturated lactam **14.7**. Finally, we introduced the eventual C(17) methyl group by cuprate addition (**14.7**→**16.2**). Such reactions with lactams are not well known, but this one worked well (96%) in the presence of Me₃SiCl, and the stereochemical outcome was exactly as required.



SCHEME 15 Formation of enone **14.7**.



SCHEME 16 Introduction of the C(17) methyl group.

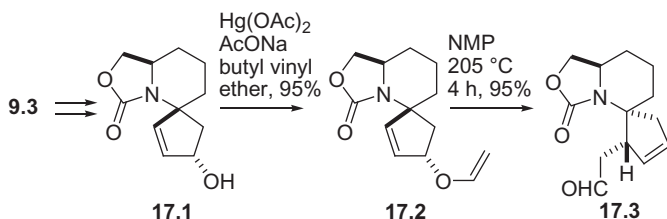
6. A STEREOCHEMICAL DISASTER—BUT A BLESSING IN DISGUISE

During the above studies, another route from alcohol **9.2** was also explored [19] and had led, via a ring closing metathesis, to the alcohol **17.1** (Scheme 17). This gave an enol ether **17.2** by reaction with butyl vinyl ether, and thermal Claisen rearrangement then produced the spirocycle **17.3**. This route was taken a few steps further, but the carbamate subunit resisted our attempts to open it, and by the time we had found that Me_3SiONa is an effective reagent for this purpose, the route described above had been fully developed. One important result from the Claisen rearrangement approach was the finding that crystals of **17.1**, examined by single crystal X-ray diffraction, were racemic, and this is the point at which we were alerted to the fact that the asymmetric allylation (**8.2**→**9.1**) was far less effective than we had assumed. We decided to accept the situation for the time being with the serious intention of later returning to this matter.

7. THE RING A PROBLEM AND THE DEVELOPMENT OF A GENERAL ANNULATION METHOD

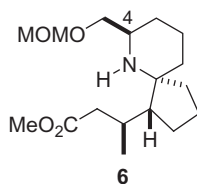
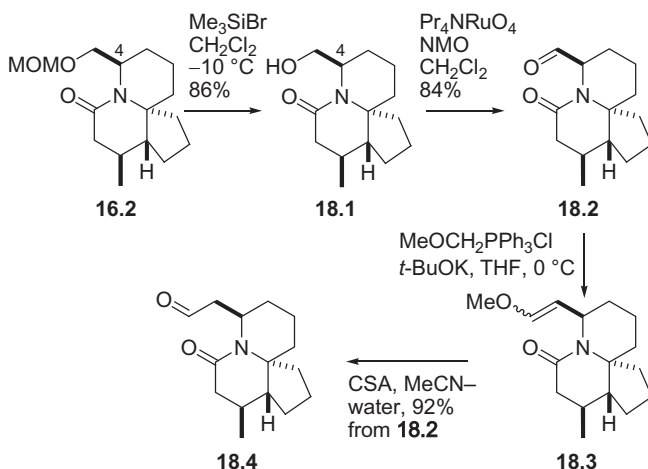
When the structure of **16.2** is compared with that of halichlorine, it is clear that the next task is to construct ring A, and to this end, we needed, either at this stage or shortly thereafter, to open the lactam ring. To our dismay, this seemingly straightforward operation was extremely troublesome and it took us a good many weeks to solve. Hydrolysis under a variety of conditions, or semireduction of the carbonyl group, was uniformly unsuccessful, but we eventually found that O-alkylation of the carbonyl with Meerwein's reagent, followed by treatment with aqueous Na_2CO_3 , afforded **6** in 71% yield (Figure 4). After our prolonged struggle with this step, we were definitely satisfied with the result.

Well before this stage had been reached, Danishefsky's pioneering and influential² synthesis [16] had been reported and this imposed a restriction—in the event a beneficial restriction—on what we should do next, because we wanted our route to ring A to be original. Our response was to go back to



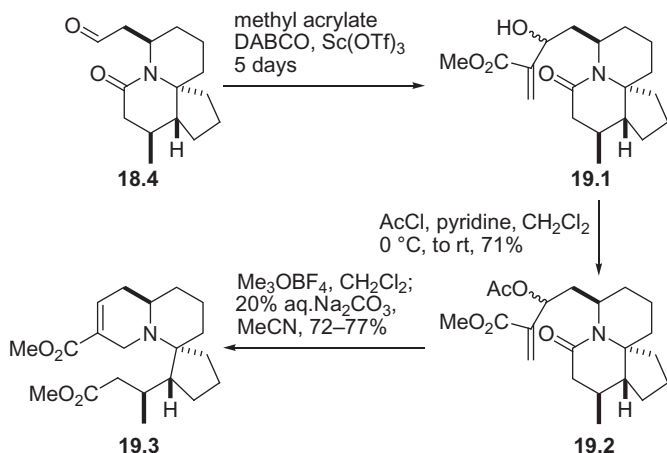
SCHEME 17 Claisen rearrangement approach.

2. It forms the basis of several formal syntheses.

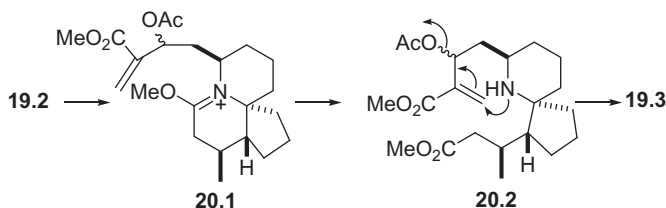
**FIGURE 4** The product of lactam opening.**SCHEME 18** Formation of the homologated aldehyde **18.4**.

lactam **16.2**, in which the nitrogen is internally protected, and we extended the chain at C(4) (Scheme 18). Removal of the MOM protecting group with Me_3SiBr and then TPAP oxidation gave aldehyde **18.2**, which was then subjected to Wittig reaction with $\text{Ph}_3\text{P}=\text{CH}(\text{OMe})$ (**18.2**→**18.3**). Finally, acid hydrolysis released the homologated aldehyde **18.4**, a key intermediate for the halichlorine synthesis. Both the oxidation and the Wittig reaction had to be done under carefully controlled conditions in order to avoid epimerization α to the aldehyde; the Swern method was unsatisfactory in this respect and the Wittig reaction was best done at 0 °C. With these precautions, aldehyde **18.4** could be obtained as a single isomer.

For the construction of ring A (Scheme 19), the aldehyde was subjected to Baylis–Hillman reaction with methyl acrylate in the presence of DABCO and $\text{Sc}(\text{OTf})_3$ [21]. After 5 days—the reaction is slow—we could isolate a mixture of alcohols (**19.1**) and a small amount of unchanged starting aldehyde. Evidently, no epimerization (by *retro*-Michael elimination and readdition) occurred during the Baylis–Hillman reaction. The mixture of epimeric alcohols was acetylated with AcCl (Ac_2O is unsuitable). When the individual acetates **19.2** were treated with Meerwein's salt and then with aqueous Na_2CO_3 under the conditions we had established with **16.2**, they were each



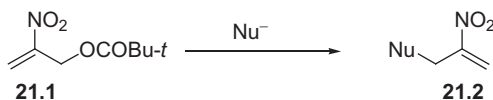
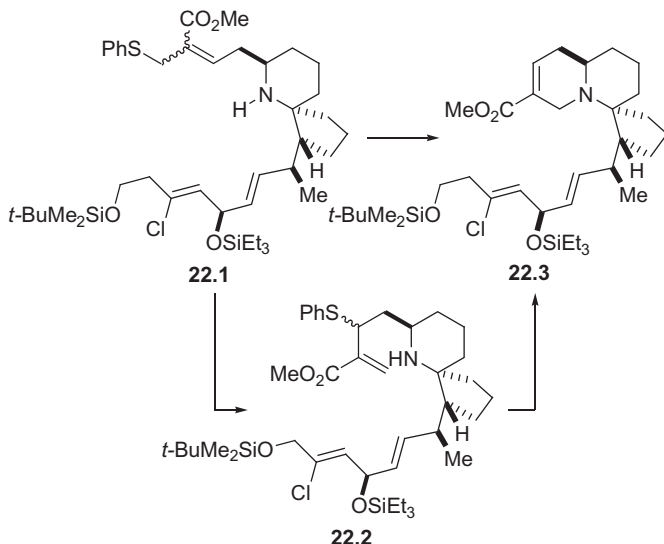
SCHEME 19 Generation of ring A.



SCHEME 20 Mechanism of the ring closure.

converted (72% and 77%, respectively) into **19.3**. There is clearly quite a lot going on here: the Meerwein's salt must generate the iminium ethers **20.1** (Scheme 20), base hydrolysis gives the esters **20.2**, and these undergo rapid cyclization (**20.2**→**19.3**) by a process that appears to be a blend of a Michael addition and an $\text{S}_{\text{N}}2'$ displacement, which we call an *intramolecular conjugate displacement* (ICD).

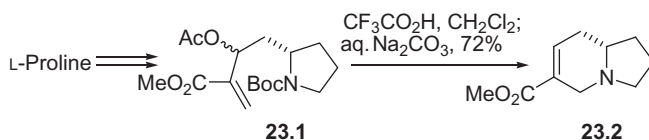
This procedure for making ring A represents an example of a general route to nitrogen-containing rings. Its development was prompted by the circumstances of the halichlorine synthesis and it evolved from an awareness of the then current spate of publications on the Baylis–Hillman reaction. A number of O-acetates of Baylis–Hillman alcohols were reported to undergo *intermolecular* $\text{S}_{\text{N}}2'$ displacement [22, 23], and I wondered if the *intramolecular* pathway (see **20.2** arrows) would also work. Such a reaction would require that no competing stereoelectronic or reactivity factors would intervene to cause $\text{O} \rightarrow \text{N}$ acetyl transfer or to direct cyclization onto the CO_2Me group of **20.2**. Fortunately, none of these possibilities arose and we have carried out many similar reactions [24]. During these studies, we acquired a proper knowledge of the background literature. The enhanced reactivity of compound

SCHEME 21 Reactivity of **21.1**.

SCHEME 22 Heathcock and Christie's approach.

21.1 toward nucleophiles was reported by Seebach and Knochel [25], who found that it reacted with a wide range of nucleophiles to give vinyl nitro compounds **21.2** (Scheme 21). As the reactions could easily be stopped at the stage of **21.2**, the latter must be less reactive than **21.1**. The synthetic opportunities available by using such reagents in an *intramolecular* manner do not appear to have been widely appreciated and I could find examples only of occasional use for cross-linking protein strands [26] (which was the original application in this area) and to make azamacrocycles [27]. During our development of the ICD process [28], Heathcock and Christie reported [29] a synthesis of racemic halichlorine in which a process that is mechanistically very similar to ours was used for constructing ring A: The olefins **22.1** were warmed with PhSH and K₂CO₃ in DMF to give **22.3**, presumably by way of **22.2** (Scheme 22).

We have made an extensive study of the ICD reaction: it represents a powerful method for making nitrogen heterocycles [24]. Scheme 23 shows an application starting from L-proline, which gave optically pure **23.2**. Compounds **7–13** (Figure 5) represent several other ICD products; in each of these cases, an arrow marks the newly formed bond from nitrogen that is generated by the ICD process.



SCHEME 23 Example of ICD reaction.

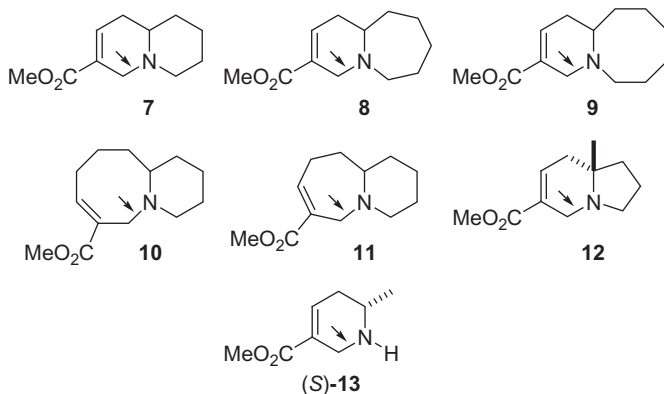
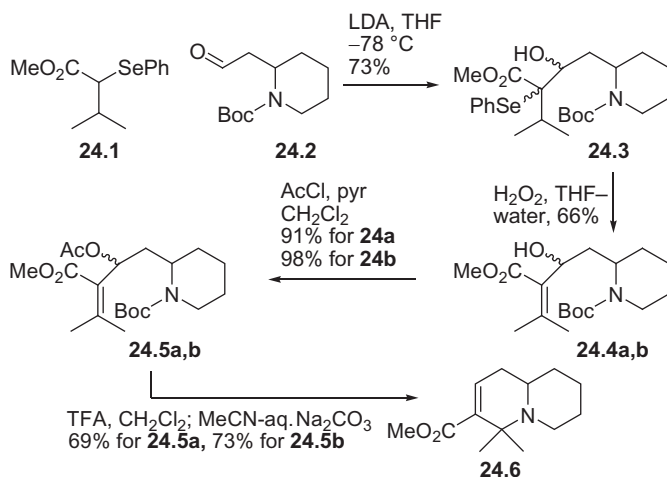


FIGURE 5 Examples of ICD products.

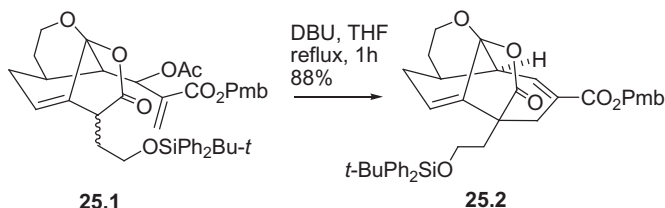
The development of the ICD reaction, while crucially helpful in our route to halichlorine, as described later, brought with it additional responsibilities. The slowness of the Baylis–Hillman step was irksome and we sought a remedy for this factor by calling on our extensive experience in the area of selenium chemistry. The selenide **24.1** (among others) was deprotonated and allowed to react with aldehyde **24.2**. This operation produced a mixture of hydroxy selenides (**24.3**), and oxidation with H_2O_2 gave the Baylis–Hillman alcohols **24.4a,b**. The regiochemistry of the selenoxide elimination (elimination *away* from the hydroxyl-bearing carbon) is a long-known outcome [30]. From **24.4a,b**, acetylation, removal of the *N*-Boc group, and basification gave **24.6**, the product of ICD. This selenium-based version of the Baylis–Hillman reaction is general. It has been used [24] with ester, nitrile, and sulfone groups as the electron-withdrawing substituent. The example in Scheme 24 is noteworthy because the alcohols **24.4a,b** would not be accessible by the classical Baylis–Hillman process because of the geminal substitution present on the double bond of the Michael acceptor.

Thus our studies on the construction of ring A provided two useful synthetic methods—the ICD and a rapid method for making Baylis–Hillman alcohols.

All the ICD reactions I have discussed so far involve nitrogen as the nucleophile, but the process also works with sulfur [31] and with carbon as the nucleophile. Our most significant example [32] of the latter type is summarized in Scheme 25. The product (**25.2**) resembles the core structure of the very complex natural product CP-263,114 [33].



SCHEME 24 Selenium version of Baylis-Hillman reaction.



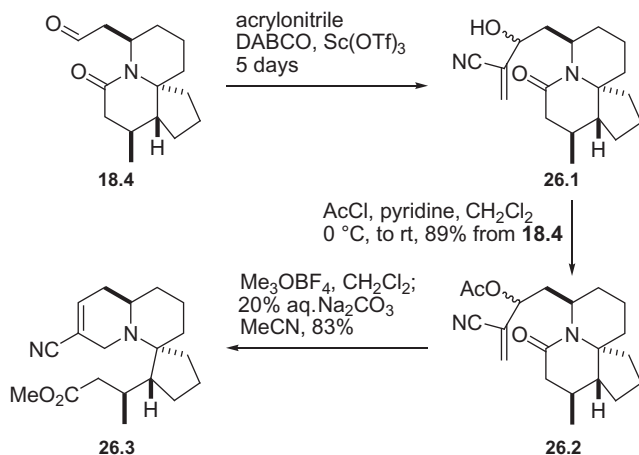
SCHEME 25 An all-carbon ICD reaction.

8. THE CONTINUING SAGA OF RING A

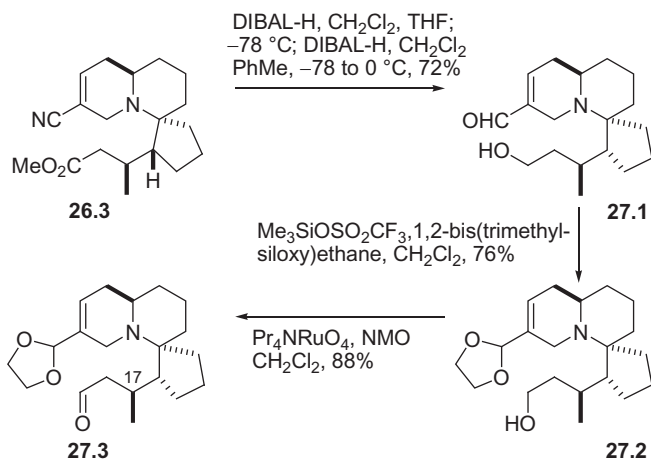
Of necessity, our further plans for **19.3** required selective manipulation of the two methyl ester groups. We wanted to selectively reduce the saturated ester, but trial experiments to this end were inefficient, and so we repeated the ICD sequence with acrylonitrile instead of methyl acrylate to obtain **26.3** (Scheme 26) in which we now had to discriminate between a nitrile and an ester instead of between two esters.

9. FORMATION OF THE MACROLACTONE

The route we followed in order to reach halichlorine from **26.3** required that the side chain on the five-membered ring be extended in a way that introduces the chlorohydroxy diene unit of the natural product. Of the several approaches we tried, the best involved initial reduction with DIBAL-H. This was done in two stages (Scheme 27): first we used 2 mol of DIBAL-H per mol of **26.3** in CH_2Cl_2 -THF at -78°C . After workup, the crude material was again exposed to the action of DIBAL-H (4mol/mol **26.3**) in CH_2Cl_2 -PhMe at -78 to 0°C .



SCHEME 26 Use of acrylonitrile in the ICD reaction.



SCHEME 27 Regioselective manipulation of nitrile and ester groups.

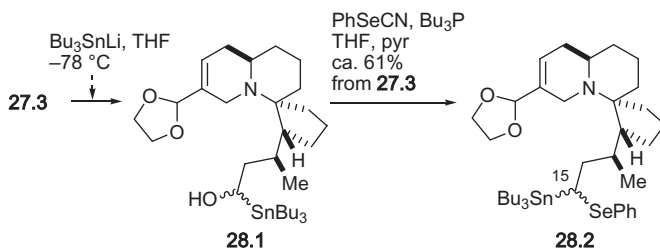
This protocol delivered the desired hydroxy aldehyde **27.1** in a respectable yield (72%) and the aldehyde group was then protected as a ketal, using 1,2-bis(trimethylsiloxy)ethane under catalysis by Me_3SiOTf .

Several methods for extending the hydroxyl-bearing side chain of **27.2** were examined, but we eventually fell back on a conservative approach via the aldehyde **27.3**, which was prepared by TPAP oxidation (**27.2**→**27.3**). The stereogenic center at C(17) is β to the aldehyde, as opposed to α , and so we had no worries about its stereochemical integrity during the remaining steps.

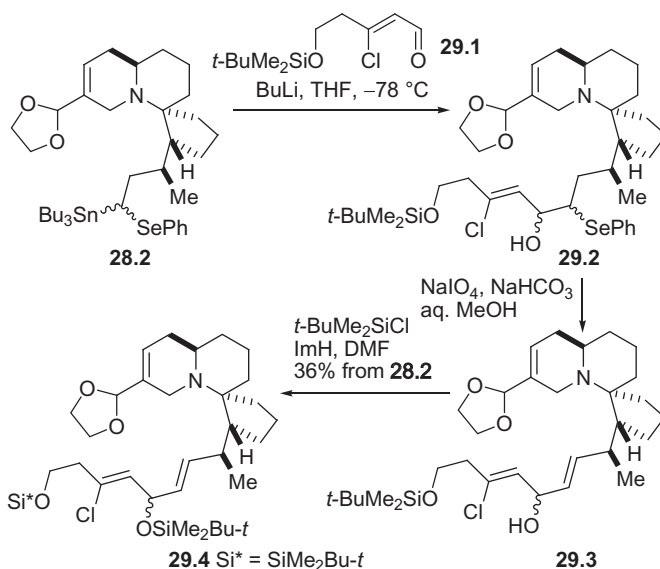
At this point, we wanted to form a selenium-stabilized carbanion at C(15) of **27.3**. The conventional method is to generate a selenoacetal, but the preparation of selenoacetals normally requires the use of a Brønsted or Lewis acid

and we had formed the impression that compounds similar to **27.3** were damaged by acids. Consequently, we decided to avoid acidic reagents. Aldehyde **27.3** was treated with Bu_3SnLi and the resulting unstable stannyl alcohols **28.1** were immediately treated with PhSeCN and Bu_3P to afford the selenides **28.2** in about 61% yield from the aldehyde (Scheme 28).

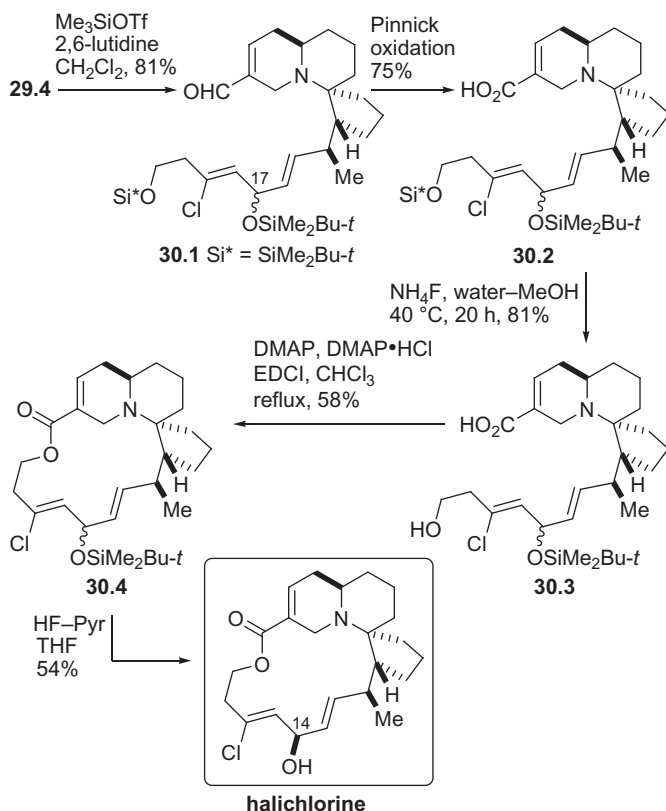
Exposure of **28.2** to BuLi at -78°C resulted in selective Sn-C heterolysis to generate a selenium-stabilized carbanion, which condensed with the known and readily available aldehyde **29.1** [3,16], affording a mixture of hydroxy selenides **29.2** (Scheme 29). Oxidation in the usual way with NaIO_4 then generated an *E*-double bond, as expected [34], and the resulting allylic alcohol was protected by silylation.



SCHEME 28 Formation of stannyl selenides.



SCHEME 29 Extension of the lower chain.



SCHEME 30 Access to halichlorine.

The Sn/Se method we used to build up the lower side chain is general [35] but does not give a really high yield. Fortunately, its performance in the present case was satisfactory, and we were now ready to complete the macrocyclic portion of halichlorine.

The ketal unit was first removed by using Me₃SiOCOCF₃ in the presence of 2,6-lutidine (Scheme 30), and the aldehydes released in this experiment—they are epimeric at C(17)—were subjected to Pinnick oxidation (29.4→30.1→30.2) [36]. Next, the silicon masking the primary hydroxyl was removed with NH₄F, which is a fine reagent for this selective deprotection [16,37] and had been used by the Danishefsky team. The resulting hydroxy acids were then subjected to the Keck macrolactonization protocol [38]. In the last step, the residual silicon group was removed with HF·pyridine, and chromatographic separation of a small amount of the undesired (14*S*)-isomer gave halichlorine. But our synthetic work was by no means finished!

10. THE OPTICAL PURITY PROBLEM

All along, our aim had been to find a route to the optically pure alkaloid and, as indicated earlier, we had discovered that the key allylation step **8.2**→**9.1** gave a poor ee—only 69%. We accepted that result but planned to later devise an effective route either to optically pure **9.1** or to a more advanced intermediate. To this end, we explored a number of chemical and enzymatic approaches, but none generated intense enthusiasm until we recognized that the structure of **9.1** should be viewed as a derivative of serine. From that perspective, the amino acid would have to be converted into a piperidine with a fully substituted asymmetric carbon α to the nitrogen, and these thoughts led us to consider compounds of type **14** (Pg, Pg'=protecting groups) (Figure 6). The hope was that C(6) (IUPAC numbering), the asymmetric center derived from the amino acid, could be used to control the stereochemistry at C(2) when that was converted to sp^3 hybridization.

We considered several routes to the requisite dihydropyridinones, but the best one was developed from a known method that is well illustrated by the reported [39] conversion of **31.1** to **31.2** (Scheme 31). From the dihydropyridinone system **14**, we tried a number of approaches to change the status of C(2) from sp^2 to sp^3 with control of the stereochemical outcome; however, only the use of a Claisen rearrangement (**32.1**→**32.2**) was successful (Scheme 32) [40,41].

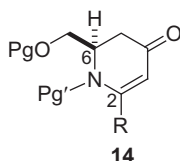
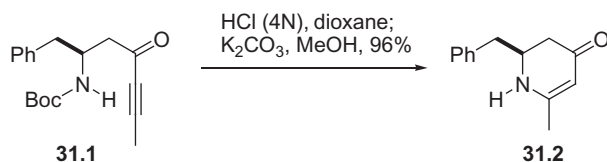


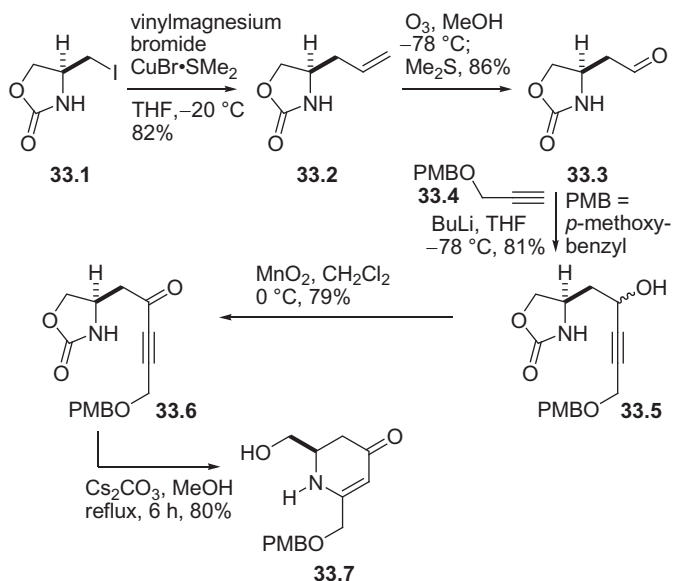
FIGURE 6 The required dihydropyridinones.



SCHEME 31 The literature synthesis of dihydropyridinones.



SCHEME 32 Claisen rearrangement to generate a quaternary center.



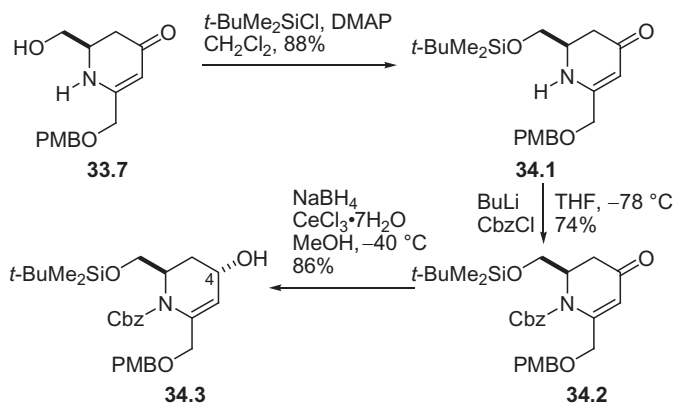
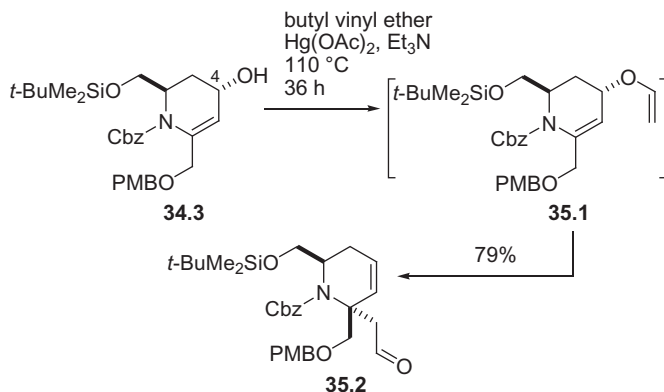
SCHEME 33 Preparation of the key dihydropyridinone.

L-Serine methyl ester hydrochloride was converted by a four-step literature procedure into iodide **33.1** (Scheme 33). Coupling with lithium divinyl cuprate gave the known [42] oxazolidinone **33.2**, from which aldehyde **33.3** was obtained by ozonolysis. The aldehyde reacts efficiently with lithium acetylides; in particular, reaction with the acetylide generated from **33.4** gave the expected alcohols **33.5**, and oxidation with MnO_2 furnished ketone **33.6**. This ketone was converted in 80% yield into the desired dihydropyridinone **33.7** on treatment with Cs_2CO_3 in hot MeOH. Each of the steps from L-serine to **33.7** occurred without loss of stereochemical integrity.

Mechanistic investigations [41], carried out at a later stage, suggest that the conversion **33.6**→**33.7** involves conjugate addition of MeOH to the triple bond, cyclization to a dihydropyridinone system, and then hydrolysis of the oxazolidinone subunit. In any event, with **33.7** in hand, the free hydroxyl was protected as a silyl ether and the nitrogen as a benzyl carbamate (**33.7**→**34.1**→**34.2**) (Scheme 34). Luche reduction of **34.2** was highly stereoselective and afforded **34.3**.

Initially, we had protected the nitrogen with a benzyl group, but compounds protected in this way gave complex mixtures or underwent saturation of the double bond on attempted carbonyl reduction; with carbamate protection, these problems disappeared [43].

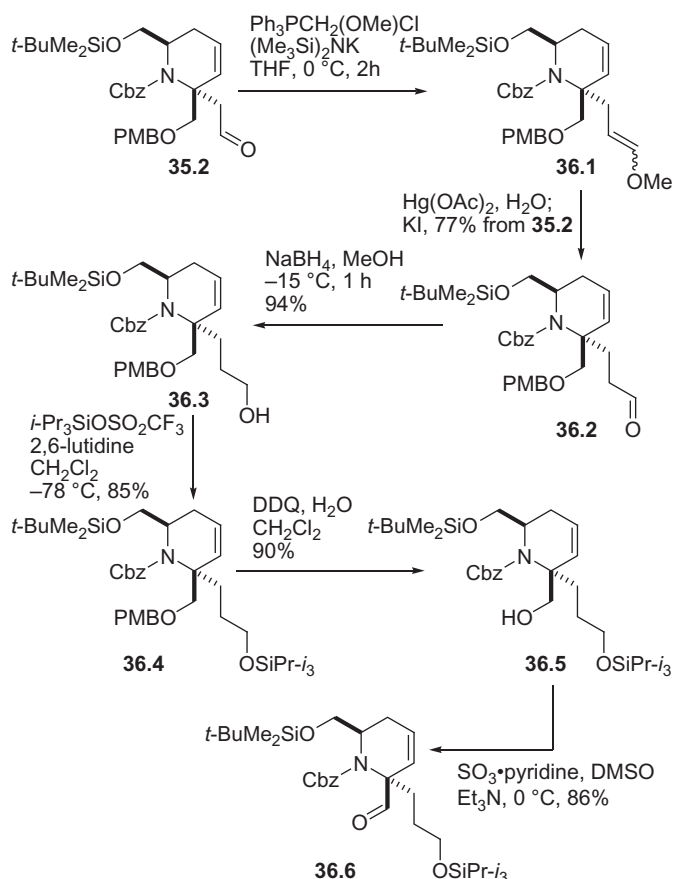
When alcohol **34.3** was heated in butyl vinyl ether in the presence of $\text{Hg}(\text{OAc})_2$ and Et_3N (sealed tube, 110°C , 36h), it was converted into **35.2** in

SCHEME 34 Stereocontrolled reduction of the dihydropyridinone **33.7**.

SCHEME 35 Claisen rearrangement.

79% yield, presumably via the vinyl ether **35.1**, although attempts to isolate this intermediate were not successful (Scheme 35). It later turned out that the stereochemistry at C(4) of **34.3** is crucial; related compounds with the epimeric C(4) stereochemistry do not undergo the Claisen rearrangement—at least under the few conditions we tried. Fortunately, the appropriate C(4) stereochemistry (as in **34.3**) is the readily accessible and direct result of Luche reduction.

From **35.2**, it was possible to make an optically pure intermediate that corresponded with one of the intermediates in our earlier work: Aldehyde **35.2** was subjected to Wittig olefination with $Ph_3P=CH(OMe)$ and the resulting enol ethers were converted into aldehyde **36.2** (Scheme 36). This was reduced and silylated (**36.2**→**36.3**→**36.4**). Removal of the PMB group and oxidation afforded aldehyde **36.6**, and this was converted without incident into **37.8**



SCHEME 36 Elaboration of Claisen rearrangement product.

by methods modeled on those we had used earlier (Scheme 37). Lactam **37.8** is optically pure and corresponds to the intermediate **12.3**, which we had used previously and which had been derived from **9.1** of only 69% ee. The formation of optically pure **37.8** constitutes a formal synthesis, based on our own route, of (+)-halichlorine.

The method we used to make **35.2** is general [41], and we have prepared a number of piperidines by this process; a few of these are shown in Figure 7. Such substances obviously lend themselves to further elaboration.

11. CONCLUSION

Looking back over our route to halichlorine brings to my mind the opinion expressed by Sir Jack Baldwin in a 2006 *ChemComm* interview:³ "... if

3. <http://www.rsc.org/Publishing/Journals/cc/News/BaldwinInterview.asp>.

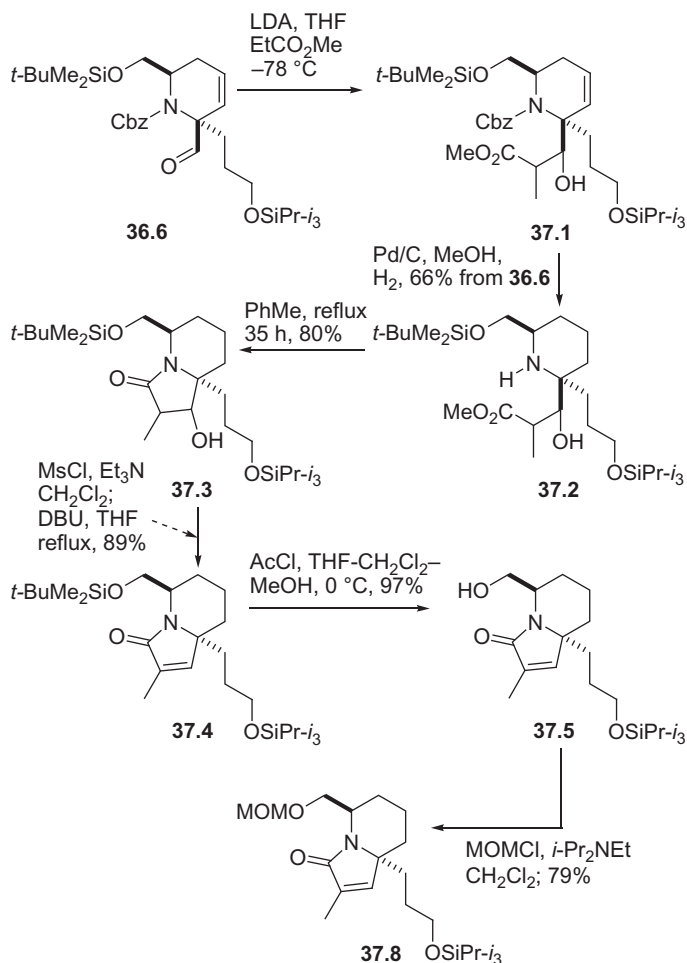
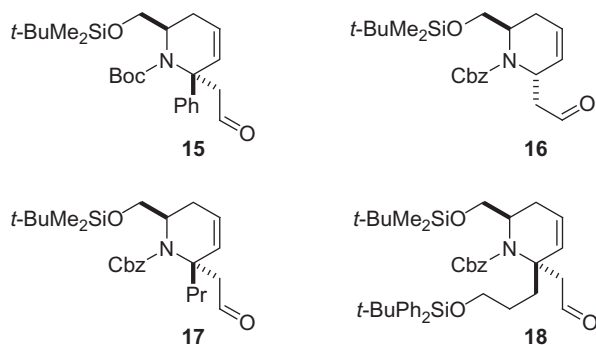
SCHEME 37 Formation of the optically pure intermediate **37.8**.

FIGURE 7 Examples of substituted piperidines made by Claisen rearrangement.

you set out to make even a simple compound, which has never been made before, you soon encounter problems, so there is still a need for new ways to synthesize complex structures.” By no stretch of the imagination is halichlorine a “simple” compound, and we certainly had our share of problems, but in every case the context allowed us to find solutions. At the outset we had, of course, no inkling that we would become involved in sulfone chemistry, in what I call ICD reactions, in a selenium version of the Baylis–Hillman reaction, or in methodology for the construction of piperidines; always the synthesis of a complex natural product leads to a substantial dividend of new information.

ACKNOWLEDGMENTS

I sincerely thank my coworkers on the halichlorine and associated projects; they were (in alphabetical order) Dr. H. P. Acharya, Dr. B. Prabhudas, Z. Chen, Dr. C. Chiruta, Dr. S. M. Jachak, S. Kang, Z. Li, D. Liu, J. Wang, L. Wang, V. S. C. Yeh, and M. Yu. Financial support from NSERC and AHFMR is gratefully acknowledged.

REFERENCES

- [1] For a personal, and early, overview of marine natural products chemistry, see: D.J. Faulkner, *Tetrahedron* 33 (1977) 1421–1443. For memorial issues of *J. Nat. Prod.* honoring three pioneers, see: *J. Nat. Prod.* 67 (8) (2004) and *J. Nat. Prod.* 70 (3) (2007).
- [2] M. Kuramoto, C. Tong, K. Yamada, T. Chiba, Y. Hayashi, D. Uemura, *Tetrahedron Lett.* 37 (1996) 3867–3870.
- [3] S.P. Keen, S.M. Weinreb, *J. Org. Chem.* 63 (1998) 6739–6741.
- [4] H. Arimoto, S. Asano, D. Uemura, *Tetrahedron Lett.* 40 (1999) 3583–3586.
- [5] Review of synthetic work related to halichlorine and the pinnaic acids: D.L.J. Clive, M. Yu, J. Wang, V.S.C. Yeh, S. Kang, *Chem. Rev.* 105 (2005) 4483–4514.
- [6] For references to model studies and formal syntheses not included in Ref. 5: (a) R.B. Andrade, S.F. Martin, *Org. Lett.* 7 (2005) 5733–5735; (b) E. Roulland, A. Chiaroni, H.-P. Husson, *Tetrahedron Lett.* 46 (2005) 4065–4068; (c) A. Sinclair, L.G. Arini, M. Rejzek, P. Szeto, R.A. Stockman, *Synlett* (2006) 2321–2324; (d) H. Kim, J.H. Seo, K.J. Shin, D.J. Kim, D. Kim, *Heterocycles* 70 (2006) 143–146; (e) H. Wu, H. Zhang, G. Zhao, *Tetrahedron* 63 (2007) 6454–6461; (f) S.-H. Yang, V. Caprio, *Synlett* (2007) 1219–1222; (g) S. Xu, H. Arimoto, D. Uemura, *Angew. Chem. Int. Ed.* 46 (2007) 5746–5749; (h) P.B. Hurley, G.R. Dake, *J. Org. Chem.* 73 (2008) 4131–4138; (i) G.E. Keck, S.A. Heumann, *Org. Lett.* 10 (2008) 4783–4786; (j) Y. Yamamoto, Y. Yasuda, H. Nasu, K. Tomioka, *Org. Lett.* 11 (2009) 2007–2009; (k) S.-H. Yang, G.R. Clark, V. Caprio, *Org. Biomol. Chem.* 7 (2009) 2981–2990; (l) A.C. Flick, M.J.A. Caballero, H.I. Lee, A. Padwa, *J. Org. Chem.* 75 (2010) 1992–1996; (m) B. Stevenson, W. Lewis, J. Dowden, *Synlett* (2010) 672–674.
- [7] (a) D. Uemura, Y. Hirata, Atta-ur-Rahman (Ed.), *Studies in Natural Products Chemistry*, Elsevier, Amsterdam, 1989, pp. 377–398 vol. 5, Part B; (b) D. Uemura, P.J. Scheuer (Ed.), *Bioactive Polyethers, Bioorganic Marine Chemistry*, Springer, Berlin, 1991, pp. 1–31 vol. 4.
- [8] (a) T.A. Springer, *Cell* 76 (1994) 301–314; (b) T.M. Carlos, J.M. Harlan, *Blood* 84 (1994) 2068–2101.

- [9] (a) C.A. Foster, *J. Allergy Clin. Immunol.* 98 (1996) S270–S277; (b) A.A. Postigo, J. Teixidó, F. Sánchez-Madrid, *Res. Immunol.* 144 (1993) 723–735.
- [10] F. Vidal-Vanaclocha, G. Fantuzzi, L. Mendoza, A.M. Fuentes, M.J. Anasagasti, J. Martín, T. Carrascal, P. Walsh, L.L. Reznikov, S.-H. Kim, D. Novick, M. Rubinstein, C. A. Dinarello, *Proc. Nat. Acad. Sci. USA* 97 (2000) 734–739.
- [11] T. Chou, M. Kuramoto, Y. Otani, M. Shikano, K. Yazawa, D. Uemura, *Tetrahedron Lett.* 37 (1996) 3871–3874.
- [12] D.L.J. Clive, V.S.C. Yeh, *Tetrahedron Lett.* 40 (1999) 8503–8507.
- [13] G. Kokotos, J.M. Padrón, T. Martín, W.A. Gibbons, V.S. Martín, *J. Org. Chem.* 63 (1998) 3741–4744.
- [14] S. Hanessian, T.A. Grillo, *J. Org. Chem.* 63 (1998) 1049–1057.
- [15] D.L.J. Clive, V.S.C. Yeh, *Synth. Commun.* 30 (2000) 3267–3274.
- [16] D. Trauner, J.B. Schwarz, S.J. Danishefsky, *Angew. Chem. Int. Ed.* 38 (1999) 3542–3545.
- [17] M.W. Carson, G. Kim, S.J. Danishefsky, *Angew. Chem. Int. Ed.* 40 (2001) 4453–4456.
- [18] N.J. Goldspink, N.S. Simpkins, M. Beckmann, *Synlett* (1999) 1292–1294.
- [19] (a) D.L.J. Clive, J. Wang, M. Yu, *Tetrahedron Lett.* 46 (2005) 2853–2855; (b) J. Wang, Ph.D. thesis, University of Alberta, Edmonton, Alberta, 2004.
- [20] A.L.J. Beckwith, D. Crich, P.J. Duggan, Q. Yao, *Chem. Rev.* 97 (1997) 3273–3312.
- [21] V.K. Aggarwal, A. Mereu, G.J. Tarver, R. McCague, *J. Org. Chem.* 63 (1998) 7183–7189.
- [22] Review on the Baylis–Hillman reaction: D. Basavaiah, A.J. Rao, T. Satyanarayana, *Chem. Rev.* 103 (2003) 811–891.
- [23] (a) For example, see: A.B. Charette, M.K. Janes, A.A. Boezio, *J. Org. Chem.* 66 (2001) 2178–2180; (b) C.-W. Cho, J.-R. Kong, M. Krische, *J. Org. Lett.* 6 (2004) 1337–1339; (c) D. Nilov, R. Räcker, O. Reiser, *Synthesis* (2002) 2232–2242.
- [24] D.L.J. Clive, Z. Li, M. Yu, *J. Org. Chem.* 72 (2007) 5608–5617.
- [25] (a) D. Seebach, P. Knochel, *Helv. Chim. Acta* 67 (1984) 261–283; (b) P. Knochel, D. Seebach, *Tetrahedron Lett.* 22 (1981) 3223–3226.
- [26] (a) S. Mitra, R.G. Lawton, *J. Am. Chem. Soc.* 101 (1979) 3097–3110; (b) S.J. Brocchini, M. Eberle, R.G. Lawton, *J. Am. Chem. Soc.* 110 (1988) 5211–5212.
- [27] (a) P. Bauchat, N. Le Bras, L. Rigal, A. Foucaud, *Tetrahedron* 50 (1994) 7815–7826; (b) P. Bauchat, A. Foucaud, *Tetrahedron Lett.* 30 (1989) 6337–6338.
- [28] D.L.J. Clive, M. Yu, Z. Li, *Chem. Commun.* (2005) 906–908.
- [29] H.S. Christie, C.H. Heathcock, *Proc. Nat. Acad. Sci. USA* 101 (2004) 12079–12084.
- [30] (a) K.B. Sharpless, R.F. Lauer, *J. Am. Chem. Soc.* 95 (1973) 2697–2699; (b) H.J. Reich, S.K. Shah, *J. Am. Chem. Soc.* 97 (1975) 3250–3252.
- [31] Z. Chen, D.L.J. Clive, *J. Org. Chem.* 75 (2010) 7014–7017.
- [32] (a) B. Prabhudas, D.L.J. Clive, *Angew. Chem. Int. Ed.* 46 (2007) 9295–9297; (b) L. Wang, B. Prabhudas, D.L.J. Clive, *J. Am. Chem. Soc.* 131 (2009) 6003–6012.
- [33] D.A. Spiegel, J.T. Njardarson, I.M. McDonald, J.L. Wood, *Chem. Rev.* 103 (2003) 2691–2727.
- [34] S. Raucher, G.A. Koolpe, *J. Org. Chem.* 43 (1978) 4252–4253.
- [35] S.C. Fernandopulle, D.L.J. Clive, M. Yu, *J. Org. Chem.* 73 (2008) 6018–6021.
- [36] B.S. Bal, W.E. Childers Jr., H.W. Pinnick, *Tetrahedron* 37 (1981) 2091–2096.
- [37] (a) T.D. Nelson, R.D. Crouch, *Synthesis* (1996) 1031–1069; (b) J.D. White, W.J. Porter, T. Tiller, *Synlett* 1993 (1993) 535–538.
- [38] E.P. Boden, G.E. Keck, *J. Org. Chem.* 50 (1985) 2394–2395.
- [39] B.J. Turunen, G.I. Georg, *J. Am. Chem. Soc.* 128 (2006) 8702–8703.

- [40] D. Liu, H.P. Acharya, M. Yu, J. Wang, V.S.C. Yeh, S. Kang, C. Chiruta, S.M. Jachak, D.L. J. Clive, *J. Org. Chem.* 74 (2009) 7417–7428.
- [41] H.P. Acharya, D.L.J. Clive, *J. Org. Chem.* 75 (2010) 5223–5233.
- [42] S.-G. Kim, K.H. Ahn, *Synth. Commun.* 28 (1998) 1387–1397.
- [43] D.L. Comins, M.A. Foley, *Tetrahedron Lett.* 29 (1988) 6711–6714.

An Adventure in Synthesis Inspired by the Pseudolaric Acids

Pauline Chiu

Department of Chemistry, The University of Hong Kong, Hong Kong, P. R. China

Chapter Outline

1. How this Chemist Came to Be	55	7. Case 2: When Model Reactions Fail	68
2. Pseudolaric Acids	56	8. Too Happy too Quickly, and the Importance of IR Spectroscopy	71
3. The First Strategy	58	9. But it was not Time to Give Up	74
4. Development of the Copper Hydride-Induced Reductive Aldol Cyclization	60	10. Other Natural Products	75
5. The Second Strategy to Pseudolaric Acid A	63	11. Epilogue	75
6. Case 1: When Model Reactions Fail	67		

1. HOW THIS CHEMIST CAME TO BE

I had not planned on being a chemist and having a career in research and teaching from the beginning. I “blame” that on my Chinese roots: according to Confucian doctrine, the most noble professions are those of statesmen and physicians. My family, like many others, hoped to have their children become doctors one day. So from an early age I was primed to think that the medical profession was my destiny, and science studies were only a means to that end. Another reason I had never considered a career in chemistry was that I was not acquainted with any role models, people who were researchers or professors. So this career was not one to which I naturally aspired.

In North America, most M.D. programs require up to 4 years of university studies as a prerequisite. Thus any sensible M.D. hopeful would enroll in a

program first, then apply for medical school after having completed all the requisites. When I thought about which program to enroll in, I decided on chemistry. I remember that in junior high, I was fascinated by the balanced equation for photosynthesis that our science teacher, Mr. Frohlinger, showed us on the blackboard for the first time. I thought that the conservation of material and the symmetry were simply beautiful. This fondness for chemistry continued through an experiment-based chemistry curriculum in Thornlea Secondary School and the University of Toronto.

Life did not turn out as originally planned and I did not become a doctor—and a good thing too—I find that I am entirely unsuited for such a profession. My becoming a chemist echoes the experience of so many other authors in this Series: that I met some wonderful teachers in chemistry over my years of education, and professors who challenged and inspired me to do research. I was also very fortunate to have the support of NSERC all of these years, which also encouraged me to pursue postgraduate studies. Thus, after my B.Sc. Honours program in Chemistry, I enrolled in the M.Sc. program and became the last postgraduate student working on silene chemistry under Prof. Adrian Brook, who was soon to retire. After completing the Master's studies, I had thought about entering and working in the pharmaceutical industry, but in the end, decided to pursue my Ph.D. working with Prof. Mark Lautens, who had been recruited to succeed Prof. Brook in the area of organometallic chemistry in the department. My parents were supportive of my education all along, but after seeing me finish degree after degree, towards the end of the Ph.D., they were anticipating that surely this was to be the end of my long education and that I was finally going to get done with school and get a job myself; most of my friends by that time had long since graduated and gotten “real” jobs. But at that time, I applied and was accepted for postdoctoral studies with Prof. Sam Danishefsky at Columbia University. I forgot how exactly I broke the news to them that I was heading to New York next. Much to the surprise of my folks, they mused, “We didn’t know that there is still school *after* the Ph.D.!”

Another unexpected turn of events was that, for family reasons, after my postdoctoral work I left North America, which I considered home up until then, and ended up working in the Department of Chemistry at the University of Hong Kong. After arriving in Hong Kong, I landed a job in the Department as a relatively independent researcher. However, I was not prepared to initiate my own research program immediately, and I had little idea what project or idea to pursue to start, still reeling somewhat from the transcontinental physical and cultural displacement. It was at that time that my research mentor in the group at the University of Hong Kong, Prof. K. F. Cheng, suggested that I could try to synthesize pseudolaric acid.

2. PSEUDOLARIC ACIDS

The pseudolaric acids (Figure 1) are a family of natural products that were first isolated in the 1980s at the Shanghai Institute of Materia Medica from

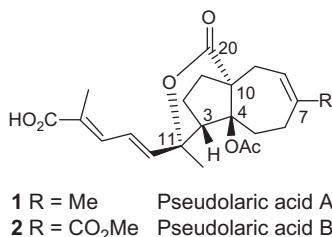


FIGURE 1 The pseudolaric acids.

the medicinal herb, *tujingpi* [1,2]. This herb is the harvested and dried bark of *Pseudolarix amabilis*, a tree which is indigenous to China, but had been introduced to the West in 1854. Known as the golden larch, it is a deciduous conifer whose leaves turn yellow before shedding. In traditional Chinese medicine, *tujingpi* was used against eczema, fungal infections and other skin conditions. The major antifungal constituents turned out to be pseudolaric acids A and B [3]. Furthermore, pseudolaric acid B was also found to have nonestrogenic antifertility effects [4], as well as anticancer [5] and antiangiogenic activity [6].

We became interested in the pseudolaric acids not only as synthetic targets, but also in further understanding and possibly harnessing their anticancer activity. I spent some time searching for potential partners and approaching them to consider a collaboration in this area, but many established researchers were not very open to pick up another new project, without knowing where the trail of investigation may lead. It was very fortunate for us that eventually, a talented research assistant professor, Dr. Ben Ko, was recruited to join our Department. At the start of his own independent career, Ben was also looking for projects and was open to working with us in these efforts. Through Ben's persistence and the hard work of a jointly supervised Ph.D. student, Vincent Wong, we found that the target of the pseudolaric acids are the microtubules, cell structures that are crucial to cell division and mitosis, and this may explain the antitumor activity of pseudolaric acid B as well as its antiangiogenic effects. We found that pseudolaric acid B was able to suppress tumor growth in spite of an overexpression of the P-gp efflux pump, a common acquired drug resistance response mechanism. Finally, we also demonstrated its efficacy *in vivo* in a nude mouse model against a taxol-resistant liver cancer [7]. Pseudolaric acid proved itself to be a worthy target for study.

Relatively abundant quantities of pseudolaric acids are found in the bark of mature trees. These compounds are likely produced by the trees for self-protection against disease and are accumulated on the bark over their lifetimes. It is probably due to these defense chemicals that *P. amabilis* can survive for a long time and grow very tall. However, to obtain these compounds from the bark means that old trees need to be sacrificed. Botanists

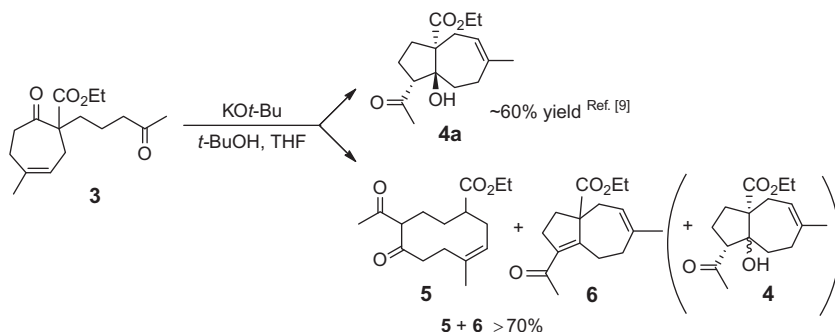
have tried to cultivate *P. amabilis* for harvesting the pseudolaric acids, but the bark of the saplings did not contain high concentrations of these antifungal compounds. We undertook an isolation study hoping to find these compounds in the foliage, which could be managed as a sustainable and renewable plant resource; however, we found that the pseudolaric acids only occurred in minute amounts there [8]. Due to the biological activity and limited resource pool, it was desirable to synthesize the pseudolaric acids.

3. THE FIRST STRATEGY

At the time we began this project, we were aware of three separate research efforts on the synthesis of pseudolaric acid A. One study from the Shanghai Institute of Materia Medica, where this molecule was isolated and structurally characterized, reported that the base-induced intramolecular aldol reaction of **3** resulted in the requisite perhydroazulene ring of pseudolaric acid A (Scheme 1) [9]. The yield was about 60%, and the stereochemistry of the aldol product **4a** was said to coincide with a degradation product from authentic pseudolaric acid. However, the experimental details were scant, and nothing had been published by the same group after this communication in 7 years.

At that time I was joined by our first Master's student, Mr. Rex Szeto, and our first Ph.D. student, Mr. Bin Chen. We initially thought that optimizations of the aldol conditions to improve the reported moderate yield would enable us to continue the synthesis from **4a**. However, when Bin tried the aldol cyclization of **3** under a variety of basic conditions, the hydroxyketones **4** were obtained only as minor compounds in the product mixture. The chief product was the "carbon zip" ring-opened **5** [10], and the next most abundant was the dehydrated product **6**, which together accounted for over 70% of the product mixture (Scheme 1) [11]. Both of these were obviously derived from further reactions of the hydroxyketone aldol product **4** under the basic conditions.

Therefore, we explored alternative ways to execute the aldol cyclization that would not involve strong bases. We thought of generating the enolate



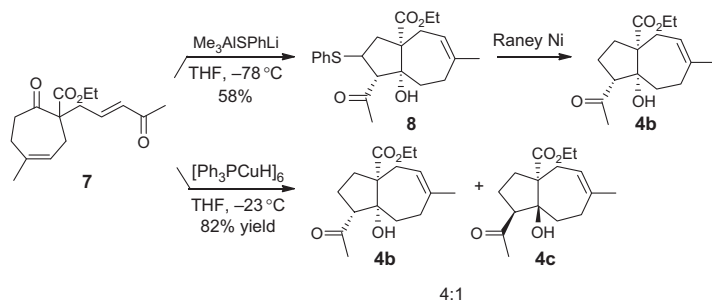
SCHEME 1 Previous and our own efforts in the aldol cyclization.

through a conjugate addition of a nucleophile that could be subsequently extruded to yield the desired aldol product. I was reminded of work previously published in the Danishefsky lab, in which an enolate, generated from a conjugate addition of a thiolate nucleophile, was allowed to further participate in an intramolecular aldol cyclization in the total synthesis of avermectin [12,13]. Accordingly, we synthesized **7**, the enone derivative of **3**, and using the ate complex $\text{Me}_3\text{AlSPhLi}$, which Danishefsky used in his work, a tandem conjugate addition-intramolecular aldol sequence yielded **8** as a single diastereomer in 58% yield, this aldol cyclization being already more efficient than the base-induced aldol previously used (Scheme 2). Instead of eliminating the sulfide residue as in the synthesis of avermectin, reduction of **8** by Raney–Nickel generated **4b**.

We contemplated that further economy in this two-step conjugate addition-reduction could be achieved if we could execute a one-step conjugate reduction-aldol cyclization cascade reaction. The reducing reagent for this process must be chemoselective for the electron-poor alkene over the unactivated $\text{C}=\text{C}$ and the isolated carbonyl group in **7**, and nonbasic to prevent the subsequent decomposition of the hydroxyketone product.

I remembered from my Ph.D. days, that Fluka annually named one new compound as a Reagent of the Year, and in 1991, Stryker's reagent, $[\text{Ph}_3\text{PCuH}]_6$, was accorded this title [14]. This hexameric copper hydride was a relatively nonbasic complex, and chemoselective for the conjugate reduction of electron-poor alkenes. However, up to that time, Stryker's reagent had been used mainly for conjugate reductions, and its applications in domino reactions had not yet been reported in the literature. When **7** was treated with Stryker's reagent at -23°C , we were delighted that conjugate reduction-aldol cyclization occurred as hoped to give cleanly **4b** and **4c** in 82% combined yield (Scheme 2).

This was one example of an aldol reaction that proceeded more efficiently under reductive conditions via copper hydride. Subsequently, other researchers have also revealed additional cases in which reductive aldol cyclization using Stryker's reagent outperformed its classical base-induced variation, in the synthetic studies of other natural products [15].



SCHEME 2 Strategies for conjugate addition-aldol cyclization.

4. DEVELOPMENT OF THE COPPER HYDRIDE-INDUCED REDUCTIVE ALDOL CYCLIZATION

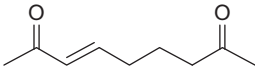
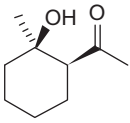
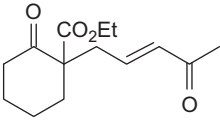
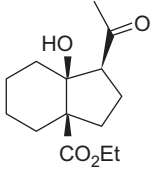
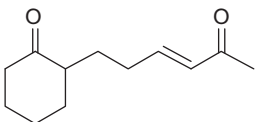
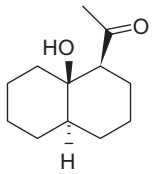
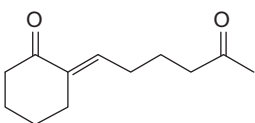
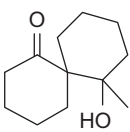
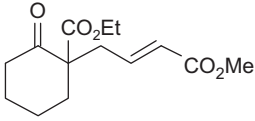
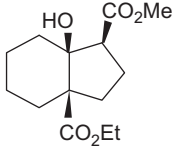
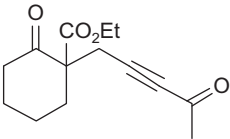
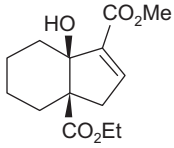
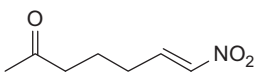
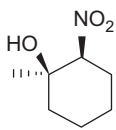
Little did we know when we attempted to solve the problem of the total synthesis of pseudolaric acid via a copper hydride-induced aldol reaction, that we would find ourselves entering a period of intense concurrent activity in the chemistry and applications of copper hydrides, with publications produced almost contemporaneously by the groups of Lipshutz [16] and Buchwald [17], ensued by a surge of work in the chemical community on this area [18,19].

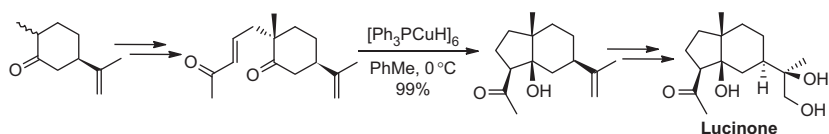
Our Master's student, Mr. Rex Szeto, began from the finding of the first copper hydride-induced reductive aldol reaction of **7**, to extend the investigation and develop this reaction as a synthetic methodology in its own right.

The reductive cyclizations induced by $[\text{Ph}_3\text{PCuH}]_6$ are generally highly diastereoselective, and at low reaction temperatures, good yields of aldol products are obtained without dehydration [20]. In addition to preventing the decomposition of the product under more alkaline conditions, the reductive aldol reaction offers other advantages over the traditional base-induced process. Selective enolate formation in compounds bearing multiple carbonyl groups, as in the context of an intramolecular aldol reaction, is quite challenging to achieve using base-induced aldol reaction conditions, whereas the enolate is exclusively derived from hydride addition to the electron-deficient olefin unambiguously and regioselectively at low temperatures in the reductive aldol cyclization (Table 1, entries 3, 4). There was no evidence of conversion of the initially formed enolate to alternative or regioisomeric enolates via inter- or intramolecular proton transfer. Secondly, using reduction, ester enolates can be generated even in the presence of the more reactive and acidic ketones to undergo directed aldol reactions (Table 1, entry 5). Finally, there are aldol products that can be synthesized via a reductive aldol reaction of an alkynone (Table 1, entry 6) [21] that could not be obtained directly via a base-induced protocol. In addition to these substrates, Ph.D. student, Wing Ki Chung also demonstrated that nitroalkenes undergo the analogous reductive Henry aldol reaction (Table 1, entry 7) [22]. We have used the reductive aldol cyclization of an enedione as the key step in the asymmetric synthesis of an iphionane sesquiterpenoid, lucinone (Scheme 3) [23].

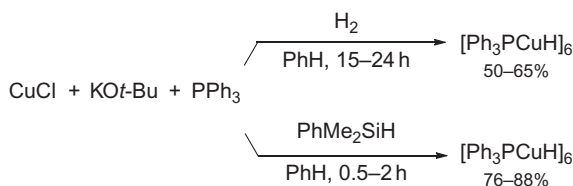
Owing to our need of $[\text{Ph}_3\text{PCuH}]_6$ for all of these studies, and finding several shipments of this commercially available reagent to be of inconsistent quality, we decided to synthesize it ourselves. Stryker had greatly simplified the synthetic procedure of preparing $[\text{Ph}_3\text{PCuH}]_6$ first published by Caulton [24], by obviating the need to prepare the air-sensitive copper *t*-butoxide separately, forming it instead from the metathesis of KOtBu and CuCl in situ (Scheme 4) [25]. He also demonstrated that atmospheric pressures of hydrogen over 15–24 h were able to generate good yields of $[\text{Ph}_3\text{PCuH}]_6$. This had been the standard protocol to prepare Stryker's reagent for the ensuing 15 years. In our lab, inspired by the results from the Brunner [26] and

TABLE 1 Reductive Aldol Cyclizations Using Stryker's Reagent

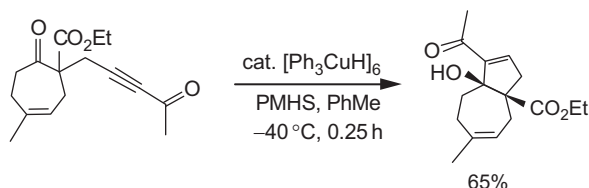
Entry	Substrate	<i>T</i> (°C)	<i>T</i> (h)	Product	Yield (%)
1		-40	1		80
2		-40	0.5		86
3		-40	1		72
4		-25	2		89
5		25	2		74
6		25	0.25		65
7		-40	1		77 (2:1)



SCHEME 3 Reductive aldol cyclization as the key step in the asymmetric synthesis of lucinone.



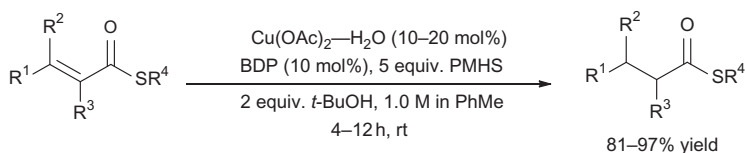
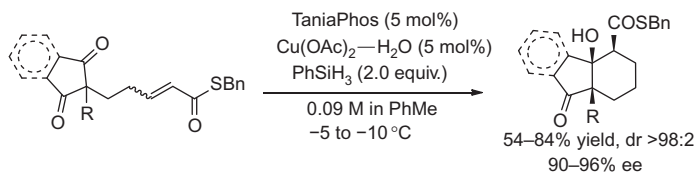
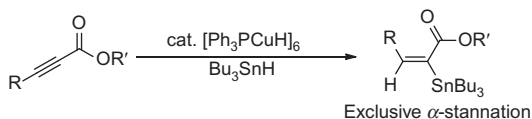
SCHEME 4 Synthesis of Stryker's reagent.



SCHEME 5 Reductive aldol cyclization of alkynediones catalyzed by copper hydride.

Lipshutz groups, who established that silanes were able to regenerate copper hydride [16], our postdoctoral fellow, Dr. Zhengning Li, and Ph.D. student Kelvin Fung, developed a homogeneous synthetic protocol using silanes instead of hydrogen to generate Stryker's reagent in as little as 0.5–1 h (Scheme 4) [27]. Other researchers have since published variations on this protocol [28].

While our initial studies employed stoichiometric amounts of copper hydride, our continued research further developed catalytic reductive aldol reactions. Ph.D. student Skarlett Leung found that alkynones underwent reductive aldol cyclizations catalyzed by Stryker's reagent with PMHS as the stoichiometric reductant (Scheme 5) [21]. More recently, a Master's student, Ally Li, found that conjugate reductions of unsaturated thioesters were catalyzed by in situ-generated *bis*(diphenylphosphino)benzene or dppe-ligated copper hydride, with PMHS as reductant (Scheme 6) [29]. This reaction was further developed by Ph.D. student Jack Ou into a desymmetrizing catalytic reductive aldol reaction with TaniaPhos as chiral ligand for the copper hydride, to afford β -hydroxythioesters with up to 97% ee (Scheme 7) [30]. Other than reductive aldol reactions, Bonnie Leung, during her undergraduate thesis research, explored the copper hydride-catalyzed hydrostannation of activated alkynes, and found that this hydrostannation occurred more

**SCHEME 6** Conjugate reduction catalyzed by copper hydride.**SCHEME 7** Desymmetrizing asymmetric reductive aldol cyclization.**SCHEME 8** Regioselective hydrostannation catalyzed by copper hydride.

regioselectively than that employing the traditionally used palladium catalysts (Scheme 8) [31].

5. THE SECOND STRATEGY TO PSEUDOLARIC ACID A

Although the reductive aldol cyclization became a useful carbon–carbon bond formation methodology to afford good yields of hydroxyketone **4**, only **4b** and **4c** were obtained as products (Scheme 2), their relative stereochemistries having been unambiguously determined by X-ray crystallography of their dinitrophenylhydrazone derivatives. Unfortunately, neither diastereomer had the correct relative stereochemistry for pursuing the synthesis of pseudolaric acid. The epimerization of **4c** to give **4a** did not seem promising, as **4b** and **4c** were also found to be the most energetically stable diastereomers by computation.

Without a solid strategy to further modify the aldol reaction to yield the desired relative stereochemistry, advancement in the total synthesis of pseudolaric acids was difficult. It was painful but necessary to go back to the drawing board to come up with another strategy that would yield the required stereochemistry with certainty. It appeared that added stereochemical constraints would help to generate the desired stereochemistry. Based on my previous work in the area of oxabicyclic compounds during my Ph.D. studies, the *trans*-fused perhydroazulene of pseudolaric acid A would be guaranteed in the context of an

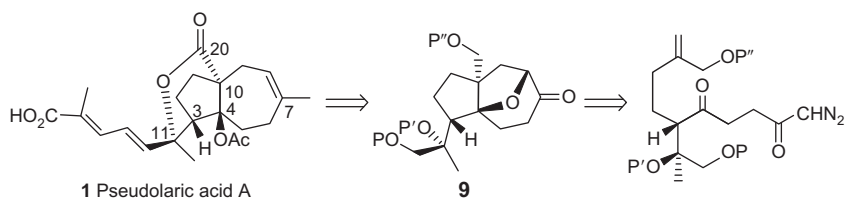
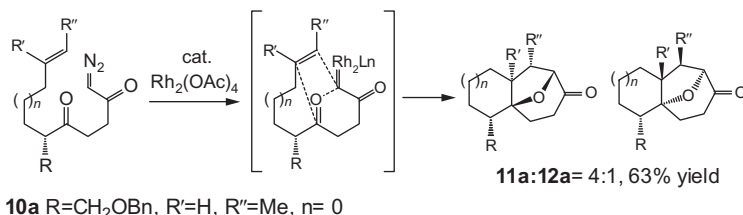


FIGURE 2 Retrosynthesis of pseudolaric acid A.

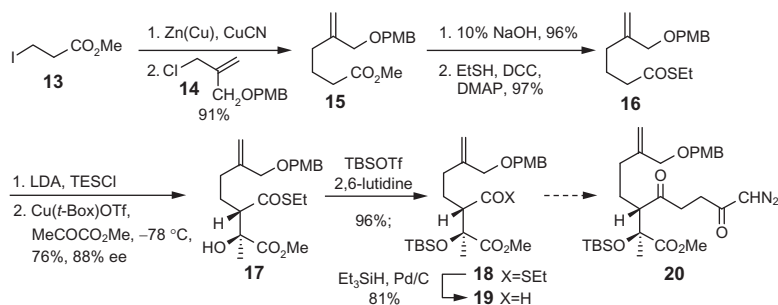


SCHEME 9 Carbene cyclization cycloaddition cascade (CCCC) reaction.

oxygen-bridged system such as **9** (Figure 2). Moreover, the tertiary alcohol masked as the oxygen bridge would be more resistant to dehydration.

Therefore, we decided to explore the synthesis of pseudolaric acid A using a carbene cyclization cycloaddition cascade (CCCC) as the key step [32]. Discovered by Iyata and further developed by Padwa, this is a domino reaction initiated by the formation of the metal carbene from decomposition of a diazoketone such as **10** under catalysis by rhodium (II) or other metals. The electrophilic carbene undergoes cyclization with a proximate carbonyl group to form a carbonyl ylide, then intramolecular cycloaddition proceeds with a dipolarophile to assemble the oxatricyclic framework from an acyclic compound in one step (Scheme 9). A total of three bond formations and installation of up to four stereocenters was possible in this elegant one-step transformation. Around this time, asymmetric variants of this reaction were being developed [33].

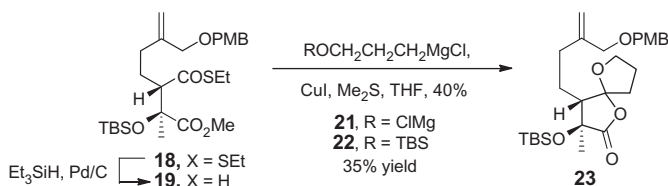
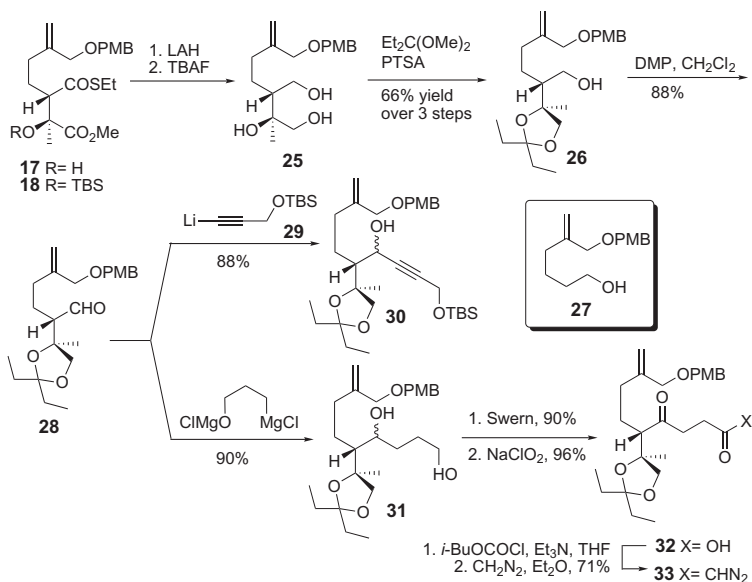
Bin was charged with reinitiating the total synthesis of pseudolaric acid using this reaction as the key strategy. At the time we began our studies, there had not been enough examples and applications of the CCCC reaction in contexts that informed us of the extent of the directing effect by substituents ($R \neq H$) in diazoketones **10** on the diastereoselectivity of this reaction to give **11** or **12**. A Ph.D. student, Rebecca Ko, studied the CCCC reaction and synthesized a model substrate **10a** ($R = \text{Me}$, $R' = \text{CH}_2\text{OBn}$, $R'' = \text{H}$, $n = 0$). It was found that the CCCC reaction produced **11a** as the major diastereomeric product with the correct relative stereochemistry for the synthesis of the pseudolaric acids with a selectivity of about 4:1 (Scheme 9) [34]. With these preliminary results in hand, we proceeded to the enantioselective synthesis of the pseudolaric acids.

SCHEME 10 Bin's synthesis of **18**.

Bin started the enantioselective synthesis via the CCCC strategy as shown in Scheme 10. The zinc homoenolate derived from iodoester **13** was alkylated with allylic chloride **14** to give an 91% yield of the homologated ester **15**. We converted **15** to the corresponding thioester **16**, and employed Evans' catalytic asymmetric aldol reaction using $[\text{Cu}\{(S,S)\text{-Box}\}][\text{OTf}]_2$ as catalyst and methyl pyruvate as the electrophile. According to optimizations carried out by the Evans group [35], these copper-catalyzed aldol reactions proceeded more efficiently in the coordinating solvent THF compared with dichloromethane, because THF promoted the turnover of the copper catalyst by aiding its decomplexation from the product. However, we found that the aldol reaction of **16** proceeded at a higher rate in dichloromethane, and this may indicate a change in the rate determining step from catalyst decomplexation to the reaction of methyl pyruvate with the silyl enol ether derived from **16**, a thioester more sterically demanding than those surveyed in the literature. We were pleased to find that in one step, the absolute stereochemistry of the two stereocenters destined to be C3 and C11 of pseudolaric acid were set, to produce hydroxythioester **17** with an optimized 88% ee.

After TBS protection of the free hydroxy group, thioester **18** seemed to be poised for the desired homologation to diazoketone **20**, as the thioester in **18** should be more reactive than the oxoester and should succumb to nucleophilic addition more readily. Unfortunately, the steric environment of thioester **18** was quite hindered, such that a variety of nucleophiles either failed to react with **18** under mild conditions, or attempts to promote reaction by increasing the temperature resulted in a mixture—due to interference by the concomitant reactivity of the ester. For example, the only carbon nucleophile that underwent any addition with **18** was Normant's Grignard reagent **21**, catalyzed by copper (Scheme 11). However, the product isolated was a low yield of *bis*-cyclized **23**, which we could not manage to unravel cleanly.¹ On the other

1. Unpublished results of the group.

SCHEME 11 Homologation attempts from **18**.SCHEME 12 Homologation from **28**.

hand, protected **22** did not undergo appreciable addition. Even after converting the thioester to the more electrophilic aldehyde **19** via a Fukuyama reduction [36], we did not observe a selective reaction.

After several months of effort that did not yield any positive results, Bin's time was up and he wrote up his thesis on the model studies and attempts and progress he made thus far to synthesize pseudolaric acid. It was then up to the next Ph.D. student, Ms. Zhe Geng, to continue the synthesis of pseudolaric acid.

Ms. Geng was a prudent and industrious student, having taught and worked at the Beijing Normal University for several years before joining our group. After studying Bin's attempts to effect addition, she became convinced that relying on the addition reaction to differentiate the two electrophilic sites was going to be nonselective. Instead, **17** was fully reduced to the triol **25**, then selectively protected as dioxolane **26** by treatment with 3,3-dimethoxypentane (Scheme 12). The reduction of **17** proceeded with

low yield; however, a major side product (**27**) resulted from the reduction of **16**, which was derived from a retroaldol reaction under the reduction conditions. To prevent the retroaldol reaction, TBS-protected **18** was treated with LAH instead and this resulted in a much higher reduction yield. Treatment with fluoride finally produced triol **25**.

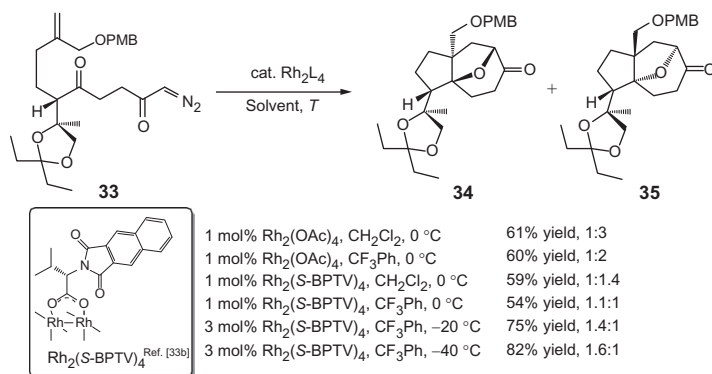
Alcohol **26** was oxidized to give aldehyde **28**, which could undergo various additions, such as with acetylide **29** to give a good yield of **30**, and also with Normant's Grignard reagent to give diol **31**. Diol **31** was carried forward, by *bis*-oxidation to yield the ketoacid **32**, which was then converted to the diazoketone **33**.

6. CASE 1: WHEN MODEL REACTIONS FAIL

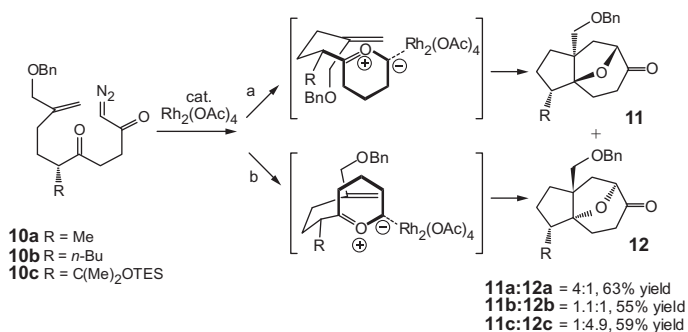
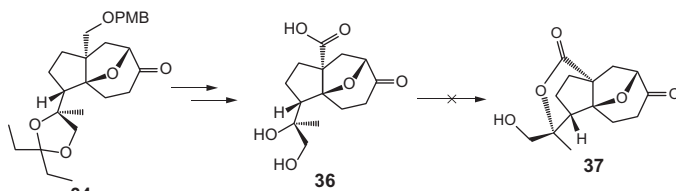
With the key diazoketone **33** in hand, we examined its CCCC reaction (Scheme 13). We were not amused to find that the $\text{Rh}_2(\text{OAc})_4$ -catalyzed reaction of **33** generated two diastereomers **34** and **35**, in which the undesired isomer **35** was the major cycloadduct!

Our model reaction from Scheme 9 showed that the mode of cycloaddition to produce the cycloadduct **11a** with the desired relative stereochemistry was favored, but this turned out not to be general. Additional model substrates (Scheme 14) showed that this selectivity was diminished when the substituent R increased in size, such as in **10b** and **10c**, probably due to transannular interactions that arise in the process of cycloaddition by this mode (Pathway a). Therefore, cycloaddition by the alternative mode (Pathway b), which avoids these interactions, became the favored pathway.

Zhe further screened various chiral rhodium catalysts to see if reagent control could be used to override the substrate cycloaddition preference to produce the desired diastereomer. This was achieved to a certain extent: using Hashimoto's catalyst $\text{Rh}_2(\text{S-BPTV})_4$ [33b], in the optimized solvent CF_3Ph , and at lower temperatures ($-40\text{ }^\circ\text{C}$), the diastereoselectivity of the cycloaddition improved



SCHEME 13 Rhodium-catalyzed CCCC reactions of **33**.

SCHEME 14 CCCC Reactions of **10a–10c**.

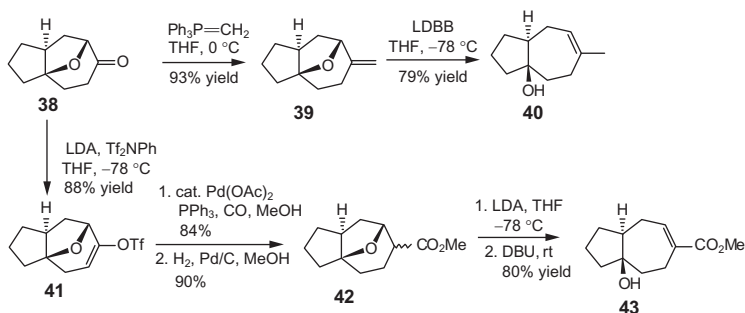
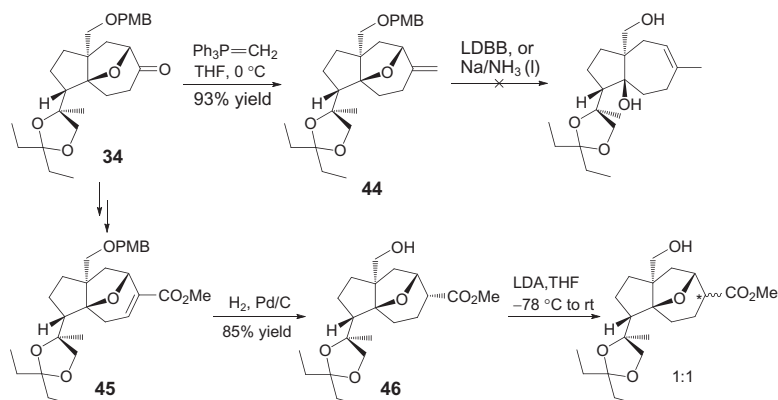
SCHEME 15 Failed lactonizations.

to 1.6:1 in our favor (Scheme 13). At the time, after months of effort exploring quite a few strategies to improve the diastereoselection, this was the best result we could achieve. While it would certainly be desirable to see an even better diastereoselectivity, it was not certain how much more time and effort would be needed and to what extent the selectivity could be further improved. Nevertheless, this outcome represented a 50% yield of the desired diastereomer **34**, in which all four of the stereocenters of pseudolaric acid had been established. We decided to devote our energies to move **34** forward instead, and explore the completion of the total synthesis.

Initially, we explored lactonization before the ring opening of the oxygen bridge, because having the hydroxyl group masked as the bridging ether protected against dehydration at that site. However, after transformation of **34** to **36**, lactonization failed under all conditions tried (Scheme 15). We finally conceded that the formation of the final ring may not be possible in the context of the bicyclic ether, which drastically altered the conformation of the perhydroazulene framework from that found in the natural product.

7. CASE 2: WHEN MODEL REACTIONS FAIL

Thus, we explored the next transformation, which was to induce the ring opening of the oxygen bridge, a reaction with which I had some experience in my Ph.D. studies with Prof. Mark Lautens [37]. Of course, we first

SCHEME 16 Cleavage of ether from model compound **38**.

SCHEME 17 Failed oxygen bridge cleavage.

explored this transformation in the context of a model perhydroazulene ketone **38** (Scheme 16). Methylenation and treatment with LDBB realized the ring-opened perhydroazulene skeleton **40**, as found in pseudolaric acid A (**1**). Alternatively, triflation of **38** yielded **41**. Carbonylation in the presence of methanol generated an alkenoate, which was reduced to give ester **42**. Treatment with LDA readily generated the more oxidized perhydroazulene framework **43**, as found in pseudolaric acid B (**2**).

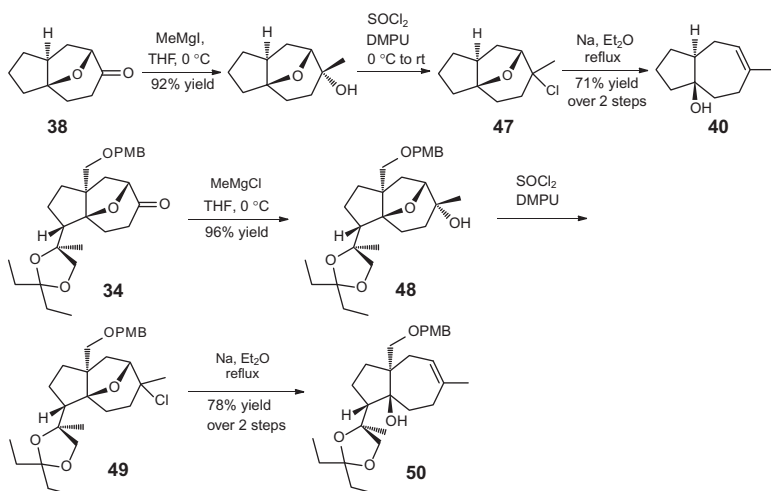
Having a number of ring-opening methods at our disposal, we applied them to the actual oxatricyclic ketone **34**. It was very annoying, and quite depressing as weeks passed, that none of the reactions induced the oxygen bridge cleavage of synthetic intermediate **34** (Scheme 17). While methylenation of **34** occurred to give **44**, many reducing agents, including LDBB and sodium in liquid ammonia, only resulted in the cleavage of the PMB group, but utterly failed to promote any ring opening. A similar enol triflation and palladium-catalyzed carbonylation sequence converted **34** to **45**. Reduction generated a single diastereomeric ester and cleaved the PMB group to

give **46**. Treatment with base from -78°C up to room temperature, with or without crown ethers and HMPA, only served to epimerize **46**, but failed to induce the E1_{cb} elimination required for ring opening.

We were at this for months—there was no way to bypass this transformation at the present stage of our strategy. If we could not open the oxygen bridge, we would not be able to accomplish the synthesis. We could not understand why ring opening was so successful in the model compounds **39** and **42**, and yet so poor with **44** and **46**. These compounds bore substituents that appeared to be rather distant from the site of the ring-opening reaction, yet these substituents apparently prevented the desired reaction. Somehow, these distal substituents unexpectedly raised the energy of the transition state of the elimination, perhaps by distorting the conformation and orbital alignment that had made the elimination possible in the model compounds **39** and **42**.

At this stage of the project, I would meet with Zhe and suggest some new ideas she could try for the coming few days, but when I was alone, I started to have doubts myself—would this strategy work? Should I have the team keep going at it, or, was I wasting their energy leading them down the garden path toward an eventual dead end?

Finally, we applied the harshest ring-opening conditions we knew, which we refrained from even considering initially—using an alkali metal reductive elimination at this rather late stage of the total synthesis. This transformation successfully induced ring opening in the model compound **47**, but by now we were quite aware that this was no guarantee that the method would be applicable to the pseudolaric acid intermediate (Scheme 18). We methylated **34**, then converted tertiary alcohol **48** to chloride **49**. Only sodium could induce



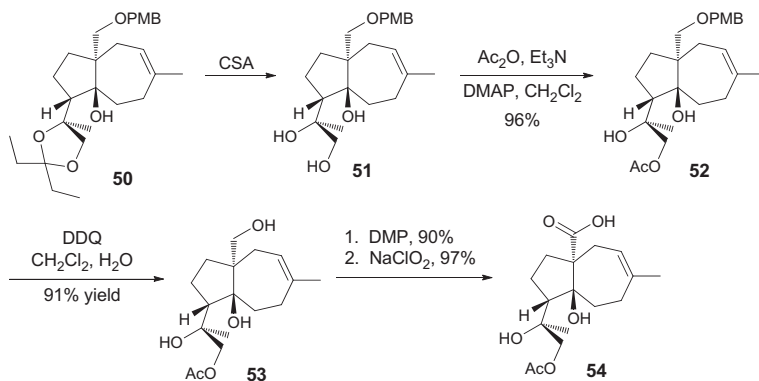
SCHEME 18 Successful oxygen bridge cleavage.

reduction of the chloride but fortunately, all the functional groups of **49** at this stage were able to tolerate these conditions. Gratifyingly, in this manner we were finally able to induce the reductive opening to give **50**. In hindsight, we rationalized that the activation barrier of the elimination was overcome and resulted in successful ring opening by forming an unstabilized organometallic species, and the ring opening became irreversible. Perhydroazulene derivative **50**, having the carbobicyclic platform of pseudolaric acid A, was in fact obtained in quite a decent overall yield of 78% over two steps. Zhe and I thought we saw the light at the end of the tunnel.

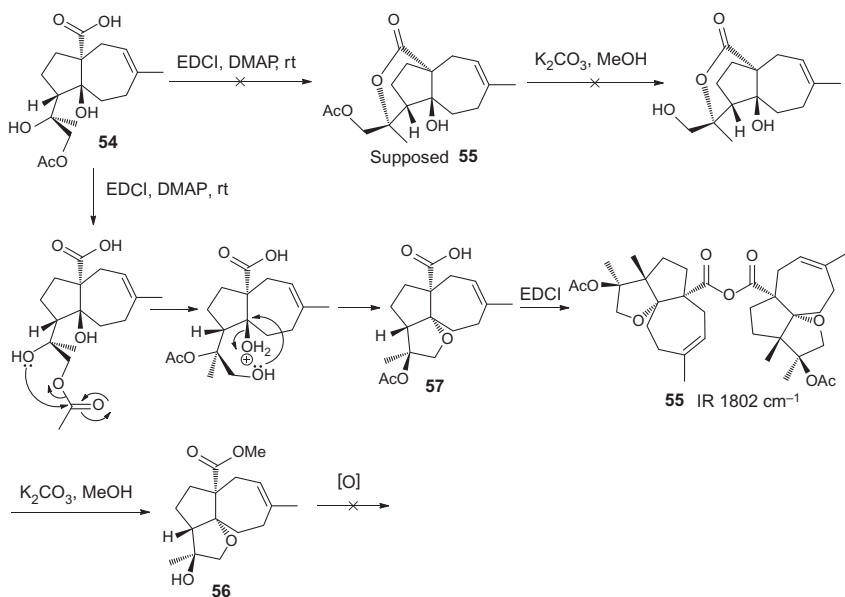
8. TOO HAPPY TOO QUICKLY, AND THE IMPORTANCE OF IR SPECTROSCOPY

We were extremely excited by this time and it appeared that we would just be able to complete the total synthesis by the deadline of Zhe's Ph.D. candidature! The most significant transformation that remained was the final lactonization. Deketalization of **50** yielded diol **51**, and to ensure lactonization with the desired tertiary hydroxyl group in the presence of the primary alcohol, the latter was selectively acetylated to give **52** (Scheme 19). Deprotection of the PMB group revealed the primary alcohol at the ring junction and this was fully oxidized to acid **54**.

To effect lactonization, **54** was treated with EDCI, which generated a single product **55** cleanly (Scheme 20). At this late stage of the synthesis, Zhe repeated this reaction several times on small scale, found them to be as clean as the first run, ascertaining the structure of **55** by NMR, before subjecting all of her material to this reaction to have enough of the compound to do the rest of the characterizations. We had to wait for a few days to get the MS results after submission to the MS lab.



SCHEME 19 Synthesis of lactonization precursor **54**.



SCHEME 20 Failed lactonization of **54**.

In the meantime, Zhe proceeded to deacetylate **55** using $K_2CO_3/MeOH$, to further oxidize it to generate the aldehyde for the HWE reaction (Scheme 20). However, methanolysis product **56** was found to be a methyl ester which could not be oxidized under a variety of conditions. At this point we started to panic, because all of our material had by then been converted to **55** that was starting to look like it was not our expected product.

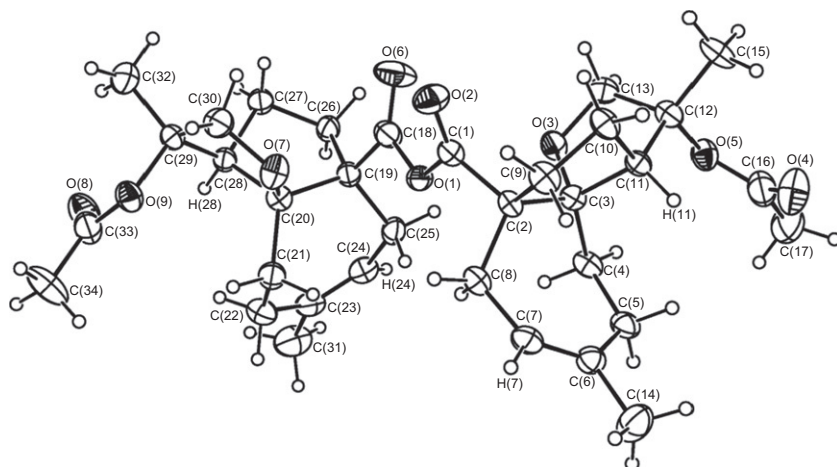
“Come to think of it, this compound had a strange IR stretch....,” Zhe remarked.

“Where is it?” I asked.

“At 1802 cm^{-1} .”

Gasp. Something had gone terribly wrong—this was no typical ester carbonyl stretch.

Zhe by this time had accumulated a considerable amount of this material and she was able to grow crystals of this compound. X-ray crystallographic analysis confirmed that it was a stable anhydride **55** (Figure 3). Something quite unexpected obviously had occurred under the seemingly innocuous EDCI coupling conditions. All of this plus deducing a plausible mechanism could be the stuff of a good “cume” question. Acetyl transfer to the tertiary alcohol had occurred before any other process, then S_N1 substitution occurred at the ring junction to give acid **57**, which was activated by EDCI in the absence of any other nucleophile to dimerize and form anhydride **55** (Scheme 20).

**FIGURE 3** ORTEP of **55**.

From this chapter of our total synthesis journey, we learned some valuable lessons. One is that no matter how much we hope a chemical transformation will proceed in our favor, it is important to look squarely at what the evidence is telling us. The other lessons may be too old-school for some readers. I still believe that we should faithfully and fully characterize all synthetic compounds and intermediates, as this adds to and enriches the database of information on chemical compounds that will be a lasting reference and resource for all organic chemists. I have observed that there is increasingly a trend for researchers to omit the IR spectral characterization of compounds, and in most cases, I do not think there is any good excuse for it. The IR spectrometer is a common laboratory instrument in all institutions, that even undergraduates have learned how to operate, and the cost to run an experiment is minimal. The use of IR spectroscopy is underrated: it provides functional group information that is sometimes not easily distinguishable by NMR spectroscopy. In the case of **55**, its NMR characterization was quite consistent with the presumed compound, and that is what misled us to think we had the desired intermediate. The more complex the structure, the more that IR spectroscopic characterization is needed for verification or as corroborating evidence. IR spectroscopy can also give meaningful information on ring sizes and hydrogen bonding, which in turn can be utilized for stereochemical and structural determinations. In an earlier volume of STOS, Prof. Aubé also cites the use of Bohlmann bands in the IR for stereochemical elucidation [38].

Having pushed all of the frontline material to this dead-end compound, we had suffered a major set-back. Zhe's Ph.D. candidature was almost due and it did not seem feasible to restart the synthesis from the beginning again. We decided that Zhe should write up her thesis based on her work so far. And so she did, and submitted her Ph.D. thesis for examination.

9. BUT IT WAS NOT TIME TO GIVE UP

During the time that Zhe's thesis was being examined, I thought she would be spending her time mainly on studying for the upcoming oral. Instead, she managed to repeat the *entire* synthesis almost from the beginning to reach intermediate **50**, a real testament to her initiative and persistence.

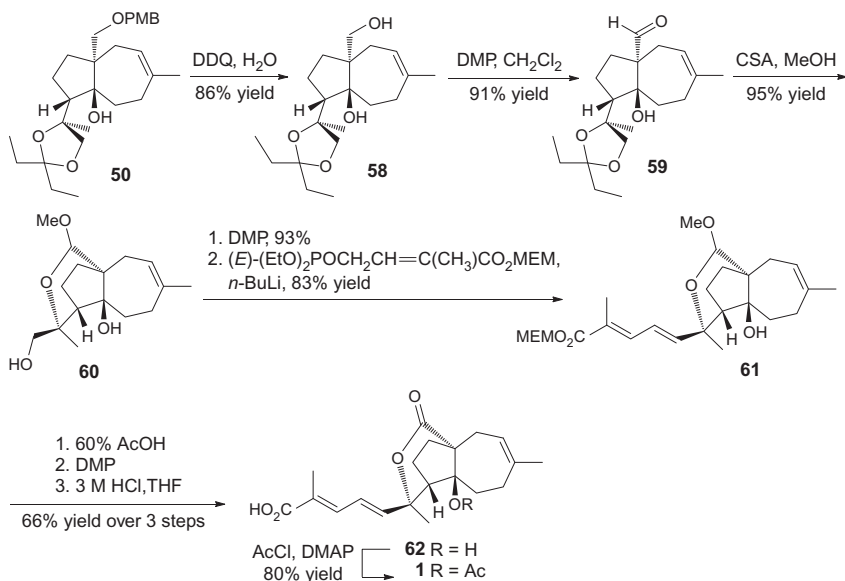
To proceed forward in the synthesis, acetylation was omitted and **50** was instead directly deprotected and oxidized to aldehyde **59** (Scheme 21). Treatment with acid served not only to deprotect the diethyl ketal but also induced intramolecular acetal formation to give **60**, confirming that in the absence of the oxygen bridge, the propensity to form the final ring was favored, as is found in the natural product. Oxidation of the primary alcohol **60** generated the aldehyde, which was homologated by an HWE reaction to generate the desired (*E,E*)-diene **61**. Hydrolysis of the mixed cyclic acetal and oxidation produced the lactone. Removal of the MEM group and acetylation finally generated pseudolaric acid A (**1**).

I think I must have been engrossed in thought when Zhe came into my office that day and said, "It's finished!" She laid some spectra on my desk. I looked up from my desk and replied, "Which step?"

Zhe exclaimed, "No, I mean the whole thing!"

And there it was, the NMR spectra of the pseudolaric acid A she synthesized, along with the spectra of the natural material, which matched perfectly [39].

Now that was a good day.



SCHEME 21 Total synthesis of pseudolaric acid A (**1**).

10. OTHER NATURAL PRODUCTS

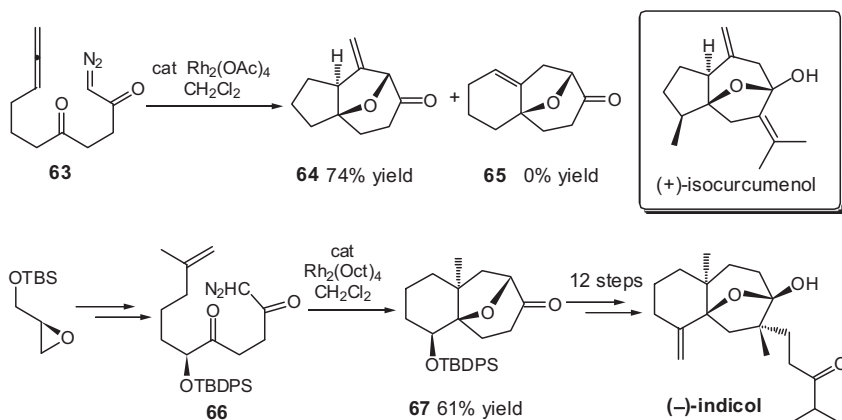
As a result of attempting the synthesis of pseudolaric acid, we became interested in applications of the CCCC reaction that further spurred synthetic studies of other natural products based on this reaction as a key step.

In the vasorelaxing sesquiterpenoid (+)-isocurcumenol, the exocyclic methylene group appeared to be a common feature of the biologically active members of this family of natural products. This exocyclic methylene group was installed directly via the carbene cyclization cycloaddition with a tethered allene. Although intervening five- or six-membered ring formation by cycloaddition with the internal and terminal double bond of the allene was in theory possible to give cycloadducts **64** or **65**, respectively, Ph.D. student Rebecca Ko found that the CCCC reaction of **63** generated exclusively **64**, having the carboskeleton for isocurcumenol (Scheme 22) [40].

The CCCC reaction to form an intervening six-membered ring through intramolecular cycloaddition was exploited by Ph.D. student Secant Lam for the synthesis of (–)-indicol, a secodolastane natural product isolated from the algae *Dictyota indica*. The asymmetric total synthesis was ultimately accomplished using the CCCC reaction of **66** to give **67** as the major diastereomeric cycloadduct (Scheme 22) [41].

11. EPILOGUE

I hope I did not bore you beginning with my mundane past. I shared it, not because I consider myself or my career path particularly exemplary; I only wanted to highlight through my experience that life, as it unfolds, turns out to be rather unexpected and surprising, with people and events making up an ultimate adventure and story that one cannot initially foresee.



SCHEME 22 Synthetic studies of other natural products based on the CCCC reaction.

My research program had been a similar adventure in that way. This tale tells how I landed on this project, and a very fortuitous thing that it was. In retrospect, had I carefully planned my professional chemistry career, perhaps I might not have begun it with a total synthesis project. Some regard this as career suicide, as there is a considerable risk that one could not finish the target molecule and generate enough papers in time for tenure application. However, even though we had our share of trials and tribulations, it was an exciting roller coaster ride that was ultimately successful in achieving the total synthesis of the target molecule, which was sweet in itself and provided the ultimate validation of our ideas and vindication of our efforts. The total synthesis also inspired and initiated our program in the study and applications of copper hydrides, as well as spawned the syntheses of other natural products. One thing led to another, and this grew into a very fruitful research program. I know this kind of gratification is not my unique experience but one shared by many who undertake total synthesis.

Those of us who continue to do research in the total synthesis of natural products are subjecting ourselves to this kind of agony and thrill everyday. It is an exciting life! Each natural product synthesis is like embarking on a new journey or an expedition for which we have to find our way. One never knows that a piece of information learned previously could be the key to unlocking the next level. The proposed route, and what one actually finds along the way and the new things that are learned and gained, are what makes the synthetic journey a surprising, exciting, and rewarding adventure.

ACKNOWLEDGMENTS

This adventure in total synthesis would not have turned out as exciting as it did without the members of the traveling troupe: postgraduate students, postdoctoral fellows and collaborators who contributed their talent to this mental and physical journey. We have shared many joys, disappointments and life lessons along the way, and the human factor of this journey has been as rewarding as the science itself. I thank all of them for their hard work, and I am truly grateful for the privilege to have been able to interact with as intellectually stimulating a group as them. I dedicate this account to all my research students and collaborators, past and present. I also thank the many mentors I met along the way for their contribution of ideas, encouragement, and support. The funding and support from the University of Hong Kong, the Research Grants Council of Hong Kong SAR, PR China (Project No. HKU 7017/04P), and the Areas of Excellence Scheme (Project No. AoE/P-10/01) administered by the University Grants Committee (HKSAR) are gratefully acknowledged.

REFERENCES

- [1] (a) B.N. Zhou, B.P. Ying, G.Q. Song, Z.X. Chen, J. Han, Y.F. Yan, *Planta Med.* 47 (1983) 35; (b) M.O. Hamburger, H.L. Shieh, B.N. Zhou, J.M. Pezzuto, G.A. Cordell, *Magn. Res. Chem.* 27 (1989) 1025.

- [2] L.T. Leung, B.C.B. Ko, P. Chiu, *Nat. Prod. Rep.* 26 (2010) 1066–1083.
- [3] E. Li, A.M. Clark, C.D. Hufford, *J. Nat. Prod.* 58 (1995) 57.
- [4] Y. Zhang, R. Lu, A. Yan, *Acta Pharmacol. Sin.* 11 (1990) 60–62.
- [5] D.J. Pan, L.Z. Li, C.Q. Hu, K. Chen, J.J. Chang, K.H. Lee, *Planta Med.* 56 (1990) 35–38.
- [6] Y. Tong, X. Zhang, M. Geng, J. Yue, X. Xin, F. Tian, X. Shen, L. Tong, M. Li, C. Zhang, W. Li, L. Lin, J. Ding, *Mol. Pharmacol.* 69 (2006) 1226–1233.
- [7] V.K.M. Wong, P. Chiu, S.S.M. Chung, L.M.C. Chow, Y.Z. Zhao, B.B. Yang, B.C.B. Ko, *Clin. Cancer Res.* 11 (2005) 6002–6011.
- [8] T. Zhou, H. Li, N. Zhu, P. Chiu, *Tetrahedron* 60 (2004) 4931–4936.
- [9] B.C. Pan, H.Y. Chang, G.L. Cai, Y.S. Guo, *Pure Appl. Chem.* 61 (1989) 389–392.
- [10] Y. Nakashita, M. Hesse, *Angew. Chem. Int. Ed.* 20 (1981) 1021.
- [11] P. Chiu, B. Chen, K.F. Cheng, *Tetrahedron Lett.* 39 (1998) 9229–9232.
- [12] (a) S.J. Danishefsky, D.M. Armistead, F.E. Wincott, H.G. Selnick, R. Hungate, *J. Am. Chem. Soc.* 109 (1987) 8117–8119; (b) D.M. Armistead, S.J. Danishefsky, *Tetrahedron Lett.* 28 (1987) 4959–4962.
- [13] Prof. Danishefsky called this reaction, the “Nozaki” process: A. Itoh, S. Ozawa, K. Oshima, H. Nozaki, *Tetrahedron Lett.* 21 (1980) 361–364.
- [14] W.S. Mahoney, D.M. Brestensky, J.M. Stryker, *J. Am. Chem. Soc.* 110 (1988) 291–293.
- [15] (a) H. Mukherjee, N.T. McDougal, S.C. Virgil, B.M. Stoltz, *Org. Lett.* 13 (2011) 825–827; (b) K.D. Schwartz, J.D. White, *Org. Lett.* 13 (2011) 248–251.
- [16] B.H. Lipshutz, J. Keith, P. Papa, R. Vivian, *Tetrahedron Lett.* 39 (1998) 4627–4630.
- [17] D.H. Apella, Y. Moritani, R. Shintani, E.M. Ferreira, S.L. Buchwald, *J. Am. Chem. Soc.* 121 (1999) 9473–9474.
- [18] (a) Review of copper hydride in synthesis: S. Rendler, M. Oestreich, *Angew. Chem. Int. Ed.* 46 (2007) 498; (b) C. Deutsch, N.J. Krause, B.H. Lipshutz, *Chem. Rev.* 108 (2008) 2916–2927.
- [19] Representative contributions: (a) J. Deschamp, O. Chuzel, J. Hannedouche, O. Riant, *Angew. Chem. Int. Ed.* 45 (2006) 1292–1297; (b) C. Czekelius, E.M. Carreira, *Angew. Chem. Int. Ed.* 42 (2003) 4793–4795; (c) H.W. Lam, P.M. Joensuu, *Org. Lett.* 7 (2005) 4225–4228; (d) D. Lee, D. Kim, J. Yun, *Angew. Chem. Int. Ed.* 45 (2006) 2785–2787; (e) T.M. Kamenecka, L.E. Overman, S.K. Ly Sakata, *Org. Lett.* 4 (2002) 79–82; (f) K. Agapiou, D.F. Cauble, M.J. Krische, *J. Am. Chem. Soc.* 126 (2004) 4528–4529; (g) D. Zhao, K. Oisaki, M. Kanai, M. Shibasaki, *Tetrahedron Lett.* 47 (2006) 1403–1407; (h) J.-N. Desrosiers, A.B. Charette, *Angew. Chem. Int. Ed.* 46 (2007) 5955–5957; (i) H. Kaur, F.K. Zinn, E.D. Stevens, S.P. Nolan, *Organometallics* 23 (2004) 1157–1160; (j) S. Rendler, G. Auer, M. Oestreich, *Angew. Chem. Int. Ed.* 44 (2005) 7620–7624; (k) C. Deutsch, B.H. Lipshutz, N. Krause, *Angew. Chem. Int. Ed.* 46 (2007) 1650–1653.
- [20] P. Chiu, C.P. Szeto, Z. Geng, K.F. Cheng, *Org. Lett.* 3 (2001) 1901–1903.
- [21] P. Chiu, S.K. Leung, *Chem. Commun.* (2004) 2308–2309.
- [22] P. Chiu, W.K. Chung, *Synlett* (2005) 55–58.
- [23] P. Chiu, C.P. Szeto, Z. Geng, K.F. Cheng, *Tetrahedron Lett.* 42 (2001) 4091–4093.
- [24] G.V. Goeden, K.G. Caulton, *J. Am. Chem. Soc.* 103 (1981) 7354–7355.
- [25] D.M. Brestensky, D.E. Huseland, C. McGettigan, J.M. Stryker, *Tetrahedron Lett.* 29 (1988) 3749–3752.
- [26] H. Brunner, W. Miehl, *J. Organomet. Chem.* 275 (1984) c17–c21.
- [27] P. Chiu, Z. Li, K.C.M. Fung, *Tetrahedron Lett.* 44 (2003) 455–457.
- [28] D. Lee, J. Yun, *Tetrahedron Lett.* 45 (2004) 5415–5417.
- [29] N. Li, J. Ou, M. Miesch, P. Chiu, *Org. Biomol. Chem.* 9 (2011) 6143–6147.

- [30] (a) J. Ou, W.T. Wong, P. Chiu, *Tetrahedron* 68 (2012) 3450–3456 (b) J. Ou, W.T. Wong, P. Chiu, *Org. Biomol. Chem.* 10 (2012) DOI:10.1039/C2OB25206F.
- [31] (a) L.T. Leung, S.K. Leung, P. Chiu, *Org. Lett.* 7 (2005) 5249–5252; (b) R. Miao, S. Li, P. Chiu, *Tetrahedron* 63 (2007) 6737–6740.
- [32] (a) G. Mehta, S. Muthusamy, *Tetrahedron*, 58 (2002) 9477–9504; (b) A. Padwa, *J. Organometal. Chem.*, 690 (2005) 5533–5540; (c) A. Padwa, M.D. Weingarten, *Chem. Rev.* 96 (1996) 223–269; (d) M.P. Doyle, M.A. McKervey, T. Ye, *Modern Catalytic Methods for Organic synthesis with Diazo Compounds*, J. Wiley & Sons, New York, 1998 Chapter 7, pp. 397–416.
- [33] (a) D.M. Hodgson, P.A. Stuppel, C. Johnstone, *Chem. Commun.* (1999) 2185–2186; (b) S. Kitagaki, M. Anada, O. Kataoka, K. Matsuno, C. Umeda, N. Watanabe, S.I. Hashimoto, *J. Am. Chem. Soc.* 121 (1999) 1417–1418.
- [34] B. Chen, R.Y.Y. Ko, M.S.M. Yuen, K.F. Cheng, P. Chiu, *J. Org. Chem.* 68 (2003) 4195–4205.
- [35] (a) D.A. Evans, M.C. Kozlowski, J.A. Murry, S. Burgey, K.R. Campos, B.T. Connell, R. J. Staples, *J. Am. Chem. Soc.* 121 (1999) 669–685; (b) D.A. Evans, C.S. Burgey, M. C. Kozlowski, S.W. Tregay, *J. Am. Chem. Soc.* 121 (1999) 686–699.
- [36] T. Fukuyama, S.C. Lin, L. Li, *J. Am. Chem. Soc.* 112 (1990) 7050–7051.
- [37] (a) P. Chiu, M. Lautens, *Top. Curr. Chem.* 190 (1997) 1–85; (b) M. Lautens, P. Chiu, J. T. Colucci, *Angew. Chem. Int. Ed Engl.* 32 (1993) 281–283; (c) M. Lautens, P. Chiu, *Tetrahedron Lett.* 34 (1993) 773–776; (d) M. Lautens, C. Gajda, P. Chiu, *J. Chem. Soc., Chem. Commun.* (1993) 1193–1194; (e) M. Lautens, P. Chiu, S. Ma, T. Rovis, *J. Am. Chem. Soc.* 117 (1995) 532–533; (f) M. Lautens, S. Ma, P. Chiu, *J. Am. Chem. Soc.* 119 (1997) 6478–6487.
- [38] K.J. Frankowski, A. Wroblewski, J. Aube, *Strategies and Tactics in Organic Synthesis*, (2008) vol. 7. pp. 408–459.
- [39] Z. Geng, B. Chen, P. Chiu, *Angew. Chem. Int. Ed.* 45 (2006) 6197–6201.
- [40] X. Zhang, R.Y.Y. Ko, S. Li, R. Miao, P. Chiu, *Synlett* (2006) 1197–1200.
- [41] S.K. Lam, P. Chiu, *Chem. Eur. J.* 13 (2007) 9589–9599.

Total Synthesis of Papulacandin D

Tetsuya Kobayashi¹, Christopher S. Regens² and Scott E. Denmark

Department of Chemistry, University of Illinois at Urbana-Champaign, Urbana, Illinois, USA

Chapter Outline

1. Introduction and Background	80		
2. Retrosynthetic Analysis	85		
3. Preparation of the Spirocyclic Aryl Glycoside	86		
3.1. Development of Cross-Coupling Conditions	86	Aldol Addition Reactions	102
3.2. Optimization of Protecting Groups for the Glucal Silanol	90	4.3. Model Study of an Asymmetric Allylation Reaction	105
3.3. Optimization of Protecting Groups for the Aromatic Iodide	95	4.4. Asymmetric Allylation of Aldehyde 28 and Proof of Configuration	108
3.4. Implementation of the Key Cross-Coupling Sequence	97	4.5. Acylation of tris-SEM Protected Aryl Glycoside	109
3.5. Oxidative Spiroketalization and C(2)-Hydroxyl Group Protection	97	5. Studies on the Global Deprotection to Synthesize Papulacandin D	111
3.6. Completion of the Synthesis of the Spirocyclic Aryl Glyco-Pyranoside	99	5.1. Model Study of SEM Deprotection	111
4. Synthesis of Fatty Acid Side Chain 26 and Acylation	100	6. New Protecting Group Strategy	114
4.1. Preparation of the Dienylaldehyde 28	100	6.1. Introduction of TEOC Protecting Groups	114
4.2. Model Study of Lewis-Base-Catalyzed Asymmetric		6.2. Studies on the Removal of TEOC Groups	117
		7. Global Deprotection	119
		8. Conclusion	122

1. Current address: Gilead Sciences, Inc., Foster City, California, USA

2. Current address: Bristol-Meyers Squibb, New Brunswick, New Jersey, USA

1. INTRODUCTION AND BACKGROUND

The papulacandins are a family of antifungal agents, isolated from the deuteromycetous fungus *Papularia sphaerosperma* [1] that have demonstrated potent *in vitro* antifungal activity against various pathogens [1–3]. Interestingly, the papulacandins are inactive against filamentous fungi, bacteria, and protozoa [1a]. Compounds effective in treating fungal infections in mammals by mechanisms that do not interfere with metabolic pathways are rare and so the discovery and synthesis of such new antifungal agents is of great importance to human health [2,4].

All members of the papulacandin family target the enzyme (1,3)-beta-D-glucan synthase [2,4]. Inhibition of this enzyme prevents the uptake of glucose in the biosynthesis of glucan. Therefore, this enzyme is essential for the construction of plant cell walls, otherwise the cell wall becomes fragile and easily susceptible to lysis [2a]. As with many secondary metabolites displaying potential medical applications, the papulacandins have stimulated interest in their isolation, structural elucidation, investigation into their biological activity, and chemical synthesis [1a–c,5,6]. Specifically, the interest in the biological activity of these compounds has focused on their value as potential therapeutic agents to combat human fungal infections, which are linked to the high mortality of immunocompromised hosts such as AIDS patients [7].

The papulacandins are amphipathic molecules: each contains a hydrophilic, glycoside domain, and a hydrophobic domain in the form of a modified fatty acid. This hydrophobic domain is thought to be essential for activity [1c]. Papulacandins A–C are complex molecules, linked via a spirocyclic structure to a lactose moiety with two different aliphatic acyl side chains, one shorter fatty acid chain at the O-(6') position of the β -galactoside and a second longer side chain at the O-(3) position of the glucose moiety [1b]. The simplest member of the papulacandin family, papulacandin D, lacks the O-(6'-acyl- β -galactoside) at the O-(4) position of the glucose residue (Figure 1) [1c].

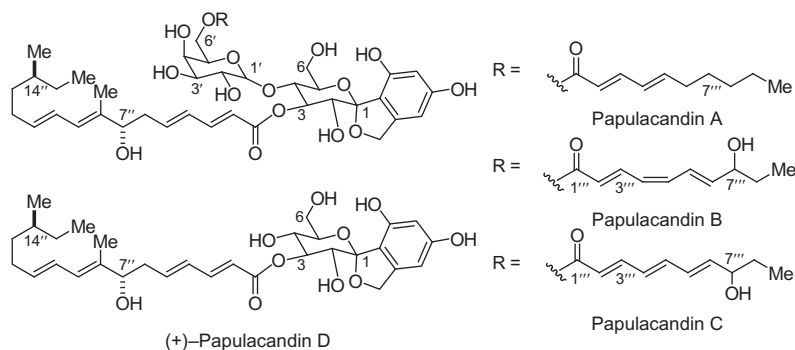


FIGURE 1 Representative papulacandins from the fermentation of *P. sphaerosperma*.

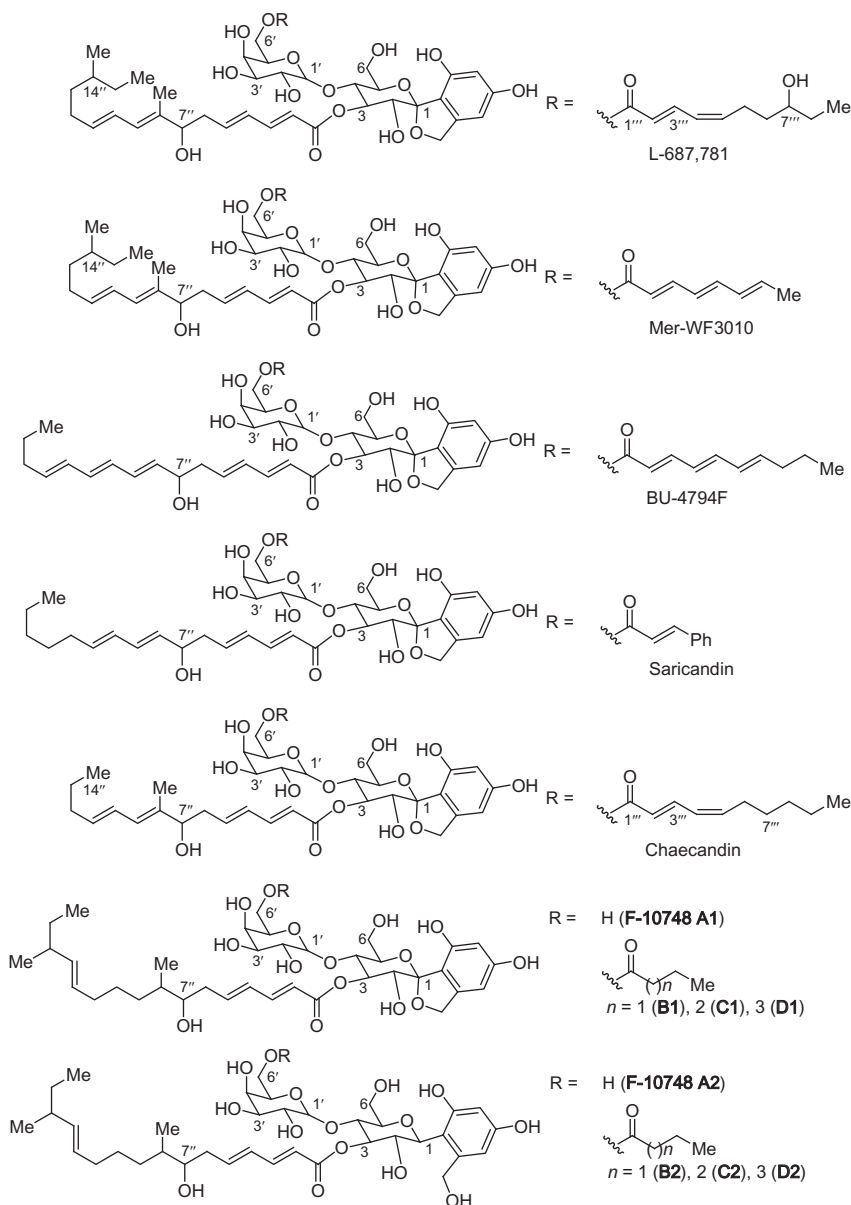


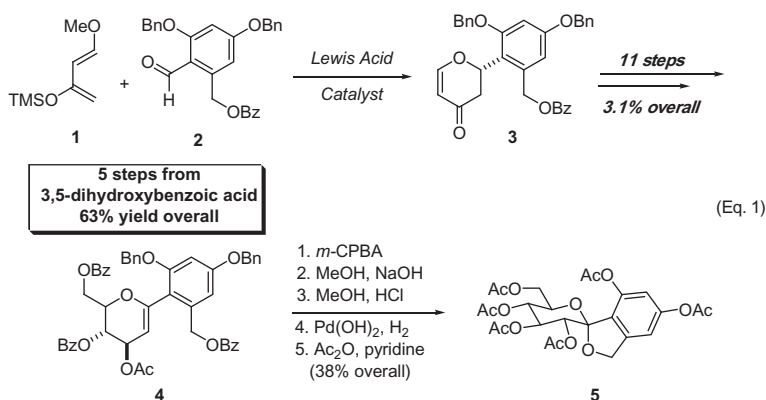
FIGURE 2 Representative papulacandin congeners.

Several new compounds structurally related to the papulacandins have also been isolated (Figure 2) [5]. These papulacandin congeners vary with respect to the degree of oxidation and unsaturation of the shorter acyl side-chain; however, some analogs display more drastic modifications to the overall

papulacandin structure [5a–d,f–h]. Papulacandins devoid of their fatty acid side chain(s) are found to be ineffective as inhibitors of (1,3)-beta-D-glucan synthase [1b].

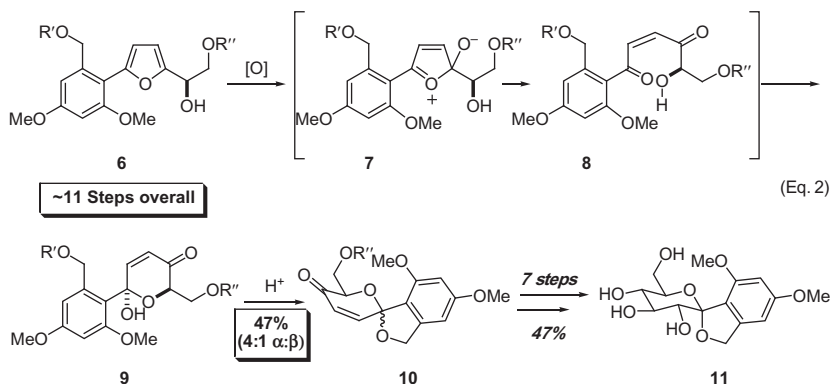
The antibiotic and antifungal properties, together with the structural complexity of these unique spiro C-arylated glycopyranoside derivatives have stimulated the development of creative solutions for the construction of the tricyclic spiro ketal ring system. The core glycopyranoside of papulacandin D has been extensively studied as a formidable target for the design of new and more potent antifungal agents. Representative examples for the synthesis of the spiro C-arylated glycopyranoside include: a racemic spiroketal unit via a hetero-Diels–Alder [6a] reaction of **1** and **2** followed by a series of oxidation reactions to install the necessary oxygen functionality of glucose (Scheme 1,

Hetero Diels-Alder Approach



(Eq. 1)

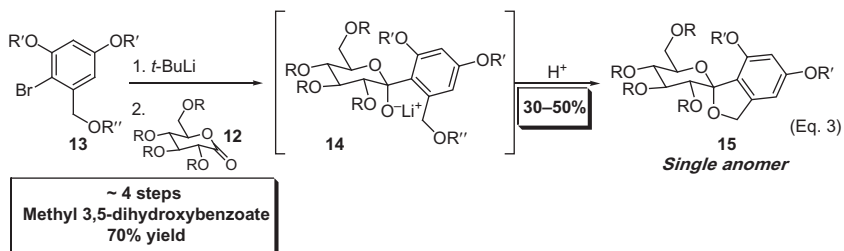
Achmatowicz Rearrangement



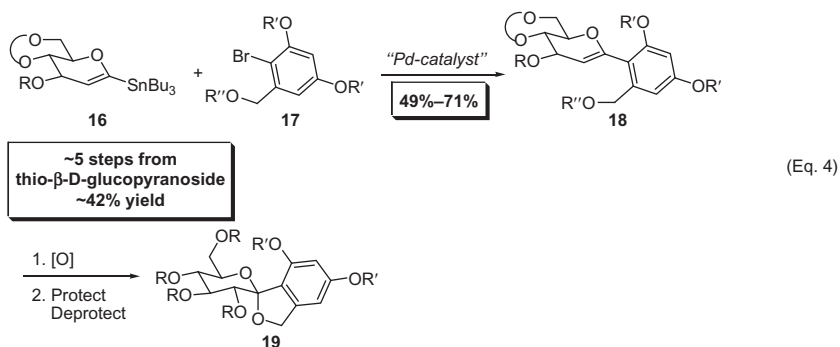
SCHEME 1

continued

Organolithium Addition to Glucolactone



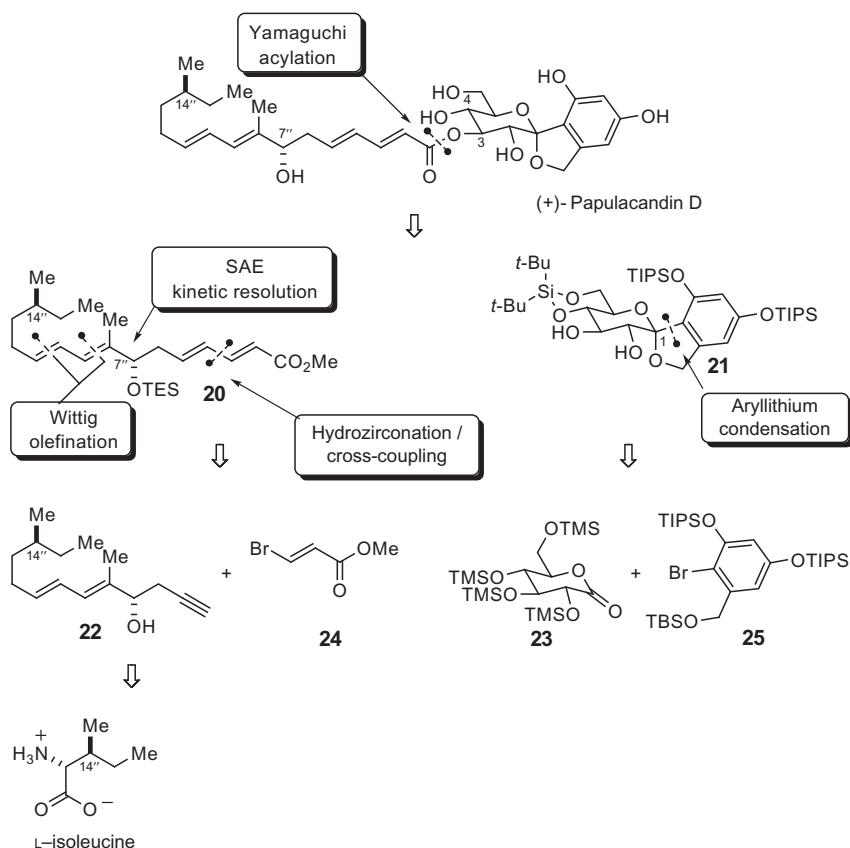
Palladium-Catalyzed Cross-Coupling



SCHEME 1 Representative methods for the preparation of C-aryl glycosides.

Eq. 1). An alternative strategy was invented by subjecting the dihydroxylated product (**6**) of 5-aryl-2-vinylfurans to Achmatowicz rearrangement/Luche reduction (Eq. 2) [6b–d]. The majority of work has focused on the addition of functionalized organolithium reagents generated from **13** with cyclic or acyclic derivatives of D-glucolactone (Eq. 3) [6e–j]. These methods provide rapid access to the spiro ketal core, but suffer from moderate to low yields. In addition, nucleophilic 1,2-addition of a lithiated hexenopyranose to a functionalized quinone has been utilized to access the aryl-β-D-C-glycopyranoside [6k]. Furthermore, a (tributyl)stannylhexenopyranose has been employed in a palladium(0)-catalyzed cross-coupling reaction with sterically hindered aryl bromides **17** (Eq. 4). Unfortunately, excess amounts of the tin reagent **16** are required because of dimerization of the organotin donor [6l–q].

Although these methods provide access to the arylglycopyranoside core of the papulacandins, there has been only one total synthesis of a member of the papulacandin family, that of papulacandin D by Barrett and coworkers in 1996 [6r]. They accomplished the first total synthesis and assigned the



SCHEME 2 Key disconnections in Barrett's total synthesis of (+)-papulacandin D.

absolute configuration of the C(7'') and C(14'') stereogenic centers of papulacandin D (Scheme 2). Barrett's approach involved addition of a functionalized aryllithium reagent, generated from bromide **25**, to a trimethylsilyl D-glucosyl lactone **23**, with subsequent acid-catalyzed spiroketalization and protecting group manipulation to assemble spiroketal **21**.

The C(14'') stereogenic center in side chain **20** was derived from L-isoleucine, and kinetic resolution via Sharpless asymmetric epoxidation (SAE) was employed to separate the C(7'') epimers. The side chain was assembled through a series of Wittig olefination reactions followed by a tandem hydrozirconation/cross-coupling sequence of **22** with methyl (*E*)-bromoacrylate (**24**). Finally, the two fragments were coupled via acylation using a mixed anhydride of the side chain; then global deprotection to give synthetic (+)-papulacandin D (Scheme 2).

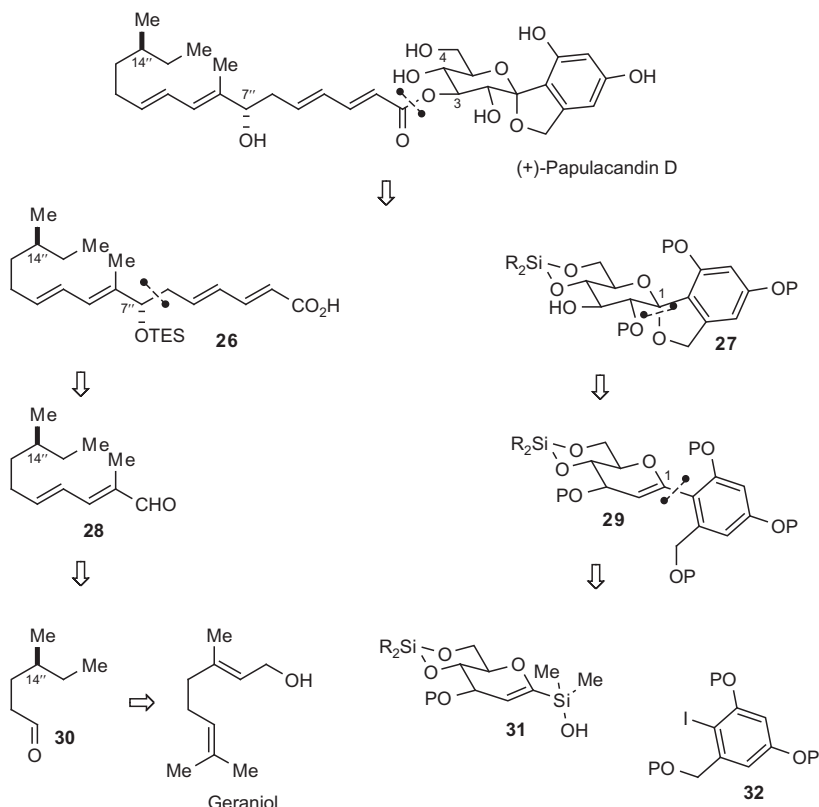
Although Barrett and coworkers were able to synthesize papulacandin D, their synthesis suffered from the following drawbacks: (1) the protecting group strategy did not allow for differential protection of the C(2) and C(3) hydroxyl groups; therefore, a mixture of acylated products was isolated, (2) the spirocyclic core was assembled rapidly via the aryllithium condensation to glycolactone, but the process was plagued by a poor yield and a cumbersome purification, and (3) more than half of an advanced intermediate was sacrificed to set the stereogenic center because an achiral method was used to create the C(7'') hydroxyl group.

Our interest in designing a total synthesis of papulacandin D was two-fold: (1) to develop general and reliable methods for the synthesis of *C*-aryl glycosides that were lacking at the time of this investigation and (2) to develop an enantioselective sequence to set the C(7'') stereogenic center with high diastereoselectivity. As part of our program on the development of new silicon-based, cross-coupling reactions, we have recently demonstrated the synthetic utility of fluoride-free activation for a variety of silanol containing reagents (Hiyama-Denmark coupling) [8]. The plan was to amalgamate this new technology with the previous success in the cross-coupling reaction of 2-pyranylsilanols with aryl iodides [9]. We felt that the total synthesis of papulacandin D was well suited to highlight the synthetic potential of silanols in complex molecule synthesis.

2. RETROSYNTHETIC ANALYSIS

The synthetic plan for papulacandin D makes the obvious disconnection at the O—C(3) ester linkage to acid **26** and glycopyranoside **27** (Scheme 3). The major challenges in the synthesis resided in these independent units, namely: (1) the construction of the aryl glycoside bond and (2) control of the C(7'') and C(14'') stereogenic centers. Moreover, potential solutions to both of these problems could be addressed by ongoing methodological studies in our laboratories. First, the *C*-spirocyclic aryl glycopyranoside **27** could be reduced to aryl-hexenopyranose **29**, where the C(2) hydroxyl group and C(1) spiroketal could be installed through an oxidative spiroketalization event. Disconnection of **29** at C(1) reduced the problem to a palladium-catalyzed cross-coupling reaction of glucal silanol **31** and aryl iodide **32**. Although this approach makes rational disconnections, it provides for challenging reaction sequences. Namely, in the cross-coupling reaction, the aromatic iodide is both electron-rich and 2,6-disubstituted. Both of these features lead to problematic cross-coupling reactions. In addition, the cross-coupling reaction conditions need to be tolerant of the array of protecting groups on **31** and **32**.

Second, disconnection of side chain **26** at the C(6'')—C(7'') bond essentially divides the molecule in half. A routine carbonyl addition reaction (aldol or



SCHEME 3 Retrosynthesis of (+)-papulacandin D.

allylation) to the unsaturated aldehyde **28** would set the configuration of the C(7'') hydroxyl group, concurrently providing a locus for further elaboration to **26**. The diene aldehyde **28** could arise from a vinylogous Horner–Wadsworth–Emmons olefination reaction of substituted hexenal **30**. Finally, the C(14'') stereogenic center could be set through an asymmetric hydrogenation of geraniol. Therefore, the crucial components to this strategy would be the fluoride-free, silicon-based, cross-coupling reaction of a glucal silanol **31** with a sterically hindered, electron-rich aromatic iodide **32**, as well as the diastereoselective installation of the C(7'') hydroxyl group in key intermediate **26**.

3. PREPARATION OF THE SPIROCYCLIC ARYL GLYCOSIDE

3.1 Development of Cross-Coupling Conditions

Previous studies from our laboratories have described the synthesis of *C*-aryl-2-*H*-pyrans from 2-pyranylsilanol **33**, under fluoride activation [9]. These conditions were successfully applied to the cross-coupling reaction of **33** with

electron-rich and sterically hindered aromatic iodides such as **34** prepared as shown below (Chart 1) [10] that are similar to those that would be required for the total synthesis of papulacandin D (Scheme 4, Eq. 5). However, extension of these conditions to the cross-coupling reaction of glucal silanol **36** and **34** led to protidesilylation of the silanol and concomitant deprotection of the C(3)-triisopropylsilyl (TIPS) ether (Eq. 6).

Given these disappointing results, we believed that either the use of hydrated TBAF·3H₂O or free protons in both silanol **36** and aromatic iodide **34** could have provided the proton source necessary for protidesilylation. Therefore, attempts were made to exclude all free protons in the following model study.

Hiyama has demonstrated that trimethylsilylalkenes can be activated for cross-coupling under anhydrous conditions using tris(diethylamino)sulfonium difluorotrimethylsilicate (TASF) [11]. Hence, we decided to synthesize trimethylsilylglucal **38**. The cross-coupling of **38** was attempted with protected iodide **39** in the presence of [allylPdCl]₂ with a combination of Ph₃As and Ag₂O (Scheme 5). Although the reaction proceeded at 70°C over 7h, the desired product was isolated in only 32% yield, accompanied by a significant

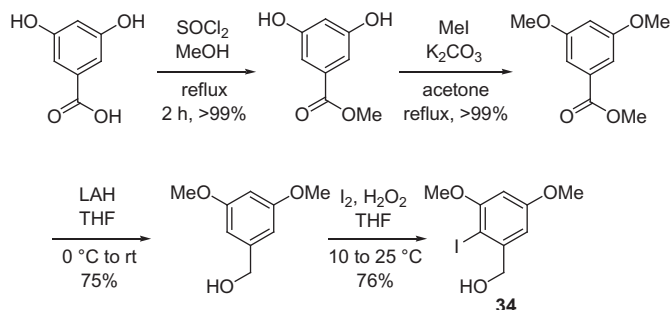
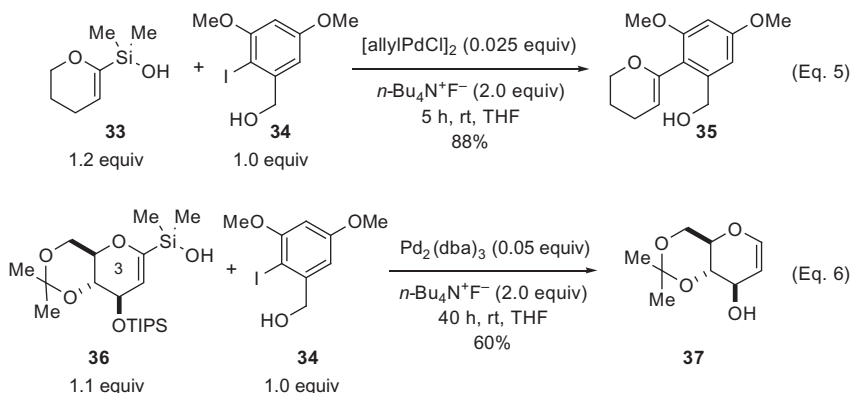
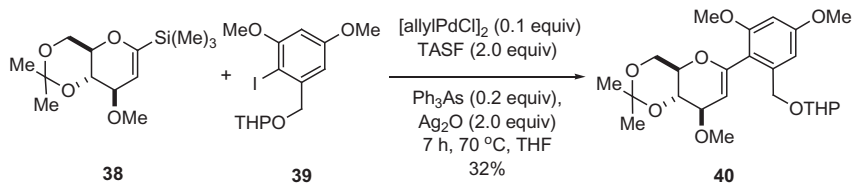


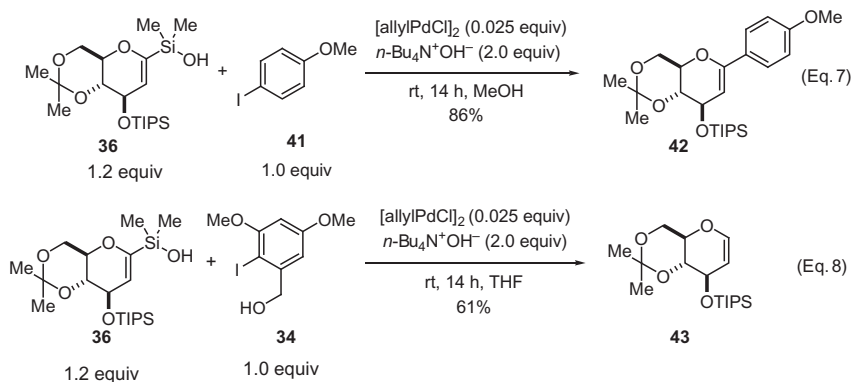
CHART 1 Preparation of resorcinol coupling partner.



SCHEME 4 Early attempts at the cross-coupling of **34** under fluoride activation.



SCHEME 5 Fluoride promoted cross-coupling of trimethylsilylglucal **38** with **39**.



SCHEME 6 Early attempts at fluoride-free cross-coupling.

amount of homodimerization of silane **38** (~17%). Interestingly, it was found that Ag_2O was necessary for cross-coupling to proceed [12]. This result suggests that Ag_2O may play a dual role in the cross-coupling reaction: (1) to aid in the displacement of the halogen from the ligated aryl–Pd–I complex, generating a cationic palladium species [13], and (2) to aid in activation of the silane for transmetalation to palladium. In addition to Ag_2O , the use of a strong fluoride source, TASF, is important for further activation of TMS group.

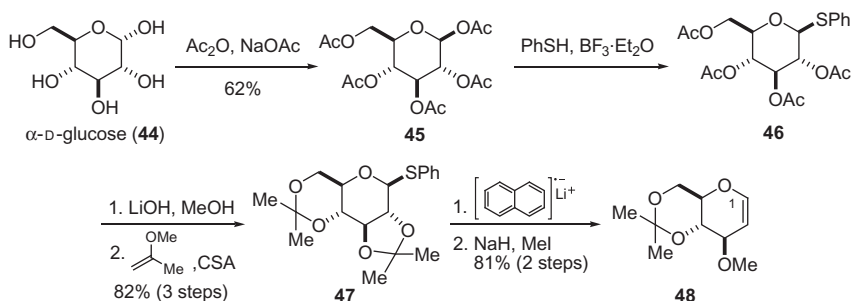
The unsatisfactory results for fluoride activation, the notion that a silylglucal could be activated in the absence of fluoride ion, and the results depicted in Scheme 5 prompted us to examine various nonfluoride additives (Hiyama–Denmark coupling) [8]. The major questions that needed to be addressed were: (1) how is a silicon donor, such as a silanol, activated for productive cross-coupling reaction and (2) would these conditions be compatible with the protecting groups on the silanol and aromatic iodide. Therefore, one of the first requirements in the total synthesis was the development of fluoride-free cross-coupling conditions that could be adapted for the desired coupling.

Preliminary results for the cross-coupling reaction of **36** with 4-iodoanisole (**41**) under activation by tetrabutylammonium hydroxide ($n\text{-Bu}_4\text{N}^+\text{OH}^-$) were encouraging (Scheme 6, Eq. 7). Once again, for more complex substrates, such as **34**, protodesilylation was a major issue (Eq. 8). Given these results, a complete survey of reaction variables (solvent, temperature, activator, etc.) was needed to develop a general and robust cross-coupling reaction.

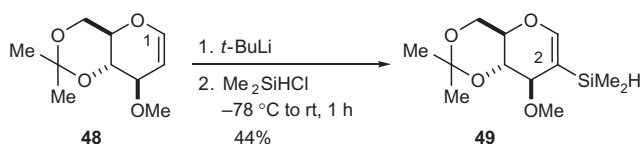
To evaluate different reaction parameters, a simple model study was conducted using acetonide protected glucal silanol **53** (Scheme 9). The preparation of silanol **53** began with peracetylation of α -D-glucose (**44**) with Ac_2O and NaOAc to provide pentaacetylglucose **45** selectively as its β -isomer in 62% yield after recrystallization (Scheme 7). The β -isomer was treated with thiophenol in the presence of $\text{BF}_3 \cdot \text{OEt}_2$ to afford β -phenylthioglycoside **46** [14]. The acetyl groups were saponified using LiOH in MeOH to provide the corresponding tetrol, which was immediately protected as the bis-acetonide **47** in 82% yield over the three steps [15]. The bis-acetonide was subjected to reductive cleavage using lithium naphthalenide in THF, providing the desired glucal quantitatively. The C(3) hydroxy group of glucal acetonide was protected as its methyl ether using NaH and MeI to give an 81% yield, over the two steps, of protected glucal **48** (Scheme 7).

A silyl moiety needed to be selectively introduced at the C(1) position of glucal **48** to prepare the desired dimethylsilanol **53** [16]. Attempts to directly silylate the C(1) position of glucal **48** proved to be difficult as lithiation/silylation occurred preferentially at the C(2) position (Scheme 8).

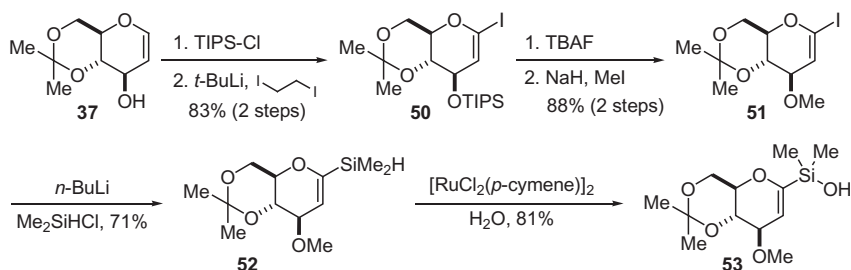
To circumvent this problem, an alternative route for the preparation of the C(1) silane was considered (Scheme 9). First, glucal **37** was protected as its TIPS ether. This was followed by selective metalation at the C(1) position and trapping with diiodoethane to provide iodo-glucal **50** in 83% yield in two steps. The TIPS ether was cleaved using TBAF and the C(3)-hydroxyl group was protected as the methyl ether using NaH and MeI (88% in two steps). Finally, lithium–iodine exchange and trapping with chlorodimethylsilane provided the desired C(1) silane **52** in 71% yield. The silane **52** was subjected to oxidative



SCHEME 7 Preparation of protected glucal **48**.



SCHEME 8 Attempted selective silylation at the C(1)-position of **48**.



SCHEME 9 Preparation of glucal silanol **53**.

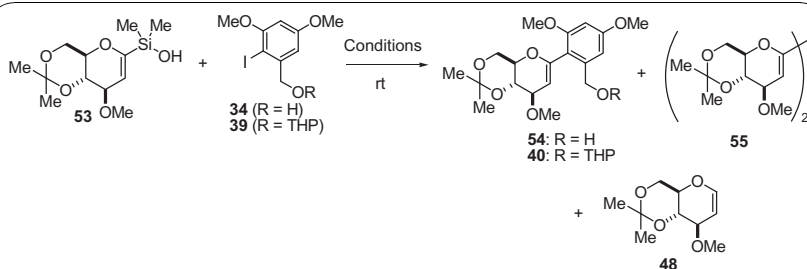
hydrolysis catalyzed by bis[chloro(*p*-cymene)ruthenium(II)] in the presence of 2.0 equiv of water to give the desired silanol **53** in 81% yield [17].

Finally, with both cross-coupling partners in hand, the palladium-catalyzed reaction of **34** with **53** could be tested using a variety of Brønsted base activators (Table 1). Unfortunately, the cross-coupling reaction of **34** and **53** under standard Brønsted base activation conditions [8,9] failed to give the desired product (Table 1, entries 1–3). In these cases, protodesilylation was the major pathway. Tetrahydropyran (THP) protected aromatic iodide **39** was studied next and, with 2.0 equiv of NaOt-Bu in toluene at ambient temperature for 12h, this iodide afforded a 69% yield of the desired cross-coupled product **40** along with trace amounts of **48** (entry 4).

In the initial studies on the cross-coupling of **53** with **34**, both TBAOH and KOSiMe₃ (Table 1, entries 1 and 2) were unsuitable activators as they afforded the protodesilylated glucal **48** exclusively. This outcome is not surprising, because these types of activators have been problematic in the cross-coupling reaction of substituted enol silanols and heteroarylsilanols [8c,9]. It is believed that the coexistence of such silanols and silanolate causes protodesilylation. Therefore, a strong, soluble Brønsted base, such as NaOt-Bu, was needed to bring about rapid formation of the sodium silanolate *in situ* and thus suppress protodesilylation. This idea in combination with protection of **39** as the corresponding THP acetal finally provided for successful cross-coupling.

3.2 Optimization of Protecting Groups for the Glucal Silanol

With successful cross-coupling reaction conditions in hand, the focus shifted to designing the global protection/deprotection strategy for the *C*-spirocyclic aryl glycopyranoside hydroxyl groups. The protecting group strategy needed to meet the following criteria (Figure 3): (1) the conditions for the final global deprotection must be extremely mild due to the acid-, base-, photo-sensitivity, incompatibility with hydrogenolysis and oxidation of the pendant unsaturated side chain of **i**, (2) the protecting group for the C(3) hydroxyl group of **v** has to be complementary to P², P³, P⁴, P⁵, and P⁶ for selective deprotection prior

**TABLE 1** Cross-Coupling of **53** With **34** or **39**

Entry	R	Conditions ^a	Yield (%) ^b			
			40 or 54	55	48	Aryl-I
1	H	[allylPdCl] ₂ , <i>n</i> -Bu ₄ N ⁺ OH ⁻ , MeOH, 5h	–	–	38	62
2	H	[allylPdCl] ₂ , KOSiMe ₃ , THF, 5h	–	–	12	44
3	H	Pd ₂ (dba) ₃ ·CHCl ₃ , NaOt-Bu, toluene, 4h	–	40	–	17
4	THP	Pd ₂ (dba) ₃ ·CHCl ₃ , NaOt-Bu, toluene, 12h	69	20	~2	27

^aPd catalyst (0.05equiv) and activator (2equiv) were used in all cases.^bYield of isolated product.

to acylation at the C(3) position of the aryl glycopyranoside, (3) the C(3) protecting group needs to be sterically hindered to direct the metalation to the C(1) position to form glucal silanol **viii**, (as was the case direct the metalation to the C(2) position in **48**) but not so sterically demanding as to prevent introduction of P² and, (4) the protecting group for the benzylic alcohol of the aromatic iodide **vii** has to be cleaved in the presence of P⁴, P⁵, P⁶, P⁷ prior to oxidative spiroketalization. Therefore, we decided that fluoride deprotection conditions should be mild and selective enough for a late stage global silyl deprotection. This decision mandated that the protecting groups for the C-spirocyclic aryl glycopyranoside must be fluoride cleavable and be carried through the synthesis.

First, the protecting group optimization strategy focused on the protection of the C(3)-hydroxyl group. The C(3)—O—methyl group was replaced with a bulky silyl protecting group such as triethylsilyl (TES, **56**) or triisopropylsilyl (TIPS, **36**). When the cross-coupling reaction was performed at room temperature, the effect of the protecting group was obvious (Table 2, entries 1–3). However, at elevated temperature, 50°C for 4h, the effect became negligible



FIGURE 3 Protecting group strategy.

(entries 4–6). Therefore, we chose to protect the C(3) hydroxyl group be as its TES ether, which should provide for a more selective deprotection prior to acylation.

The C(4) and C(6) hydroxyl groups would be converted to the di-*t*-butylsilylene acetal [18], because the acidic deprotection conditions needed for the acetonide group would not be compatible with the side chain in a late stage global deprotection. The preparation of silanol **63** began by saponification of triacetate **59** [19], resulting in the free hexenopyranose, which was immediately protected as its di(*t*-butyl)silylene acetal in good yield (89% in two steps, Scheme 10).¹ Protection of the C(3)-hydroxyl group with

1. It was found through deuterium incorporation experiments 1.0–1.5 equiv *t*-BuLi was sufficient to lithiate C(1).

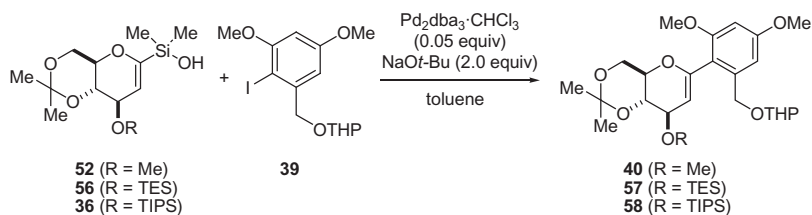
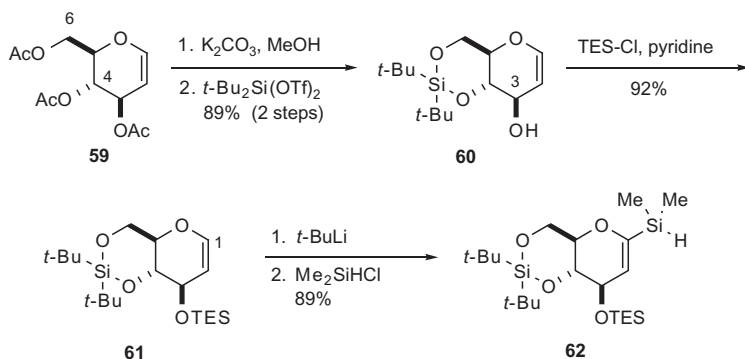


TABLE 2 Influence of the Protecting Group on the C(3)-Hydroxyl Group on Cross-Coupling Reaction

Entry	R	Temp, Time (h)	Yield (%)
1	Me	rt, 12	69
2	TES	rt, 12	<50 ^a
3	TIPS	rt, 12	20
4	Me	50°C, 4	71
5	TES	50°C, 4	67
6	TIPS	50°C, 4	<70 ^a

^aThe product obtained was contaminated with the a side product.



SCHEME 10 Preparation of fully silylated glucal silane **62**.

TES-Cl provided fully protected hexenopyranose **61** in 92% yield. Silylglucal **61** was metalated exclusively at the C(1) position with *t*-BuLi and trapped with chlorodimethylsilane to provide **62** in 89% yield.

Silane **62** was then subjected to oxidative hydrolysis catalyzed by bis [chloro(*p*-cymene)-ruthenium(II)] [20] in the presence of 2.0 equiv of water

to give silanol **63** in 73% yield on small scale (Table 3, entry 1). However, silane **62** was insoluble in CH₃CN and therefore not amenable to larger scale hydrolyses (entries 2 and 3). Hence, finding scalable oxidative hydrolysis conditions of **62** was important for the efficient synthesis of the spirocyclic C-aryl glycopyranoside. To this end, a number of conditions and catalysts were surveyed. Hydrolysis of **62** using 0.03 equiv of [IrCl(C₈H₁₂)]₂ [21], gave **63** in

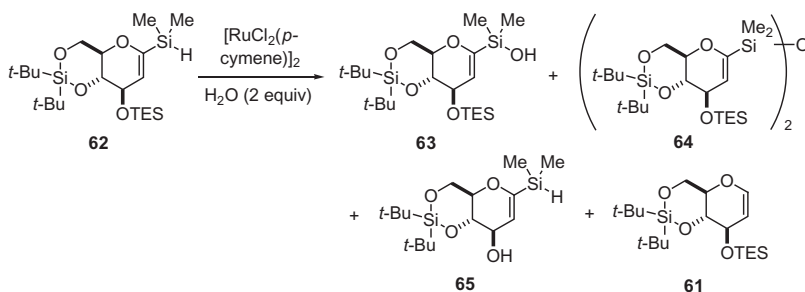


TABLE 3 Survey of Oxidative Hydrolysis Conditions for Hydrosilane **62**

Entry ^a	"Ru" equiv	Solvent	Time (h)	Yield (%) ^b				
				62	63	64	65	61
1 ^c	0.04	CH ₃ CN	4	–	73	–	–	–
2 ^d	0.04	CH ₃ CN	1	–	70	–	–	–
3 ^e	0.08	CH ₃ CN	2	–	47	–	–	–
4 ^{f,g}	0.03	CH ₃ CN	3	19	52	3	23	–
5	0.08	<i>n</i> -BuCN	2	–	87	2	–	–
6	0.03	<i>n</i> -BuCN	4	–	84	4	–	–
7	0.03	THF	4	–	54	5	–	27
8	0.04	PhCN	4	–	90	4	–	–
9	0.03	C ₆ H ₆ /CH ₃ CN (1:1)	1	–	86	7	–	–
10 ^h	0.03	C ₆ H ₆ /CH ₃ CN (1:1)	1	–	84	8	–	–

^aAll the reactions were carried out on 100mg scale, unless otherwise stated.

^bIsolated yields.

^c110 mg scale.

^d564 mg scale.

^e950 mg scale.

^f[Ir(cod)Cl]₂, H₂O (2.0 equiv) were used.

^gTES ether cleavage was observed.

^hThe reaction was run on 1.6 mmol scale and the yield of **63** is of analytically pure material.

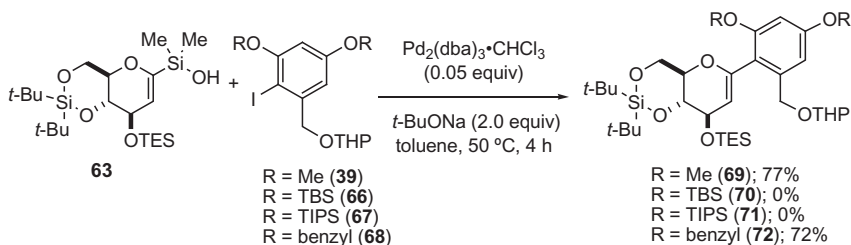
moderate yield, but cleavage of the TES ether was a major side process (entry 4). In a less polar solvent, *n*-BuCN, the reaction proceeded cleanly to the desired silanol in 87% and 84% yield (entries 5 and 6). However, in THF, a significant amount of protodesilylated product was observed (entry 7).

Switching the solvent to benzonitrile gave an excellent yield of **63**. Unfortunately, the higher boiling point of PhCN made purification tedious. Finally, after extensive optimization of mixed solvent systems it was found that a 1:1 mixture of CH₃CN/benzene afforded **63** in 86% yield (entry 9). To our delight, these conditions were amenable to larger scale preparations (>2 g) of **63** in excellent 84% yield (entry 10).

3.3 Optimization of Protecting Groups for the Aromatic Iodide

In the next stage of the synthesis, suitable protecting groups for the resorcinol moiety of the aromatic iodide were investigated. The cross-coupling reaction of glucal silanol **63** with iodide **39** proceeded very smoothly to afford the aryl glucal **69** in 77% yield (Scheme 11). When the protecting groups were changed from methyl ethers to *t*-butyldimethylsilyl (TBDMS) or TIPS ethers, the cross-coupling reaction did not provide any of the desired product. Employing benzyl protecting groups gave the desired product **72** in a reasonable 72% yield; however, the benzyl ethers would need to be replaced at some point prior to global silyl deprotection.

Finally, different protecting groups for the benzylic alcohol portion of the aromatic iodide were evaluated (Table 4). Interestingly, protection of the benzylic alcohol had a significant impact on the yield of the cross-coupling reaction. The aromatic iodide bearing a 1-ethoxyethyl (EE), 1-methoxy-1-methylethoxy (MME) or trimethylsilyl (TMS) ether afforded the desired product, albeit in low yield (entries 2–5). Protection as a pivaloyl ester provided the aryl glucal **80** in good yield (entry 6). The pivaloyl ester could be cleaved quantitatively using DIBAL-H (Scheme 12, Eq. 9), whereas the acidic conditions for deprotection of the THP ether led to nonoxidative spiroketalization and TES cleavage (Eq. 10). Therefore, we decided that the pivaloyl protecting group would be used for the synthesis.



SCHEME 11 Influence of the protecting groups on the resorcinol moiety on the cross-coupling reaction.

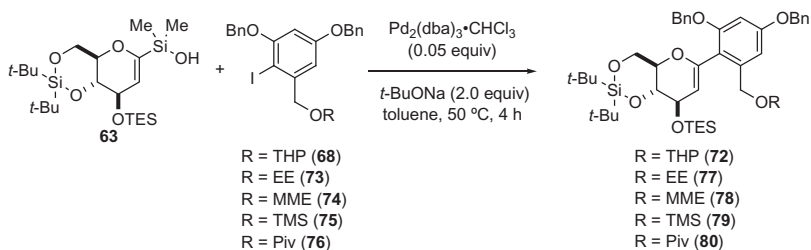
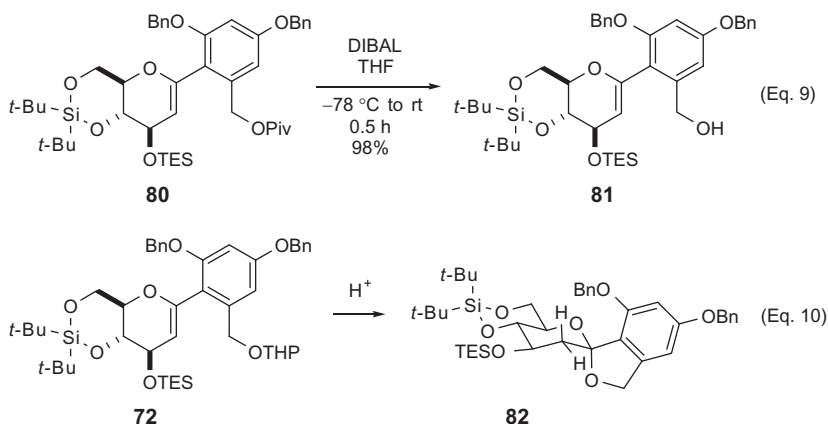


TABLE 4 Survey of Protecting Groups for the Benzylic Alcohol of the Aromatic Iodide

Entry	R	Product (yield, %)
1	THP	72 (72)
2	EE	77 (28)
3	MME	78 (26)
4	TMS	79 (28)
5 ^a	TMS	79 (52)
6	Piv	80 (75)

^aThe reaction was heated at 110 °C for 1 h.



SCHEME 12 Comparison of deprotection conditions for the benzylic alcohol.

Protection of the benzylic alcohol had two benefits: (1) it removed a proton source for potential protidesilylation and (2) it suppressed coordination of the free benzylic alcohol to the Pd(II) intermediate after oxidative addition. We believe that the rate of displacement of this alkoxide palladium

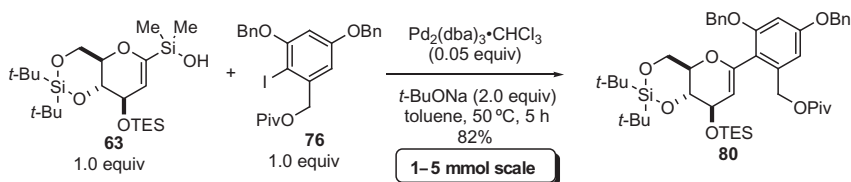
intermediate by silanolate may be slow, and thus significantly decrease the rate of cross-coupling relative to undesirable side processes. The dramatic impact that the benzylic alcohol protecting group had on the rate and yield of the cross-coupling reaction could be rationalized in terms of the coordinating ability of the protecting group (**68**, **73**, **74**, and **76**) to a Pd(II) intermediate. The pivaloyl protecting group was ultimately chosen for the following reasons: (1) the reduced ability of the carbonyl group to coordinate to the Pd(II) intermediate, compared to the free alkoxide, MME, and EE protecting groups and (2) the near quantitative deprotection with DIBAL-H that also did not induce nonoxidative spirocyclization of the corresponding aryl glucal (Scheme 12, Eq. 10).

3.4 Implementation of the Key Cross-Coupling Sequence

The next objective in the synthesis was to generate large quantities of the 1-aryl-hexenopyranose **80**. In order to achieve this goal, the cross-coupling reaction needed to be scaleable (i.e., >1.0 mmol scale). Gratifyingly, the key cross-coupling reaction of an equimolar ratio of the silanol **63** and the electron-rich aryl iodide **76** proceeded smoothly to afford **80** in a reproducible 82% yield (Scheme 13).² The crucial cross-coupling reaction was executed with 0.05 equiv of $\text{Pd}_2(\text{dba})_3 \cdot \text{CHCl}_3$ as the catalyst and 2.0 equiv of NaOt-Bu as activator at 50°C for 5 h. In addition, the pivaloyl ester was selectively cleaved in near quantitative yield using DIBAL-H reduction to give desired benzylic alcohol **81** in 98% yield, giving more credence to the choice of pivaloyl ester as the ideal protecting group for the synthesis (Scheme 12, Eq. 9).

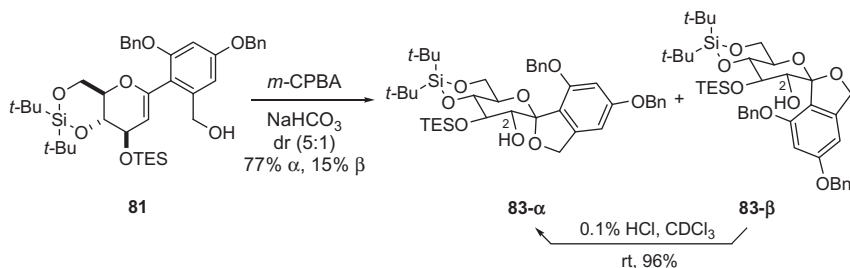
3.5 Oxidative Spiroketalization and C(2)-Hydroxyl Group Protection

To assemble the carbon framework of the C-spirocyclic aryl glycopyranoside of papulacandin D, the next challenge was to effect both a stereocontrolled installation of the C(2) hydroxyl moiety and oxidative spiroketalization. The conditions for oxidative spiroketalization need to be basic to prevent the undesired Brønsted acid-catalyzed spiroketalization (Scheme 12, Eq. 10) [6p].



SCHEME 13 Key Brønsted base promoted silanol cross-coupling reaction of **63** and **76**.

2. The 82% yield was consistently reproducible on both 1.0 and 5.0 mmol scales.



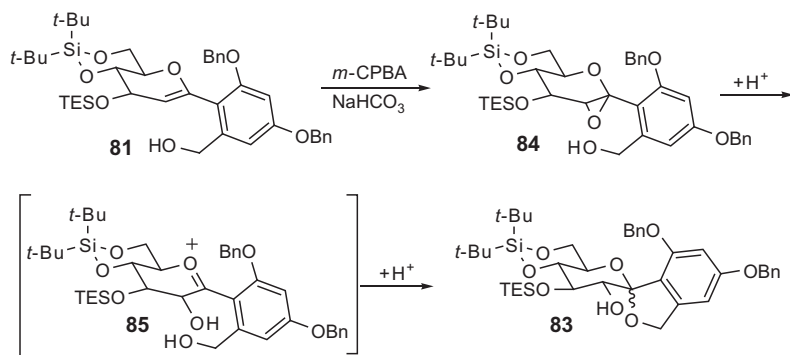
SCHEME 14 Oxidative spiroketalization of **81**.

Selective formation of α -glycosyl anhydrides from 1,2-dehydrosugars using dimethyldioxirane (DMDO) is well known [22]. For the current study, *m*-chloroperbenzoic acid (*m*-CPBA) was used as the oxidant under nonequilibrating conditions [6q]. Treatment of **81** with *m*-CPBA in CH_2Cl_2 at 0°C in the presence of NaHCO_3 , smoothly provided the chromatographically separable spiro ketals **83- α** and **83- β** in a 5:1 ratio (Scheme 14).

The configuration of the C(2) hydroxyl group was confirmed by inspection of the ^1H NMR spectra of each anomer as well as more extensive NMR analyses. The spectrum of **83- α** in dry, neutralized CDCl_3 displayed diagnostic signals at δ 4.32 ppm and δ 3.84 ppm corresponding to the HC(2) and HC(3) proton resonances, respectively. The structure of α -anomer was confirmed by the vicinal coupling constants of the glucose ring in the spiroketal **83- α** , which were also particularly diagnostic. The key constants ($J_{2,3}=10.0$ Hz, $J_{3,4}=10.0$ Hz, $J_{4,5}=10.2$ Hz) were consistent with a chair conformation, where the large coupling constants suggest that mutual trans-diaxial relationships exists between HC(2)/HC(3) and HC(3)/HC(4). The distorted chair conformation of the β -anomer was also confirmed by vicinal coupling constants ($J_{2,3}=8.2$ Hz, $J_{3,4}=8.2$ Hz, $J_{4,5}=9.4$ Hz), which are consistent with the observations of Dubois and Beau for a similar system [6q].

Finally, the β -anomer could be isomerized to the α -anomer with a 96% recovery using a solution of chloroform containing 0.1% dry HCl (Scheme 14). This experiment also aided in the assignment of the absolute configuration of the **83- β** C(2) hydroxyl group.

The oxidative spiro ketalization of 1-aryl glucal **81**, most likely proceeds via: (1) α -selective epoxidation of the enolic double bond, generating a glycosyl anhydride **84** or Brigl's intermediate [23], (2) opening of the internal epoxide to generate an oxocarbenium ion **85**, and (3) trapping of the oxocarbenium ion with the pendant hydroxyl group of the C(1) aromatic moiety to provide the desired C-spirocyclic aryl glycopyranoside (Scheme 15). Crucial to the success of this transformation is the selective epoxidation of the glucal, by *m*-CPBA from the α -face of the enol ether. This process sets the configuration of the C(2)-hydroxyl group of the spirocyclic aryl glycopyranoside **83- α** . The epoxidation of **81** relies upon substrate-controlled diastereoselectivity in the initial oxidation event. The use of sterically demanding protecting



SCHEME 15 Rationalization for selective oxidative apiroketalization.

groups on the C(3)-, C(4)-, and C(6)-hydroxyl groups shielded the β -face, allowing epoxidation to proceed exclusively from the α -face. The diastereoselectivity of the oxidation was supported by determination of the absolute configuration of the C(2)-hydroxyl group in both α - and β -anomers.

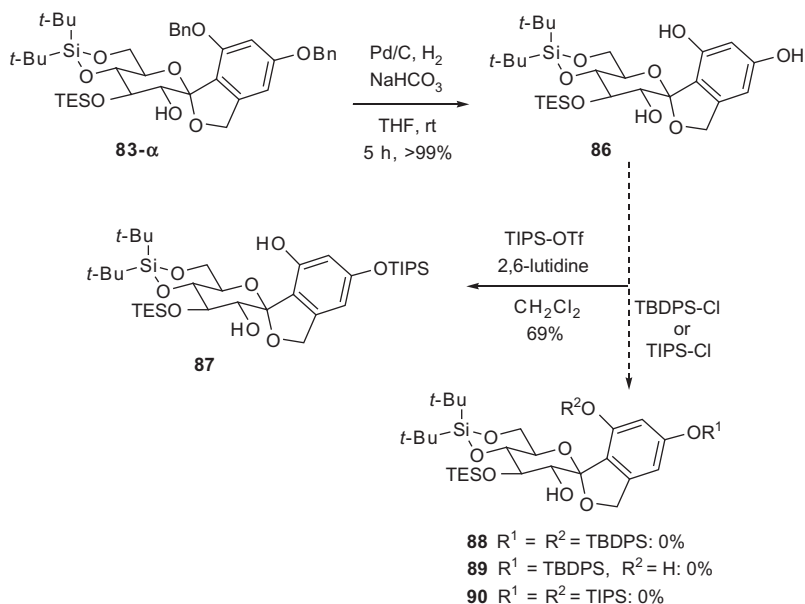
The 5:1 mixture of α - and β -anomers represented the kinetic ratio, as no isomerization was observed when the β -anomer was exposed to *m*-CPBA and NaHCO_3 in CH_2Cl_2 [24]. However, the use of CHCl_3 containing 0.1% of dry HCl provided a source of activation for the anomeric center of the β -anomer, inducing complete isomerization to the desired α -anomer.

3.6 Completion of the Synthesis of the Spirocyclic Aryl Glyco-Pyranoside

To complete the synthesis of the *C*-spirocyclic aryl glycopyranoside, the following protecting group manipulations needed to be completed: (1) the aromatic benzyl ethers had to be switched to silicon-based protecting group for the late stage global deprotection, and (2) the C(2) hydroxyl group needed to be replaced with a protecting group complementary to the C(3) TES ether, thus allowing for selective deprotection and acylation.

Hydrogenolytic debenzylation of **83- α** , using Pd/C in the presence of NaHCO_3 proceeded smoothly to afford triol **86** quantitatively (Scheme 16). Initially, it was envisioned that the phenolic hydroxyl groups could be fitted with bulky silicon protecting groups such as *tert*-butyldiphenylsilyl (TBDPS) or TIPS ethers. Treatment of triol **86** with either TBDPS chloride or TIPS chloride in the presence of 2,6-lutidine did not afford any of the desired silyl ethers. Therefore, silylation with a more reactive silylating agent, TIPSOTf, was attempted. In this case, only the mono-TIPS-protected product **87** was isolated in 69% yield and characterized by ^1H NMR analyses.

At this point, a less sterically demanding protecting group such as 2-(trimethylsilyl)ethoxymethyl (SEM) ether was considered for the protection of the all three hydroxyl groups of triol **86** [25]. Unfortunately, bis-SEM ether **91** was isolated as the major product, presumably due to a slow alkylation



SCHEME 16 Initial attempts at the protection of triol **86**.

of the C(2) hydroxyl group (Table 5, entries 1–4). In an attempt to improve the yield of alkylation at the C(2) hydroxyl group, additives such as tetrabutylammonium iodide (TBAI) [26] and AgOTf [27] were tested (Table 5, entries 2–4). However, only moderate success was obtained in this survey.

Resubjecting **91** to SEM-Cl in a more polar solvent, DMF, in the presence of TBAI, again did not afford any of the tris-SEM ether **92** (Table 5, entry 5). Finally, **92** was synthesized in good yield, using a combination of 3 equiv of TBAI and 9 equiv of AgOTf in DMF (Table 5, entry 6).

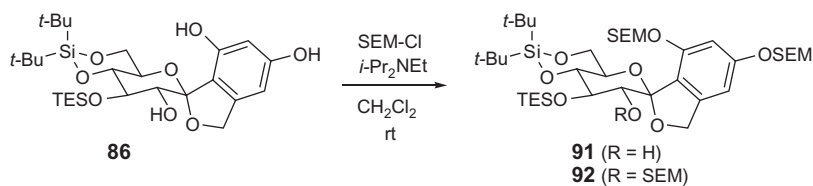
The final step in the synthesis of the spirocyclic aryl glycopyranoside was selective deprotection of the C(3) TES ether. This was accomplished using PPTS in ethanol albeit in moderate yield (52%), presumably due to a partial deprotection of SEM groups (see Section 6 for the solution to this problem) (Scheme 17).

4. SYNTHESIS OF FATTY ACID SIDE CHAIN 26 AND ACYLATION

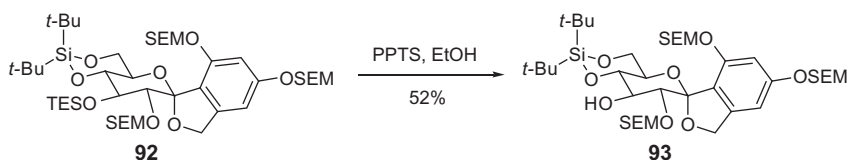
4.1 Preparation of the Dienylaldehyde 28

Synthesis of the unsaturated acid **26** began by asymmetric hydrogenation of geraniol³ with $\text{Ru}(\text{OAc})_2[(S)\text{-BINAP}]$ [28] to provide (*S*)-citronellol

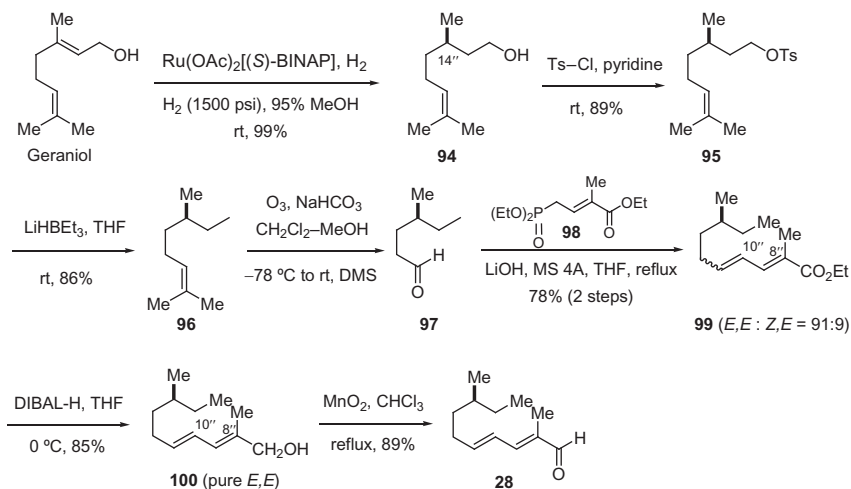
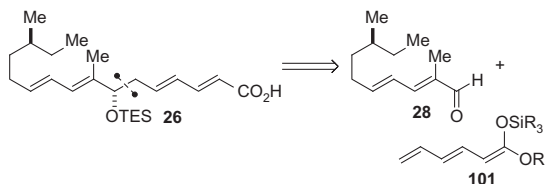
3. Commercially available geraniol was enriched by spinning band distillation (GC analysis 99.8%, geraniol; 0.2% nerol).

**TABLE 5** SEM Protection of Triol **86**

Entry	SEM-Cl (equiv)	<i>i</i> -Pr ₂ NEt (equiv)	Additive (equiv)	Yield (%) ^a		
				Conc. (86 , M)	Time (h)	91 92
1	2.5	5.0	None	0.06	3	52 –
2	9.0	15.0	TBAI (4)	0.06	10	66 8
3	9.0	15.0	TBAI (4)	0.16	10	36 31
4	9.0	15.0	AgOTf (9)	0.016	1	53 19
5 ^b	3.0	5.0	TABI (3)	0.6	10	82 ^c –
6 ^b	12.0	20.0	TABI (3), AgOTf (9)	0.6	1	– 74

^aIsolated yield of **91** and **92**.^bObtained product **91** was resubjected to the reaction in DMF.^cRecovery of the starting material.**SCHEME 17** Selective deprotection of the C(3) TES ether.

(**94**) in excellent yield and enantiomeric purity (99%, 97:3er) ([Scheme 18](#)). Tosylation of the alcohol followed by deoxygenation with LiHBEt₃ afforded hydrocarbon **96** in 88% yield for the two steps. Alkene **96** was then subjected to ozonolysis and vinylogous Horner–Wadsworth–Emmons olefination using phosphonate **98** [29d] to afford unsaturated ester **89** as an inseparable mixture of isomers ($\Delta^{10'',11''}$ *E/Z*, 91:9). Subsequent, DIBAL-H reduction of the ester followed by chromatographic separation of the geometrical isomers of the allylic alcohol and oxidation afforded aldehyde **28** in 89% yield.

SCHEME 18 Preparation of dienylaldehyde **28**.

SCHEME 19 Double vinylogous aldol addition.

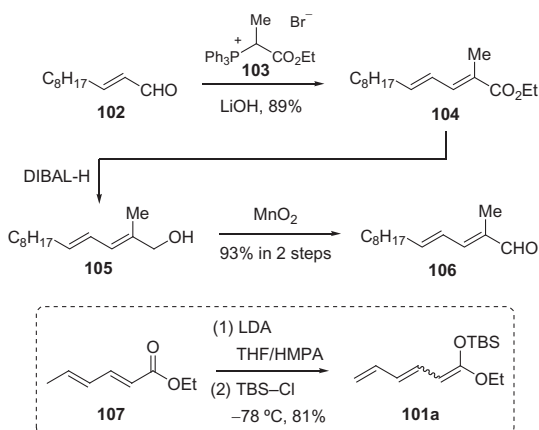
4.2 Model Study of Lewis-Base-Catalyzed Asymmetric Aldol Addition Reactions

4.2.1 Doubly Vinylogous Aldol Addition

To set the C(7'') stereogenic center of acid **26**, one of the most convergent routes would employ an asymmetric aldol addition reaction of a doubly vinylogous enolate **101** to aldehyde **28** (Scheme 19).

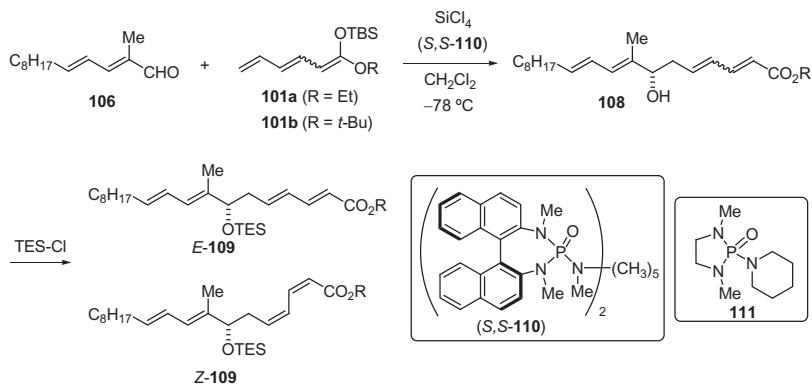
To test this hypothesis, model aldehyde **106** was prepared from commercially available undecenal (**102**) (Scheme 20). Olefination of **102** afforded dienoate **104** in 89% yield as a mixture (*E/Z*, 93:7) of olefin isomers. Dienoate **104** was then reduced with DIBAL-H to alcohol **105**, which was oxidized with MnO₂ to afford aldehyde **106** in 93% yield over the two steps. Instead of using the precious advanced intermediate **28**, the aldehyde **106** was employed for the model study.

Next, the addition of trienyl silyl ketene acetal **101a** (easily prepared from ethyl sorbate, Scheme 20) to model aldehyde **106**, was tested under



SCHEME 20 Preparation of the precursors.

Lewis-base activation [30]. In the presence of silicon tetrachloride (1.0 equiv) and 0.01equiv of bisphosphoramidate catalyst (*S,S*)-**110** [31], the reaction provided only a 27% yield of product **108** after 3 h with exclusive ϵ -selectivity (Table 6, entry 1). To test if an increase in catalyst loading could effect a higher conversion, 0.4 equiv of monomeric, achiral catalyst **111** was used (entry 2). After 3 h, the reaction was quenched and a 44% yield of the desired product was isolated as a mixture of geometrical isomers (*E:Z*, 75:25), which suffered elimination of the $\text{C}(7'')$ hydroxyl group. To circumvent this problem, it was found that immediate silyl protection of **108** provided a stable mixture of geometrical isomers, which were separable by preparative HPLC. Once again the asymmetric doubly vinylogous aldol addition was attempted with 0.1 equiv of bisphosphoramidate (*S,S*)-**110** (entry 3). The tetraenoate was isolated in 53% yield as a 62:38 (*E:Z*) mixture of isomers. The mixture was immediately subjected to the TES protection conditions to afford a mixture of silyl ethers **109** in 93% yield, with little change to the isomeric ratio. The isomeric mixture was separated by HPLC and the enantiomeric purity of both isomers was determined by SFC analysis to be (61:39 er) for the *E*-isomer and (79:21 er) for the *Z*-isomer. To increase the yield of the aldol addition the reaction was run for 25 h; however, little change in the yield and enantiomeric purity of either isomer was observed (entry 4). Previous studies in these laboratories with ester-derived dienolates demonstrated the site and enantioselectivity of the addition is largely influenced by the size of the alkoxy substituents. Therefore, the *t*-butyl hexenoate-derived *t*-butyldimethylsilyl ketene acetal **101b** was synthesized and subjected to the asymmetric aldol reaction [32]. Unfortunately, the enantiomeric ratio was not significantly improved (*E*-isomer, 60:40 er; *Z*-isomer, 78:22, entry 5). Because of the low

**TABLE 6** Lewis-Base-Catalyzed Double Vinylogous Aldol Reaction

Entry ^a	R	Catalyst (equiv)	Time (h)	<i>E/Z</i> (ratio) ^b	er (<i>E</i>)/(<i>Z</i>) ^c	Yield (%) ^d
1	Et (101a)	(<i>S,S</i>)- 110 (0.01)	3	—	—	27
2	Et (101a)	111 (0.4)	3	75:25	—	44
3	Et (101a)	(<i>S,S</i>)- 110 (0.1)	3	62:38	(61:39)/(79:21)	53
4	Et (101a)	(<i>S,S</i>)- 110 (0.01)	25	60:40	(57:43)/(76:24)	55
5	<i>t</i> -Bu (101b)	(<i>S,S</i>)- 110 (0.1)	3	64:34	(60:40)/(78:22)	63

^aConditions: **101** (1.2 equiv), SiCl₄ (1.1 equiv), *i*-Pr₂NEt (0.4 equiv), -78 °C, CH₂Cl₂.

^bThe isomer ratio was determined by coupling constants and nOe analysis. The isomers were separated by preparative HPLC.

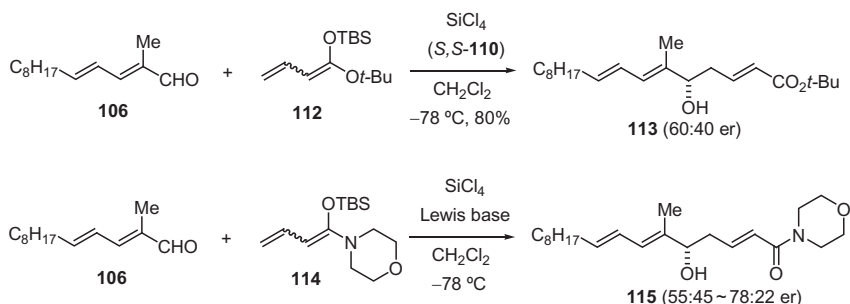
^cer determination from TES ether **109** using CSP-SFC analysis.

^dYield of isolated, isomeric mixture.

enantioselectivity, tedious separation and poor geometric selectivity, of the doubly vinylogous aldol reaction, this approach was abandoned.

4.2.2 Vinylogous Aldol Addition

On the basis of extensive studies on Lewis base-catalyzed, vinylogous aldol reaction of silyl dienol ethers [33], it was anticipated that higher enantioselectivity and exclusive γ -site selectivity could be achieved. However, now a two-carbon homologation would be required to complete the synthesis of the fatty acid **26**. Thus, the *t*-butyl propanoate-derived silyl ketene acetal **112** [31] was



SCHEME 21 Vinylogous aldol reactions.

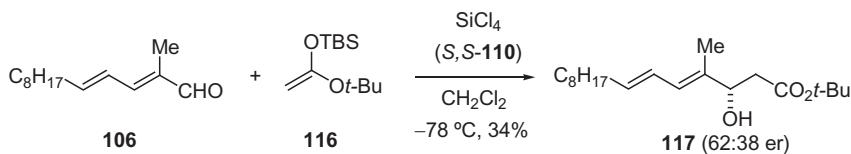
employed in the aldol reaction of **106**, under the action of (*S,S*)-**110** at -78°C for 3 h (Scheme 21). The aldol product **113** was isolated as a single olefin isomer with high γ -selectivity, but unfortunately with poor enantioselectivity (60:40 er). Given these disappointing results, a vinylogous, asymmetric ketene acetal aldol reaction was tested [34]. A series of Lewis bases was surveyed. However, again, enantioselectivity was not satisfactory (Scheme 21).⁴

4.2.3 Simple Aldol Addition: Is the α -Methyl Group of the Aldehyde Problematic?

The disappointing results from vinylogous aldol reactions forced us to consider the simple aldol reaction to see if the substrate was causing the problem [31a]. Silyl ketene acetal **116** was chosen as the nucleophile. Once again, the enantiomeric ratio was found to be 62:38. It was therefore concluded that the α -methyl substituted aldehyde is not suitable substrate for the Lewis-base-catalyzed aldol reaction (Scheme 22). Because we were not able to achieve satisfactory stereoselectivity, alternative asymmetric carbonyl addition reactions were explored.

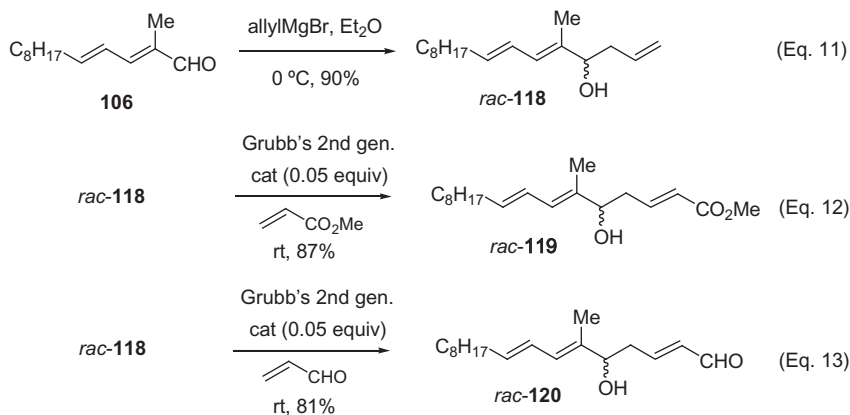
4.3 Model Study of an Asymmetric Allylation Reaction

An alternative strategy for the construction of the C(7'') stereogenic center would employ an asymmetric allylation reaction [30a,35]. The allyl group



SCHEME 22 Simple aldol reaction.

4. See the supporting information for Ref. [6v].



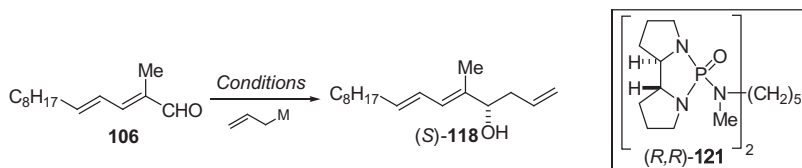
SCHEME 23 Alkylation followed by cross-metathesis.

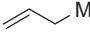
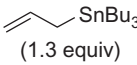
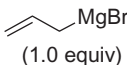
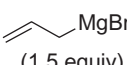
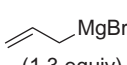
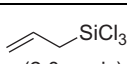
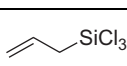
was of interest because it provides a handle for further elaboration of the side chain of papulacandin D through a sequential cross-metathesis and two-carbon homologation. To investigate this plan, the cross-metathesis reaction of model homoallylic alcohol **118** was tested, before starting the investigation into asymmetric allylation reaction.

The cross-metathesis of racemic homoallylic alcohol **118** (prepared by the addition of allylmagnesium bromide into aldehyde **106**) was tested with both methyl acrylate and acrolein using 0.05 equiv of Grubbs' second-generation catalyst (Scheme 23) [36]. The reactions afforded the desired α,β -unsaturated ester **119** and aldehyde **120** in 87% and 81% yield, respectively (Scheme 23, Eqs. 12 and 13).

Next, a variety of asymmetric allylation reactions were evaluated. The use of allyltributyltin in the presence of 0.2equiv BINOL/Ti(Oi-Pr)₄ and 4 Å molecular sieves as described by Keck [37] provided excellent enantioselectivity (99.4:0.6), albeit in only 30% yield (Table 7, entry 1). The chiral borane reagent, allyl(Ipc)₂B, developed by Brown [38], afforded an improved yield (entry 2), and the enantiomeric ratio reflected the purity of the reagent. The enantiomeric purity of the borane reagent can be enriched by synthesizing methoxy(Ipc)₂B rather than using chloro(Ipc)₂B [38a]. Therefore, (–)-methoxy(Ipc)₂B was prepared from (+)- α -pinene [38b,c]. The allylation using (–)-methoxy(Ipc)₂B at –78 °C afforded homoallylic alcohol (*S*)-**118** in 73% yield with a 96:4 enantiomeric ratio (entry 3). A lower temperature (–100 °C) did not improve the enantioselectivity (entry 4). Although successful, the Brown-type allylation was not ideal because it required the preparation and use of stoichiometric amounts of a chiral reagent.

An enantioselective allylation method developed in these laboratories, namely the chiral bisphosphoramidate-catalyzed allylation reaction of allyltri-chlorosilanes and aldehydes, was tested for this purpose [39]. Thus, the

**TABLE 7** Survey of Asymmetric Allylation Reactions

Entry	 M	Conditions	Yield (%) ^a	er ^b
1	 (1.3 equiv)	(<i>S</i>)-BINOL (0.24 equiv), Ti(O <i>i</i> -Pr) ₄ (20mol%), −78 to −20 °C	30	99:1
2	 (1.0 equiv)	(+)-Ipc ₂ B—Cl (1 equiv), −78 °C	70	90:10
3	 (1.5 equiv)	(+)-Ipc ₂ B—OMe (1 equiv), −78 °C	73	96:4
4	 (1.3 equiv)	(+)-Ipc ₂ B—OMe (1 equiv), −100 °C	71	96:4
5	 (2.0 equiv)	(<i>R,R</i>)- 121 (0.05 equiv), Et ₃ N/ CH ₂ Cl ₂ , −78 °C	11	93:7
6	 (2.0 equiv)	(<i>R,R</i>)- 121 (0.05 equiv), <i>i</i> -Pr ₂ NEt/ CH ₂ Cl ₂ , −78 °C	76	95:5

^aYield corresponds to isolated product.^bThe enantiomeric ratio was determined by CSP-SFC.

addition of allyltrichlorosilane (2.0 equiv) to **106** using 0.05 equiv of chiral bisphosphoramidate (*R,R*)-**121** in the presence of triethylamine at −78 °C for 8 h afforded the desired homoallylic alcohol (*S*)-**118** only in 11% yield. However, the enantiomeric ratio was acceptable and proven to be 93:7 (entry 5). It was determined that the Lewis-base catalyst (*R,R*)-**121** was not efficiently turning over. Therefore, it was anticipated that switching to a more Lewis basic cosolvent such as *i*-Pr₂NEt instead of Et₃N would facilitate a more

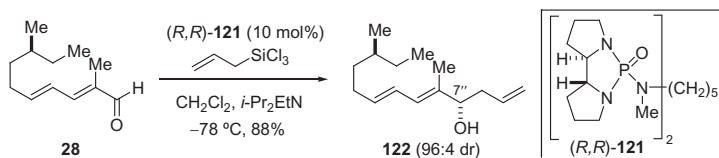
efficient catalyst turnover [39]. Use of *i*-Pr₂NEt gave the product in 76% yield and the selectivity improved (95:5). Because the Lewis base-catalyzed reaction provided excellent enantioselectivity and yield in the model system, it was applied in the synthesis of the side chain of papulacandin D.

4.4 Asymmetric Allylation of Aldehyde **28** and Proof of Configuration

Now, the enantioselective allylation of the substrate could be tested (Scheme 24). Gratifyingly, allylation of **28** using chiral bisphosphoramidate (*R,R*)-**121** smoothly provided **122** in good yield and excellent diastereomeric selectivity (88%, dr 96:4).

On the basis of our stereochemical analysis of the allyltrichlorosilane allylation, the (*R,R*)-**121** catalyst should produce the *S*-configuration at the homoallylic position (Figure 4).

To confirm this stereochemical outcome, the allylated product **122** was subjected to Mosher ester analysis [40] (Figure 5). The Mosher ester was prepared by the reaction of **122** with 1-methoxy-1-trifluoromethyl-phenylacetyl (MTPA) chloride in pyridine/CDCl₃ and was analyzed by ¹H NMR of the crude reaction mixture. Both diastereomers of the *S*- and *R*-MTPA esters (*S*-MTPA-**122** (**123**) and *R*-MTPA-**122** (**124**), respectively) were analyzed, and



SCHEME 24 Asymmetric allylation of aldehyde **28**.

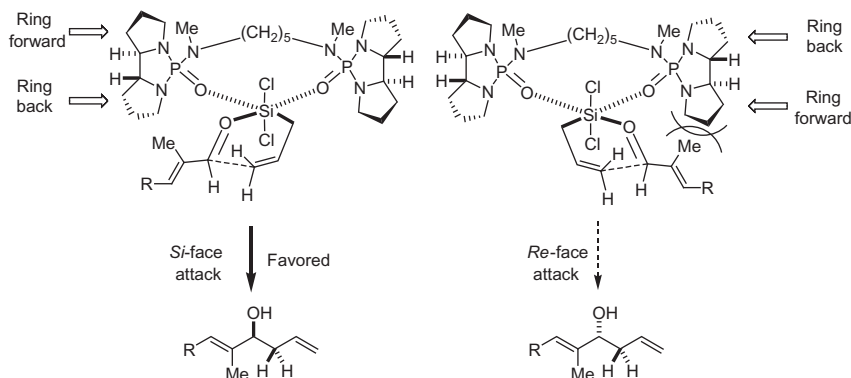


FIGURE 4 Hypothetical model for the reaction promoted by (*R,R*)-**121**.

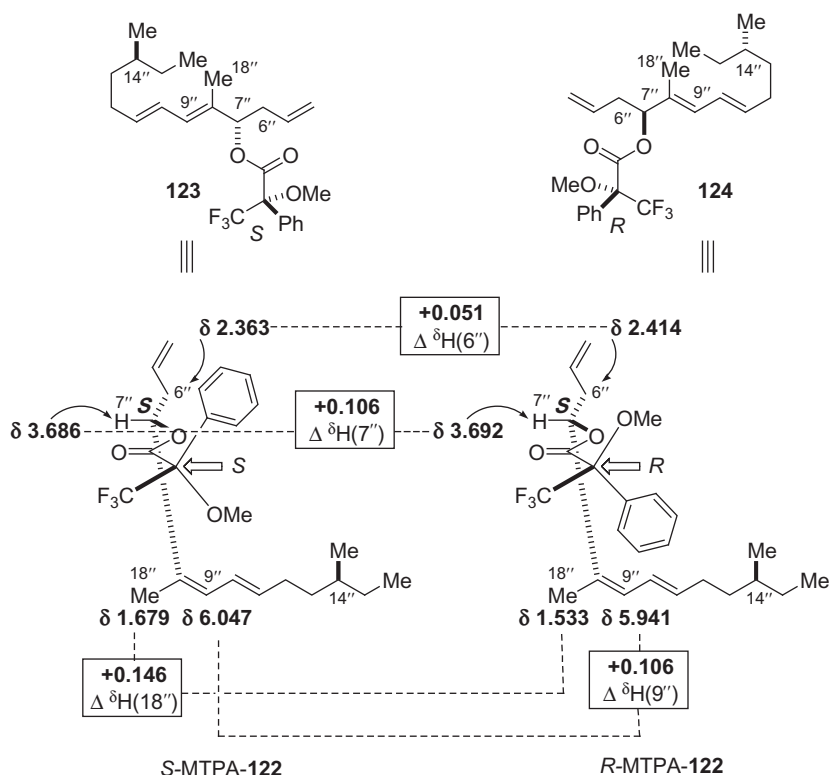


FIGURE 5 Mosher ester analysis of MTPA-122.

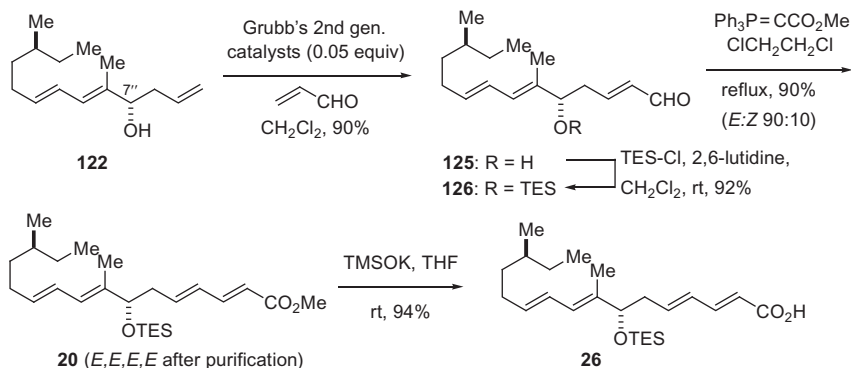
their chemical shift differences were measured (Figure 5). From the Mosher ester analysis it was determined that the configuration at the homoallylic position was indeed of the *S*-configuration, which correlated with the model in Figure 4.

Olefin metathesis of the allylated product **122** with acrolein using Grubbs' second-generation catalyst, and protection of the C(7'') hydroxyl group with TES-Cl gave **126** in 91% yield for the two steps. The synthesis of **26** was completed by Wittig olefination and saponification with KOTMS [41] in 90% yield over two steps (Scheme 25).

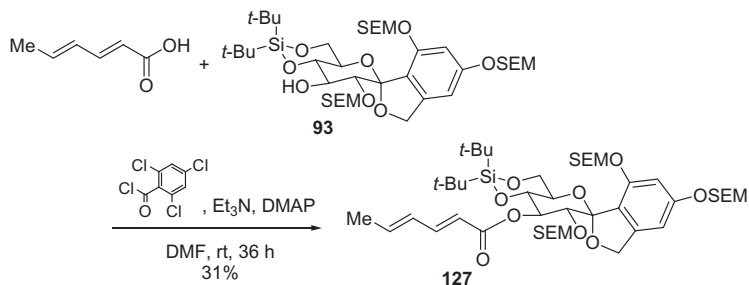
4.5 Acylation of tris-SEM Protected Aryl Glycoside

4.5.1 Model Acylation with Sorbic Acid

The next challenge in the synthesis was the union of fragments **93** and **26**, through an acylation reaction. Because of the sensitivity of the side chain acid **26**, the Yamaguchi mixed anhydride protocol was first tested [42]. Barrett [6r] reported the use of such a mixed anhydride derived from **26** in combination



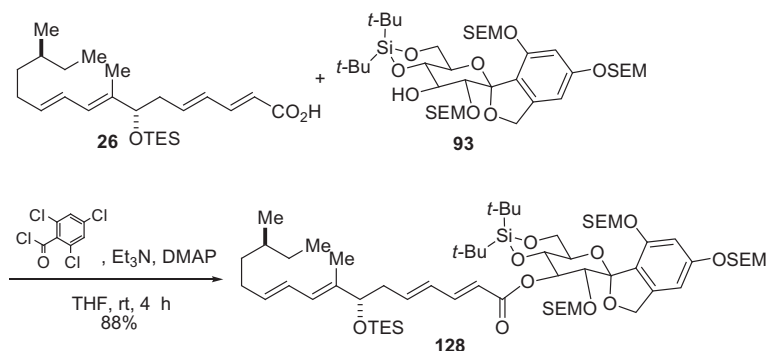
SCHEME 25 Preparation of the side chain carboxylic acid **26**.



SCHEME 26 Acylation of precursor **93** with sorbic acid.

with *O*-4,*O*-6-di-*t*-butylsilylene acetal and TIPS protecting groups on the spiricyclic aryl glycopyranoside to improve the site selectivity of the acylation. In this study, the C(2) hydroxyl group is protected and therefore, the acylation should be selective for the C(3) hydroxyl group. However, the secondary hydroxyl group is in significantly more hindered environment compared to Barrett's substrate. Hence, the acylation was tested using sorbic acid (**27**) before committing precious acid **26**.

Sorbic acid was activated via a mixed anhydride using 2,4,6-trichlorobenzoyl chloride in the presence of DMAP and DMF and then a solution of **93** and DMAP in DMF was added to the mixed anhydride at ambient temperature. The acylated product **127** was isolated in 31% yield, where the remaining mass corresponded to unreacted **93** (Scheme 26). Although the yield of the reaction was poor presumably due to moisture, it demonstrated that acylation can proceed at the C(3) position. Applying the above conditions to the crucial coupling of fragments **26** and **93** in absolute THF for 4 h, however, afforded the desired ester **128** in good yield (88%) (Scheme 27).



SCHEME 27 Acylation of precursor **93** with side chain carboxylic acid **26**.

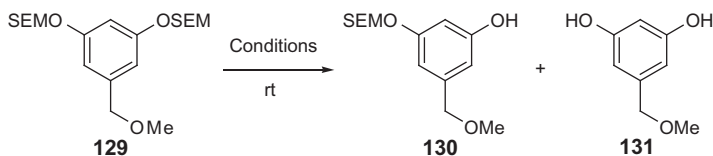
5. STUDIES ON THE GLOBAL DEPROTECTION TO SYNTHESIZE PAPULACANDIN D

5.1 Model Study of SEM Deprotection

The last step in the synthesis was the global deprotection of all the silicon protecting groups in **128**. Standard fluoride sources such as TASF, TBAF, HF·Et₃N, etc., were expected to cleave the protecting groups in one step, thus revealing the natural product. To find optimal conditions for the cleavage of the SEM protecting groups, we decided to work with a simple model compound, bis-*O*-SEM-protected 5-(methoxymethyl)-resorcinol **129**, prepared from methyl 3,5-dihydroxybenzoate.

A variety of conditions were surveyed that are known for silicon and SEM ether deprotection (Table 8) [43]. Only a combination of MgBr_2 and *n*-BuSH provided the fully deprotected resorcinol derivative. These SEM deprotection conditions were then applied to a more appropriate model compound, acyl spirocyclic aryl glycopyranoside **127**. Because of the stability of SEM ethers to fluoride treatment (*vide infra*), a two-step deprotection sequence was employed. First, to cleave the silyl ether protecting groups, **127** was treated with 10 equiv of a 1.0 M solution of TBAF in THF at room temperature for 1.5h (Scheme 28). Unfortunately, acyl migration took place and the product (isolated in low yield) was a mixture of C(3) and C(4) acylated isomers **132** and **133**, respectively.

Nevertheless, sufficient material was secured to investigate the SEM ether cleavage. Therefore, the mixture of **132** and **133** was subjected to the action of 25 equiv of MgBr₂ and 23 equiv *n*-BuSH in Et₂O at room temperature for 1 h. The reaction became biphasic and only a trace of the desired SEM-deprotected product **134** was isolated. Next, the inverse of the above sequence was employed; **127** was first treated with 60 equiv of MgBr₂ and 60 equiv of *n*-BuSH in the presence of MeNO₂ as a cosolvent to provide the desired product **135** quantitatively.

**TABLE 8** Survey of SEM Ether Deprotection Conditions

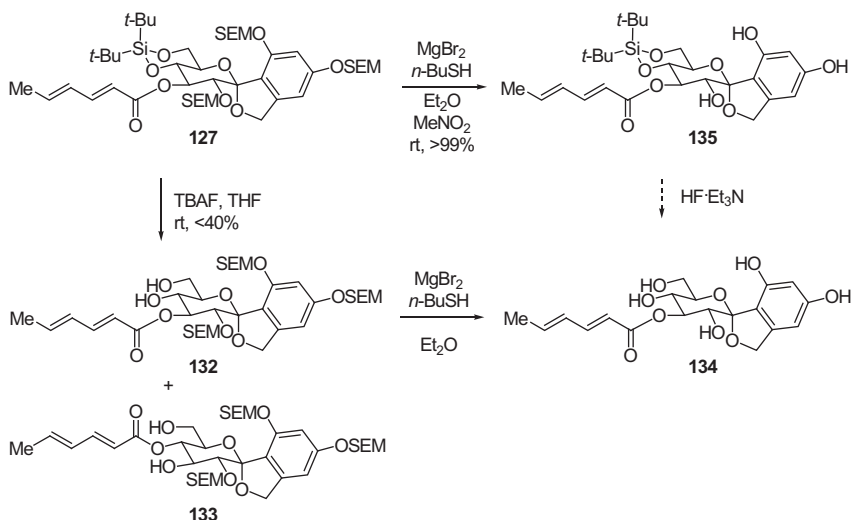
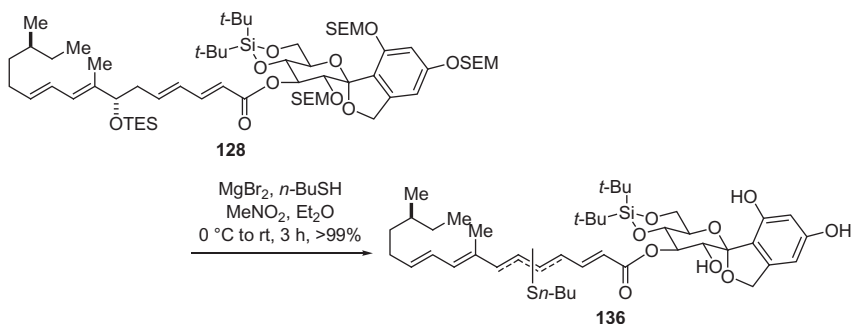
Entry	Conditions	Yield (%) ^a	
		130	131
1	TBAF·3H ₂ O (10 equiv), MS 4 Å, HMPA, 1 h	72	–
2	TBAF·3H ₂ O (10 equiv), MS 4 Å, HMPA, 12 h	12	21
3 ^b	TBAF·3H ₂ O (10 equiv), MS 4 Å, HMPA, 2 h	– ^c	–
4 ^d	TMAF·H ₂ O (10 equiv), HMPA, 40 h	15	–
5 ^e	TASF (15 equiv), THF, 48 h	38	–
6	TASF (15 equiv) HMPA, 48 h	68	32
7	HF·NEt ₃ (70:30) (12 equiv), H ₂ O/CH ₃ CN, 48 h	– ^f	–
8	ZnBr ₂ (20 equiv), MeOH (40 equiv), CH ₂ Cl ₂ , 1 h	– ^c	–
9	ZnF ₂ (20 equiv), CH ₂ Cl ₂ , 12 h	– ^c	–
10	MgBr ₂ (20 equiv), CH ₃ NO ₂ (40 equiv) Et ₂ O, 3 h	– ^c	–
11	MgBr ₂ (20 equiv), <i>n</i> -BuSH (40 equiv), Et ₂ O, 1 h	–	99

^aYields of isolated products.^b50 °C.^cExtensive decomposition was observed.^d**129** was recovered in 76%.^eProduct was isolated as a 62:38 mixture of **130:131**.^f**129** was recovered quantitatively.

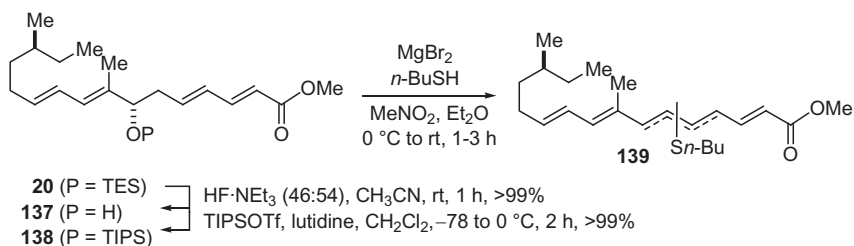
Treatment of **135** with HF·Et₃N solution should cleave the silyl ether protecting groups to afford the fully deprotected product.

These results encouraged attempts at the global deprotection of **128** (Scheme 29). The SEM-protected papulacandin D precursor **128** was treated with 60 equiv MgBr₂ and 60 equiv *n*-BuSH in Et₂O/MeNO₂ from 0 °C to room temperature. After 3 h consumption of **128** was observed by TLC analysis; however, a mixture of butanethiol-incorporated products was isolated and tentatively assigned as **136**.

The failure of the deprotection strategy at the last step in the synthesis was very disappointing. Clearly, the removal of the SEM protecting group required more forcing conditions than anticipated. Thus, the search for a

SCHEME 28 Model study of SEM deprotection with **127**.SCHEME 29 Attempt at the global deprotection of papulacandin D precursor **128**.

new protecting group that could be removed without damage to the sensitive C(7'') hydroxyl group was needed. Therefore, a couple of different protecting groups were examined to increase the stability of the C(7'') hydroxyl group under the SEM deprotection conditions (Scheme 30). Regardless of the C(7'') hydroxyl protecting group, elimination was always the major pathway. Thus, the identification of milder deprotection conditions became paramount. The stability of the C(7'') TES ether **20** was tested using a solution of 5 equiv TASF in THF. Surprisingly, TASF induced the elimination of the silyl ether, even though Barrett and coworkers used similar conditions for their global silyl deprotection [6r]. In the course of our studies, the side chain was fairly stable in the presence of a buffered hydrofluoric acid solution in CH₃CN (HF·NEt₃ (46:54)) (**20**–**137**). Unfortunately, it was observed that neither



SCHEME 30 Incompatibility of C(7)-oxygen functionality with deprotection conditions.

HF·NEt₃ (70:30) nor HF·pyridine (60:40) were strong enough to induce SEM ether cleavage (Table 8, entry 7).

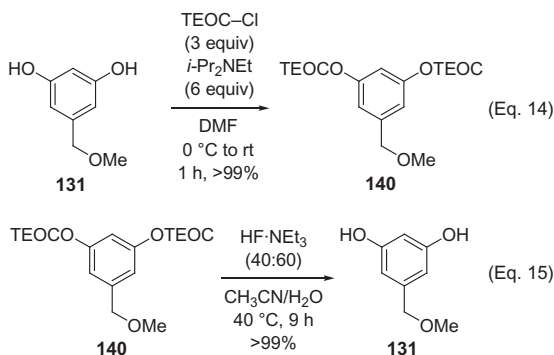
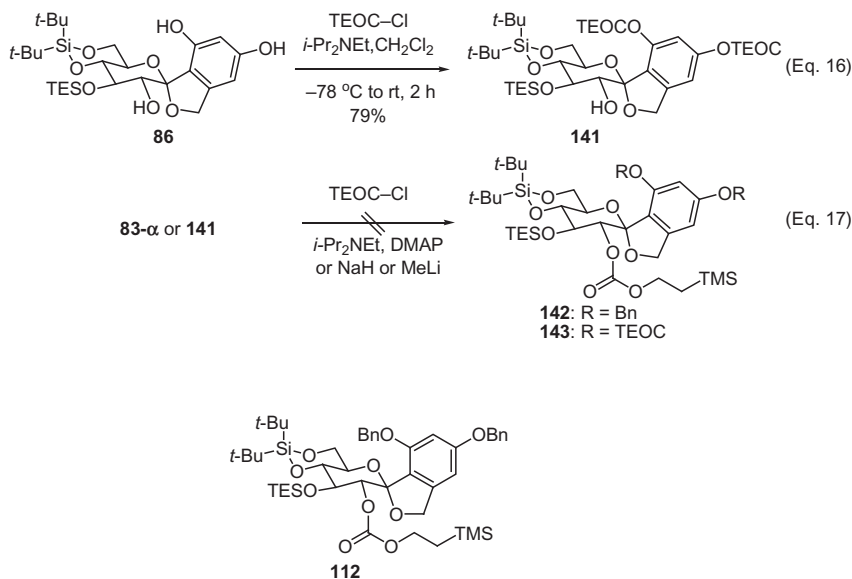
6. NEW PROTECTING GROUP STRATEGY

6.1 Introduction of TEOC Protecting Groups

The failure to cleave the SEM groups shifted the focus to revising the initial protecting group strategy so that it would accommodate the sensitivity of the pendant side chain. The study focused on silicon-based protecting groups that could be easily cleaved with HF·NEt₃ or HF·pyridine, because of the observed stability of the side chain to these conditions. The survey began with trialkylsiloxymethyl ethers (TBSCH₂OR and TIPSCH₂OR) using methyl 3,5-dihydroxybenzoate as a model compound [44]. However, it was observed that the protection afforded a mixture of trialkylsilyl and trialkylsilyloxymethyl ethers. Because the introduction of a trialkylsilyloxymethyl protecting group was unsuccessful, 2-(trimethylethylsilylethoxy-carbonyl) (TEOC) was then investigated [45]. It was anticipated that the TEOC protecting group could be easily cleaved under HF·NEt₃ conditions, and was small enough to protect the sterically encumbered C(2) hydroxyl group. The model substrate 5-(methoxymethyl)resorcinol (**131**) was transformed into the bis-TEOC carbonate **140** quantitatively using 3 equiv of TEOC-Cl [46] in the presence of 6 equiv of *i*-Pr₂NEt. To our delight, the TEOC groups in **140** could be quantitatively removed using HF·NEt₃ (40:60) in CH₃CN at 40°C for 9 h (Scheme 31).

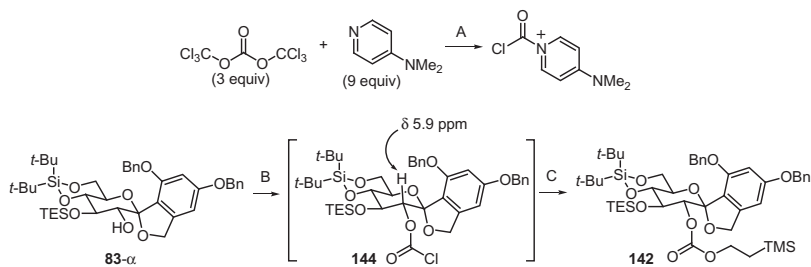
TEOC protection of all three hydroxyl groups in triol **86** was attempted first. However, only the aromatic hydroxyl groups could be protected (Scheme 32, Eq. 16). Surprisingly, when the aromatic hydroxyl groups were protected as TEOC or benzyl ethers, TEOC protection failed at the C(2)-hydroxyl group (Eq. 17). The acylation of **142** or **143** was slow because of the steric congestion at the C(2) hydroxyl group.

The C(2) hydroxyl group of **83-α** could be acylated, with acetic anhydride and pyridine, albeit very slowly. Even after 12 h the reaction did not go to completion and the acetate was isolated along with some of the starting material. The failure to attach a TEOC group at C(2) most likely arises from insufficient reactivity of TEOC-Cl. To circumvent this problem, the TEOC

SCHEME 31 Installation of TEOCS onto resorcinol **131** and their removal.SCHEME 32 TEOC protection of triol **86**.

protecting group was affixed in a stepwise manner to allow use of a more reactive acylating agent, namely triphosgene. The resulting chloroformate could then be combined with 2-(trimethylsilyl)ethanol to complete the TEOC protection.

This idea was put into practice by generating a chlorocarbonyl-pyridinium cation with triphosgene and DMAP in a mixture of *i*-Pr₂NEt and CH₂Cl₂. To this solution was added alcohol **83-α**. However, the reaction did not afford any of the desired product (Table 9, entries 1 and 2). The experiment was

**TABLE 9** TEOC Protection of **83-α**

Entry	Solvent	Result
1 ^a	CH ₂ Cl ₂	83-α (>99%)
2 ^b	CH ₂ Cl ₂	83-α (>99%)
3 ^c	CDCl ₃	biphasic mixture
4 ^d	CDCl ₃	24 h; 144 : 142 =52:48 48 h; 144 : 142 =16:84 72 h; 144 : 142 =0:100
5 ^e	CDCl ₃	142 (92%)
6 ^f	CHCl ₃	142 (92%)

^a**A**: *i*-Pr₂NEt (1055 equiv), −78 °C, 20 min; **B**: −78 °C, 1 h (0.002 M); **C**: TMS-ethanol (18 equiv), −78 °C to rt, 4 h (0.0012 M).

^b**A**: *i*-Pr₂NEt (1055 equiv), −78 °C, 20 min; **B**: −78 °C to rt, 1 h (0.002 M); **C**: TMS-ethanol (72 equiv), −78 °C to rt, 9 h (0.0012 M).

^c**A**: *i*-Pr₂NEt (28 equiv), −78 °C to rt, 30 min (DMAP 0.6 M); **B**: −78 °C to rt, 1 h (0.002 M); **C**: TMS-ethanol (72 equiv), −78 °C to rt, 9 h (0.0012 M).

^d**A**: −78 °C to rt, 1 h (DMAP, 1.2 M); **B**: *i*-Pr₂NEt (28 equiv), −78 °C to rt, 1 h (0.043 M); **C**: TMS-ethanol (26 equiv), rt (0.0041 M).

^e**A**: −78 °C to rt, 30 min (DMAP, 1.2 M); **B**: *i*-Pr₂NEt (28 equiv), −78 °C to rt, 1 h (0.043 M); **C**: TMS-ethanol (26 equiv), rt, 12 h (0.043 M).

^f**A**: −56 °C to rt, 30 min, DMAP (2 equiv); **B**: *i*-Pr₂NEt (7 equiv), −78 °C to rt, 1 h; **C**: TMS-ethanol (4 equiv), rt, 12 h.

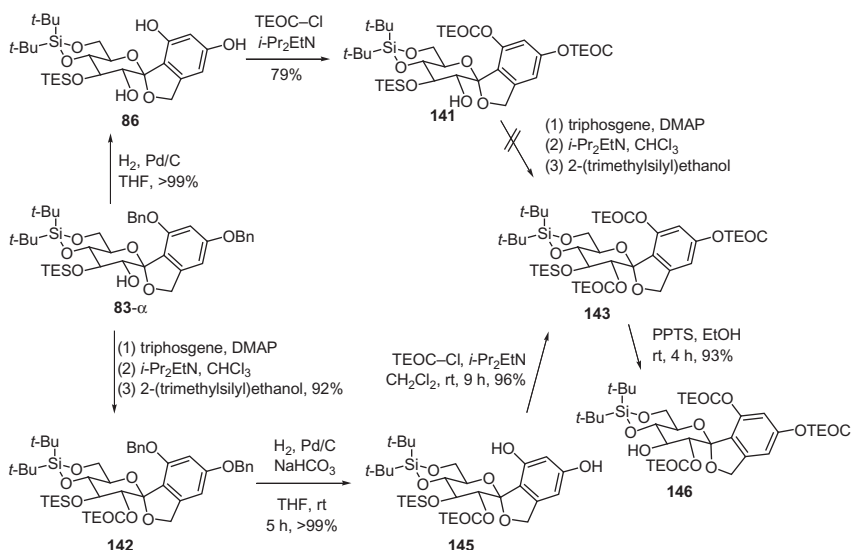
repeated in CDCl₃ and was monitored by ¹H NMR spectroscopy. In CDCl₃, the reaction mixture became biphasic when *i*-Pr₂NEt was added to the solution of DMAP and triphosgene (entry 3). Therefore, *i*-Pr₂NEt was added later along with **83-α**. When the chlorocarbonyl-pyridinium cation was observed, this solution was transferred to a solution of **83-α** in CDCl₃/*i*-Pr₂NEt. To observe the formation of chloroformate **144**, the reaction mixture was diluted with CDCl₃ (conc. 0.0014 M). Once complete conversion of **83-α** to **144** was confirmed, the solution was treated with 2-(trimethylsilyl)ethanol. At this low concentration, the rate of reaction was very slow and required ca. 70 h for complete conversion (entry 4). However, at 0.043 M, complete conversion

was observed within 12 h to afford **142** in 92% yield (entry 5). It is of note that all the attempts listed in Table 9 except for entry 6 were accomplished using a total of 2.4 mg of **83- α** , demonstrating the power of ^1H NMR for reaction monitoring. Gratifyingly, only with minor modification to the reagent stoichiometry, treatment of **83- α** with a preformed acylpyridinium species followed by the addition of 2-(trimethylsilyl)ethanol gave the 2-TEOC protected spiroketal in 92% yield on preparative scale (entry 6).

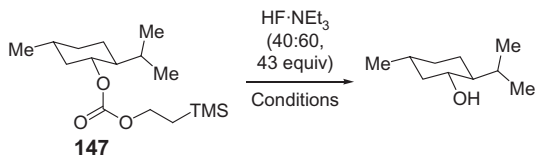
Initially, we thought that bis-TEOC carbamate **141** derived from **83- α** , could be transformed into tris-TEOC carbamate **143** (Scheme 33). Thus, **141** was subjected to the new acylation conditions, but only decomposition was observed. In an alternative approach, **142** (also derived from **83- α**) was converted to **145** quantitatively by hydrogenolysis. Subsequent protection of the phenolic groups of **145** was achieved under standard TEOC protection conditions to produce the fully silylated spiroketal **143** in 96% yield. Finally, selective removal of the C(3) TES ether with PPTS/ETOH afforded acylation precursor **146** in 93% yield.

6.2 Studies on the Removal of TEOC Groups

To evaluate if the sterically congested C(2)-TEOC protecting group could be removed using $\text{HF}\cdot\text{NEt}_3$ solution, TEOC protected menthol **147** was used as a test substrate. A variety of reaction variables were systematically surveyed (time, concentration of fluoride, $\text{HF}\cdot\text{NEt}_3$ ratio, temperature, and solvent) and some representative examples are presented in Table 10. These studies concluded that the rate of TEOC cleavage in DMSO was significantly faster



SCHEME 33 Preparation of acylation precursor **146**.

**TABLE 10** Model Study for the TEOC Deprotection on **147**

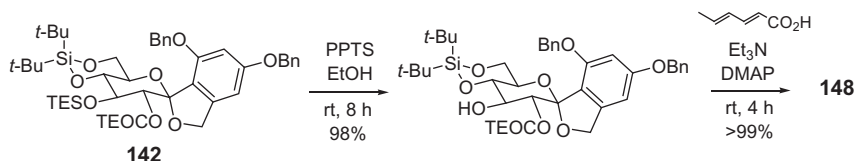
Conditions					
Entry ^{a,b}	Solvent	Conc. (Fluoride, M)	Temp (°C)	Time (h)	Ratio (147 :Menthol)
1	CH ₃ CN/H ₂ O	1.67	40	9	90:10
2	CH ₃ CN/H ₂ O	1.67	40	42	76:24
3	CH ₃ CN/H ₂ O	2.51	40	9	87:13
4 ^c	CH ₃ CN/H ₂ O	2.88	40	9	86:14
5	CH ₃ CN/H ₂ O	1.67	60	9	74:26
6	THF/H ₂ O	1.67	60	9	Decomp.
7	DMSO/H ₂ O	1.67	60	9	22:78
8	DMSO/H ₂ O	1.67	40	9	72:28

^aThe each reaction was carried out in a poly styrene test tube using 5 mg of TEOC protected L-menthol.

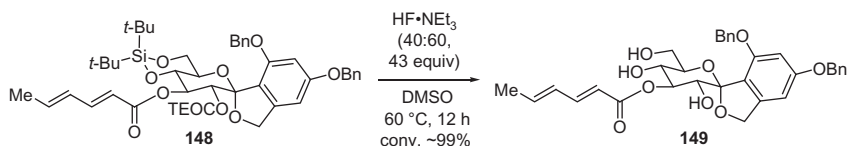
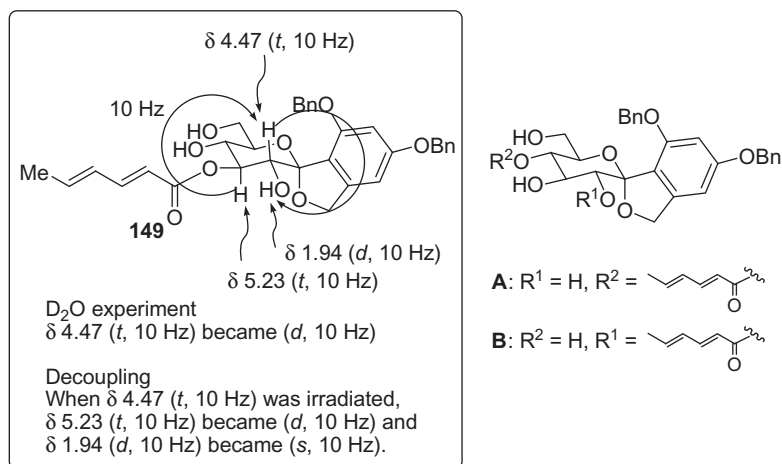
^bTime (entries 1, 2), concentration (entries 1, 3); HF:NEt₃-ratio (entries 3, 4), reaction temp. (entries 1, 5), and solvent (entries 5, 6, 7 and entries 1, 8) were systematically surveyed.

^cThe HF:NEt₃-ratio was 46:54.

than the other solvents (Table 10, entries 7 and 8). Applying these conditions to the TEOC cleavage of a sorbyl ester **148** (prepared from **142**)



demonstrated that at 40°C in DMSO the cleavage was not complete, but at 60°C after 12 h complete deprotection to **149** was observed (Scheme 34). Although deprotection of **147** did not go to completion, that for **148** did under similar reaction conditions. This is not only because of an extended reaction time, but also presumably because of the increased acidity of C(2)-alcohol due to three extra oxygen functionalities at the β-position on **148**. Finally,

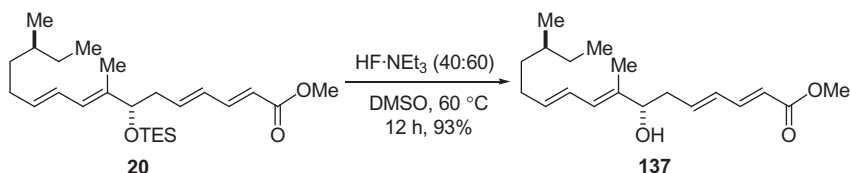
SCHEME 34 Global deprotection model study on **148**.FIGURE 6 Assignment of esterification site in **149**.

to establish that acyl migration did not occur (a problem observed during the initial SEM-*t*-butyldisilylene-acetal deprotection studies of **127**, Scheme 28), structure **149** was confirmed (and structures **A** and **B** were eliminated) through a series of NMR experiments (Figure 6).

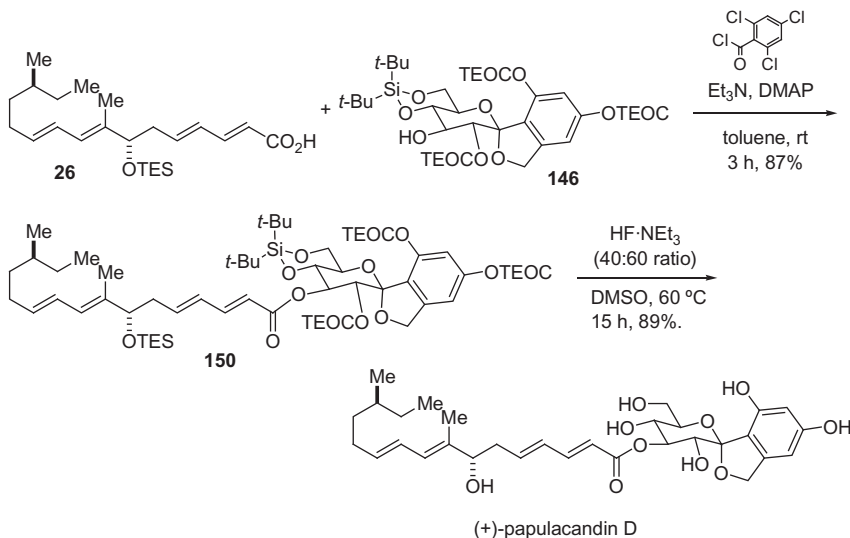
Finally, the side chain must not degrade under the deprotection reaction conditions. Before subjecting the very precious, fully protected papulacandin D to the HF·NEt₃ deprotection conditions, the stability of the side chain was once again tested. In a Teflon flask, a biphasic solution of DMSO and HF·NEt₃ (40:60) was added to methyl ester **20** (Scheme 35) and the mixture was heated to 60 °C. Deprotection of the C(7'')-silyl ether was rapid under these conditions. However, heating for 15 h was required to remove all the TEOC groups of the 1-aryl glycopyranoside. Therefore, the stability of the unprotected side chain, upon extended heating, needed to be tested. Fortunately, it was determined that the side chain was stable under prolonged heating and alcohol **137** was isolated in 93% yield.

7. GLOBAL DEPROTECTION

With routes for the side chain **26** (Scheme 25) and the protected spirocyclic aryl glycopyranoside **146** secured, the penultimate challenge was the coupling of the two fragments via the mixed anhydride of **26** from 2,4,6-



SCHEME 35 Compatibility of C(7)-oxygen functionality with deprotection conditions.



SCHEME 36 Completion of the total synthesis of papulacandin D.

trichlorobenzoyl chloride. The two fragments were united (1.3 equiv **26**, toluene, rt, 3 h) in 87% yield, with only slight modification from the original acylation protocol⁵ (Schemes 27 and 36).

Finally, the most daunting step in the synthesis could be attempted, namely deprotection of all the silicon protecting groups in protected papulacandin D, **150**. Gratifyingly, the extensive optimization of protecting groups and deprotection conditions proved worthwhile. Global deprotection of **150** proceeded smoothly on >80 mg scale using a buffered HF·Et₃N (40:60 ratio) in DMSO at 60 °C for 15 h to afford an 89% yield of synthetic (+)-papulacandin D.

The physical and spectroscopic data for the synthetic sample were nearly identical in all respects [m.p. 126–128 °C (lit. 127–130 °C), ¹H NMR, ¹³C NMR, IR, UV–Vis, [α]_D²⁴ +8.78 (*c*=0.21, MeOH)]; lit. 7 ± 1 (MeOH) to

5. Use of THF for the acylation caused a cleavage of TEOC on the phenols followed by acylation of them with the acyl donor.

those reported for natural (+)-papulacandin D and that of Barrett's synthetic material.

One of the most challenging aspects of the total synthesis was the successful implementation of the protecting group strategy. In the previous section, the criteria for the protecting group strategy was discussed; however, this proved to be much more challenging in practice than initially anticipated. Early in the synthesis, we decided that the hydroxyl groups of papulacandin D would be protected with silicon-based protecting groups to facilitate a global silicon deprotection as the last step in the synthesis. This strategy limited the choice of protecting groups to those that are easily cleaved in the presence of fluoride and thus required a very delicate balance between the protecting groups chosen. For instance, when the resorcinol portion of the aromatic iodide contained TIPS or TBS silyl ethers, the cross-coupling reaction did not proceed. However, when the hydroxyl groups were protected as the benzyl ethers, productive cross-coupling was achieved. Although the benzyl protecting groups were optimal for cross-coupling, the reductive deprotection conditions would not be compatible with the unsaturated side chain **2**. Therefore, these groups needed to be removed and replaced before the introduction of the side chain.

The first attempt at the synthesis of papulacandin D employed SEM protection because, at the time, SEM was the only protecting group that would efficiently protect the aromatic hydroxyl groups and the sterically hindered C(2) hydroxyl group. Unfortunately, SEM ethers could not be cleaved in the presence of the usual fluoride sources that would also allow the side chains to emerge intact. Thus, the related TEOC group was selected as a slightly more labile alternative.

The sequence for the introduction of the TEOC groups was crucial for the successful preparation of the tris-TEOC aryl glycopyranoside **143** (Scheme 33). If the phenolic hydroxyl groups were protected first, then C(2)-hydroxyl group protection was very difficult, because of an instability of the bis-TEOC carbamate **141** under the reaction conditions. Therefore, the following sequence was employed: (1) the C(2)-hydroxyl group was protected first, through an *in situ* formation of a chlorocarbonate **144** and trapping with 2-(trimethylsilyl)ethanol, (2) the benzyl groups were removed under hydrogenolysis conditions, and (3) the phenolic hydroxyl groups were protected using TEOC-Cl in the presence of *i*-Pr₂NEt. This three step sequence (**83-α** to **143**, Scheme 33) proceeded in 88% overall yield compared to the 49% yield for the three step sequence for the SEM protection (**83-α** to **92**, Scheme 16, Table 5).

Finally, the successful global deprotection required extensive optimization for the cleavage of all the TEOC groups. The C(2)-TEOC was the most difficult to remove of all the silicon protecting groups in **150**. Manipulation of the fluoride concentration, ratio of HF to Et₃N, changing the solvent from CH₃CN to DMSO, and raising the temperature from 40 to 60°C were all required to effect complete desilylation and provide excellent yield (89%) of the natural product.

8. CONCLUSION

The total synthesis of (+)-papulacandin D has been accomplished in a convergent approach (31 steps overall, 9.2%, over 80 mg) from commercially available triacetoxylglucal and geraniol. The synthetic strategy breaks the molecule into two nearly equal subunits, the C-spirocyclic aryl glycoside **146** and polyunsaturated fatty acid side chain **26**. The key significant features of the synthetic strategy are (1) the palladium-catalyzed, organosilanolate-based, cross-coupling of a protected glucal silanol and (2) a catalytic enantioselective allylation reaction using chiral bisphosphoramidate (*R,R*)-**121** for the construction of the C(7'') stereogenic center.

ACKNOWLEDGMENTS

Funding was provided by the National Institutes of Health (Grant R01 GM63167). CSR thanks Eli Lilly research laboratories and Johnson & Johnson PRI for graduate fellowships. We are also grateful to Prof. A. G. M. Barrett for providing spectra for synthetic (+)-papulacandin D.

REFERENCES

- [1] Isolation: (a) P. Traxler, J. Gruner, J.A.L. Auden, *J. Antibiot.* 30 (1977) 289–296; Structural determination: (b) P. Traxler, H. Fritz, W. Richter, *J. Helv. Chim. Acta* 60 (1977) 578–584; (c) P. Traxler, H. Fritz, H. Fuhrer, W. Richter, *J. Antibiot.* 33 (1980) 967–978.
- [2] Biological evaluations: (a) P. Pérez, R. Varona, I. Garcia-Acha, A. Durán, *FEBS Lett.* 129 (1981) 249–252; (b) R. Varona, P. Pérez, A. Durán, *FEMS Microbiol. Lett.* 20 (1983) 243–247; (c) B.C. Baguley, G. Rommele, J. Gruner, W. Wehrli, *Eur. J. Biochem.* 97 (1979) 345–351; (d) A. Murgui, M. Victoria Elorza, R. Sentandreu, *Biochem. Biophys. Acta* 841 (1985) 215–222; (e) P. Pérez, I. Garcia-Acha, A. Durán, *J. Gen. Microbiol.* 129 (1983) 245–250; (f) M. Kopecka, *Folia Microbiol.* 29 (1984) 441–449; (g) D.M. Schmatz, M. A. Romancheck, L.A. Pittarelli, R.E. Schwartz, R.A. Fromtling, K.H. Nollstadt, F. L. VanMiddlesworth, K.E. Wilson, M. Turner, *J. Proc. Natl. Acad. Sci. USA.* 87 (1990) 5950–5954; (h) K. Bartizal, G. Abruzzo, C. Trainor, D. Krupa, K. Nollstadt, D. Schmatz, R. Schwartz, M. Hammond, J. Balkovec, F. VanMiddlesworth, *Antimicrob. Agents Chemother.* 36 (1992) 1648–1657; (i) P. Traxler, W. Tosch, O. Zak, *J. Antibiot.* 40 (1987) 1146–1164; (j) D.M. Schmatz, *US* 5,089,478, 1992.
- [3] Patents: (a) P. Traxler, *US* 4,374,129, 1983. (b) P. Traxler, *US* 4,251,517, 1981. (c) P. Traxler, J. Gruner, J. Nuesch, *US* 4,278,665, 1981.
- [4] Review: M. Debono, R.S. Gordee, *Annu. Rev. Microbiol.* 48 (1994) 471–497.
- [5] For L-687,781 (Merck, Sharp & Dohme) isolation: (a) F. VanMiddlesworth, M.N. Olmstead, D. Schmatz, K. Bartizal, R. Fromling, G. Bills, K. Nollstadt, S. Honeycutt, M. Zweerink, G. Garrity, K. Wilson, *J. Antibiot.* 44 (1991) 45–51; Structural elucidation: (b) F. VanMiddlesworth, C. Dufresne, J. Smith, K.E. Wilson, *Tetrahedron* 47 (1991) 7563–7568; Biological evaluations: see Refs. 2g and 2h. For Mer-WF3010 (Mercian Corp.) isolation and structural elucidation: (c) R. Kaneto, H. Chiba, H. Agematu, N. Shibamoto, T. Yoshioka, H. Nishida, R. Okamoto, *J. Antibiot.* 46 (1993) 247–250; (d) H. Chiba,

- R. Kaneto, H. Agematu, N. Shibamoto, T. Yoshioka, H. Nishida, R. Okamoto, *J. Antibiot.* 46 (1993) 356–358; For BU-4794F (Bristol-Myers Squibb, Tokyo) isolation and structural elucidation: (e) M. Aoki, T. Andoh, T. Ueki, S. Masuyoshi, K. Sugawara, T. Oki, *J. Antibiot.* 46 (1993) 952–960; For saricandin, see: (f) R.H. Chen, S. Tennant, D. Frost, M.J. O'Beirne, J. P. Karwowski, P.E. Humphrey, L.H. Malmberg, W. Choi, K.D. Brandt, P. West, S. K. Kadam, J.J. Clement, J.B. McAlpine, *J. Antibiot.* 49 (1996) 596–598; For chaetiacandin isolation: (g) T. Komori, Y. Itoh, *J. Antibiot.* 38 (1985) 544–546; Structural elucidation: (h) T. Komori, M. Yamashita, Y. Tsurumi, M. Kohsaka, *J. Antibiot.* 38 (1985) 455–459; For F-10748 A1, A2, B1, B2, C1, C2, D1 and D2 (Daiichi-Sankyo) isolation and structural elucidation: (i) T. Ohyama, Y. Iwade-Kurihara, T. Hosoya, T. Ishikawa, S. Miyakoshi, K. Hamano, M. Inukai, *J. Antibiot.* 55 (2002) 758–763.
- [6] For aryl glycoside synthesis, see: (a) S. Danishefsky, G. Phillips, M. Ciufolini, *Carbohydrate Res.* 171 (1987) 317–327; (b) D. Balachari, G.A. O'Doherty, *Org. Lett.* 2 (2000) 863–866; (c) D. Balachari, G.A. O'Doherty, *Org. Lett.* 2 (2000) 4033–4036; (d) M.M. Ahmed, G. A. O'Doherty, *Tetrahedron Lett.* 46 (2005) 4151–4155; (e) F.E. McDonald, H.Y.H. Zhu, C.R. Holmquist, *J. Am. Chem. Soc.* 117 (1995) 6605–6606; (f) R.R. Schmidt, W. Frick, *Tetrahedron* 44 (1988) 7163–7169; (g) A.G.M. Barrett, M. Peña, J.A. Willardsen, *J. Chem. Soc., Chem. Commun.* (1995) 1145–1146; (h) A.G.M. Barrett, M. Peña, J.A. Willardsen, *J. Chem. Soc., Chem. Commun.* (1995) 1147–1148; (i) S.B. Rosenblum, R. Bihovsky, *J. Am. Chem. Soc.* 112 (1990) 2746–2748; (j) S. Czernecki, M.-C. Perlat, *J. Org. Chem.* 56 (1991) 6289–6292; (k) K.A. Parker, A.T. Georges, *Org. Lett.* 2 (2000) 497–499; (l) R.W. Friesen, C.F. Sturnio, *J. Org. Chem.* 55 (1990) 2572–2574; (m) R.W. Friesen, C.F. Sturnio, *J. Org. Chem.* 55 (1990) 5808–5810; (n) R.W. Friesen, C.F. Sturnio, A.K. Daljeet, A. Kolaczewska, *J. Org. Chem.* 56 (1991) 1944–1947; (o) E. Dubois, J.-M. Beau, *J. Chem. Soc. Chem. Commun.* (1990) 1191–1192; (p) E. Dubois, J.-M. Beau, *Tetrahedron Lett.* 36 (1990) 5165–5168; (q) E. Dubois, J.-M. Beau, *Carbohydr. Res.* 223 (1992) 157–167; (r) For the total synthesis of papulacandin D see, A.G.M. Barrett, M. Peña, J.A. Willardsen, *J. Org. Chem.* 61 (1996) 1082–1100; (s) S.A. Hitchcock, H. Chafig, C. Sanchez-Martinez, A.R. Esteban, *US* 6,069,238; Our earlier communication, see: (t) S.E. Denmark, C. S. Regens, T. Kobayashi, *J. Am. Chem. Soc.* 129 (2007) 2774–2776; (u) T. Kobayashi, C. S. Regens, S.E. Denmark, *J. Syn. Org. Chem. Jpn.* 66 (2008) 616–628; (v) S.E. Denmark, T. Kobayashi, C.S. Regens, *Tetrahedron* 66 (2010) 4745–4759.
- [7] R.F. Hector, *Clin. Microbiol. Rev.* 6 (1993) 1–21.
- [8] (a) S.E. Denmark, R.F. Sweis, A. de Meijere, F. Diederich (Eds.), *Metal-Catalyzed Cross-Coupling Reactions*, Wiley-VCH, Weinheim, Germany, 2004, pp. 163–216; (b) S.E. Denmark, S.-M. Yang, M. Harmata (Ed.), *Strategies and Tactics in Organic Synthesis*, Elsevier, Amsterdam, 2005 Volume 6; Chapt. 4; (c) S.E. Denmark, J.D. Baird, *Chem. Eur. J.*, 12 (2006) 4954–4963; (d) S.E. Denmark, C.S. Regens, *Acc. Chem. Res.*, 41 (2008) 1486–1499; (e) S. E. Denmark, *J. Org. Chem.*, 74 (2009) 2915–2927.
- [9] S.E. Denmark, L. Neuville, *Org. Lett.* 2 (2000) 3221–3224.
- [10] C.S. Swindell, W.J. Fan, *Org. Chem.* 61 (1996) 1109–1118.
- [11] (a) Y. Hatanaka, T. Hiyama, *J. Org. Chem.* 53 (1988) 918–920; (b) P. Pierrat, P. Gros, Y. Fort, *Org. Lett.* 7 (2005) 697–700.
- [12] AgO activation of silanols see: K. Hirabayashi, A. Mori, J. Kawashima, M. Suguro, Y. Nishihara, T. Hiyama, *J. Org. Chem.* 65 (2000) 5342–5349.
- [13] D.M. Grove, G. van Koten, J.N. Louwen, J.G. Noltjes, A.L.J. Spec, *J. Am. Chem. Soc.* 104 (1982) 6609–6616.

- [14] R.J. Ferrier, R.H. Furneaux, *Carbohydr. Res.* 52 (1976) 63–68.
- [15] (a) A. Fernandez-Mayoralas, A. Marra, M. Trumtel, A. Veyrieres, P. Siney, *Tetrahedron Lett.* 30 (1989) 2537–2540; (b) Idem, *Carbohydr. Res.* 188 (1989) 81–95; (c) C. Jäkel, K. H. Dötz, *J. Organometallic Chem.* 624 (2001) 172–185 Although the glycal acetonide can be prepared from glucose via triacetyl glycal, it has been proven to be low yielding.; (d) B. Fraser-Reid, D.L. Walker, S.Y.-K. Tam, N.L. Holder, *Can. J. Chem.* 51 (1973) 3950–3954; (e) R.W. Franck, T.V. John, *J. Org. Chem.* 48 (1983) 3269–3276.
- [16] (a) Direct formation of silanol from metalation of glucals and trapping with D3 the yields and scale were irreproducible. S.E. Denmark, C.R. Butler, *e-EROS Encyclopedia of Reagents for Organic Synthesis*, (2007). doi:10.1002/047084289X.rm00785.
- [17] M. Lee, S. Ko, S.J. Chang, *Am. Chem. Soc.* 122 (2000) 12011–12012.
- [18] (a) E.J. Corey, P.B. Hopkins, *Tetrahedron Lett.* 23 (1982) 4871–4874; (b) B.M. Trost, C. D. Caldwell, *Tetrahedron Lett.* 22 (1981) 4999–5002.
- [19] W. Roth, W. Pigman, *Methods in Carbohydr. Chem.* 2 (1963) 405–408.
- [20] M. Lee, S. Ko, S. Chang, *J. Am. Chem. Soc.* 122 (2000) 12011–12012.
- [21] Y. Lee, D. Seomoon, S. Kim, H. Han, S. Chang, P.J. Lee, *Org. Chem.* 69 (2004) 1741–1743.
- [22] (a) R.L. Halcomb, S.J. Danishefsky, *J. Am. Chem. Soc.* 111 (1989) 6661–6666; (b) S. J. Danishefsky, M.T. Bilodeau, *Angew. Chem. Int. Ed Engl.* 35 (1996) 1380–1419 and references cited therein.
- [23] P.Z. Brigl, *Physiol. Chem.* 122 (1922) 245–262.
- [24] G. Liu, J.M. Wurst, D.S. Tan, *Org. Lett.* 11 (2009) 3670–3673.
- [25] (a) (TMS-ethanol) M.L. Mancini, J.F. Honek, *Tetrahedron Lett.* 23 (1982) 3249–3250; (b) (SEM-Cl) B.H. Lipshutz, J.J. Pegram, *Tetrahedron Lett.* 21 (1980) 3343–3346; (c) B.H. Lipshutz, R. Moretti, R. Crow, *Tetrahedron Lett.* 30 (1989) 15–18; (d) K.C. Nicolaou, E.W. Yue, S.L. Greca, A. Nadin, Z. Yang, J.E. Leresche, T. Tsuru, Y. Naniwa, F.D. Riccardis, *Chem. Eur. J.* 1 (1995) 467–494.
- [26] J. Inanaga, K. Hirata, H. Saeki, T. Katsuki, M. Yamaguchi, *Bull. Chem. Soc. Jpn.* 52 (1979) 1989–1993.
- [27] E.D. Laganis, B.L. Chenard, *Tetrahedron Lett.* 25 (1984) 5831–5834.
- [28] (a) H. Takaya, T. Ohta, S.-I. Inoue, M. Tokunaga, M. Kitamura, R. Noyori, *Org. Synth.* 72, (1995) 169–175; (b) H. Takaya, K. Mashima, K. Koyano, M. Yagi, H. Kumobayashi, T. Taketomi, S. Akutagawa, R. Noyori, *J. Am. Chem. Soc.* 109 (1987) 1596–1597.
- [29] (a) K. Tanaka, H. Mori, M. Yamamoto, S. Katsumura, *J. Org. Chem.* 66 (2001) 3099–3110; (b) G. Alvernhe, A. Laurent, K. Touhami, *J. Fluorine Chemistry* 29 (1985) 363–384; (c) K. C. Nicolaou, J.-J. Liu, Z. Yang, H. Ueno, E.J. Sorensen, C.F. Claiborne, R.K. Guy, C.-K. Hwang, M. Nakada, P.G. Nantermet, *J. Am. Chem. Soc.* 117 (1995) 634–644; (d) N. Yamazaki, W. Dokoshi, C. Kibayashi, *Org. Lett.* 3 (2001) 193–196.
- [30] Lewis base catalysis: (a) S.E. Denmark, N.G. Almstead, J. Otera (Ed.), *Modern Carbonyl Chemistry*, Wiley-VCH, Weinheim, 2000 Chapt. 10; (b) S.E. Denmark, R.A. Stavenger, *J. Am. Chem. Soc.*, 122 (2000) 8837–8847; (c) S.E. Denmark, G.L. Beutner, *Angew. Chem. Int. Ed.*, 47 (2008) 1560–1638; (d) S.E. Denmark, *Chimia*, 62 (2008) 37–40.
- [31] Lewis base-catalyzed asymmetric aldol reaction employing dimeric catalyst: (a) S.E. Denmark, T. Wynn, G. Beutner, *J. Am. Chem. Soc.* 124 (2002) 13405–13407; (b) J.R. Heemstra, S.E. Denmark, *Encyclopedia of Reagents for Organic Synthesis*. (2008) doi:10.1002/047084289Xg.rm00771.
- [32] Effect of *t*-Bu: S.E. Denmark, G.L. Beutner, T. Wynn, M.D. Eastgate, *J. Am. Chem. Soc.* 127 (2005) 3774–3789.

- [33] Lewis base-catalyzed vinylogous aldol reactions: (a) S.E. Denmark, G.L. Beutner, J. Am. Chem. Soc. 125 (2003) 7800–7801; (b) S.E. Denmark, J.R. Heemstra Jr., J. Org. Chem. 72 (2007) 5668–5688.
- [34] S.E. Denmark, J.R. Heemstra, J. Am. Chem. Soc. 128 (2006) 1038–1039.
- [35] Reviews: (a) S.E. Denmark, J. Fu, Chem. Rev. 103 (2003) 2763–2793; (b) J.-A. Ma, D. Cahard, Angew. Chem. Int. Ed. 43 (2004) 4566–4583.
- [36] (a) Grubbs' 2nd generation catalysts: (1,3-bis-(2,4,6-trimethylphenyl)-2-imidazolidinylidene) dichloro(phenylmethylene)(tricyclohexylphosphine)ruthenium: (b) M. Lautens, M.L. Maddes, Org. Lett. 6 (2004) 1883–1886; (c) S. BouzBouz, R. Simmons, J. Cossy, Org. Lett. 6 (2004) 3465–3467; (d) A.K. Chatterjee, J.P. Morgan, M. Scholl, R.H. Grubbs, J. Am. Chem. Soc. 122 (2000) 3783–3784; (e) A.K. Chatterjee, T.L. Choi, D.P. Sanders, R.H. Grubbs, J. Am. Chem. Soc. 125 (2003) 11360–11370.
- [37] (a) G.E. Keck, K.H. Tarbet, L.S. Geraci, J. Am. Chem. Soc. 115 (1993) 8467–8468; (b) G. E. Keck, L.S. Geraci, Tetrahedron Lett. 34 (1993) 7827–7828; (c) D. Meng, D.-S. Su, A. Balog, P. Bertinato, E.J. Sorensen, S.J. Danishefsky, Y.-H. Zheng, T.-C. Chou, L. He, S.B. Horwitz, J. Am. Chem. Soc. 119 (1997) 2733–2734.
- [38] (a) P.K. Jadhav, K.S. Bhat, T. Perumal, H.C. Brown, J. Org. Chem. 51 (1986) 432–439; (b) H.C. Brown, N.N. Joshi, J. Org. Chem. 53 (1988) 4059–4062; (c) M. Lautens, M. L. Maddes, E.L.O. Sauer, S.G. Ouellet, Org. Lett. 4 (2002) 83–86; Salt free conditions: (d) U.S. Racherla, H.C. Brown, J. Org. Chem. 56 (1991) 401–404.
- [39] Allylations: (a) S.E. Denmark, J. Fu, D.M. Coe, X. Su, N. Pratt, B.D. Griedel, J. Org. Chem. 71 (2006) 1513–1522; (b) S.E. Denmark, J. Fu, M.J. Lawler, J. Org. Chem. 71 (2006) 1523–1536.
- [40] (a) J.A. Dale, H.S.J. Mosher, Am. Chem. Soc. 95 (1973) 512–519; (b) J.M. Seco, E. Quinoa, R. Riguera, Chem. Rev. 104 (2004) 17–117.
- [41] E.D. Langanis, B.L. Chenard, Tetrahedron Lett. 25 (1984) 5831–5834.
- [42] J. Inanaga, K. Hirata, H. Saeki, T. Katsuski, M. Yamaguchi, Bull. Chem. Soc. Jpn. 52 (1979) 1989–1993.
- [43] Removal of SEM from alcohols: CsF, HMPA (a) R.E. Ireland, D.W. Norbeck, J. Am. Chem. Soc. 107 (1985) 3279–3285; TFA (b) R.H. Schlessinger, M.A. Poss, S. Richardson, J. Am. Chem. Soc. 108 (1986) 3112–3114; Ammonium fluoride sources in HMPA or THF (c) T. Kan, M. Hashimoto, M. Yanagiya, H. Shirahama, Tetrahedron Lett. 29 (1988) 5417–5418; TBAF, MS 4 Å; DMPU (d) B.H. Lipshutz, T.A. Miller, Tetrahedron Lett. 30 (1989) 7149–7152; MgBr₂, *n*-BuSH, Et₂O (e) S. Kim, I.S. Kee, Y.H. Park, J.H. Park, Synlett. (1991) 183–184; MgBr₂, MeNO₂, Et₂O (f) A. Vakalopoulos, H.M.R. Hoffmann, Org. Lett. 2 (2000) 1447–1450; ZnBr₂, MeOH, Et₂O or MgBr₂, MeNO₂, Et₂O (g) A. Vakalopoulos, H.M.R. Hoffmann, Org. Lett. 3 (2001) 2185–2188; ZnX₂ in CH₂Cl₂ (h) H.C. Kolb, H.M. R. Hoffmann, Tetrahedron: Asymmetry 1 (1990) 237–250; MgBr₂, EtSH, Et₂O (i) D. B. Berkowitz, S. Choi, J.-H. Maeng, J. Org. Chem. 65 (2000) 847–860; SEM deprotection from phenol (j) (TBAF, HMPA) H. Saimoto, T. Hiyama, Tetrahedron Lett. 27 (1986) 597–600; P₂I₄ (k) H. Saimoto, Y. Kusano, T. Hiyama, Tetrahedron Lett. 27 (1986) 1607–1610; H₂SO₄ (l) T.L. Shih, M.J. Wyvratt, H. Mrozik, J. Org. Chem. 52 (1987) 2029–2033; TBAF, MS 4 Å, DMPU (m) M. Koreeda, L.A. Dixon, J.D. His, Synlett (1993) 555–556; HCl (n) T.L. Graybill, E.G. Casillas, K. Pal, C.A. Townsend, J. Am. Chem. Soc. 121 (1999) 7729–7746; “Anhydrous TBAF” (o) T. Sugimura, L.A. Paquette, J. Am. Chem. Soc. 109 (1987) 3017–3024; HF, CH₃CN (p) J.D. White, M. Kawasaki, J. Am. Chem. Soc. 112 (1990) 4991–4993; I₂, hv (q) S. Karim, E.R. Parmee, E.J. Thomas, Tetrahedron Lett. 32 (1991) 2269–2272.

- [44] Preparation of trialkylsilyloxymethyl chlorides: (a) S. Pitsch, P.A. Weiss, X. Wu, D. Ackermann, T. Honegger, *Helv. Chim. Acta* 82 (1999) 1753–1761; (b) S. Pitsch, P. A. Weiss, L. Jenny, A. Stutz, X. Wu, *Helv. Chim. Acta* 84 (2001) 3773–3795.
- [45] C. Gioeli, N. Balgobin, S. Josephson, J.B. Chattopadhyaya, *Tetrahedron Lett.* 22 (1981) 969–972.
- [46] (a) M. Sekine, M. Tobe, T. Nagayam, T. Wada, *Lett. Org. Chem.* 1 (2004) 179–182; (b) R.E. Shute, D.H. Rich, *Synthesis* (1987) 346–349.

Asymmetric Total Synthesis of the Antitumor Sesquiterpenoid (+)-Eremantholide A

Karl J. Hale and Yi Li

The School of Chemistry and Chemical Engineering, Queen's University Belfast, Belfast, Northern Ireland, United Kingdom

Chapter Outline

1. Prologue (Karl J. Hale)	127	3. The Hale–Li	
2. Introduction: Background and Previous Total Syntheses of (+)-Eremantholide A	131	Retrosynthetic Analysis of (+)-Eremantholide A	138
		4. The Hale–Li Total Synthesis of (+)-Eremantholide A	142

1. PROLOGUE (KARL J. HALE)

The present story has its origins in the summer of 1987 at the University of Pennsylvania where, one afternoon, Professor Amos B. Smith III very kindly invited me into his office for a quick informal chat about my next total synthesis project in his lab. His invitation followed our successful joint completion of a total synthesis of the phyllanthostatin natural products [1] and our collective desire to carry out another research project together.

I remember sitting there in Amos' office and his unveiling of a most enchanting set of exquisitely drawn out natural product structures. Each was characterized by a rich and highly decorated molecular framework that offered massive challenges for asymmetric total synthesis. Each molecule also had an intriguing biological profile that would render future analogue synthesis potentially worthwhile and insightful. The target molecules that were on offer that day were totally inspiring for the time, since synthetic organic chemistry was then in a far lower degree of refinement than it is currently,

and the preparation of compounds of that level of complexity presented massive scientific challenges.

I stared intently at Professor Smith's target list (part of which is shown in Figure 1), enthralled by the large number of unusual structures that were on show: extraordinary molecules such as penitrem D [2], (–)-FK506 [3], hitachimycin [4], (–)-echinosporin [5], breynolide [6], calyculin A [7], and (+)-eremantholide A, to name but a few, molecules that, in the vast majority cases, Professor Smith would later go on to synthesize [2–7]. I carefully surveyed each molecule, wondering what the future would hold with each possible choice. The key for me that day was to try to select a molecule that would offer excellent opportunities for new reaction development and novel chemistry. In the end, (–)-FK506 was the molecule I selected because of the

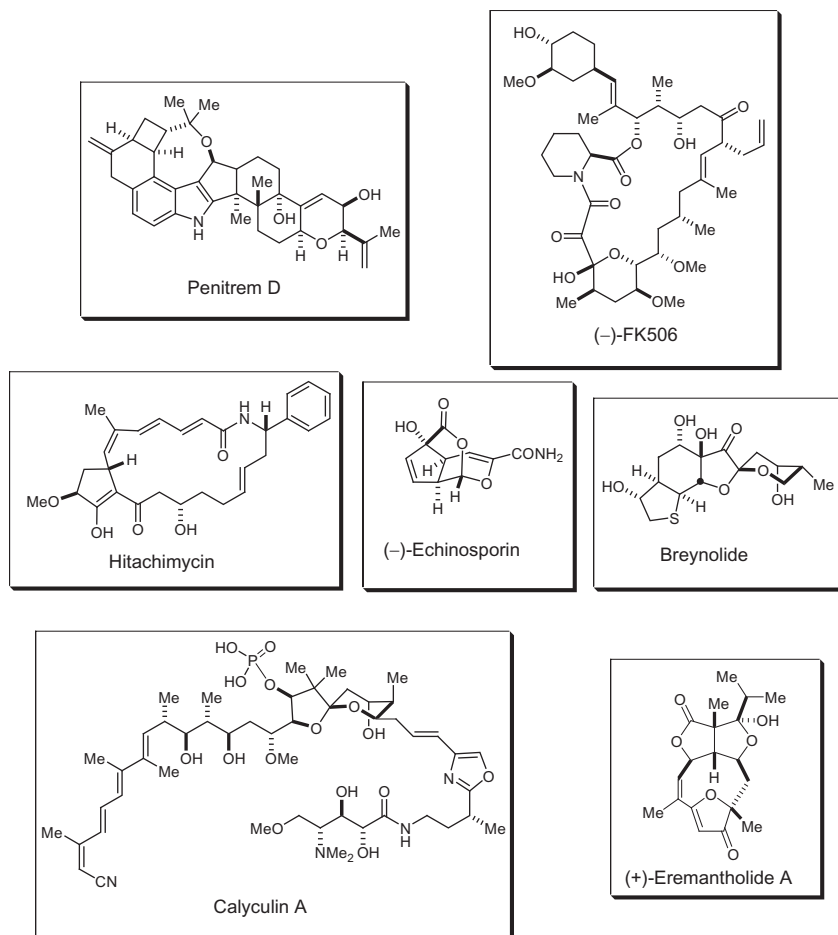
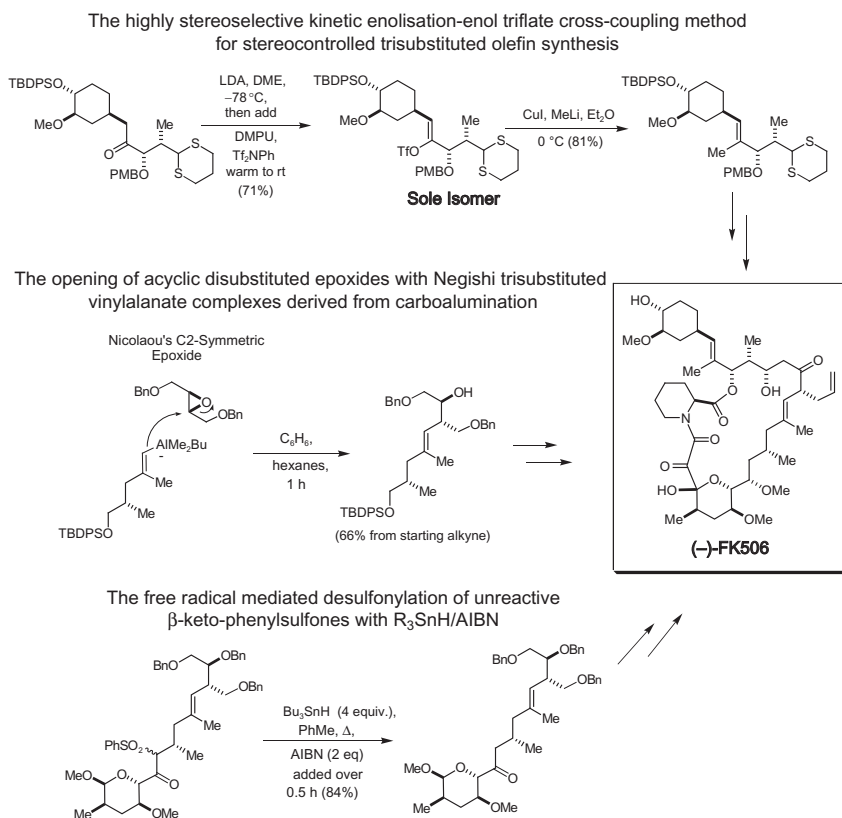


FIGURE 1 Some of the target molecules of the Amos B. Smith III group in 1997.

longstanding interest I had in stereocontrolled olefin synthesis in acyclic systems and because this structure presented me with the greatest opportunities to apply my very latest ideas in that sphere.

The rather unusual structure of (+)-eremantholide A also caught my eye but, with that particular molecule, I felt that it would probably be best to delay our future chemical encounter to some further point down the line, to a time when I had secured an independent academic position in a good university, and funding was available to carry out an independent synthesis.

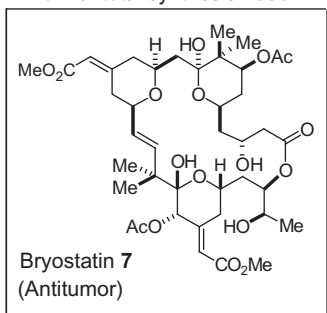
It transpired that my decision to work on the (–)-FK506 project was a good one, for considerable success accrued in that venture with Professor Smith [3,8–10]. The highly stereoselective kinetic enolization-enol triflate cross-coupling method [8] emerged as a powerful and highly predictable new method for constructing trisubstituted olefins in complex systems (Scheme 1). The viability of using Negishi trisubstituted vinylalane complexes to open up acyclic chiral disubstituted epoxides was also demonstrated



SCHEME 1 Some of the important new methodological advances that emerged from Amos B. Smith III's total synthesis of (–)-FK506.

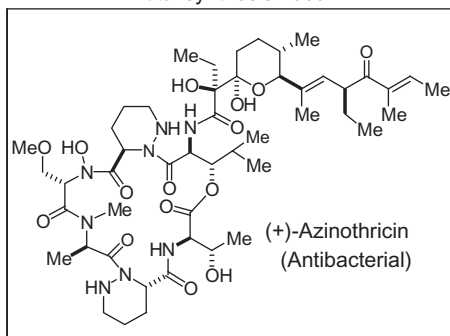
for the first time [9]. A new free radical-based method for the desulfonation of β -keto-sulfones [10] was also invented on our pathway to the challenging (–)-FK-506 structure. Because of the many excellent papers that flowed from that program, I managed to secure my very first permanent academic appointment at University College London (UCL), where Professor Robin J. H. Clark FRS hired me as a Lecturer in Organic Chemistry in August 1990.

Formal total synthesis 2006



Hale, Manaviyar et al. [11]

Total synthesis 2009



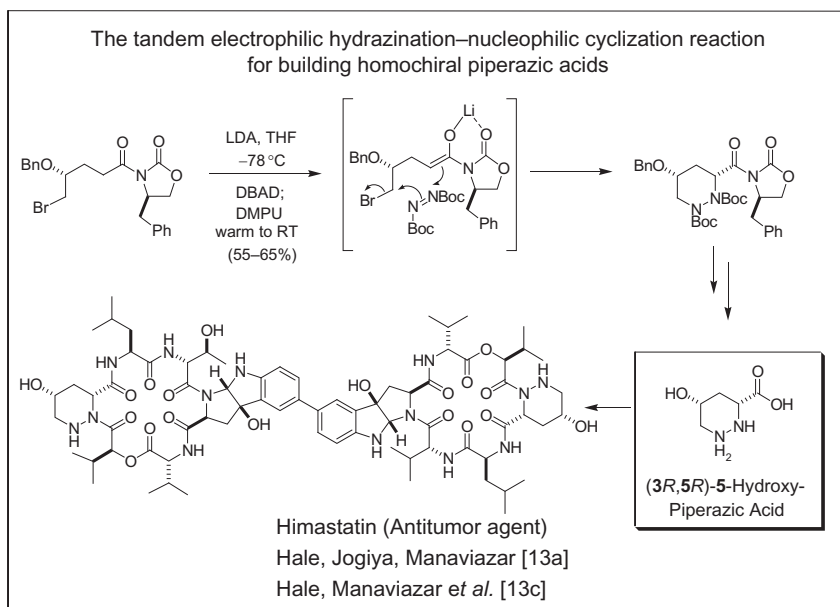
Hale, Manaviyar et al. [12a]

Hale, Manaviyar, George [12b]

In my early years at UCL, I decided to undertake the total synthesis of macrolide structures such as bryostatin 7 [11] and (+)-azinothricin [12], rather than (+)-eremantholide A. My reasons for this were twofold. First, I believed that I would have a much better chance of securing research funding for proposals that were submitted on the former two molecules, due to their exceptional bioactivity. Second, I felt that these two targets would offer greater opportunities for publishing syntheses of various advanced fragments. Clearly, such publications could help establish my group's credentials for doing independent high-level total synthesis in the complex natural product arena, and I considered this to be an important priority at this early stage in my career. I also believed that these two target molecules would be much more likely to yield important new methodological discoveries rapidly, and in the case of (+)-azinothricin, the tandem asymmetric electrophilic hydrazination–nucleophilic cyclization method [13] ultimately emerged as a powerful new method for building up piperazic acid structures (Scheme 2).

While my long-term objective of synthesizing (+)-eremantholide A still endured throughout my first decade at UCL, I recognized that the challenges posed by this particular target would almost certainly involve me in a lengthy battle royal and good papers would probably only emerge at the very final stages of this project, after the molecule had ultimately succumbed to full total synthesis.

I also had to address the challenging issue of securing the very considerable funding that would be required to commence such a venture. However,



SCHEME 2 Tandem asymmetric electrophilic hydrazination–nucleophilic cyclization.

good fortune did eventually smile on me in 2003, when the UK EPSRC awarded me a 3-year postdoctoral project grant to begin our group's work on the total synthesis of (+)-eremantholide A, which ultimately led to my recruiting the talented postdoctoral fellow, Dr Yi Li, from Professor Tony Barrett's group at Imperial College. The scene was thus set for the tale that Dr. Li and I are now about to tell about our total synthesis of (+)-eremantholide A.

2. INTRODUCTION: BACKGROUND AND PREVIOUS TOTAL SYNTHESSES OF (+)-EREMANTHOLIDE A

In 1975, Le Quesne and Brennan reported the isolation and structure determination of the structurally novel sesquiterpenoid, (+)-eremantholide A [14]. They had encountered this molecule in the extracts of aerial parts of the Brazilian shrub *Eremanthus elaeagnus*. Its structure was elucidated by single-crystal X-ray analysis, which revealed the presence of an extraordinarily complex, multiply-annulated, ring system in which there was a unique dioxabicyclo[3.3.0]octanone grafted onto a nine-membered oxonene that itself was partially juxtaposed upon a 3(2*H*)-furanone. Importantly, the significant ring strain that was present within the nine-membered oxonene was sufficiently high to distort the C(4)—C(5)-double bond out of conjugation from the 3(2*H*)-furanone structure, and when considered alongside the remaining

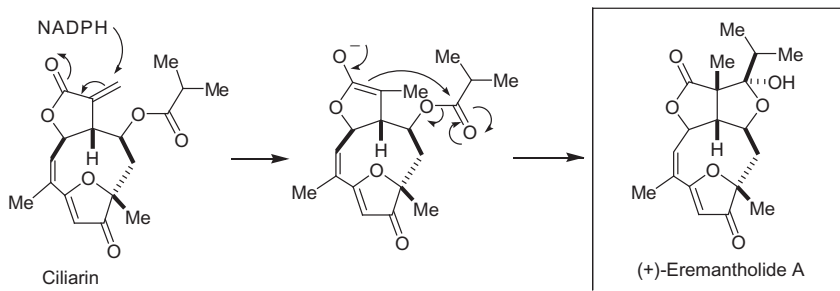
stereochemical complexity of the molecule, these combined features made this a target of the very highest quality and challenge for asymmetric total synthesis.

The primary reason why Le Quesne and Brennan went to such efforts to elucidate the molecular structure of (+)-eremantholide A was because of its very pronounced growth inhibitory effects against human KB nasopharyngeal carcinoma cells at 2 $\mu\text{g/mL}$ [14]. Such data helped establish its credentials as a potentially novel drug design lead.

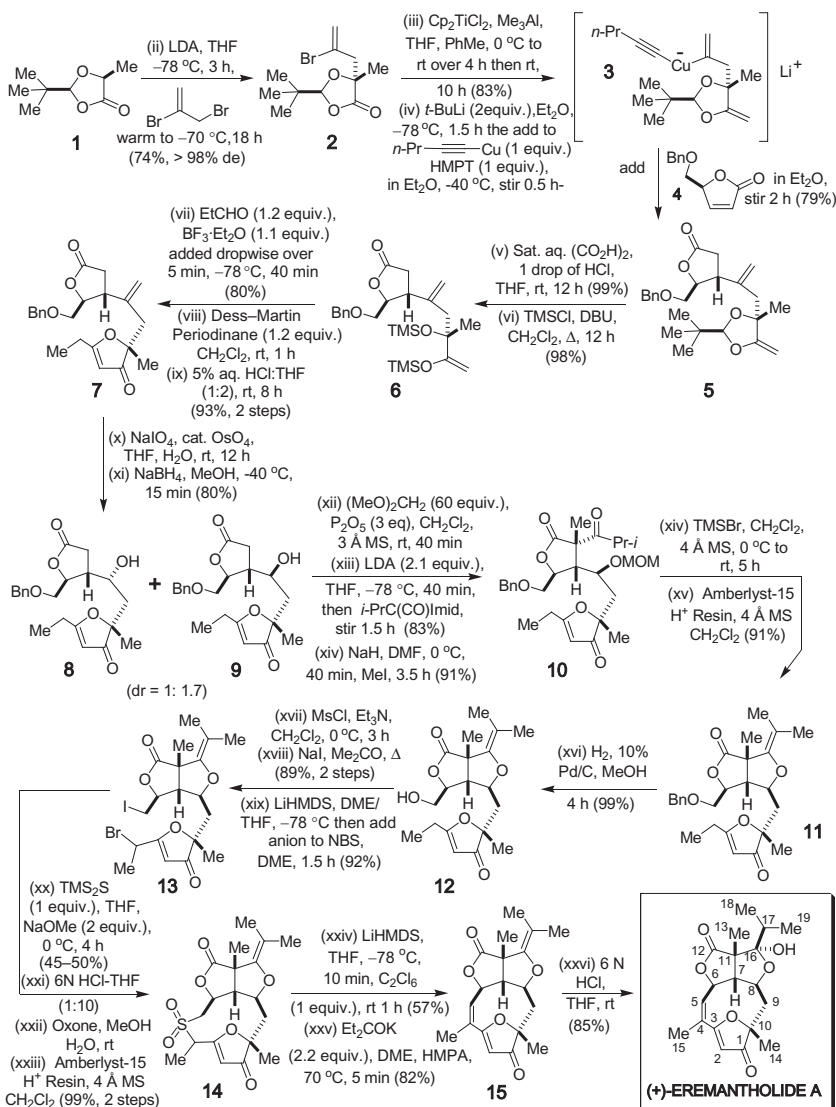
As regards biosynthetic provenance, nothing conclusive has ever been established for (+)-eremantholide A. The only clue as to its possible biosynthetic origins came from Le Quesne and Brennan's proposal that it is generated from ciliarin by NADPH-mediated 1,4-reduction and internal Dieckmann cyclization, although no experimental evidence was ever gathered to support this hypothesis (Scheme 3) [14].

The first ever total synthesis of (+)-eremantholide A was by Boeckman and coworkers in 1991 (Scheme 4) [15]. The Rochester synthesis stands out not only for its extraordinary beauty and simplicity of design but also for the logic of its planning, and the many unusual reactions it expounds *en route* to the final target. Indeed, one of the more noteworthy reactions it exemplified for nine-membered oxonene ring construction was the Ramberg–Backlund rearrangement. At the time, this represented a completely new methodological departure for building up such strained ring systems.

Boeckman's synthesis set off with the highly stereoselective 1,4-conjugate addition of cuprate **3** to butenolide **4**, which delivered the chiral butyrolactone **5** as a single product in 79% yield. Cuprate **3** was itself created from the known lactone **1** by a three-step sequence that commenced with Seebach enantioretentive C-alkylation to afford **2**. Tebbe olefination of **2** converted it to the corresponding enol ether, and metal–halogen exchange and transmetalation led to organometallic **3**. The transmetalation was performed with pentynylcopper, which allowed a nucleophilic delivery of only 1 equiv. of the precious transferrable vinylmetal unit to **4**.



SCHEME 3 Le Quesne and Brennan's biosynthetic proposal for (+)-eremantholide A.



SCHEME 4 Boeckman's 1991 synthesis of (+)-eremantholide A.

With **5** in hand, the 3(2*H*)-furanone moiety was elaborated by a multi-step procedure that involved aqueous oxalic acid-induced cleavage of the enol ether moiety, silyl enol ether formation with TMSCl/DBU, $\text{BF}_3\cdot\text{Et}_2\text{O}$ -mediated aldol reaction of **6** with propionaldehyde, Dess–Martin oxidation of this aldol to obtain the 1,3-diketone, and finally, acid-induced cyclization. This combined set of reactions proceeded without a hitch to deliver **7** in high yield.

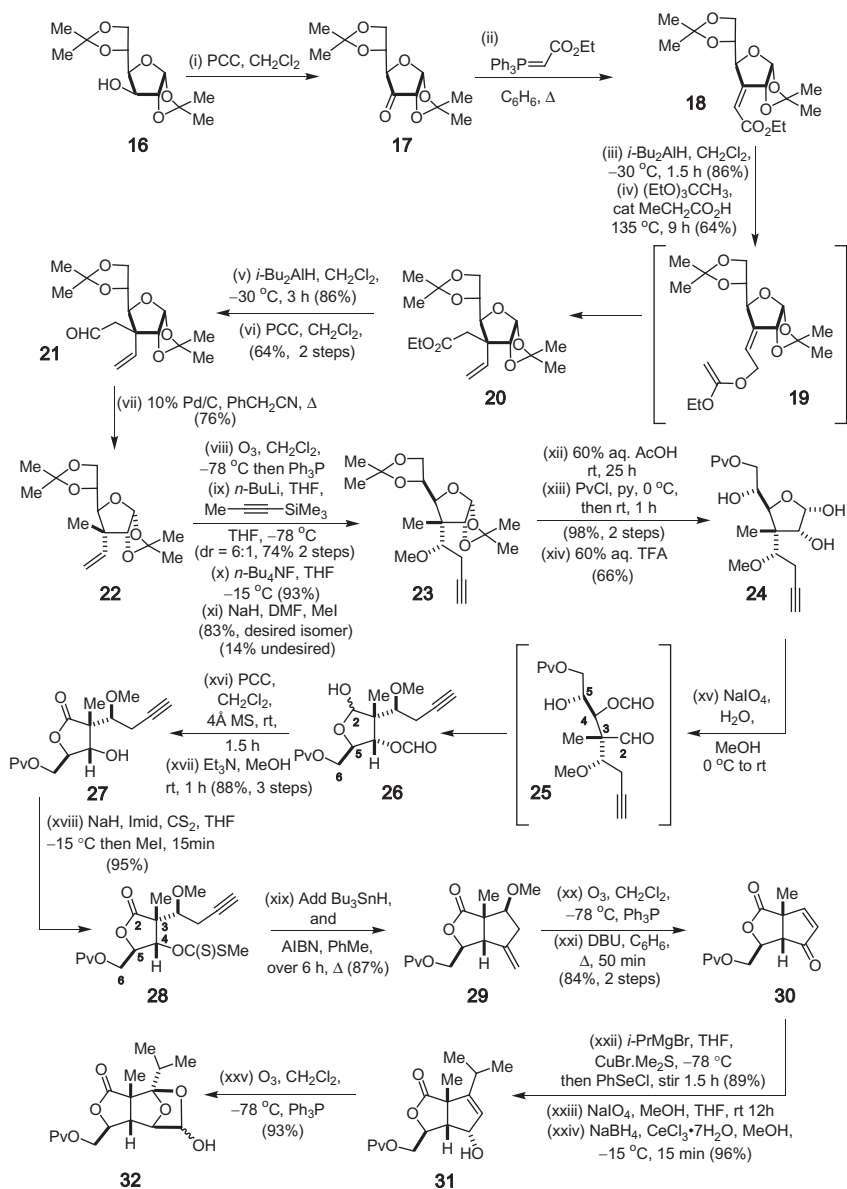
Having served its purpose in allowing the C(7)-stereocenter to be installed with high stereocontrol, the olefin at C(8) was oxidatively degraded with catalytic osmium tetroxide and sodium periodate to give a ketone that was reduced with sodium borohydride in methanol at low temperature (-40°C). The latter process furnished a mixture of two epimeric alcohols **8** and **9** in 1:1.7 ratio, but fortunately, these were both readily separable by SiO_2 flash chromatography with the minor component **8** being recyclable by oxidation and borohydride reduction.

MOM-protection of **9** and a double enolization-trapping sequence next procured **10** with high stereocontrol, and TMSBr-induced cleavage of the MOM-group thereafter allowed hemiketalization to proceed. Dehydration of this hemiketal was now deemed operationally strategic for performing the key chemical conversion of this intermediate into **13**. The dehydration was itself effected with Amberlyst-15 H^+ resin in CH_2Cl_2 and furnished **11** in 91% yield. Hydrogenation thereafter cleaved the *O*-benzyl group without perturbation of any of the alkenic bonds. Two-step iodination of the alcohol in **12** and enolate bromination thereafter afforded **13**.

A Harpp–Ando double thioalkylation was now effected on **13** with sodium methoxide and TMS_2S . It afforded the desired thioether in 45–50% yield. Because the B-ring enol ether of this product was highly susceptible to oxidative damage when exposed to oxone, Boeckman temporarily hydrated this feature, thereby allowing oxidation of the sulfide to the cyclic sulfone. However, the newly installed hemiketal-OH did need to be excised subsequently to allow the requisite chloro substituent to be installed at C(4) and permit implementation of the desired Ramberg–Backlund rearrangement. The latter chlorination was best performed with LiHMDS and 1,1,1,2,2,2-hexachloroethane at -78°C .

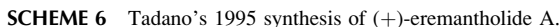
Brief treatment with Et_3COK in HMPA and DME at 70°C was all that was needed to bring about the desired ring closure and the accompanying tri-substituted olefin-forming event. The product **15** was formed in 82% yield by this method, and this thereafter allowed a highly chemoselective hydrolysis of the exocyclic enol ether at C(16) to give (+)-eremantholide A in 85% yield, completing what was a truly excellent synthesis.

The next synthesis of (+)-eremantholide A to be accomplished was that of Tadano and coworkers at Keio University in 1995 [16]. Their route (Schemes 5 and 6) set off from commercially available diacetone D-glucose **16** and had many appealing features. Although much longer than Boeckman's original 1991 strategy (40 steps from **16**), its main synthetic highlights were the novel way in which it formed the quaternary center at C(11), its imaginative and highly concise strategy for setting the dihydrofuranone quaternary center at C(10), and its novel aldol/elimination tactic for building up the strained nine-membered oxonene system. All these were interesting pieces of chemistry in their own right and broke much new methodological ground at the time of publication. Tadano's opening move was to set the quaternary



SCHEME 5 Tadano's 1995 synthesis of (+)-eremantholide A.

center at C(11) of the target. For this, he assembled the Johnson orthoester Claisen rearrangement substrate **19** by a four-step sequence that commenced with the PCC oxidation of **16** to afford **17**. Subsequent Wittig olefination gave **18** in 75% yield, alongside an 18% yield of its opposite (*Z*)-geometric isomer.



The ester group in **18** was then reduced with DIBAL and the allylic orthoester **19** fashioned by treatment with triethyl orthoacetate in the presence of a catalytic amount of propionic acid. Heating of this substrate for 9 h at 135 °C afforded a single rearranged product **20** in 64% yield, where the newly introduced quaternary stereocenter was set with complete stereocontrol. A DIBAL reduction now transformed this ester into an alcohol that was reoxidized to the aldehyde **21**. Then, in a truly noteworthy step, Tadano effected the very efficient thermal decarbonylation of **21** in benzonitrile at reflux over 30 min using 10% Pd/C (50% wt. with respect to **21**) as the reaction mediator.

Typically, one sees thermal decarbonylations of this sort performed with Rh (I)-type catalysts. However, such reactions can often be difficult to effect in complex substrates of this sort, and so this most useful new alternative (that often gives superior results) is of special interest, most especially since Pd is much less expensive than Rh.

With **22** now acquired, its manipulation into **23** and thereafter **24** was investigated. Ozonolysis delivered an aldehyde that reacted with the anion of 1-(trimethylsilyl)propyne to give a 6:1 mixture of adducts enriched in the desired product. C-desilylation with TBAF and O-methylation with NaH/MeI subsequently furnished a separable mixture of epimers from which the desired product **23** was isolated in 83% yield. Its 5,6-*O*-isopropylidene acetal (sugar numbering) was then hydrolyzed by 60% aqueous acetic acid, the resulting diol selectively *O*-pivaloylated, and the 1,2-*O*-acetal clipped off with 60% aqueous trifluoroacetic acid. The product diol **24** was then oxidatively degraded to give aldehyde **25**, which immediately internally engaged the C(5)-hydroxyl to give the hemiacetal **26**, which itself was oxidized with PCC and *O*-deformylated to obtain **27**.

The plan now was to effect a free radical cyclization of the xanthate **28** to obtain **29**, ozonize the exocyclic alkene to expose a cyclopentanone, and thereafter effect a β -elimination of the OMe group to secure **30**. All these reactions worked well and nicely set the stage for isopropylcuprate addition, *in situ* enolate trapping with PhSeCl, and subsequent selenoxide elimination and Luche reduction to afford the allylic alcohol **31**. This combined set of reactions very nicely set the C(7)- and C(8)-stereocenters of the target with complete stereocontrol and concurrently positioned the isopropyl group needed in ring B. However, in cyclopentene **31**, all these features were in a latent format and were only revealed after an ozonolysis of the cyclopentene unit in **31**, which unveiled **32**, in which the newly set C(8)-hydroxyl cyclized upon the unmasked ketone and the resulting hemiketal in turn was internally trapped by the C(9)-aldehyde.

In order to release the C(9)-O-atom from this internal hemiacetal **32**, it was carefully reduced at low temperature ($-50\text{ }^{\circ}\text{C}$) with sodium borohydride, taking care not to over-reduce the newly liberated hemiketal whose primary alcohol was subsequently *O*-acetylated. This tactic proved necessary because an internal ketalization of the C(9)-hydroxyl onto that hemiketal proceeded when attempts were made to prepare the methyl glycoside by Fischer glycosylation. *O*-acetylation prevented this, so allowing the methyl glycoside **34** to be formed. Although the *O*-acetate in **34** could be detached selectively, and the resulting alcohol converted to a triflate ester, this intermediate reacted with the kinetic K^+ -enolate derived from **39** in an unsatisfactory manner. Accordingly, other *O*-protecting groups were now positioned at C(5) and similar couplings with **39** attempted. Eventually, it was found that triflate **38** reacted with the kinetically generated potassium enolate of **39** to give a 2.59:1 mixture of **40** and **41** enriched in the desired product **41**. This really

was a big breakthrough, for it very nicely allowed the difficult C(10)-quaternary center to be rapidly set and it also established the challenging C(9)—C(10)-bond. It thus allowed the synthesis of (+)-eremantholide A to be completed by a four-step sequence that commenced with base-mediated intramolecular aldol cyclization of **42**, under conditions of quite high dilution (0.01 M), which proceeded in 41% yield over two steps. The aldol adducts were then dehydrated by O-mesylation and DBU-promoted elimination, and the methyl glycoside finally detached by simple 6 M aqueous HCl acid hydrolysis to complete the synthesis.

3. THE HALE-LI RETROSYNTHETIC ANALYSIS OF (+)-EREMANTHOLIDE A

Apart from the intrinsic chemical challenge that (+)-eremantholide A provides for asymmetric total synthesis, we had other reasons for undertaking this exercise [17], and one of these centered around the desire to find out more about the possible mechanism(s) of antitumor action of this compound [18]. Nothing had ever been reported on this topic at the very outset of our work, and it was our belief that a new pathway to this structure might potentially facilitate the creation of novel biotinylated probe molecules that could assist us in cancer cell lysate protein retrieval by affinity chromatographic methods. The latter, in turn, might potentially yield novel new protein targets of central importance to human cancer onset and progression and assist our oncological drug discovery efforts, which is a major priority of our laboratory.

Another exciting possibility with such biotinylated probes could come from their use as chemical inducers of protein dimerization within yeast cells. (Figure 2) Such cells could be genetically engineered to express all of the proteins found inside a human cancer cell but appended to a Gal4-transactivation domain. Significantly, they could also be engineered to express a streptavidin-Gal4 DNA-binding domain that could control a His-3 reporter gene which, in turn, could undergo transcriptional activation when a biotinylated-eremantholide probe had entered inside the yeast and bound to a candidate Gal-4-tagged target oncogenic protein expressed within the cell. This is the so-called yeast three-hybrid technology [19]. The latter is potentially a more sensitive and illuminating technique than affinity chromatography, as it can allow every protein that binds to a small molecule drug to be identified and later expressed in *Escherichia coli*. Another reason for synthesizing (+)-eremantholide A would be to access a synthetic sample that could be more thoroughly screened as an antitumor agent. An appropriately designed synthetic strategy could also potentially test out the likely chemical validity of the Le Quesne–Brennan biosynthetic proposal [14] and be modified to provide other novel analogues for biological testing.

With all these considerations in mind, we initially formulated the retrosynthetic plan shown in Scheme 7 for the securement of (+)-eremantholide A [17]. It was predicated upon asymmetric alkylation of the AB-iodide **46**

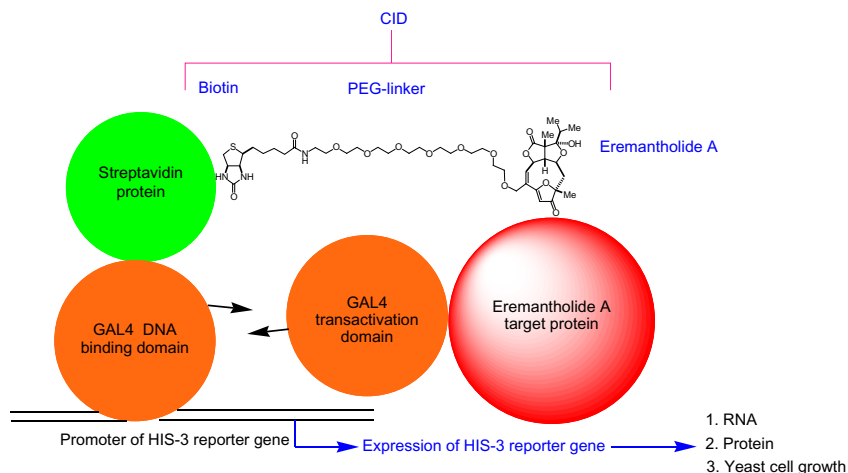
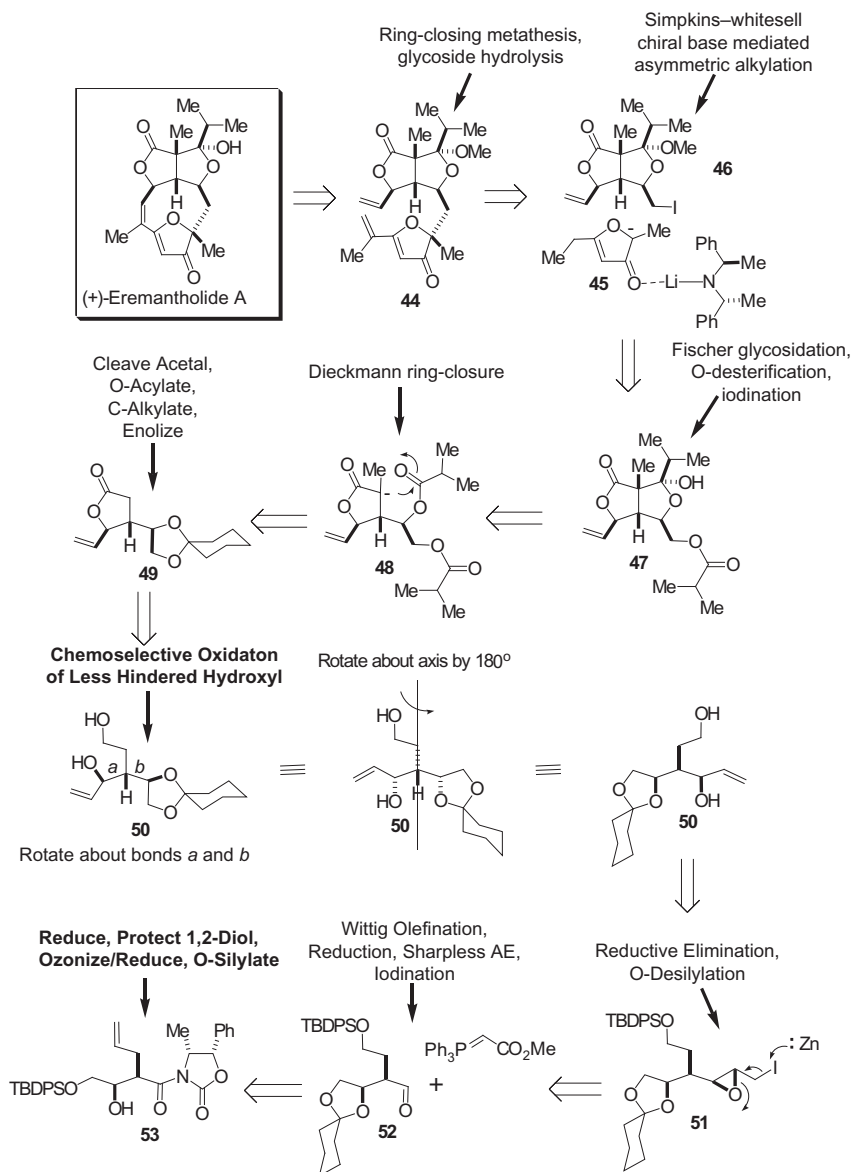


FIGURE 2 A possible way of isolating Gal4-transactivation domain-tagged oncogenic proteins via yeast three-hybrid technology [19]. This shows the potential use of a biotinylated-eremantholide as a chemical inducer of protein dimerization (CID) to create a functionally active heterodimeric Gal4 transcription factor that could turn on HIS-3 transcriptional activation and yeast cell growth when an eremantholide-binding protein had been captured inside the yeast.

with the 3(2*H*)-furanone kinetic enolate **45** generated from **39** [20] using the Simpkins–Marshall–Whitesell chiral lithium amide base [21]. Although Professor Simpkins has reported some truly excellent results on the asymmetric deprotonation of functionalized nonsymmetric ketones with various chiral bases when his methodology has been allied with enolate trapping using silyl halides, we were curious to investigate whether such bases could have a beneficial effect on the stereochemical course of the direct alkylation of 3(2*H*)-furanone kinetic enolates. Why we wished to use a chiral enolate in the present synthesis was because we were cognizant of Tadano's earlier work on the alkylation of **38** with **39** (Scheme 6), where he showed that the nature of A-ring C(6)-substituent could profoundly affect the stereochemical course of alkylation. In the present instance, we were desirous of having a vinyl substituent emanating from that carbon, and given that we were conscious that it would be a much smaller group than the $-\text{CH}_2\text{OTBDPS}$ system found in **38** (see Scheme 6), we thought that a stereochemically matched chiral enolate might have a beneficial influence on reaction outcome to favor the desired C-alkylation product. Olefin elaboration could then take place at C(4) to give the triene **44**, which then presented an intriguing and previously unprecedented test case for Grubbs ring-closing metathesis (RCM).

The RCM of **44** would be challenging for several reasons. First and foremost, the ring closure would have to be effected on a triene substrate whose 3(2*H*)-furanone could itself open up and react in an unpredictable way. Second,



SCHEME 7 The Hale-Li initial retrosynthetic synthesis of (+)-eremantholide A.

the nine-membered oxonene ring undergoing construction was very highly strained and, as such, it could possibly undergo rapid ring-opening, once closed, followed by cross-metathesis and polymerization, which might relieve ring strain. Together these complicating issues could potentially break our planned synthesis at its very final stages.

However, on a more positive note, there would be considerable “turn” character within triene **44** imposed by its three connected rings and the 1,1,-disubstituted alkene emanating from C(3) of the 3(2*H*)-furanone. When allied with the potentially powerful Thorpe–Ingold effect that would be imparted by the C(10)-quaternary substituent in this cyclization precursor, these collective facets could work positively to assist the final ring-closure event. Of course, what we are basically saying here is that it was simply not possible to be certain about the outcome of this RCM reaction *a priori*, and that actual real-life investigation would be a necessity. Obviously, if it worked well, this could perhaps make us dramatically rethink the application of RCM reactions in the construction of highly strained oxonene rings, most especially if the starter substrates had beneficial conformation-constraining influences.

If successful, the ring closure of **44** could ultimately link into Tadano’s final intermediate, the methyl glycoside of (+)-eremantholide A, and based upon his previous findings, we could be highly confident that this precursor of the natural product could be successfully hydrolyzed with 6*N* aqueous HCl.

Naturally, it would be essential to have a fallback position in the event of failure with this high-risk RCM step on **44**. In this regard, we would convert the primary alcohol precursor of iodide **46** into Tadano’s advanced AB-intermediate **37** (see [Scheme 6](#)) and again intersect with his route, but potentially we would now build up his advanced intermediate in far fewer steps.

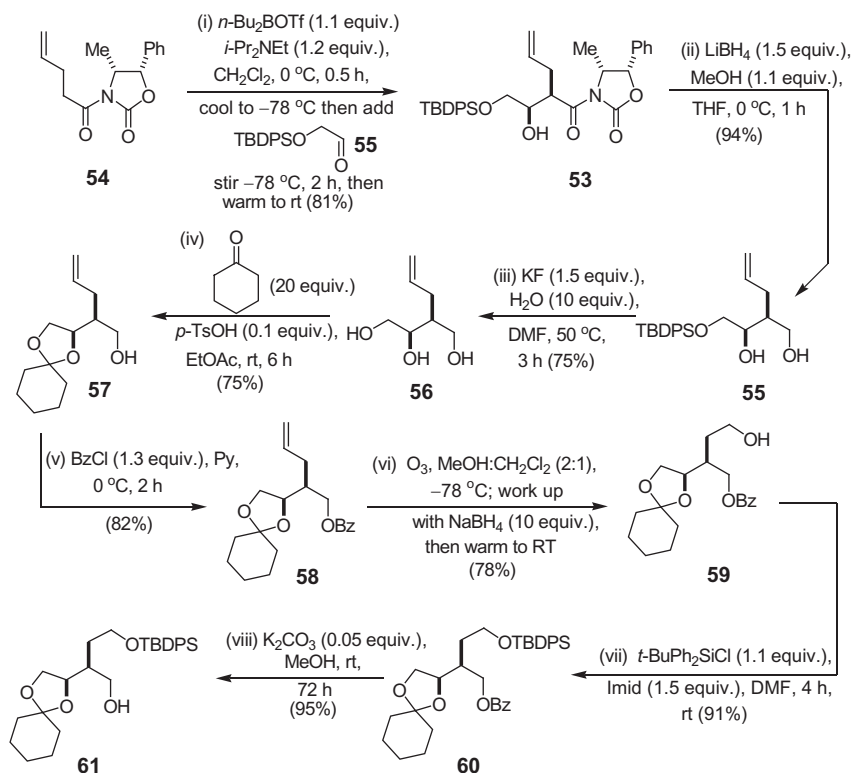
With iodide **46** selected as a key subtarget, we retrosynthetically worked toward the bicyclic hemiketal **47** as a precursor and we envisioned Fischer glycosidation with methanol, deesterification, and iodination as the reactions needed in the forward direction. Of course, selecting **47** as an intermediate now raised the interesting possibility of testing out the feasibility of the Le Quesne/Brennan biosynthetic hypothesis to some degree, since, clearly, if we could somehow selectively generate the enolate **48**, by conventional deprotonation methods, we might be able to successfully arrive at **47**. If we did, then this would at least illustrate that the Le Quesne/Brennan biosynthetic proposal was on track from a Dieckmann ring-closure perspective. Naturally, if it failed, we would still have to seek another potential genesis of iodide **46**, but we felt that this could be achieved from lactone **49**.

With **49** selected, we now had to think about how it could be prepared. One possible avenue to **49** was to chemoselectively oxidize the less hindered primary alcohol in **50**, internally hemiacetalize the resulting hydroxy-aldehyde, and then further oxidize. However, this was a high-risk approach, since although the secondary-OH in **50** would be more hindered, it would be significantly more electronically activated by virtue of it being allylic, which would render it fairly nucleophilic toward many reactive electrophilic oxidants, and therefore potentially oxidizable. Therefore, this was a significant worry for us but, with due oxidant screening, we felt that such an obstacle might be surmounted. We now duly rotated bonds a and b in structure **50**, and thereafter, we rotated the resulting projection about the imaginary axis

depicted in [Scheme 7](#) to expose all the *syn*-arrangement of stereocenters shown, which itself would be crafted through the implementation of a reductive elimination on iodide **51**. The latter would be fashioned through Wittig olefination, ester reduction, Sharpless asymmetric epoxidation [\[22\]](#), and iodination. The *syn*-stereochemistry within protected aldol **52** naturally called for an Evans' asymmetric aldol reaction to fashion adduct **53**.

4. THE HALE-LI TOTAL SYNTHESIS OF (+)-EREMANTHOLIDE A (**17**)

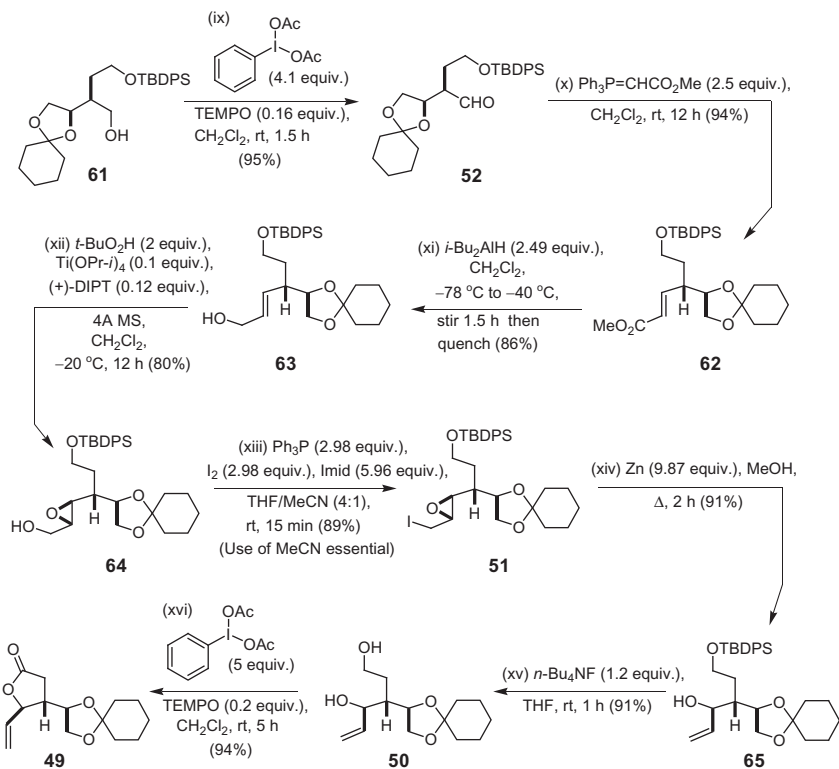
The aforementioned low-temperature Evans' aldol reaction [\[23\]](#) between oxazolidinone **54** and aldehyde **55** [\[24\]](#) delivered a single *syn*-aldol adduct **53** in 81% yield ([Scheme 8](#)). The chiral auxiliary was then reductively removed with LiBH_4 in MeOH/THF to give the diol **55**, which was O-desilylated with KF in aqueous DMF to provide the triol **56** in 71% combined yield. Although $n\text{-Bu}_4\text{NF}$ was also very effective at cleaving the TBDPS group from **55**, it proved extremely difficult to rid **56** of tetrabutylammonium salt by-products,



SCHEME 8 The Hale and Li asymmetric aldol route to alcohol intermediate **61**.

which eventually made KF the ideal choice for performing this particular operation. Next, we selectively protected the terminal 1,2-diol grouping in **56** to allow the C(6) primary alcohol to be selectively manipulated at a later point in the route. For this, O-cyclohexylidenation with cyclohexanone and *p*-TsOH proved optimal [25]; the desired alcohol **57** was formed in 75% yield and none of the 1,3-dioxane was detected in the reaction mixture. Following O-benzoylation of **57** with benzoyl chloride and pyridine, the double bond of **58** was ozonolytically cleaved and the resulting ozonides were reduced with NaBH₄; alcohol **59** was isolated in 78% overall yield. The latter was then O-silylated to obtain **60**, and its *O*-benzoate group was removed with K₂CO₃/MeOH (without inducing O-silyl migration). The desired alcohol **61** had now been appended with protecting groups appropriate for further oxidation and Wittig homologation.

Various methods were investigated for converting the alcohol **61** into aldehyde **52** (Scheme 9) including Swern oxidation (COCl₂/Me₂SO), which rather surprisingly, caused catastrophic loss of the cyclohexylidene grouping. Most unusually, the normally reliable catalytic TPAP/NMO oxidation [26] protocol



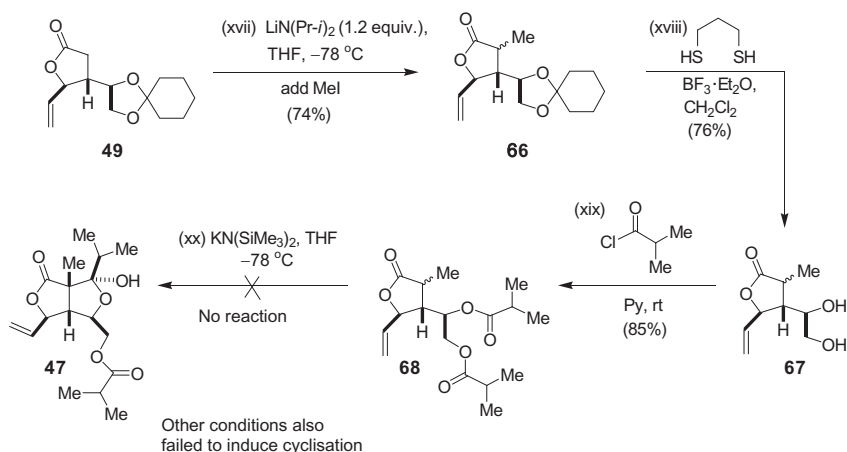
SCHEME 9 The Hale and Li route to lactone **49**.

also proved problematical in this system, causing significant epimerization (ca. 10–15%) of the C(7) stereocenter, notwithstanding it performing efficiently in the actual chemical conversion of **61** into the aldehyde (95% yield). As a result, we evaluated alternative oxidants for accomplishing this transformation, and after much effort, we eventually discovered that catalytic TEMPO and excess [bis(acetoxy)iodo]benzene (BAIB) [27] in CH_2Cl_2 were able to successfully produce the desired aldehyde **52** without causing any epimerization at C(7). Aldehyde **52** was thereafter condensed with carbomethoxymethylene triphenylphosphorane in CH_2Cl_2 to give the (*E*)-enoate **62** as a single geometric isomer in 94% yield.

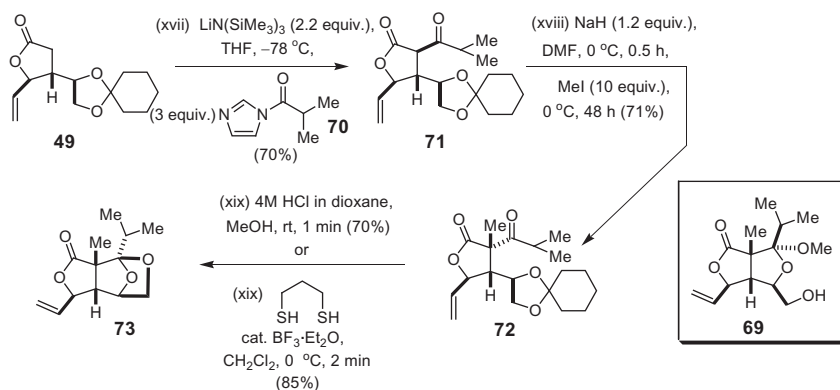
Compound **62** underwent smooth reduction to **63** with DIBAL-H in $\text{PhMe}/\text{CH}_2\text{Cl}_2$ at -78°C over a 1.5 h period. However, it was most important to preserve the temperature of this reduction at -78°C throughout, otherwise unwanted cleavage of the primary TBDPS group began to occur, even at temperatures as low as -40°C . However, by sticking to the -78°C procedure, excellent results (86% yield) were generally obtained. With the desired allylic alcohol **63** in hand, we now proceeded to investigate the Sharpless asymmetric epoxidation needed to secure 2,3-epoxy alcohol **64**. Again, the latter was produced with high stereocontrol, as essentially a single diastereoisomer. It was immediately iodinated at room temperature with Ph_3P , I_2 , and imidazole [28] in THF and MeCN. Significantly, the inclusion of MeCN as a solvent proved critical to the success of this reaction, enabling the desired iodo epoxide **51** to be formed efficiently in good yield (89–97%). Treatment of **51** with Zn dust in MeOH then effected the desired reductive elimination process to provide the allylic alcohol **65** in 91% yield. O-Desilylation with *n*- Bu_4NF now followed to provide **50**. We did attempt the direct conversion of epoxy alcohol **64** into **65**, using Yadav's titanocene chloride ($\text{Cp}_2\text{TiCl}/\text{THF}$) reduction procedure [29]. Disappointingly, we were unable to detect any alkene **65** in the reaction mixture.

The time had now come for us to attempt the all-important chemoselective oxidation of **50** into the chiral butyrolactone **49**. Following a thorough evaluation of the many different oxidants reported to be effective for generating γ -butyrolactones from 1,4-diols, we eventually discovered that the catalytic TEMPO/BAIB oxidation system [27] was highly effective at delivering the desired lactone **49** in 94% yield. To our surprise, the TPAP/NMO proved nonselective in this capacity, which was most unusual since both our own group and that of Steve Ley have successfully used TPAP/NMO to chemoselectively oxidize such systems [30,31]. However, the secondary alcohol in **50** is not especially hindered, and given its electronic activation by the proximal double bond, the latter undoubtedly imparts significant nucleophilicity on this hydroxyl, making chemoselectivity more difficult to achieve with this oxidant.

With our pathway to lactone **49** secure, attention turned to the synthesis of diol **67**, which was accessed by successive LDA-mediated alkylation with



SCHEME 10 Our failed attempt at building up **47** via Dieckmann ring closure.



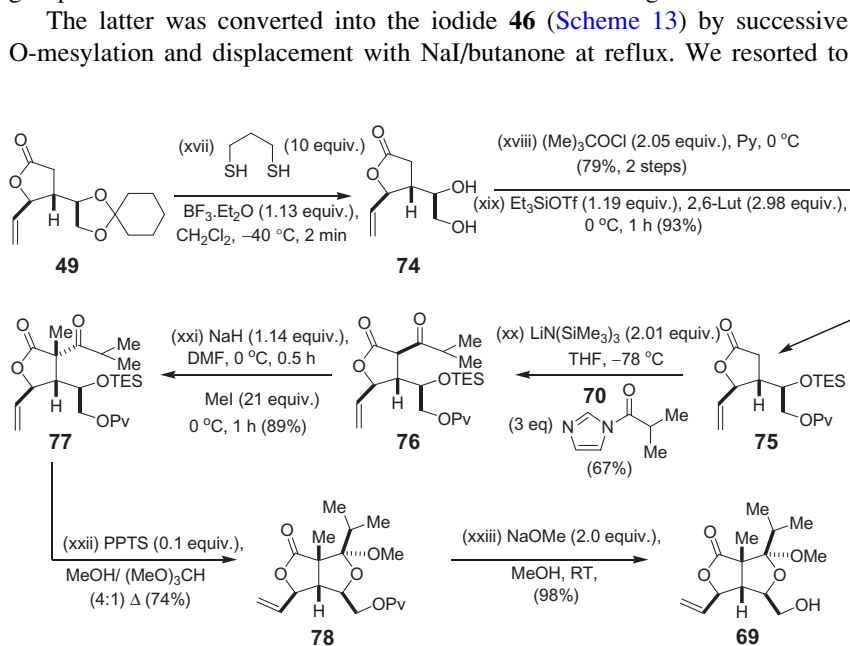
SCHEME 11 Our initial failed attempts at securing alcohol **69** that led to **73** instead.

MeI (which proceeded nonstereoselectively) and O-deacetalization of **66** induced by boron trifluoride etherate and 1,3-propanedithiol (Scheme 10) [25]. Diol **67** was thereafter O-acylated with isobutyryl chloride to afford the dibutyrate **68** in 85% yield. We next investigated the KHMDS-induced “kinetic” enolization of lactone **68** at -78°C in THF and PhMe, on multiple occasions, but always a mixture of slower-moving products was formed, with nothing corresponding to the desired hemiketal **47** ever being isolated.

As a result of this failure, the synthesis of alcohol **69** (Scheme 11) became our new objective. Initially, we successfully C-acylated **49** with isobutyryl imidazolidide **70** and thereafter C-methylated the resulting β -keto ester **71** with NaH/MeI but observed that the subsequent Fischer glycosidation of **72** with MeOH/(MeO)₃CH/PPTS did not yield any of the desired methyl glycoside **69**. Further, when 4 M HCl in dioxane and dry methanol were used for this Fischer

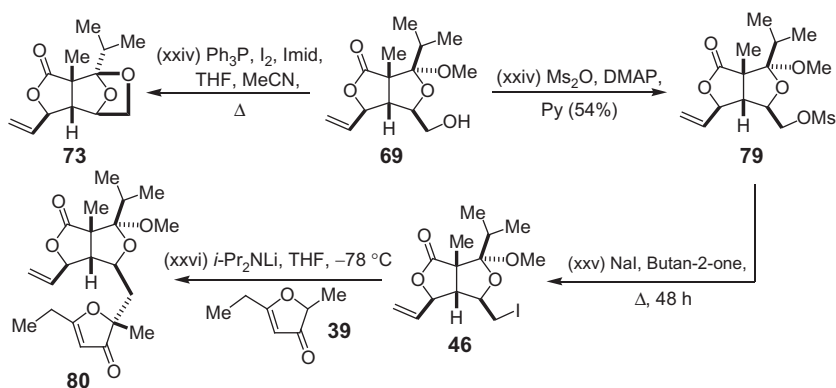
glycosidation at room temperature, the internal acetal **73** was formed involving the C(9) oxygen (Scheme 11), and this subsequently proved extremely difficult to manipulate. Likewise, when we attempted to prepare the 1,3-dithiane derivative of ketone **72** while simultaneously deprotecting the cyclohexylidene acetal, yet again, the only product that we could isolate was **73** in 85% yield.

In light of these problems, we elected to cleave the cyclohexylidene grouping from **49** with 1,3-propanedithiol and $\text{BF}_3 \cdot \text{Et}_2\text{O}$ at low temperature [25] (Scheme 12), and while this did successfully deliver **74**, it did so with concomitant formation of an accompanying butyrolactone migration product.¹ We then selectively O-pivaloylated the C(9)-OH of diol **74** and O-silylated the product monopivaloate with Et_3SiOTf . This furnished the pure product **75** in 93% yield. C-Acylation of the lithium enolate derived from **75**, using $\text{LiN}(\text{SiMe}_3)_2$ as the base, proceeded efficiently with isobutyryl imidazolidine **70** [15]. The enolate derived from **76** was thereafter reacted with MeI to give **77** with the C(11)-quaternary center set with complete stereocontrol. Exposure of **77** to PPTS/ $\text{MeOH}/(\text{MeO})_3\text{CH}$ now cleaved the TES group from O(8) and brought about the desired Fischer glycosidation at C(16) to give **78**. The Piv group was then detached from **78** with NaOMe/MeOH to give alcohol **69**.



SCHEME 12 The Hale and Li route to AB-alcohol **69**.

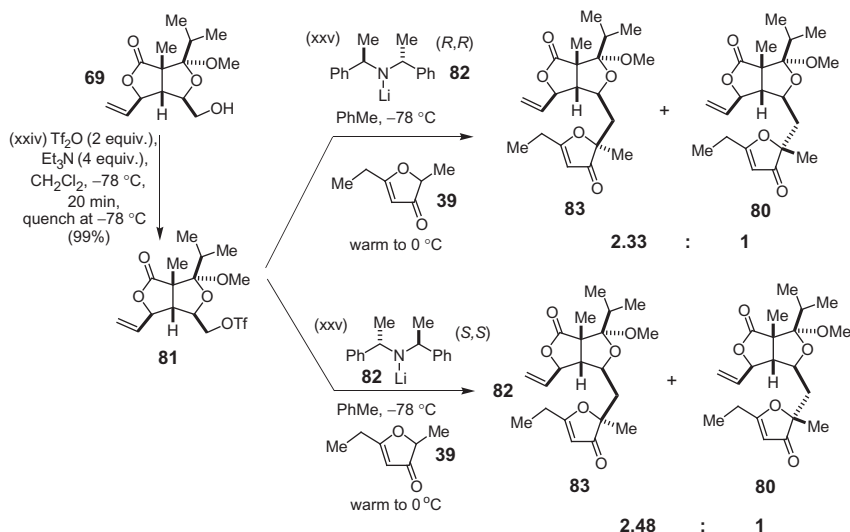
1. Under these conditions, we observed that **74** was always formed alongside approximately 14–17% of a lactone migration product that was difficult to remove at this stage; the latter impurity arises from attack of the C(8)-OH in **74** on its own lactone carbonyl. It can be removed at a later stage.



SCHEME 13 Our attempts at preparing iodide **46** and using it to alkylate **39**.

application of this two-step Finkelstein protocol on **69**, as the more convenient Garegg iodination procedure of $\text{Ph}_3\text{P}/\text{I}_2/\text{imidazole}$ [28] caused methyl glycoside cleavage with concomitant internal acetalization to give **73**; the latter was a most unexpected result to say the least! Presumably, small quantities of HI brought about the initial glycoside cleavage and the pendant hydroxy at C(9) then swung around before phosphonium ion formation and iodide displacement could occur. The two-step iodination protocol avoided this problem. Unfortunately, however, iodide **46** proved unreactive toward all metal enolates that were generated from **39**. We therefore conducted all subsequent alkylation chemistry with the *O*-triflate **81** (Scheme 14), in a manner analogous to Tadano and his team [16].

Initially, we employed the “chiral” lithium enolate formed from exposing **39** to lithium bis[(*S*)- α -methylbenzylamide] [21] in PhMe at low temperature (-78 to 0°C) (Scheme 14), not knowing what the likely stereochemical outcome would be in the alkylation with **81**. In the event, we observed that a 2.48:1 mixture of **83/80** was formed, in which the undesired isomer **83** was predominant (Scheme 14). Buoyed by this encouraging result, even if it was in the opposite stereochemical sense to that which was desired, we duly examined the corresponding alkylation with the chiral kinetic lithium enolate generated from **39** with the enantiomeric base, lithium bis[(*R*)- α -methylbenzylamide] in PhMe, expecting to see an identical but opposite stereochemical outcome, except now in the desired sense. However, to our surprise, we again discovered that a similar ratio of the very same products (2.33:1 of **83/80**) was formed! Although, in hindsight, we had no real basis to expect an inverted stereochemical outcome, it was our belief that that we would see an inversion of the configurational ratio, if reagent control was to dominate. However, our thinking proved incorrect in this instance, with some very subtle effects clearly operating with this pair of chiral bases. The fact that both had a near identical

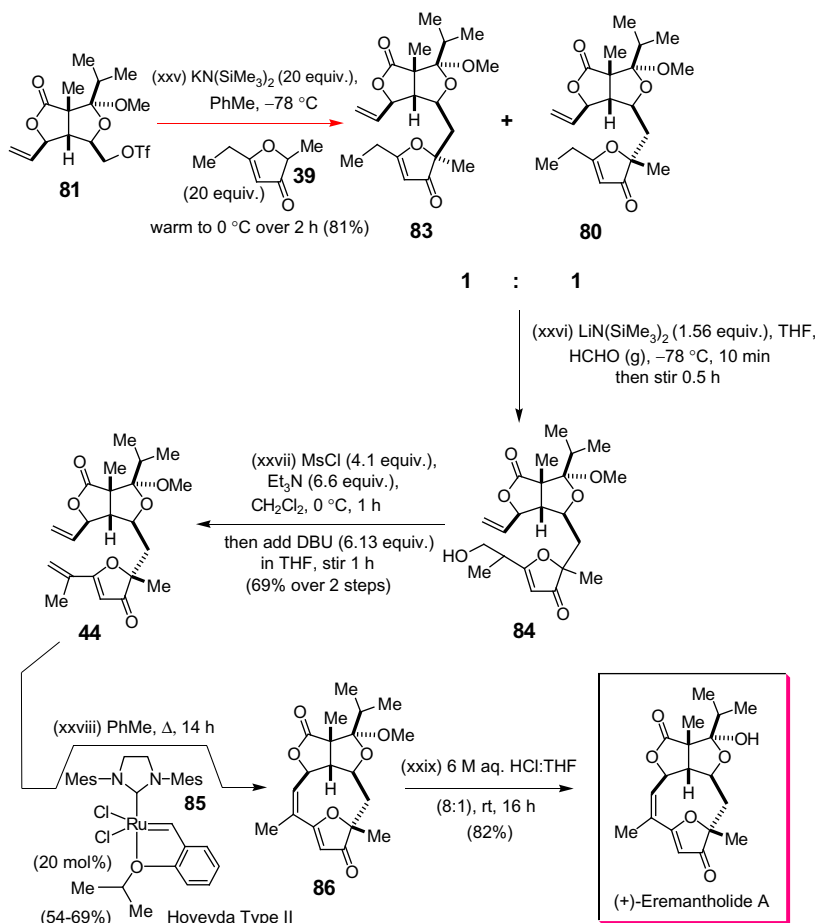


SCHEME 14 The stereochemical outcome of the alkylation between **39** and **81** mediated by the enantiomeric chiral bases **82**.

effect on the stereochemical outcome could never have been anticipated *a priori*, most especially in light of the result that we will now share.

The fact that the aforementioned two chiral enolates were clearly having a genuine effect on the stereochemistry of alkylation (even if poorly understood) was soon appreciated when the union of **39** and **81** was examined under “achiral” enolization conditions. In this system (Scheme 15), with KHMDS as the base in PhMe at 0°C , a 1:1 mixture of **83/80** was produced, as one might expect from Tadano’s previous work [16], where a bulky substituent at C(5) was found to be necessary for observing a predominance of the product with the desired stereochemistry at C(10). Clearly, with our triflate **81**, the C(5)-vinyl was insufficiently bulky to have any truly profound effect on the stereochemical outcome. However, this peculiar set of results in the asymmetric alkylation of 3(2*H*)-furanones using the Simpkins–Marshall–Whitesell chiral bases [21] shows that our approach might yield some potentially useful results in future years, provided further research effort is expended upon this problem, and a range of other chiral bases are surveyed in this capacity.

Returning now to the story at hand, we found it exceedingly difficult and sacrificial to separate the 1:1 mixture of **83:80** at this stage, and so, instead of doing this, we opted to simultaneously deprotonate **83** and **80** at C(4) with LiHMDS in THF at -78°C and react the resulting pair of dienolates with gaseous formaldehyde (passed over the reaction mixture as a gentle stream); this afforded **84** as a mixture of diastereomers in 94% yield. Exposure of **84** to $\text{MsCl}/\text{Et}_3\text{N}$ now yielded four diastereomeric O-mesylate esters, which were

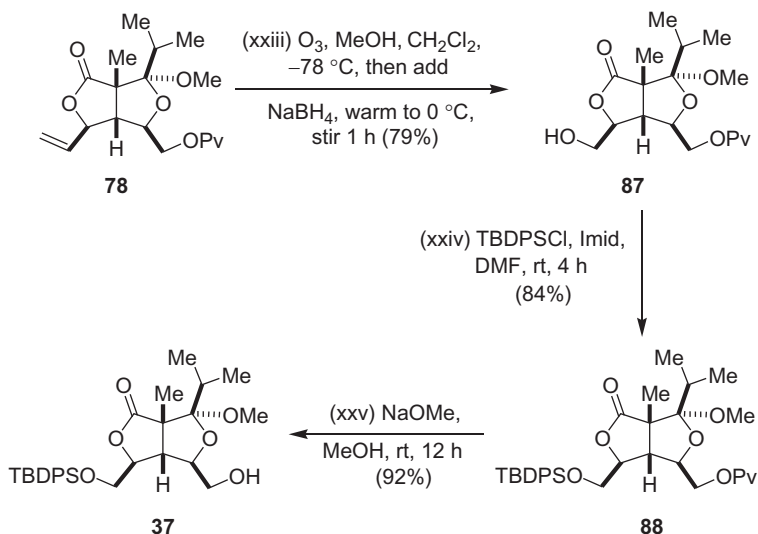


Grubbs I & II Catalysts Unsuccessful

SCHEME 15 The completion of our asymmetric total synthesis of (+)-eremantholide A.

subjected to base-induced elimination with DBU. The latter provided **44** in 69% yield following separation of the two triene products by silica gel chromatography.

In a further very surprising twist, triene **44** was found to cyclize to **86** in respectable yield (54–69%) when subjected to RCM with the Hoveyda–Grubbs type II catalyst **85** [32], whereas its C(10)-epimer showed no tendency to cyclize at all! Instead, it preferentially cross-metathesized. Significantly, the Grubbs type II catalyst gave a complex mixture of products when it was heated with **44** in CH_2Cl_2 at reflux for 12 h, and nothing that remotely corresponded to the desired product **86** was ever isolated from the reaction mixture!



SCHEME 16 A greatly shortened and improved pathway to the Tadano advanced intermediate **37**, a new formal asymmetric total synthesis of (+)-eremantholide A.

We completed our new total synthesis by repeating the acid-induced hydrolysis of methyl glycoside **86** under the conditions that had been reported by Tadano, which entailed reacting **86** with 6 M aqueous HCl in THF for 16 h [16]. This proved to be a remarkably clean reaction that produced (+)-eremantholide A in highly commendable 82% yield.

Following this success, we now decided to see if we could reduce the number of steps needed to arrive at Tadano's alcohol **37** for (+)-eremantholide A. Our new approach to **37**, which is shown in Scheme 16, commences from lactone **78** and now shortens the pathway needed to access Tadano's AB-alcohol by eight steps and provides it by a route that is only 25 steps overall from chiral oxazolidinone **54**. Our new strategy to **37** thus greatly shortens and improves Tadano's earlier route to (+)-eremantholide A.

In the near future, we are hoping to use our new total synthesis of (+)-eremantholide A to construct various eremantholide analogues and photoaffinity probes to help us clarify the mechanism(s) of antitumor action of (+)-eremantholide A. Hopefully, this work will lead to exciting new antitumor chemical biology discoveries.

ACKNOWLEDGMENT

We are grateful to the EPSRC for postdoctoral funding via project grant GR/S81582/01.

REFERENCES

- [1] For Amos B. Smith's total synthesis efforts on the phyllanthostatins, see: (a) A.B. Smith III, K.J. Hale, H.A. Vaccaro, *J. Chem. Soc., Chem. Commun.* (1987) 1026–1028; (b) A. B. Smith III, K.J. Hale, H.A. Vaccaro, *Tetrahedron Lett.* 28 (1987) 5591–5594; (c) A. B. Smith III, R.A. Rivero, K.J. Hale, H.A. Vaccaro, *J. Am. Chem. Soc.* 113 (1991) 2092–2112; (d) A.B. Smith III, K.J. Hale, H.A. Vaccaro, R.A. Rivero, *J. Am. Chem. Soc.* 113 (1991) 2112–2122.
- [2] For Smith's total synthesis of (–)-penitrem D, see: A.B. Smith III, N. Kanoh, H. Ishiyama, R.A. Hartz, *J. Am. Chem. Soc.* 122 (2000) 11254–11255.
- [3] For Smith's formal total synthesis of (–)-FK506, see: A.B. Smith III, K. Chen, D.J. Robinson, L.M. Laakso, K.J. Hale, *Tetrahedron Lett.* 35 (1994) 4271–4274.
- [4] For Smith's synthesis of (+)-hitachimycin, see: A.B. Smith III, T.A. Rano, N. Chida, G.A. Sulikowski, *J. Org. Chem.* 55 (1990) 1136–1138.
- [5] For the total synthesis of (–)-echinosporin, see: A.B. Smith III, G.A. Sulikowski, M.M. Sulikowski, K. Fujimoto, *J. Am. Chem. Soc.* 114 (1992) 2567–2576.
- [6] Total synthesis of (±)-breynolide: A.B. Smith III, J.R. Empfield, R.A. Rivero, H.A. Vaccaro, J.J.-W. Duan, M.M. Sulikowski, *J. Am. Chem. Soc.* 114 (1992) 9419–9434.
- [7] Total Synthesis of (+)-calyculin A and (–)-calyculin B: A.B. Smith III, G.K. Friestad, J.J.-W. Duan, J. Barbosa, K.G. Hull, M. Iwashima, Y. Qiu, P.G. Spoors, E. Bertounesque, B.A. Salvatore, *J. Org. Chem.* 63 (1998) 7596–7597.
- [8] A.B. Smith III, K.J. Hale, L.M. Laakso, K. Chen, A. Riéra, *Tetrahedron Lett.* 30 (1989) 6963–6966.
- [9] A.B. Smith III, K.J. Hale, *Tetrahedron Lett.* 30 (1989) 1037–1040.
- [10] A.B. Smith III, K.J. Hale, J.P. McCauley Jr., *Tetrahedron Lett.* 30 (1989) 5579–5582.
- [11] For our recent enantiospecific formal total synthesis bryostatins 7, see: S. Manaviyar, M. Frigerio, G.S. Bhatia, M.G. Hummersone, A.E. Aliev, K.J. Hale, *Org. Lett.* 8 (2006) 4477–4480.
- [12] For our total syntheses of (+)-azinothricin and (+)-kettapeptin, see: (a) K.J. Hale, S. Manaviyar, J.H. George, M.A. Walters, S.M. Dalby, *Org. Lett.* 11 (2009) 733–736; (b) K.J. Hale, S. Manaviyar, J. George, *Chem. Commun.* 46 (2010) 4021–4042.
- [13] For the synthesis of (3S,5S)-5-hydroxypiperazic acid via tandem asymmetric hydrazination-nucleophilic cyclization, see: (a) K.J. Hale, N. Jogiya, S. Manaviyar, *Tetrahedron Lett.* 39 (1998) 7163–7166; (b) For the synthesis of homochiral piperazic acid itself, see: K. J. Hale, J. Cai, V. Delisser, S. Manaviyar, S.A. Peak, G.S. Bhatia, T.C. Collins, N. Jogiya, *Tetrahedron* 52 (1996) 1047–1068; For the synthesis of (3S,5S)-5-hydroxypiperazic acid via tandem asymmetric hydrazination-nucleophilic cyclization, see: (c) K.J. Hale, M.G. Hummersone, J. Cai, S. Manaviyar, G.S. Bhatia, J.A. Lennon, M. Frigerio, V. M. Delisser, A. Chumnongsaksarp, N. Jogiya, A. Lemaitre, *Pure Appl. Chem.* 72 (2000) 1659–1670; (d) See also: W. Jiang, J.R. Heemstra, R.R. Forseth, C.S. Neumann, S. Manaviyar, F.C. Schroeder, K.J. Hale, C.T. Walsh, *Biochemistry* 50 (2011) 6063–6072.
- [14] (+)-Eremantholide A isolation, structure determination, and initial antitumor evaluation: (a) R.F. Raffauf, P.-K.C. Huang, P.W. Le Quesne, S.B. Levery, T.F. Brennan, *J. Am. Chem. Soc.* 97 (1975) 6884–6886; (b) P.W. Le Quesne, S.B. Levery, M.D. Menachery, T.F. Brennan, R.F. Raffauf, *J. Chem. Soc., Perkin Trans. 1* (1978) 1572–1580.
- [15] For Boeckman's total syntheses of (+)-eremantholide A, see: R.K. Boeckman Jr., S.K. Yoon, D.K. Heckendorn, *J. Am. Chem. Soc.* 113 (1991) 9682–9684.

- [16] For Tadano's synthesis of (+)-eremantholide A, see: K. Takao, H. Ochiai, K. Yoshida, T. Hashizuka, H. Koshimura, K. Tadano, S. Ogawa, *J. Org. Chem.* 60 (1995) 8179–8193.
- [17] Y. Li, K.J. Hale, *Org. Lett.* 9 (2007) 1267–1270.
- [18] (a) B. Hladon, T. Twardowski, *Pol. J. Pharmacol. Pharm.* 31 (1979) 35–43; (b) Although 15-acetoxy-eremantholide B inhibits NF- κ B at 5 μ M in Jurkat T cells, (+)-eremantholide A does not inhibit this target at the concentrations needed to inhibit cancer cell growth. See: P. Rungeler, V. Castro, G. Mora, N. Goren, W. Vichniewski, H.L. Pahl, I. Merfort, T.J. Schmidt, *Bioorg. Med. Chem.* 7 (1999) 2343–2352.
- [19] (a) K. Baker, D. Sengupta, G. Salazar-Jimenez, V.W. Cornish, *Anal. Biochem.* 315 (2003) 134–137; (b) M.L. Alcaide-German, A. Vara-Vega, L.F. Garcia-Fernandez, M. O. Landazuri, L. del Peso, *BMC Cell Biol.* 9 (2008) 18.
- [20] S. Chimichi, M. Boccacini, B. Cosimelli, F. Dall'Acqua, G. Viola, *Tetrahedron* 59 (2003) 5215–5223.
- [21] (a) J.K. Whitesell, S.W. Felman, *J. Org. Chem.* 45 (1980) 755–756; (b) J.A. Marshall, J. Lebreton, *J. Am. Chem. Soc.* 110 (1988) 2925–2931; (c) C.M. Cain, R.P.C. Cousins, G. Coumbarides, N.S. Simpkins, *Tetrahedron* 46 (1990) 523–544.
- [22] Y. Gao, R.M. Hanson, J.M. Klunder, S.Y. Ko, H. Masamune, K.B. Sharpless, *J. Am. Chem. Soc.* 109 (1987) 5765–5780.
- [23] D.A. Evans, J. Bartroli, T.L. Shih, *J. Am. Chem. Soc.* 103 (1981) 2127–2129.
- [24] K.J. Hale, M. Frigerio, S. Manaviyar, *Org. Lett.* 3 (2001) 3791–3794.
- [25] K.J. Hale, M.G. Hummersone, G.S. Bhatia, *Org. Lett.* 2 (2000) 2189–2192.
- [26] S.V. Ley, J. Norman, W.P. Griffith, S.P. Marsden, *Synthesis* (1994) 639–666.
- [27] A. De Mico, R. Margarita, L. Parlanti, A. Vescovi, G. Piancatelli, *J. Org. Chem.* 62 (1997) 6974–6977.
- [28] P.J. Garegg, B. Samuelsson, *J. Chem. Soc., Perkin Trans. 1* (1980) 2866–2869.
- [29] J.S. Yadav, T. Shekharam, V.R. Gadgil, *Chem. Commun.* (1990) 843–844.
- [30] H. Shi, H. Liu, R. Bloch, G. Mandville, *Tetrahedron: Asymmetry* 13 (2002) 1423–1428.
- [31] T.M. Hansen, G.J. Florence, P. Lugo-Mas, J. Chen, J.N. Abrams, C.J. Forsyth, *Tetrahedron Lett.* 44 (2003) 57–59.
- [32] (a) J.S. Kingsbury, J.P.A. Harrity, P.J. Bonitatebus Jr., A.H. Hoveyda, *J. Am. Chem. Soc.* 121 (1999) 791–799; (b) R.H. Grubbs, S. Chang, *Tetrahedron* 54 (1998) 4413–4450; For the successful application of **85** in build-up of the highly strained ring system of ingenol, see; (c) A. Nickel, T. Maruyama, H. Tang, P.D. Murphy, B. Greene, N. Yusuff, J. L. Wood, *J. Am. Chem. Soc.* 126 (2004) 16300–16301.

A Chemo- and Diastereoselective Ring Closing Metathesis Macrocyclization Approach to the Total Syntheses of Aigialomycin C and D

Naval Bajwa and Michael P. Jennings

Department of Chemistry, The University of Alabama, Tuscaloosa, Alabama, USA

Chapter Outline

1. Introduction	153	4. Third Retrosynthetic Analysis of Aigialomycin D	163
2. Initial Retrosynthetic Analysis of Aigialomycin D	154	5. Conclusion	167
3. Second Generation Retrosynthetic Analysis of Aigialomycin D	157		

1. INTRODUCTION

There has been a great interest in the total syntheses of various biologically active natural products for synthetic chemists over a number of years [1]. Along this line, the aigialomycin family of natural products are resorcinyl compounds that possess a 14-membered macrolide core structure fused to a benzenoid unit, as shown in Figure 1 [2]. This family of compounds possesses potentially exploitable patterns of antitumor, antibiotic, and antimalarial activities, making them a valuable class of compounds for chemical genetics [3]. The impressive levels of biological activity of the structurally related macrocyclics render them desirable for total synthesis and serve as an excellent scaffold for the development and validation of new synthetic methodologies. Aigialomycin D (**4**) was first isolated from the mangrove fungus, *Aigialus parvus* BCC 5311, by Isaka and coworkers in 2002, and was been shown to

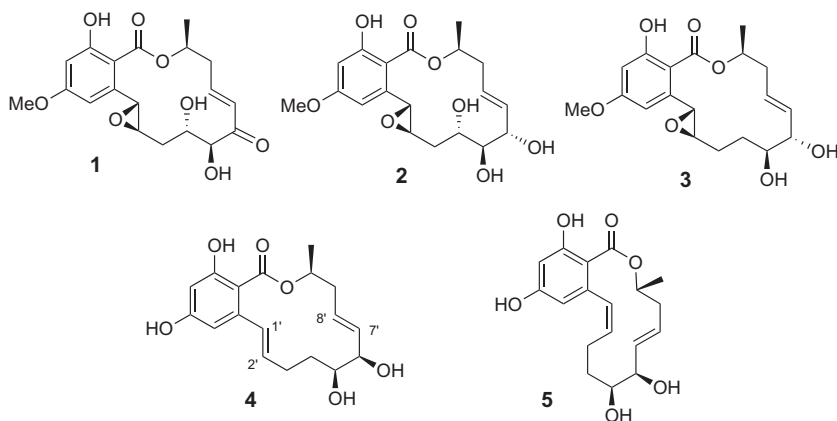


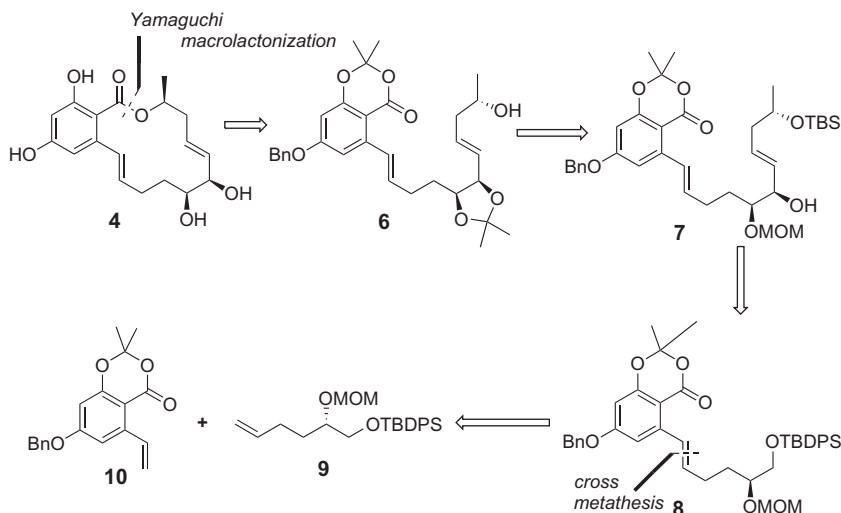
FIGURE 1 The aigialomycin family of natural products.

exhibit modest antimalarial activities (IC_{50} : 6.6 $\mu\text{g/mL}$) against *Plasmodium falciparum* K1, as well as cytotoxicity toward the KB and Vero cancer cell lines with IC_{50} values of 3.0 and 1.8 $\mu\text{g/mL}$, respectively [2]. In addition, **4** has recently been shown to bind to HSP90, but does not function as an indiscriminate ATP antagonist [4]. Also, Winssinger has demonstrated that **4** is a selective kinase inhibitor for CDK1/cyclin and CDK/5p25 (5.7–5.8 M) [4]. Based on HRMS and NMR data of **4**, Isaka and coworkers proposed the structure of aigialomycin D as shown in Figure 1. The key ^1H NMR features revealed that this compound bears a *trans*-olefin at the styrene linkage [$C_1'-C_2'$ ($J = 15.9$ Hz)] and also at $C_7'-C_8'$. It should be noted that most aigialomycins display an epoxide at $C_1'-C_2'$, except for **4** and aigialomycin E (**5**).

Based on the biological data of **4** and other structurally similar resorcinol natural products, it is not surprising that there has been great interest in these compounds [5]. The first total synthesis of **4** was reported by the Danishefsky group in 2004 and utilized a ring-closing metathesis (RCM) reaction to forge the macrocycle at the $C_7'-C_8'$ linkage and a very elegant late stage Diels–Alder reaction for the construction of the aromatic core [5]. A second synthesis was reported by She and Pan, in which they employed a Julia–Kocienski olefination reaction for the construction of both double bonds and a Yamaguchi macrolactonization finished the targeted compound **1** [5]. Similarly, a macrocyclic RCM strategy at the $C_7'-C_8'$, similar to the Danishefsky effort, was recently utilized by Winssinger for the completion of **4** and structurally related analogues via both solution and solid phase protocols [4]. More recently, a variety of novel and innovative approaches have been reported for the synthesis of aigialomycin D [6].

2. INITIAL RETROSYNTHETIC ANALYSIS OF AIGIALOMYCIN D

Our initial approach toward the synthesis of aigialomycin D centered on a cross-metathesis (CM) reaction. As shown in Scheme 1, the most evident disconnection would be the formation of the macrolide ester **4** via a Yamaguchi



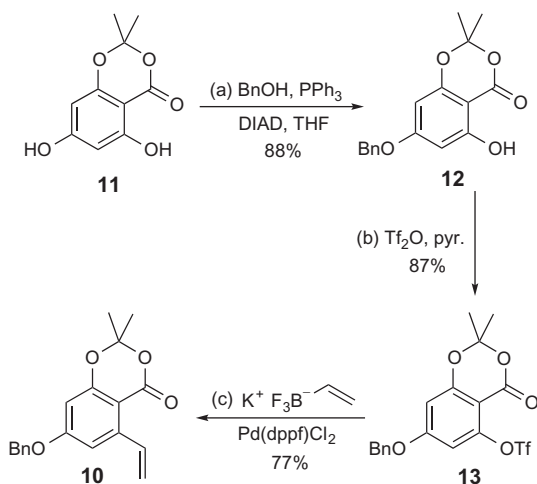
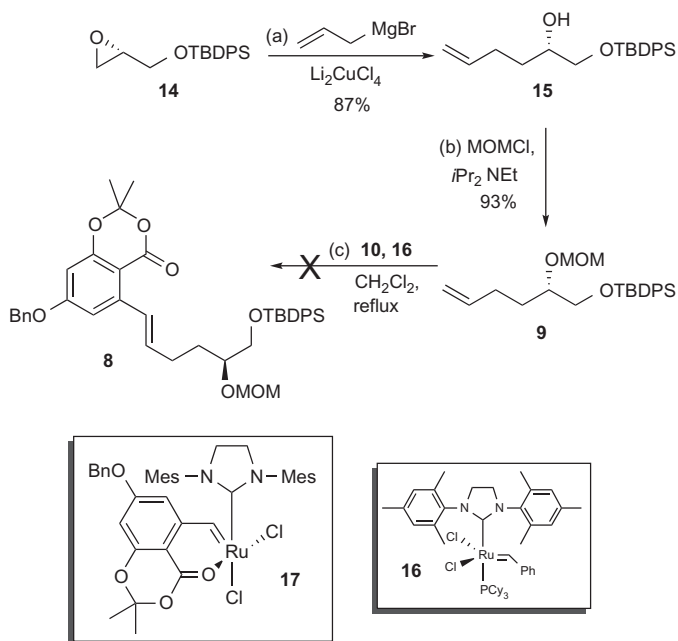
SCHEME 1 First retrosynthetic analysis of aigialomycin D.

macrolactonization. Thus, the acyclic precursor **7** could be formed by a chelation-controlled addition utilizing the MOM acetal as a directing group. A key disconnection is made in going from **8** to **9** and **10** corresponding to the CM reaction using Grubbs' second generation catalyst. We envisioned that compound **10** could be prepared from the commercially available 5,7-dihydroxy-2,2-dimethyl-1,3-benzodioxan-4-one. Compound **9** would be prepared starting from commercially available (*R*)-(+)-glycidol over a series of steps.

We initially anticipated that the CM reaction between two olefinic moieties **9** and **10** using Grubbs' second generation catalyst would result in the formation of **8**, thereby constructing the desired *trans*-olefin (Scheme 1).

The synthesis of styrene **10** started from commercially available 5,7-dihydroxy-2,2-dimethyl-4H-1,3-benzodioxin-4-one (**11**). The hydroxy group at C4 of **11** was chemoselectively protected by Mitsunobu conditions [7] using DIAD and PPh₃ in the presence of benzyl alcohol and provided **12** in 88% yield (Scheme 2). Ensuing treatment of **12** with Tf₂O and pyridine readily provided the corresponding triflate **13** in 88% yield [8]. The resulting triflate **13** underwent Suzuki cross-coupling reaction with potassium vinyl trifluoroborate and in the presence of Pd(dppf)Cl₂ as described by Molander, to furnish the substituted styrene **10** in 77% yield [9].

With the completion of olefin coupling partner **10**, we turned our attention to the synthesis of the aliphatic alkene **9**. We envisaged that the completion of the CM partner **9** could be accomplished from commercially available (*R*)-glycidol as shown in Scheme 3. Thus, the primary hydroxyl group of (*R*)-glycidol was first protected as a TBDPS ether under standard silylating conditions of TBDPSCl, Et₃N, and DMAP to provide **14**. The resulting epoxide **14** on treatment with allyl magnesium bromide and 2 mol% of Li₂CuCl₄

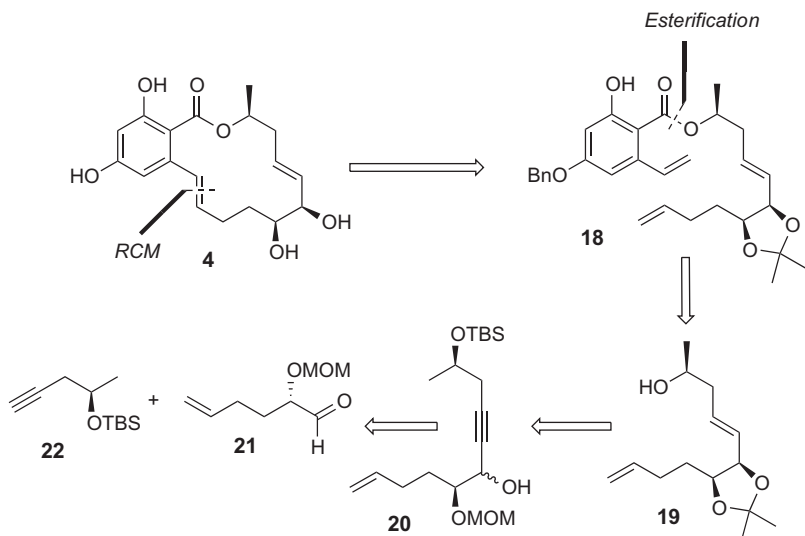
SCHEME 2 Synthesis of the aromatic segment **10**.SCHEME 3 Attempted CM between **9** and **10** with **16**.

afforded the desired terminal olefin **15** in 87% yield (Scheme 3) [10]. Subsequent protection of the free secondary hydroxyl group as MOM ether furnished **9** in 93% yield. Having substrates **9** and **10** in hand, we initiated our investigation into the CM reaction.

At first glance, the CM between **9** and **10** appeared to be fairly straightforward, as the aliphatic olefin should be classified as a type I and the styrene portion as a type II alkene. There are numerous reports in the literature of type I and II olefins selectively cross-metathesizing to afford a single product [11]. Thus, we initially anticipated very little problems with the coupling. However, the reaction between **9** and **10** using 5 mol% of Grubbs' second generation catalyst (**16**) did not yield the desired product **8** and returned mostly the starting materials plus a trace of styrene (~5%) [12]. Upon further thought, we proposed that the Ru-catalyst initially inserted into the styrene olefin to provide compound **17**, even though one might assume that insertion into the aliphatic alkene would be favored. Fürstner and coworkers reported a comparable reaction with a catalyst similar to **16** and a styrene having an *ortho*-carbonyl group that resulted in a Ru-carbonyl chelate complex similar to **17** [13]. However, in the Fürstner example, RCM readily proceeded, even via the intermediate chelate complex. Two very important observations were made by Fürstner and are applicable to our synthetic issue. The first was that the *ortho*-carbonyl exerts an influence on the Ru catalyst with respect to chemoselective insertion within an unsymmetrical diene, when lone electron pairs on the carbonyl oxygen are free and available. In our case, it would appear that the insertion of **16** into styrene **10** would be preferred to that of the aliphatic alkene **9**. The second observation was that the carbonyl-Ru chelate would allow for an RCM reaction to proceed. However, in the Fürstner example, the ester carbonyl maintained freedom of rotation, thus yielding a fairly weak Ru-chelate. In our case, described in Scheme 3, the 2,2-dimethyl-1,3-benzodioxan-4-one functional group formed an extremely stable chelate complex (due to limited freedom of rotation as it is locked as an acetone) by means of a proximity effect and impeded the CM with alkene **9**. With this knowledge, we abandoned this route and examined formation of the styrene linkage of **4** via an RCM reaction process, avoiding the problems with chelate complex formation.

3. SECOND GENERATION RETROSYNTHETIC ANALYSIS OF AIGIALOMYCIN D

With the initial failure with the CM reaction, an alternate strategy to construct the styrene double bond was devised and is shown in Scheme 4. We envisioned that the synthesis of aigialomycin D (**4**) would require a highly chemoselective RCM protocol for the completion of the 14-membered macrocycle. While RCM had been previously utilized by both Danishefsky and Winssinger for the C7'-C8' olefin formation, our approach to **4** relied on a disconnection at the C1'-C2' styrene linkage, which would require a highly chemoselective macrocyclization versus a six-membered ring formation from triene **18**. The synthesis of **18** would arise from the coupling of **19** with the previously synthesized styrene derivative **10**. Working backward, diene **19**

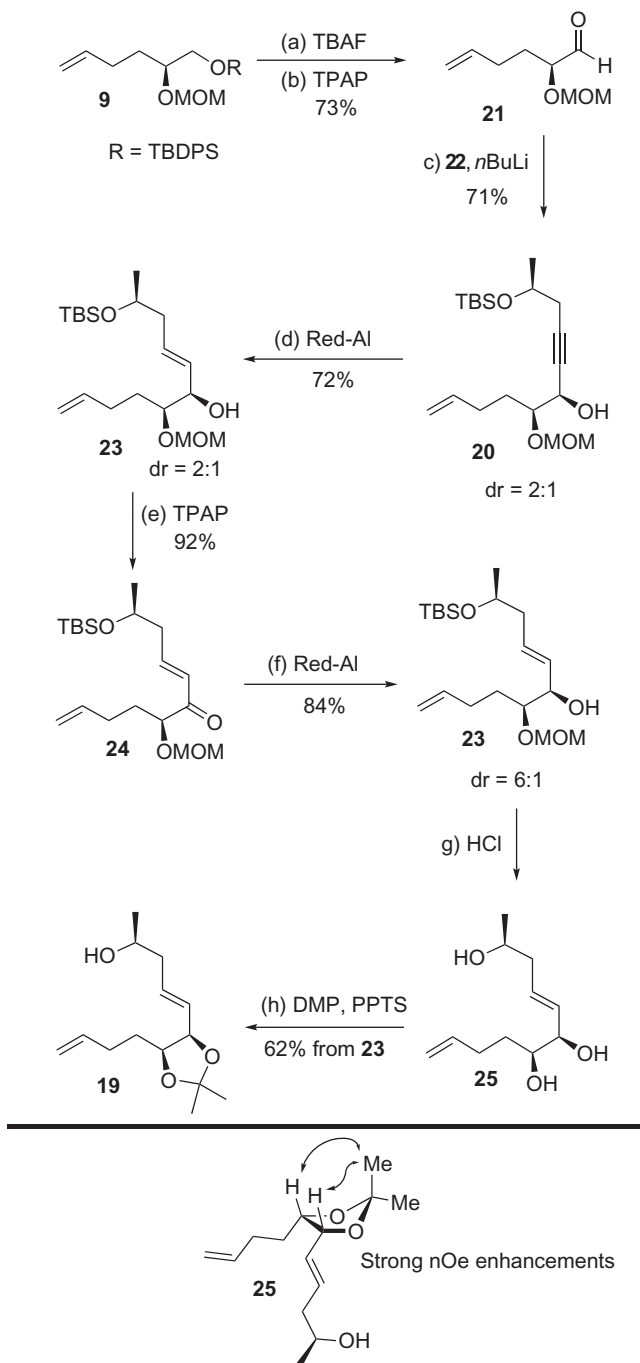


SCHEME 4 Second retrosynthetic analysis of aigialomycin D.

could be envisaged from a coupling of two readily available chiral synthons, **21** and **22**. Finally, **22** would be a simple desilylation and oxidation away from compound **9**.

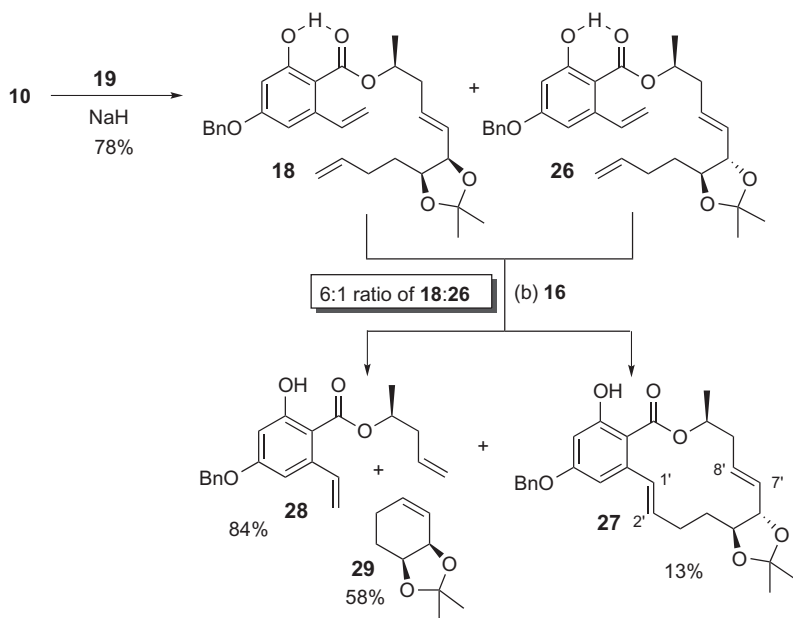
As described earlier, the synthesis of substituted styrene **10** was accomplished starting from a commercially available 5,7-dihydroxy-2,2-dimethyl-4H-1,3-benzodioxan-4-one over number of steps as delineated in [Scheme 2](#). With the aromatic segment readily in hand and in gram quantities, we next focused our effort on the completion of the aliphatic portion of **4** as delineated in [Scheme 5](#). Commencing with the already synthesized compound **9**, selective removal of the silyl ether with TBAF afforded the free primary alcohol, which was further oxidized with TPAP–NMO to furnish the MOM-protected chiral α -hydroxy aldehyde **21** in 73% yield over two steps from **9** [14]. With **21** in hand, treatment of the known TBS-protected propargylic alcohol **22** [15] with *n*BuLi provided the corresponding lithium alkynyl nucleophile, which smoothly underwent addition to the aldehyde moiety of **21** to provide **20** in 71% yield. Compound **20** contains the entire carbon framework of the aliphatic portion of **4**. We initially surmised that the nucleophilic addition to **21** might display modest selectivity for the anti-Cram product due to the ability of the MOM group to undergo chelation-controlled additions. Somewhat surprisingly, the addition of **22** to **21** gave rise to a 2:1 diastereomeric ratio (dr) favoring the Cram product **20**.

Ensuing diastereoselective reduction of the acetylenic moiety of **20** was accomplished upon addition of Red-Al via chelation–hydroalumination to selectively ($\geq 15:1$, *E:Z*) afford the corresponding allylic alcohol **23** in

SCHEME 5 Synthesis of intermediate **19**.

72% yield, while maintaining the 2:1 dr at the C_{6'} hydroxyl group. With the olefin geometry set, attention was turned to final induction of the required diol stereochemistry of **19**. Thus, oxidation of the allylic alcohol resident in **23** with TPAP–NMO readily removed the redundant 2:1 dr at C_{6'} and provided the α,β -unsaturated ketone **24** in 92% yield, which set the stage for a chelation-controlled reduction in anticipation of forming the *cis*-diol **23**. Both lithium and sodium borohydrides failed to exhibit selectivity though the product alcohol was isolated in good yields (80–88%). Unfortunately and contrary to Burke's report, LiBH₄ appeared not to undergo a chelation-controlled addition as a modest amount of the Cram alcohol was isolated (2:1) [16]. Attempted reduction of **24** with LAH in THF (0 °C) provided the desired alcohol **23** in very high yield. However, the selectivity for the LAH reduction just simply replicated the dr from the addition of **22** to **21**. With the LAH result in hand, it appeared that aluminum “ate” based reducing reagents showed a propensity for a chelation-controlled reduction of ketone **24**. Based on this observation, we decided to investigate Red-Al as a chelating reagent for the reduction of **24** to **23**. Much to our delight, treatment of **24** with Red-Al in toluene at 0 °C readily afforded alcohol **23** with a satisfactory diastereomeric ratio (dr = 6:1 by ¹H NMR of the crude product) in a very acceptable 84% yield [17]. With **23** in hand, only a couple of protecting group removals and a selective reprotection of the 1,2-diol subunit as the acetonide was left to complete the aliphatic portion of **4**. Hence, treatment of the protected triol **23** with conc. HCl in refluxing methanol readily cleaved both the silyl ether, as well as the MOM protecting group to provide the triol intermediate **25**. Ensuing ketal formation of the *cis*-diol functionality of **25** to afford the acetonide-protected compound **19** was accomplished via 2,2-dimethoxypropane and PPTS as the acid catalyst in a 62% yield over two steps from **23**. The absolute configuration of the *cis*-diol moiety was unequivocally defined via NOE enhancements between C5' and C6' hydrogen atoms.

With the two subunits readily in our hands, we proceeded to couple advanced intermediates **10** and **19** as described in Scheme 6. Thus, deprotonation of **19** with NaH in 1:1 THF/DMF at 0 °C provided the corresponding alkoxide anion, which was then esterified with the aromatic compound **10** to afford the macrocyclic precursors **18** and **26** as an inseparable 6:1 ratio of diastereomers in 78% yield. With the two subunits coupled, the stage was finally set for our proposed macrocyclization via a chemoselective RCM reaction. Much to our surprise, treatment of **18** and **26** with **16** in refluxing toluene (0.0002 M) did not provide any of the desired macrocycle, but resulted in the decomposition of the starting material. Switching the medium from toluene to CH₂Cl₂, led to the formation of a 14-membered macrocycle **27** and the acyclic compound **28** in 13% and 84% yields, respectively. In addition, the cyclohexene diol **29** that accompanies the acyclic compound **28** was isolated in 58% yield.

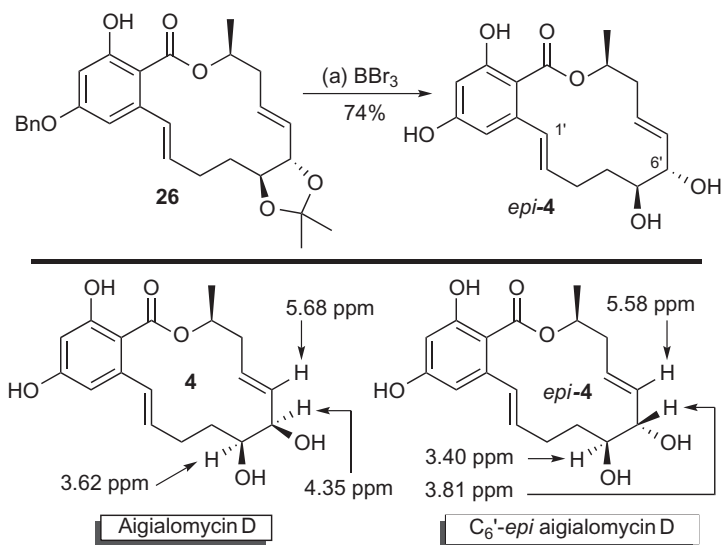


SCHEME 6 Synthesis of intermediate **27** via a chemo- and diastereoselective RCM reaction.

Final treatment of **27** with 4 equiv. of BBr_3 at -78°C in CH_2Cl_2 furnished the macrocycle *epi-4* in a respectable 74% yield, as shown in [Scheme 7](#). Unfortunately, the spectral data (^1H NMR, 360 MHz; ^{13}C NMR, 90 MHz) were not in agreement with the natural sample **4** [2]. Close inspection of the ^1H NMR of *epi-4* and **4** coupled with the comparison of the structural data of aigialomycin C (**3**) suggested that the synthesized compound was that of *epi-C'_6* aigialomycin D. The methine proton of C'_6 possessed a dramatic upfield shift of 3.81 ppm versus that of 4.35 ppm in **4**. In addition, both protons α - to the C'_6 methine displayed an upfield shift with respect to that of **4**.

Thus, it appeared that the stereochemistry resident at C'_6 influenced macrocyclization by means of a stereodivergent reaction of the two diastereomers (**18** and **26**) with Grubbs' catalyst **16**. The initial insertion of **16** must have taken place at the more accessible terminal alkene moiety of **18** and **26**, followed either by 6- or 14-membered ring formation via RCM. The formation of the *cis*-acetonide-protected cyclohexene diol **29** appeared to be favored over macrocyclization (also leading to the production of **28**). However, the construction of the *trans*-substituted six-membered ring was not viable due to strain, and RCM of **26** exclusively led to the desired macrocyclic framework **27**.

A few observations merit noting and further discussion. As described earlier, the carbonyl resident on the aromatic ring of **10** defined the site of catalyst **16** initiation into the styrene olefin with respect to the attempted CM

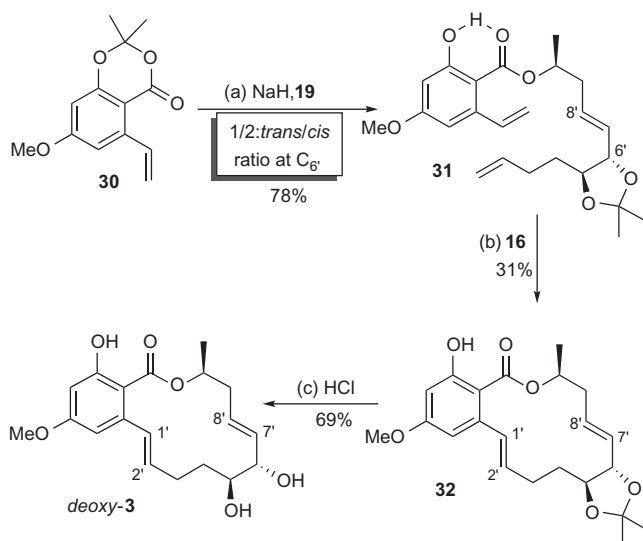


SCHEME 7 Synthesis of *epi*-aigialomycin D.

between **10** and **9**. However, in the case of compounds **18** and **26**, initial insertion of **16** did not take place into the aromatic alkene. This presumably was due to the reduced proximity effect resulting from the hydrogen bonding between the phenol and the *ortho*-carbonyl. Thus, simple coordination of the carbonyl lone pair in a hydrogen bond played a significant role with respect to metathesis initiation, as was originally thought. The second observation worth discussing is that the RCM macrocyclization readily took place while the lone pair of electrons of the carbonyl were “tied-up” in the hydrogen bond. Additionally, catalyst **16** was not deactivated via any type of carbonyl chelation when initial insertion took place into the terminal alkene of **18** and **26**. This observation parallels that of the Fürstner report [13]. In addition to this molecule, we have since used this exact strategy with respect to the synthesis of the purported structure of the pochonin J [18].

As shown in Scheme 8, we took advantage of such a diastereoselective RCM reaction to additionally synthesize *deoxy*-aigialomycin C (*deoxy*-**3**). As described above, esterification of **19** (1:2 *trans*:*cis* ratio at C_6') with styrene **30**¹ provided **31** in 78% yield. Subsequent RCM of **31** with catalyst **16** furnished macrocycle **32** in virtually quantitative yield with respect to the *trans*-dioxolane diastereomer (31% overall due to the 1:2 ratio at C_6'). Final deprotection of the acetonide moiety with aq. HCl provided *deoxy*-**3** in 69% yield.

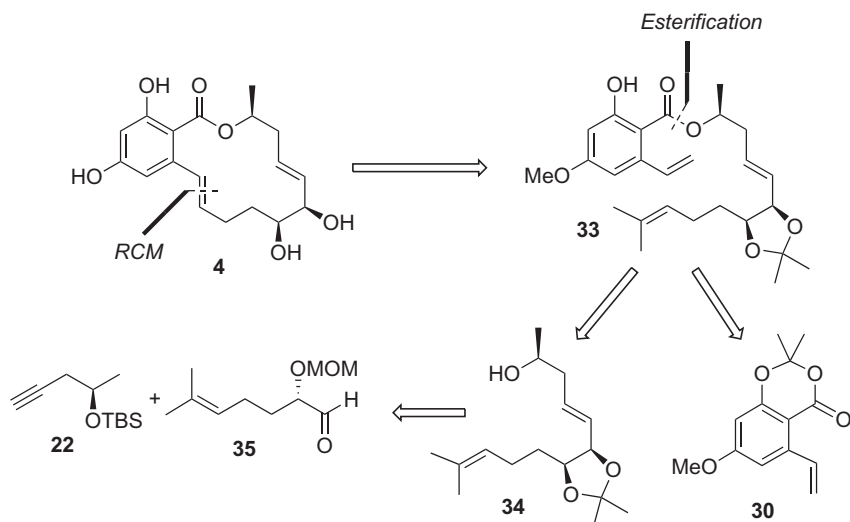
1. Styrene **30** was synthesized in the same manner as compound **10**.

SCHEME 8 Synthesis of *deoxy*-aigialomycin C.

4. THIRD RETROSYNTHETIC ANALYSIS OF AIGIALOMYCIN D

As already observed, the RCM reaction of the macrocyclic precursors **18** and **26** resulted in the formation of a 14-membered macrocycle **27** and the acyclic compound **28** as highlighted in Scheme 6. The initial insertion must have taken place at the more accessible terminal alkene moiety of **18** and **26** followed either by 6- or 14-membered ring formation via RCM. In addition, the acyclic compound **28** was isolated in good yields, which suggested that diene **28** does not undergo an intramolecular RCM reaction in the presence of Grubbs' catalyst **16**. We hoped to take advantage of this observation and anticipated that if we could force the initial insertion of **16** to the styrene olefin, the intermediate would eventually cyclize to furnish the desired 14-membered macrocyclic framework of aigialomycin D. Along this line, we envisaged that RCM of macrocyclic precursor **33** would furnish the desired 14-membered macrocycle. The macrocyclic precursor, in turn, would be synthesized by the esterification reaction between the styrene intermediate **30** and the aliphatic substrate **34** as delineated in Scheme 9. With this idea in mind, we recognized that it would be necessary to "block" the insertion of **16** into the terminal alkene of precursor **33**. We envisioned replacing the terminal alkene with a geminally substituted dimethyl analogue, in which the extraneous substituents would be cleaved during the proposed RCM process.

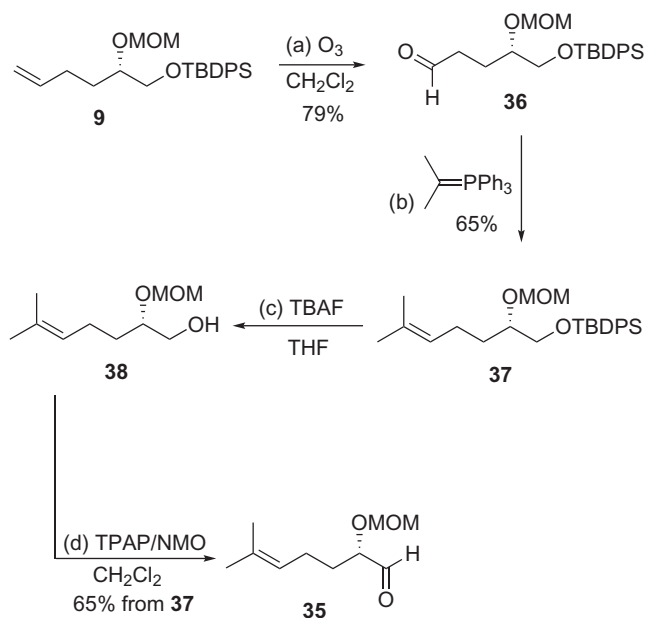
In order to test our hypothesis, we decided to investigate the Wittig olefination reaction between aldehyde **36** and isopropylidene triphenylphosphorane. Thus, ozonolysis of the terminal olefin **9** afforded the corresponding



SCHEME 9 Third generation retrosynthetic analysis of aigialomycin D.

aldehyde **36** in 79% yield. The phosphorus ylide was generated *in situ* by treatment of isopropyl triphenylphosphonium iodide with lithium hexamethyldisilazide in THF. Upon treatment with aldehyde **36**, the desired olefinic product **37** was obtained in 65% overall yield. Subsequent TBDPS deprotection of **37** with TBAF afforded the primary alcohol **38**, which was immediately further oxidized with TPAP–NMO to afford the MOM-protected chiral α -hydroxy aldehyde **35** in 55% yield over two steps from **37** as described in Scheme 10.

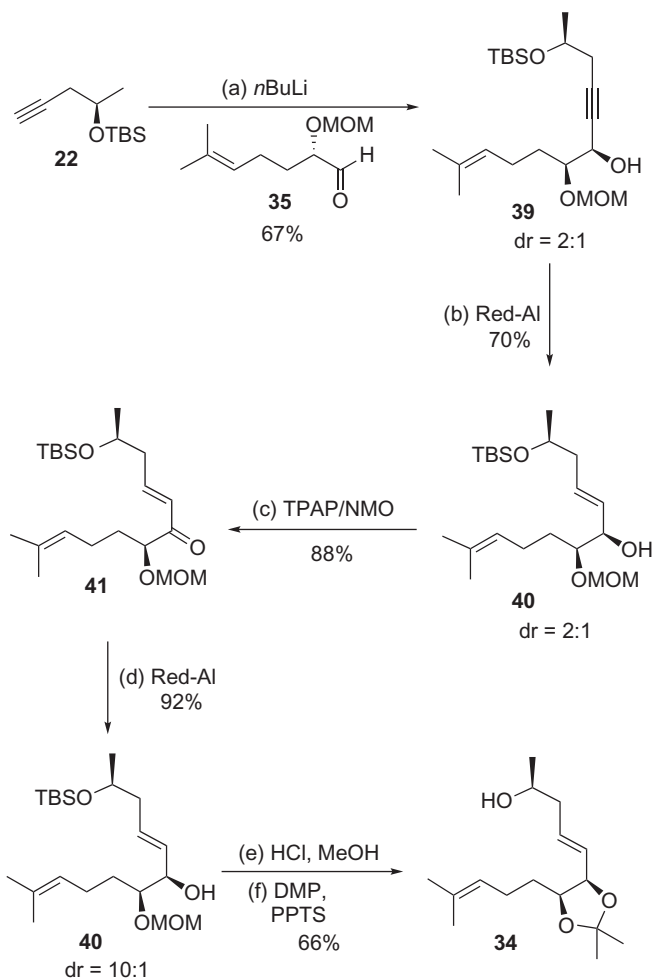
With **35** in hand, we next focused our attention on the completion of **34** via an alkynyl addition to the resident aldehyde moiety. As in the synthetic pathway in Scheme 3, treatment of the TBS-protected propargylic alcohol **22** with *n*BuLi provided the lithium alkynyl nucleophile that underwent smooth addition to the aldehyde moiety of **35** to afford **39** in 67% yield (Scheme 11). Diastereoselective reduction of the acetylenic moiety of **39** was accomplished upon addition of Red-Al via chelation–hydroalumination to selectively ($>15:1$, *E:Z*) afford the corresponding allylic alcohol **40** in 70% yield, while maintaining the $\sim 2:1$ dr at the C_6' hydroxyl group. With the olefin geometry set, attention was turned to final induction of the required diol stereochemistry of **34**. Thus, oxidation of the allylic alcohol resident in **40** with TPAP–NMO readily removed the redundant stereochemistry at C_6' and provided the α,β -unsaturated ketone **41** in 88% yield. This set the stage for a chelation-controlled reduction in anticipation of forming selectively the *cis*-diol **40**. Treatment of **41** with Red-Al in toluene at 0°C readily afforded alcohol **40** with an excellent dr (10:1 by ^1H NMR of the crude product) in a very acceptable 92% yield. It is worth noting that the dr for the reduction of

SCHEME 10 Synthesis of chiral aldehyde **35**.

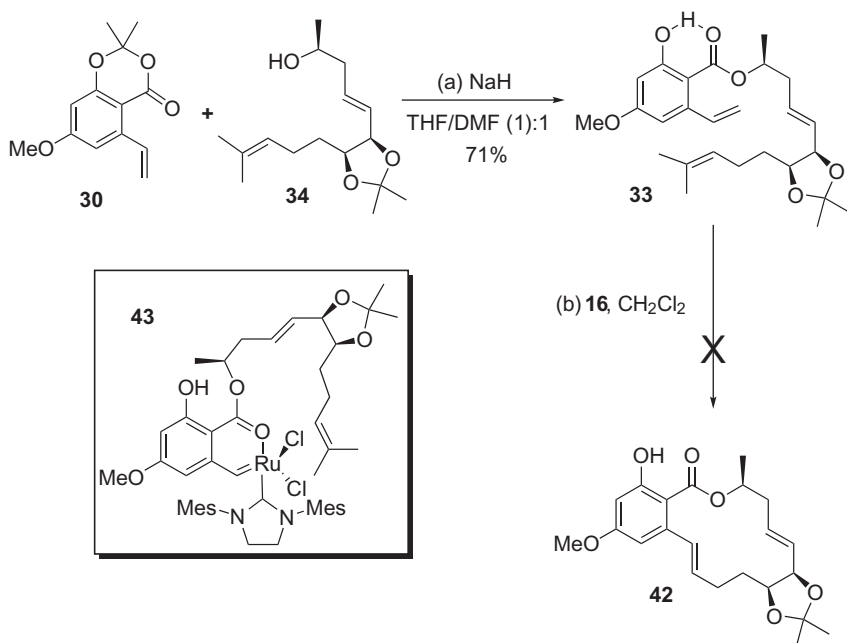
41 is greater than was previously observed with ketone **24** (see Scheme 5). With **40** in hand, only a couple of protecting group removals and a selective reprotection of the 1,2-diol subunit as the acetonide was left to complete the aliphatic portion of **4**. Hence, treatment of the protected triol **40** with conc. HCl in refluxing methanol readily cleaved both the silyl ether, as well as the MOM protecting group to provide the triol intermediate. Ketal formation of the *cis*-diol functionality to afford the acetonide-protected compound **34** was accomplished via 2,2-dimethoxypropane and PPTS as the acid catalyst in a 66% yield over two steps from **40**.

With the two subunits readily in our hands, we proceeded to couple the advanced intermediates **30** and **34** as described in Scheme 12. Thus, deprotonation of **34** with NaH in 1:1 THF/DMF at 0 °C proceeded to provide the alkoxide anion, which was then *trans*-esterified with the aromatic compound **30** to afford the macrocyclic precursor **33** in 71% yield. With the two subunits coupled, the stage was finally set for our proposed macrocyclization via a chemoselective relay RCM reaction.

With styrene **10**, we postulated that Grubbs' catalyst forms a very stable six-membered chelate with the carbonyl oxygen at *ortho*-position of styrene double bond. We initially surmised that in the macrocyclic precursor **33**, the hydrogen bond between hydroxyl group on aromatic ring and carbonyl oxygen would be strong enough to prevent the formation of six-membered chelate between carbonyl oxygen and ruthenium metal. We also envisaged that initial

SCHEME 11 Synthesis of diene intermediate **34**.

insertion of Grubbs' catalyst would take place at styrene double bond, which would then undergo the desired RCM reaction with the trisubstituted olefin (vs. the C_7' – C_8' olefin) to afford the macrocyclic framework **42**. We decided to investigate the RCM reaction of macrocyclic precursor **33** under variety of conditions as highlighted in Scheme 12. Much to our disappointment, treatment of **34** with Grubbs' second generation catalyst (**16**) in refluxing CH_2Cl_2 (0.001 M) did not provide any of the cyclized product; only the starting material was recovered ($\sim 95\%$). Unfortunately, changing the solvent from CH_2Cl_2 to toluene and attempting the RCM at elevated temperatures also did not allow for ring closure. With these results in hand, we postulated that the hydrogen bond between phenol group and carbonyl oxygen is not strong



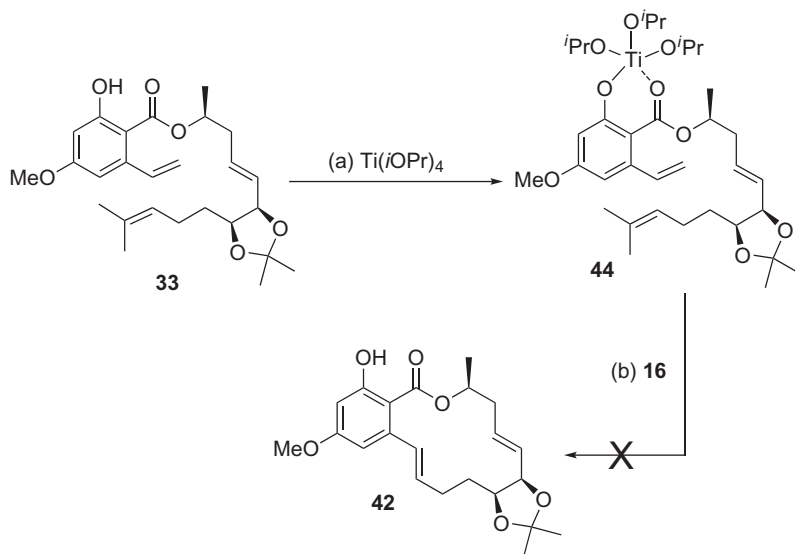
SCHEME 12 Unsuccessful attempts of “directed” RCM to furnish **42**.

enough to prevent the formation of very stable chelate **43** with catalyst **16** upon initial insertion of the catalyst into the styrene olefin. However, it is worth noting, this is only part of the issue. Once initial insertion of **16** into the styrene olefin of **33** took place, it is quite possible that the *gem*-dimethyl alkene would not undergo RCM due to steric hindrance.

Being fairly desperate at this point, we decided to pursue an alternative route wherein we would prechelate the carbonyl oxygen with a Lewis acid such as Ti(^{*i*}OPr)₄ [19]. However, attempted RCM reaction of **44** with **16** in the presence of a Ti(^{*i*}OPr)₄ in refluxing CH₂Cl₂ did not lead to any of the desired cyclized product **42**, but resulted in the decomposition of the starting material (Scheme 13). Thus, it appeared that the construction of styrene olefin of **4** was not viable by means of a RCM with a geminally substituted dimethyl analogue.

5. CONCLUSION

In conclusion, we have highlighted our approach to the syntheses of aigialomycin C and D via a RCM approach. While we did not succeed in reaching the final desired targets, the syntheses of *epi*-aigialomycin D and *deoxy*-aigialomycin C are described via a remote stereocontrolled RCM macrocyclization. The key reaction involved a highly chemo- and diastereoselective RCM protocol for



SCHEME 13 Final attempt at RCM of **33** with added Lewis acid.

the formation of the macrocyclic core. In addition, we observed that a remote stereocenter influenced the RCM reaction with respect to macrocyclization. During the synthetic approaches to **4**, we observed a delicate balance between steric blocking and electronic effects of catalyst insertion during a CM and RCM macrocyclization process, which ultimately will have value with respect to future synthetic planning. Unfortunately, through our efforts it emerged that the construction of styrene olefin resident in **4** was not viable by means of a RCM macrocyclization.

REFERENCES

- [1] (a) K.C. Nicolaou, D. Vourloumis, N. Winssinger, P.S. Baran, *Angew. Chem. Int. Ed.* 39 (2000) 44–122; (b) G.M. Cragg, D.J. Newman, *Pure Appl. Chem.* 77 (2005) 7–24.
- [2] M. Isaka, C. Suyarnsestakorn, M. Tanticharoen, P. Kongsaree, Y. Thebtaranonth, *J. Org. Chem.* 67 (2002) 1561–1567.
- [3] (a) P. Delmotte, J. Delmotte-Plaquee, *Nature* 171 (1953) 344–345; (b) G.A. Ellestad, F. M. Lovell, N.A. Perkinson, R.T. Hargreaves, W.J. McGahren, *J. Org. Chem.* 43 (1978) 2339–2343; (c) W.A. Ayer, S.P. Lee, A. Tsuneda, Y. Hiratsuka, *Can. J. Microbiol.* 26 (1980) 766–773; (d) W.A. Ayer, L. Pena-Rodriguez, *Phytochemistry* 26 (1987) 1353–1355; (e) F. Sugawara, K.W. Kim, K. Kobayashi, J. Uzawa, S. Yoshida, N. Murofushi, N. Takahashi, G.A. Strobel, *Phytochemistry* 31 (1992) 1987–1990; (f) S.V. Sharma, T. Agatsuma, H. Nakano, *Oncogene* 16 (1998) 2639–2645.
- [4] S. Barluenga, P.-Y. Dakas, Y. Ferandin, L. Meijer, N. Winssinger, *Angew. Chem. Intl. Ed.* 45 (2006) 3951–3954.

- [5] (a) X. Geng, S.J. Danishefsky, *Org. Lett.* 6 (2004) 413–416; (b) J. Lu, J. Ma, X. Xie, B. Chen, X. She, X. Pan, *Tetrahedron Asymmetry* 17 (2006) 1066–1073.
- [6] (a) N.Q. Vu, C.L.L. Chai, K.P. Lim, S.C. Chia, A. Chen, *Tetrahedron* 63 (2007) 7053–7058; (b) C.C. Chrovian, B. Knapp-Reed, J. Montgomery, *Org. Lett.* 10 (2008) 811–814; (c) L. J. Baird, M.S.M. Timmer, P.H. Teesdale-Spittle, J.E. Harvey, *J. Org. Chem.* 74 (2009) 2271–2277; (d) F. Calo, J. Richardson, A.G.M. Barrett, *Org. Lett.* 11 (2009) 4910–4913.
- [7] S. Takahashi, S. Kamisuki, Y. Mizushina, K. Sakaguchi, F. Sugawara, T. Nakata, *Tetrahedron Lett.* 44 (2003) 1875–1877.
- [8] R.G. Dushin, S.J. Danishefsky, *J. Am. Chem. Soc.* 114 (1992) 655–659.
- [9] G.A. Molander, M.R. Rivero, *Org. Lett.* 4 (2002) 107–111.
- [10] D.J. Dixon, S.V. Ley, D.J. Reynolds, *Angew. Chem. Intl. Ed.* 39 (2000) 3622–3626.
- [11] (a) For a very recent review, see: G.C. Vougioukalakis, R.H. Grubbs, *Chem. Rev.* 110 (2010) 1746–1787; (b) A.K. Chatterjee, T.L. Choi, D.P. Sanders, R.H. Grubbs, *J. Am. Chem. Soc.* 125 (2003) 11360–11370.
- [12] M. Scholl, S. Ding, C.W. Lee, R.H. Grubbs, *Org. Lett.* 1 (1999) 953–956.
- [13] A. Fürstner, O.R. Thiel, C.W. Lehmann, *Organometallics* 21 (2002) 331–335.
- [14] S.V. Ley, J. Norman, W.P. Griffith, S.P. Marsden, *Synthesis* (1994) 639–666.
- [15] D. Romo, R.M. Rzasa, H.A. Shea, K. Park, J.M. Langenhan, L. Sun, A. Akhiezer, J.O. Liu, *J. Am. Chem. Soc.* 120 (1998) 12237–12254.
- [16] S.D. Burke, D.N. Deaton, R.J. Olsen, D.M. Armistead, B.E. Blough, *Tetrahedron Lett.* 28 (1987) 3905–3906.
- [17] N. Bajwa, M.P. Jennings, *J. Org. Chem.* 71 (2006) 3646–3649.
- [18] D. Martinez-Solorio, K.A. Belmore, M.P. Jennings, *J. Org. Chem.* 76 (2011) 3898–3908.
- [19] A.K. Ghosh, J. Cappiello, D. Shin, *Tetrahedron Lett.* 39 (1998) 4651–4654.

Regio- and Stereoselective Metal-Catalyzed Reactions and Their Application to a Total Synthesis of (–)-Dactylolide

Daesung Lee and Ivan Volchkov

Department of Chemistry, University of Illinois, Chicago, Illinois, USA

Chapter Outline

1. Introduction and Background	172	2.8. Altmann and Gertsch Synthesis of (–)-Dactylolide	181
2. Review of Previous Total Syntheses	172	2.9. Ghosh Synthesis of (–)-Dactylolide and (–)-Zampanolide	182
2.1. Smith Synthesis of (+)-Dactylolide	173	3. Retrosynthetic Analysis	184
2.2. Hoye Synthesis of (–)-Dactylolide and (–)-Zampanolide	174	4. New Synthetic Methods Development and Application	185
2.3. Jennings Synthesis of (–)-Dactylolide	175	4.1. Preparation of the Pyran Subunit	185
2.4. Floreancig Synthesis of (+)-Dactylolide	176	4.2. Preparation of the (Z)-Trisubstituted Vinyl Boronate	189
2.5. Keck Synthesis of (+)-Dactylolide	177	4.3. Macrocyclic Ring-Closing Metathesis	192
2.6. McLeod Synthesis of (–)-Dactylolide	179	5. Completion of Dactylolide Synthesis	193
2.7. Uenishi and Tanaka Synthesis of (–)-Dactylolide	180	6. Summary	194

1. INTRODUCTION AND BACKGROUND

(+)-Dactylolide was isolated from the marine sponge of the genus *Dactylospongia* by Riccio and coworkers off the coast of the Vanuatu islands in 2001 (Figure 1) [1]. It exhibited 63% inhibition of lymphatic leukemia in mice (L1210) and 40% inhibition of ovarian carcinoma (SK-OV-3) at 3.2 $\mu\text{g/mL}$. Structurally, dactylolide is a highly unsaturated 18-membered macrolactone containing a 2,6-*cis*-disubstituted tetrahydropyran and an aldehyde functionality. The complete stereochemical assignment of the relative and absolute stereochemistry of dactylolide was realized by Smith via total syntheses of both (+)-dactylolide [2] as well as (+)-zampanolide [2b,3] (Figure 1).

(-)-Zampanolide was isolated by Higa and Tanaka as a minor constituent of the completely different marine sponge *Fasciospongia rimosa*, collected off Cape Zampa on the island of Okinawa, Japan in 1996 [4]. (-)-Zampanolide has shown more potent cytotoxicity than (+)-dactylolide against the P388, A549, HT29, and MEL28 tumor cell lines (on the order of 1–5 ng/mL), blocking the G to M transition in the cell cycle through the stabilization of microtubules [5], similar to the characteristic actions of taxol [6], laumalide, and the pelorusides [7].

The similarity between dactylolide and zampanolide in their structures and the metabolite makeup of the host sponges imply a common biosynthetic precursor, possibly the result of two genetically related symbiotic microorganisms. However, the total synthesis of (+)-dactylolide revealed the absolute stereochemistry of the two natural products is opposite [2]. Therefore, dactylolide is not a degradation product of, or biosynthetic precursor for, zampanolide.

2. REVIEW OF PREVIOUS TOTAL SYNTHESSES

Because of their structural complexity and promising biological activities, dactylolide and zampanolide have attracted considerable synthetic interest [2,3,8]. To date, nine and four total syntheses of dactylolide and zampanolide, respectively, have been reported since their first synthesis in 2002 [2] and 2001 [3]. In 2003, Hoye reported a one-step conversion of (-)-dactylolide into (-)-zampanolide [8a], demonstrating that the synthesis of dactylolide

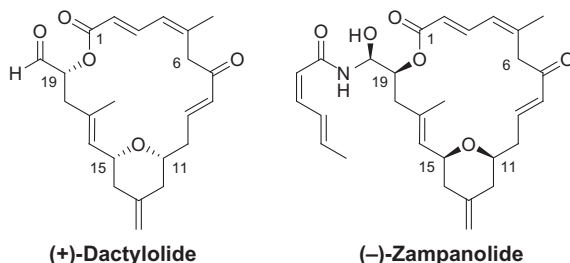
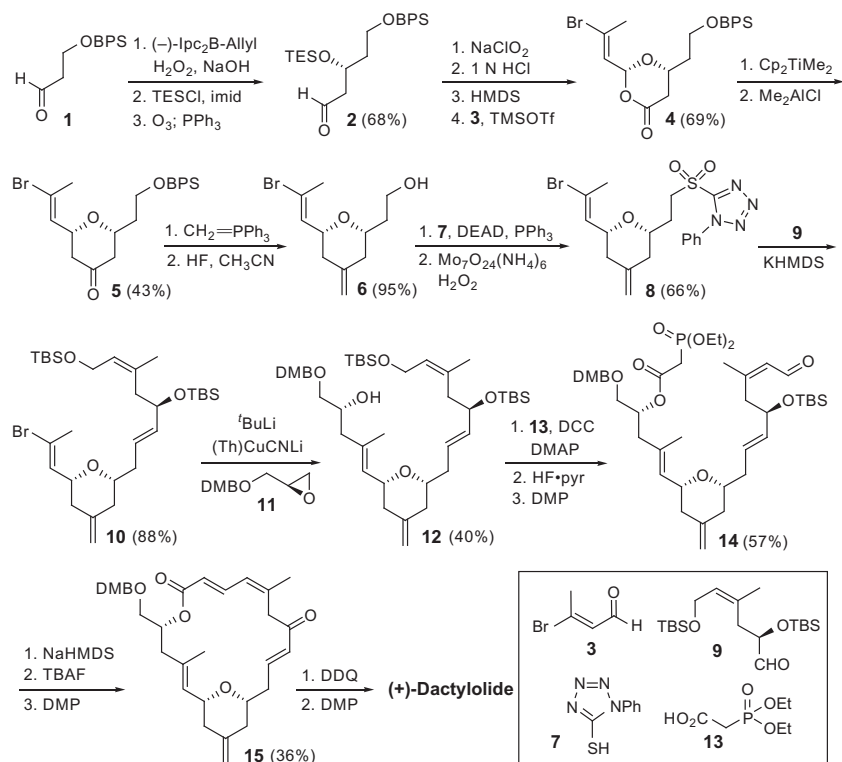


FIGURE 1 Naturally occurring (+)-dactylolide and (-)-zampanolide.

constitutes a formal synthesis of zampanolide. These syntheses are reviewed here, with a focus on the major structural challenges including the formation of the *cis*-2,6-disubstituted-4-methylene tetrahydropyran, the *E*- and *Z*-trisubstituted double bonds, and the 18-membered ring lactone.

2.1 Smith Synthesis of (+)-Dactylolide

Smith's strategy [2] involved a Horner–Wadsworth–Emmons olefination to form the macrocycle at the C2–C3 double bond and a Petasis–Ferrier rearrangement [9] to generate the pyran subunit (Scheme 1). The synthesis started with Brown asymmetric allylation of aldehyde **1** followed by protection of the resulting alcohol as the TES ether. Ozonolysis afforded aldehyde **2**, which was subsequently oxidized to the carboxylic acid. *Bis*-silylation with HMDS followed by condensation with aldehyde **3** promoted by TMSOTf led to dioxanone **4** (10:1 dr). Methylenation of **4** and the Petasis–Ferrier rearrangement afforded pyranone **5**. The installation of the *exo*-methylene group via Wittig olefination, silyl ether deprotection, and Mitsunobu reaction with thiotetrazole **7** provided sulfone **8** after oxidation. Sulfone **8** was coupled with aldehyde **9**



SCHEME 1 Smith synthesis of (+)-dactylolide.

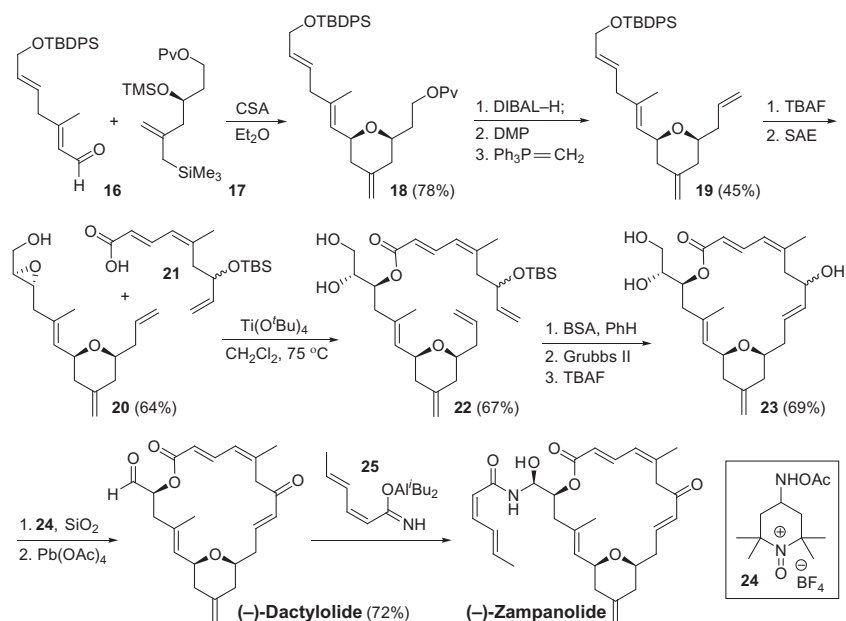
under the Julia–Kocienski protocol to install the C8–C9 double bond. The cuprate derived from vinyl bromide **10** was then merged with epoxide **11**, giving alcohol **12**. For the macrocyclization, phosphonate **14** was prepared by initial esterification between **12** and **13** followed by selective primary TBS-ether deprotection and oxidation. Macrocyclization via Horner–Wadsworth–Emmons olefination, deprotection of the TBS and DMB groups followed by oxidation of the C20 hydroxyl group afforded (+)-dactylolide.

(+)-Dactylolide could also be accessed by degradation of (+)-zampanolide. The authors demonstrated that heating (+)-zampanolide in benzene at 85 °C for 1.5 h led to clean formation of (+)-dactylolide, giving further confirmation of their relative and absolute stereochemistry.

2.2 Hoya Synthesis of (–)-Dactylolide and (–)-Zampanolide

Hoya and Hu reached zampanolide by direct addition of the *N*-acyl hemiaminal side chain to dactylolide via an aza-aldol reaction [8a]. Other key steps include the formation of the ester by titanium-mediated opening of a 2,3-epoxy alcohol with a carboxylic acid and a ring-closing metathesis to generate the macrocycle.

The synthesis commenced with formation of the *cis*-2,6-disubstituted-4-methylene tetrahydropyran **18** via coupling of aldehyde **16** with allylsilane **17** (Scheme 2). A three-step manipulation of the primary pivalate in **18** to



SCHEME 2 Hoya synthesis of (–)-dactylolide.

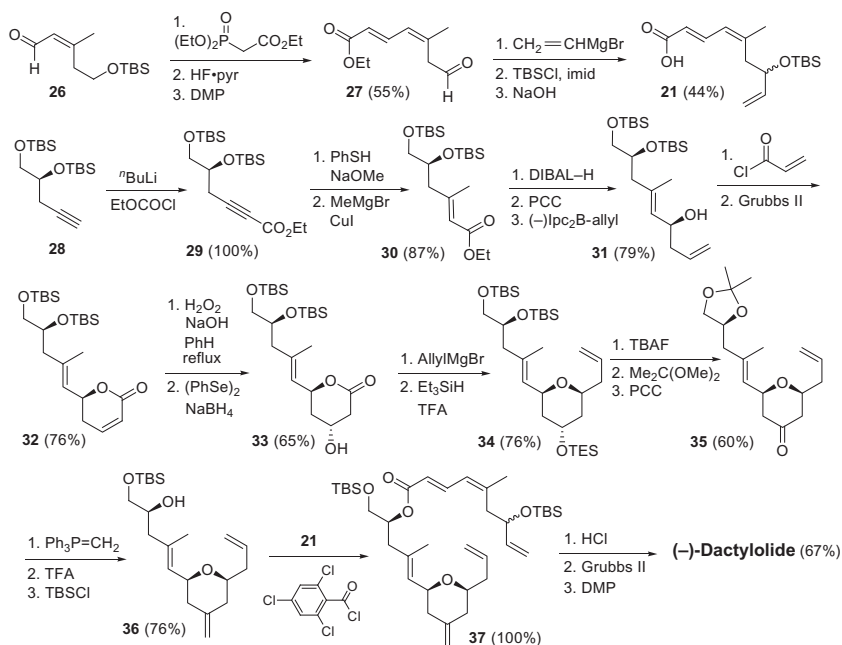
the corresponding terminal alkene provided **19**, which was subjected to silyl deprotection and the Sharpless asymmetric epoxidation to install important C19 stereochemistry, delivering epoxide **20**. Treatment of **20** and carboxylic acid **21** with $\text{Ti}(\text{O}^t\text{Bu})_4$ at 75 °C delivered ester **22** in 67% yield. The regiochemistry of the epoxide opening is the consequence of titanium chelate formation on the epoxy alcohol, leading to nucleophilic attack at the carbon distal to the alcohol [10]. Macrocyclization via ring-closing metathesis to form the C8–C9 bond gave allylic alcohol **23**, which was selectively oxidized with oxoammonium salt **24**. The final oxidative cleavage of the 1,2-diol afforded (–)-dactylolide ($[\alpha]_{\text{D}}^{\text{RT}} = -128^\circ$, $c = 0.39$, MeOH). (–)-Dactylolide was further converted to (–)-zampanolide as a 1:1 mixture of C20 epimers by aza-aldol addition of **25**, derived from (*Z,E*)-sorbamide and DIBAL-H.

2.3 Jennings Synthesis of (–)-Dactylolide

In 2005, Jennings reported a synthesis of (–)-dactylolide relying on ring-closing metathesis as the key macrocyclization step [8b]. Similar to the Hoye's synthesis, 1,3-dienoic acid **21** was esterified with the pyran-containing subunit at a late stage prior to the macrocycle formation (Scheme 3). The preparation of **21** commenced with aldehyde **26** via Horner–Wadsworth–Emmons olefination, deprotection of the silyl ether, and oxidation of primary alcohol, leading to the (*E,Z*)-conjugated ester **27**. Addition of vinylmagnesium bromide to provide a racemic allylic alcohol, its TBS-protection and saponification afforded acid **21**.

For the preparation of pyran moiety via a tandem nucleophilic addition–diastereoselective reduction of an *in situ*-generated oxonium ion, the C16–C17 trisubstituted alkene in **30** was installed via a two-step protocol involving an initial conjugate addition of benzenethiol to ynoate **29**, followed by an addition–elimination reaction with methylmagnesium bromide. Conversion of the ester to an aldehyde followed by Brown allylation afforded **31**. Acylation of alcohol **31** with acryloyl chloride and subsequent ring-closing metathesis gave lactone **32**, epoxidation of which with basic hydroperoxide followed by regioselective C–O bond cleavage using PhSeH [11] afforded **33**. The conversion of **33** to 2,6-*cis*-disubstituted tetrahydropyran was achieved in 76% yield via the addition of allylmagnesium bromide to the lactone and subsequent reduction of corresponding lactol with Et_3SiH and TFA.

The required 2,6-*cis*-stereochemistry was set by the axial attack of an incoming hydride onto a half-chair conformation of an oxonium intermediate. Installation of the *exo*-methylene functionality was accomplished by manipulation of **34** to ketone **35** and its Wittig methylenation. Esterification of **36** with **21** under Yamaguchi conditions, ring-closing metathesis, and final oxidation of both the primary and allylic alcohols afforded (–)-dactylolide ($[\alpha]_{\text{D}}^{\text{RT}} = -136^\circ$, $c = 1.2$, MeOH).



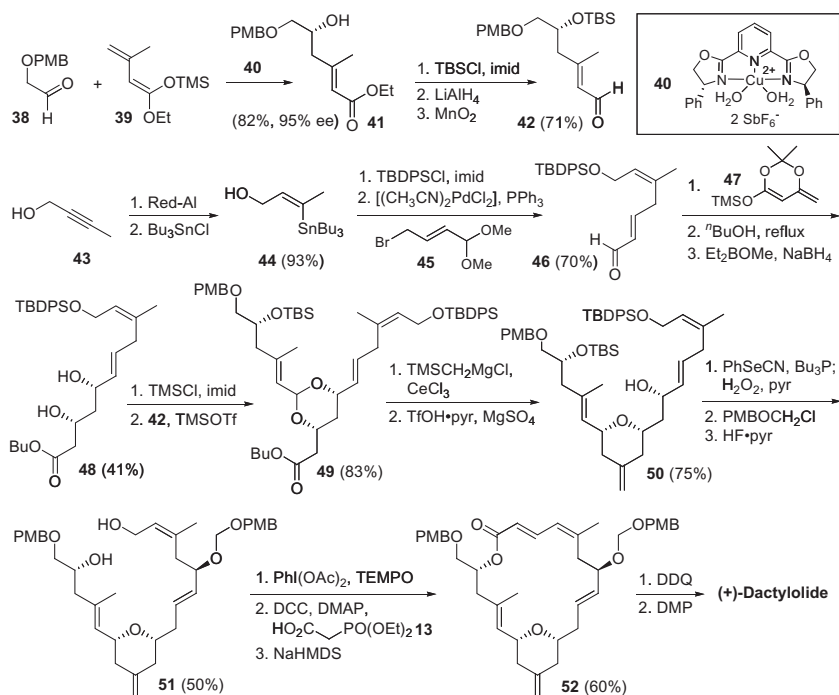
SCHEME 3 Jennings synthesis of (–)-dactylolide.

2.4 Floreancig Synthesis of (+)-Dactylolide

The Floreancig synthesis published in 2005 [8c] relies on the asymmetric vinylogous Mukaiyama aldol reactions [12] by which two advanced fragments for the *cis*-2,6-disubstituted-4-methylene tetrahydropyran were prepared. The macrocycle was formed via Horner–Wadsworth–Emmons olefination at the C2–C3 position as in Smith’s synthesis.

The synthesis commenced with an asymmetric vinylogous Mukaiyama aldol reaction between **38** and **39**, which was catalyzed by Cu–Pybox complex **40** [13] (Scheme 4). This reaction established the *E*-trisubstituted double bond as well as the C19 stereocenter with 95% ee. Silyl protection and reduction of the ester afforded aldehyde **42**. The C4–C5 double bond was set by hydroalumination of 2-butynol **43** followed by trapping of aluminum intermediate with tributylstannyl chloride to form vinyl stannane **44**.

After protection as the TBDPS ether, **44** was coupled with bromide **45**, and the product was then hydrolyzed upon workup, giving aldehyde **46**. A second Mukaiyama aldol reaction between **46** and **47**, catalyzed by Denmark’s bisphosphoramidate ligand [14] (not shown), set the stereochemistry of the newly formed allylic hydroxyl group. With ester **48** in hand, the two coupling partners were joined. Acid-catalyzed condensation of **48** with **42** provided acetal **49**, which was treated with excess $\text{TMSCH}_2\text{MgCl}$ and CeCl_3

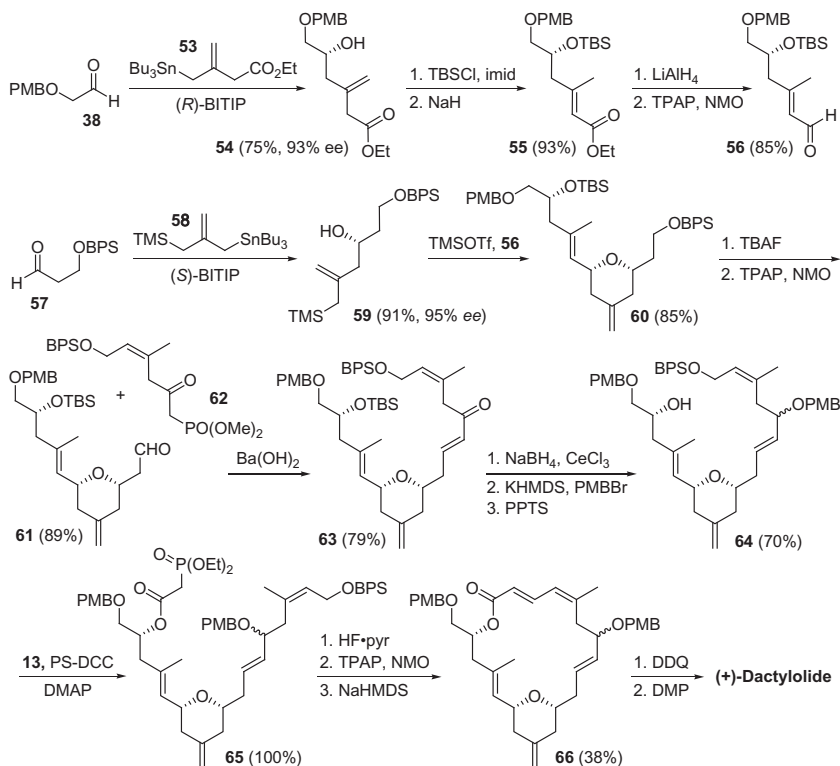


SCHEME 4 Floreancig synthesis of (+)-dactylolide.

and worked up under acidic conditions. This multistep transformation includes addition of two equivalents of the nucleophile to the ester, inducing a Peterson olefination [15] to generate an allyl silane. Upon acidic workup, the acetal ionized, forming an oxonium ion, which was trapped intramolecularly by the allylic silane, generating desired pyran **50** in 75% yield. With the pyran formed, an allylic [1,3]-transposition of the C7–C9 allylic alcohol was required. Toward this end, alcohol **50** was converted to a selenide by displacement with PhSeCN and Bu₃P. Upon oxidation, the resultant selenoxide underwent a [2,3]-sigmatropic rearrangement, delivering the transposed alcohol [16,17], which was subjected to protecting group manipulations to give **51**. Selective oxidation at the primary alcohol and esterification with **13** provided macrocycle **52** via Horner–Wadsworth–Emmons olefination upon treatment with NaHMDS. Deprotection of the C7 and C19 hydroxyl groups and *bis*-oxidation provided (+)-dactylolide. ($[\alpha]_{\text{D}}^{\text{RT}} = +163^\circ$, $c = 0.29$, MeOH) in 49% yield over two steps.

2.5 Keck Synthesis of (+)-Dactylolide

The synthesis by Sanchez and Keck [8d] shares strategic similarity with that of others. This includes a macrocyclization via Horner–Wadsworth–Emmons olefination to establish the C2–C3 bond and the pyran formation via



SCHEME 5 Keck synthesis of (+)-dactylolide.

intramolecular attack of an allylic silane to an incipient oxonium species. One of the unique features of this synthesis involves the catalytic asymmetric allylation using allyl silanes and stannanes developed in the same group [18].

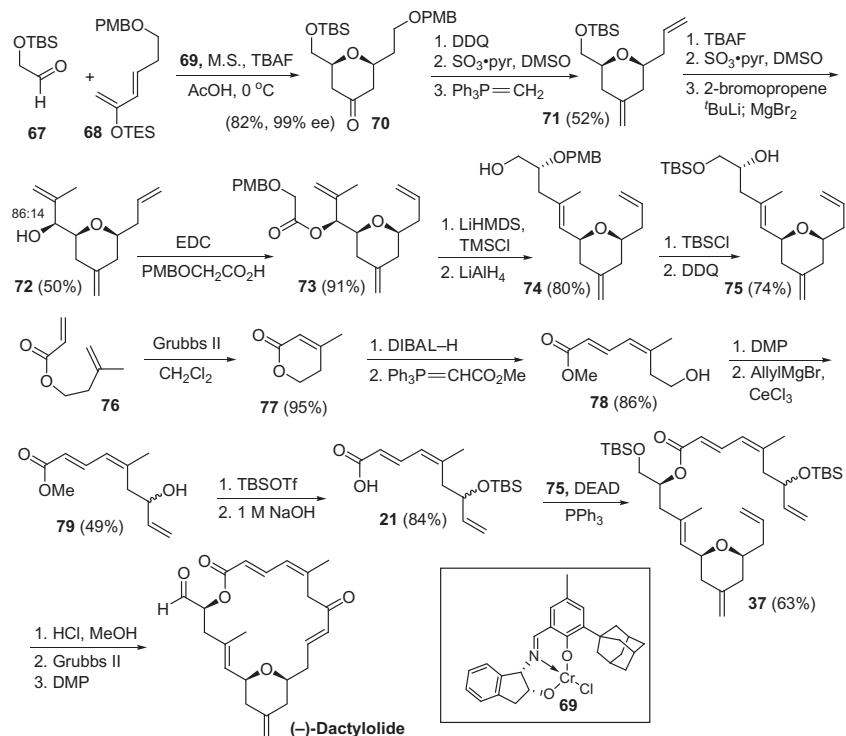
The synthesis started with the asymmetric allylation of aldehyde **38** with functionalized allylic stannane **53** (Scheme 5). The reaction was catalyzed by BINOL–titanium tetraisopropoxide (BITIP) [19], which provided **54** in 93% ee. The trisubstituted alkene was accessed by isomerization of the β,γ -unsaturated ester to a more stable α,β -unsaturated isomer. This reaction gave best results for the desired *E*-isomer when the counteraction was sodium. A second BITIP-catalyzed allylation between aldehyde **57** and allylic stannane **58** afforded allylic silane **59** in 91% yield and 95% ee. The pyran annulation reaction occurred between **59** and **56**, giving the pyran subunit **60** in 85% yield. The right arm of pyran **60** was homologated by conversion to aldehyde **61** followed by Horner–Wadsworth–Emmons olefination with ketophosphonate **62** to install the C8–C9 alkene. The trisubstituted alkene of **62** was derived from conjugate addition of methyl cuprate to an ynoate similar to that described in Smith’s synthesis. With **63** in hand, the final elaboration to dactylolide closely followed

those of Floreancig and Smith. After minor protecting group manipulations, **63** was coupled with **13** using polymer bound DCC to simplify isolation. Horner–Wadsworth–Emmons macrocyclization gave **66**, the deprotection and oxidation of which led to (+)-dactylolide ($[\alpha]_{\text{D}}^{\text{RT}} = +134^\circ$, $c = 0.065$, MeOH).

2.6 McLeod Synthesis of (–)-Dactylolide

McLeod and coworkers reported a synthesis of (–)-dactylolide in 2006 [8e]. This approach implements a macrocyclic RCM to form the C8–C9 double bond employing C1–C8 subunit **21**, which is a common feature in the syntheses of Hoyer and Jennings. However, the synthesis of the *exo*-methylene tetrahydropyran subunit via an asymmetric hetero Diels–Alder reaction is unique in this approach. An Ireland–Claisen rearrangement was implemented for the installation of the trisubstituted C16–C17 double bond.

The synthesis began with an asymmetric hetero-Diels–Alder reaction between **67** and **68** with Jacobsen’s chiral chromium(III) catalyst **69**, affording **70** in 82% yield and 99% ee (Scheme 6). Deprotection of the PMB-ether and oxidation to the aldehyde followed by Wittig reaction of both the aldehyde



SCHEME 6 McLeod synthesis of (–)-dactylolide.

and ketone afforded **71**. Deprotection of the silyl ether, oxidation and alkylation with isopropenyllithium, in the presence of magnesium bromide, delivered **72** (86:14 dr). Esterification of **72** to **73** followed by an Ireland–Claisen rearrangement and reduction gave **74**, which simultaneously set both the C16–C17 double bond geometry and the C19 stereochemistry. Protecting group manipulations of **74** provided secondary alcohol **75** necessary for the esterification with subunit **21**, which was synthesized from acrylate **76**.

A three-step sequence involving an RCM, partial reduction of the lactone moiety, and Horner–Wadsworth–Emmons olefination delivered (2*E*,4*Z*)-diene ester **78**. Conversion of **78** to allylic alcohol **79** followed by TBS-protection and saponification afforded acid **21**.

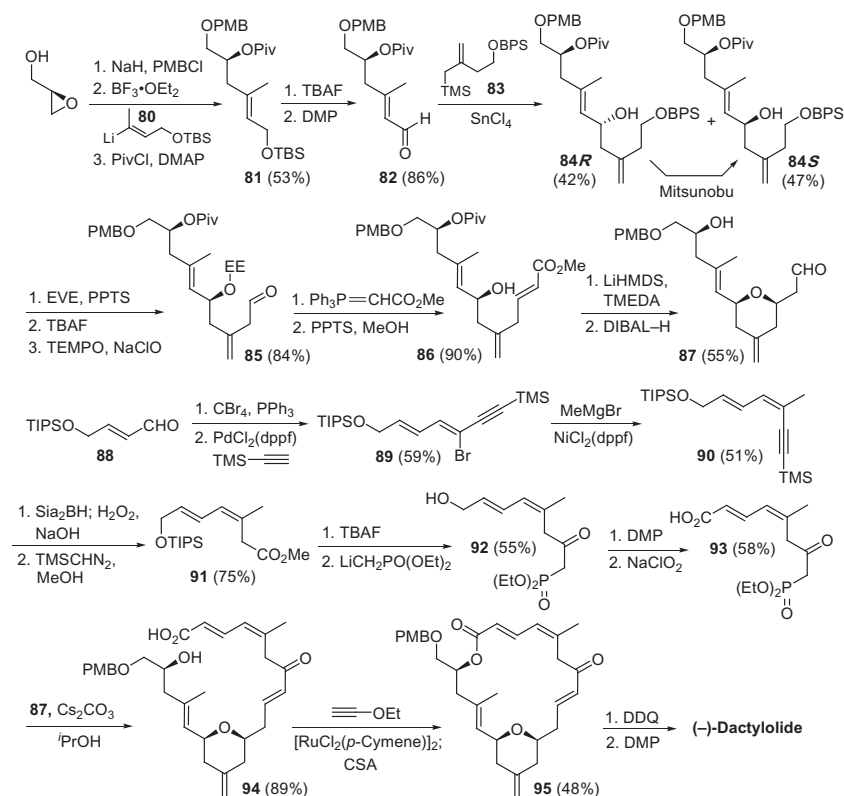
The union of **75** and **21** was achieved to afford **37** via a Mitsunobu reaction with the inversion at the C19 stereocenter. Desilylation of **37** followed by an RCM to form the macrocycle and the final TBS deprotection and oxidation completed the synthesis of (–)-dactylolide ($[\alpha]_{\text{D}}^{\text{RT}} = -169^\circ$, $c = 0.42$, MeOH).

2.7 Uenishi and Tanaka Synthesis of (–)-Dactylolide

The strategy of Uenishi *et al.* [8f] for (–)-dactylolide involved a Trost–Kita method [20] to close the macrocycle and a Sakurai reaction similar to the syntheses of Hoye and Keck to assemble the tetrahydropyran subunit. Other key steps include a stereoselective intramolecular *O*-Michael reaction for the 2,6-*cis*-tetrahydropyran moiety and a stepwise metal-catalyzed cross-coupling of 1,1-dibromodiene to install *Z*-trisubstituted alkene [21] in the C1–C8 subunit.

The synthesis started with ring opening of PMB-protected (*R*)-glycidol with lithium reagent **80** followed by pivalate formation to afford **81** (Scheme 7). Removal of the silyl ether and oxidation gave aldehyde **82**, which was coupled with allylic silane **83** under Sakurai conditions, providing diastereomers **84R** and **84S**. The stereochemistry at C15 of **84R** was inverted by a Mitsunobu reaction followed by methanolysis. Conversion of **84S** to the cyclization precursor **86** was realized via ethoxyethyl protection of secondary alcohol, cleavage of silyl ether and oxidation to form **85**. This was followed by a Wittig reaction, and hydrolysis of the ethoxyethyl ether to give **86**. The *O*-Michael reaction of **86** gave separable *cis/trans* tetrahydropyrans (1.8:1 dr). Reduction of the ester with DIBAL-H afforded aldehyde **87**.

The C1–C8 subunit was synthesized from aldehyde **88**. Dibromomethylation and stereoselective Sonogashira coupling gave dienyne **89**, which upon Kumada coupling with methylmagnesium bromide afforded **90** with an inversion of olefin geometry. The stereochemical outcome can be explained by the isomerization of a (*Z*)-alkenyl Ni-intermediate [21] to the corresponding (*E*)-alkenyl Ni-complex via a reversible 1,3-metal migration whereby the unfavorable steric repulsions are attenuated. Subsequent transmetallation and reductive elimination from this intermediate would provide the observed



SCHEME 7 Uenishi and Tanaka synthesis of (–)-dactylolide.

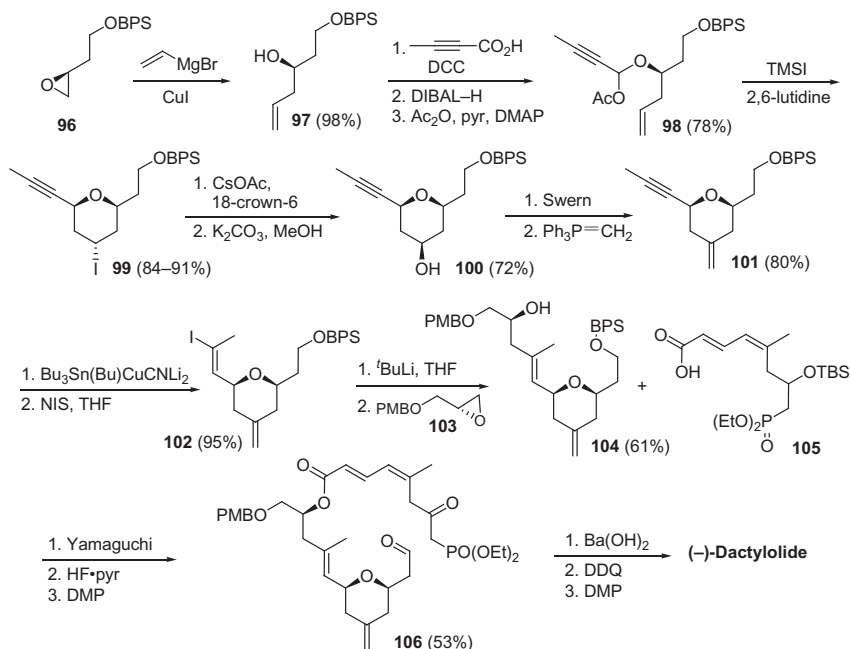
product. Dieneyne **90** was elaborated to β -ketophosphonate **93** in four steps via the intermediacy of methyl ester **91**.

The Horner–Wadsworth–Emmons reaction between **87** and **93** installed C8–C9 double bond and Trost–Kita macrocyclization of **94** afforded cyclic product **95** in modest yield. Final deprotection of PMB-ether and oxidation delivered (–)-dactylolide. ($[\alpha]_D^{RT} = -167.8^\circ$, $c = 0.45$, MeOH).

2.8 Altmann and Gertsch Synthesis of (–)-Dactylolide

Published in 2010 [8g], the Altmann and Gertsch synthesis of (–)-dactylolide relied on Horner–Wadsworth–Emmons olefination to install C8–C9 double bond as a macrocyclization step. The synthesis of the tetrahydropyran subunit was unique in that it employed a highly stereoselective Prins-type reaction involving a segment coupling originally developed by Rychnovsky [22] (Scheme 8).

The synthesis commenced with the copper-catalyzed opening of epoxide **96** with vinylmagnesium bromide, generating homoallylic alcohol **97**. Alcohol

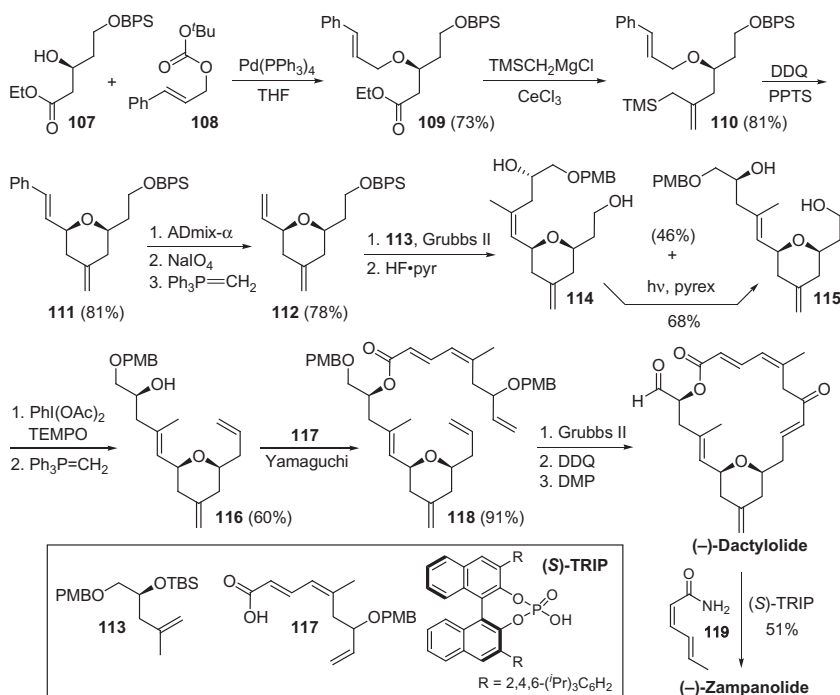


SCHEME 8 Altmann and Gertsch synthesis of (–)-dactylolide.

97 was then elaborated to the acetal **98** via esterification with 2-butynoic acid, reduction with DIBAL-H and trapping of the aluminate intermediate with Ac_2O . Treatment of **98** with TMSI resulted in stereoselective Prins-type cyclization to generate *cis*-2,6-disubstituted 4-iodotetrahydropyran core [22f]. The *exo*-methylene functionality was installed by converting iodide **99** to secondary alcohol **100**, followed by oxidation and Wittig methylenation. The internal triple bond in **101** was then converted to *E*-vinyl iodide **102** by stannyl cupration with $\text{Bu}_3\text{Sn(Bu)CuCNLi}_2$ followed by Sn–I exchange with NIS. The necessary three-carbon unit was introduced by opening of epoxide **103** with the vinyl lithium reagent derived from iodide **102**. Yamaguchi esterification with phosphonate **105**, desilylation, and oxidation afforded macrocyclization precursor **106**. Intramolecular Horner–Wadsworth–Emmons reaction of **106** in the presence of activated Ba(OH)_2 , deprotection of PMB-ether, and oxidation of the C20 primary alcohol delivered (–)-dactylolide ($[\alpha]_{\text{D}}^{\text{RT}} = -258.3^\circ$, $c = 0.11$, MeOH).

2.9 Ghosh Synthesis of (–)-Dactylolide and (–)-Zampanolide

The most recent synthesis of (–)-dactylolide and (–)-zampanolide was reported by Ghosh in 2011 [8h]. This route involves the synthesis of dactylolide on which the *N*-acyl hemiaminal side chain was directly introduced via a stereoselective organocatalytic reaction. The 18-membered macrocycle was



SCHEME 9 Ghosh synthesis of (–)-dactylolide and (–)-zampanolide.

installed by forming the C8–C9 alkene by an RCM reaction as in the syntheses of Hoyer and Jennings. The C1–C8 building block, similar to **21** in Hoyer's synthesis, was prepared via the sequence of Reformatsky and Wittig reactions. For the synthesis of the pyran subunit, DDQ-mediated generation of an oxonium intermediate and its trapping with a tethered allyl silane moiety was employed.

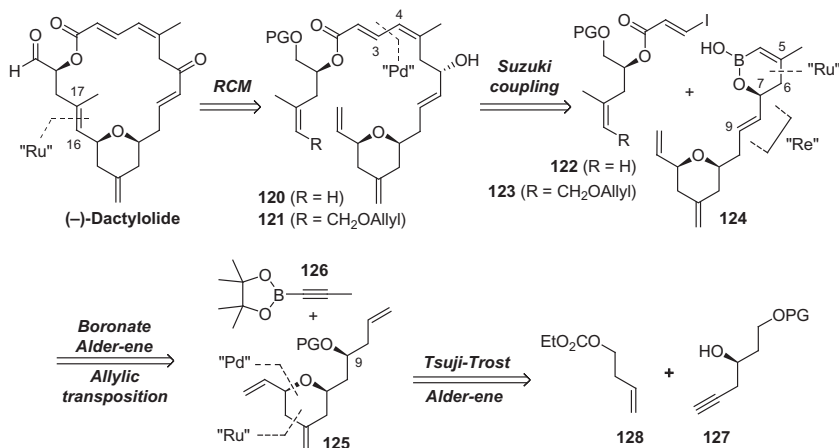
The synthesis was initiated by Pd-catalyzed etherification of secondary alcohol **107** with *tert*-butylcinnamyl carbonate **108** to generate cinnamyl ether **109** (Scheme 9). Conversion of the ester moiety of **109** to allyl silane **110** was achieved 81% yield via a one-step protocol developed by Narayanan and Bunelle [23]. Treatment of allyl silane **110** with DDQ and PPTS provided *cis*-2,6-disubstituted tetrahydropyran **111** in good yield. At this point, the cross metathesis to install the trisubstituted alkene at C16–C17 was not successful probably due to the low reactivity of styrene moiety, which thus was converted to the corresponding terminal alkene **112** via dihydroxylation, diol cleavage, and Wittig olefination.

Cross metathesis of **112** and **113** provided a separable 1.7:1 mixture of *Z*-alkene **114** and *E*-alkene **115** in 46% overall yield after desilylation. *Z*-alkene **114** was converted to **115** by photochemical isomerization. Selective oxidation of primary alcohol in **115** followed by methylenation afforded **116**,

which was coupled with acid **117** under Yamaguchi conditions. RCM of **118**, PMB-deprotection and oxidation delivered (–)-dactylolide in 52% yield ($[\alpha]_{\text{D}}^{\text{RT}} = -148^\circ$, $c = 0.09$, MeOH). (–)-Dactylolide was converted to (–)-zampanolide by Bronsted acid-catalyzed addition of **119** to C20 formyl group. The chemoselectivity and stereoselectivity of this reaction using chiral phosphoric acid (*S*)-TRIP was significantly higher (51% of (–)-zampanolide and 18% of its epimer) than that of Uenishi *et al.* [8f]. No aminor formation was observed in this reaction.

3. RETROSYNTHETIC ANALYSIS

Although there have been a multitude of syntheses reported for dactylolide and zampanolide, they share quite similar key bond disconnections and overall synthetic strategies. We envisioned a new strategy involving completely different bond disconnections from the reported approaches. In order to achieve this, we developed several new synthetic methodologies that rely on transition metal-catalyzed manipulations of unsaturated functional units. The ability of these catalysts to engage relatively unactivated alkenes and alkynes as substrates is a key to minimize the number of synthetic steps, especially for synthetic targets containing multiple units of unsaturation, such as dactylolide. Our strategy for the macrocyclization relies on a late stage ring-closing metathesis [24] to form the C16–C17 double bond from **120** or its corresponding relay metathesis [25] substrate **121** (Scheme 10). This novel bond disconnection is adventurous considering the number of alkenes in the molecule and a predisposed difficulty in forming trisubstituted double bonds via metathesis, let as well as the desired *E*-stereochemistry. The C3–C4 bond was planned to be constructed via Suzuki coupling between iodoacrylate **122**



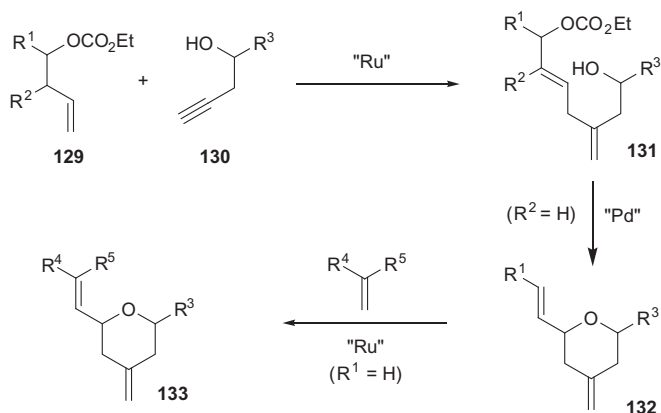
SCHEME 10 Retrosynthetic approach toward (–)-dactylolide.

or **123** and cyclic boronic acid half ester **124**. Alkenyl boron species **124** would be accessed by using a ruthenium-catalyzed Alder-ene reaction (RCAER) [26] between terminal alkene **125** and borylated alkyne **126** to form the C5–C6 bond followed by a regioselective [27] rhenium(VII)-catalyzed [28] allylic [1,3]-transposition [29]. The pyran subunit in **125** would be installed using a tandem RCAER and subsequent palladium-catalyzed ring closure [30] from readily accessible building blocks **127** and **128**.

4. NEW SYNTHETIC METHODS DEVELOPMENT AND APPLICATION

4.1 Preparation of the Pyran Subunit

For the synthesis of the pyran subunit of dactyloide, we have developed a general approach [30] to construct this substructure via a streamlined use of three transition metal-catalyzed transformations; RCAER, π -allyl-Pd-mediated cyclization, and ruthenium alkylidene-catalyzed cross metathesis (Scheme 11). The key step of our strategy is the Ru-catalyzed Alder-ene [26b,31] reaction between alkene **129** and alkyne **130** to directly install the *exo*-methylene unit and the precursor functionality for the π -allyl-Pd-mediated cyclization [32]. Subsequent ring closure of **131** would provide tetrahydropyran **132**, containing not only an *exo*-methylene but also the pendent vinyl group. One potential limitation of this strategy would be the difficulty in forming the C16–C17 trisubstituted alkene. This is because of the low reactivity of the π -allyl-Pd species containing a branched carbon at the allylic center (R^2) as well as the tedious installation of a tertiary carbonate with defined configuration on the alkene substrate. Faced with this encumbrance, we envisioned a cross metathesis reaction between the terminal alkene of **132** ($R^1 = H$) and appropriate 1,1-disubstituted alkene, but the execution of the plan

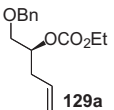
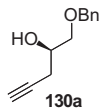
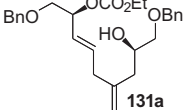
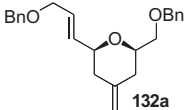
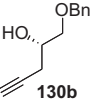
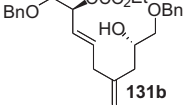
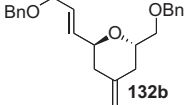
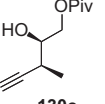
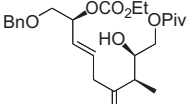
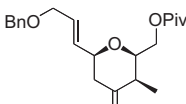
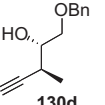
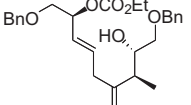
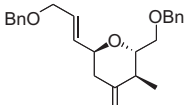
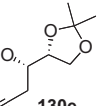
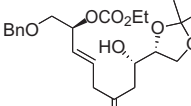
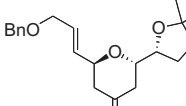


SCHEME 11 General strategy for pyran synthesis.

was hampered by the relatively low reactivity of sterically hindered vinyl group in **132**.

We explored the synthesis of a variety of functionalized 2-vinyl-4-methylene-tetrahydropyrans from enantiomerically enriched homoallylic and homo-propargylic alcohols (Table 1). The ruthenium-catalyzed coupling proceeded with excellent selectivity in most cases, generating branched isomer products **131** either predominantly or exclusively. The typical mechanism involving a metallacyclopentene intermediate derived from **129** and **130** accounts for the product distribution of RCAER [26b]. Subsequently, a palladium-catalyzed cyclization of branched dienes **131** afforded 4-methylene tetrahydropyrans **132** with good efficiency. The only minor side product in this reaction is the conjugated triene, which results from the β -hydride elimination of the π -allyl-Pd complex. In case of secondary allyl carbonates **131** ($R^2=H$, $R^1\neq H$) both *cis*- and *trans*-2,6-disubstituted tetrahydropyrans could be

TABLE 1 Substrate Controlled Synthesis of Functionalized Tetrahydropyrans

Entry	Alkene	Alkyne	Coupled product	Yield (%) (BORSM)	Cyclized product	Yield (%)
1				45 (63)		71
2	129a			61		68
3	129a			55		70
4	129a			51 (72)		85
5	129a			41		85

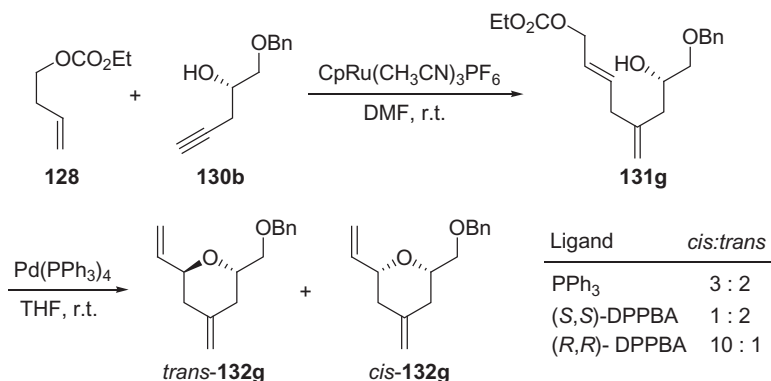
accessed by choosing appropriate stereochemistry of the substrate carbonates and homopropargylic alcohols.

The transfer of stereochemistry from the starting materials to the final tetrahydropyrans is exemplified in Table 1. Starting with suitable stereochemistry on alkenes and alkynes, both *cis*- and *trans*-2,6-disubstituted tetrahydropyrans can be synthesized relying on the stereospecificity of the formation of π -allyl-Pd intermediates and their subsequent displacement with oxygen nucleophiles. Thus, the stereochemical information of allylic carbonate will be retained in the product by double inversion during allylic alkylation, which enables the formation either *cis*- or *trans*-product depending on the stereochemistry of homoallylic alcohols. The more thermodynamically favorable *cis*-2,6-disubstituted tetrahydropyran **132a** was obtained in 71% yield (entry 1), yet the reversed stereochemistry of the homopropargylic alcohol gave the *trans*-2,6-disubstituted isomer with equal efficiency (entry 2).

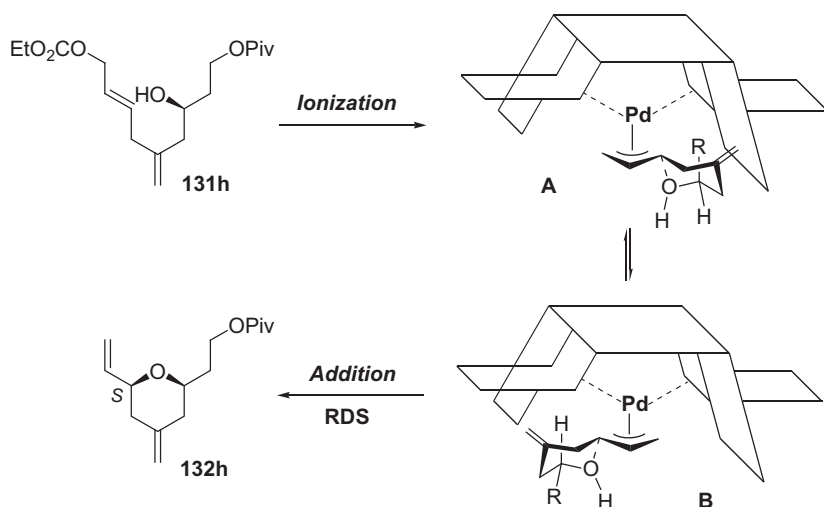
Reactions of other homopropargylic alcohols containing an additional stereogenic substituent provided the corresponding tetrahydropyran products in a similar manner (entries 3–5).

For the preparation of 4-*exo*-methylene-2,6-disubstituted tetrahydropyrans containing a vinyl substituent as a handle for metathesis-based homologation, alkene **128** was coupled with alkyne **130b** to give the terminal allylic carbonate **131g** in 44% yield (92% BORSM) (Scheme 12). Palladium-catalyzed cyclization of **131g** under substrate control afforded both *cis*- and *trans*-isomers in a 3:2 ratio and 77% overall yield. Selective formation either the *cis*- or *trans*-isomer can be realized by using Trost's diphenylphosphinobenzoic acid (DPPBA)-based chiral ligands [33]. The selectivity for *cis*-**132g** in the Pd-catalyzed ring closure could be increased to 10:1 by using (*R,R*)-DPPBA ligand, while that with (*S,S*)-DPPBA ligand reversed the ratio to 1:2 in favor of the *trans*-isomer.

The stereochemical outcome of the cyclization can be predicted / explained by the working model [33] proposed by Trost for the reactions with DPPBA



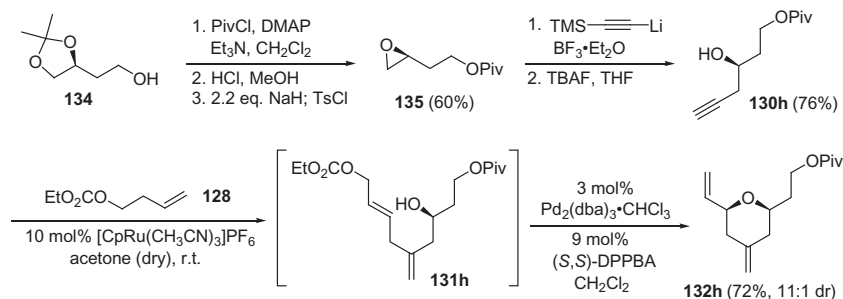
SCHEME 12 Ligand-based stereocontrol in pyran synthesis.



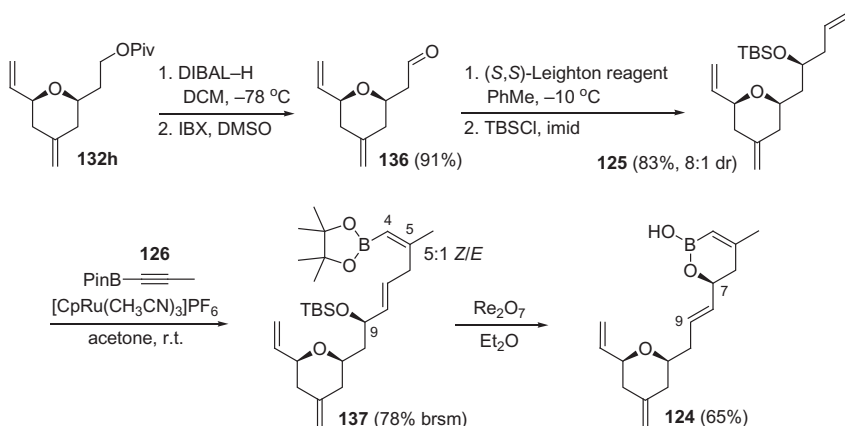
SCHEME 13 Stereocontrol of cyclization.

ligands (Scheme 13). In this Pd-catalyzed allylic alkylation mechanism, there are two possible stereochemistry-determining steps: ionization of the leaving group and addition of a nucleophile. If the rate of equilibration of diastereomeric π -allyl-Pd complexes is slower than the rate of nucleophilic addition, the ionization step is stereochemistry determining. On the other hand, if the rate of equilibration is faster than the nucleophilic addition, the stereochemical outcome will be determined at this stage. The nature of the nucleophile is of profound importance for high selectivity in these reactions. “Soft” nucleophiles react faster with π -allyl-Pd complexes, which makes the ionization step stereochemistry determining. With “hard” nucleophiles, the rate of trapping becomes comparable to or slower than η^1 - and η^3 -allyl interconversion. Alcohols are relatively poor nucleophiles for Pd-catalyzed allylic alkylations due to their “hard” nature. Therefore, the rate of addition is lower than that of π -allyl interconversion, and thus nucleophilic addition becomes stereochemistry determining. Under this model, allylic carbonate **131h** in the presence of (*S,S*)-DPPBA-complexed palladium catalyst would undergo an ionization dictated by chiral environment of the ligand to form π -allyl-Pd complex **A**. While the intermediate **A** is in equilibrium with an isomeric complex **B**, an addition of the oxygen nucleophile onto a matched face of **B** would lead to (*S*)-stereochemistry of the newly created stereogenic center in **132h**.

With this methodology in hand, we explored the synthesis of the pyran subunit of (–)-dactylolide. Homopropargylic alcohol **130h**, the substrate for the Alder-ene reaction, was synthesized from commercially available (4*S*)-(+)-4-(2-hydroxyethyl)-2,2-dimethyl-1,3-dioxolane **134** via epoxide **135** according to the known procedure (Scheme 14) [34]. The Alder-ene reaction between **130h** and homoallylic carbonate **128** followed by a cycloetherification under



SCHEME 14 Synthesis of the pyran subunit of dactylolide.

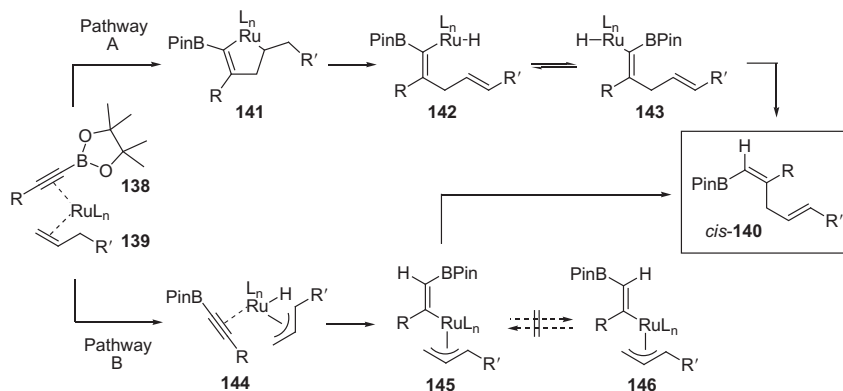


SCHEME 15 Synthesis of cyclic boronic acid half ester.

the palladium-catalyzed conditions led to the formation of pyran **132h**. In general, this transformation was best achieved in DMF employing the procedure developed by Trost *et al.* [35], but in case of the conversion of **131h** to **132h** the stereoselectivity was only modest (*cis:trans* = 4:1) under the standard conditions (0 °C to r.t.) with (*S,S*)-DPPBA [33]. Gratifyingly, running the reaction in acetone, followed by its evaporation, and addition of a premixed solution of Pd-catalyst and ligand in CH₂Cl₂ at -25 °C, improved the selectivity for *cis*-**132h** to an 11:1 ratio with a 72% isolated yield.

4.2 Preparation of the (Z)-Trisubstituted Vinyl Boronate

The pyran subunit **132h** was elaborated into triene **125** in four steps (Scheme 15). Removal of the pivalate group from **132h** with DIBAL-H and oxidation of the resultant alcohol with *o*-iodoxybenzoic acid (IBX) afforded aldehyde **136**. Leighton asymmetric allylation [36] and subsequent TBS-protection of the homoallylic alcohol gave **125** in 83% yield (8:1 dr). At this point, all necessary functionality had been introduced for the sequence of

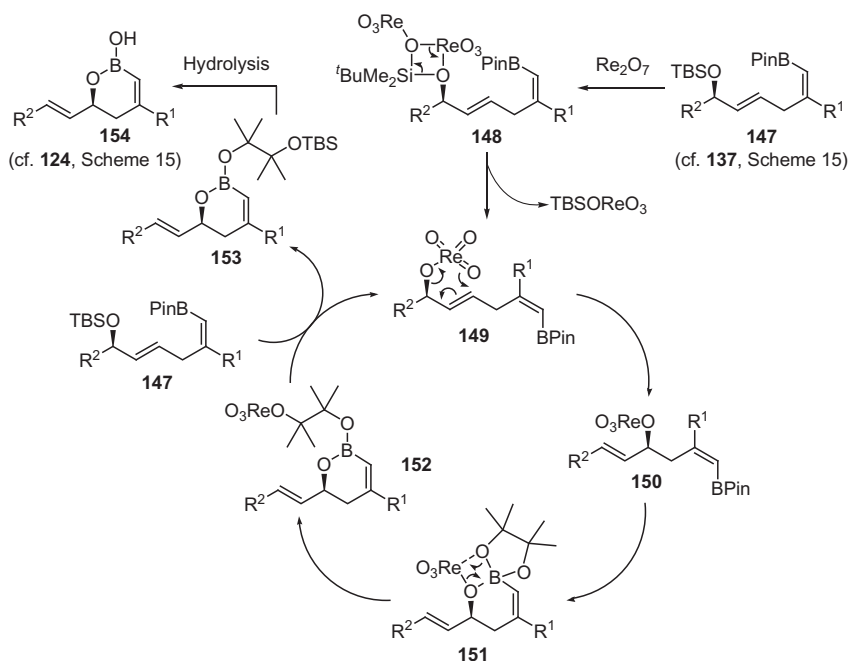


SCHEME 16 Possible mechanisms for the formation of *cis*-vinyl boronates.

Alder-ene reaction with borylated alkynes [26a] and an allylic transposition [27c] for the stereoselective construction of C4–C9 fragment of dactylolide.

RCAER of **125** and borylated alkyne **126** [37] occurred selectively with least hindered double bond at the C7 position and afforded vinyl boronate **137** exclusively with the expected *Z*-selectivity of C4–C5 trisubstituted alkene (*Z*:*E* = 5:1). The conversion of **125** was low; however, acceptable yields were obtained by recycling this compound. Exclusive formation of the branched product in the Alder-ene reaction is assumed to be the result of a strong directing effect of a boronate to form ruthenacyclopentene intermediate **141** (Scheme 16). The tendency for internal alkynes with bulky substituents favoring this pathway is well established for silicon- [38] and carbon-containing [39] alkynes. In order to explain the unusual *cis*-stereochemistry, two possible mechanisms were formulated by the extension of the general mechanisms of the Alder-ene reaction proposed by Trost [31a,c,e,40]. The formation of *cis*-**140** would be the consequence of an isomerization of **142** to **143** after β -hydride elimination from ruthenacyclopentene **141** (pathway A). An alternate mechanism involves an allylic C–H activation to form a π -allyl ruthenium hydride complex **144** and *trans*-hydridoruthenation [41] sequence, where the isomerization of **145** to **146** would be slower than its reductive elimination (pathway B).

Installation of the allylic hydroxyl group at C7 requires a regioselective transposition of C–O bond of boronate **137** either before or after the planned Suzuki coupling. In general, metal-catalyzed allylic transposition of allylic alcohols leads to the formation of an equilibrium mixture of regioisomeric products due to the reversible nature of the reaction [28,29]. While electronic biasing elements such as conjugation and steric pressure around the allylic alcohol moiety have been utilized to achieve the regiocontrol of transposition [27a,b], we envisioned a Lewis acid–base interaction between the boronate and the rearranged oxygen-based functional group. To pursue this idea, we developed a two-step sequence to generate the allylic hydroxy-transposed boronic esters,



SCHEME 17 Plausible mechanisms for the allylic transposition.

wherein the TBS-protecting group of homoallylic alcohol was found to be most suitable for both the Alder-ene reaction and allylic transposition step (Scheme 15). The allylic transposition of **137** proceeded at room temperature in the presence of 5 mol% Re_2O_7 to generate the cyclic boronic acid half ester **124** in 65% yield with complete chirality transfer of transposed alcohol.

A plausible mechanism that accounts for the formation of the cyclic boronic acid is shown in Scheme 17. Upon activation of the Si–O bond of substrate **147** with rhenium oxide via **148**, the resultant intermediate **149** will undergo an allylic transposition into **150** via either a [3,3]-sigmatropic rearrangement or an ion pair of the corresponding allylic carbocation. A ligand exchange via the expected Lewis acid–base interaction on **151** will lead to a penultimate intermediate **152**, which upon another ligand exchange with a substrate will release product **153**, regenerating intermediate **149**. The initially formed boronate **153** readily hydrolyzed during the purification on silica gel, providing the final product **154**.

The generality of this allylic transposition was explored with a variety of boronates **147a–e** (Table 2). Under typical conditions (Re_2O_7 ; CH_2Cl_2 or Et_2O , 25 °C), these boronates rearranged to generate products **154a–e** in good yields. In case of **147c**, transposition occurred during the Alder-ene reaction, to produce **154c** in 43% yield, probably via a cationic intermediate that readily formed under the reaction conditions (entry 3).

TABLE 2 Synthesis of Cyclic Boronic Esters

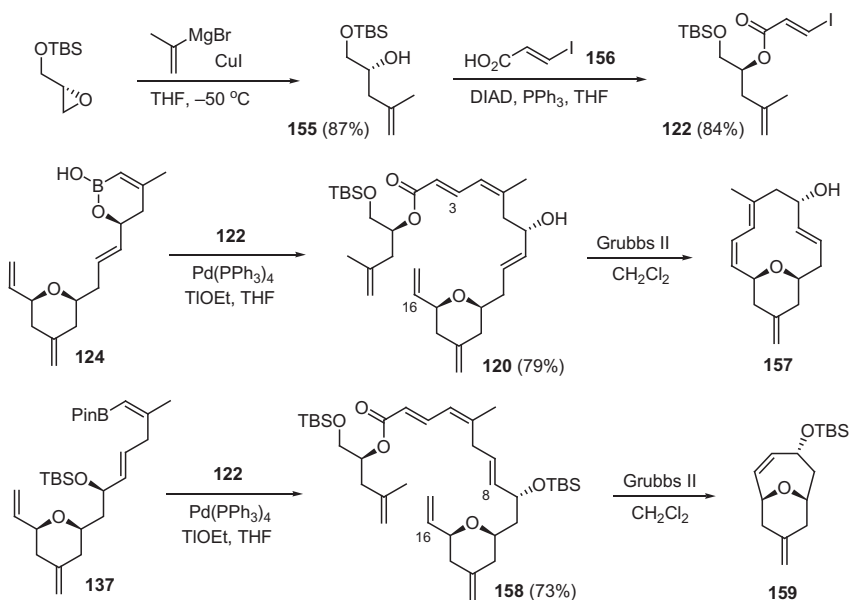
Entry	Coupled product	Yield (%)	Rearranged product	Yield (%)
1	147a	62	154a	92
2	147b	60	154b	73
3	147c	—	154c	43
4	147d	60	154d	72
5	147e	65	154e	70

Allylic transposition of **147d** and **147e** provided **154d** and **154e** with complete stereochemical integrity (entries 4 and 5), which is assumed to be the result of a predominant [3,3]-sigmatropic rearrangement over the formation of an ion pair of allylic carbocation.

4.3 Macrocyclic Ring-Closing Metathesis

E-vinyl iodide coupling partner **122** for the Suzuki reaction was prepared from TBS-protected (*S*)-glycidol (Scheme 18). The epoxide opening with 2-propenylmagnesium bromide to form **155** and its subsequent Mitsunobu reaction [42] in the presence of 2-iodoacrylic acid **156** [43] provided ester **122**.

The coupling between **122** and **124** proceeded smoothly using conditions developed by Roush et al. [44], providing **120** in 79% yield. At this stage, a

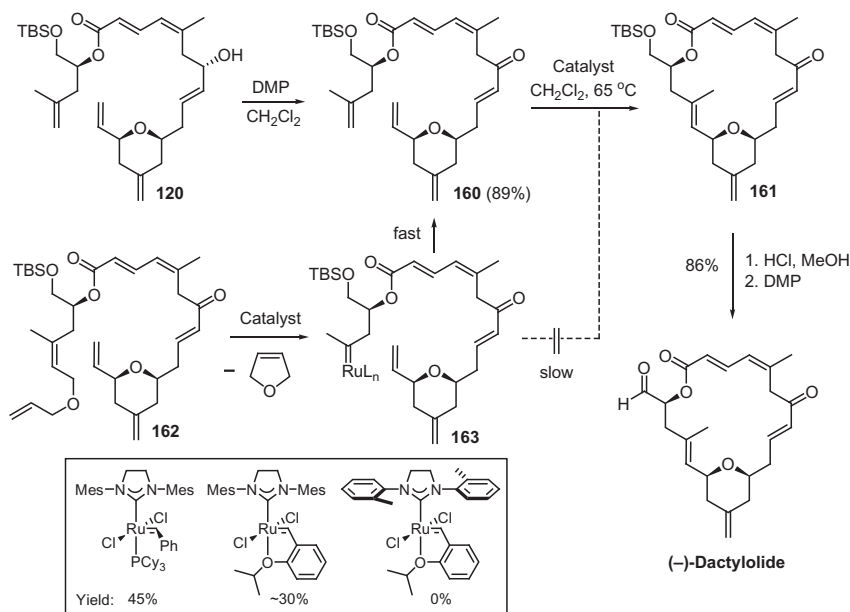
**SCHEME 18** Suzuki coupling and ring closure attempts.

ring-closing metathesis was attempted by treating a dilute solution of **120** with Grubbs second-generation catalyst. However, the desired ring closure product was not observed. Instead, an alternative mode of ring closure involving the C2–C3 double bond led to **157**. Surprisingly, the RCM of **158**, bearing the allylic TBS-ether before an allylic transposition, afforded a rather strained bridged bicycle **159**, which is the consequence of a ring closure onto the nearest C7–C8 double bond.

5. COMPLETION OF DACTYLOLIDE SYNTHESIS

To steer the ring-closing metathesis toward the formation of desired 18-membered macrolactone, we oxidized the C7 alcohol of **120** with Dess–Martin periodinane in 89% yield (Scheme 19).

This conversion is based on the notion that the local conformation of the resultant ketone **160** around C7 would resemble that of dactylolide more closely than alcohol **120**, such that the desired ring closure would become more accessible. Gratifyingly, treatment of **160** with Grubbs second-generation catalyst in the presence of benzoquinone [45] produced desired macrocycle **161** in 45% yield. To improve the efficiency of cyclization, we explored other catalysts such as Grubbs–Hoveyda second-generation catalyst and sterically less encumbered catalysts as well as the first-generation Grubbs catalyst, but none of them provided an increased yield. We expected that ring closure would be facilitated



SCHEME 19 Completion of the synthesis.

by generating propagating alkylidene species on the more sterically hindered trisubstituted double bond. To test this hypothesis, an RCM substrate **162** that contains a relay metathesis tether was prepared. However, **162** did not cyclize directly into **161**, it rather deactivated itself to **160** by cleaving off the relay tether. This futile metathesis is the result of a faster methylene transfer with intermediate **163** compared to its macrocyclic ring closure. Based on the RCM behaviors of **120**, **158**, **160**, and **162**, we concluded that the local conformation of the linear substrates plays a more important role than the steric hindrance on or near the reacting alkene moieties.

Completion of (–)-dactylolide was accomplished by removal of the TBS group from **161** followed by oxidation of the resultant alcohol with Dess–Martin periodinane. The spectroscopic data of the synthetic material identical to those reported in the literature for dactylolide ($[\alpha]_{\text{D}}^{\text{RT}} = -140.0^\circ$, $c = 0.03$, MeOH).

6. SUMMARY

In conclusion, a concise total synthesis of (–)-dactylolide was achieved via a longest linear sequence of 13 steps with a 7.5% overall yield. This synthetic process highlights several new synthetic methodologies designed for the construction of the delicate functionalities present in the target molecule. A RCAER of homoallylic carbonates and homopropargylic alcohols followed by a palladium-catalyzed π -allyl etherification was used for stereoselective construction of 2,6-disubstituted-4-methylene-tetrahydropyrans. A tandem sequence of RCAER of

alkynyl boronates and a rhenium-catalyzed allylic transposition was implemented to install the C4–C5 Z-trisubstituted and C8–C9 disubstituted double bonds with a good regio- and stereochemical control. The novel late stage ring-closing metathesis was employed to simultaneously construct the macrocycle and the trisubstituted double bond at C16–C17. The effectiveness and versatility of transition metal-catalyzed reactions for the synthesis of complex and delicate carbon frameworks has been demonstrated in the current synthesis of dactylolide.

ACKNOWLEDGMENTS

The authors thank Ph.D. students, postdoctoral fellows, and colleagues listed in the references for their fine collaboration. We are indebted to Dr. S. Y. Yun, Dr. E. C. Hansen, and Dr. E. J. Cho for their motivation, enormous effort, and intelligence in these investigations. We are grateful to Mr. Furong Sun of the University of Illinois at Urbana-Champaign for high resolution mass spectrometry data. The studies described in this chapter were founded by NIH, NSF, and UIC. We appreciate their generous support.

REFERENCES

- [1] A. Cutignano, I. Bruno, G. Bifulco, A. Casapullo, C. Debitus, L. Gomez-Paloma, R. Riccio, *Eur. J. Org. Chem.* (2001) 775–778.
- [2] (a) A.B. Smith III, I.G. Safonov, *Org. Lett.* 4 (2002) 635–637; (b) A.B. Smith III, I.G. Safonov, R.M. Corbett, *J. Am. Chem. Soc.* 124 (2002) 11102–11113.
- [3] A.B. Smith, I.G. Safonov, R.M. Corbett, *J. Am. Chem. Soc.* 123 (2001) 12426–12427.
- [4] J. Tanaka, T. Higa, *Tetrahedron Lett.* 37 (1996) 5535–5538.
- [5] J.J. Field, A.J. Singh, A. Kanakkanthara, T. Halafihi, P.T. Northcote, J.H. Miller, *J. Med. Chem.* 52 (2009) 7328–7332.
- [6] P.B. Schiff, J. Fant, S.B. Horwitz, *Nature* 277 (1979) 665–667.
- [7] E. Hamel, B.W. Day, J.H. Miller, M.K. Jung, P.T. Northcote, A.K. Ghosh, D.P. Curan, M. Cushman, K.C. Nicolaou, I. Paterson, E.J. Sorenson, *Mol. Pharmacol.* 70 (2006) 1555–1564.
- [8] (a) T.R. Hoyer, M. Hu, *J. Am. Chem. Soc.* 125 (2003) 9576–9577; (b) F. Ding, M.P. Jennings, *Org. Lett.* 7 (2005) 2321–2324; (c) D.L. Aubele, S. Wan, P.E. Floreancig, *Angew. Chem., Int. Ed.* 44 (2005) 3485–3488; (d) C.C. Sanchez, G.E. Keck, *Org. Lett.* 7 (2005) 3053–3056; (e) I. Louis, N.L. Hungerford, E.J. Humphries, M.D. McLeod, *Org. Lett.* 8 (2006) 1117–1120; (f) J. Uenishi, T. Iwamoto, J. Tanaka, *Org. Lett.* 11 (2009) 3262–3265; (g) D. Zurwerra, J. Gertsch, K.-H. Altmann, *Org. Lett.* 12 (2010) 2302–2305; (h) A.K. Ghosh, X. Cheng, *Org. Lett.* 13 (2011) 4108–4111.
- [9] N.A. Petasis, S.-P. Lu, *Tetrahedron Lett.* 37 (1996) 141–144.
- [10] M. Caron, K.B. Sharpless, *J. Org. Chem.* 50 (1985) 1557–1560.
- [11] M. Miyashita, T. Suzuki, M. Hoshino, A. Yoshikoshi, *Tetrahedron* 53 (1997) 12469–12486.
- [12] G. Casiraghi, F. Zanardi, G. Appendino, G. Rassu, *Chem. Rev.* 100 (2000) 1929–1972.
- [13] D.A. Evans, M.C. Kozlowski, J.A. Murry, C.S. Burgey, K.R. Campos, B.T. Connell, R.J. Staples, *J. Am. Chem. Soc.* 121 (1999) 669–685.
- [14] S.E. Denmark, T. Wynn, G.L. Beutner, *J. Am. Chem. Soc.* 124 (2002) 13405–13407.
- [15] T.J. Mickelson, J.L. Koviach, C.J. Forsyth, *J. Org. Chem.* 61 (1996) 9617–9620.
- [16] D.L.J. Clive, G. Chittattu, N.J. Curtis, S.M. Menchen, *J. Chem. Soc. Chem. Comm.* (1978) 770–771.
- [17] H.J. Reich, *Acc. Chem. Res.* 12 (1979) 22–30.

- [18] G.E. Keck, J.A. Covell, T. Schiff, T. Yu, *Org. Lett.* 4 (2002) 1189–1192.
- [19] G.E. Keck, K.H. Tarbet, L.S. Geraci, *J. Am. Chem. Soc.* 115 (1993) 8467–8468.
- [20] (a) B.M. Trost, J.D. Chisholm, *Org. Lett.* 4 (2002) 3743–3745; (b) Y. Ohba, M. Takatsuji, K. Nakahara, H. Fujioka, Y. Kita, *Chem. Eur. J.* 15 (2009) 3526–3537.
- [21] J. Uenishi, K. Matsui, M. Ohmi, *Tetrahedron Lett.* 46 (2005) 225–228.
- [22] (a) S.D. Rychnovsky, Y. Hu, B. Ellsworth, *Tetrahedron Lett.* 39 (1998) 7271–7274; (b) S.D. Rychnovsky, D.J. Kopecky, *J. Org. Chem.* 65 (2000) 191–198; (c) J.J. Jaber, K. Mitsui, S.D. Rychnovsky, *J. Org. Chem.* 66 (2001) 4679–4686; (d) S.D. Rychnovsky, S. Marumoto, J. Jaber, *Org. Lett.* 3 (2001) 3815–3818; (e) S. Marumoto, J.J. Jaber, J.P. Vitale, S.D. Rychnovsky, *Org. Lett.* 4 (2002) 3919–3922; (f) R. Jasti, J. Vitale, S.D. Rychnovsky, *J. Am. Chem. Soc.* 126 (2004) 9904–9905; (g) J.P. Vitale, S.A. Wolckenhauer, M.D. Nga, S.D. Rychnovsky, *Org. Lett.* 7 (2005) 3255–3258; (h) R. Jasti, S.D. Rychnovsky, *J. Am. Chem. Soc.* 128 (2006) 13640–13648.
- [23] B.A. Narayanan, W.H. Bunnelle, *Tetrahedron Lett.* 28 (1987) 6261–6264.
- [24] (a) R.H. Grubbs, S. Chang, *Tetrahedron* 54 (1998) 4413–4449; (b) In: R.H. Grubbs (Ed.), *Handbook of Metathesis*, Vol. 2, Wiley-VCH, Weinheim, Germany, 2003; (c) R.R. Schrock, A.H. Hoveyda, *Angew. Chem., Int. Ed.* 42 (2003) 4592–4633; (d) S.J. Connon, S. Blechert, *Angew. Chem., Int. Ed.* 42 (2003) 1900–1923; (e) A. Deiters, S.F. Martin, *Chem. Rev.* 104 (2004) 2199–2238; (f) K.C. Nicolaou, P.G. Bulger, D. Sarlah, *Angew. Chem., Int. Ed.* 44 (2005) 4490–4527.
- [25] (a) T.R. Hoye, C.S. Jeffrey, M.A. Tennakoon, J. Wang, H. Zhao, *J. Am. Chem. Soc.* 126 (2004) 10210–10211; (b) E.C. Hansen, D. Lee, *Org. Lett.* 6 (2004) 2035–2038; (c) For a review, see: D.J. Wallace, *Angew. Chem., Int. Ed.* 44 (2005) 1912–1915.
- [26] (a) E.C. Hansen, D. Lee, *J. Am. Chem. Soc.* 127 (2005) 3252–3253; (b) For a review, see: B.M. Trost, M.U. Frederiksen, M.T. Rudd, *Angew. Chem., Int. Ed.* 44 (2005) 6630–6666.
- [27] (a) C. Morrill, R.H. Grubbs, *J. Am. Chem. Soc.* 127 (2005) 2842–2843; (b) C. Morrill, G.L. Beutner, R.H. Grubbs, *J. Org. Chem.* 71 (2006) 7813–7825; (c) E.C. Hansen, D. Lee, *J. Am. Chem. Soc.* 128 (2006) 8142–8143; (d) A.T. Herrmann, T. Saito, C.E. Stivala, J. Tom, A. Zakarian, *J. Am. Chem. Soc.* 132 (2010) 5962–5963; (e) I. Volchkov, S. Park, D. Lee, *Org. Lett.* 13 (2011) 3530–3533.
- [28] (a) S. Bellemin-Laponnaz, H. Gisie, J.P. Le Ny, J.A. Osborn, *Angew. Chem., Int. Ed.* 36 (1997) 976–978; (b) S. Bellemin-Laponnaz, J.P. Le Ny, A. Dedieu, *Chem. Eur. J.* 5 (1999) 57–64; (c) S. Bellemin-Laponnaz, H. Gisie, J.P. Le Ny, J.A. Osborn, *Tetrahedron Lett.* 41 (2000) 1549–1552.
- [29] (a) K. Takai, H. Nozaki, K. Oshima, T. Okazoe, S. Matsubara, *Bull. Chem. Soc. Jpn.* 58 (1985) 844–849; (b) K. Narasaka, H. Kusama, Y. Hayashi, *Tetrahedron* 48 (1992) 2059–2068; (c) M.S. Gordon, J.H. Jensen, J.H. Espenson, J. Jacob, *Organometallics* 17 (1998) 1835–1840; (d) G. Wang, A. Jimtaisong, R.L. Luck, *Organometallics* 23 (2004) 4522–4525; (e) For a review, see: J.-P. Le Ny, S. Bellemin-Laponnaz, *C. R. Chimie* 5 (2002) 217–224.
- [30] E.C. Hansen, D. Lee, *Tetrahedron Lett.* 45 (2004) 7151–7155.
- [31] (a) B.M. Trost, A.F. Indolese, T.J.J. Mueller, B. Treptow, *J. Am. Chem. Soc.* 117 (1995) 615–623; (b) B.M. Trost, G.D. Probst, A. Schoop, *J. Am. Chem. Soc.* 120 (1998) 9228–9236; (c) B.M. Trost, A.B. Pinkerton, F.D. Toste, M. Sperrle, *J. Am. Chem. Soc.* 123 (2001) 12504–12509; (d) For a review, see: B.M. Trost, *Acc. Chem. Res.* 35 (2002) 695–705; (e) B.M. Trost, F.D. Toste, A.B. Pinkerton, *Chem. Rev.* 101 (2001) 2067–2096.
- [32] (a) B.M. Trost, *Chem. Pharm. Bull.* 50 (2002) 1–14; (b) B.M. Trost, C. Lee, I. Ojima (Ed.), *Catalytic Asymmetric Synthesis II*, Wiley-VCH, New York, 2000, pp. 593–650; (c) For review see: B.M. Trost, *Angew. Chem. Int. Ed.* 28 (1989) 1173–1192.

- [33] (a) B.M. Trost, D.L. Van Vranken, C. Bingel, *J. Am. Chem. Soc.* 114 (1992) 9327–9343; (b) B.M. Trost, F.D. Toste, *J. Am. Chem. Soc.* 121 (1999) 4545–4554; (c) L. Jiang, S.D. Burke, *Org. Lett.* 4 (2002) 3411–3414; (d) B.M. Trost, M.L. Crawley, *Chem. Rev.* 103 (2003) 2921–2943; (e) B.M. Trost, M.R. Machacek, A. Aponick, *Acc. Chem. Res.* 39 (2006) 747–760.
- [34] G. Pattenden, M.A. Gonzalez, P.B. Little, D.S. Millan, A.T. Plowright, J.A. Tornos, T. Ye, *Org. Biomol. Chem.* 1 (2003) 4173–4208.
- [35] B.M. Trost, M.R. Machacek, B.D. Faulk, *J. Am. Chem. Soc.* 128 (2006) 6745–6754.
- [36] J.W.A. Kinnaird, P.Y. Ng, K. Kubota, X. Wang, J.L. Leighton, *J. Am. Chem. Soc.* 124 (2002) 7920–7921.
- [37] H.C. Brown, N.G. Bhat, M. Srebnik, *Tetrahedron Lett.* 29 (1988) 2631–2634.
- [38] B.M. Trost, M. Machacek, M.J. Schnaderbeck, *Org. Lett.* 2 (2000) 1761–1764.
- [39] B.M. Trost, H.C. Shen, A.B. Pinkerton, *Chem. Eur. J.* 8 (2002) 2341–2349.
- [40] (a) B.M. Trost, D.F. Toste, *J. Am. Chem. Soc.* 121 (1999) 9728–9729; (b) B.M. Trost, D.F. Toste, *J. Am. Chem. Soc.* 124 (2002) 5025–5036.
- [41] (a) R.S. Tanke, R.H. Crabtree, *J. Am. Chem. Soc.* 112 (1990) 7984–7989; (b) B.M. Trost, Z.T. Ball, *J. Am. Chem. Soc.* 125 (2003) 30–31; (c) L.W. Chung, Y.-D. Wu, B.M. Trost, Z.T.J. Ball, *J. Am. Chem. Soc.* 125 (2003) 11578–11582.
- [42] O. Mitsunobu, *Synthesis* (1981) 1–28.
- [43] R. Takeuchi, K. Tanabe, S.J. Tanaka, *Org. Chem.* 65 (2000) 1558–1561.
- [44] S.A. Frank, H. Chen, R.K. Kunz, M.J. Schnaderbeck, W.R. Roush, *Org. Lett.* 2 (2000) 2691–2694.
- [45] S.H. Hong, D.P. Sanders, C.W. Lee, R.H. Grubbs, *J. Am. Chem. Soc.* 127 (2005) 17160–17161.

Development of a General Approach to the *Leucetta*-Derived Alkaloids

Carl J. Lovely

Department of Chemistry and Biochemistry, The University of Texas at Arlington, Arlington, Texas, USA

Chapter Outline

1. Introduction	199	5. Naphthimidazole	
2. Strategic Considerations	200	Derivatives	209
3. C4-Substituted Derivatives	203	5.1. Kealiinine C	209
3.1. Preclathridine and Clathridine A	203	5.2. Kealiquinone	211
3.2. Isonaamine C and Isonaamidine E	204	5.3. New C2-Oxidation Chemistry	213
4. C4,C5-Substituted Derivatives	205	6. Oxidized Derivatives	217
4.1. Naamidine G	205	6.1. Calcaridine A	217
4.2. Naamidine H	205	7. Summary	222

1. INTRODUCTION

The *Leucetta* alkaloids are a moderately sized family of marine natural products isolated from *Leucetta* and *Clathrina* sponges found in a variety of locations around the globe [1,2]. These alkaloids are characterized by the presence of a polysubstituted 2-aminoimidazole moiety with substituents at the N1, C4, and typically C5 positions (1–10, Figure 1) [3]. In most cases, the N1 substituent is a methyl group and the C4- and C5-substituents are oxygenated benzyl groups, but variations on this theme do exist [3]. The parent system is exemplified by naamine A (1) [4,5], which like many examples in this family has a closely related derivative, that is, naamidine A (4) in which the C2-amino group is functionalized with a methyl parabanic acid substituent [4,5]. An

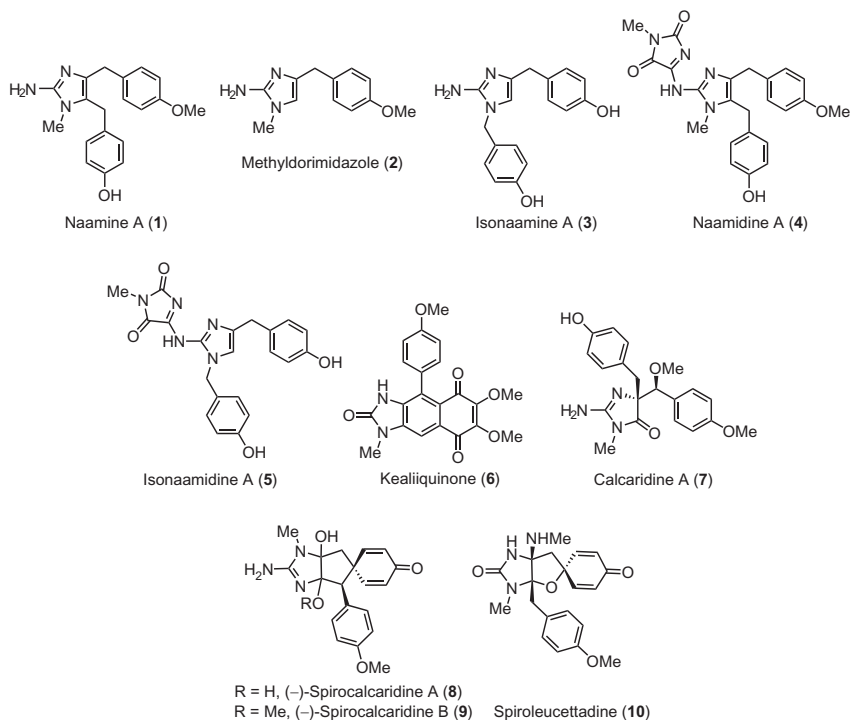


FIGURE 1 Structural diversity in the *Leucetta* alkaloids.

isomeric series of derivatives have also been isolated, termed the isonaamines (e.g., isonaamine A (3)) and isonaamidines (e.g., isonaamidine A (5)) in which one of the benzyl groups is on N1 [5]. In addition to these basic derivatives, a series of more highly oxidized congeners has recently been described possessing more elaborate frameworks, including kealiiquinone (6) [6], calcaridine A (7) [3], spirocalcaridine A (8) [3], and spiroleucettadine (10) [7]. The structure of 10 was revised [8] after several synthetic approaches to the originally assigned structures were unsuccessful [9–12].

2. STRATEGIC CONSIDERATIONS

Several years ago, we initiated a program toward the development of methods for the total synthesis of members of the oroidin family of alkaloids [13], molecules that have attracted the attention of many research groups around the world. As our methodologies evolved, we began to search for other targets that might be accessible through the application of this chemistry, and in the course of this search, we identified that calcaridine (7), the spirocalcaridines (8 and 9), and spiroleucettadine (10) were particularly attractive, as we had developed chemistry that would allow entry into the high oxidation states of these

alkaloids from simple imidazoles. As we considered the details of constructing the precursors, we recognized that our strategies would in fact be ideal for extremely concise approaches to the naamidines and related molecules depicted in [Figure 1](#).

Generally speaking, we have attempted to pursue approaches to many of the more elaborate molecules in this family guided by (hypothetical) biomimetic strategies, which when assessed globally result in these molecules' being traced back to a common type of precursor (see **11** in [Figure 2](#)). Further, as we developed our approach, we recognized that this strategy would provide general access to many members of this family of alkaloids, and with modest modification, most family members would be accessible. This global strategy is depicted schematically in [Figure 2](#), wherein a naamine type of system **11** serves as the divergence point for the assembly of a variety of natural products. Specifically, it was envisioned that calcaridine A (**7**) might be accessible through an oxidative rearrangement of **11** based on some prior precedent with such chemistry from other programs in our lab [[14–16](#)]. The same type of precursor would also permit construction of the spirocalcaridines (e.g., **8**) through a dearomatizing alkylation if “Z” were a suitable leaving group. We have shown that imidazoles can be dihydroxylated across the 4,5-imidazole bond [[17](#)], which in tandem with an oxidative dearomatization of the phenol offers a potential route toward spiroleucettadine (**10**). An intramolecular Friedel–Crafts reaction/oxidation would allow formation of the kealiinine group of alkaloids **12–14** [[18](#)], which upon further oxidation would offer an entry toward kealiiquinone (**6**) [[19,20](#)].

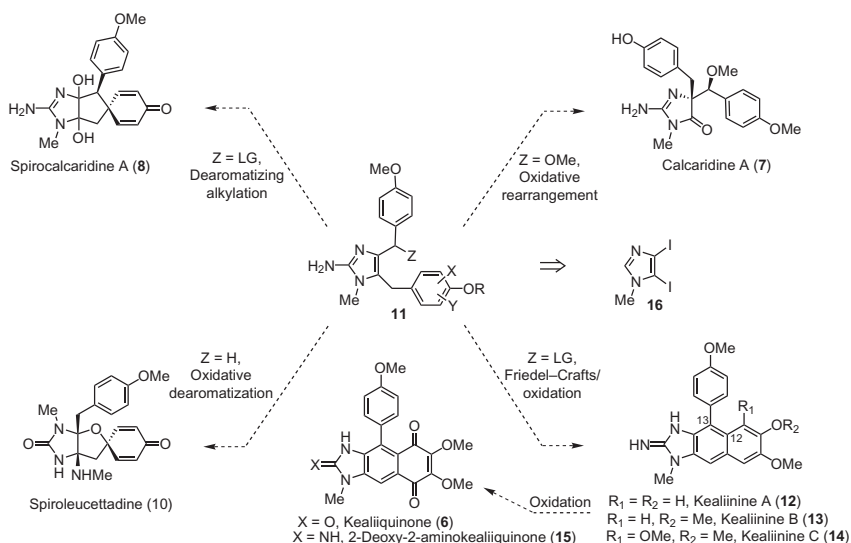
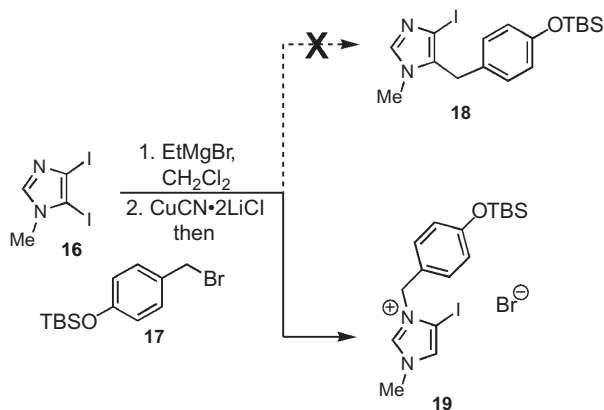


FIGURE 2 Biomimetic-guided strategy toward various *Leucetta*-derived alkaloids.

As a strategic paradigm in our lab, we have chosen to pursue an approach to imidazole-containing systems through the elaboration of a *preexisting* imidazole rather than the *de novo* construction of the heterocycle [13]. We anticipated that such a strategy would not only permit the total synthesis of a variety of natural products, but it would also facilitate the development of new chemistry of this important heterocyclic molecule. A somewhat similar tactic of functionalizing imidazole derivatives has been utilized for the construction of this family of alkaloids by the Ohta lab and relies on sequential metalation through deprotonation with alkylolithium bases and electrophilic quench [19–29]. While this approach provides access to several examples of these natural products, it requires protection of the more reactive C2 position as the thioether (which is then converted to an amino group) and in some cases C5 must be protected. Obviously, this adds to the step counts of the syntheses and as a result reduces the overall efficiency. In our approach, we chose to employ readily available 4,5-diiodimidazoles, for example, **16** (Figure 1), as they have been shown by several groups [30–35], including our own [36–38], to undergo position-specific metalation upon treatment with Grignard reagents (C5 then C4) with C2 being functionalized last by deprotonation with a strong base (typically *n*-BuLi) and electrophilic quench (typically TsN₃ or TrisN₃) [39]. This strategy avoids the need to protect the more acidic positions in the imidazole. As indicated above, our initial interests were aroused by the more highly oxidized congeners; however, the key intermediate **11** embodies the skeleton of several simpler congeners and thus we have also used this strategy to access some of these molecules.

In initial studies with this chemistry, we found, at least with imidazoles containing an *N*-methyl group (e.g., **16**), that we were not able to introduce a benzyl substituent directly via metalation, transmetalation to the cuprate, and reaction with benzyl halides, as this led to the formation of the deiodinated benzyl imidazolium salt **19** (Scheme 1). To circumvent this issue, we have



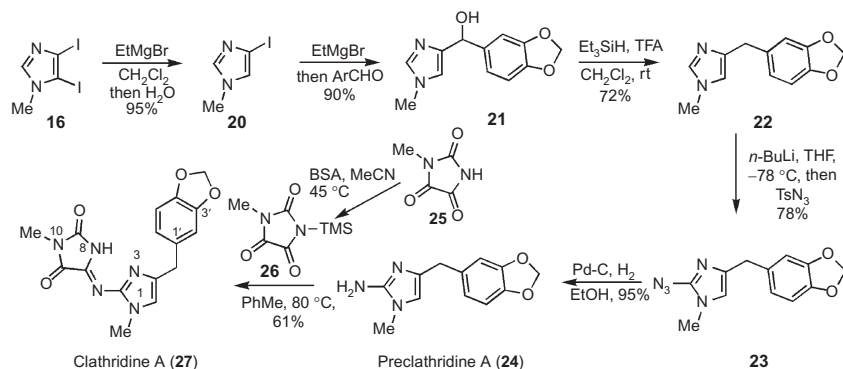
SCHEME 1 Attempted direct alkylation of Grignard reagents derived from iodoimidazoles.

employed a two-step sequence via addition of the corresponding Grignard reagent to an aldehyde followed by ionic reduction in many cases; although recently we have developed chemistry that permits the use of benzyl halides, a tactic that has substantially improved efficiency (see [Scheme 6](#) for details).

3. C4-SUBSTITUTED DERIVATIVES

3.1 Preclathridine and Clathridine A

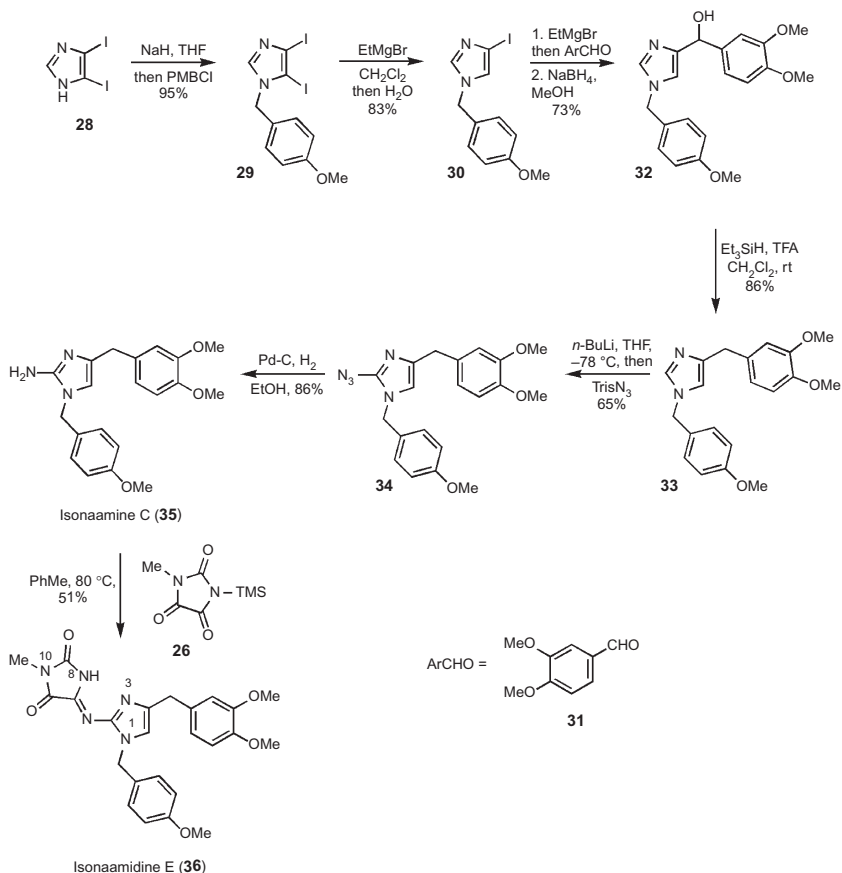
Among the first targets that we attempted to synthesize were the simple mono-benzylic derivatives preclathridine A (**24**) and clathridine A (**27**) ([Scheme 2](#)) [40]. These natural products were reported by Crews and Fattoruso, respectively, almost 20 years ago [41,42] and are among some of the simplest members in this family of alkaloids. While several total syntheses of these derivatives had been reported previously [23,43,44], a successful execution of our strategy would place it among the shortest described to date. Our synthesis commenced from the readily prepared 4,5-diiodimidazole derivative **16** [45], which undergoes metalation with EtMgBr followed by hydrolysis to provide the monoiodoimidazole derivative **20** ([Scheme 2](#)). This iodoimidazole **20** is commercially available but rather expensive, and our chemistry results in a cost-effective, large-scale synthesis of this material. A second metalation with EtMgBr and subsequent reaction with the piperonal provided the alcohol **21**, which undergoes ionic reduction upon treatment with TFS and Et₃SiH to produce **22**. The C2-position of **22** can be metalated by deprotonation with *n*-BuLi and upon exposure of the resulting organolithium to TsN₃ provides the corresponding 2-azido derivative **23**. Catalytic hydrogenation then affords preclathridine A (**24**). Treatment with methyl parabanic acid derivative (**26**) [46], prepared by silylation of **25** with *N,O*-bis(trimethylsilyl)acetamide by a known procedure [9], then produces clathridine A (**27**). The highly crystalline product was subjected to X-ray crystallography, which unequivocally confirmed the connectivity of the synthetic material.



SCHEME 2 Total synthesis of preclathridine A and clathridine A.

3.2 Isonaamine C and Isonaamidine E

Isonaamine C (**36**), along with the related isonaamidine E (**35**), was described in 2002 and was reported to possess modest anticancer activity against several different cell lines [47]. These alkaloids differ from the naamine/naamidine group with respect to the location of one of the benzyl groups on N1. Prior to this point in our synthetic investigations, we had not examined the construction of this subgroup and so we initiated a total synthesis of this target. 4,5-Diiodoimidazole (**28**) was converted to the *p*-methoxybenzyl derivative **29** through treatment with the corresponding benzyl chloride (Scheme 3). Exposure to EtMgBr followed by treatment with water provided the 4-iodo derivative **30** and set up the second metalation step. One issue with metalations of benzyl-substituted imidazoles is that the benzylic position is susceptible to deprotonation with strong bases [48,49], and in fact, this is one of the reasons we have utilized Grignard reagents in modestly polar solvents, as



SCHEME 3 Total syntheses of isonaamine C and isonaamidine E.

these are less prone to function as bases. Accordingly, compound **30** was treated with EtMgBr followed by the 3,4-dimethoxybenzaldehyde (**31**) to afford a mixture of the expected alcohol **32** and corresponding ketone. In practice, this mixture was subjected to NaBH₄ reduction, resulting in the formation of the alcohol **32** in 73% yield. Interestingly, when we increased the number of aldehyde equivalents, the formation of the ketone appeared to decrease but was never completely suppressed. Subjection of the alcohol to ionic reduction provided **33**, which was converted to the azide **34** via lithiation and treatment with trisyl azide. Catalytic hydrogenation then produced isonaamine C (**35**), which was readily converted into isonaamidine E (**36**) with the methyl parabanic acid derivative **26** under standard conditions, providing material that matched the natural product in all respects [50].

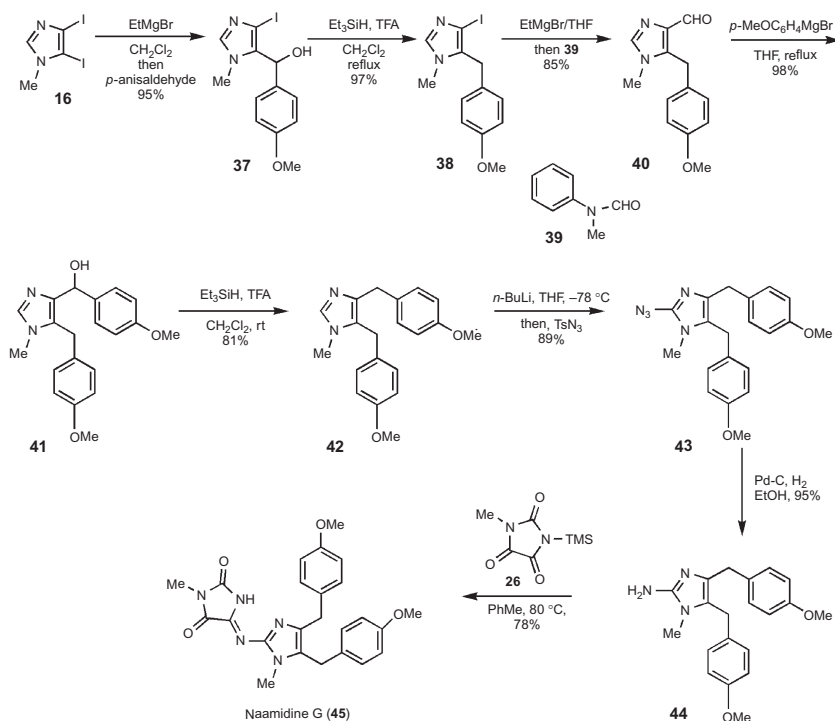
4. C₄,C₅-SUBSTITUTED DERIVATIVES

4.1 Naamidine G

The final basic framework that has been assembled through this Grignard/reduction strategy was naamidine G (**45**), which was originally isolated by Pietra and coworkers from a *Leucetta* sp. of the Coral Sea [51]. The partially purified extract was shown to be cytotoxic toward KB cells, but no biological studies were reported on the purified individual components. Strategically, we anticipated that this alkaloid could be prepared through metalation with EtMgBr and reaction of the resulting Grignard with anisaldehyde. Reduction would then provide the benzylated imidazole; repetition of this sequence would then provide the dibenzylated core [52]. The first part of this sequence proceeded uneventfully, resulting in the synthesis of the 5-benzyl derivative **38** (Scheme 4). However, attempts to introduce the second benzyl group via this chemistry were unsuccessful, resulting in the formation of the ketone in modest yield. Subsequently, it was found that the alcohol **41** could be obtained through a two-step sequence via **40**, by metalation and trapping with *N*-methyl formanilide (**39**), and then reaction with the corresponding anisyl Grignard (**38** → **40** → **41**, Scheme 4). Reduction of **41** with Et₃SiH/TFA in the presence of TFA furnished the dibenzyl derivative **42**. Introduction of the 2-amino substituent was accomplished by reduction of the azide **43** with Pd-C/H₂. The azide was prepared by metalation of **42** at C2 with BuLi and trapping with TsN₃. Functionalization of the 2-amino group was performed by exposure to **26**, thus providing naamidine G (**45**).

4.2 Naamidine H

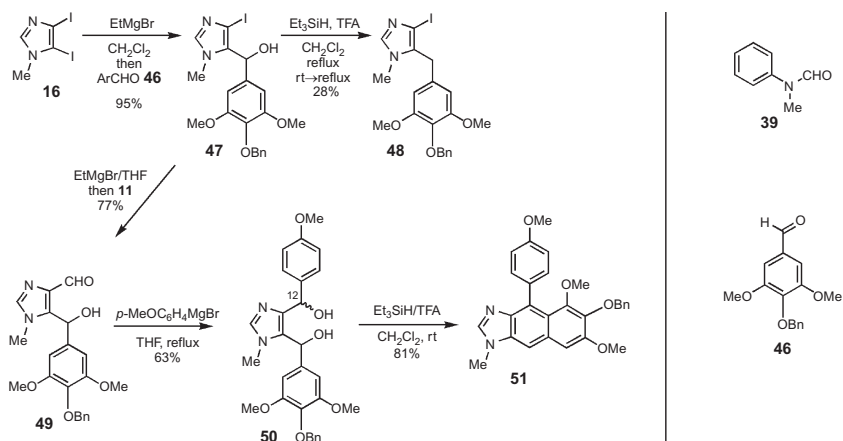
Naamidine H (**60**) was isolated by Tsukumoto and coworkers from *Leucetta chagosensis* collected from North Sulawesi, Indonesia, and was reported to exhibit modest anticancer activity against HeLa cells [53]. Our synthesis plan was to employ a similar approach to that described above for the preparation



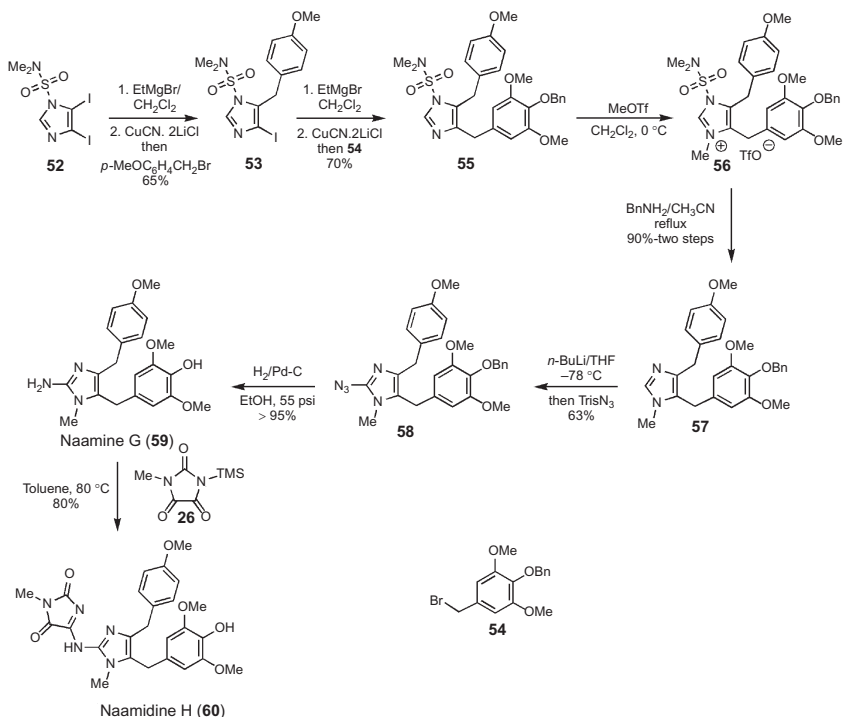
SCHEME 4 Total synthesis of naamidine G.

of naamidine G (**45**) (Scheme 4) [52]. The chemistry proceeded uneventfully through the first few steps, specifically the incorporation of the lower substituent, that is, the formation of **47**, but attempts to reduce the doubly benzylic alcohol to **48** through treatment with $\text{Et}_3\text{SiH/TFA}$ were not efficient (Scheme 5) [54]. Undeterred, we deferred this reduction until later in the synthesis and incorporated the second benzyl moiety via formylation (EtMgBr then *N*-methyl formanilide (**39**)) and treatment of the aldehyde derivative **49** with the corresponding Grignard reagent to afford **50**. Our plan was to simultaneously remove both of the benzylic alcohols in **50** through treatment with $\text{Et}_3\text{SiH/TFA}$. However, rather than forming the required reduction product (see **57**, Scheme 6), the corresponding naphthimidazole derivative **51** was obtained, presumably through a Friedel–Crafts cyclization and dehydration. While this result was not useful in the context of this total synthesis, the outcome did suggest an approach to another subfamily of natural products (see Scheme 7 below).

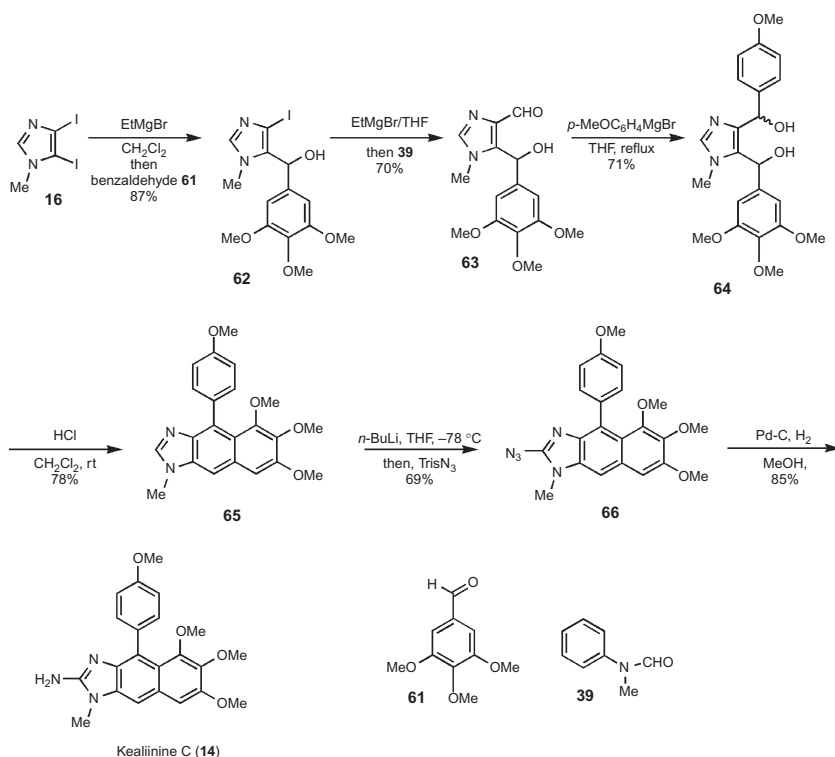
We still required a solution to the problem presented by naamidine H (**60**). From a purely pragmatic perspective, if the formation of a carbocationic species could be avoided, the propensity for Friedel–Crafts cyclization would be



SCHEME 5 First-generation approach to naamidine H.



SCHEME 6 Second-generation approach to naamidine H and naamine G.



SCHEME 7 Synthesis of the reported structure of kealiinine C.

circumvented and then a solution would be forthcoming. One option that appeared attractive was direct C-alkylation, but this chemistry did not appear to be feasible when the imidazole is *N*-methyl substituted (see [Scheme 1](#)). However, in earlier work, Lindell had demonstrated that if the imidazole was protected on nitrogen with a DMAS (dimethylaminosulfonyl) group, alkylation with benzyl groups was successful [\[35\]](#). Accordingly, we prepared the corresponding sulfonyl urea **52** and subjected it to metalation with EtMgBr, transmetalated with CuCN·2LiCl, and then reacted the resulting organometallic species with *p*-methoxybenzyl bromide to produce the corresponding C-alkylated derivative **53** ([Scheme 6](#)) [\[54\]](#). Repetition of the sequence with **53** and benzyl bromide **54** provided the dibenzyl derivative **55** in good overall yield. With this intermediate in hand, the removal of the imidazole-protecting group and installation of the methyl substituent needed to be accomplished; the latter had to be performed in a position-specific manner. Fortunately, this was readily achieved by formation of the methyl imidazolium salt **56** and treatment with a nucleophilic amine, leading to **57** [\[55\]](#). Completion of the synthesis required C2-metalation and reaction with trisyl azide to form **58**, which upon reduction provided naamine G (**59**) [\[18\]](#).

Reaction with the silyl parabanic acid derivative **26** gave naamidine H (**60**) [54]. Interestingly, this approach using the DMAS-protected derivative led to an overall shorter sequence of reactions than our original strategy through the use of aldehydes for these 4,5-disubstituted derivatives.

5. NAPHTHIMIDAZOLE DERIVATIVES

5.1 Kealiinine C

Given that our original approach to naamidine H (**60**) via diol **50** (Scheme 5) had resulted in formation of the naphthimidazole derivative **51** related to the framework found in kealiinine C (**14**), we decided to take advantage of this observation through a minor modification of the substrate to allow completion of the natural product **14** [18]. Accordingly, we used the trimethoxy-substituted aldehyde **61** as the electrophile in the first metalation step to provide alcohol **62** (Scheme 7). Subsequent conversion of the alcohol **62** first to the aldehyde derivative **63** and then to the diol **64** was accomplished through what were now standard manipulations for our lab. Treatment of the diol with HCl triggered a Friedel–Crafts/elimination sequence to provide the naphthimidazole derivative **65**, the structure of which was confirmed by X-ray crystallography. Metalation at C2 with *n*-BuLi followed by treatment with trisyl azide provided the corresponding azide **66**, which upon reduction with Pd-C/H₂ afforded the reported structure of kealiinine C (**14**).

Comparison of the reported ¹H NMR data of the natural product with that obtained for the synthetic material revealed that there were some significant discrepancies between the two; unfortunately, no ¹³C NMR data for the natural product were available for comparison. An X-ray analysis of the synthetic material confirmed that the constitution of the molecule had been correctly assigned and thus we contacted Prof. Proksch to establish the possible source of the inconsistency. In the course of this exchange, it was noted that in our case, at least based on the X-ray structure coupled with the fact that we saw a two-proton absorption in the ¹H NMR spectrum for the 2-amino protons, that we had prepared the 2-amino derivative **14'** (Figure 3). However, the Proksch group reported isolation of the tautomeric imino derivative **14**—based on analogy to two other family members, kealiinine A and B reported in the same isolation paper as kealiinine C (**14**)—although this was not confirmed through experimental observation [18]. For comparative purposes, small differences in the spectroscopic data have been observed between synthetic (**6**) and natural kealiiquinone (**6'**), particularly for one of the methyl groups (Figure 3) [6,20]. These discrepancies were attributed to tautomeric differences between the natural and synthetic materials. In part, this hypothesis was based on the ¹H NMR data, which showed differences in the low field signals at $\delta=8.14$ (for **6'** and OH) versus $\delta=11.01$ (for **6** and NH) (Figure 3). Only relatively minor differences were noted for the signals attributed to the *N*-methyl group

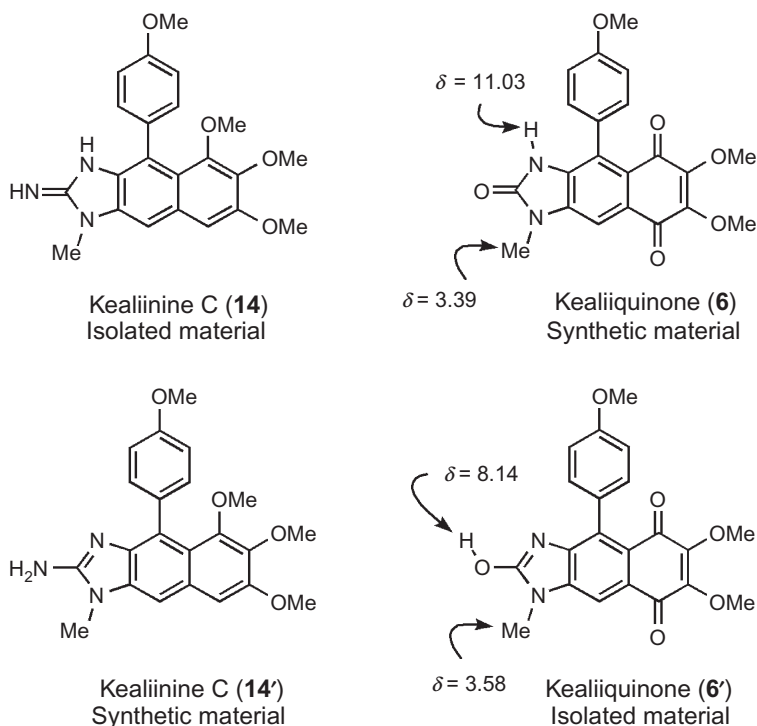
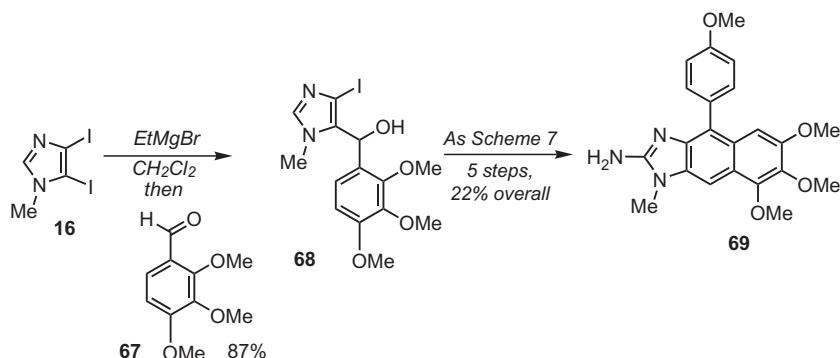


FIGURE 3 Tautomeric isomers of kealiinine C and kealiiquinone.

(Figure 3), but all other signals were in excellent agreement ($\Delta\delta = 0.01$ – 0.02). The constitutions were corroborated by the fact that X-ray crystal structure determinations had been performed in both cases, and for the natural material, the 2-hydroxyimidazole derivative **6'** was obtained, whereas for the synthetic material, the 2-oxo derivative **6** was obtained. Similar issues may be at play in the case of synthetic and natural kealiinine C, but the spectroscopic differences are more pronounced in this case. Other factors may be involved, for example, natural products are often isolated in very small quantities and invariably these isolates contain impurities, both factors can influence chemical shifts and the position of the tautomeric equilibrium, particularly with polar compounds. Our attempts to reproduce the reported data by diluting the NMR sample, adding TFA, or by adding water, failed to induce any significant changes in the spectrum.

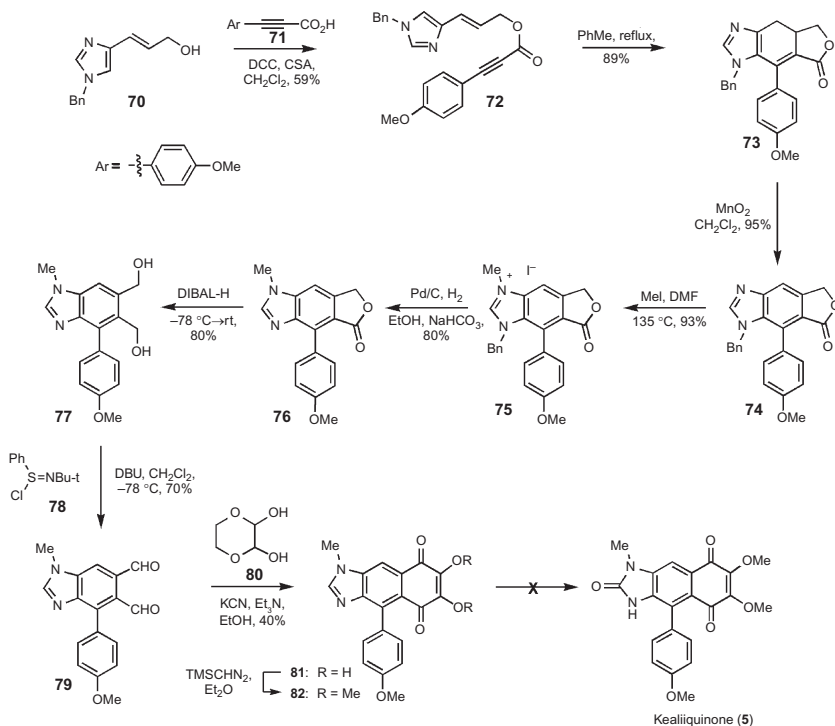
Given our inability to induce any changes in the ^1H NMR spectra in the presence of additives or on dilution, we became concerned that the discrepancies in the data were too significant to be attributable to differences in the tautomeric distribution. Specifically, one of the methyl groups in the synthetic material was significantly upfield from that reported in the literature, as was one of the aromatic protons. We hypothesized that it was conceivable that

**SCHEME 8** Synthesis of an isomeric kealiinine C derivative.

the location of the methoxy groups on the C-ring had been incorrectly assigned and that one methoxy group was located at C8, rather than at C11. Fortunately, our synthetic strategy allowed us to address this issue readily by preparing the corresponding isomeric derivative through a series of largely analogous reactions and employing the isomeric aldehyde **67** (Scheme 8). While the ^1H NMR data for this isomeric material (**69**) are a better fit for that reported for the natural product, they do not match exactly.

5.2 Kealiiquinone

We had an interest in developing a total synthesis of kealiiquinone (**5**) for some time and in fact this interest predated the initiation of our efforts toward other *Leucetta* family members. One previous synthesis of this natural product has been described in the literature by the Ohta lab using an approach that is related to that depicted in Figure 2 involving oxidation of a kealiinine C-like intermediate [20,56]. It should be noted that this approach preceded the isolation of the kealiinine group of natural products by almost a decade. The genesis of our own strategy was rooted in the use of an intramolecular Diels–Alder reaction to construct the benzimidazole core of this natural product, an area in which we were already active due to our efforts toward the oroidin family of alkaloids (Scheme 9) [15,16,45,57]. We have quite extensively investigated the Diels–Alder chemistry of 4-vinylimidazoles and building off these studies anticipated that the heterocyclic core could be constructed quite rapidly. The assembly of the Diels–Alder substrate **72** was accomplished through standard transformations, with the imidazole portion **70** derived from urocanic acid. Heating a toluene solution of **72** to reflux resulted in the formation of the dihydrobenzimidazole **73**; aromatization to **74** was then achieved on exposure to MnO_2 . Again we were confronted with the issue of the imidazole substituent being on the wrong nitrogen. In this case, we relied on the imidazolium trick (cf. **56** in Scheme 6), but instead



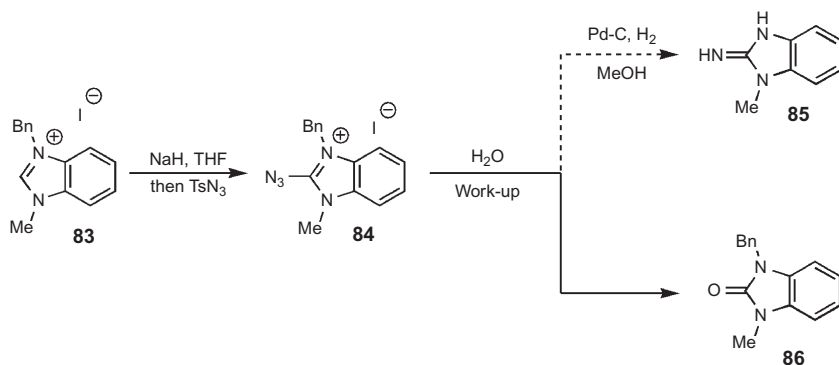
SCHEME 9 First-generation approach to kealiiquinone (6).

of using a nucleophile to remove the unwanted group, reductive debenzoylation was effected with Pd-C/H₂ to afford **76** from **75**. Reduction of the lactone with DIBAL-H provided the diol **77**, which then was converted to the dialdehyde **79** by oxidation with the sulfimide derivative **78**. As might be imagined, this oxidant was not the first reagent that we assessed to effect this conversion. Many of the obvious oxidants (e.g., MnO₂, PCC, IBX, DMP) resulted in transformation of the diol to a lactone or formation of complex mixtures, with the exception of Swern-type conditions. However, traditional Swern-type protocols (DMSO, (COCl)₂, Et₃N) were unreliable in this transformation. Reagent **78**, developed by the Mukaiyama group, provided a solution to these problems [58]. Subsequent application of a seldom-used quinone-forming reaction using the protected glyoxal derivative **80** in the presence of cyanide ion and base led to the formation of the dihydroxy quinone **81** [59]. Presumably, this reaction occurs by way of a benzoin-type pathway and subsequent oxidation. Methylation of the vinylogous diacid **81** with TMS-diazomethane resulted in the preparation of the dimethoxy quinone **82**. At this stage, our plan for completion of the kealiiquinone (and the related 2-amino congener) rested on application of our usual metalation and electrophilic amination or oxidation chemistry. However, to our great disappointment, we were unable

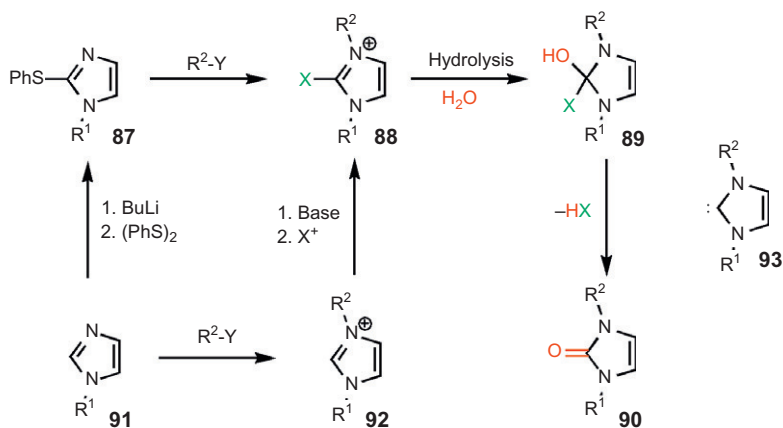
to effect these reactions on advanced intermediate **82**. While the precise fate of the substrate in these attempted metalations is uncertain, as highly colored and water-soluble materials were produced, it was clear that the quinone was not stable to typical bases used for deprotonation [60].

5.3 New C2-Oxidation Chemistry

Obviously, we were disappointed that our synthesis had failed at such a late stage in the proceedings and we began to mull over other options for rescuing the synthesis. One option considered was to introduce an oxo or amino surrogate at the beginning of the synthesis; however, it was quickly dismissed as it would have required a significant reengineering of the synthesis and thus other alternatives were required. One possibility that occurred to us was that the imidazolium salt **75** might represent an intermediate that would undergo deprotonation under relatively mild conditions forming a carbene species that would react with an appropriate electrophilic species. In an initial iteration of this strategy, we attempted such a reaction with imidazolium salt **83** by deprotonation with NaH followed by treatment with TsN₃ (then aqueous work-up), thus producing what we assumed to be **84** (Scheme 10). Our plan was then to remove the benzyl group under reductive conditions such that the azide would be converted to the amino moiety simultaneously thereby providing **85**. However, although it was clear that reaction had taken place, the product obtained was not the one we had initially anticipated. It quickly emerged from the IR data that, rather than introduction of the azido group, a 2-oxo moiety was incorporated, providing the corresponding urea **86** (Scheme 10) [19]. While this reaction did not go as originally anticipated, we did view this as an exciting opportunity for further exploration. Mechanistically we assumed that this reaction occurred through the formation of the expected 2-azido imidazolium species **84** (Scheme 10), which on aqueous work-up underwent hydrolysis–tautomerization to provide the urea **86**. It should be noted that we cannot rule



SCHEME 10 Unexpected formation of a 2-benzimidazolone.

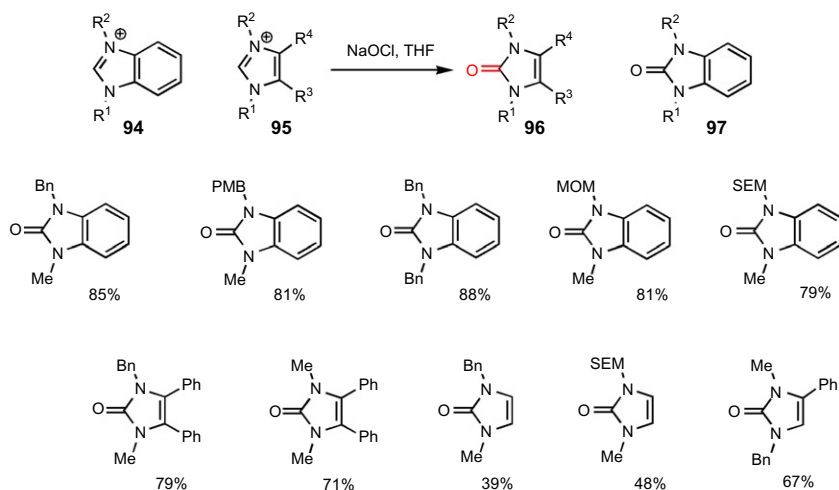


SCHEME 11 Mechanistic design toward a direct C2-activation–oxidation.

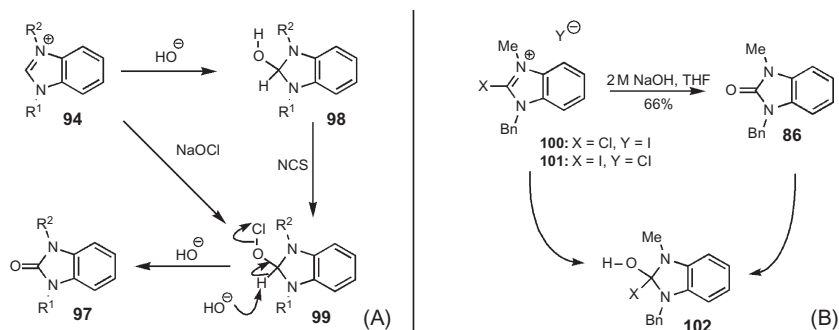
out the intermediacy of a 2-phenylsulfonylbenzimidazolium species, which would be expected to result in the same overall process. A related approach for the introduction of the oxo substituent on imidazolium salts has been reported by the Ohta lab in which a 2-thiophenyl substituted derivative **87** underwent hydrolysis on conversion to the imidazolium salt **88** (Scheme 11). With this as a working mechanistic hypothesis, we designed what we hoped would be a more convenient sequence to convert imidazoles to the corresponding 2-imidazolones in which we substituted the azide (or thiophenyl) moiety with a chloro leaving group (i.e., X=Cl) in compound **88**.

In the first and perhaps naïve iteration of this chemistry, we reacted imidazolium salt **83** with NaH in THF followed by treatment with NCS and subsequently added water. Gratifyingly, the corresponding imidazolone **86** was obtained in good yield. We evaluated a number of different bases and found that several weaker aqueous bases (NaOH, K₂CO₃, Na₂CO₃) in combination with NCS provided the corresponding 2-imidazolone in modest to good yield. However, given that these bases in combination with NCS provided the imidazolone, we wondered whether simply using NaOCl solutions might effect the same overall transformation. Pleasingly, we found that this was the case on using commercial bleach solution (ca. 5% NaOCl), and in many cases, the yields were improved (Scheme 12) [61].

Although at this stage the mechanistic details of this transformation remain to be fully elucidated, two pathways can be envisioned. The first is along the lines of the hypothesized reaction in which the imidazolium salt is converted to the 2-chloroimidazolium species, which then undergoes the addition–elimination sequence. A second possibility involves the addition of water (or hydroxide) to the imidazolium ion **98**, conversion to hypochlorite **99**, and

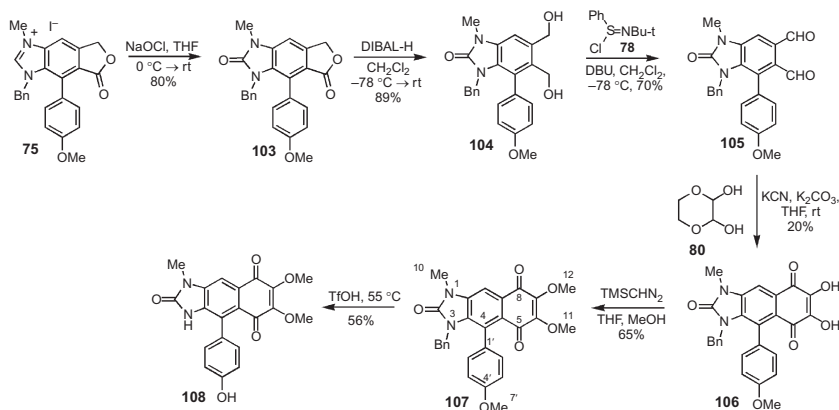


SCHEME 12 C2-Oxidation of imidazolium salts.



SCHEME 13 Mechanistic hypotheses.

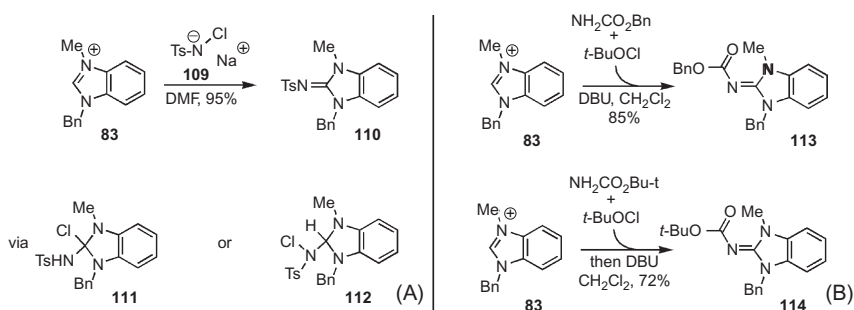
then loss of HCl (Scheme 13A). In the case of the reaction with bleach, it is feasible that the hypochlorite ion may add to the imidazolium species directly ($94 \rightarrow 99$, Scheme 13A). It has been shown by others that chloroimidazolium salts undergo hydrolysis to provide the imidazolones and are thus viable intermediates in this chemistry [62,63]. However, we have not yet demonstrated that it is an intermediate in the conversion of the imidazolium ion to the imidazolone. We did attempt to confirm this by the preparation of the 2-chloroimidazolium salt **100** from the corresponding 2-chlorobenzimidazole. As anticipated, the salt underwent hydrolysis to the imidazolone **86** (Scheme 13B), but we found during characterization from the mass spectrum that the precursor was in fact the 2-iodoimidazolium salt **101**. Presumably, the exchange occurred during



SCHEME 14 Second-generation synthesis of kealiquinone—total synthesis of 7'-desmethylkealiquinone (**108**).

methylation with MeI, suggesting that the imidazolium salts are prone to addition–elimination reactions.

The mechanistic nuances of imidazolone formation notwithstanding, we had discovered a mild procedure for the introduction of the key functional group that avoided using strong bases that should be applicable in our total synthesis of kealiquinone (Scheme 14). Accordingly, we treated the imidazolium salt **75** with bleach. This led uneventfully to the corresponding imidazolone derivative **103**. Subjecting this derivative to reduction with DIBAL-H provided the crystalline diol **104**, whose structure was confirmed through X-ray crystallography. Subsequent oxidation under Mukaiyama conditions provided the dialdehyde derivative **105** (Scheme 14) [58]. Exposure to the glyoxal derivative **80** in the presence of basic KCN resulted in the formation of the dihydroxy quinone **106**, which was methylated as before with TMS-diazomethane forming **107**. At this stage, all that remained to be done was the removal of the *N*-benzyl group. While in many cases this can be accomplished by hydrogenolysis, *N*-benzyl amides oftentimes do not engage in this chemistry and this was the case with our substrate. Attempted removal of the benzyl group under even quite forcing conditions did not occur. In some cases, a benzyl moiety can be removed under oxidative conditions, but again our substrate failed to react. A recent report described a method wherein a treatment with triflic acid removes *N*-benzyl groups from amides [64]. Treatment of **107** with triflic acid gave a red crystalline solid, which in addition to removal of the benzyl moiety resulted in demethylation of the phenolic oxygen and the production of 7'-desmethylkealiquinone (**108**) (kealiquinone numbering see **107**) [6]. Initial attempts to selectively *O*-methylate the phenolic hydroxyl group have been unsuccessful due to competitive methylation of the imidazolone [60]. Current efforts are focused on using alternative protecting groups that will ultimately be easier to remove and thus circumvent the unwanted demethylation.

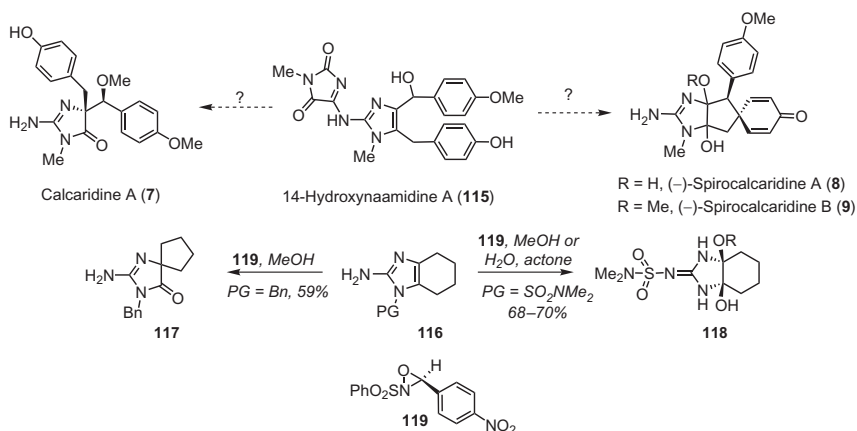
**SCHEME 15** New approach to C2-amination of imidazoles.

We have been able to extend the hydrolysis chemistry to the incorporation of amino groups through the use of *N*-chloroamides. For example, chloramine-T (**109**) reacts with imidazolium salts to provide the corresponding imine derivative. We have also developed a method for introducing carbamates via the *in situ* preparation of *N*-chlorocarbamate [65] (Scheme 15). While the yields for these reactions are still modest, these initial experiments provide optimism for the development of convenient methods for C2-amination via this net addition–elimination chemistry.

6. OXIDIZED DERIVATIVES

6.1 Calcaridine A

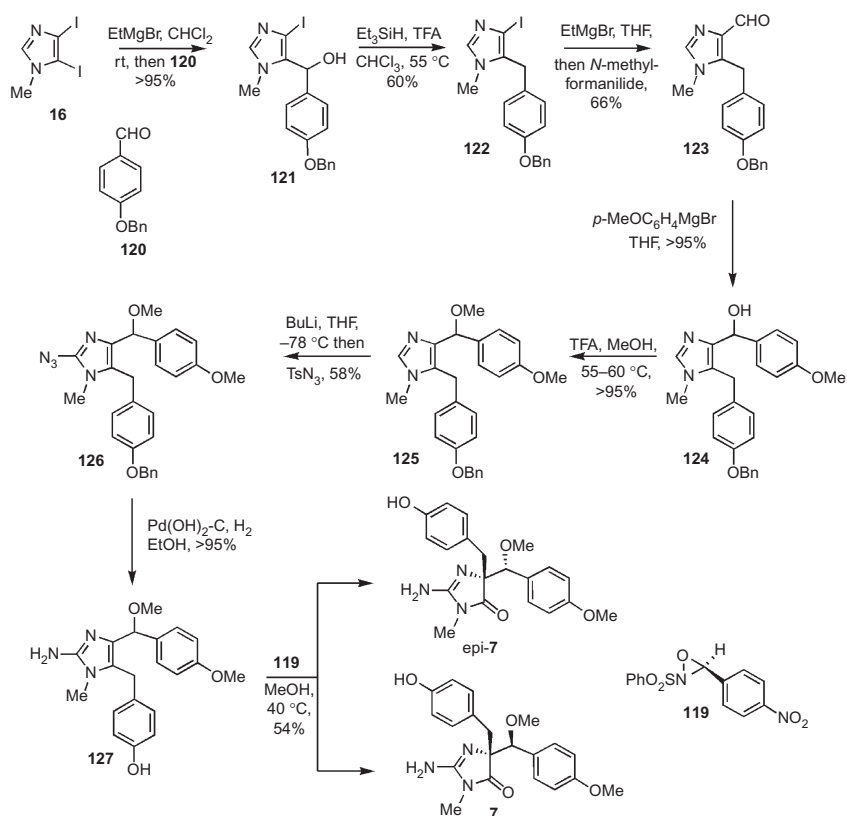
In many respects, this natural product was the driving force behind our whole program that developed in the *Leucetta* alkaloids. This imidazolone derivative **7** was reported by the Crews lab in 2003 along with two other unusual and highly oxidized 2-aminoimidazole alkaloids, spirocalcaridine A (**8**) and B (**9**) [3]. Part of the attraction of these natural products for us, in addition to the challenges in their structures, lay in the fact that we had recently discovered in the course of a related synthetic program that we could convert 2-aminoimidazole derivatives to either 5-imidazolones (**116** → **117**, Scheme 16) or 4,5-dihydroxy derivatives (**116** → **118**, Scheme 16) through treatment with an oxidizing agent [14,17]. At the time this project was initiated, we had only performed this oxidative chemistry on a limited number of tetrahydrobenzimidazole derivatives and so there were questions of generality and scope that would emerge from this effort. Further, as indicated in the introduction, we have pursued a loosely biomimetic approach to these alkaloids and implementation of such a rearrangement would provide circumstantial evidence at least that the biosynthetic hypothesis was valid. It is of note that oxygenated naamidine derivatives such as 14-hydroxynaamidine (**115**) have been reported and thus may serve as a biosynthetic precursor to calcaridine A (**7**) [66,67] and the spirocalcaridines (**8**) and (**9**), but there is no experimental evidence to support this claim.



SCHEME 16 Oxidative chemistry of aminoimidazoles.

In order to execute such a strategy, access to an intermediate related to **115** was required that we anticipated would arise through application of our usual strategy from diiodoimidazole **16** (Scheme 17). Metalation of **16** with EtMgBr, followed by treatment with *p*-benzyloxybenzaldehyde, afforded the alcohol **121**, which was then deoxygenated by treatment with Et₃SiH/TFA to afford **122**. We attempted to introduce the second benzyl moiety by formation of the Grignard (EtMgBr) and reaction with anisaldehyde. Unfortunately, this reaction was inefficient, providing mixtures of the required alcohol **124**, the corresponding ketone, and the deiodinated product. We were able to access the required alcohol through a two-step sequence by first introducing a formyl group and then subjecting the imidazolyl aldehyde **123** to reaction with *p*-methoxyphenyl Grignard reagent to give **124**. Initial attempts to convert the alcohol into the methyl ether under basic conditions were compromised by the formation of the imidazolium salt; however, under acidic conditions (TFA, MeOH), the methyl ether **128** was secured. Metalation at the imidazole C2-position was accomplished with *n*-BuLi. Reaction with TsN₃ resulted in the formation of the 2-azido derivative **126**. Subjection of the azide **126** to catalytic hydrogenation led to simultaneous reduction of the azide and the hydrogenolysis of the benzyl moiety forming **127**. With this substrate in hand, we were ready to evaluate the key oxidative rearrangement. Subjection of **127** to reaction with a Davis oxaziridine **119** resulted in a smooth oxidative rearrangement and formation of a 2:1 mixture of diastereomeric imidazolones in modest (but unoptimized) yield. Unfortunately at this stage of the proceedings, we were unable to separate the two stereoisomers **7** and *epi*-**7** but were able to determine from the ¹H NMR data that the major isomer was in fact the epimer of the natural product.

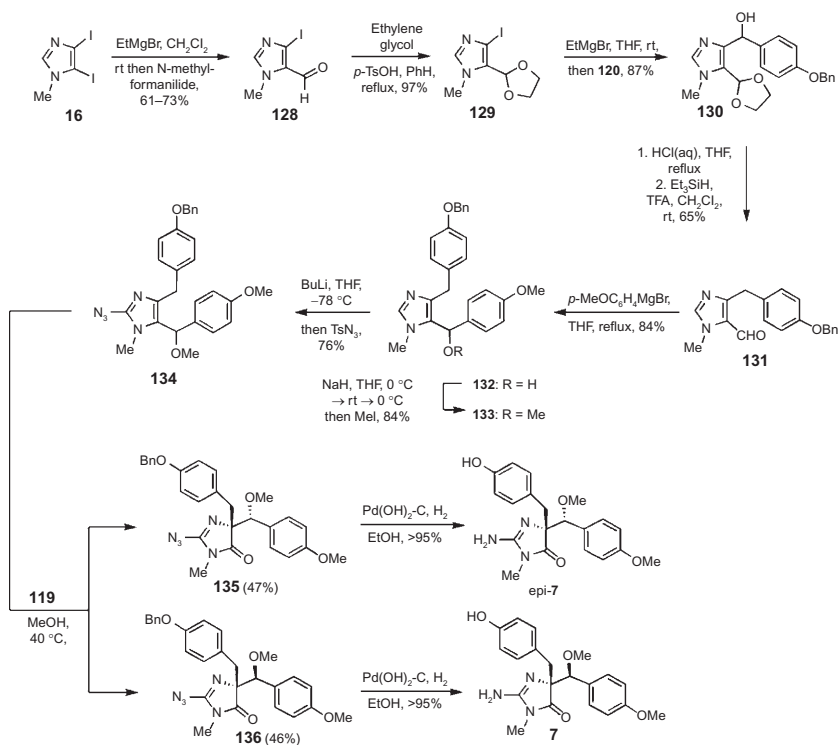
Our mechanistic hypothesis for the oxidative rearrangement involved oxygen transfer to C5 followed by a pinacol-type rearrangement leading to the



SCHEME 17 First-generation total synthesis of calcaridine A (7).

imidazolone. With this in mind, we envisioned that moving the ether-substituted stereocenter to the C5 carbon should result in an increase in the diastereoselectivity in the rearrangement due to proximity. To test this hypothesis, we prepared the regioisomeric substrate through largely similar transformations. Starting from aldehyde **128**, which was protected as the ethylene ketal **129**, and then application of the Grignard exchange protocol and subsequent reaction with a protected benzaldehyde derivative produced the alcohol **130** (Scheme 18). Attempts to deoxygenate with $\text{Et}_3\text{SiH/TFA}$ at this stage led to complex mixtures. However, upon removal of the ketal-protecting group, the hydroxyl group could be removed to give **131**. Introduction of the second aryl moiety was accomplished through addition of the Grignard derivative to the appropriate aldehyde moiety to afford alcohol **132**, which was then converted to the methyl ether **133** via a Williamson reaction.

Introduction of the 2-amino group was performed as described previously through C2-metalation, trapping with azide and reduction (also removes the benzyl group) providing the corresponding amine. Oxidative rearrangement

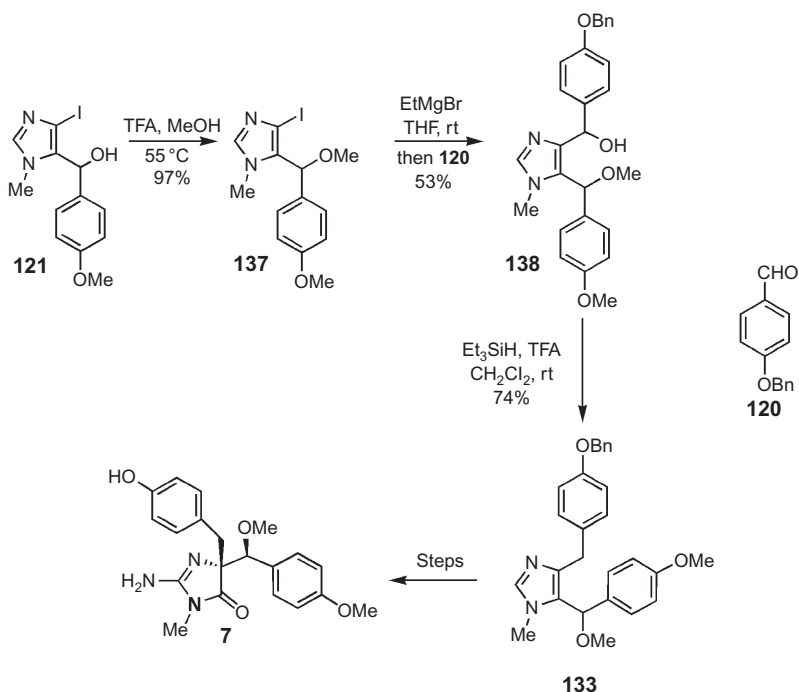


SCHEME 18 Second-generation total synthesis of calcaridine A (7).

of this amine with the Davis reagent **119** proceeded to provide a 1:1 mixture of the diastereomeric imidazolones, so although there was a small increase in the amount of the natural diastereomer, the overall change in the diastereomer ratio was not significant. This result was also disappointing from a separation perspective as we were still unable to isolate the individual diastereomers from the mixture. However, we had learned in the course of the methodology studies that the reaction was fairly tolerant of a variety of C2 substituents, including a 2-azido moiety [17]. Accordingly, we subjected imidazole **134** to the oxidative rearrangement and found that not only did this derivative engage in the oxidative rearrangement chemistry, but it also now provided a chromatographically separable 1:1 mixture of diastereomers **135** and **136**. Subjection of each diastereomer individually to catalytic hydrogenation resulted in reduction of the azido moiety and cleavage of the *O*-benzyl protecting group providing the two isomeric 2-aminoimidazolones **7** and *epi*-**7**. The spectroscopic data for one of the diastereomers matched exactly with the data reported by Crews. At this stage, we got a lucky break in that one imidazolone, *epi*-**7**, crystallized out from the solvent (CD_3OD) used to acquire the NMR data and provided material suitable for X-ray analysis. Our colleague

Rasika Dias was able to obtain the structure of this material, which in turn allowed us to determine the relative configuration of the epimer and by extension that of the synthetic natural product. An added benefit of obtaining this crystalline diastereomer was that we were now able to use it to seed fractional crystallizations in order to separate all of the diastereomeric mixtures that we had prepared previously. Through this means, we were able to obtain relatively large quantities of both the natural and nonnatural diastereomers that have been submitted to various venues for biological testing.

Although we were happy with the fact that we had accomplished the total synthesis of calcaridine A, the efficiency of the synthesis of the precursor for the oxidative rearrangement did leave something to be desired. Accordingly, we have attempted to develop a more concise approach. In this case, the Grignard reagent prepared from **7** and EtMgBr was reacted with anisaldehyde to provide the corresponding alcohol. Conversion of **121** into the methyl ether was readily accomplished by treatment with MeOH and TFA. The second benzylic fragment was introduced by metalation and reaction with benzaldehyde **120** producing **138** (Scheme 19). At this point, we found that the hydroxyl moiety was removed effectively simply upon treatment with Et₃SiH and TFA to provide **133**, which intersects with the route depicted in Scheme 18.



SCHEME 19 Third-generation total synthesis of calcaridine A (**7**).

7. SUMMARY

Hopefully in the preceding pages, we have been able to convey a sense of how this program has evolved to allow the assembly of a variety of different members of this alkaloid family through the functionalization of simple imidazole derivatives. The basic tetrasubstituted imidazole frameworks are assembled through sequential metalation reactions, typically through Grignard-halogen exchange or lithiation and electrophilic capture. Oxidation chemistry has featured in these endeavors, including the development of a simple method for introducing a C2-oxo group or a C2-amino group. We anticipate that this latter chemistry will have broader applications in our alkaloid total synthesis programs. Strategically, we have employed a biomimetic-guided strategy to construct the more complex derivatives. Current efforts in this program in our laboratory are directed toward developing syntheses of spirocalcaridine and spiroleucettadine.

ACKNOWLEDGMENTS

The work described in this account would not be possible without the hard work and intellectual contributions of a number of talented individuals, specifically Dr. Rasapalli Sivappa, Dr. Panduka Koswatta, Dr. Heather M. Lima, and Jayanta Das. To them I extend my heartfelt gratitude. My colleagues Prof. H.V. Rasika Dias and Dr. Muhammed Yousufuddin have been invaluable in collecting and determining X-ray crystal structures. We have been fortunate to have received continuous funding from the Robert A. Welch Foundation (Y-1362) over a number of years; we are immensely grateful for the faith shown in our programs. We are also grateful to the NIH (GM065503) for partial support of these efforts and the NSF (CHE-0234811, CHE-0840509) who have provided funding for the NMR spectrometers used in this research.

REFERENCES

- [1] P.B. Koswatta, C.J. Lovely, *Nat. Prod. Rep.* 28 (2011) 511–528.
- [2] J.D. Sullivan, R.L. Giles, R.E. Looper, *Curr. Bioact. Compd.* 5 (2009) 39–78.
- [3] R.A. Edrada, C.C. Stessman, P. Crews, *J. Nat. Prod.* 66 (2003) 939–942.
- [4] S. Carmerly, Y. Kashman, *Tetrahedron Lett.* 28 (1987) 3003–3006.
- [5] S. Carmerly, M. Ilan, Y. Kashman, *Tetrahedron* 45 (1989) 2193–2200.
- [6] R. Akee, T.R. Carroll, W.Y. Yoshida, P.J. Scheuer, T.J. Stout, J. Clardy, *J. Org. Chem.* 55 (1990) 1944–1946.
- [7] P. Ralifo, P. Crews, *J. Org. Chem.* 69 (2004) 9025–9029.
- [8] K.N. White, T. Amagata, A.G. Oliver, K. Tenney, P.J. Wenzel, P. Crews, *J. Org. Chem.* 73 (2008) 8719–8722.
- [9] N. Aberle, S.P.B. Ovenden, G. Lessene, K.G. Watson, B.J. Smith, *Tetrahedron Lett.* 48 (2007) 2199–2203.
- [10] J.J. Chang, B. Chan, M.A. Ciufolini, *Tetrahedron Lett.* 47 (2006) 3599–3601.
- [11] C. Li, S.J. Danishefsky, *Tetrahedron Lett.* 47 (2006) 385–387.
- [12] P.B. Koswatta, Ph.D. Dissertation, 2010, University of Texas at Arlington.

- [13] Y. He, H. Du, R. Sivappa, C.J. Lovely, Synlett (2006) 965–992.
- [14] C.J. Lovely, H. Du, Y. He, H.V.R. Dias, Org. Lett. 6 (2004) 735–738.
- [15] R. Sivappa, N.M. Hernandez, Y. He, C.J. Lovely, Org. Lett. 9 (2007) 3861–3864.
- [16] R. Sivappa, S. Mukherjee, H.V.R. Dias, C.J. Lovely, Org. Biomol. Chem. 7 (2009) 3215.
- [17] R. Sivappa, P. Koswatta, C.J. Lovely, Tetrahedron Lett. 48 (2007) 5771.
- [18] W. Hassan, R.A. Edrada, R. Ebel, V. Wray, A. Berg, R.W.M. van Soest, S. Wiryowidagdo, P. Proksch, J. Nat. Prod. 67 (2004) 817–822.
- [19] S. Nakamura, N. Tsuno, M. Yamashita, I. Kawasaki, S. Ohta, Y. Ohishi, J. Chem. Soc. Perkin Trans. I (2001) 429–436.
- [20] I. Kawasaki, N. Taguchi, M. Yamashita, S. Ohta, Chem. Pharm. Bull. 45 (1997) 1393–1398.
- [21] I. Kawasaki, N. Sakaguchi, N. Fukushima, N. Fujioka, F. Nikaido, M. Yamashita, S. Ohta, Tetrahedron Lett. 43 (2002) 4377–4380.
- [22] I. Kawasaki, N. Sakaguchi, A. Khadeer, M. Yamashita, S. Ohta, Tetrahedron 62 (2006) 10182–10192.
- [23] S. Ohta, N. Tsuno, S. Nakamura, N. Taguchi, M. Yamashita, I. Kawasaki, M. Fujieda, Heterocycles 53 (2000) 1939–1955.
- [24] S. Nakamura, I. Kawasaki, M. Kunimura, M. Matsui, Y. Noma, M. Yamashita, S. Ohta, J. Chem. Soc. Perkin Trans. I (2002) 1061–1066.
- [25] I. Kawasaki, S. Nakamura, S. Yanagitani, A. Kakuno, M. Yamashita, S. Ohta, J. Chem. Soc. Perkin Trans. I (2001) 3095–3099.
- [26] S. Ohta, T. Yamamoto, I. Kawasaki, M. Yamashita, Y. Nagashima, T. Yoshikawa, Chem. Pharm. Bull. 42 (1994) 821–825.
- [27] I. Kawasaki, N. Taguchi, Y. Yoneda, M. Yamashita, S. Ohta, Heterocycles 43 (1996) 1375–1379.
- [28] M. Yamashita, M. Oda, K. Hayashi, I. Kawasaki, S. Ohta, Heterocycles 48 (1998) 2543–2550.
- [29] I. Kaswasaki, M. Yamashita, S. Ohta, J. Chem. Soc. Chem. Commun. (1994) 2085–2086.
- [30] R.M. Turner, S.V. Ley, S.D. Lindell, Synlett (1993) 748–750.
- [31] X. Yang, P. Knochel, Chem. Commun. (2006) 2170–2172.
- [32] M. Abarbri, J. Thibonnet, L. Bérillon, F. Dehmel, M. Rottländer, P. Knochel, J. Org. Chem. 65 (2000) 4618–4634.
- [33] F. Dehmel, M. Abarbri, P. Knochel, Synlett (2000) 345–346.
- [34] P. Knochel, W. Dohle, N. Gommermann, F. Kneisel, F. Kopp, T. Korn, I. Sapountzis, V. Vu, Angew. Chem. Int. Ed. 42 (2003) 4302–4320.
- [35] D.S. Carver, S.D. Lindell, E.A. Saville-Stones, Tetrahedron 53 (1997) 14481–14496.
- [36] Y. Chen, H.V.R. Dias, C.J. Lovely, Tetrahedron Lett. 44 (2003) 1379–1383.
- [37] C.J. Lovely, Y. Chen, E.V. Ekanayake, Heterocycles 74 (2007) 873–894.
- [38] M.K. Bhandari, R. Sivappa, C.J. Lovely, Org. Lett. 11 (2009) 1535.
- [39] T. Lindel, M. Hochguertel, J. Org. Chem. 65 (2000) 2806–2809.
- [40] P.B. Koswatta, C.J. Lovely, Tetrahedron Lett. 50 (2009) 4998.
- [41] K.A. Alvi, B.M. Peters, L.M. Hunter, P. Crews, Tetrahedron 49 (1993) 329–336.
- [42] P. Ciminiello, C. Dell’Aversano, E. Fattorusso, S. Magno, Eur. J. Org. Chem. (2001) 55–60.
- [43] P. Molina, P.M. Fresneda, M.A. Sanz, J. Org. Chem. 64 (1999) 2540–2544.
- [44] D.S. Ermolat’ev, V.L. Alifanov, V.B. Rybakov, E.V. Babaev, E.V. van der Eycken, Synthesis (2008) 2083–2088.
- [45] C.J. Lovely, H. Du, R. Sivappa, M.K. Bhandari, Y. He, H.V.R. Dias, J. Org. Chem. 72 (2007) 3741–3749.
- [46] S. Nakamura, I. Kawasaki, M. Yamashita, S. Ohta, Heterocycles 60 (2003) 583–598.

- [47] H. Gross, S. Kehraus, G.M. Koenig, G. Woerheide, A.D. Wright, *J. Nat. Prod.* 65 (2002) 1190–1193.
- [48] M. Moreno-Manas, J. Bassa, N. Llado, R. Pleixas, *J. Heterocycl. Chem.* 27 (1990) 673–678.
- [49] A.J. Carpenter, D.J. Chadwick, *Tetrahedron* 42 (1986) 2351–2358.
- [50] H.M. Lima, B.J. Garcia-Barboza, N.N. Khatibi, C.J. Lovely, *Tetrahedron Lett.* 52 (2011) 5725–5727.
- [51] I. Mancini, G. Guella, C. Debitus, F. Pietra, *Helv. Chim. Acta* 78 (1995) 1178–1184.
- [52] P. Koswatta, C.J. Lovely, *Tetrahedron Lett.* 51 (2010) 164–166.
- [53] A.W. Grubbs, G.D. Artman III, S. Tsukamoto, R.M. Williams, *Angew. Chem. Int. Ed.* 46 (2007) 2257–2261.
- [54] P. Koswatta, C.J. Lovely, *Chem. Commun.* 46 (2010) 2148.
- [55] B. Delest, P. Nshimyumukiza, O. Fasbender, B. Tinant, J. Marchand-Brynaert, F. Darro, R. Robiette, *J. Org. Chem.* 73 (2008) 6816–6823.
- [56] I. Kawasaki, N. Taguchi, T. Yamamoto, M. Yamashita, S. Ohta, *Tetrahedron Lett.* 36 (1995) 8251–8254.
- [57] Y. He, P. Krishnamoorthy, H.M. Lima, Y. Chen, H. Wu, R. Sivappa, H.V.R. Dias, C.J. Lovely, *Org. Biomol. Chem.* 9 (2011) 2685.
- [58] J.-i. Matsuo, D. Iida, K. Tatani, T. Mukaiyama, *Bull. Chem. Soc. Jpn.* 75 (2002) 223–224.
- [59] M.C. Venuti, *Synthesis* (1982) 61–63.
- [60] H.M. Lima, S. Rasapalli, M. Yousefuddin, C.J. Lovely, *Org. Lett.* 14 (2012) 2274–2277.
- [61] H.M. Lima, C.J. Lovely, *Org. Lett.* 13 (2011) 5736–5739.
- [62] H. Wamhoff, W. Kleimann, G. Kunz, C.H. Theis, *Angew. Chem. Int. Ed.* 93 (1981) 601–602.
- [63] M. Kitamura, M. Yano, N. Tashiro, S. Miyagawa, M. Sando, T. Okauchi, *Eur. J. Org. Chem.* (2011) 458–462.
- [64] F. Rombouts, D. Franken, C. Martínez-Lamenca, M. Braeken, C. Zavattaro, J. Chen, A.A. Trabanco, *Tetrahedron Lett.* 51 (2010) 4815–4818.
- [65] R. Tsuruoka, T. Nagamachi, Y. Murakami, M. Komatsu, S. Minakata, *J. Org. Chem.* 74 (2009) 1691–1697.
- [66] P.B. Koswatta, R. Sivappa, H.V.R. Dias, C.J. Lovely, *Org. Lett.* 10 (2008) 5055–5058.
- [67] P. Koswatta, R. Sivappa, H.V.R. Dias, C.J. Lovely, *Synthesis* (2009) 2970–2983.

The Adventure of Abudinol and the Misadventure of Muzitone

Frank E. McDonald^{*}, Rongbiao Tong[†], Matthew A. Boone[‡] and Jason C. Valentine[§]

^{*}*Department of Chemistry, Emory University, Atlanta, Georgia, USA*

[†]*The Hong Kong University of Science and Technology, Department of Chemistry, Clear Water Bay, Kowloon, Hong Kong*

[‡]*Eastman Chemical Company, Research Laboratories, P.O. Box 1972, Kingsport, Tennessee, USA*

[§]*Kenyon & Kenyon LLP, Washington, DC, USA*

Chapter Outline

- | | | | |
|---|------------|--|------------|
| 1. Introduction: Identification of Marine Polyether Terpenes as a Synthetic Target | 226 | | |
| 1.1. Polyepoxide Cyclizations as a Possible Biomimetic Synthetic Route to Brevetoxins | 226 | | |
| 1.2. Abudinol A and B, and Muzitone | 229 | | |
| 2. First-Generation Synthesis of Abudinol B | 233 | | |
| 2.1. Synthesis of the Bicyclic Segment by Cascade Oxacyclization | 233 | | |
| 2.2. Retrosynthesis of Abudinol B, First Generation | 236 | | |
| 2.3. Synthesis of the Tricyclic Segment by Cascade Oxacyclization | 236 | | |
| | | 2.4. Coupling the Two Segments and Completion of the First Synthesis of Abudinol B | 239 |
| | | 3. Second-Generation Synthesis of Abudinol B | 242 |
| | | 3.1. Preparation of a Partially Epoxidized Polyene Precursor | 242 |
| | | 3.2. Sequential Cascade Cyclizations to Provide the Structure of Abudinol B | 245 |
| | | 3.3. Synthesis of Squalene Tetraepoxide | 248 |
| | | 4. Synthesis of the Purported Structure of Muzitone | 249 |
| | | 4.1. Preparation of a Regioisomeric Partially Epoxidized Polyene Precursor | 249 |

4.2. Sequential Cascade Cyclizations to a Fused Pentacyclic Structure	250	5. Conclusion: Biosynthetic Considerations in the Proposal of Other Structures for Muzitone	255
4.3. Disappointment upon Arriving at the Purported Structure of Muzitone	252		

1. INTRODUCTION: IDENTIFICATION OF MARINE POLYETHER TERPENES AS A SYNTHETIC TARGET

1.1 Polyepoxide Cyclizations as a Possible Biomimetic Synthetic Route to Brevetoxins

The lead author has long been fascinated by the concept of cascade cyclizations for efficiently preparing polycyclic organic compounds, dating back to the mid-1980s when he was a graduate student at Stanford University. The pioneering studies of the Stanford laboratories of Johnson [1] directed toward polyene cyclizations as a biomimetic route to the synthesis of steroids and polycyclic triterpenes were particularly inspirational (i.e., **1** \rightarrow **2**, Figure 1), as were contemporary reports from the laboratories of Still and Schreiber [2,3] describing stereospecific and regioselective cascade cyclizations of di- and triepoxides (i.e., **3** \rightarrow **4**) prepared by stereoselective epoxidations of macrolactone dienes and trienes (Figure 1).

In 1989, the lead author encountered an article from Koji Nakanishi's laboratory describing a provocative proposal of *endo*-mode cascade cyclization of a hypothetical polyepoxide **5** as a possible biosynthetic pathway for *trans*-*syn*-*trans* polycyclic ether natural products such as brevetoxin B₂ (**6**, Figure 2) [4]. Upon viewing the structure of **5** in its extended state, it was apparent that although each epoxide would have to be formed stereoselectively, the sense of stereochemistry would be identical for each of the 10

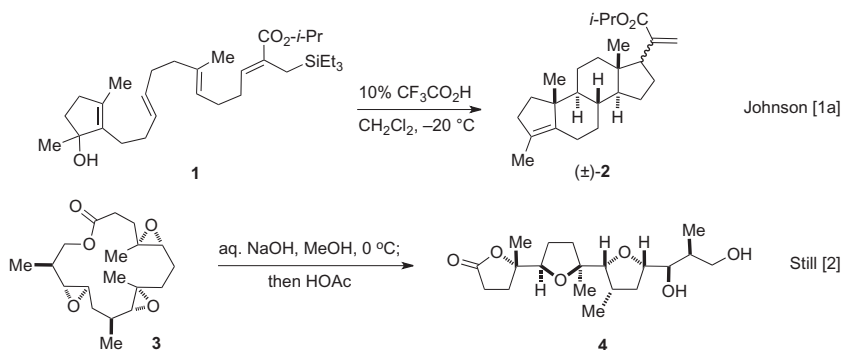


FIGURE 1 Representative early examples of biomimetic cascade cyclizations.

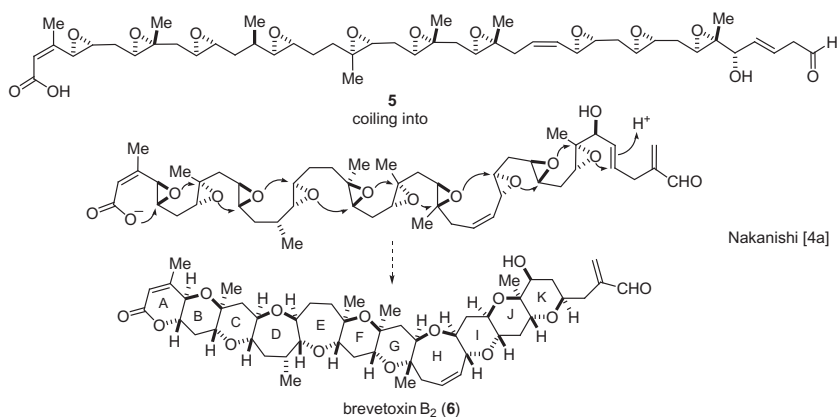


FIGURE 2 Biosynthetic proposal for *trans-syn-trans*-fused polycyclic ethers.

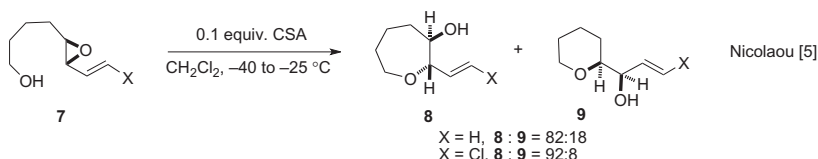


FIGURE 3 An early example of *endo*-mode oxacyclization.

epoxides, and thus one could envision that a single enzyme might provide the polyepoxide **5** from multiple epoxidations of an acyclic polyene precursor. Nicolaou's laboratory concurrently reported that oxacyclizations of hydroxyepoxides **7** could be steered to favor *endo*-mode regioselectivity with certain vinylic substituents at the epoxide carbon distal to the hydroxyl-bearing tether, although their studies were limited to monocyclization processes (Figure 3) [5].

Failing to heed Nakanishi's admonition that "the cyclization cascade of the polyepoxides ... as an intriguing biogenetic scheme... should not be taken seriously" [4a], over the next 10 years, the lead author occasionally contemplated how polyepoxide cyclizations might be more generally transformed from *exo*-mode cyclizations into *endo*-selective *cascade* cyclization pathways, while we examined other avenues for *endo*-selective oxacyclizations [6]. A rhenium-promoted process for cascade oxidative cyclizations of hydroxy-polyenes remained stubbornly *exo*-regioselective [7], although an alternative approach involving oxacyclization of cyclic sulfates (arising from vicinal diols obtained by enantioselective dihydroxylation) provided modest yields of *endo*-selective cyclization products [8].

We initially avoided directly exploring the Nakanishi hypothesis of *endo*-mode polyepoxide cyclizations, as we originally perceived that the *stereo-selective* synthesis of a polyepoxide corresponding to **5** or even a much

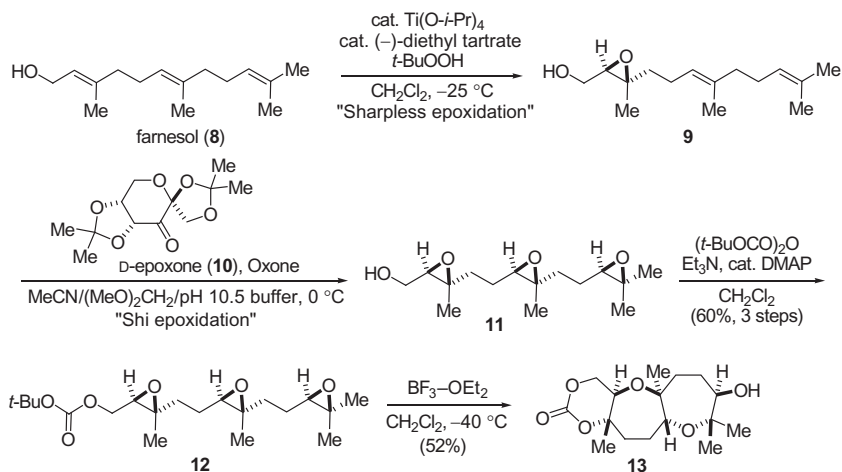


FIGURE 4 Synthesis and cascade tricyclization of triepoxide (12).

simpler model compound would be impractical. However, the 1996 report of enantioselective epoxidations of alkyl-substituted *trans*-alkenes arising from Shi's laboratory abruptly changed our thinking [9]. We realized that the Shi epoxidation could be applied to preparing polyepoxides *with the same sense of stereochemistry* upon multiple epoxidations of a polyene, quite reasonably in a single step.

In 1999, Emory University graduate student Xia Wang began to explore polyepoxide cyclizations. She discovered that Lewis acid-promoted cyclizations of terpene-derived polyepoxide 12 terminated with a carbonyl nucleophile provided *trans-syn-trans*-fused polycyclic ether 13 reminiscent of the brevetoxins arising from *endo*-oxacyclization (Figure 4) [10]. As the Shi epoxidation had been demonstrated to give lower stereoselectivity for alkenes bearing allylic hydroxyl groups [11], we first conducted the hydroxyl-directed Sharpless enantioselective epoxidation of farnesol (8) to provide the monoepoxide 9 [12], which then underwent double Shi epoxidation of both remaining alkenes in a single step to provide triepoxide 11 [10,13]. Postdoctoral associate Dr. Fernando Bravo and graduate student Jason Valentine subsequently optimized these reactions and more broadly explored the generality of this approach [14].

In 2001, postdoctoral associate Dr. Xudong Wei took advantage of the lower reactivity of alkenes bearing allylic hydroxyl groups in the Shi epoxidation [11] to prepare the farnesol-derived diepoxide 14 (Figure 5). He demonstrated that the same conditions utilized for polyepoxide cascade cyclization could also accommodate alkene reactants, affording the fused tricyclic product 15 bearing a central cyclohexane ring [13]. At that time, Dr. Wei brought to our attention the structural similarity of his cyclization product 15 with bicyclic substructures of natural products such as siphonolol A (16) [15].

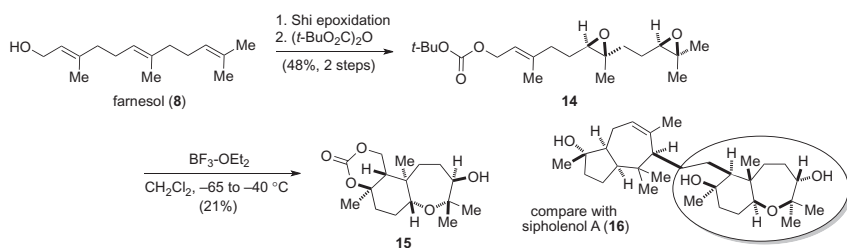


FIGURE 5 Synthesis and cascade tricyclization of ene-diepoxide (14).

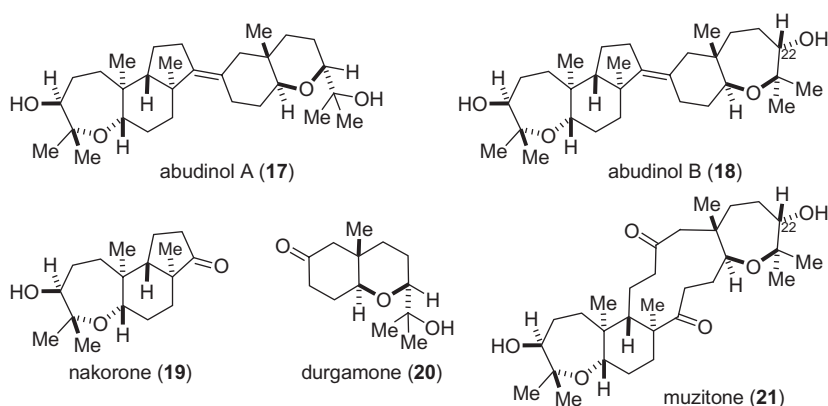


FIGURE 6 Structures of terpenoid cyclic ether marine natural products.

1.2 Abudinols A and B, and Muzitone

1.2.1 Structure Determination Reports

In 2004, Jason Valentine suggested again the idea of combining polyepoxide oxacyclizations with alkene carbocyclizations, this time in the context of a possible application to the synthesis of a pentacyclic triterpene natural product, abudinol B (18, Figure 6). Abudinols A (17) and B were discovered by the laboratory of Kashman, isolated from *Axinellidae* sponges collected at 10 m below sea level in the Red Sea waters of the Dahlak Archipelago of Eritrea [16,17]. The structure of abudinol A was first described in 1998, with the stereochemistry of the tetrasubstituted alkene unambiguously established by X-ray crystallography [16]. A subsequent full report in 1999 provided more details, revealing that ozonolysis of abudinol A provided two polycyclic ketones, matching the characterization data recorded for nakorone (19) and durgamone (20), which were also isolated from the same collection [17]. The absolute configuration of abudinol A (17) was deduced by examination of the Cotton effects from circular dichroism studies on nakorone (19) and durgamone (20). The 1999 publication also described the isomeric structure of abudinol B (18), as well as several other triterpene natural products including

the macrocyclic diketone, muzitone (**21**). The structure of abudinol B (**18**) was determined primarily by comparisons with the spectroscopic data for abudinol A (**17**).

However, the stereochemistry of the C₂₂ alcohol of abudinol B (**18**) and the corresponding secondary alcohol of muzitone (**21**) was inconsistently rendered in the 1999 paper [17]. Although it was unclear if the stereochemistry of these chiral centers was *R* or *S*, from the way that the paper was written, it appeared that the authors had determined the stereochemistry to be *S* for these chiral centers in both compounds. We contacted Prof. Kashman by e-mail, and he quickly responded by acknowledging the error and confirming that the stereochemistry for these chiral centers in both compounds was *S*, based on the similarity in coupling constants for the corresponding region of siphonol A (**16**, Figure 5), for which the relative stereochemistry had been unambiguously confirmed by X-ray crystallography [15a].

1.2.2 Proposed Biosynthetic Pathways

The Kashman laboratory proposed biosynthetic schemes for abudinols A and B involving bidirectional cyclizations of a squalene-derived tetraol **23** (Figure 7) to form the skeleta of these pentacyclic natural products [17]. The initial cascade cyclization might be initiated by oxidation of C₂₈ with a leaving group (E₁, possibly an alcohol), to induce a series of anti-Markovnikov alkene additions including nucleophilic addition of the C₂ alcohol, to produce tricyclic intermediate **24**. A second stage of cascade cyclization, initiated by electrophile E₂, might proceed by anti-Markovnikov alkene additions, with

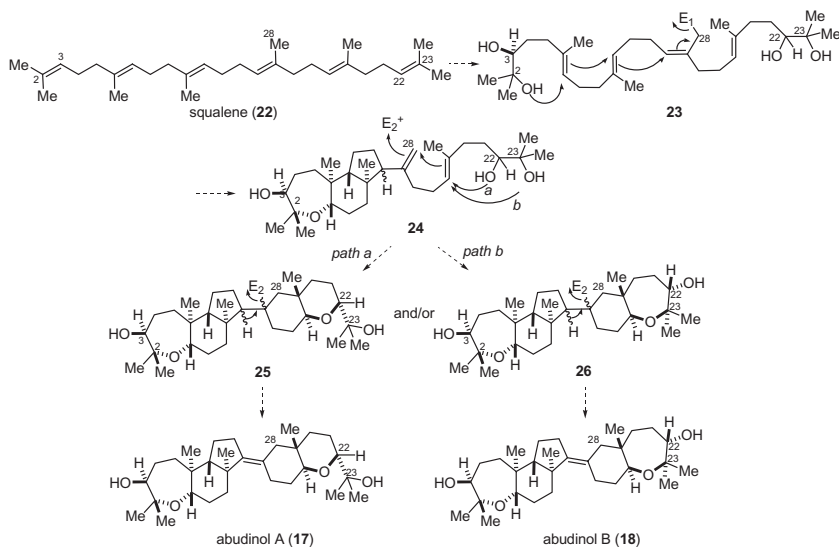


FIGURE 7 Kashman's proposal for biosynthesis of abudinols.

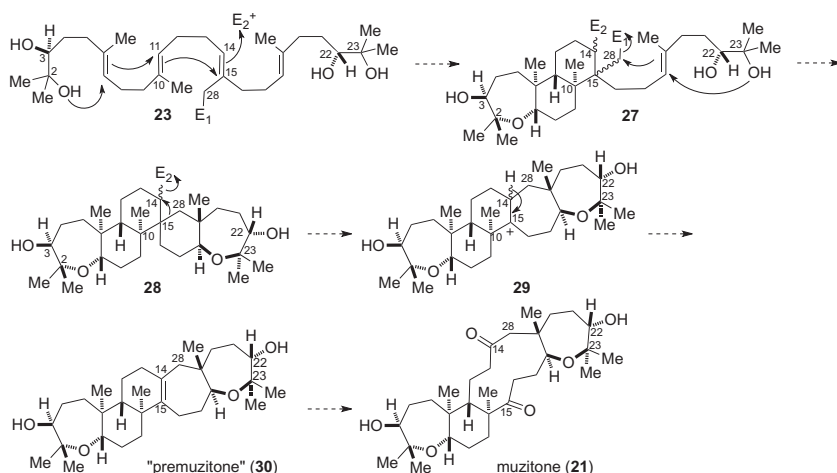


FIGURE 8 Kashman's proposal for biosynthesis of muzitone from squalene tetraol.

abudinol A arising from nucleophilic addition of the C₂₂ secondary alcohol (*path a*) and elimination of H-E₂ from the intermediate **25** to form the tetra-substituted alkene of abudinol A (**17**). Alternatively, nucleophilic addition of the C₂₃ tertiary alcohol (*path b*) would give intermediate **26** as the immediate biogenetic precursor to abudinol B (**18**).

For the biosynthesis of muzitone (**21**), Kashman presumed that an all-fused structure isomeric to the abudinols, namely compound **30** (Figure 8), was the immediate precursor to the diketone of muzitone [**17**]. He proposed two approaches: the first (Figure 8) involved a different regioselectivity for the initial cascade cyclization of the squalene 2,3-diol promoted by electrophile (E₂) to afford tricyclic **27**, followed by a second cascade bicyclization for substitution of functionalized C₂₈ (albeit at a neopentyl primary carbon) to provide spirocyclic **28**. Subsequent ring expansion of **28** with displacement of E₂ to give the cation **29** would lead to deprotonation to provide what we came to call “premuzitone” (**30**).

Kashman also proposed a second alternative, involving electrophilic reaction with the tetrasubstituted alkene of abudinol B to generate the C₁₅ cation **31** (Figure 9). Ring expansion with migration of C₁₀ to bond with C₁₅ in spirocyclic intermediate **32** would be followed by a second ring expansion to cation **33**, which upon loss of electrophilic residue “E” would also provide a route to “premuzitone” (**30**) [**17**].

The Norte laboratory proposed a different biosynthetic scheme for abudinols and muzitone in their 2000 review on marine triterpenoids [**18**], based on a sequence of cyclizations of the squalene-derived tetraepoxide **34** (Figure 10). The Norte hypothesis described initial formation of the tricyclic substructure of abudinols by sequential reaction of each alkene with one diepoxide set, concluding with proton elimination at C₂₈ to generate a new alkene in

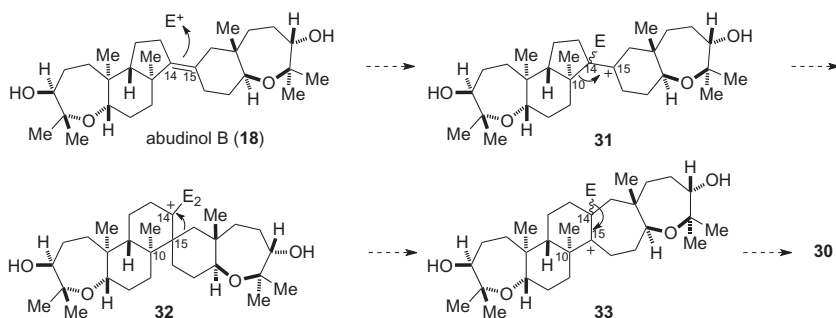


FIGURE 9 Kashman's proposal for biosynthesis of muzitone from abudinol B.

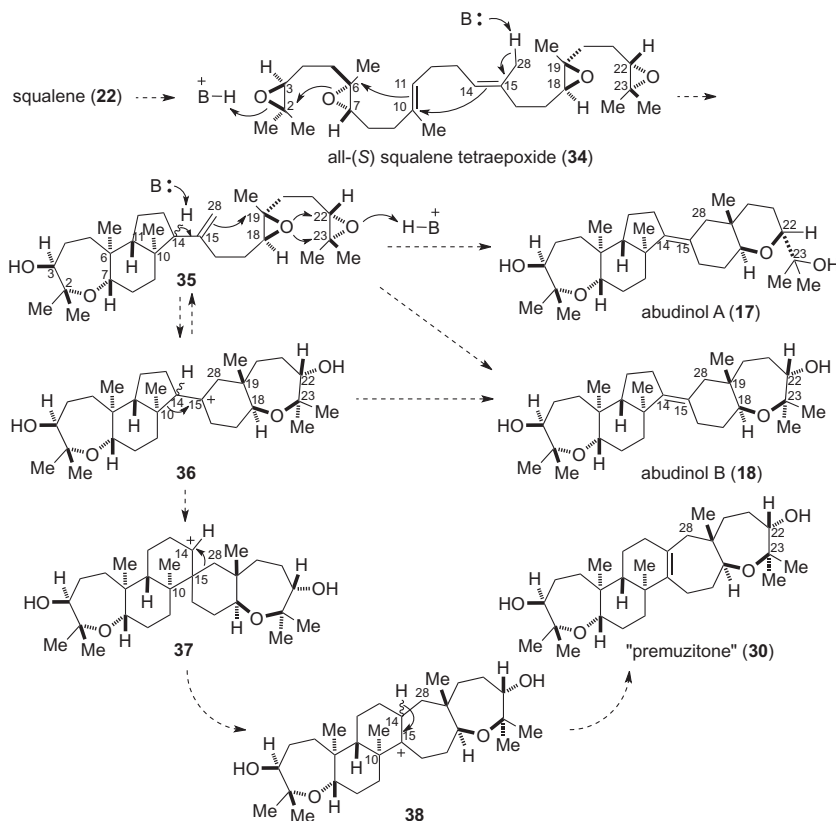


FIGURE 10 Norte's proposal for the biosynthesis of abudinols and "premuzitone."

compound 35. A second cyclization cascade with the remaining diepoxide set would then ensue, leading to both abudinols A and B (17, 18), perhaps through the carbocation 36, although a direct pathway from 35 can also be envisioned. For muzitone, Norte proposed that sequential 1,2-alkyl shifts

triggered by ring expansion might provide the all-fused isomeric structure of a pentacyclic precursor to muzitone, not unlike one of Kashman's proposals. In this case, migration of the C₁₀–C₁₄ bond from tertiary carbocation **36** to form a new C₁₀–C₁₅ bond in **37** was proposed, although the secondary carbocation at C₁₄ of **37** did not escape notice. Migration of the C₁₅–C₂₈ bond to the C₁₄–C₂₈ bond of **38** and proton elimination would afford “premuzitone” (**30**).

Given the similarities of the individual stages of Norte's hypothesis for abudinol biosynthesis to the demonstrated biosynthesis pathway for steroids from squalene monoepoxide [19], as well as the connection of diepoxide cyclization pathways with our own results, we decided to explore polyepoxide cyclization cascades terminated by carbon nucleophiles, directed toward the synthesis of abudinol B.

2. FIRST-GENERATION SYNTHESIS OF ABUDINOL B

2.1 Synthesis of the Bicyclic Segment by Cascade Oxacyclization

2.1.1 Termination of the Bicyclization Cascade with Carbon Nucleophiles

Jason Valentine developed a model system for preparing the bicyclic ketone arising from oxidative cleavage of abudinol B, based on diepoxide cyclizations coupled with alkene cyclizations to form the carbocyclic ring of this compound. The keto-diepoxide **40** (Figure 11) was prepared from geranylacetone (**39**) by three different routes. Xia Wang had initially prepared keto-diepoxide in a single step by double Shi epoxidation [10], but due to modest stereoselectivity attributed to competitive formation of a dioxirane intermediate from the ketone, Jason modified the synthesis to protect the ketone as the dimethyl ketal **41** prior to double Shi epoxidation with high diastereoselectivity, followed by Lewis acid-

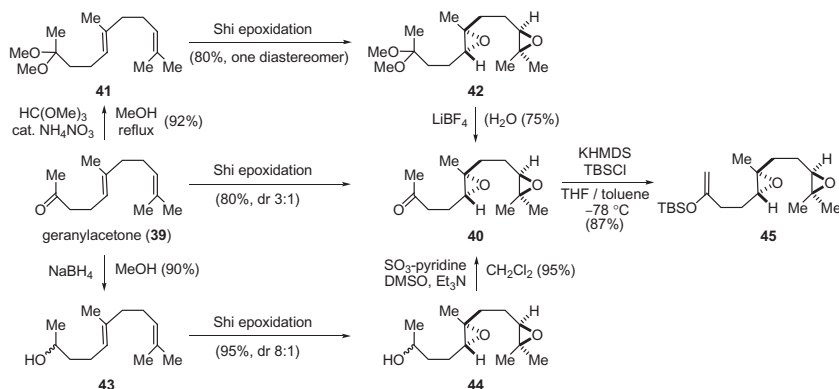


FIGURE 11 Preparation of keto-diepoxide **40** and enol silane **45**.

promoted hydrolysis of ketal **42** [20]. Subsequently, graduate student Rongbiao Tong developed a third alternative involving simple reduction of the ketone to the racemic secondary alcohol **43**, prior to double Shi epoxidation and Parikh–Doering oxidation [21] of **44** to afford the ketone **40**, with a diepoxide diastereomeric ratio of 8:1 favoring the targeted stereochemistry. Notably, the hydroxy-diepoxide **44** did not undergo “spontaneous” oxacyclization [22], even surviving silica gel chromatography prior to the oxidation step. Generation of the kinetic enolate in the presence of *tert*-butyldimethylsilyl chloride (TBSCl) provided the enol silane **45** in good yield, without detectable side reactions of the epoxides [23,24].

Our very first double cyclization experiment had been conducted with a diastereomeric mixture of the keto-diepoxide **40**, demonstrating the formation of an oxepane-diol by tandem *endo*-selective cyclization and nucleophilic termination by the ketone oxygen [10]. We then asked whether the corresponding enol silane **45** might similarly act as a terminating carbon nucleophile [25]. Although initial results with BF_3 -etherate and methylaluminum dichloride were promising, affording mixtures of silyl ether **46** and alcohol **48**, we ultimately discovered that the best yields were obtained with substoichiometric TBSOTf in the presence of 2,6-di-*tert*-butyl-4-methylpyridine (DTBMP) as a proton trap, providing **46** in reasonably good yield (Figure 12) [26]. By following the reaction with thin layer chromatography, Rongbiao observed that the minor diastereomer **47** (arising from the minor diepoxide diastereomer) was formed at a much slower rate than diastereomer **46**. This opportunity for kinetic separation was never optimized as a preparative method, as the silyl ether diastereomers could be separated by silica gel chromatography [24]. The structural assignments of our products were confirmed by X-ray crystal structures of the corresponding alcohols **48** and **49** [26].

Our mechanistic hypothesis is that the terminal epoxide is activated by the Lewis acid, followed by nucleophilic addition of the oxygen of the second epoxide to provide a bicyclic oxonium ion intermediate **51**. The carbacyclic

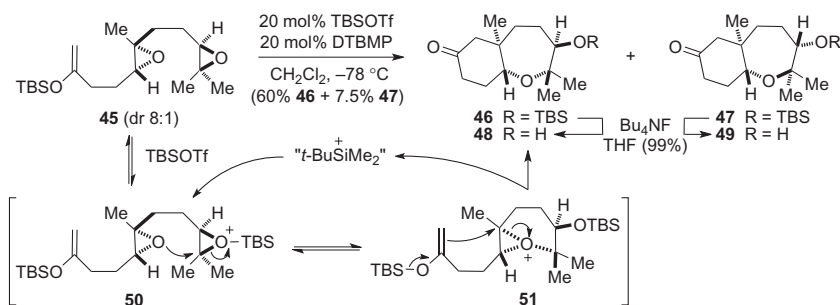


FIGURE 12 Bicyclization of enol silane-diepoxide **45**.

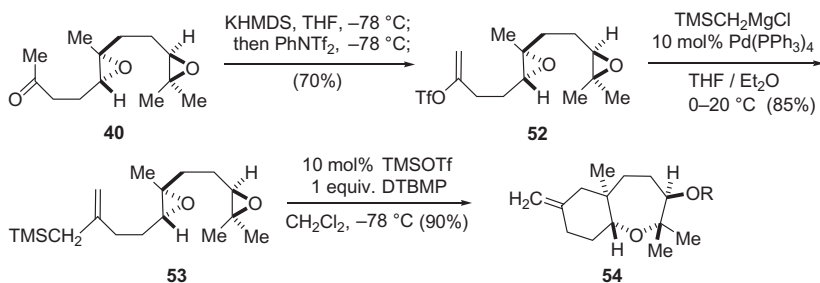


FIGURE 13 Bicyclization of allylsilane-diepoxyde **53**.

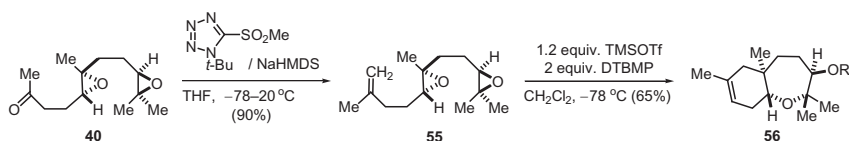


FIGURE 14 Bicyclization of diepoxyde terminated with 1,1-disubstituted alkene.

ring then arises by nucleophilic addition of the enol silane to the nearest fully substituted carbon of the oxonium ion to afford the bicyclic product **46**, and simultaneously regenerating the trialkylsilyl Lewis acid. We have assumed that the initial activation of the epoxide is an equilibrium process, as the internal epoxide might be only slightly more hindered than the terminal epoxide. Despite the modest yield of **46**, we did not find byproducts arising from activation of the internal epoxide.

This bicyclization approach was subsequently demonstrated with the allylic silane **53** (Figure 13) [27], giving the exocyclic alkene **54**, reminiscent of the alkene of abudinol B. Again, the choice of Lewis acid was important for optimizing yields, with substoichiometric trimethylsilyl triflate (TMSOTf) in the presence of DTBMP as the ideal reagents for a bicyclization transformation [24,28].

Of course, the application of silicon-containing nucleophiles did not truly correspond to a biosynthetic pathway, given the virtual absence of organosilicon compounds in living organisms. The 1,1-disubstituted alkene of **55** (Figure 14) represented a better model as a biosynthetic cyclization precursor [29]. In the presence of *stoichiometric* TMSOTf and DTBMP, cyclization of compound **55** provided the bicyclic product **56**, albeit as the endocyclic alkene [24,28].

2.1.2 Synthesis of ent-Durgamone

With the bicyclic keto alcohol **48** in hand, we wondered if the seven-membered ring oxepane might be rearranged into the structure of durgamone. This was readily accomplished by modifying a rearrangement originally developed by Nakata for ring expansion [22a,30] but applied in our case to a stereospecific ring contraction via the chloromesylate derivative **57** (Figure 15). The rearrangement presumably proceeds by anchimeric assistance, with initial nucleophilic

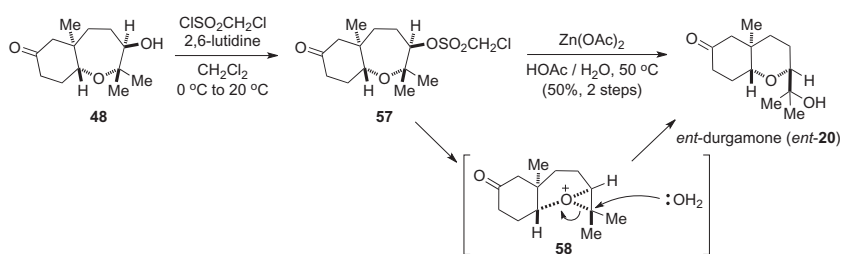


FIGURE 15 Synthesis of *ent*-durgamone (*ent*-20) by stereospecific ring contraction.

substitution of chloromethyl sulfonate by the ether ring oxygen with inversion of stereochemistry from *R* to *S*, followed by addition of water to the more substituted carbon of the oxonium ion **58** to generate *ent*-durgamone (*ent*-20) [26].

It was only at this stage that we realized that the Kashman laboratory had reported only partial ^1H NMR data for durgamone, specifically only for hydrogens at the secondary ether positions and for the three methyl groups [17]. Although our data was in close agreement with the partial ^1H NMR data as well as the ^{13}C NMR resonances, we were troubled by discrepancies in the optical rotations. As we had deliberately prepared the enantiomer of the natural product (ultimately arising from the fact that the chiral ketone for Shi epoxidation was much more easily prepared from commercial D-fructose than from synthetic L-fructose) [9,31], the magnitude of our measured optical rotation (+14, $c = 0.13$, methanol) was substantially lower than reported for the natural product (−28.5, $c = 0.1$, methanol), although the sign of our measured rotation corresponded to that expected for the directed synthesis of the enantiomer of the naturally occurring compound.

2.2 Retrosynthesis of Abudinol B, First Generation

At this time, we began to seriously consider a total synthesis of one or both of the abudins. A conservative approach would be to combine two sectors, one bearing the bicyclic substructure **48** already prepared in our laboratory and the other tricyclic substructure corresponding to *ent*-nakorone (*ent*-19), which might also arise from cascade cyclization. In preparation for a synthesis of *ent*-abudinol B, our next goal was the synthesis of *ent*-nakorone (*ent*-19) from tricyclization of diepoxy enyne **59** (Figure 16).

2.3 Synthesis of the Tricyclic Segment by Cascade Oxacyclization

2.3.1 Electronic Effects Harnessed for Regioselective Epoxidation

With sound precedents from the Johnson laboratory on the termination of polyene cyclizations with propargylic silanes [32], we envisioned preparing the tricyclic sector represented by *ent*-19 by the analogous diepoxy alkene

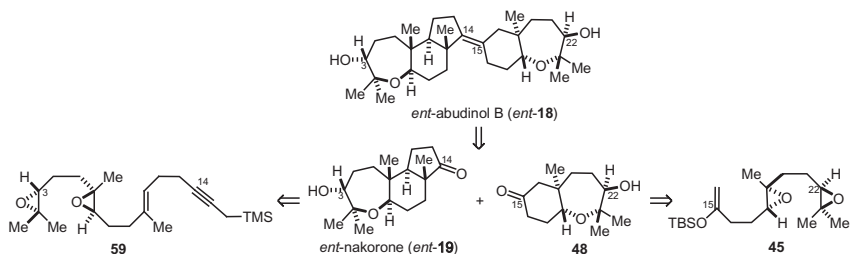


FIGURE 16 Retrosynthesis of abudinol B via polycyclic ketones **48** and *ent*-**19**.

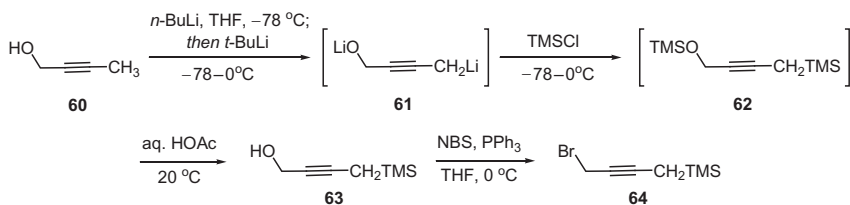


FIGURE 17 Synthesis of 1-bromo-4-trimethylsilyl-2-butyne (**64**).

cyclization terminated by a propargylic silane. For introduction of the propargylic silane, we required a good supply of the known compound 1-bromo-4-trimethylsilyl-2-butyne (**64**, Figure 17). In our hands, we obtained relatively low yields following the literature procedure from commercial but expensive 1-trimethylsilyl-2-propyne [33]. Rongbiao Tong found that the alcohol predecessor was more easily prepared from 2-butyne-1-ol (**60**), by generation of the dianion **61**, double silylation to **62**, and chemoselective hydrolysis of the silyl ether. This new procedure for preparation of the alcohol **63** was subsequently optimized for multigram-scale synthesis by undergraduate student Alex Wein and published in *Organic Syntheses* [34].

After conversion of farnesol (**8**) into the known phenylsulfone **65** [35] by the intermediacy of farnesyl bromide, alkylation of the sulfone anion with bromopropargylic silane **64** afforded the racemic trienylalkyne **66** (Figure 18).

At this stage in our research, we knew that electronegative and electron-withdrawing allylic substituents greatly diminished the rate of epoxidation such that regioselective epoxidations could be realized. Thus, we were not surprised when Shi epoxidation of the trienyl-propargylsilane **66** cleanly provided only the diepoxide **67** (Figure 19). As the sulfone substituent had now completed its dual tasks of anion stabilization for carbon–carbon bond formation and protecting the nearest alkene from undesired epoxidation, it was uneventfully removed with palladium catalysis in the presence of Super-Hydride[®] ($\text{Li}^+\text{Et}_3\text{BH}^-$) [36]. We were pleased to observe that the epoxides were stable to these reaction conditions, thus avoiding potential side reactions

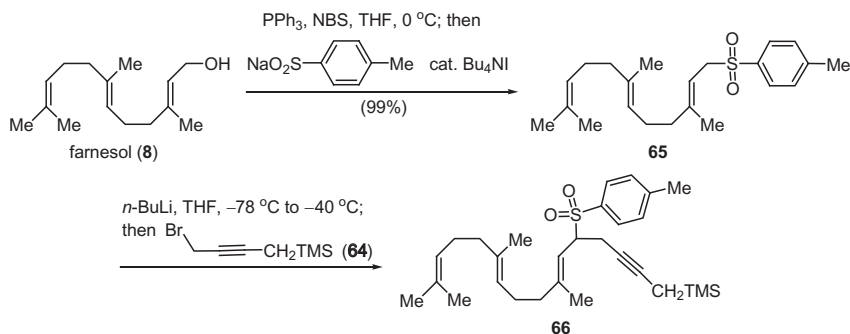


FIGURE 18 Synthesis of trienyl-propargylsilane **66**.

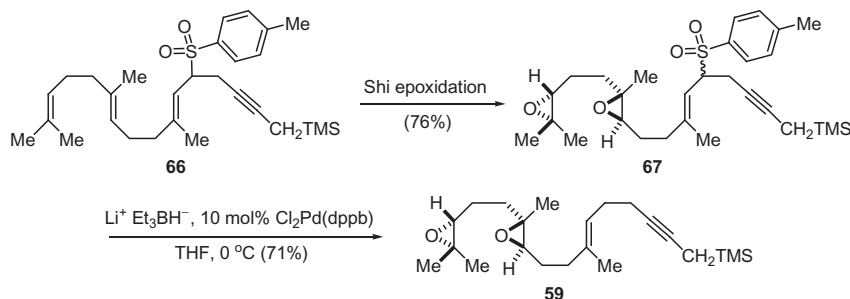


FIGURE 19 Regioselective Shi epoxidation and desulfonylation.

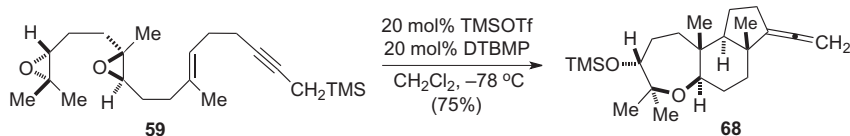


FIGURE 20 Tricyclization of diepoxide **59**.

such as reductive opening of the epoxide or premature initiation of the cascade cyclization of the epoxides.

2.3.2 Synthesis of ent-Nakorone

The diepoxy-enyne **59** underwent cascade cyclization using our now standard conditions of substoichiometric TMSOTf and DTBMP, to provide the *trans*–*anti*–*trans*-tricyclic structure **68** (Figure 20) bearing an exocyclic allene [24,26]. Although stereoselective formation of the oxepane ring was consistent with stereospecific anti opening of the two epoxides, being controlled by the stereochemistry of the two epoxides, we also observed that the stereochemistry of the ring fusion between the two carbocyclic rings was delivered with complete stereoselectivity, consistent with the possible concerted

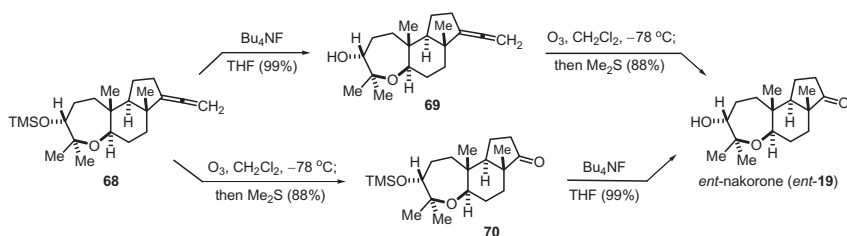


FIGURE 21 Conversion to *ent*-Nakorone (*ent*-19).

mechanism of enyne cyclization onto an activated bicyclic epoxonium ion. The yield of this tricyclization reaction was superior to yields observed in any of our previous cascade cyclization work.

Desilylation of the tricyclic product **68** afforded a crystalline alcohol **69** (Figure 21), providing unambiguous substantiation of the structure by X-ray crystallography. Ozonolysis of the allene then furnished the structure of the enantiomer of nakorone (*ent*-19). The final steps could also be conducted in the opposite order through silyl ether **70**, with the same yield [24,26].

We then compared our spectroscopic data with the partial data provided in Kashman's 1999 publication [17]. Whereas our ^1H and ^{13}C NMR data showed a fairly good match with the published tabulated data, we were alarmed to find that the optical rotation data of our synthetic *ent*-nakorone (-50 , $c = 0.25$, methanol) *had the same sign as that reported for the natural product* (-210.0 , $c = 0.2$, methanol)! We hurriedly sent another e-mail to Prof. Kashman inquiring into his level of confidence in the optical rotation data for durgamone and nakorone, and requesting copies of spectral data. As the publication of these compounds was nearly 10 years previous to our inquiries, Prof. Kashman reported that the original natural products were no longer available or had decomposed. He sent us by fax and subsequently by mail copies of the ^1H NMR spectrum of nakorone, which unfortunately was of lower quality than desired, but clearly did show the same types of coupling patterns in diagnostic regions of the NMR spectrum of our synthetic material.

2.4 Coupling the Two Segments and Completion of the First Synthesis of Abudinol B

With the silyl ethers of bi- and tricyclic ketones in hand, we sought to connect these two segments to form the pentacyclic structure of abudinol B. We essentially needed to conduct a “retro-ozonolysis”, specifically the heterocoupling of ketones **46** and **70**, thus ruling out methods such as McMurry coupling [37]. Due to the sterically hindered nature of the tricyclic ketone **70**, our initial attempts failed, including coupling **70** with the titanium carbene from reduction of the *gem*-dichloride **71** prepared from the bicyclic ketone [38] or addition of the vinylolithium **72** arising from Shapiro reaction of a bicyclic

trisylylhydrazone [39] (Figure 22). A variation on the Barton–Kellogg reaction proceeded as far as the diazine-linked structure **75** [40] (which we optimistically dubbed “azo-abudinol”) but then resisted carbon–carbon bond formation under a variety of conditions [24].

Ultimately, Rongbiao linked the segments of abudinol B to form the C₁₄–C₁₅ bond, employing palladium-catalyzed Suzuki–Miyaura cross-coupling of a vinylic triflate with a vinylic boronate [41]. Thus, enolate formation from bicyclic ketone **46** provided the enol triflate **76** with complete regioselectivity, and the corresponding enol triflate **77** was uneventfully prepared from tricyclic ketone **70** (Figure 23). Each enol triflate was then converted into the corresponding vinylboronates **78/79** by palladium-catalyzed substitution [42], and in the same pot, palladium-catalyzed Suzuki–Miyaura cross-coupling with the opposite enol triflate partner provided the desired diene **80**. The most attractive feature of this approach (in addition to its success!)

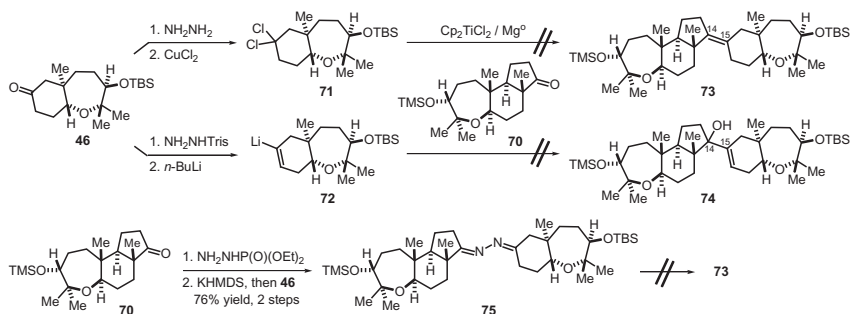


FIGURE 22 Unsuccessful approaches to link ketones **46** and **70**.

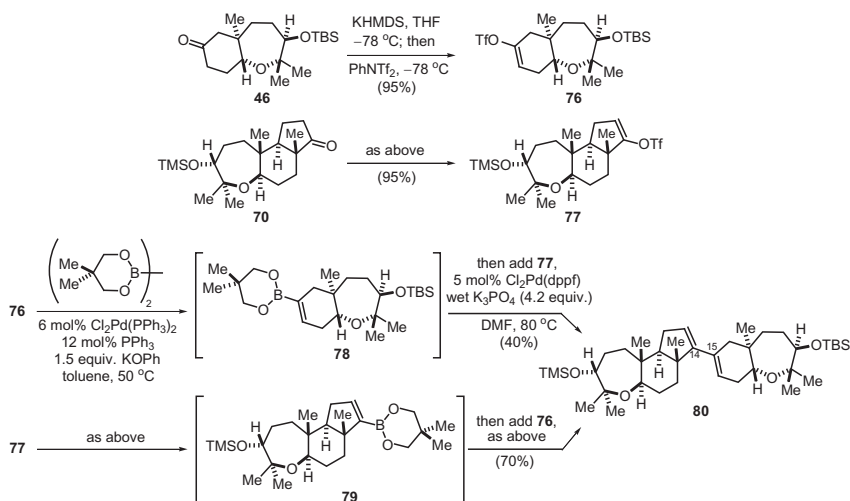


FIGURE 23 Synthesis of diene **80** by palladium-catalyzed cross-coupling.

was the flexibility for swapping the electrophilic and nucleophilic partners. Indeed, both approaches provided the same diene **80**, although better yields were obtained by coupling the less hindered bicyclic enol triflate **76** with tricyclic vinyl boronate **79** [24,27].

Having formed the C₁₄–C₁₅ bond, we now faced considerable difficulty in converting the diene **80** (dehydroabudinol) into the tetrasubstituted alkene of abudinol B. We ruled out methods based on 1,3-diene-coordination [43], as such an approach would have favored the undesired *Z*-alkene stereochemistry by enforcing an *s-cis* conformation between C₁₄–C₁₅. However, Rongbiao found a good precedent for conditions developed by Shibasaki for an analogous hydrogenation of a bicyclic prostaglandin analog [44], and these conditions produced the bis-silyl ether **81** in modest yield, along with the isomeric trisubstituted alkene **82** (Figure 24). At this stage, the structure of **81** including the all-important *E*-alkene stereochemistry was confirmed by X-ray crystallography [24,27].

Several unsuccessful attempts were made to isomerize the trisubstituted alkene of **82** to abudinol B (cat. sulfuric acid, KAPA, Pd-catalysis) [45]. Hole-transfer promoted hydrogenation of **80** (with [*p*-BrPh]₃N⁺.SbCl₆[−] and Bu₃SnH) [46] produced primarily the trisubstituted alkene **82**, along with approximately 5% of a tetrasubstituted alkene, which may have been the *Z*-alkene isomer of **81**. Upon desilylation of **81**, the enantiomer of abudinol B was obtained (*ent*-**18**, Figure 25), which exhibited spectroscopic characteristics similar to those described by Kashman's publication, including good overlap with an ¹H NMR spectrum of abudinol B kindly provided by Prof Kashman. In this case, the sign of our synthetic material (+23, *c* = 0.05, methanol) was consistent with that expected in comparison with the naturally occurring antipode (−5.0, *c* = 0.05, methanol), although now the magnitude of our optical rotation was significantly greater. Nonetheless, we judged that we

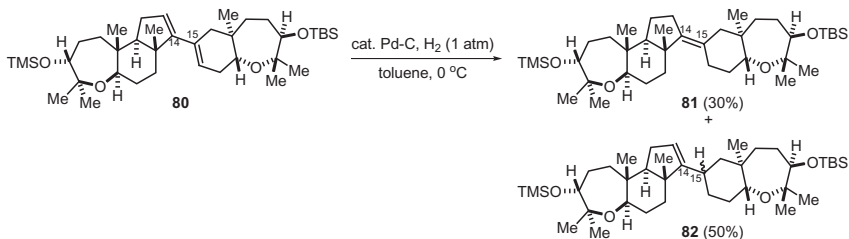


FIGURE 24 Partial hydrogenation of diene **80**.

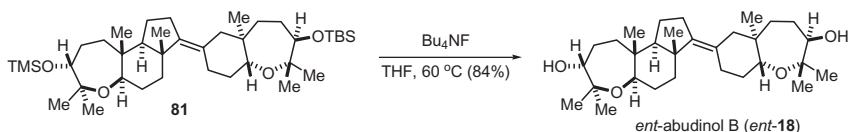


FIGURE 25 Synthesis of *ent*-abudinol B (*ent*-**18**).

had indeed prepared the enantiomer of the natural product, and thus we could confirm Kashman's structural assignment to the extent possible with the data available from Kashman's publication and his primary spectral data [17].

We were unable to come to a conclusion regarding the discrepancies in the optical rotation data. The Kashman laboratories based their stereochemical assignments of nakorone (**19**) and durgamone (**20**) from circular dichroism measurements, with both ketones exhibiting a positive Cotton effect, which were also compared with several other triterpene natural products isolated and characterized by their laboratory [17]. Thus, we believe that the Kashman assignments for nakorone, durgamone, and by extension, abudinol B (**17**) are correct and have been confirmed by our syntheses of the antipodal forms.

Of course, the discrepancy in the order of magnitude could also be explained by poor control of absolute stereochemistry on our part. Indeed if the stereochemistry of durgamone and nakorone had been introduced by a single transformation of lower enantioselectivity, and control of the remaining chiral centers had resulted from substrate-induced diastereinduction, the generation of scalemic products would be a realistic concern. However, *our application of two independent enantioselective transformations*, namely the Shi epoxidations, means that *any deficiencies in the enantioselectivity of the epoxidations would be expressed in the form of the minor diastereomer*, rather than the enantiomer [47]. The diastereomeric diepoxides were not separable (even difficult to distinguish by ^1H NMR spectroscopy), but after these materials underwent cascade cyclization, the bi- and tricyclic products were purified as single diastereomers, thus removing vestiges of any imperfection in the enantioselectivity of the Shi epoxidations.

Although we did not prepare chiral ester derivatives of alcohols **48** and **69** (in retrospect, perhaps an oversight) [48], the synthetic route provided another proof of the high enantiomeric purity: *the cross-coupling product 80 was produced as a single diastereomer*. Specifically, the ^{13}C NMR spectrum of **80** showed only 34 peaks (35 expected, two overlapping resonances at 18.2 ppm), and ^1H NMR clearly exhibited seven distinct methyl singlets. Note that a mixture of diastereomers would have shown some additional peaks in the NMR spectra, especially for atoms near the connection point of $\text{C}_{14}\text{--}\text{C}_{15}$.

3. SECOND-GENERATION SYNTHESIS OF ABUDINOL B

3.1 Preparation of a Partially Epoxidized Polyene Precursor

Having completed the synthesis of *ent*-abudinol B by cross-coupling bi- and tricyclic sectors, we had some confidence in a more direct synthesis from an acyclic analog of squalene epoxides, not unlike the squalene tetraepoxide (**34**) proposed by Norte as a hypothetical biosynthetic precursor [18]. We first considered preparing a bis-silyl tetraepoxide **83** (Figure 26), but we failed to conceive a synthetic plan for introducing the two trimethylsilyl groups that

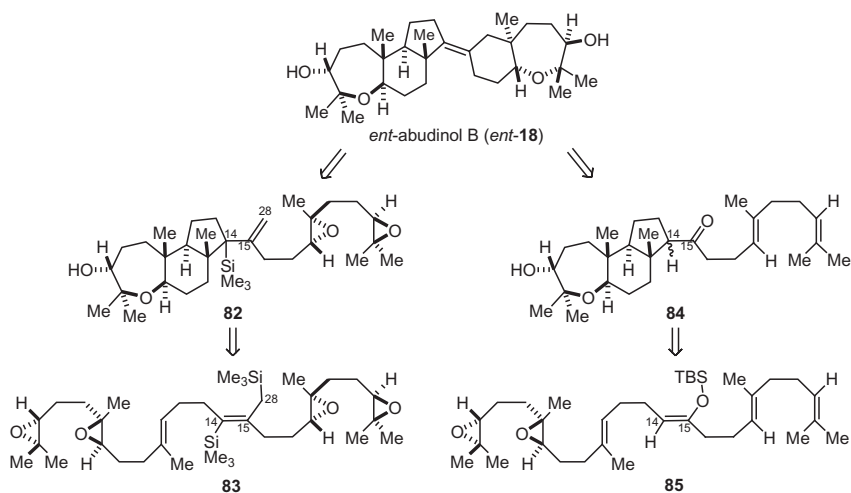
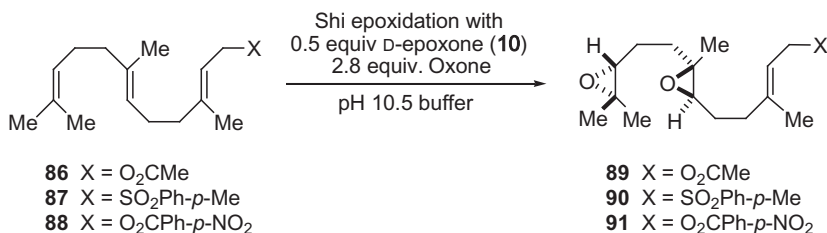


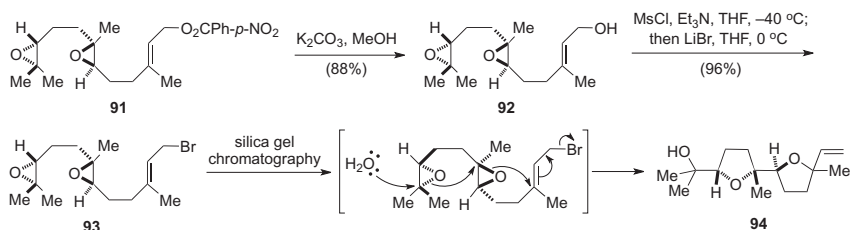
FIGURE 26 Retrosynthesis of abudinol B, second generation.

anyone wished to risk. On the other hand, we realized that squalene tetraepoxide itself (**34**, Figure 10) might be produced fairly easily, but any production of abudinol B from Lewis acid-promoted polycyclizations of squalene tetraepoxide might also be accompanied by many other compounds, not unlike a crude mixture in a natural product extract, and thus this was also unattractive as a possible “needle-in-a-haystack” problem that was ill-suited to the analytical and separation competency of our laboratory. We ultimately prepared a derivative of squalene **85** in which one of the central methyl groups was replaced by a silyloxy substituent in order to direct cyclization by a highly nucleophilic enol silane. Moreover, we introduced only two epoxides at the outset, to simplify the problem of epoxide activation by cleanly separating the tricyclization and bicyclization processes.

The first order of business was to prepare the diepoxide-containing sector of **85**, which would arise from farnesol (**8**). Alluding again to our experience in the regioselective application of Shi’s enantioselective epoxidation methodology with farnesol and its derivatives, we observed that farnesyl acetate (**86**) provided the diepoxide **89** with 10:1 dr, although a significant quantity of the triepoxide was consistently obtained (Table 1), with poor stereoselectivity for epoxidation of the alkene bearing the allylic acetate. Given that farnesyl *p*-tolyl sulfone (**87**) clearly provided only the diepoxide **90**, we felt that a more strongly electron-withdrawing ester would more strongly suppress epoxidation of the alkene near the electron-withdrawing group. Early attempts with farnesyl *tert*-butyl carbonate and farnesyl benzoate proceeded with poor conversion, due to the low solubility of the hydrophobic triene derivative in the polar protic reaction solvent. However, graduate student Matt Boone discovered that Shi epoxidation of farnesyl *p*-nitrobenzoate (**88**) primarily produced the diepoxide **91**

TABLE 1 Regioselectivity of Shi Epoxidations with Farnesol Derivatives

Triene	Monoepoxides yield	Diepoxide yield	Triepoxide yield
86	Trace	35–55%	40%
87	Trace	71%	Trace
88	28%	49–61%	Trace

**FIGURE 27** An exciting preparation of diepoxide-allylic bromide **93**.

accompanied by only a trace of the triepoxide, along with modest quantities of two monoepoxide regioisomers, which were generally further transformed into additional diepoxide **91** by another cycle of the Shi epoxidation [49,50].

After mildly basic methanolysis of the ester **91**, we sought to convert the resulting alcohol **92** into the allylic bromide **93** (Figure 27). However, Rongbiao discovered that an attempt to purify this allylic bromide by silica gel chromatography resulted in a highly exothermic tandem *exo*-mode bicyclization when the material touched silica gel pretreated with hexane/ethyl acetate (the wet silica literally appeared to explode within the column!), from which the bis-tetrahydrofuran **94** could be isolated and partially characterized [24]. As the allylic bromide **93** was also sensitive to light, moisture, and air, he subsequently prepared this material immediately before it was needed, without further incident.

Rongbiao proposed a short synthesis of the enol silane **85** by a three-component synthesis originally described by Reich [51] and subsequently extended by Kuwajima [52], involving addition of a vinyl lithium or vinylic Grignard reagent to acylsilane, followed by Brook rearrangement of the lithium alkoxide and alkylation of the resulting silyloxy-substituted allyllithium with a reactive carbon electrophile. Any trepidation that epoxides would be incompatible with these basic reaction conditions was soon soothed by the realization that Corey's laboratory had used this method on several occasions with monoepoxide components in their cascade carbocyclization approaches to all-carbocyclic triterpenoid natural products [53]. Our application of this methodology began with alkylation of the metalloenamine from **95** [54] with geranyl bromide (**96**), leading to the acylsilane **97** (Figure 28). Addition of vinylmagnesium chloride provided a stable magnesium alkoxide, which was protonated to give **98**. However, the corresponding lithium alkoxide **100** underwent Brook rearrangement to the beta-silyloxyallyllithium intermediate **101**, with alkylation with freshly prepared allylic bromide **93** providing the desired enol silane as the *Z*-isomer, in 50% yield. The formation of byproducts arising from protonation and/or oxidative dimerization of the organolithium **101** could not be completely prevented despite our attention to stringently maintaining air- and moisture-free reaction conditions, but the procedure was robust enough to provide more than 2 g of **85** [24,55].

3.2 Sequential Cascade Cyclizations to Provide the Structure of Abudinol B

With the enol silane **85** in hand, Rongbiao triggered the first stage of biomimetic tricyclization with 1.1 equiv. of TMSOTf and DTBMP. He initially obtained the product as a mixture of C₁₄ diastereomers, and when quenching

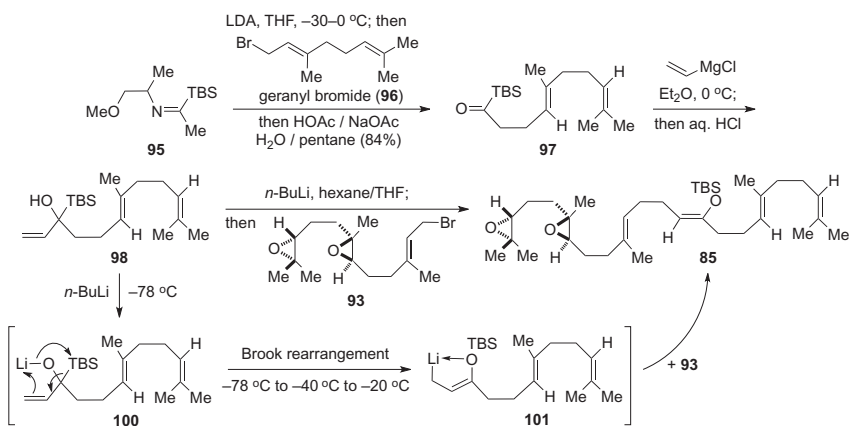


FIGURE 28 Synthesis of **85** by tandem Brook rearrangement–alkylation.

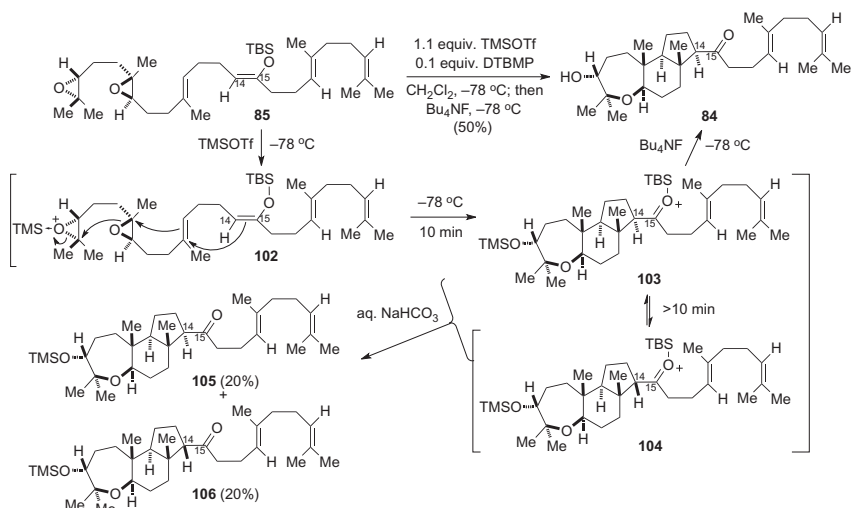


FIGURE 29 Tricyclization studies with diepoxide **85**.

with aqueous sodium bicarbonate was able to isolate and characterize trimethylsilyl ether products **105** and **106** (Figure 29). He found that both the isolated yield and the product diastereoselectivity greatly improved when the reaction mixture was quenched with 1.1 equiv. of tetrabutylammonium fluoride at $-78\text{ }^{\circ}\text{C}$ within 10 min of initiating the tricyclization, giving **84** as the only tricyclic product and small amounts of mono- and bicyclic side-products from truncated cyclization processes. We have attributed the mixture of C_{14} diastereomers to the possible equilibration between relatively long-lived silyloxonium ions **103** and **104** as a mechanism for epimerization of the C_{14} chiral center upon longer reaction times [24,54].

To prepare for the final bicyclization stage, methylenation of the acyclic ketone of **84** was conducted. Several methods were explored before we found that Wittig methylenation with methyltriphenylphosphonium bromide and potassium *tert*-butoxide in refluxing benzene [53b] provided the desired alkene **107**. However, we could not suppress epimerization at the C_{14} position so that the diastereomer **108** was actually the major product (Figure 30). We suspect that the basic Wittig reagent competitively deprotonates the ketone so that additional Wittig reagent cannot react with the enolate intermediate. However, the presence of *tert*-butanol can presumably protonate the enolate to regenerate the ketone, which eventually is driven through this acid–base equilibrium by Wittig methylenation. Diastereomers **107** and **108** were separable only by careful column chromatography, and for preparative purposes, the mixture of diastereomers was generally carried forward through the subsequent Shi epoxidation step.

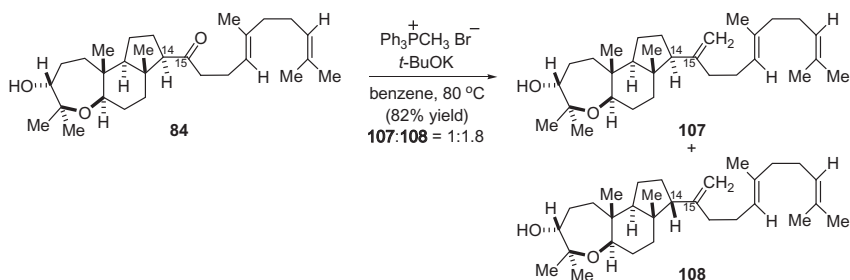
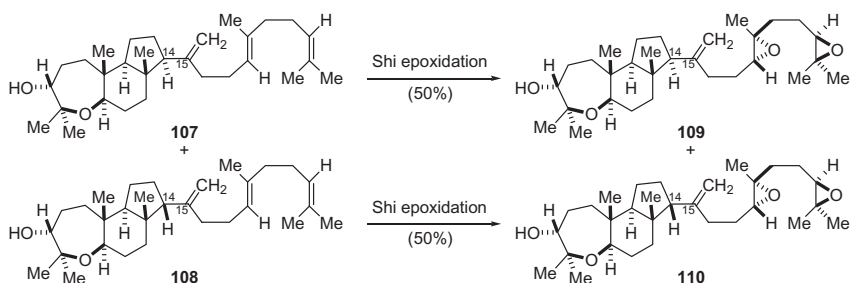


FIGURE 30 Wittig methylation.

FIGURE 31 Shi epoxidations of trienes **107** and **108**.

The Shi epoxidations of the trienes **107** and **108** were carefully conducted to minimize formation of the triepoxide, which would have been a useless compound for our purposes. Thus, we avoided carrying the epoxidations to complete conversion, relying on the subtle differences in nucleophilicity of trisubstituted versus 1,1-disubstituted alkenes, to provide mixtures of both monoepoxides and the desired diepoxides **109** and **110** (Figure 31), with the option for resubjecting monoepoxides to another cycle of epoxidation. Note that epoxidation was necessary after the ketone had undergone methylenation, otherwise competitive formation of the dioxirane might have occurred with the ketone, with the correspondingly poor diastereoselectivities observed for geranylacetone **39** (Figure 11). Similar results for the Shi epoxidations were observed whether conducted on the separated diastereomers **107** and **108**, or with mixtures of **107** and **108** from which diastereomers **109** and **110** were chromatographically separated.

Our excitement at having generated the structures implicated in the biosynthetic cyclizations was tempered by the scrambling of C_{14} stereochemistry in the methylenation step leading to **109** and **110**. However, it was unclear which diastereomer would give abudinol B, so we might be considered fortunate to have the opportunity to study both epimers. At the time, we had not assigned the stereochemistry at C_{14} for either diastereomer **109** or **110**, and so the first bicyclization study was conducted with the diastereomer that was later shown to be **109**. Bicyclization of **109** with TMSOTf/DTBMP

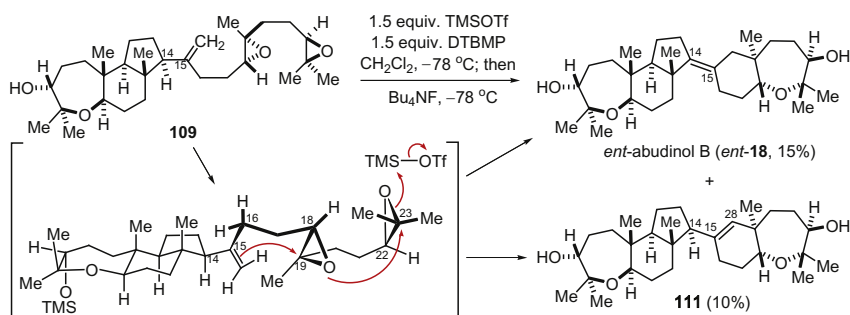


FIGURE 32 Biomimetic cyclization of diastereomer **109** gives *ent*-abudinol B.

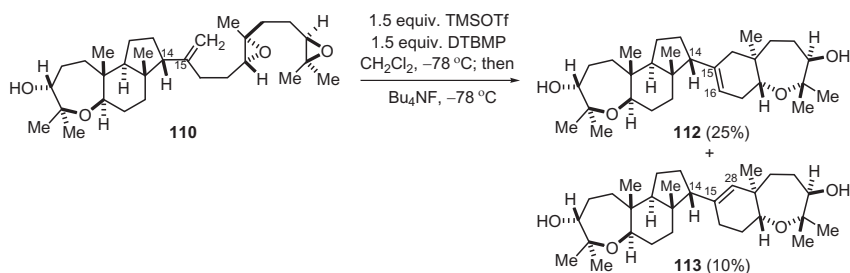


FIGURE 33 Biomimetic cyclization of diastereomer **110** does *not* give abudinol B.

produced two bicyclic products, albeit in relatively low yields, one of which was clearly *ent*-abudinol B (*ent*-**18**), along with a trisubstituted alkene isomer **111**, but this time with the double bond in the six-membered ring (Figure 32).

On the other hand, cyclization experiments on the C_{14} diastereomer **110** gave absolutely no trace of *ent*-abudinol B. The only pentacyclic products found were isomeric trisubstituted alkenes **112** and **113** (Figure 33). The structure of **112** was confirmed by X-ray crystallography of the bis-bromobenzoate derivative, and with assignment of the stereochemistry at C_{14} of **112**, the corresponding stereochemical assignments were made for compounds **84**, **105–110**, and **113**.

3.3 Synthesis of Squalene Tetraepoxide

We subsequently completed a short and stereoselective synthesis of all-*R*-squalene tetraepoxide, the enantiomer of the tetraepoxide proposed by Norte as the biosynthetic precursor for abudinol and other triterpenoid natural products [18]. This compound had been reported half a century ago, arising as a mixture of enantio- and diastereomers from perbenzoic acid epoxidation of squalene [56]. As the enantio- and regioselective Shi epoxidations had provided us with good routes to a variety of farnesol-derived diepoxides, including diepoxy-allylic

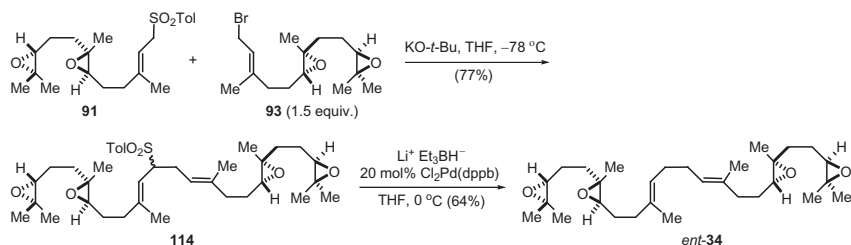


FIGURE 34 Synthesis of all-(*R*)-squalene tetraepoxide (*ent*-34).

sulfone **91** and diepoxy-allylic bromide **93**, we successfully coupled **91** and **93** under basic conditions to assemble intermediate **114**, which upon palladium-catalyzed desulfonylation provided squalene tetraepoxide *ent*-34 (Figure 34) [50].

As feared, the reaction of synthetic tetraepoxide *ent*-34 with TMSOTf/DTBMP gave only a complex mixture of over 20 minor products, none of which could be sufficiently purified for structural characterization [49]. Nonetheless, our procedure for squalene tetraepoxide synthesis, especially if conducted with the antipode of the Shi catalyst [31] to prepare the all-*S*-enantiomer **34**, may provide useful material for biosynthetic studies with the cyclic ether triterpene-producing organisms.

4. SYNTHESIS OF THE PURPORTED STRUCTURE OF MUZITONE

4.1 Preparation of a Regioisomeric Partially Epoxidized Polyene Precursor

We recognized that our strategy might be applied to the structure of the pentacyclic compound *ent*-30 as the precursor to *ent*-muzitone (*ent*-21), simply by shifting the position of the enol silane on the squalene diepoxide analog, that is, compound **116** (Figure 35). In this case, the enol silane reaction onto the alkene would also need to be an *endo*-selective process via intermediate **115**, in order to provide both fused six-membered carbocyclic rings of *ent*-30.

Matt Boone prepared the required enol silane **116** by switching the order of introduction of the two allylic bromides (Figure 36). Thus the metalloenamine from **95** [54] was first alkylated with the sensitive diepoxy-allylic bromide **93**, which was then subjected to the Reich–Kuwajima methodology of vinyl Grignard addition to the acylsilane **117**, Brook rearrangement of the lithium alkoxide of **118**, and alkylation with geranyl bromide (**96**). Although the yields were lower for the synthesis of **116** when compared with the regioisomer **85** utilized earlier for the abudinol synthesis, the reader is reminded that the diepoxide sector of **116** survived anionic conditions in each of the three steps.

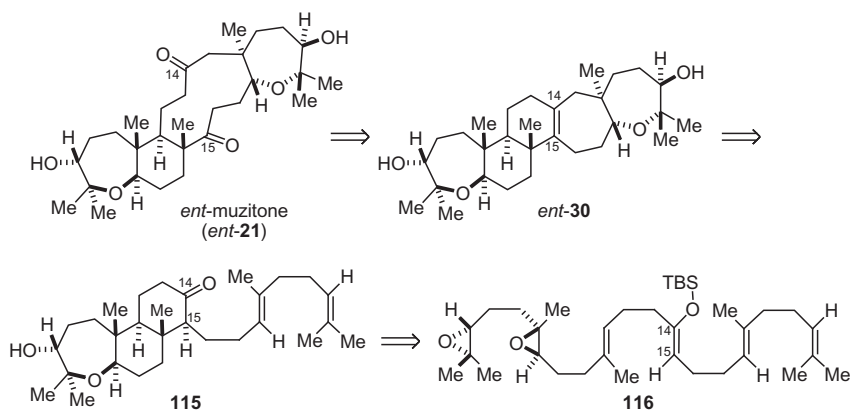


FIGURE 35 Retrosynthetic analysis of muzitone.

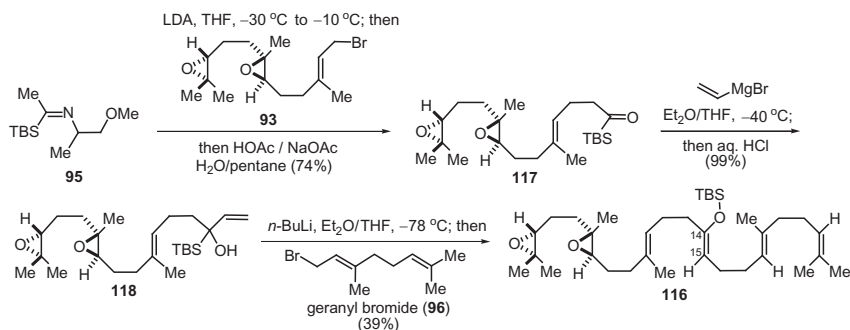


FIGURE 36 Synthesis of 116 by tandem Brook rearrangement-alkylation.

4.2 Sequential Cascade Cyclizations to a Fused Pentacyclic Structure

The biomimetic tricyclization was conducted with 116 under the same conditions developed in our abudinol synthetic work, providing the desired tricyclic product 115 as a 1:1 mixture of epimers, mixed with an unknown but inseparable byproduct. The inseparable mixture containing both C₁₅ diastereomers of tricyclic product 115 was first epimerized under basic conditions, to provide a single diastereomer corresponding to the equatorially substituted cyclohexanone. After derivatization as the *para*-nitrobenzoate ester 119, the tricyclic product was obtained in pure form, albeit in relatively low yield overall. Nonetheless, the brevity of the synthesis to this stage enabled our preparation of over 700 mg of pure 115 (slightly more than 1.5 mmol) (Figure 37) [28,49].

The Wittig reaction proceeded smoothly to provide the triene 120, in this case without apparent epimerization of the adjacent chiral center (Figure 38). The stereoselective nature of this reaction meant that we would be denied the

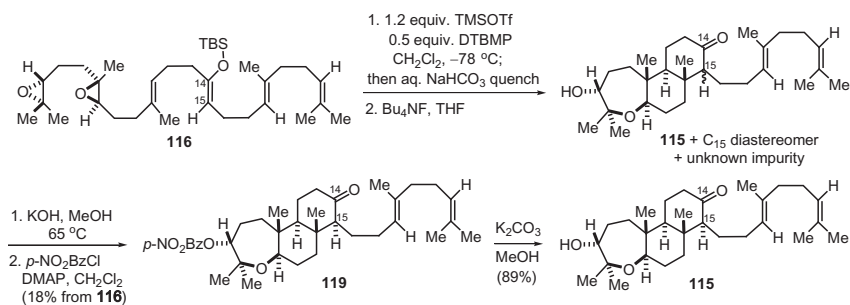
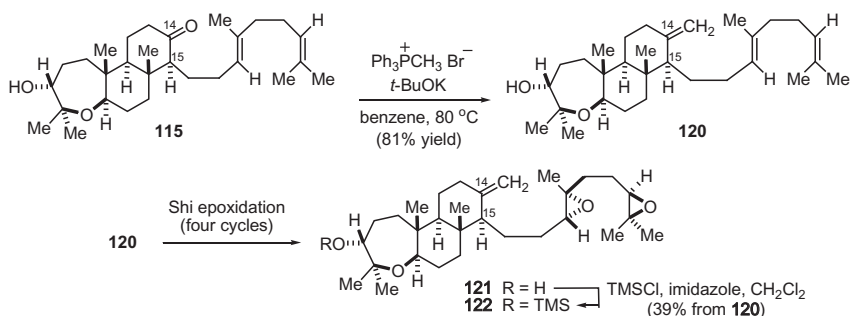
FIGURE 37 Tricyclization studies with diepoxide **116**.

FIGURE 38 Wittig methylation and Shi epoxidation.

opportunity to study the outcome of the final bicyclization stage with both diastereomers of the diepoxide substrate, which was unfortunate since the C_{15} chiral center would not be present in the final product. However, the bigger problem proved to be the regioselectivity of the Shi epoxidation of triene **120**. In contrast to our good experience with the low reactivity of the acyclic 1,1-disubstituted alkene in our abudinol B synthesis, the difference in rates was not as great for triene **120**. Ultimately the best approach for generating enough diepoxide for the final cyclization studies was to quench the epoxidation reaction as soon as significant triepoxide was observed upon TLC visualization, even though some triene and both monoepoxides were also present in addition to the desired diepoxide **121**. After the diepoxide was separated, the recovered triene and monoepoxides were resubjected to Shi epoxidation conditions, with appropriate modifications for the stoichiometry of Oxone[®] and the base. After four cycles of this procedure, and protection of the alcohol of the combined fractions of diepoxide (to facilitate chromatographic removal of D-epoxone), a useful yield of diepoxide **122** was produced for exploring the final bicyclization.

The second bicyclization cascade from **122** worked better than the corresponding second cascade for abudinol, even though the carbocyclic ring

formed was now a seven-membered ring. This transformation was performed on sufficient scale to provide 0.47 mmol (250 mg) of the pentacyclic product. The only problem was that the pentacyclic product **123** was formed as a single *trisubstituted alkene* isomer, instead of the desired tetrasubstituted alkene of *ent*-**30**, “premuzitone.” Although alkene isomerization had not succeeded in our earlier work directed toward the synthesis of abudinol B, we now had no choice but to focus on the isomerization, after a few experiments demonstrated that changes in the bicyclization reaction conditions did not afford any trace of the desired tetrasubstituted alkene. Given some precedents on HI-catalyzed alkene isomerization [57], we elected to explore this as our first approach. The alcohols were protected as the diacetate **124**, in order to inductively deactivate the oxepane oxygens from protonation. Matt quickly discovered that addition of 0.6 equiv. of HI in benzene heated slightly below its boiling point (specifically, at 70 °C) gave near quantitative conversion to the tetrasubstituted alkene (**125**:**124** = 20:1). As the diacetates of both the trisubstituted alkene **124** and the tetrasubstituted alkene **125** were crystalline, their structures were confirmed by X-ray crystallography, confirming that all the stereochemical elements of compounds **124** and **125** were consistent with the enantiomer of the hypothetical pentacyclic precursor to muzitone (Figure 39).

4.3 Disappointment upon Arriving at the Purported Structure of Muzitone

At this stage, all that remained was oxidative cleavage of the tetrasubstituted alkene of *ent*-**30**. However, initial studies with ozonolysis were inconclusive. Matt was initially concerned that unprotected alcohols would undergo side reactions with ruthenium-catalyzed oxidative cleavage, and his first successful experiment was conducted with the diacetate **125**, which cleanly provided the desired diketone **126** (Figure 40). He then treated the crude diketone **126** with potassium carbonate in methanol, intending to cleave the acetate esters. Instead, he discovered that a transannular aldol reaction [58] had occurred more rapidly than acetate ester methanolysis, giving products judged as

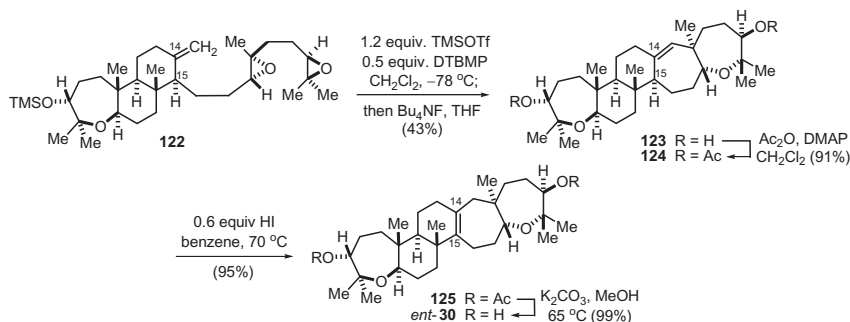


FIGURE 39 Bicyclization of **122** and isomerization of **123** to *ent*-**30**.

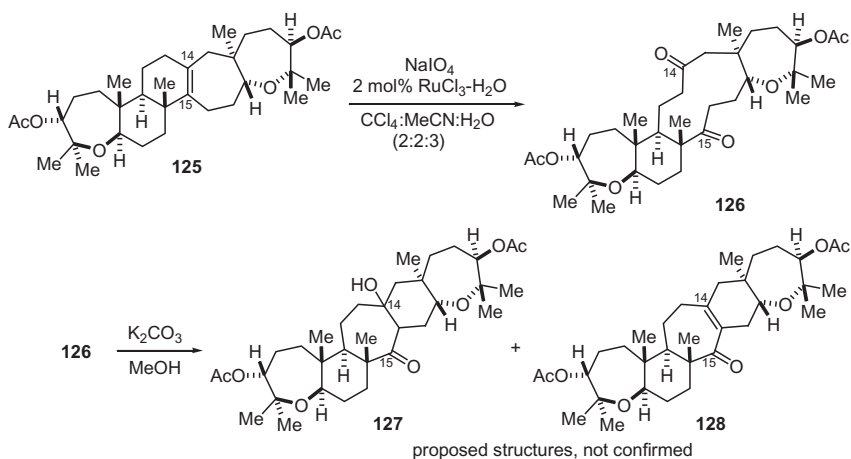


FIGURE 40 Oxidative cleavage of alkene followed by undesired transannular aldol.

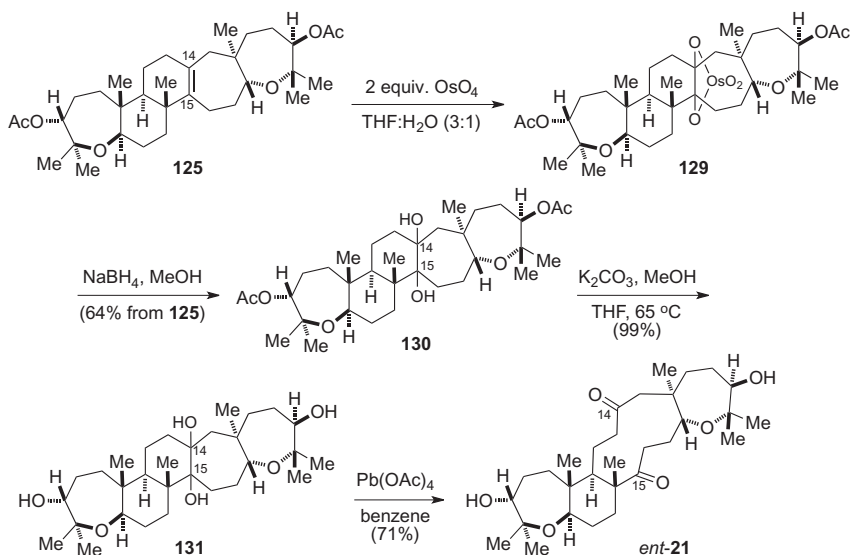


FIGURE 41 First synthesis of the purported structure of *ent*-muzitone (*ent*-**21**).

structures **127** and **128** (although the other aldol regioisomer could not be excluded).

Thus Matt elected to dissect the oxidative cleavage operation into separate mechanistic steps, namely dihydroxylation of the alkene, then basic methanolysis of the acetate esters, and finally periodate cleavage of the geminal diol at C₁₄ and C₁₅. In practice, the dihydroxylation of **125** required stoichiometric osmium tetroxide, as the stable osmate ester **129** was produced (Figure 41).

This osmate ester proved to be resistant to mild reductive methods including bisulfite and sulfite reduction, but sodium borohydride reduction [59] provided the desired diol **130**. The acetate esters were then removed by basic methanolysis in refluxing methanol/tetrahydrofuran, with the C₁₄–C₁₅ sigma bond scission as the final step. The reaction of tetraol **131** with sodium periodate was extremely slow, and after 2 days, only a trace of the diketone *ent*-**21** was obtained. However, the corresponding reaction with lead tetraacetate [60] was completed in less than a minute, providing us with the material that was expected to be *ent*-muzitone (*ent*-**21**).

Unfortunately, we observed significant differences in physical and spectroscopic characteristics between our synthetic product and the data reported for muzitone. For instance, our synthetic product was a white crystalline solid with a relatively high melting point of 210–213 °C, whereas naturally occurring muzitone was described as an oil [17]. Our spectroscopic data (compared not only with published data but also with a copy of the ¹H NMR spectrum of impure muzitone provided by Kashman) showed general similarities but also some key differences in the spectral data. After substantial additional experimentation, we found that the diol *ent*-**30** could be converted into the spectroscopically identical diketone *ent*-**21** more directly by ozonolysis followed by dimethyl sulfide reduction or by ruthenium-catalyzed oxidative cleavage [61], albeit in much lower yield than the multistep process described above (Figure 42).

Our confidence in the structural assignment of our synthetic material was bolstered by finding that the same diketone *ent*-**21** could be prepared by multiple different approaches from the pentacyclic alkene *ent*-**30**. By this time, the structure of the alkene precursors **124** and **125** had been authenticated by crystallography, confirming that we had not inadvertently prepared a different diastereomer. Examination of the structure showed no obvious mechanism for epimerization of the chiral centers in the final steps from **125** to *ent*-**21**. Matt prepared the bis-*p*-nitrobenzoate **132** (Figure 43) from his synthetic product, and after carefully growing crystals, compound **132** was subjected to X-ray crystallographic analysis. The structure initially was difficult to solve, but in the hands of our talented crystallographer, Dr. Kenneth Hardcastle, we conclusively determined that the structure of

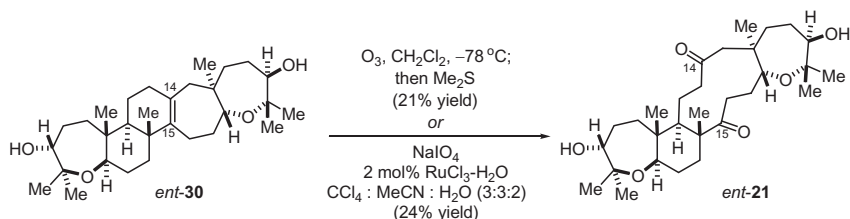


FIGURE 42 Preparation of *ent*-**21** by single-step oxidative cleavage of *ent*-**30**.

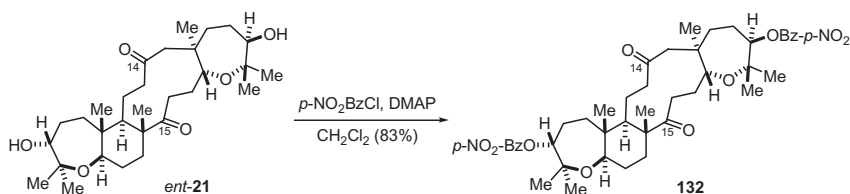


FIGURE 43 Preparation of bis-*para*-nitrobenzoate **132**.

our synthetic material was indeed identical to the expected structure of *ent*-muzitone [28]. Thus, muzitone must be added to the long list of natural product structures that were initially misassigned [62].

5. CONCLUSION: BIOSYNTHETIC CONSIDERATIONS IN THE PROPOSAL OF OTHER STRUCTURES FOR MUZITONE

In comparing the spectroscopic data for our synthetic compound *ent*-**21** with that tabulated by Kashman for the macrocyclic diketone dubbed muzitone [17], we focused on the four most deshielded hydrogens, and especially the C₂₂ hydrogen. In our synthetic material, this hydrogen appeared at 4.24 ppm (600 MHz, C₆D₆) and was a doublet of doublets with coupling constants of 2.4 and 6.0 Hz. In contrast, the Kashman laboratory reported a chemical shift of 3.88 ppm (500 MHz, C₆D₆) and coupling constants of 5.3 and 11.3 Hz. It is notable that Kashman's coupling constant data was similar to those observed in the structurally rigid pentacyclic alkene product: 3.49 ppm (400 MHz, CDCl₃) with coupling constants of 5.2 and 11.6 Hz. Nonetheless, the Kashman laboratory clearly isolated a diketone, as they reported δ 218.0, 207.0 in C₆D₆ (we observed δ 216.3, 211.6 in C₆D₆ for our synthetic compound). Moreover, Kashman's HMBC studies indicated that each ketone carbon is connected to an ethano group (as in structure **21**).

As neither an authentic sample of muzitone nor high-quality copies of the 2D NMR spectra are available from the Kashman laboratory, our proposal for an alternative structure is purely speculative, but we take the liberty here of sharing a few ideas. Muzitone must be an isomer of the compound *ent*-**21** that we have synthesized, with molecular formula C₃₀H₅₀O₆. Although we cannot rule out the possibility of a simple diastereomer of **21** (with the corresponding implications for the stereochemistry of the probable tetraepoxide biogenetic precursor or the stereoselectivity of the biogenetic cyclization processes), other possible structures that we have considered include **133**, shown in two different orientations (Figure 44). Although this structure does not perfectly fit the published HMBC data, which played an important role in Kashman's assignment of the ketone positions, those with experience in interpreting 2D NMR data on compounds with many overlapping resonances in the ¹H and

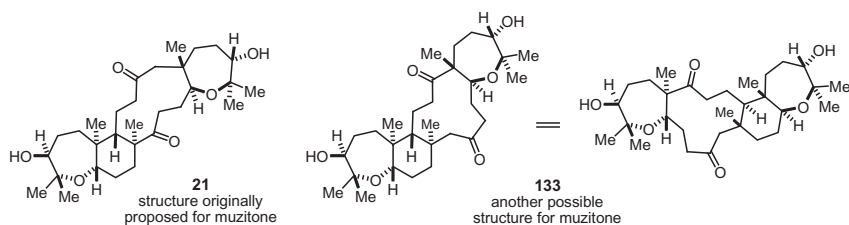


FIGURE 44 An alternative structure for muzitone.

^{13}C spectra will appreciate the difficulty of correctly assigning all resonances in such structures, especially for compounds such as abudinol B and muzitone bearing considerable complexity yet sharing two identical substructures, namely the hydroxytrimethyloxepane rings. Erroneous assignments of overlapping carbon and/or hydrogen resonances would invalidate the interpretation of some of the HMBC data.

One attractive feature of the hypothetical structure **133** is that it requires only a slight modification of the Norte hypothesis for the biosynthesis of abudinols, as depicted in Figure 45. Specifically, the abudinols probably arise from initial tricyclization of two epoxides and two alkenes to convert squalene tetraepoxide (**34**) into a tricyclic intermediate **35**, whereas a pathway in which the cyclization cascade is terminated after the participation of only one alkene would provide the bicyclic intermediate **134**. At this stage, a cyclization cascade of the remaining epoxides with both dienes of **134** could give an all-fused pentacyclic compound **135**, which upon oxidative cleavage might afford an 11-membered diketone **133**.

ACKNOWLEDGMENTS

This work was possible due to the creativity, diligence, and careful experimentation on the part of a talented group of Emory University graduate students and postdoctoral associates. As described herein, the project area of the abudinols and muzitone was proposed by coauthor Dr. Jason C. Valentine, and following his preliminary work on biomimetic oxo- and carbacyclizations, coauthors Drs. Rongbiao Tong and Matthew A. Boone completed total syntheses of the triterpene structures that were the ultimate focus of this account. We also thank Ms. Xia Wang, Dr. Fernando Bravo, and Dr. Xudong Wei for establishing our work in the area of *endo*-selective polyepoxide cyclizations, which set the stage for the subsequent total synthesis of the triterpene structures. We are also deeply indebted to Dr. Kenneth I. Hardcastle for several X-ray crystal structures obtained in support of this project. We acknowledge Prof. Yoel Kashman (Tel Aviv University) for several informative e-mail exchanges and for sharing copies of NMR spectral data from his laboratory. This research was supported by the National Science Foundation, most recently in grant CHE-0516793, with additional financial support from the Laney Graduate School and the Department of Chemistry at Emory University.

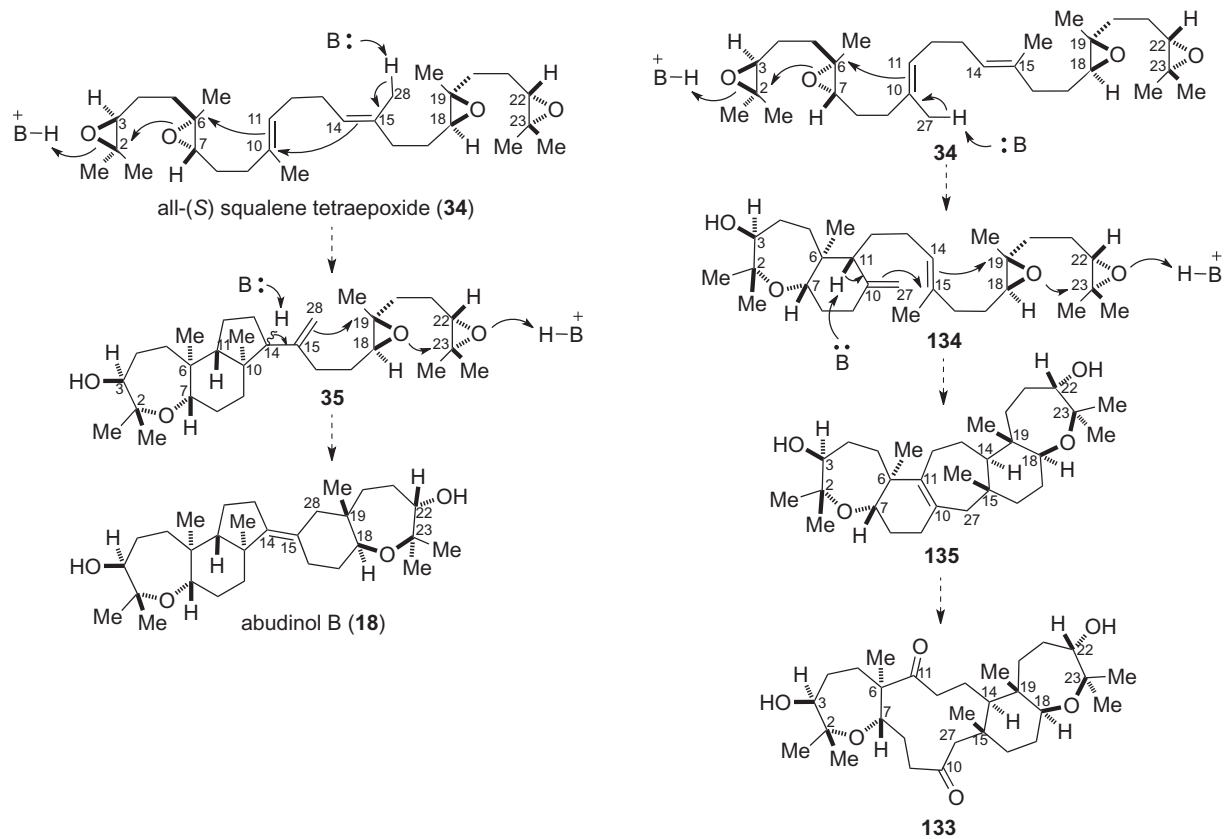


FIGURE 45 Comparison of biosynthetic pathways for abudinol B compared to an isomeric all-fused compound 135.

REFERENCES

- [1] (a) W.S. Johnson, C. Newton, S.D. Lindell, *Tetrahedron Lett.* 27 (1986) 6027–6030; (b) W.S. Johnson, S.J. Telfer, S. Cheng, U. Schubert, *J. Am. Chem. Soc.* 109 (1987) 2517–2518; (c) W.S. Johnson, S.D. Lindell, J. Steele, *J. Am. Chem. Soc.* 109 (1987) 5852–5853.
- [2] W.C. Still, A.G. Romero, *J. Am. Chem. Soc.* 108 (1986) 2105–2106.
- [3] S.L. Schreiber, T. Sammakia, B. Hulin, G. Schulte, *J. Am. Chem. Soc.* 108 (1986) 2106–2108.
- [4] (a) M.S. Lee, G.W. Qin, K. Nakanishi, M.G. Zagorski, *J. Am. Chem. Soc.* 111 (1989) 6234–6241; (b) M.S. Lee, D.J. Repeta, K. Nakanishi, M.G. Zagorski, *J. Am. Chem. Soc.* 108 (1986) 7855–7856.
- [5] (a) K.C. Nicolaou, C.V.C. Prasad, P.K. Somers, C.K. Hwang, *J. Am. Chem. Soc.* 111 (1989) 5335–5340; (b) K.C. Nicolaou, C.V.C. Prasad, P.K. Somers, C.K. Hwang, *J. Am. Chem. Soc.* 111 (1989) 5330–5334.
- [6] F.E. McDonald, M. Harmata (Ed.), *Strategies and Tactics in Organic Synthesis*, vol. 5, Elsevier, Amsterdam, 2004, pp. 391–415.
- [7] (a) T.B. Towne, F.E. McDonald, *J. Am. Chem. Soc.* 119 (1997) 6022–6028; (b) F.E. McDonald, C.C. Schultz, *Tetrahedron* 53 (1997) 16435–16448; (c) F.E. McDonald, T.B. Towne, C.C. Schultz, *Pure Appl. Chem.* 70 (1998) 355–358.
- [8] F.E. McDonald, P. Vadapally, *Tetrahedron Lett.* 40 (1999) 2235–2238.
- [9] (a) Y. Tu, Z.-X. Wang, Y. Shi, *J. Am. Chem. Soc.* 118 (1996) 9806–9807; (b) Z.X. Wang, Y. Tu, M. Frohn, J.R. Zhang, Y. Shi, *J. Am. Chem. Soc.* 119 (1997) 11224–11235; (c) Y. Shi, *Acc. Chem. Res.* 37 (2004) 488–496; (d) O.A. Wong, Y. Shi, *Chem. Rev.* 108 (2008) 3958–3987.
- [10] (a) F.E. McDonald, X. Wang, B. Do, K.I. Hardcastle, *Org. Lett.* 2 (2000) 2917–2919; (b) Novel *Endo*-Oxacyclizations of Polyepoxides Activated by Lewis Acids, (2000) M.S. thesis, X. Wang, Emory University.
- [11] Z.-X. Wang, Y. Shi, *J. Org. Chem.* 63 (1998) 3099–3104.
- [12] (a) H. Kigoshi, M. Ojika, Y. Shizuri, H. Niwa, K. Yamada, *Tetrahedron Lett.* 23 (1982) 5413; (b) E.J. Corey, D.-C. Chan, *Tetrahedron Lett.* 29 (1988) 3171–3174; (c) Y. Gao, R.M. Hanson, J.M. Klunder, S.Y. Ko, H. Masamune, K.B. Sharpless, *J. Am. Chem. Soc.* 109 (1987) 5765.
- [13] F.E. McDonald, F. Bravo, X. Wang, X. Wei, M. Toganoh, J.R. Rodríguez, B. Do, W.A. Neiwert, K.I. Hardcastle, *J. Org. Chem.* 67 (2002) 2515–2523.
- [14] (a) F. Bravo, F.E. McDonald, W.A. Neiwert, B. Do, K.I. Hardcastle, *Org. Lett.* 5 (2003) 2123–2126; (b) F. Bravo, F.E. McDonald, W.A. Neiwert, K.I. Hardcastle, *Org. Lett.* 6 (2004) 4487–4489; (c) J.C. Valentine, F.E. McDonald, W.A. Neiwert, K.I. Hardcastle, *J. Am. Chem. Soc.* 127 (2005) 4586–4587; (d) J.C. Valentine, F.E. McDonald, Synlett (2006) 1816–1828; (e) F.E. McDonald, R. Tong, J.C. Valentine, F. Bravo, *Pure Appl. Chem.* 79 (2007) 281–291.
- [15] (a) U. Shmueli, S. Carmely, A. Groweiss, Y. Kashman, *Tetrahedron Lett.* 22 (1981) 709–712; (b) I. Ohtani, T. Kusumi, Y. Kashman, H. Kakisawa, *J. Org. Chem.* 56 (1991) 1296–1298.
- [16] A. Rudi, Z. Stein, I. Goldberg, T. Yosief, Y. Kashman, M. Schleyer, *Tetrahedron Lett.* 39 (1998) 1445–1448.
- [17] (a) A. Rudi, T. Yosief, M. Schleyer, Y. Kashman, *Tetrahedron* 55 (1999) 5555–5566; (b) This account uses a different numbering scheme for muzitone from that published in Ref. 17a, for consistency in comparing muzitone with abudinolins and the likely squalene-derived precursors.

- [18] J.J. Fernández, M.L. Souto, M. Norte, *Nat. Prod. Rep.* 17 (2000) 235–246.
- [19] R.A. Yoder, J.N. Johnston, *Chem. Rev.* 105 (2005) 4730–4756.
- [20] B.H. Lipshutz, D.F. Harvey, *Synth. Commun.* 12 (1982) 267–277.
- [21] J.R. Parikh, W.E. Doering, *J. Am. Chem. Soc.* 89 (1967) 5505–5507.
- [22] (a) T. Nakata, G. Schmid, B. Vranesic, M. Okigawa, T. Smith-Palmer, Y. Kishi, *J. Am. Chem. Soc.* 100 (1978) 2933–2935; (b) M. Hashimoto, H. Harigaya, M. Yanagiya, H. Shirahama, *J. Org. Chem.* 56 (1991) 2299–2311; (c) H. Makabe, Y. Hattori, A. Tanaka, T. Oritani, *Org. Lett.* 4 (2002) 1083–1085.
- [23] Part 1. Biomimetic Synthesis of trans, syn, trans-Fused Polyoxepanes: Remarkable Substituent Effects on the endo-Regioselective Oxacyclization of Polyepoxides. Part 2. Carbon Terminating Nucleophiles in Combination with the Tandem Oxacyclization of Polyepoxides: Progress Toward the Total Synthesis of Abudinol B. Ph.D. thesis, J.C. Valentine, Emory University, 2006.
- [24] Chapter 1. Biomimetic Total Synthesis of *ent*-Durgamone, *ent*-Nakorone and *ent*-Abudinol B. Chapter 2. Biomimetic Synthesis of Fused Polypyranes. Ph.D. thesis, R. Tong, Emory University, 2008.
- [25] (a) E.J. Corey, M. Sodeoka, *Tetrahedron Lett.* 32 (1991) 7005–7008; (b) E.J. Corey, G. Lin, L.S. Lin, *J. Am. Chem. Soc.* 119 (1997) 9927–9928.
- [26] R. Tong, J.C. Valentine, F.E. McDonald, R. Cao, X. Fang, K.I. Hardcastle, *J. Am. Chem. Soc.* 129 (2007) 1050–1051.
- [27] (a) P.V. Fish, W.S. Johnson, *J. Org. Chem.* 59 (1994) 2324–2335; (b) P.V. Fish, *Tetrahedron Lett.* 35 (1994) 7181–7184.
- [28] M.A. Boone, R. Tong, F.E. McDonald, S. Lense, R. Cao, K.I. Hardcastle, *J. Am. Chem. Soc.* 132 (2010) 5300–5308.
- [29] E.J. Corey, B.E. Roberts, *Tetrahedron Lett.* 38 (1997) 8921–8924.
- [30] (a) T. Nakata, S. Nomura, H. Matsukura, *Tetrahedron Lett.* 37 (1996) 213–216; (b) N. Hori, K. Nagasawa, T. Shimizu, T. Nakata, *Tetrahedron Lett.* 40 (1999) 2145–2148; (c) N. Hayashi, K. Fujiwara, A. Murai, *Synlett* (1997) 793–794.
- [31] M.-X. Zhao, Y. Shi, *J. Org. Chem.* 71 (2006) 5377–5379.
- [32] (a) R. Schmid, P.L. Huesmann, W.S. Johnson, *J. Am. Chem. Soc.* 102 (1980) 5122–5123; (b) W.S. Johnson, M.S. Plummer, S.P. Reddy, W.R. Bartlett, *J. Am. Chem. Soc.* 115 (1993) 515–521.
- [33] (a) J. Porret, B. Randrianoelina, L. Miginiac, *Tetrahedron Lett.* 25 (1984) 651–654; (b) A.G. Angoh, D.J.L. Clive, *J. Chem. Soc., Chem. Commun.* (1984) 534–536; (c) H. Mastalerz, *J. Org. Chem.* 49 (1984) 4092–4094.
- [34] A.N. Wein, R. Tong, F.E. McDonald, *Org. Synth.* 88 (2011) 296–308.
- [35] (a) P.A. Grieco, Y. Masaki, *J. Org. Chem.* 39 (1974) 2135–2136; (b) T. Murakami, H. Furusawa, *Synthesis* (2002) 479–482.
- [36] (a) R.O. Hutchins, K. Learn, *J. Org. Chem.* 47 (1982) 4380–4382; (b) M. Mohri, H. Kinoshita, K. Inomata, H. Kotake, *Chem. Lett.* (1985) 451–454.
- [37] J.E. McMurry, *Chem. Rev.* 89 (1989) 1513–1524.
- [38] T. Takeda, R. Sasaki, T. Fujiwara, *J. Org. Chem.* 63 (1998) 7286–7288.
- [39] O.P. Törmäkängas, R.J. Toivola, E.K. Karvinen, A.M.P. Koskinen, *Tetrahedron* 58 (2002) 2175–2181.
- [40] (a) D.H.R. Barton, B.J. Willis, *J. Chem. Soc., Chem. Commun.* (1970) 1225–1226; (b) D.H.R. Barton, E.H. Smith, B.J. Willis, *J. Chem. Soc., Chem. Commun.* (1970) 1226; (c) J. Buter, S. Wassenaar, R.M. Kellogg, *J. Org. Chem.* 37 (1972) 4045–4060; (d) F. J. Hoogesteger, R.W.A. Havenith, J.W. Zwikker, L.W. Jenneskens, H. Kooijman,

- N. Veldman, A.L. Spek, *J. Org. Chem.* 60 (1995) 4375–4384; (e) M.K.J. ter Wiel, J. Vicario, S.G. Davey, A. Meetsma, B.L. Feringa, *Org. Biomol. Chem.* 3 (2005) 28–30.
- [41] (a) T. Oh-e, N. Miyaoura, A. Suzuki, *Synlett* (1990) 221–223; (b) N. Miyaoura, A. Suzuki, *Chem. Rev.* 95 (1995) 2457–2483.
- [42] J. Takagi, K. Takahashi, T. Ishiyama, N. Miyaoura, *J. Am. Chem. Soc.* 124 (2002) 8001–8006.
- [43] M. Sodeoka, M. Shibasaki, *Synthesis* (1993) 643–658.
- [44] A. Takahashi, Y. Kirio, M. Sodeoka, H. Sasai, M. Shibasaki, *J. Am. Chem. Soc.* 111 (1989) 643–647.
- [45] (a) A.J. Hubert, H. Reimlinger, *Synthesis* (1970) 405–430; (b) C.A. Brown, *J. Chem. Soc., Chem. Commun.* (1975) 222–223.
- [46] G.A. Mirafzal, J. Liu, N.L. Bauld, *J. Am. Chem. Soc.* 115 (1993) 6072–6077.
- [47] (a) J.P. Vigneron, M. Dhaenens, A. Horeau, *Tetrahedron* 29 (1973) 1055–1059; (b) S.L. Schreiber, T.S. Schreiber, D.B. Smith, *J. Am. Chem. Soc.* 109 (1987) 1525–1529; (c) I. Fleming, S.K. Ghosh, *J. Chem. Soc., Chem. Commun.* (1994) 99–100.
- [48] J.M. Seco, E. Quiñó, R. Riguera, *Chem. Rev.* 104 (2004) 17–118.
- [49] Chapter 1. Part 1: Novel Synthesis and Biological Evaluation of 1,5-Linked D-Mannoseptanosides. Part 2: Synthesis of D-Glucoseptanosides. Chapter 2. Biomimetic Total Synthesis of the Proposed Structure of *ent*-Muzitane. Ph.D. thesis, M. A. Boone, Emory University, 2009.
- [50] R.B. Tong, M.A. Boone, F.E. McDonald, *J. Org. Chem.* 74 (2009) 8407–8409.
- [51] H.J. Reich, R.E. Olson, M.C. Clark, *J. Am. Chem. Soc.* 102 (1980) 1423–1424.
- [52] J. Enda, I. Kuwajima, *J. Am. Chem. Soc.* 107 (1985) 5495–5501.
- [53] (a) E.J. Corey, G. Luo, L.S. Lin, *Angew. Chem. Int. Ed.* 37 (1998) 1126–1128; (b) J. Zhang, E.J. Corey, *Org. Lett.* 3 (2001) 3215–3216; (c) Y. Mi, J.V. Schreiber, E.J. Corey, *J. Am. Chem. Soc.* 124 (2002) 11290–11291.
- [54] J.S. Nowick, R.L. Danheiser, *Tetrahedron* 44 (1988) 4113–4134.
- [55] R.B. Tong, F.E. McDonald, *Angew. Chem. Int. Ed.* 47 (2008) 4377–4379.
- [56] B.L. van Duuren, F.L. Schmitt, *J. Org. Chem.* 25 (1960) 1761.
- [57] I.S. Marcos, A.B. Pedrero, M.J. Sexmero, D. Diez, N. García, M.A. Escola, P. Basabe, A. Conde, R.F. Moro, J.G. Urones, *Synthesis* (2005) 3301–3310.
- [58] M.E. Herr, G.S. Fonken, *J. Org. Chem.* 32 (1967) 4065–4066.
- [59] E. Herranz, K.B. Sharpless, *Org. Synth. Coll. VII* (1990) 375–381.
- [60] F.J. Wolf, J. Weijlard, *Org. Synth. Coll. IV* (1963) 124–125.
- [61] (a) P.H.J. Carlsen, T. Katsuki, V.S. Martin, K.B. Sharpless, *J. Org. Chem.* 46 (1981) 3936–3938; (b) R. Pappo, D.S. Allen, R.U. Lemieux, W.S. Johnson, *J. Org. Chem.* 21 (1956) 478–479.
- [62] K.C. Nicolaou, S.A. Snyder, *Angew. Chem. Int. Ed.* 44 (2005) 1012–1044.

In Pursuit of an Elusive Target: Our Kendomycin Story

Harry J. Martin^{*}, Thomas Magauer^{*,†} and Johann Mulzer^{*}

^{*}Institute of Organic Chemistry, University of Vienna, Vienna, Austria, [†]Department of Chemistry and Chemical Biology, Harvard University, Cambridge, Massachusetts, USA

Chapter Outline

1. Introduction	261	2.4. C19/C20 Disconnection Approach (RCM)	280
2. Synthetic Approaches to Kendomycin	264	2.5. C10/C11 Disconnection Approach (RCM)	282
2.1. C13/C14 Disconnection Approaches	264	2.6. C4a/C5 Disconnection Approach (Photo-Fries Reaction)	285
2.2. Model Studies for the Synthesis of a Kendomycin-like Quinone Methide	277	2.7. Completion of the Total Synthesis	286
2.3. C9/C10 Disconnection Approach (RCM)	278	3. Summary	287

1. INTRODUCTION

Organic compounds derived from nature have been an abundant source of drugs and drug leads and have provided a rich array of interesting synthetic targets. Among various selection criteria, novel and complex structural features combined with interesting biological activities might be the most important ones to promote a molecule to a target for natural product synthesis. Kendomycin (**1**), a novel *Streptomyces* metabolite, which was presented at a meeting in 1999, meets all these requirements and thus was selected as a new target for our research 1 year later. The compound was first described as an endothelin receptor antagonist [1] and shortly after as a molecule with anti-osteoporotic properties [2]. In the course of its reisolation from *Streptomyces violaceoruber* by Bode and Zeeck, it was found that **1** shows strong antibiotic activities against a variety of bacteria, including methicillin-resistant *Staphylococcus aureus*

strains [3,4]. Additionally, kendomycin exhibits strong cytotoxicity against multiple human tumor cell lines [3], most likely through proteasome inhibition or Bcl-xl inhibition [5]. Structurally, **1** features an aliphatic *ansa*-chain with a densely substituted tetrahydropyran ring attached to a quinone methide chromophore (Figure 1). Thus, **1** is one of the very few *ansa*-carbon natural products that have been isolated to date. Likewise, the quinone methide structure, which can be considered a 1,6-oxidation product of the corresponding benzofuran, is a unique feature, so far unprecedented in natural product chemistry. The relative and absolute configurations of the nine stereogenic centers were confirmed by both single crystal X-ray diffraction and advanced Mosher's ester analysis [3].

The biosynthesis of kendomycin (Figure 2) was first explored by Bode and Zeeck and was later elaborated by means of gene expression experiments by

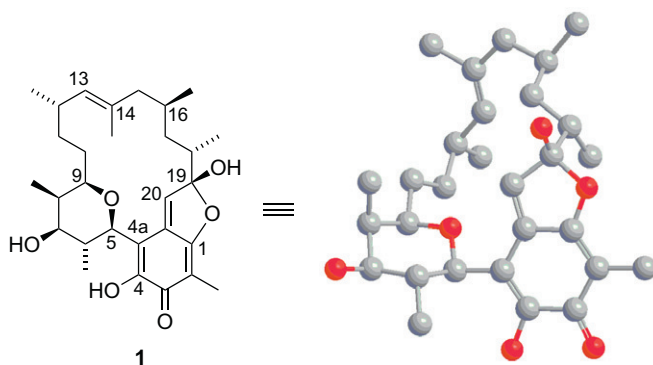


FIGURE 1 2D- and 3D (X-ray)-structure of kendomycin (**1**).

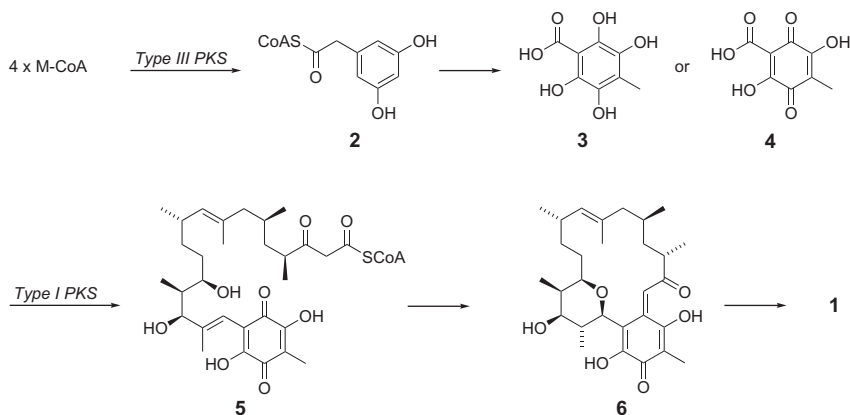


FIGURE 2 Biosynthesis of kendomycin (**1**) according to Zeeck and Müller.

Müller [3,4,6]. It was suggested that initially arene **2** is formed under the mediation of a type III polyketide synthase (PKS). Oxidation, methylation, and a degradation sequence then leads to benzoic acid **3** or a quinoid analog **4** as an unusual starter unit that is loaded onto the type I PKS complex to furnish keto ester **5**. After pyran ring closure, a previously unknown termination of the type I PKS first furnishes macrocycle **6** via decarboxylation and subsequently **1** by hemiketal formation.

The compound has attracted broad interest both from synthetic and medicinal chemists. Over a period of 10 years, 10 research groups worldwide have documented synthetic efforts towards **1**, and six total syntheses have been reported [7,8]. Remarkably, most syntheses roughly follow the biogenetic sequence of events. This means starting from an aromatic precursor similar to **3**, to which polyketide *ansa*-fragments are attached. Ring closure is then mostly achieved somewhere in the *ansa*-chain to form a macrocyclic intermediate. It seems obvious that the formation of the quinone methide chromophore should be deferred to the end of the synthesis, envisaging the oxidation of a benzyl ketone or a corresponding benzofuran (Figure 3). Thus, either the oxidation of polyphenol **7** to **8** followed by lactol formation, or the oxidation of benzofuran **9** to *ortho*-benzoquinone **10** followed by 1,6-addition of water have been used in the endgame.

During the synthesis of macrocyclic compounds, the macrocyclization is usually one of the final steps. From a retrosynthetic point of view, this means that the planned cyclization method and particularly the cyclization site, largely define the synthetic strategy. Macrocyclization at C4a/C5 and concomitant tetrahydropyran formation have been achieved by a macro-*C*-glycosidation during the first total synthesis of **1** by Lee (Figure 4) [9]. Later, an intramolecular Prins reaction was used by Rychnovsky to perform macrocyclization

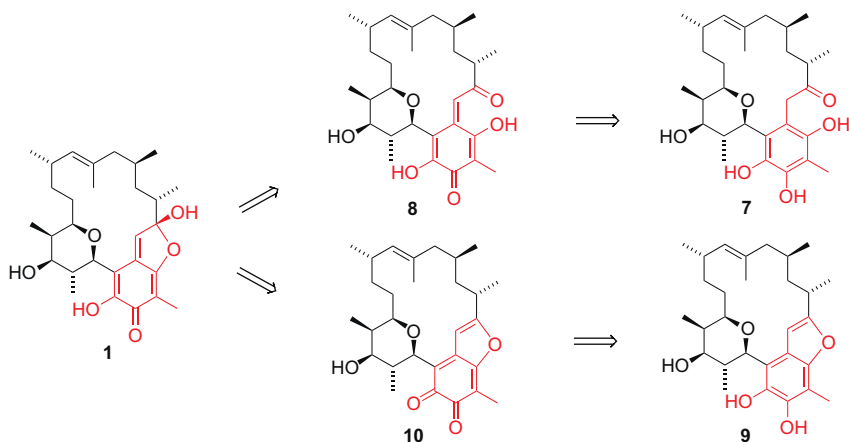


FIGURE 3 Oxidative endgame strategies for the synthesis of kendomycin (**1**).

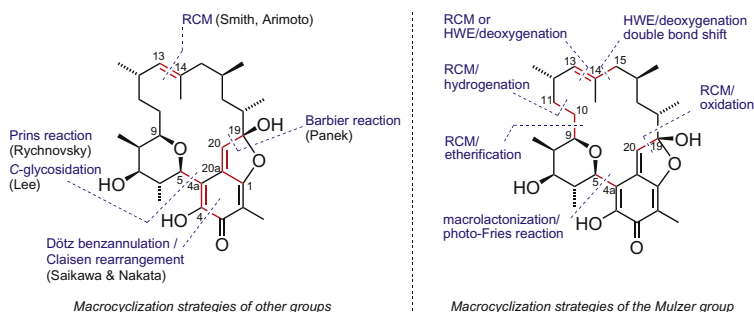


FIGURE 4 Macrocyclization strategies for the synthesis of kendomycin.

and tetrahydropyran formation at C4a/C5 [10,11]. Ring-closing metathesis (RCM) at C13/C14 was achieved by the groups of Smith [12,13] and Arimoto [14], albeit the undesired *Z*-olefin was formed and had to be inverted. Panek's total synthesis employed the macrocyclization at C19/C20 using a SmI_2 -Barbier reaction [15]. Recently, a completely different approach was described by Saikawa and Nakata using Dötz benzannulation and a macrocyclic Claisen rearrangement for the construction of the *ansa*-skeleton [8]. During our work, macrocyclizations were attempted at six different sites (Figure 4), predominantly RCM reactions at C9/C10, C10/C11, C13/C14, and C19/C20. Horner–Wadsworth–Emmons (HWE) cyclizations were attempted at C13/C14 and C14/C15, while an unusual macrolactonization/photo-Fries approach has been applied at C4a/C5. Largely in chronological order, the discussion below will present our different synthetic approaches to kendomycin and advanced intermediates thereof.

2. SYNTHETIC APPROACHES TO KENDOMYCIN

2.1 C13/C14 Disconnection Approaches

The initial synthetic plan (Figure 5) was based on a RCM of diene **11**, which was to be assembled by a Heck reaction between alkene **12** and aryl bromide **14**, or an epoxide-opening reaction with oxirane **13**. The tetrahydropyran ring was planned to be formed by an intramolecular hetero-Michael addition of enone **15**, which could be derived from a HWE olefination of aldehyde **16** and β -keto phosphonate **17**.

2.1.1 Synthesis of the Tetrahydropyran-Aryl Fragment

Our first synthetic endeavor focused on the construction of a left-hand fragment (C5–C13), which involved the installation of the densely substituted tetrahydropyran ring next to the fully substituted benzene [16]. The synthesis started from dimethoxytoluene (**18**), which was converted into ethyl ketone

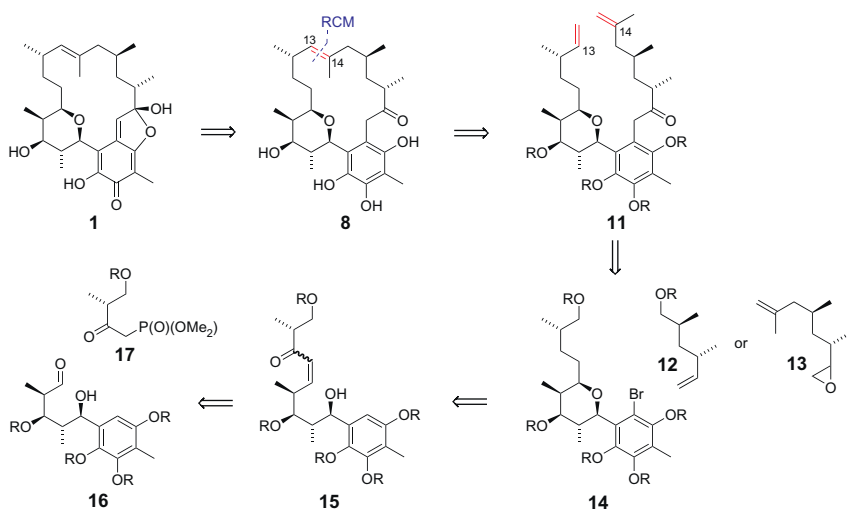


FIGURE 5 Initial retrosynthetic considerations for the C13/C14 RCM approach. R = H or suitable protecting group.

19 in a three-step sequence including Friedel–Crafts acylation, Baeyer–Villiger oxidation and *ortho*-Fries rearrangement (Figure 6). Subsequent *O*-methylation and *syn*-selective aldol addition with **20** afforded aldol **21**, which was converted to acetonide **22** via 1,3-*anti*-selective reduction, diol protection and oxidative removal of the PMB protecting group. Oxidation of **22** and subsequent LiOH-promoted HWE reaction with keto phosphonate **17** gave enone **15** which, after selective acetonide deprotection, spontaneously underwent an efficient intramolecular conjugate addition to form tetrahydropyran **23**. Subsequent carbonyl reduction via a tosylhydrazone then afforded tetrahydropyran **24**.

NMR analysis of compounds **23** and **14** (derived via a deoxygenation–desilylation–bromination sequence) revealed an important and hitherto unknown feature of this type of *C*-aryl glycoside. Both of them showed broadened proton signals for 5-H and 6-H, while carbon signals of C20a, C5, and C6 were missing. This was attributed to restricted sp^2 – sp^3 rotation around the C4a–C5 σ -bond and was confirmed with a temperature dependent ^1H -NMR study of **23**, revealing a second set of proton signals at lower temperatures. Below -10°C , the signal of the benzylic proton sharpened to a doublet with a typical coupling constant ($J=10.7$) for *trans*-diaxial J^3 -coupling in chair-like conformations. Due to distinct NOE interactions at -40°C , it was concluded that compound **23** exists as an equilibrium mixture of two individual rotamers **23a** and **23b** (93:7) (Figure 7). A considerably increased rotation barrier was observed when the arene hydrogen was replaced with bromine (**14**). In this case, ^1H -NMR signals of **14** did not vary with

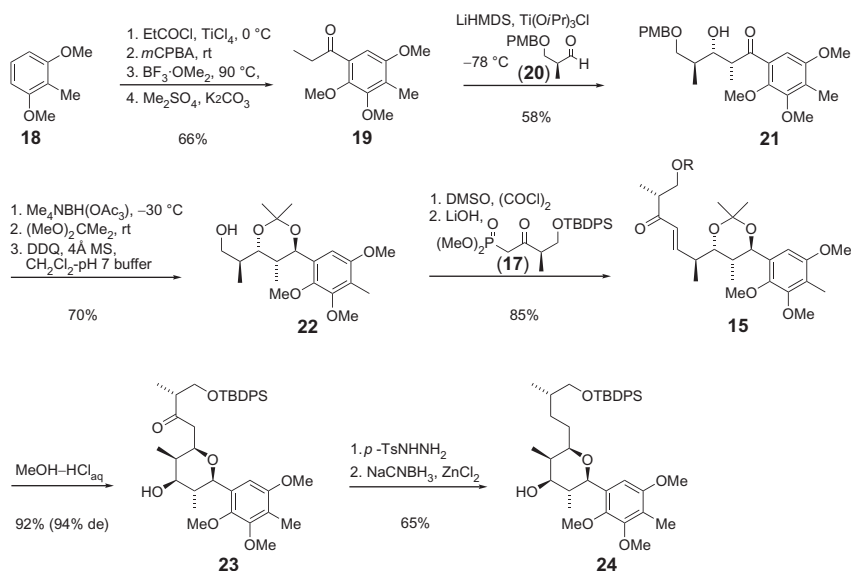


FIGURE 6 Synthesis of tetrahydropyran **24** via conjugate addition. *m*CPBA, *meta*-chloroperoxybenzoic acid; LiHMDS, Lithium bis(trimethylsilyl)amide; PMB, *p*-methoxybenzyl; DDQ, 2,3-dichloro-5,6-dicyanobenzoquinone; TBDPS, *tert*-butyldiphenylsilyl; *p*-Ts, *para*-toluenesulfonyl.

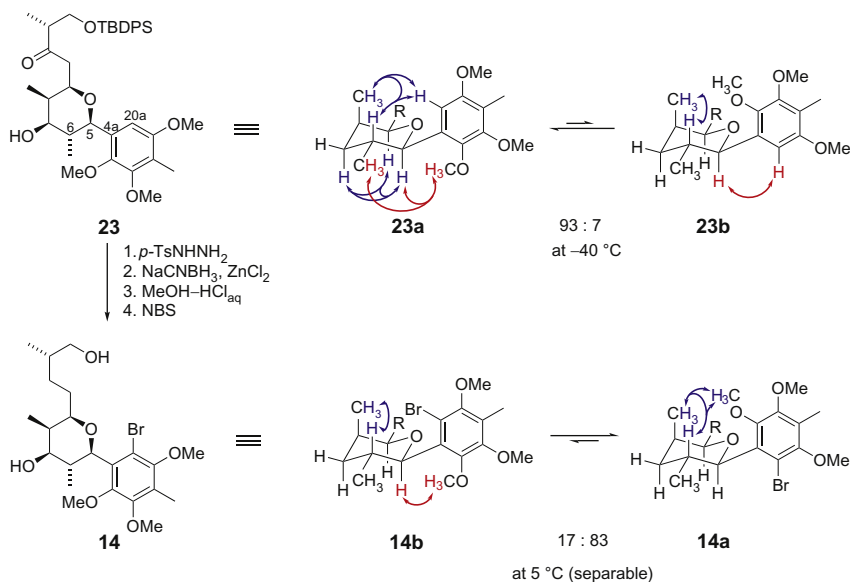


FIGURE 7 Structures and dynamic phenomena of tetrahydropyran-aryl compounds **23** and **14**. \leftrightarrow , NOE interactions.

temperature (up to 100 °C) and bromide **14** exists as a mixture of two separable atropisomers **14a** and **14b** (5:1). Although sp^2 – sp^3 hindered rotation in THP-aryl systems is known [17,18], to the best of our knowledge this was the first example of an aryl-*C*-glycoside atropisomerism. At that time, we also concluded that these dynamic phenomena might influence the reactivity at C20a as well as the reactive rotamer conformations in a later macrocyclization.

Despite the valuable insights into the dynamics of the synthesized THP-aryl compounds, there were also some drawbacks to this first approach. In particular, the number of synthetic steps and the low diastereoselectivity in the aldol step did not meet the high requirements of modern total synthesis. Thus, we adopted an alternative approach that included a more stereocontrolled and shorter synthesis of the tetrahydropyran moiety [19]. The new synthesis started from the known ester **25**, which after bromination, ester hydrolysis and *O*-methylation, gave aryl bromide **26** (Figure 8). Formylation at C4a afforded aldehyde **27**, which was reacted with the (*E*)-enol borinate derived from Evans' β -keto imide **28** to the *anti*-aldol adduct **29** almost quantitatively with high diastereoselectivity (de > 96%) [20]. Subsequent *anti*-selective reduction with $Me_4NBH(OAc)_3$, treatment with a catalytic amount of DBU and *in situ* protection with TPSCl furnished lactone **30**. The introduction of a simplified aliphatic chain was achieved via addition of allylmagnesium bromide to **30** to form the corresponding lactol, which was reduced to tetrahydropyran **31** with Et_3SiH in the presence of $SnCl_4$.

2.1.2 Attachment of the Right-Hand ansa-Chain

After we had established the two different approaches to the THP-arene moiety, we turned our attention towards the attachment of an aliphatic side chain (Figure 9) [21,22]. In our first attempts, bromide **32**, derived from TBS protection of alcohol **24**, was reacted either with alkene **33** in a Heck reaction or, after metalation, with epoxide **34** through a ring-opening reaction.

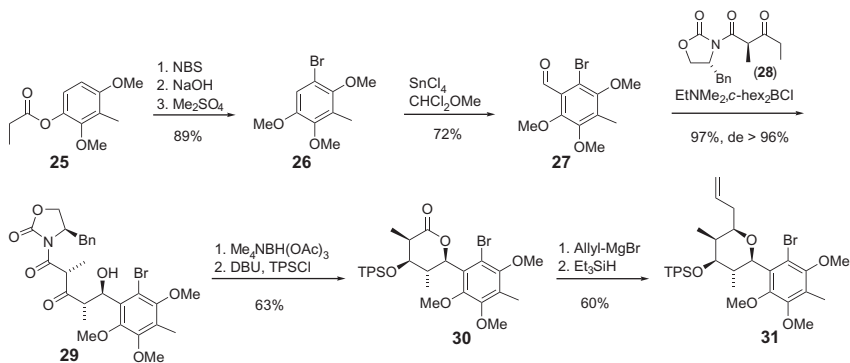


FIGURE 8 Modified approach to the aryl-tetrahydropyranyl moiety. NBS, *N*-bromosuccinimide; TPS, triphenylsilyl; DBU, 1,8-diaza-bicyclo-[5.4.0]-undec-7-ene.

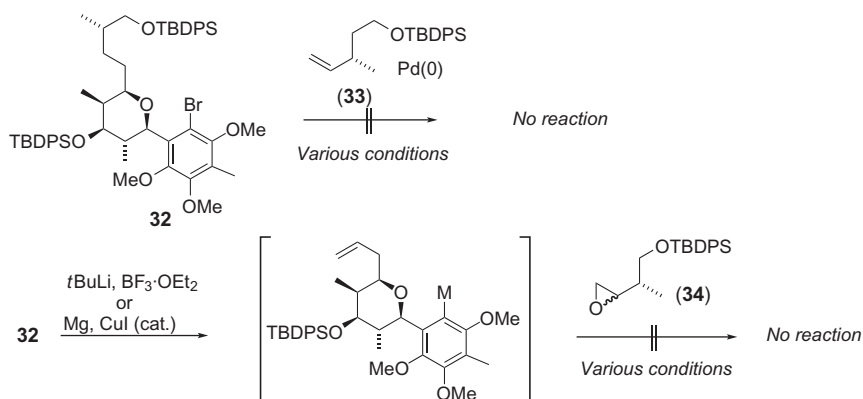


FIGURE 9 Unsuccessful attempts to attach the right-hand *ansa*-chain.

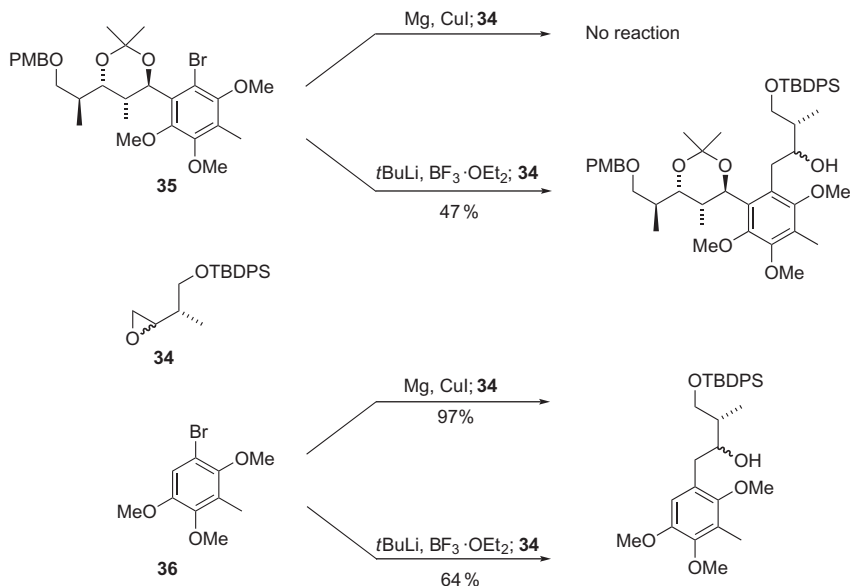


FIGURE 10 Attachment of the right-hand *ansa*-chain by epoxide-opening reactions.

Unfortunately, both reactions failed, probably due to steric hindrance or the previously discussed dynamic effects of the arene-THP moiety.

Next, we investigated the epoxide-opening reaction with organometallic intermediates derived from aryl bromide **35** (Figure 10). Again, no product was obtained using Grignard reaction conditions. In contrast, the reaction was successful (with moderate yield) when $t\text{BuLi}$ was used for halogen-metal exchange. As we assumed that the *ortho*-benzylic oxygen could be problematic for the formation of the Grignard reagent, we used the simpler aryl

bromide **36** to avoid those difficulties. To our delight, epoxide ring-opening could be achieved with both metalation methods and remarkably, the Grignard compound was now the more efficient reagent and led to nearly quantitative conversion.

2.1.3 Modified C13/C14 Disconnection Approach

As the presence of the tetrahydropyran ring turned out to be detrimental to the introduction of the second carbon chain, we decided to reverse the order of the coupling reactions (Figure 11) [21,22]. Thus, the right hand fragment **37** should be attached first by an epoxide-opening reaction with arene **38** at the angular position (C20a). Then the second angular position (C4a) was to be reacted as a nucleophile with lactone **39**, aldehyde **40** or another suitable carbonyl electrophile. Finally, it was planned to establish the tetrahydropyran ring by either lactol reduction or nucleophilic substitution at C5 or C9.

For the synthesis of the eastern fragment (Figure 12), TBDPS-protected Roche aldehyde **41** was subjected to a HWE olefination with phosphonate **42** [23] to afford the corresponding *N*-enoyl sultam. Subsequent methylation

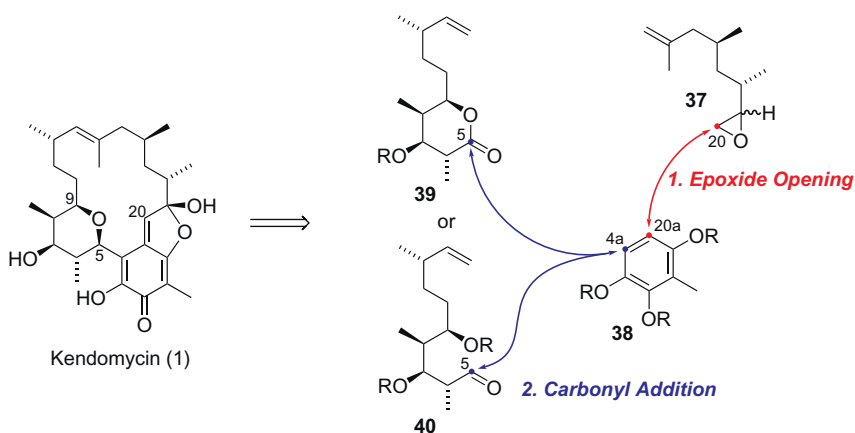


FIGURE 11 Modified approach—attachment of aliphatic side chains. R, = suitable protecting group.

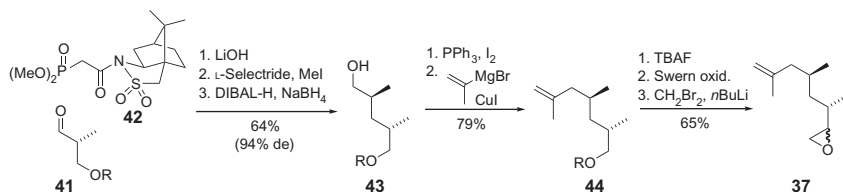


FIGURE 12 Synthesis of epoxide **37**. R, = TBDPS, L-Selectride, lithium tri-*sec*-butylborohydride, DIBAL-H, disobutylaluminium hydride, TBAF, tetrabutylammonium fluoride.

using Oppolzer's 1,4-addition/enolate-trapping protocol [24] and reductive removal of the auxiliary afforded alcohol **43** in good yield and diastereoselectivity. Conversion of the primary alcohol **43** into the iodide and coupling with isopropenylmagnesium bromide under Schlosser-Fouquet conditions furnished olefin **44** in excellent yield. Deprotection of **44** and subsequent Swern oxidation furnished the corresponding aldehyde, which was transformed directly into epoxide **37** by addition of lithiated dibromomethane [25].

The synthesis of the western fragments **39** and **40** started from (*S*)-citronellene-derived aldehyde **45** [26], which was converted into *syn*-aldol adduct **46** by extended Evans aldol methodology using keto imide **28** (Figure 13) [27]. Subsequent *anti*-selective reduction and treatment with LiOH/H₂O₂ furnished the corresponding γ -lactone **47**, which was either transformed into the protected methyl ester **48** or into OH-protected lactone **39**. Finally, a reduction-oxidation sequence on ester **48** completed the synthesis of the desired aldehyde **40**.

The known arene **49** [28], which allows a selective deprotection at C1–O, appeared to be a suitable candidate for the crucial coupling reactions. In fact, after bromination to **50** and conversion into the corresponding Grignard compound, reaction with epoxide **37** provided a diastereomeric mixture of alcohols **51** (Figure 14). Swern oxidation followed by C1–O–MOM deprotection with triflic acid then furnished benzofuran **52** in good yield. Since bromination reactions on a related benzofuran were not completely regioselective, we investigated the direct *ortho*-metalation on **52**. Treatment of **52** with *n*BuLi/TMEDA followed by D₂O-quench gave the *ortho*-deuterated product **53**. Relying on our previous results, lithiated benzofuran **52** was first treated with lactone **39**, but unfortunately no reaction product (**54**) could be detected. As a possible alternative coupling, we tried a *C*-glycosidation type reaction of the corresponding acetal **55** under Lewis acid conditions. Again, none of the desired coupling product was formed, but we found small amounts of a

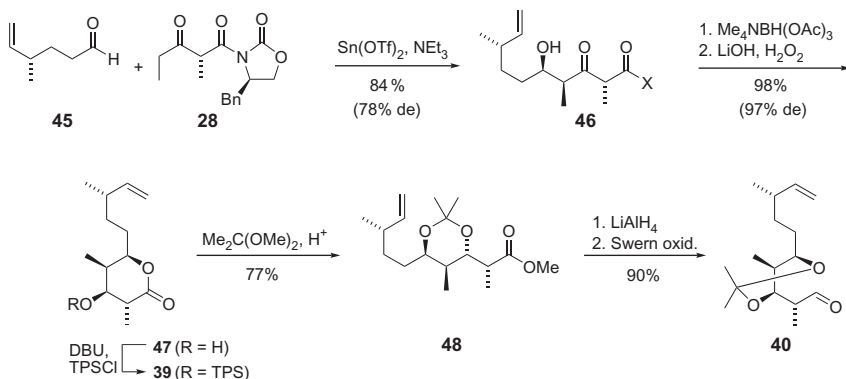


FIGURE 13 Synthesis of the left-hand fragments **39** and **40**. Tf, trifluoromethanesulfonyl.

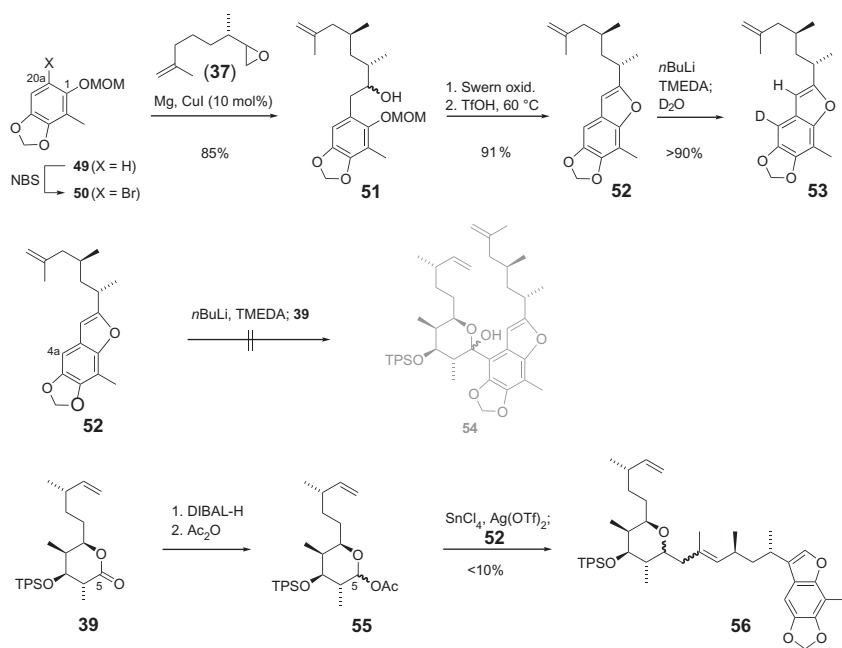


FIGURE 14 Synthesis of benzofuran **52** and initial fragment coupling experiments. TMEDA, tetramethylethylenediamine.

product mixture (**56**) resulting from an initial reaction of the corresponding oxonium intermediate with the terminal double bond of **52** in an ene-type reaction. Both of these results reemphasized the problems involved with the coupling of our sterically encumbered fragments [21,22].

Eventually, we achieved the coupling of lithiated **52** with the more reactive but less hindered aldehyde **40** (Figure 15). To our delight, the reaction proceeded smoothly and furnished benzylic alcohol **57** in a ca. 5:1 mixture of diastereomers. Compound **57** contained all the carbons of **1**, however, the problem of tetrahydropyran ring formation still remained. Owing to the stabilization of benzylic carbenium species, we focused next on a S_N1-type cyclization [29,30]. After removal of the acetonide protecting group, the resulting triol **58** did indeed cyclize readily to tetrahydropyran **59** upon treatment with a catalytic amount of *p*-TsOH in toluene at 60 °C. The cyclization could also be carried out in a single step (**57** → **59**) but suffered from a somewhat lower yield. With tetrahydropyran-arene **59** in hand, we had solved our hitherto most complex problem, namely to connect the synthetically demanding tetrahydropyran ring with the fully substituted aromatic core. Additionally, we had achieved a short and convergent synthesis of the full carbon skeleton with all stereogenic centers in place.

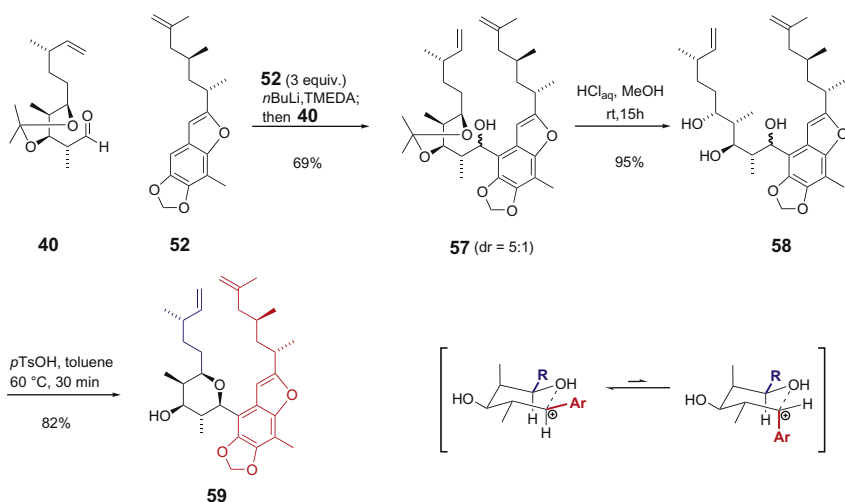


FIGURE 15 Synthesis of RCM precursor **59**.

In the course of the approach described above, we had observed some additional drawbacks. Firstly, as preliminary experiments had shown, the methylenedioxy protection group was not appropriate for secure removal at a late stage of the synthesis. Secondly, the *ortho*-lithiation step required an immoderate excess of benzofuran **52** (3 equiv.) to obtain satisfying yields. Since we had also observed a distinct influence of the substitution pattern of the aromatic core in terms of the preferred rotamer in tetrahydropyran-arene compounds (*vide supra*), a more flexible aromatic template was required. Considering all the difficulties, we chose MOM-ether **60** as the central aromatic core (Figure 16). Bromination with NBS gave **61**, which was converted into the corresponding Grignard compound. Subsequent treatment with epoxide **37** afforded alcohol **62**. Application of the previously established oxidation–condensation procedure furnished the corresponding benzofuran with a free OH at carbon C4. After reinstallation of the MOM-protecting group, we obtained benzofuran **63**, as precursor for the planned *ortho*-directed lithiation. In fact, the subsequent coupling with aldehyde **40** provided benzylic alcohol **64** without any of the above-mentioned drawbacks in a ca. 9:1 mixture of diastereomers. Since the configuration of the benzylic position was irrelevant in the ensuing reaction sequence, the diastomeric mixture was carried through the next steps. A modified removal of the acetonide protecting group had become necessary since we had observed acetonide migration in the original procedure. Thus, subsequent treatment with acetic anhydride, diluted HCl and NaOH first gave the diastomeric mixture of the corresponding triol, which was cyclized as described above to furnish tetrahydropyran **65** as a single diastereomer in good yield (71% over four steps). It is

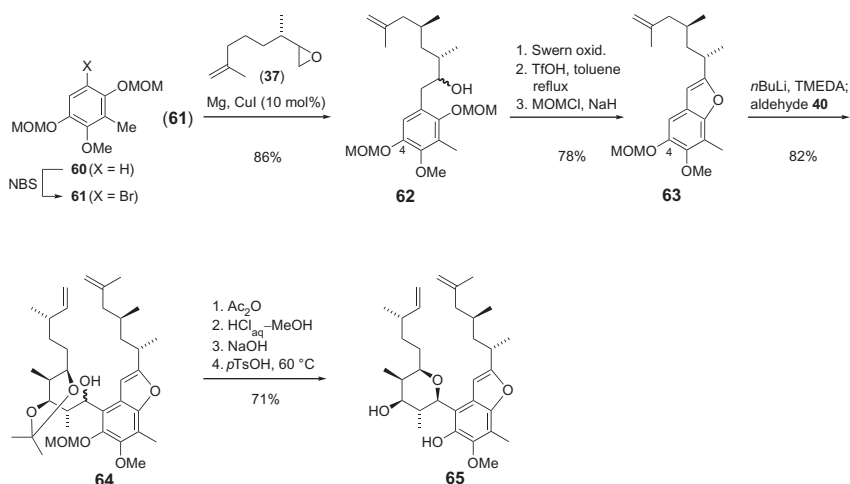


FIGURE 16 Synthesis of an alternative RCM precursor. MOM, methoxymethyl.

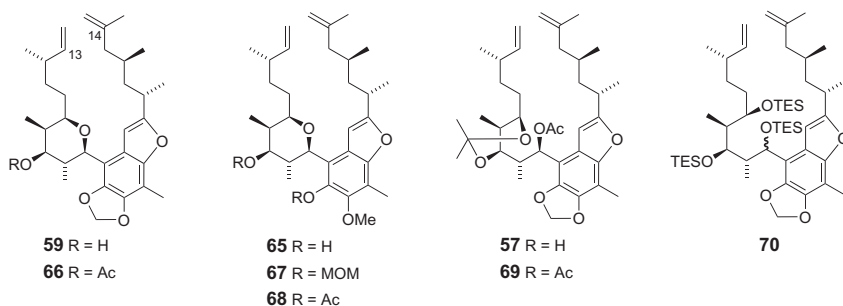


FIGURE 17 Examined substrates that proved unsuccessful for RCM reaction at C13/C14.

noteworthy that in later studies (*vide infra*), S_N1 -type cyclizations of related compounds could be performed more directly by treatment with $\text{HCl}_{\text{aq}}/\text{MeOH}$ using prolonged reaction times.

The synthesis had now arrived at the crucial macrocyclization via RCM. Unfortunately, neither **59** nor its acylated analog **66** underwent the desired cyclization, but produced complex product mixtures, presumably of dimers and oligomers, using various olefin metathesis catalysts. Compounds **65** and its *O*-protected analogs **67** and **68** gave similar results. Since RCM reactions with substrates that did not even bear the tetrahydropyran ring (**57**, **69**, and **70**) were also unsuccessful (Figure 17), we abandoned efforts towards a RCM at C13/C14. At this point, we also concluded that the rotational barriers caused by the tetrahydropyran ring might be not the only structural deficiency, but that the planar benzofuran unit also served to keep the reacting centers too far apart. Shortly afterwards, during their successful synthesis of **1**, Smith and

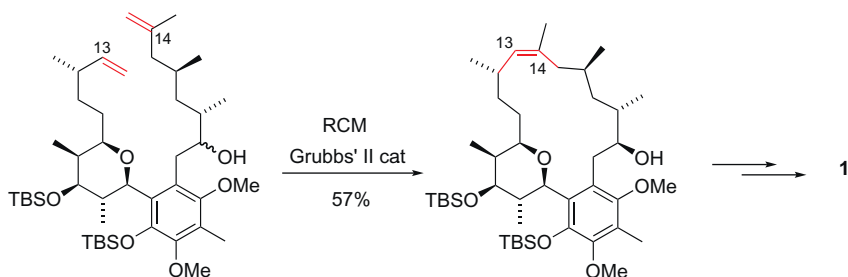


FIGURE 18 Z-selective RCM at C13/C14 according to Smith [12,13].

coworkers achieved a RCM at C13/C14 with a related substrate lacking the benzofuran unit, albeit with undesired olefin geometry (*Z*) that required a three-step procedure for the isomerization of the double bond (Figure 18) [13].

2.1.4 HWE Macrocyclization at C13/C14

As we had abandoned our initial RCM approach, we realized that another reaction type might be more successful for the cyclization at C13/C14, allowing us to easily adapt our previous synthetic strategy. HWE reactions have been successfully applied in macrocyclizations [31–34] and are generally more energetically favorable than the metathesis reaction, which would make the former the method of choice. Compared to the RCM strategy, a significant increase in synthetic operations would be unavoidable in this case, but if successful, the HWE reaction should also provide the desired *E*-geometry of the trisubstituted olefin. With regard to our system, we had either the option to perform the *Z*-selective Still–Gennari variant (**71** → **72**) or to use the common *E*-selective HWE olefination (**73** → **74**) with a β -keto phosphonate (Figure 19) [22].

For the Still–Gennari approach (Figure 20), aryl bromide **61** and epoxide **75** were condensed to benzofuran **76** using the sequence outlined in Figure 14. Appendage of the second side chain (aldehyde **40**) and subsequent S_N1 -type ring closure gave **77**, which was converted into bis-MOM-protected olefin **78**. Deprotection with TBAF afforded the corresponding primary alcohol, which was tosylated and then converted to iodide **79** by treatment with NaI in acetone. After alkylation of phosphonate ester **80**, the terminal alkene was cleaved by successive treatment with OsO_4 /NMO and $NaIO_4$, to provide *seco* aldehyde **71**. Despite numerous attempts, we were unable to identify any reaction conditions to furnish the required product.

To produce the alternative HWE substrate, silyl ether **78** was converted into aldehyde **81**, which was treated with the anion of diethyl ethylphosphonate (Figure 21). Dess–Martin oxidation, dihydroxylation, and periodate

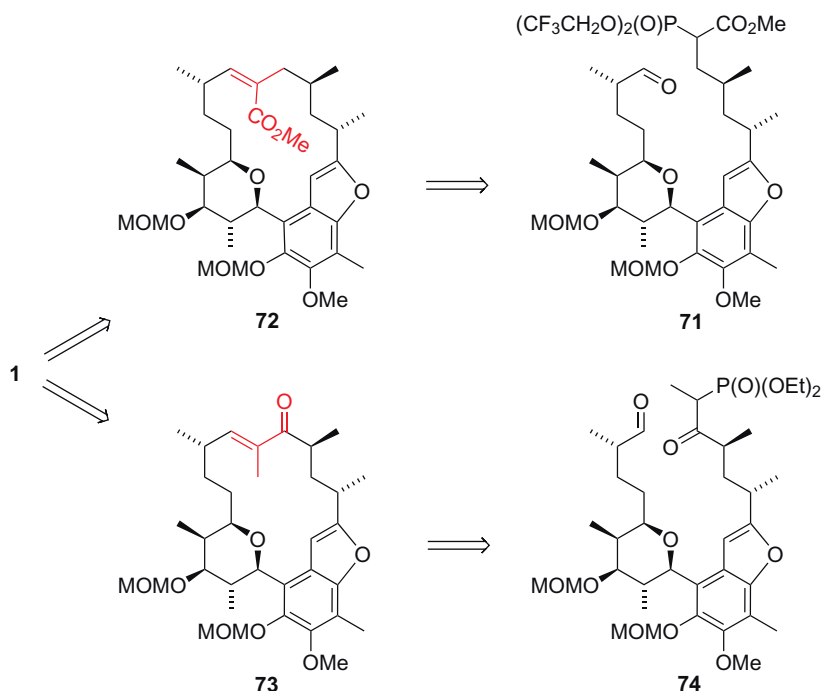


FIGURE 19 C13/C14 double bond generation by intramolecular HWE reactions.

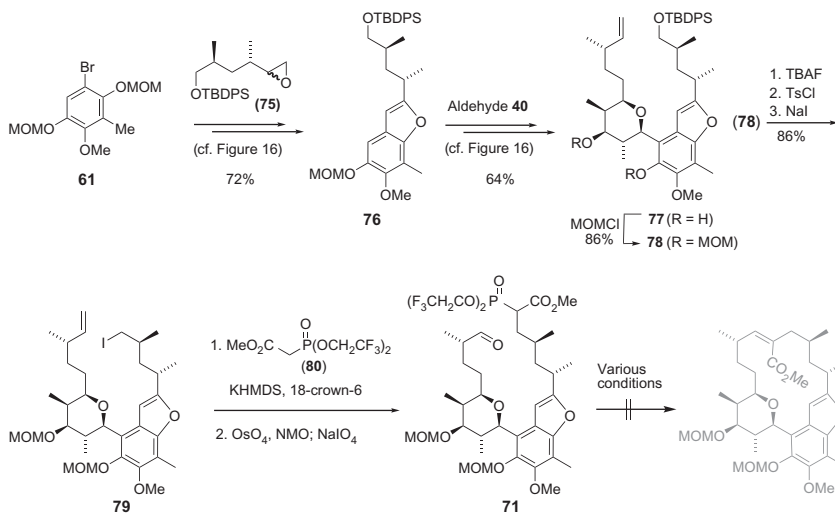


FIGURE 20 Unsuccessful Still-Gennari approach. KHMDS, potassium hexamethyldisilazane.

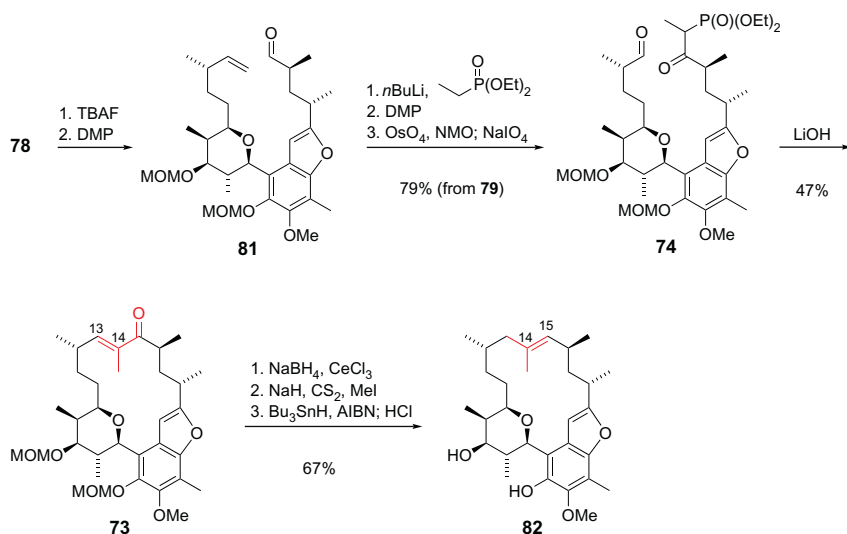


FIGURE 21 C13/C14 HWE-cyclization/deoxygenation affords the undesired C14/C15-olefin. DMP, Dess–Martin periodinane; NMO, *N*-methylmorpholine-*N*-oxide; AIBN, azobisisobutyronitrile.

cleavage furnished the desired β -keto phosphonate **74**. Moderate heating with LiOH resulted in smooth cyclization to afford the macrocyclic enone **73** in acceptable yield. The remaining undesired carbonyl function proved resistant towards direct reduction. But after extensive experimentation, a two-step procedure using Luche conditions and Barton McCombie xanthate reduction delivered a deoxygenated compound. Because of the pseudo-*C*₂-symmetry of the upper part of the molecule, it was difficult to assign the position of the trisubstituted double bond (13/14 vs. 14/15). Finally, after deprotection and careful removal of all traces of stannane residues, it could be proven with various 2D-NMR techniques (COSY, NOESY, and TOCSY) that the double bond had migrated to the 14/15 position, resulting in the undesired regioisomer **82**. Because no other olefinic isomer was detected, we concluded that the migration presumably occurred on formation of the xanthate intermediate by [3,3]-sigmatropic rearrangement [35,36].

After the failure of the C13/C14 HWE approach, caused by double bond migration during the deoxygenation step, it seemed obvious to test a modified HWE approach with reversed reactive sites. Accordingly, cyclization should now occur between C14 and C15 if we used compound **83** as the HWE substrate (Figure 22). Deoxygenation and double bond migration would then lead to the desired C13/C14 olefinic compound. HWE precursor **83** was easily prepared from aldehyde **84** in a four-step sequence. Unfortunately, although various reaction conditions were examined for the HWE reaction, we did not obtain the desired cyclization product **85**. Since both RCM and

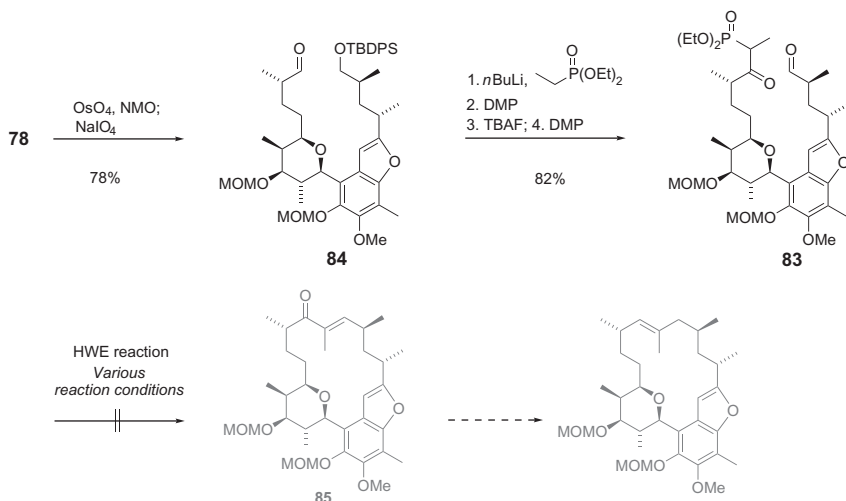


FIGURE 22 Unsuccessful C14/C15 HWE-cyclization approach.

HWE-cyclization failed, we abandoned our initial plans for macrocyclization in the C13–C15 area. Even though we did not complete the total synthesis at this stage, we developed efficient methodology for the synthesis and attachments of the polyketide side chains as well as a highly stereoselective formation of the tetrahydropyran unit.

2.2 Model Studies for the Synthesis of a Kendomycin-like Quinone Methide

During the work on the C13/C14 disconnection approach, we also carried out some model studies on the construction of the kendomycin-type quinone methide chromophore [37]. First we planned to oxidize benzofuran **86** to the corresponding orthoquinone **87**, which then should undergo a 1,6 addition of water to produce quinone methide **88** (Figure 23). After some experimentation, we found that oxidation of **86** with sodium periodate (adsorbed on silica) [38] produced a stable, deep blue colored, long-lived species, presumably semiquinone radical **89**. Evidence for this hypothesis came from the EPR spectrum, which clearly showed the presence of a free radical. On treatment with 0.1M HCl, we observed a rapid color change from blue to yellow that was attributed to the formation of orthoquinone **88** either by autoxidation or disproportionation of **89** and concomitant conjugate addition of water to produce quinone methide **88**, which could be isolated in moderate yield. In a second approach, benzofuran **86** was demethylated to catechol **90**, which was then oxidized with DMDO at -78°C to give strained epoxide **91** (not isolated). This epoxide then rearranged spontaneously to quinone methide **88**.

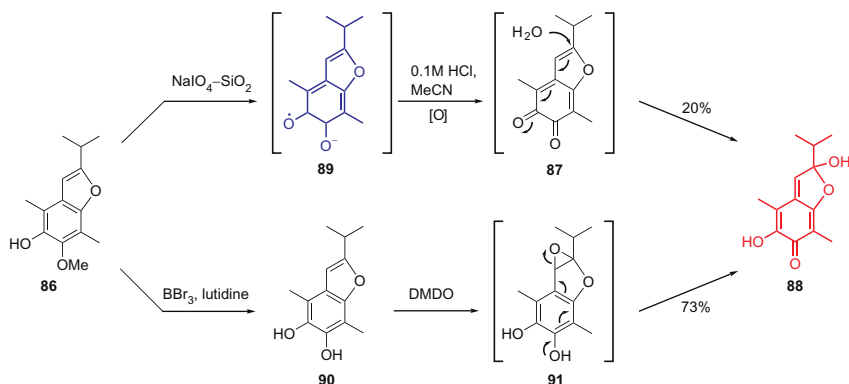


FIGURE 23 Model studies for the synthesis of a kendomycin-like quinone methide. DMDO, dimethyldioxiran.

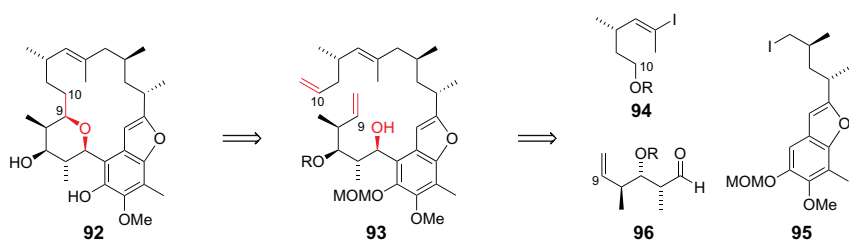


FIGURE 24 Retrosynthesis for the C9–C10 disconnection approach. R = H or suitable protecting group.

2.3 C9/C10 Disconnection Approach (RCM)

In this approach, we intended to combine carbons C9 and C10 of kendomycin precursor **92** via RCM, followed by the addition of C5–OH to olefinic C9 for tetrahydropyran ring formation [39]. For this RCM/*trans*-etherification route, the RCM precursor **93** was retrosynthetically disconnected into vinyl iodide **94**, alkyl iodide **95** and aldehyde **96** (Figure 24). The synthesis of the northern diene portion could be achieved by a Negishi cross-coupling of iodides **94** and **95**, followed by chain elongation to the 10-olefin. *Ortho*-directed lithiation and addition to aldehyde **96** should set the stage for the envisaged RCM reaction. Vinyl iodide **94** was easily available from known aldehyde **97** [40] by Colvin's one carbon chain elongation [41] followed by alkylation with MeI and subsequent hydrozirconation/iodination (Figure 25). Alkyl iodide **95** was prepared from the previously described TBS-ether **76** (cf. Figure 16) via a two-step standard procedure. Pd(0)-assisted Negishi coupling of iodides **94** and **95**, followed by deprotection gave (*E*)-olefin **98**, which was converted to 1,4-diene **99** via IBX oxidation and Wittig methylenation.

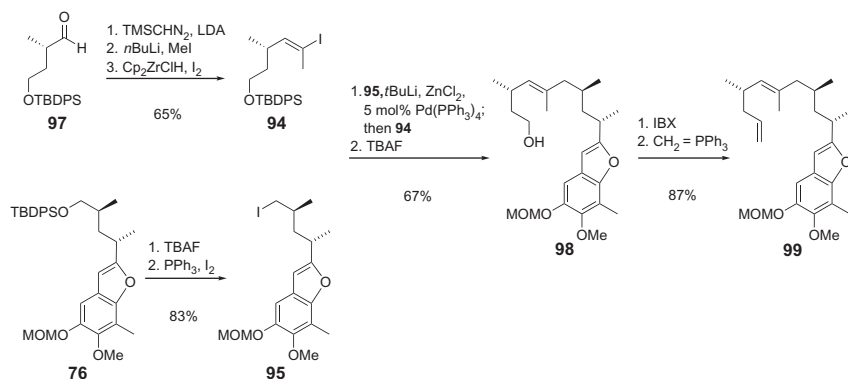


FIGURE 25 Synthesis of diene **99**. TMS, trimethylsilyl; IBX, 2-iodoxybenzoic acid.

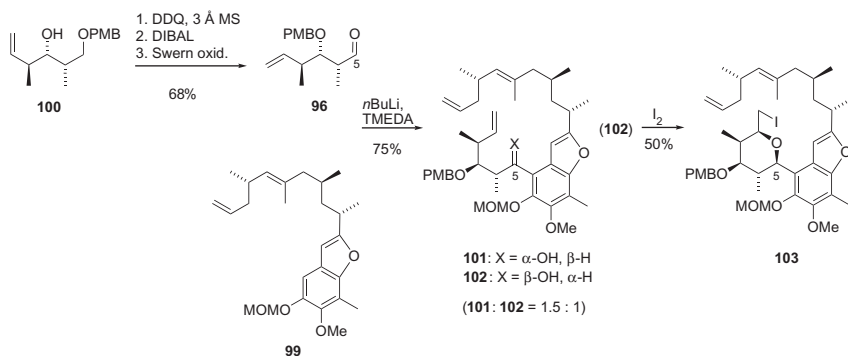


FIGURE 26 Synthesis of RCM precursors **101** and **102**.

Aldehyde **96** was available from known alcohol **100** [42] via 1,3 shift of the PMB protecting group and Swern oxidation of the primary alcohol (Figure 26). Subsequent MOM-directed *ortho*-lithiation of **99** followed by nucleophilic addition to aldehyde **96** afforded benzylic alcohols **101** and **102** as a 1.5:1 epimeric mixture. The configuration at the benzylic carbon C5 was assigned by converting compound **102** into cyclic iodoether **103**. 2D-NMR experiments (COSY, NOESY) confirmed that **103** and thus also **102** have the desired *R*-configuration at C5.

Subjecting epimer **102** to Grubbs' II catalyst [43] did not result in the desired cyclization to **104**, but led to decomposition of the starting material (Figure 27). In contrast, epimer **101** underwent the cyclization and afforded macrocycle **105**, which was used for testing purposes. Unfortunately, all attempts to form the tetrahydropyran by iodination, oxymercuration, or selencyclization failed. In addition, the RCM reaction of ketone **106** was unsuccessful. Although there would have been additional options (e.g., Mitsunobu

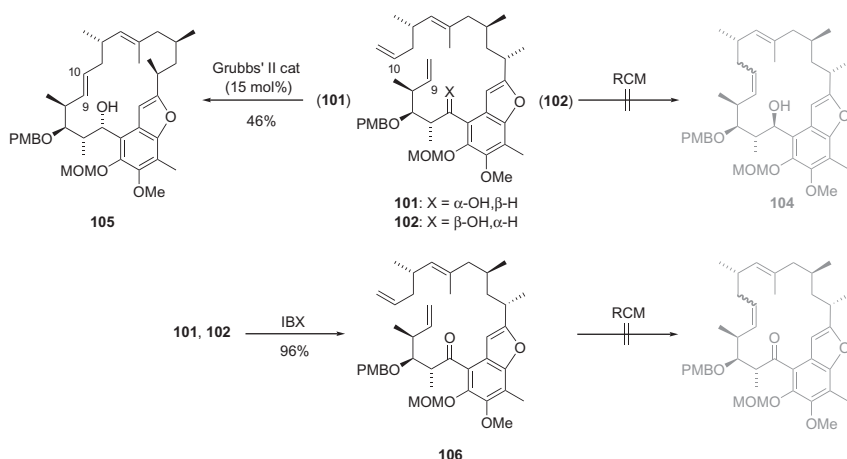


FIGURE 27 Attempted RCM reactions at C9/C10.

inversion at C5–OH), we abandoned the C9/C10 disconnection approach at this point and turned to another route.

2.4 C19/C20 Disconnection Approach (RCM)

Since the installation of the 13,14-(*E*)-double bond via Negishi coupling and C4/C5 connection via an *ortho*-lithiation aldehyde addition sequence had proven reliable and efficient, we retained them as key transformations for the C19/C20 approach [39]. In this approach, we planned that *seco* compound **107** should be available from styrene **108** and aldehyde **109**, which in turn could be formed by an Evans aldol addition of aldehyde **110** and ketoimide **28** (Figure 28). The installation of the C14/C15 double bond should be achieved by Negishi coupling of iodides **111** [11] and **112**.

The synthesis started from known aldehyde **45** [44], which was converted into the corresponding acid by Pinnick oxidation (Figure 29). Subsequent amidation with Evans' oxazolidinone **113** afforded **114**, which was converted into primary alcohol **115** by methylation and reductive removal of the auxiliary. A Finkelstein reaction delivered alkyl iodide **112**, which was subjected to a Negishi reaction with vinyl iodide **111** to give diene **116** as a key fragment. Alternatively, we envisaged the Ireland–Claisen rearrangement as an appropriate tool for generating the 13,14-(*E*)-olefin and the C16-methyl group with the desired configuration (Figure 30). For this purpose, known aldehyde **117** [9] was treated with isopropenyl bromide in a Hiyama–Kishi reaction to give a 1.4:1 mixture of the corresponding allylic alcohols, which could be separated by HPLC. Esterification of (*S*)-citronellene-derived carboxylic acid **118** with allylic alcohol **119** afforded ester **120**, which was rearranged to the corresponding ester in good yield and acceptable

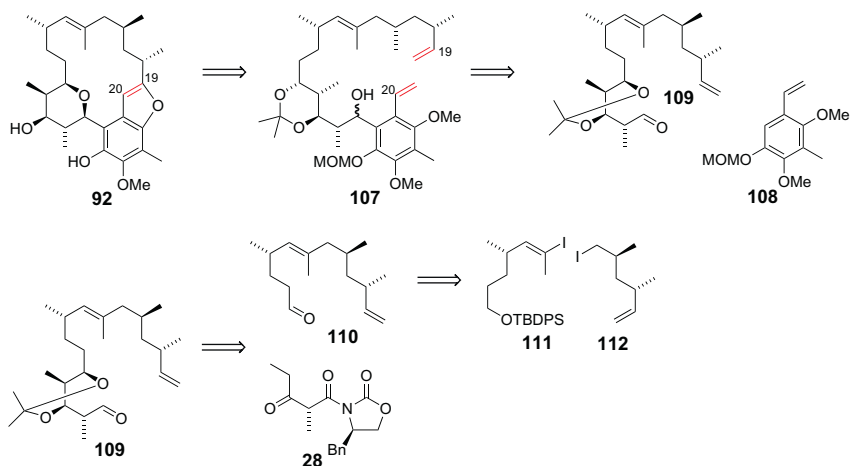


FIGURE 28 Retrosynthesis for the C19/C20 disconnection approach.

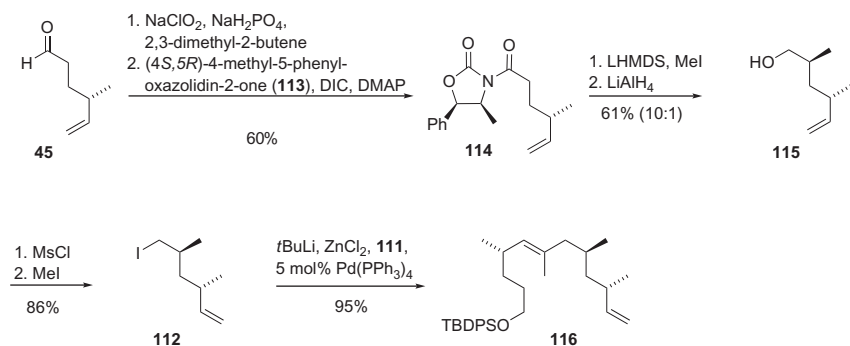


FIGURE 29 Synthesis of compound **116** via Negishi coupling. DIC, 1,3-diisopropylcarbodiimide; DMAP, 4-(dimethylamino)pyridine; Ms, methanesulfonyl.

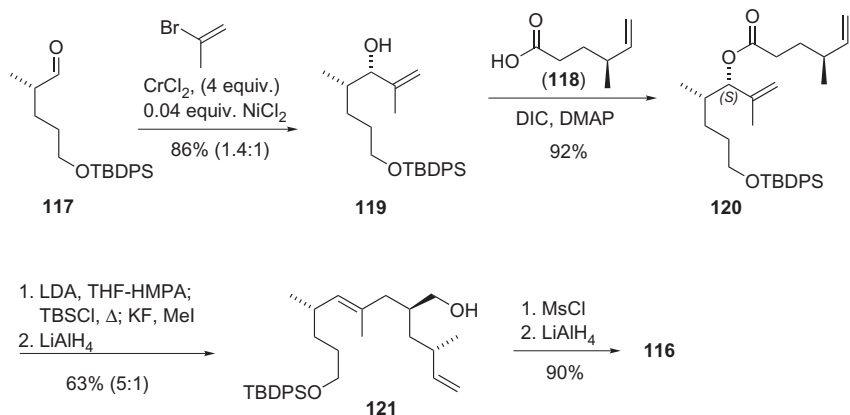


FIGURE 30 Synthesis of compound **116** via Ireland-Claisen rearrangement. HMPA, hexamethylphosphoramide; TBS, *tert*-butyldimethylsilyl.

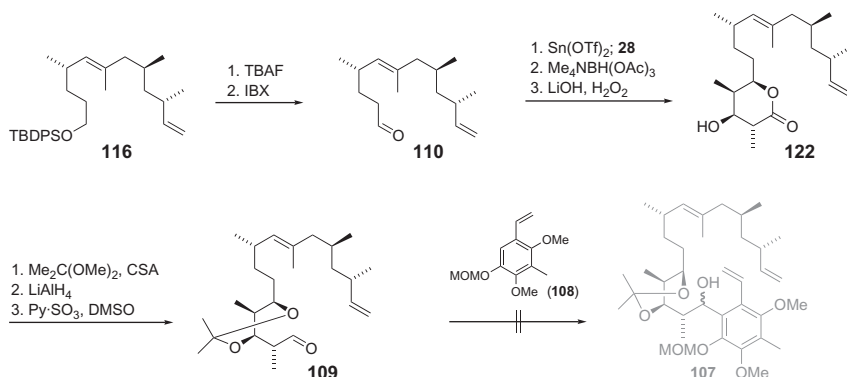


FIGURE 31 Unsuccessful carbonyl addition of the aromatic core. CSA, camphorsulfonic acid; Py, pyridine.

diastereoselectivity (5:1). Subsequent reaction with KF/MeI followed by reduction with LiAlH_4 furnished primary alcohol **121**, which was reduced to give olefin **116**.

Having two reliable syntheses of **116** in hand, we turned to the synthesis of olefin **109** (Figure 31). After deprotection and IBX oxidation, aldehyde **110** was converted into aldehyde **109** via lactone **122**, according to the previously established reaction sequence including extended Evans aldol methodology and anti-1,3 reduction (cf. Figure 13). To obtain the desired RCM precursor **107**, aldehyde **109** and arene **108** had to be coupled as before. Unfortunately, addition of $n\text{BuLi}/\text{TMEDA}$ to **108** did not give the expected *ortho*-lithiated product but only led to polymerization of the styrene unit instead.

2.5 C10/C11 Disconnection Approach (RCM)

In our third RCM approach, we planned to generate a C10/C11 olefin, which would have to be subsequently reduced in presence of the 13,14-trisubstituted olefin [39,45]. For the formation of the 13,14-trisubstituted double bond, we wanted to reapply the Ireland–Claisen approach using the known allylic alcohol **123** [46] and carboxylic acid **124** as simple precursors (Figure 32). Carboxylic acid **124** should be assembled from epoxide **125** and aryl bromide **61**. The tetrahydropyran side chain (C5–C9) should be introduced in the usual way by *ortho*-lithiation of the C4a-position and addition to aldehyde **126**.

The synthesis of acid **124** from (*S*)-citronellene-derived epoxide **125**, was achieved via the previously established epoxide-opening strategy (cf. Figure 14) using aryl bromide **61** to afford benzofuran **127** (Figure 33). An alternative synthesis of **127** started from citronellene-derived aldehyde **128**, which was converted into vinyl iodide **129** using Colvin's methodology and subsequent hydrosilylation/iodination. Negishi cross-coupling with aryl

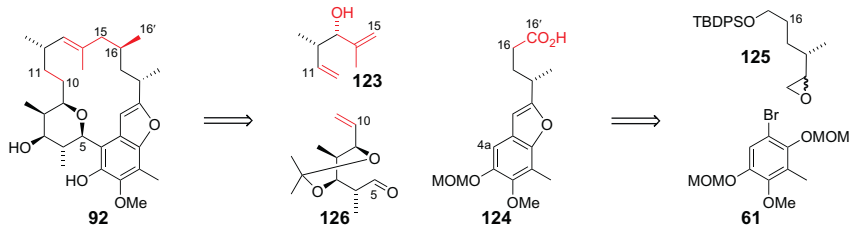


FIGURE 32 Retrosynthetic disconnections for the C10/C11-RCM approach. R = H or suitable protecting group.

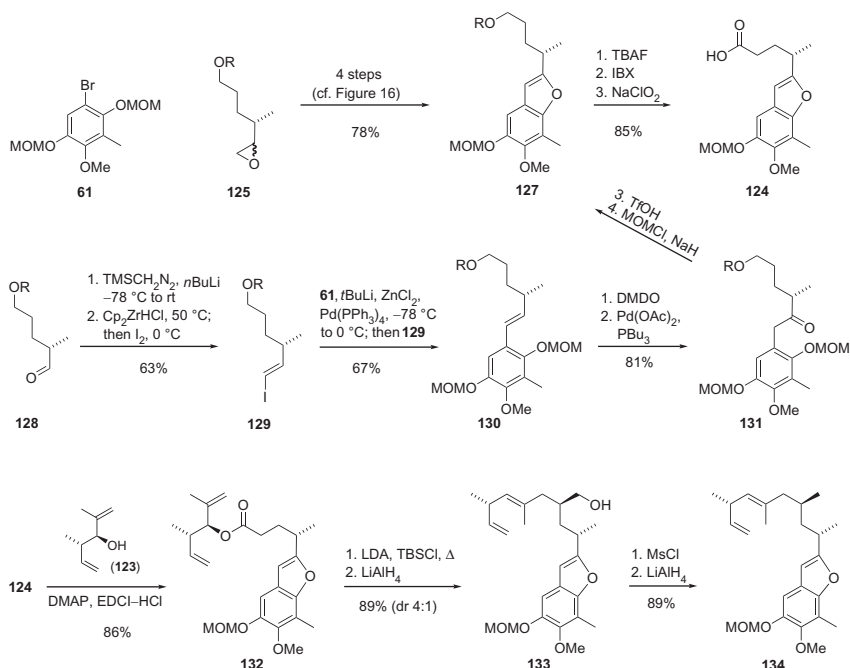


FIGURE 33 Synthesis of carboxylic acid **124** and diene **134**. R = TBDPS; EDCI, 1-ethyl-3-(3-dimethylaminopropyl) carbodiimide.

bromide **61** furnished styrene **130**, which was treated with DMDO to give the corresponding epoxide. Palladium-mediated rearrangement gave ketone **131**. Acid-catalyzed condensation to the furan ring and reinstallation of the 3-O MOM group furnished benzofuran **127**. Desilylation and two-step oxidation of the primary alcohol gave carboxylic acid **124**, which was esterified with alcohol **123** to provide the allylic ester **132**. Ireland–Claisen rearrangement and *in situ* reduction afforded primary alcohol **133**, which was reduced to give diene **134**.

Evans aldol addition of ketoimide **28** and acrolein followed by carbonyl reduction and nucleophilic removal of the auxiliary, afforded lactone **135**, which was converted into aldehyde **126** in the usual manner (Figure 34). *ortho*-Directed lithiation of **134** and addition of aldehyde **126** gave triene **136** as a 3.5:1 mixture of C5-epimers, which were separated by chromatography (the configuration at C5 was not determined at this point). The major epimer was successfully used in the subsequent RCM reaction to give macrocyclic 10,11-(*E*)-olefin **137** exclusively.

Site selective reduction of the 10,11-olefin with diimide afforded mono-olefin **138** (Figure 35). Subsequent acid-induced formation of the tetrahydropyran

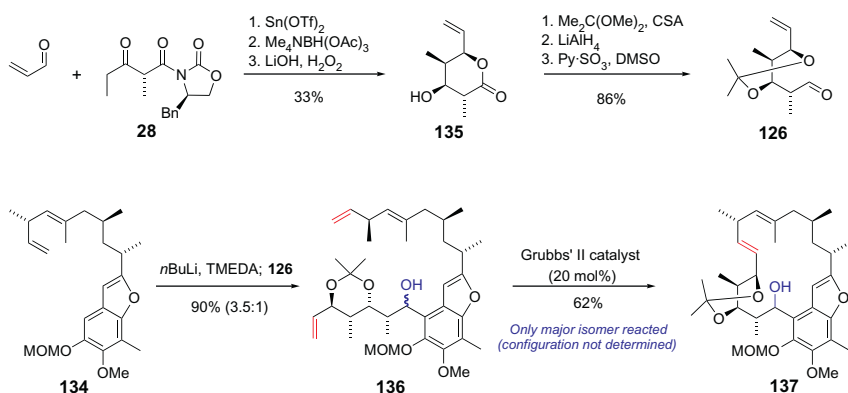


FIGURE 34 Ring-closing metathesis at C10/C11.

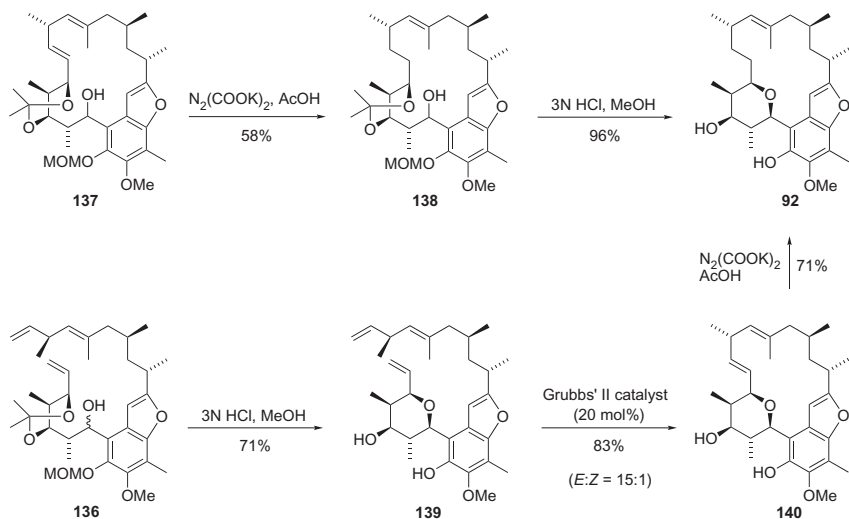


FIGURE 35 Formal total synthesis of kendomycin—achieved with the synthesis of olefin **92**.

ring and concomitant removal of the MOM group then led to key intermediate **92**. Since the minor diastereomer of alcohols **136** did not undergo the RCM reaction and the S_N1 tetrahydropyran formation is independent of the configuration at C5, we concluded that it might be advantageous to change the order of the cyclization reactions. Treatment of the epimeric mixture (**136**) with HCl resulted in clean formation of tetrahydropyran **139**, which, not surprisingly, showed the typical atropisomerism (1.5:1) of those compounds. Pleasingly, the subsequent RCM afforded the desired macrocycle in excellent yield and almost exclusively as the 10,11-(*E*)-isomer **140** (15:1). The success of this RCM was rather unexpected, as we had anticipated major problems having the tetrahydropyran ring already in place. Diene **140** was reduced with high site selectivity to olefin **92** with diimide. With the synthesis of olefin **92**, which had also been synthesized by Lee [9] and Rychnovsky [11], we had achieved our first formal total synthesis of kendomycin.

2.6 C4a/C5 Disconnection Approach (Photo-Fries Reaction)

This approach was centered on *seco* acid **141** as precursor for the envisaged macrolactonization/*ortho*-Fries rearrangement (Figure 36) [39,45]. The carbon skeleton would be assembled from the already established building blocks **118** and **124**, which would give the (*E*)-13,14-olefinic unit via Ireland–Claisen rearrangement. Again, the Evans aldol addition of a C9-aldehyde with keto-imide **28** could be used for the C8–C5-chain elongation.

For the preparation of the C13/C14 olefinic fragment, acid **124** was esterified with allylic alcohol **118** to give ester **142** (Figure 37). Subsequent Ireland–Claisen rearrangement and reduction furnished the primary alcohol **143**. Reduction of the alcohol via its mesylate gave TBS-ether **144**, which, after desilylation and oxidation, was converted into lactone **145** by the previously established aldol methodology. Subsequent removal of the MOM-protecting group, acetone formation and ester saponification gave *seco* acid **141**.

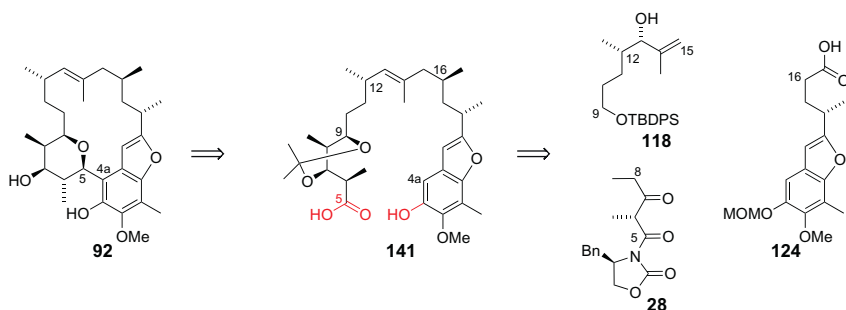


FIGURE 36 Retrosynthetic considerations for the C4a/C5 disconnection approach.

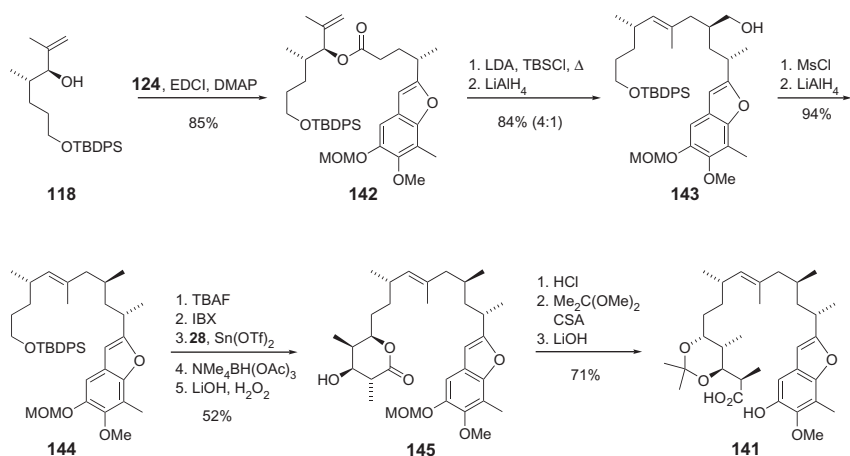


FIGURE 37 Synthesis of *seco* acid **141** via Ireland–Claisen rearrangement and Evans' extended aldol methodology.

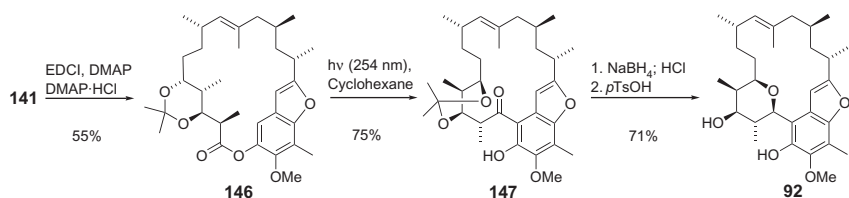


FIGURE 38 Synthesis of olefin **92** via macrolactonization/photo-Fries rearrangement.

After the successful macrolactonization of **141** using modified Keck conditions, we turned to the crucial *ortho*-Fries rearrangement of macrolactone **146** (Figure 38). Since we wanted to avoid harsh Lewis acid conditions, we decided to try the photochemical variant of the Fries rearrangement. In fact, **146** rearranged smoothly upon irradiation (254 nm) in cyclohexane to provide ketone **147**. Reduction with NaBH_4 and subsequent formation of the tetrahydropyran ring led again to Lee's intermediate **92**.

2.7 Completion of the Total Synthesis

With two successful approaches for benzofuran intermediate **92** in hand, we focused on the crucial oxidative endgame (Figure 39). Firstly, we reproduced Lee's endgame by starting with protection of the C7–OH to give the corresponding TES ether, which was then oxidized with IBX to provide the unstable yet isolable *o*-quinone **148**. On treatment of **148** with aqueous HF, the silyl group was removed and 1,6-conjugate addition of water occurred to furnish kendomycin (**1**). In an alternative approach, we tried to avoid the OTES protecting group. For this purpose, we envisaged

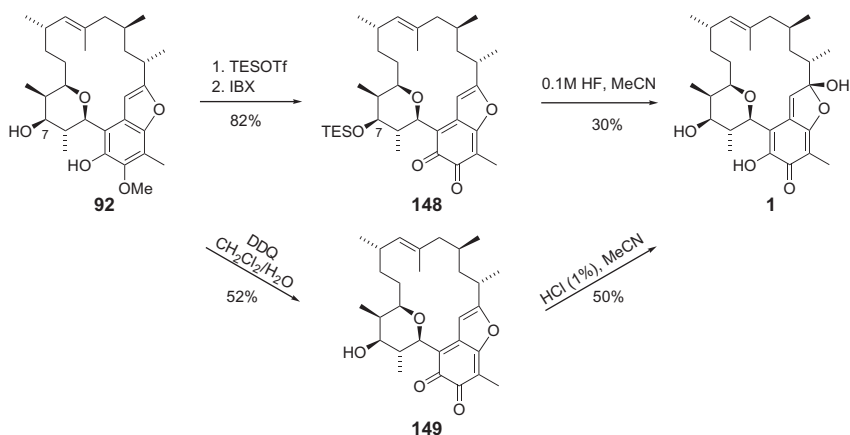


FIGURE 39 Oxidative endgame: Synthesis of kendomycin (**1**).

a biomimetic pathway, by first converting **92** into the corresponding catechol, followed by oxidation to unprotected *o*-quinone **149** and spontaneous addition of water. Unfortunately, we could not remove the phenolic methyl ether even under a variety of conditions. Finally, we discovered that DDQ in CH₂Cl₂/H₂O cleanly oxidized **92** directly to *o*-quinone **149**, which was immediately hydrolyzed to target molecule (**1**) on treatment with diluted hydrochloric acid.

3. SUMMARY

Our initial studies provided efficient methods for the synthesis and attachment of the polyketidic side chains, including epoxide-opening reactions for the introduction of the right-hand side chain and *ortho*-directed lithiation/carbonyl addition for the appendage of the left-hand side chain. A general and highly stereoselective formation of the tetrahydropyran was achieved by Evans aldol methodology and S_N1-type cyclizations of the corresponding benzylic alcohols. We also found that aryl-tetrahydropyranyl compounds display a restricted sp²–sp³ rotation, which was a hitherto unknown feature of this type of *C*-aryl glycoside. In a model study, we explored the oxidative endgame for the formation of the kendomycin-like quinone methide chromophore from the corresponding benzofurans.

Although three attempted RCM approaches (C13/C14, C9/C10, and C19/C20) failed, macrocyclization was eventually achieved by RCM at C10/C11. In another approach, we developed a novel macroglycosidation using a lactonization/photo-Fries rearrangement sequence. Both approaches included Ireland–Claisen rearrangements with unusually large fragments and led to the formation of Lee's macrocyclic benzofuran intermediate, which was converted into kendomycin by an improved oxidative endgame.

REFERENCES

- [1] Y. Funahashi, T. Ishimaru, N. Kawamura. JP Patent 1996, 08231551 [A2960910]; (b) Y. Funahashi, N. Kawamura, T. Ishimaru. JP Patent 1996, 08231552 [A2960910].
- [2] M.H. Su, M.I. Hosken, B.J. Hotovec, T.L. Johnston. US Patent 1998, 5728727 [A980317].
- [3] H.B. Bode, A. Zeeck, J. Chem. Soc., Perkin Trans. 1 (2000) 323–328.
- [4] H.B. Bode, A. Zeeck, J. Chem. Soc., Perkin Trans. 1 (2000) 2665–2670.
- [5] Y.A. Elnakady, M. Rohde, F. Sasse, C. Backes, A. Keller, H.-P. Lenhof, K.J. Weissman, R. Mueller, *Chembiochem* 8 (2007) 1261–1272.
- [6] S.C. Wenzel, H.B. Bode, I. Kochems, R. Mueller, *Chembiochem* 9 (2008) 2711–2721.
- [7] H.J. Martin, T. Magauer, J. Mulzer, *Angew. Chem. Int. Ed.* 49 (2010) 5614.
- [8] K. Tanaka, M. Watanabe, K. Ishibashi, H. Matsuyama, Y. Saikawa, M. Nakata, *Org. Lett.* 12 (2010) 1700–1703.
- [9] Y. Yuan, H. Men, C. Lee, *J. Am. Chem. Soc.* 126 (2004) 14720–14721.
- [10] K.B. Bahnck, S.D. Rychnovsky, *Chem. Commun.* (2006) 2388–2390.
- [11] K.B. Bahnck, S.D. Rychnovsky, *J. Am. Chem. Soc.* 130 (2008) 13177–13181.
- [12] A.B. Smith III, E.F. Mesaros, E.A. Meyer, *J. Am. Chem. Soc.* 127 (2005) 6948–6949.
- [13] A.B. Smith III, E.F. Mesaros, E.A. Meyer, *J. Am. Chem. Soc.* 128 (2006) 5292–5299.
- [14] T. Sengoku, D. Uemura, H. Arimoto, *Chem. Lett.* 36 (2007) 726–727.
- [15] J.T. Lowe, J.S. Panek, *Org. Lett.* 10 (2008) 3813–3816.
- [16] H.J. Martin, M. Drescher, H. Kahlig, S. Schneider, J. Mulzer, *Angew. Chem. Int. Ed.* 40 (2001) 3186–3188.
- [17] T. Hatano, R.W. Hemingway, *J. Chem. Soc., Perkin Trans. 2* (1997) 1035–1043.
- [18] J. Jimenez-Barbero, J.F. Espinosa, J.L. Asensio, F.J. Canada, A. Poveda, *Adv. Carbohydr. Chem. Biochem.* 56 (2001) 235–285.
- [19] M.M.B. Marques, S. Pichlmair, H.J. Martin, J. Mulzer, *Synthesis* (2002) 2766–2770.
- [20] D.A. Evans, H.P. Ng, J.S. Clark, D.L. Rieger, *Tetrahedron* 48 (1992) 2127–2142.
- [21] S. Pichlmair, M.M.B. Marques, M.P. Green, H.J. Martin, J. Mulzer, *Org. Lett.* 5 (2003) 4657–4659.
- [22] J. Mulzer, S. Pichlmair, M.P. Green, M.M.B. Marques, H.J. Martin, *Proc. Natl. Acad. Sci.* 101 (2004) 11980–11985.
- [23] W. Oppolzer, D. Dupuis, G. Poli, T.M. Raynham, G. Bernardinelli, *Tetrahedron Lett.* 29 (1988) 5885–5888.
- [24] W. Oppolzer, G. Poli, *Tetrahedron Lett.* 27 (1986) 4717–4720.
- [25] T.J. Michnick, D.S. Matteson, *Synlett* (1991) 631–632.
- [26] R.E. Ireland, S. Thaisrivongs, P.H. Dussault, *J. Am. Chem. Soc.* 110 (1988) 5768–5779.
- [27] D.A. Evans, J.S. Clark, R. Metternich, V.J. Novack, G.S. Sheppard, *J. Am. Chem. Soc.* 112 (1990) 866–868.
- [28] E.J. Corey, D.Y. Gin, R.S. Kania, *J. Am. Chem. Soc.* 118 (1996) 9202–9203.
- [29] M.A. Grassberger, T. Fehr, A. Horvath, G. Schulz, *Tetrahedron* 48 (1992) 413–430.
- [30] D.R. Williams, A.A. Kiryanov, U. Emde, M.P. Clark, M.A. Berliner, J.T. Reeves, *Angew. Chem. Int. Ed.* 42 (2003) 1258–1262.
- [31] J.A. Marshall, B.S. Dehoff, *Tetrahedron* 43 (1987) 4849–4860.
- [32] T.I. Richardson, S.D. Rychnovsky, *J. Am. Chem. Soc.* 119 (1997) 12360–12361.
- [33] K. Tatsuta, N. Masuda, H. Nishida, *Tetrahedron Lett.* 39 (1998) 83–86.
- [34] D.R. Williams, G.S. Cortez, S.L. Bogen, C.M. Rojas, *Angew. Chem. Int. Ed.* 39 (2000) 4612–4615.
- [35] I. Kadota, H. Takamura, Y. Yamamoto, *Tetrahedron Lett.* 42 (2001) 3649–3651.

- [36] S.F. Martin, D. Daniel, R.J. Cherney, S. Liras, *J. Org. Chem.* 57 (1992) 2523–2525.
- [37] M.P. Green, S. Pichlmair, M.M.B. Marques, H.J. Martin, O. Diwald, T. Berger, J. Mulzer, *Org. Lett.* 6 (2004) 3131–3134.
- [38] M. Daumas, Y. Voquang, L. Voquang, F. Legoffic, *Synthesis* (1989) 64–66.
- [39] T. Magauer, H.J. Martin, J. Mulzer, *Chem. Eur. J.* 16 (2010) 507–519.
- [40] J. Uenishi, R. Kawahama, O. Yonemitsu, *J. Org. Chem.* 62 (1997) 1691–1701.
- [41] E.W. Colvin, B.J. Hamill, *J. Chem. Soc. Chem. Comm.* (1973) 151–152.
- [42] W.H. Jung, C. Harrison, Y. Shin, J.H. Fournier, R. Balachandran, B.S. Raccor, R.P. Sikorski, A. Vogt, D.P. Curran, B.W. Day, *J. Med. Chem.* 50 (2007) 2951–2966.
- [43] M. Scholl, S. Ding, C.W. Lee, R.H. Grubbs, *Org. Lett.* 1 (1999) 953–956.
- [44] K. Mori, *Tetrahedron* 64 (18) (2008) 4060–4071.
- [45] T. Magauer, H.J. Martin, J. Mulzer, *Angew. Chem. Int. Ed.* 48 (2009) 6032–6036.
- [46] E. Merifield, E.J. Thomas, *J. Chem. Soc., Perkin Trans. 1* (1999) 3269–3283.

Synthesis of the *Lycopodium* Alkaloid Lyconadin A: Discovery of a Unique C—N Bond Forming Reaction

Richmond Sarpong

Department of Chemistry, University of California, Berkeley, California, USA

Chapter Outline

1. Introduction	291	5.2. Enantioselective Synthesis of Lyconadin A	304
2. The <i>Lycopodium</i> Alkaloids	292	6. Studies of the Oxidative C—N Bond Formation	307
3. The Selection of Lyconadin A	294	6.1. NMR Studies of the Dianion Intermediate	310
4. Initial Thoughts on Strategy	296	6.2. Experimental Studies on the Reactivity of the Dianion Intermediate	311
5. Successful Execution of a Strategy to Lyconadin A	298	7. Conclusion	314
5.1. Completion of the Synthesis: Discovery of a Unique Oxidative C—N Bond Formation	300		

1. INTRODUCTION

For over 60 years, total synthesis has occupied a revered position among the practitioners of chemical synthesis. However, as far back as I can remember during my professional training, there has been increasing discontent with the state of the field that seems to wax and wane depending on the financial climate for doing research. Although unhealthy at times, this sentiment has served to propel the field to new heights and inspired some truly stimulating total syntheses that have influenced not only the direction of our research program but, I trust, that of many others. Prior to beginning my independent academic career at Berkeley in 2004, I was fortunate to stumble upon an article

written by my future colleague, Prof. Clayton Heathcock, which recounted the minutes of a panel discussion from a NATO workshop on Organic Synthesis in 1994 entitled “As we head into the 21st century, is there still value in total synthesis of natural products as a research endeavor?” [1] As an academician who intended to pursue a program centered on total synthesis in the twenty-first century, I felt the need to pay attention. Two things struck me in my reading of this very educational tome:

1. It is difficult to define a central problem in chemical synthesis that galvanizes the community of practitioners.
2. If one is to pursue a total synthesis, the process of target selection should be a very important and deliberate one that takes into account the following criteria that I have paraphrased from the Heathcock account:
 - (a). The target must afford opportunities to explore new strategies or the scope of a new method.
 - (b). The function of the target must address important problems that have not been solved.
 - (c). The target must possess a high potential for training students and teaching the community something new.

It was with these humbling thoughts in mind that I selected lyconadin A as a total synthesis target in my group, with the hope that at the very least, it would serve as a good training ground for me and the students that chose to work on the synthesis of this molecule.

2. THE *LYCOPodium* ALKALOIDS

The *Lycopodium* alkaloids, which comprise over 270 natural products, are isolated from club mosses and have been the subject of chemical studies for over 130 years [2]. In the past decade, there has been a resurgence in synthetic interest in these compounds. This renaissance stems from their emergence as potential tools to combat cognitive decline (e.g., in Alzheimer’s disease) because of their documented acetylcholinesterase inhibition activity and their unique architectures, which makes them desirable targets to test new synthetic strategies and methods.

The *Lycopodium* alkaloids have been divided into four generally accepted classes as depicted in Figure 1. The first three classes are named for the

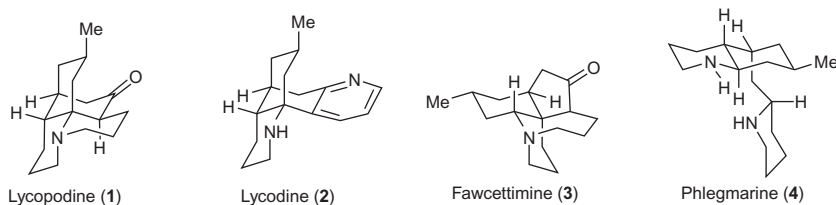


FIGURE 1 Representative members of the four classes of *Lycopodium* alkaloids.

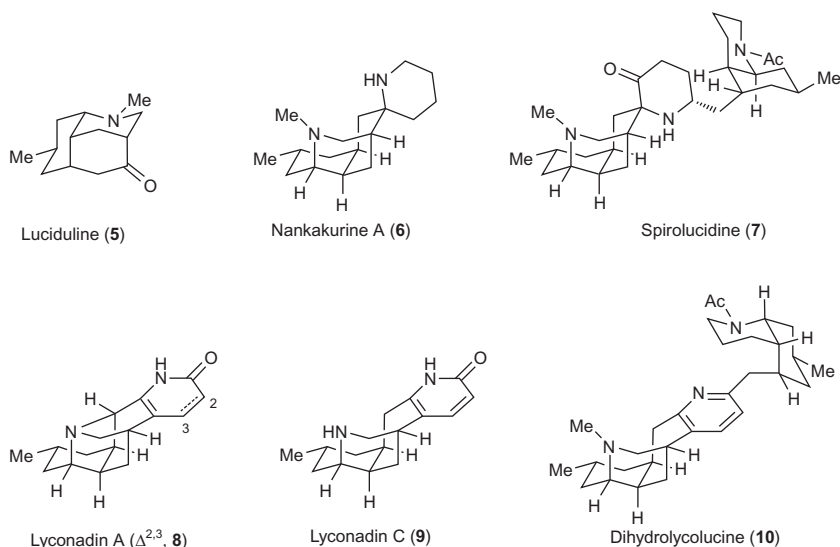
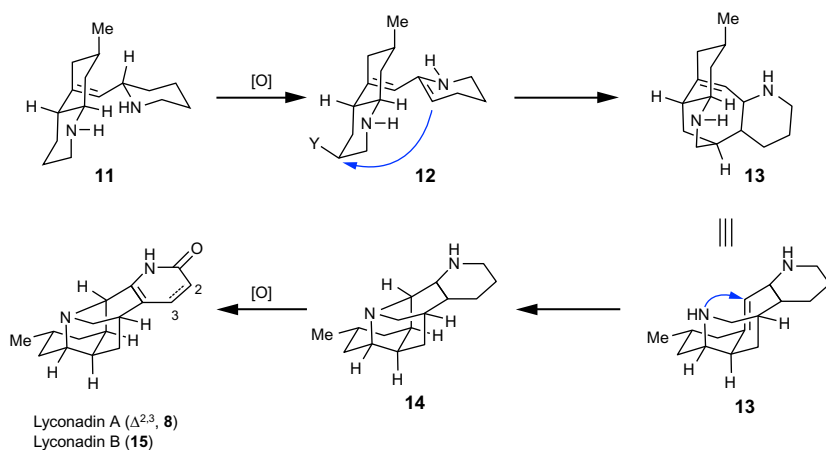


FIGURE 2 Selected congeners of the miscellaneous group of *Lycopodium* alkaloids.

compounds illustrated in Figure 1. Our target, lyconadin A, falls into the latter category, which consists of a range of skeletally diverse natural products and is therefore referred to as the miscellaneous group. Recently, the compound phlegmarine (4), which is the prototypical member of the miscellaneous group, has been proposed to be the key biosynthetic progenitor for all the *Lycopodium* alkaloids.

The miscellaneous group displays truly impressive architectural diversity (see Figure 2), which was part of our attraction to this subset of molecules as it offered an opportunity to trace their structural connections by chemical synthesis.

The biosynthesis of the miscellaneous group, for which lyconadins A and B will be used as a representative example, diverges from the other classes by the oxidation of the dehydro-phlegmarine (11, Scheme 1) piperidine ring to provide 12. For the biosynthesis of lyconadins A and B, attack from an enamine moiety yields tetracycle 13, which could suffer a transannular hydroamination to afford pentacycle 14. Subsequent oxidation and oxygenation would then afford the natural products. Several aspects of this proposed biosynthesis were intriguing from a synthetic viewpoint. First, the transannular hydroamination (13 \rightarrow 14) could provide some insight into this well-recognized, synthetically challenging, process because it is approximately thermoneutral and has a high associated negative entropy. We were therefore interested in investigating alternatives to this process, which could potentially find applications beyond the lyconadins. Second, the tertiary amine group, as well as the pyridone and dihydropyridone



SCHEME 1 Proposed biosynthesis of lyconadins A and B.

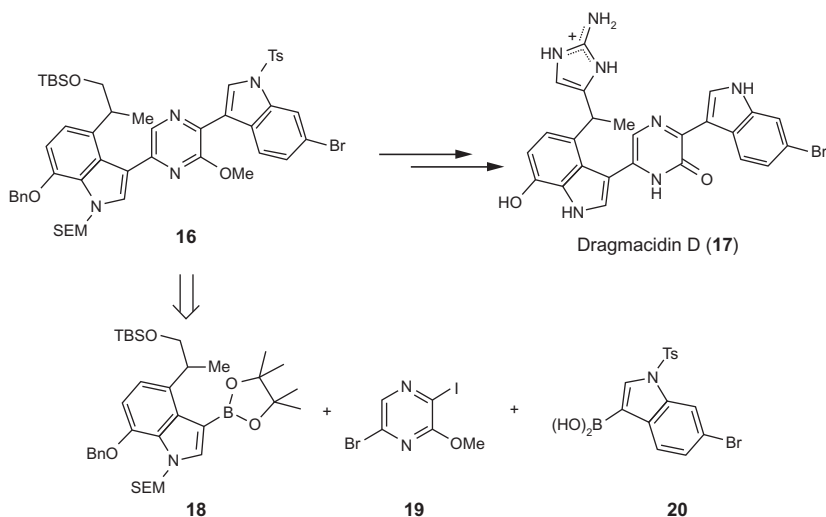
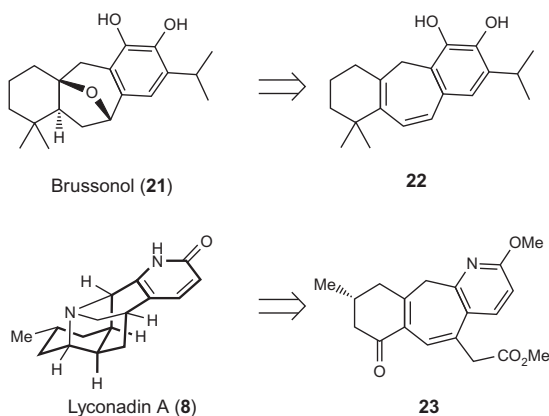
groups in lyconadins A and B, respectively, appeared to be rather challenging from a synthetic handling standpoint and so would offer an ideal (and most likely frustrating) training platform for how to handle highly nitrogenous compounds.

3. THE SELECTION OF LYCONADIN A

In addition to all the objective virtues described in the preceding sections for the choice of lyconadin A as a target, there is a very subjective reasoning to its selection, which is likely true for how many practitioners of total synthesis select their targets.

In my case, the selection of lyconadin A really begins with my experiences as a postdoctoral student in the laboratories of Prof. Brian Stoltz at Caltech. A major undertaking during my tenure at Caltech was the synthesis of the bisindole natural product dragmacidin D (**17**, [Scheme 2](#)), which was conducted in close collaboration with a then first year graduate student, Neil Garg, who is now on the faculty at UCLA. The late stage intermediates en route to dragmacidin A proved to be very polar and almost intractable materials, and the synthesis was significantly aided by introducing the cyclic guanidine heterocycle last and also carrying the pyrazinone unit as a methoxy pyrazine through most of the synthesis. This made quite the impression on me and taught me that perhaps the synthesis of other pyrazinone- and perhaps pyridone-containing compounds could be greatly facilitated by masking these groups as methoxypyrazines and methoxypyridines, respectively. Lyconadin A presented itself as a perfect case to test this latter scenario.

Another subjective attraction to lyconadin A was that our nascent laboratory at Berkeley had been working on the synthesis of a series of natural products in

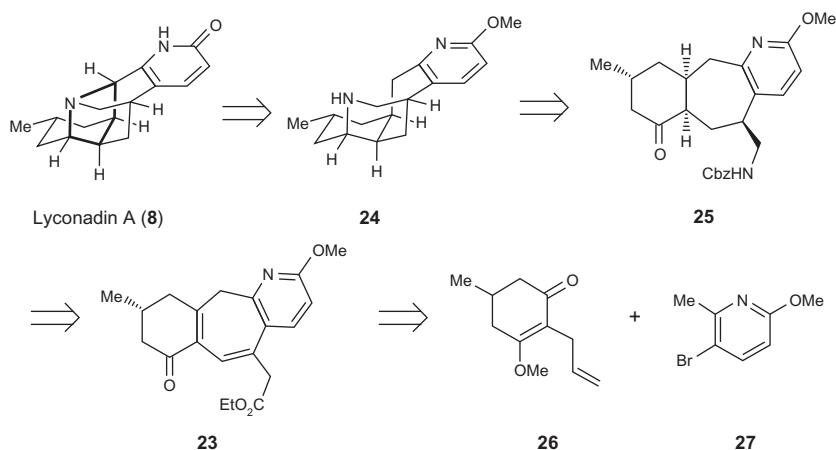
**SCHEME 2** The Stoltz approach to dragmacidin D.**SCHEME 3** A connection to annulated cycloheptadienes.

the icetexane diterpenoid family (e.g., brussanol, **21**, [Scheme 3](#)), which contain a 6-7-6 tricyclic core that we thought could be accessed from benzannulated cycloheptadienes such as **22**. In our exploration of the scope of these benzannulated cycloheptadienes, we had become interested in pyridine-annulated derivatives (e.g., **23**) and lyconadin A seemed to offer a nice opportunity for the application of these cycloheptadiene motifs.

Unbeknownst to us at the beginning of our work on lyconadin A, several other groups had taken an interest in this natural product. During the course of our synthetic studies on lyconadin A, several reports of progress toward this natural product [3], and, indeed, a total synthesis from the laboratories of Professor Amos Smith, appeared [4]. The report from Prof. Smith and his graduate student, Douglas Beshore, was significant in that it provided unequivocal support for the structure of lyconadin A and also proved the absolute stereochemistry of the natural product. Subsequent to our report on the total synthesis of lyconadin A, Prof. Fukuyama has reported a very elegant total synthesis of this natural product [5]. As a testament to the creativity of synthetic organic chemists, the three total syntheses use very different strategies.

4. INITIAL THOUGHTS ON STRATEGY

As is by now evident from Section 1, Prof. Clayton Heathcock has been very influential in my approach to natural product synthesis. So, faced with the task of devising a synthetic approach to the topologically complex framework of lyconadin A, we turned to the strategic bond disconnection approach (network analysis; introduced by Prof. E. J. Corey) that Prof. Heathcock taught for many years to droves of students in his classes at Berkeley [6]. To summarize, we first identified the maximum bridging ring (see bolded ring in **8**, Scheme 4) and then made a strategic disconnection of the C—N bond to yield secondary amine **24**. This bond was chosen for disconnection because it led back to a precursor where the atoms that were to be joined were functional positions or next to functional positions. Despite this analysis, it was unclear to us how we would make the C—N bond of lyconadin A from **24** in the forward direction.



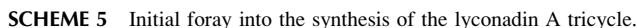
SCHEME 4 Initial retrosynthetic analysis of lyconadin A.

However, from our review of the literature, the use of a Hoffman–Löffler–Freytag (HLF) reaction for the construction of this bond seemed reasonable. Secondary amine **24** could arise from tricyclic keto-carbamate **25** through a hydrogenolysis/reductive amination sequence. Tricycle **25** could in turn be formed from pyridine-annulated cycloheptadiene **23** by manipulation of the conjugated diene moiety using a formal two-stage reduction. The cycloheptadiene-containing tricycle **23** was envisioned to arise from a union of vinylogous ester **26** and bromomethoxypicoline **27**, which had been investigated in detail by Langlois and coworkers in their syntheses of a range of alkaloids [7]. Vinylogous ester **26** was interesting in its own right. We were very inspired by the many examples of exploiting symmetry in complex molecules and became quite infatuated with the idea of a desymmetrization of a 1,3-cyclohexadione precursor to afford **26** in enantioenriched form. The lone stereocenter in **26** was then expected to guide the installation of the additional five stereocenters in the molecule.

Our initial efforts focused on a racemic synthesis of lyconadin A in order to work out issues of diastereoselectivity prior to embarking on a synthesis of enantioenriched **8**. The preparation of **26** [8] and **27** [9] were without event and followed closely the literature reports for their synthesis. Following a Stork–Danheiser protocol, lateral deprotonation of **27** followed by the addition of vinylogous ester **26** at low temperature and quenching with aqueous HCl gave the adduct **28** (Scheme 5). Following a series of false starts, we discovered that the best way to proceed at this stage was to install the enoate unit of **29**, which could be achieved effectively using a Grubbs cross metathesis. Intramolecular Heck cyclization under standard conditions afforded pyridine-annulated cycloheptadienone **23**. It was possible to hydrogenate the conjugated diene of **23** under forcing conditions. However, this was always attended by partial reduction of the ketone group. The initial reduction of the carbonyl group followed by hydrogenation led to the cleanest reactions and provided **31** as a single diastereomer, which was confirmed by X-ray crystal analysis of the *meta*-nitrobenzoate derivative (**32**).

Much to our chagrin, the relative stereochemistry of the methyl bearing stereocenter in **32** relative to the newly introduced centers was opposite to what was desired for lyconadin A. Attempts to utilize the hydroxy group in **30**, or various derivatives, to direct the hydrogenation proved to be ineffective. This unfortunate outcome, which is easily rationalized but was not predicted, led to a substantial investment in an unfruitful path that will be described here (Scheme 6).

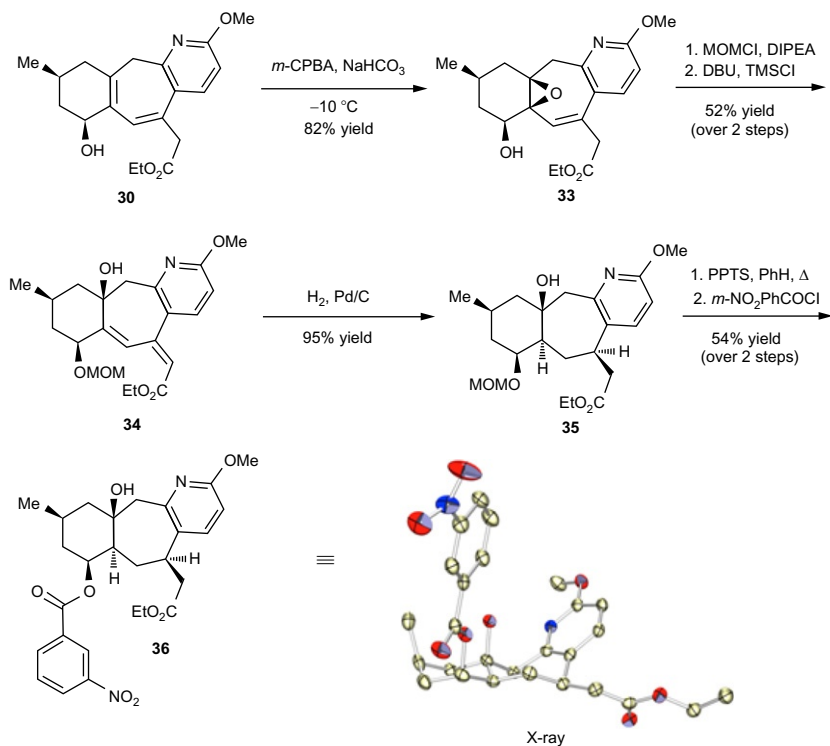
Unlike the attempted directed hydrogenation of **30**, which proceeded with the opposite selectivity to what was desired, directed epoxidation using the hydroxyl substituent was very successful, providing **33** in 82% yield. From this compound, our plan was to open the epoxide and effect hydrogenation, which could, in principle, be directed by two hydroxy groups (or their derivatives). The best path that emerged was to protect the hydroxyl of **33** as the MOM ether. Treatment of this intermediate with TMSCl in the presence of DBU led cleanly to diene **34**. To our disappointment, hydrogenation of **34**



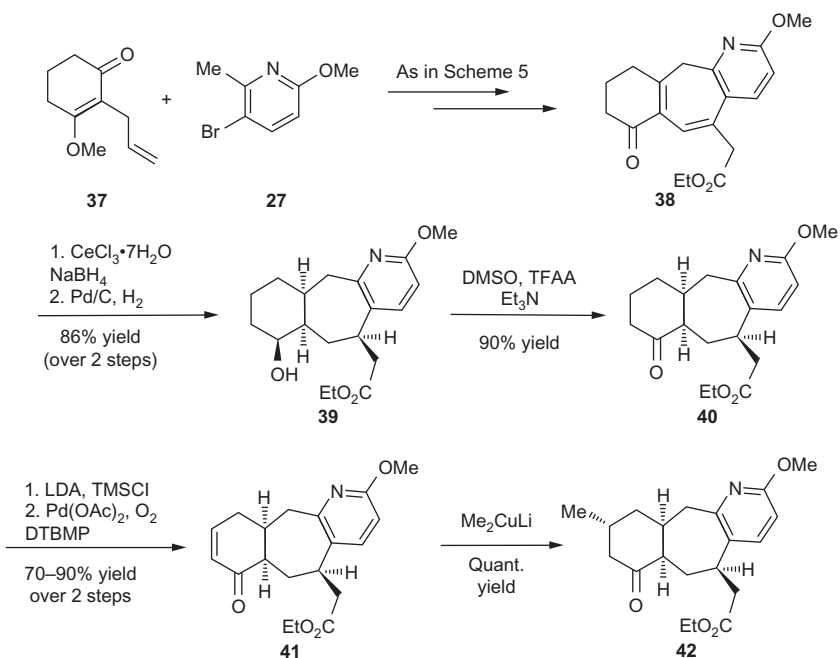
under standard conditions as well as conditions that would normally direct hydrogenation (Wilkinson's, Crabtree's, etc.) led only to **35**, which possesses the undesired stereochemistry at the newly introduced centers. This outcome was unambiguously confirmed by X-ray analysis of the meta-nitrobenzoate derivative **36** (Scheme 6).

5. SUCCESSFUL EXECUTION OF A STRATEGY TO LYCONADIN A

The difficulty associated with introducing the correct relative stereochemistry of the stereocenters in the lyconadin tricycle can be pinned directly on our strategic decision to start the synthesis with **26**, which has the key methyl group in the A ring of the natural product preinstalled. This decision, driven by a desire to exploit symmetry in the synthesis (and ultimately simplify the synthesis), had indeed created a more difficult problem. As such, we took a step back and decided to explore a route where the methyl group would be introduced late. Pyridine-annulated cycloheptadiene **38** (Scheme 7) was obtained from vinylogous ester **37** and **27** using a protocol analogous to that employed in the synthesis of **23**. Although direct hydrogenation of **38** to provide **40** could be accomplished cleanly on small scale, the reaction proved to be capricious on larger scale. In addition to the desired product (**40**),



SCHEME 6 Epoxidation route to correct relative stereochemistry.



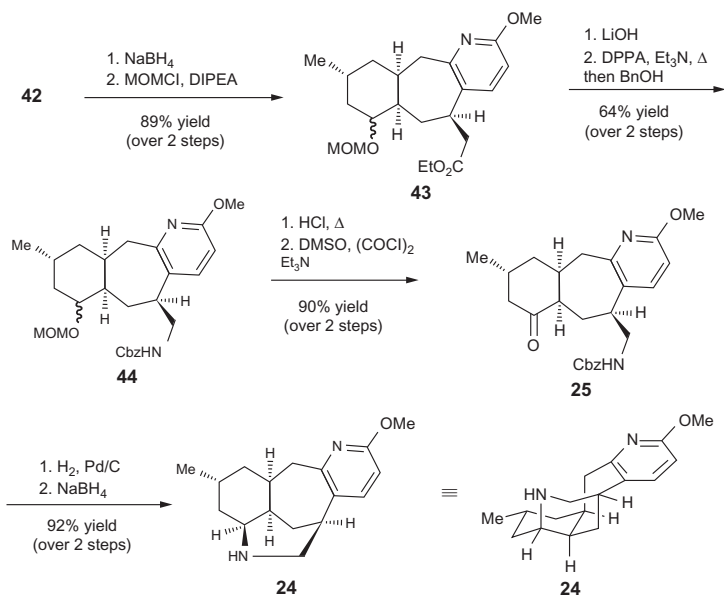
SCHEME 7 Synthesis of the lyconadin A tricycle.

over-reduction products (e.g., **39**) and the starting material were obtained. The reaction occurred cleanly and over a shorter period of time once the carbonyl group of **38** was reduced. As such, the alcohol resulting from reduction of **38** was used for the processing of material in the hydrogenation step of the synthesis. This necessitated a reoxidation of the alcohol group, to give ketone **40**, which underwent Saegusa–Ito oxidation (via the intermediate silyl enol ether) to give enone **41**. Even though the Saegusa–Ito oxidation sequence required half an equivalent of $\text{Pd}(\text{OAc})_2$, it was a very welcome alternative to our initial attempts to install the enone using the Reich protocol (LDA , PhSeCl ; then H_2O_2), IBX or HIO_3 as these proceeded in poor yield (15–40%) to the enone. Conjugate addition of a methyl nucleophile to enone **41** using the Gilman reagent proceeded in excellent yield and diastereoselectivity to afford the long sought lyconadin tricyclic diastereomer **42**.

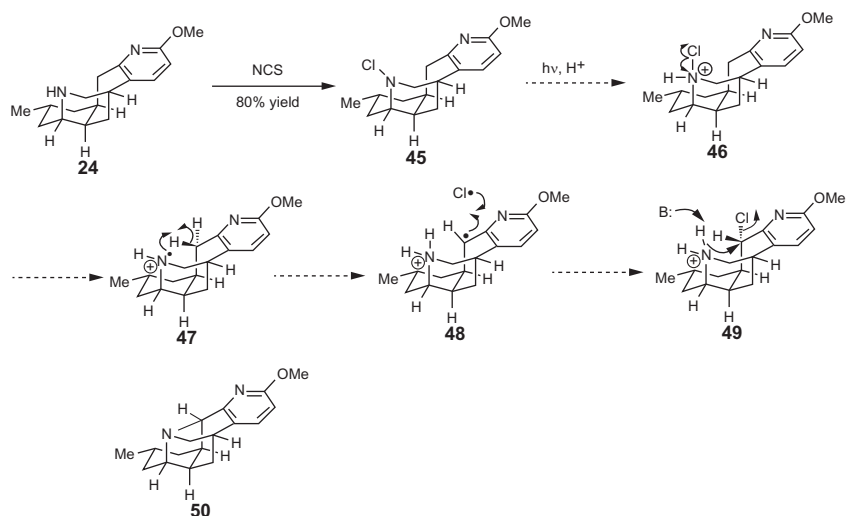
With ketoester **42** in hand, our plan was to install the piperidine ring of lyconadin A by first converting the ester group to a primary amine. This called for saponification of the ester to the acid, which would be subjected to Curtius rearrangement. Unfortunately, all attempts to saponify the ester led to epimerization of the stereocenter at the ring-fusion alpha to the ketone group. As such, reduction of the carbonyl group was required. The resulting alcohol (1:1 d.r.) was protected as the MOM ether to afford **43**. At this stage, saponification of the ester followed by Curtius rearrangement in the presence of benzyl alcohol gave Cbz-protected amine **44**. Having served its purpose, the MOM ether was cleaved to afford the corresponding alcohol, which was oxidized to ketone **25** under Swern conditions. Hydrogenolysis of the benzyl carbamate group was coupled with a reductive amination sequence using NaBH_4 as the reductant to yield tetracyclic piperidine **24** (Scheme 8).

5.1 Completion of the Synthesis: Discovery of a Unique Oxidative C—N Bond Formation

With tetracyclic piperidine **24** in hand, we were faced with the task of forging a key C—N bond to complete the highly caged pentacyclic core of lyconadin A. Our initial strategic bond disconnection analysis (see Scheme 4) had called for making this bond last and our initial plan led us to the possible use of the HLF reaction [10]. This approach was very much inspired by a report from Shibnuma, where the HLF reaction was put to powerful use in the construction of the highly caged skeleton of the diterpene alkaloid kobusine [11]. The N—Cl substrate for the HLF reaction (**45**, Scheme 9), was easily prepared by reaction of secondary amine **24** with N-chlorosuccinimide. It was expected that in the presence of a strong acid such as trifluoroacetic acid, photolysis would initiate homolysis of **45** to afford ammonium radical **47**, which would

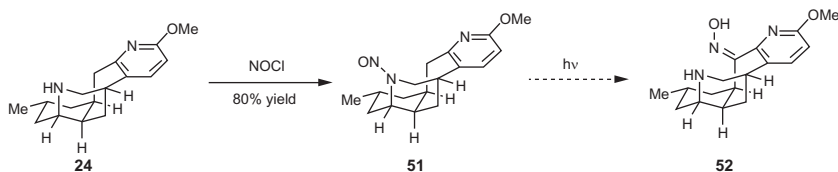


SCHEME 8 Synthesis of the tetracyclic intermediate.



SCHEME 9 Mechanism of the Hofmann-Löffler-Freytag reaction.

abstract a hydrogen atom from C-6 (via a six-membered transition state) to afford pseudo-benzylic radical **48**. Recombination of this radical with the chlorine atom would afford **49**. Upon base work up, **49** was expected to undergo C—N bond formation by $\text{S}_{\text{N}}2$ closure to give pentacycle **50**.



SCHEME 10 Attempted Barton nitrite oxidation.

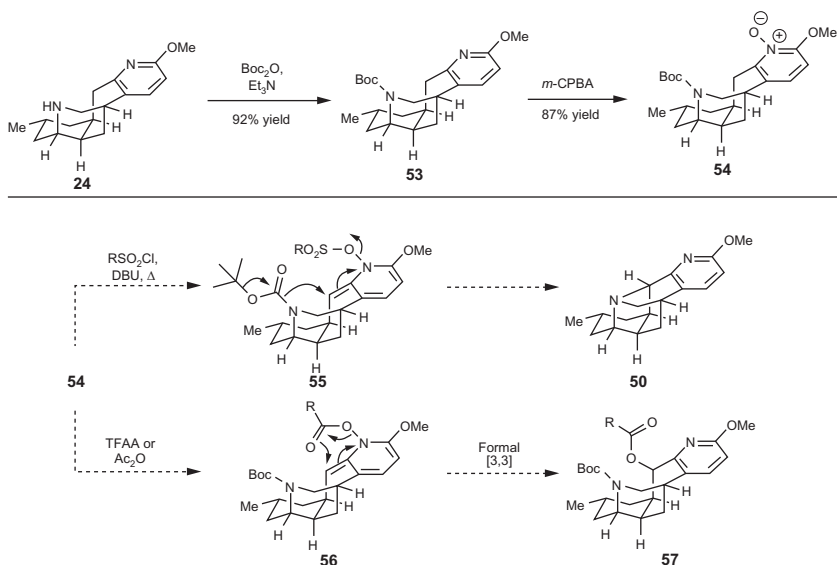
Despite our well-laid plans, exposure of N—Cl compound **45** to a variety of acidic conditions with precedent to promote the HLF reaction led to either recovered starting material or a complex mixture of products from which the desired pentacycle **50** could not be isolated. Using basic conditions, we observed either reduction of the N—Cl bond to afford piperidine **24** or the loss of HCl to yield imine byproducts.

As an alternative to the HLF reaction, we also attempted to effect a variant of the Barton nitrite ester oxidation (Scheme 10) [10]. This sequence required the synthesis of N-nitrosoamine **51**, which was readily prepared from NOCl. The expectation was that photolysis of **51** would promote homolysis of the N—N bond and then by analogy to the sequence of steps proposed for the HLF reaction (see Scheme 9), 1,5-hydrogen atom abstraction and recombination with the nitrosyl radical would follow to give oxime **52**. In this way, installation of the functional handle at C-5 would provide several possibilities for ring closure. Unfortunately, only nonspecific decomposition was observed upon irradiation of **51**. This outcome diminished all optimism about a possible photo-promoted route to C—N bond formation.

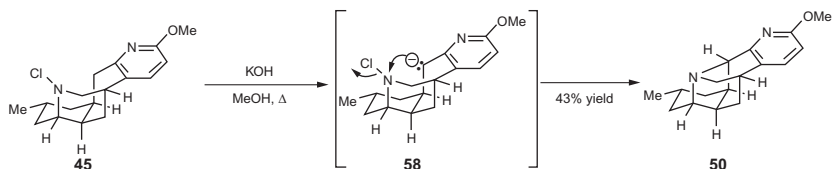
In an attempt to exploit the innate reactivity of pyridines for N-functionalization, the reactivity of the N-oxide **54** (Scheme 11) was explored. Pyridine N-oxide **54** was prepared from **24** by Boc-protection followed by reaction with m-CPBA. Two approaches to C—N bond formation were investigated at this stage. First, to directly form the desired C—N bond, we hypothesized that activation of the pyridine N-oxide by sulfonation could facilitate isomerization to enamine **55**. At this stage, thermal cleavage of the Boc group and ensuing addition of the resulting secondary amine to the alkene group would proceed with loss of a sulfate or sulfonate to directly give pentacycle **50**.

Alternatively, a Boekelheide variant [12] of the Polonovski rearrangement [13] of N-oxide **54** could yield the acyloxy compound **56**. The functionalized tetracyclic derivative **57** could serve as a precursor to pentacycle **50**. Unfortunately, all our attempts to effect the transformation of pyridine N-oxide **54** to either pentacycle **50** via **55** or to **57** were met with the formation of complex mixtures from which none of the desired products could be isolated.

With the options for C—N bond formation quickly narrowing, we were reminded of the remarkable C—N bond formation in Rabe’s synthesis of

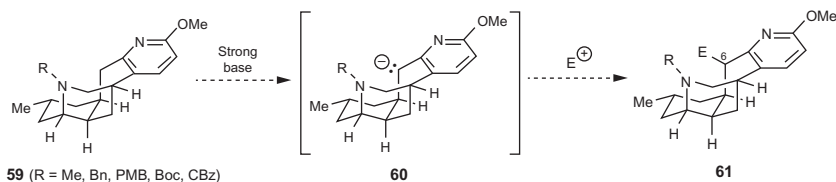


SCHEME 11 Attempted lateral functionalization approaches.

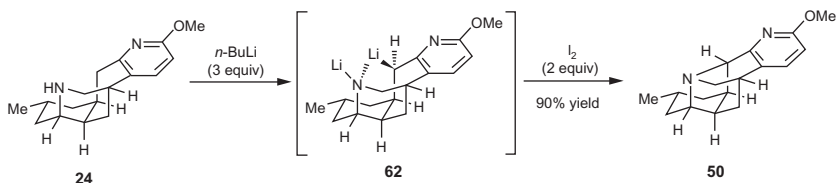
SCHEME 12 Synthesis of the pentacycle from N-Cl compound **45**.

quinine [14], which Professor Robert Williams at Colorado State had recently revisited [15]. On the basis of the Rabe/Williams account, our plan was to effect lateral deprotonation of N-chloro compound **45** (Scheme 12), which could then lead to attack of the carbanion nucleophile on the chloroamine nitrogen with the loss of a chloride nucleofuge to give pentacycle **50**. While the use of a variety of bases including LDA , LiTMP , NaHMDS , NaH , NaNH_2 , and $\text{KO}t\text{-Bu}$ led to complex mixtures of products, KOH in refluxing methanol effected the desired transformation to afford, for the first time, the lyconadin pentacycle (**50**) in low yield.

Our excitement regarding the realization of the lyconadin pentacycle (**50**) from **45** was summarily quelled by the capricious nature of the transformation. It was difficult to obtain reproducible yields of **50** and scale up the sequence in appreciable amounts. As such, we sought a more reliable sequence for the formation of the C-N bond. What we had learned from the transformation depicted in Scheme 12 was that it was possible to deprotonate the pseudo-benzylic position (which we have dubbed the picolinic position; see **58**). However, attempts to deprotonate at the picolinic position of N-protected variants of



SCHEME 13 Attempted functionalization at C6 using lateral deprotonation.



SCHEME 14 Formation of the lyconadin pentacycle via a dianion intermediate.

24 (i.e., **59**; [Scheme 13](#)) proved futile. We hypothesized that the free secondary amine, once deprotonated, could serve as a proximal, specific base to in turn deprotonate the picolinic position. Therefore, in the presence of an excess of a strong base, such as *n*-BuLi, a double deprotonation could be effected to afford a dianion, which could be oxidized to give pentacycle **50**.

Upon subjecting secondary amine **24** ([Scheme 14](#)) to *n*-BuLi (3 equiv) at -78°C for 30 min, a bright orange solution was formed, which upon exposure to I_2 (2 equiv) and slowly warming to room temperature and stirring for 6 h gave pentacycle **50** as the only product after workup in 90% yield! This was an exciting result for us from a synthetic standpoint, where in one pot we had formed the elusive C—N bond to craft the framework of lyconadin A. At this stage, a simple methyl ether cleavage using NaSEt gave lyconadin A in 76% yield. In subsequent studies, we have found that the number of equivalents of *n*-BuLi and I_2 can be reduced to 2 and 1 equiv, respectively. In addition, we discovered that depending on the workup of the reaction, the free base or salt of lyconadin A was formed. This somewhat confounded us at first because the resulting ^1H NMR spectra have some pronounced differences. As we later came to appreciate, this phenomena is not uncommon for alkaloids [16] and this lesson has stayed with us in all our subsequent syntheses of alkaloids. Our synthesis of racemic lyconadin A came as a relief for us and there was a lot of associated celebration in the group. However, it was clear even during this euphoric period that our task was not complete until an enantioselective synthesis of lyconadin A had been achieved.

5.2 Enantioselective Synthesis of Lyconadin A

Our plan to accomplish an enantioselective synthesis of lyconadin A had always rested on our ability to effect a formal enantioselective hydrogenation of cycloheptadienone **38**. This plan evolved when we discovered during the

racemic synthesis of lyconadin A (described in [Scheme 7](#)) that hydrogenation of **38** proceeds best when the ketone group was first reduced. Although this had “cost” us steps in the racemic synthesis, we thought we could exploit this “additional” step by using the stereocenter that is introduced during the reduction of the carbonyl group to govern the formation of the other stereocenters following diastereoselective hydrogenation. Oxidation of the resulting alcohol would complete the formal enantioselective hydrogenation that was initially planned. In line with this plan, the first task was to effect an enantioselective reduction of the carbonyl group of enone **38**.

A range of reducing agents that have a history of accomplishing highly enantioselective carbonyl reductions were screened for the reduction of **38**. This included *S*-Alpine-Borane[®] (**64**, [Table 1](#)) and (+)-B-chlorodiisopinocampheylborane (**65**; DIP-Cl). Reduction with *S*-Alpine-Borane[®] led to a complex mixture of products (entry 1), whereas (+)-DIP-Cl gave the desired allylic alcohol (**63**) in 40% yield with an enantiomeric excess (*ee*) of –59% *ee* (entry 2). Careful control of the temperature for the (+)-DIP-Cl reduction (entry 3) led to a cleaner conversion and higher isolated yield (63%), which was attended by higher *ee* (–65%). Even though the (+)-DIP-Cl reduction demonstrated that the enantiotopic faces of enone **38** could be differentiated, the modest *ee*'s and yields caused us to explore other possibilities for the reduction. The documented successes of the Corey–Bakshi–Shibata (CBS) reduction [[17](#)] in the enantioselective reduction of cyclic enones made it an attractive alternative. In our initial studies with (*R*)-CBS-Me catalyst (**66**) and borane-THF complex as the stoichiometric reductant, only modest conversions were achieved at –78 °C (entries 4 and 5). The use of catecholborane as the reductant in CH₂Cl₂ as the solvent led to a dramatic improvement in the conversion and *ee* (63% yield, 83% *ee*; entry 6). A brief survey of solvents identified toluene to be optimal (entry 8), affording the enantioenriched alcohol product in 85% yield and 98% *ee*.

With highly enantioenriched tricyclic alcohol **63** in hand, we proceeded with hydrogenation under standard conditions (Pd/C, H₂ at 1 atm), which was followed by Swern oxidation to give ketone **40** in good yield but with significantly diminished *ee* (77%). Our careful analysis of the two steps for the conversion of **63** to **40** revealed that the hydrogenation step proceeds with only modest diastereoselectivity to provide alcohols **39** and its diastereomer (89:11 d.r.). Oxidation of the diastereomeric alcohols affords enantiomers of ketone **40**, which is manifested in the decrease in observed *ee*. Attempts to improve the diastereoselectivity of the hydrogenation in order to proceed with the rest of the synthesis were met with little success. Ultimately, we found that we could effect a recrystallization to obtain the major alcohol diastereomer (**39**) from hexanes, which was serviceable for the rest of the synthesis. The relative and absolute stereochemistry of **39** was confirmed by X-ray crystallographic analysis ([Scheme 15](#)).

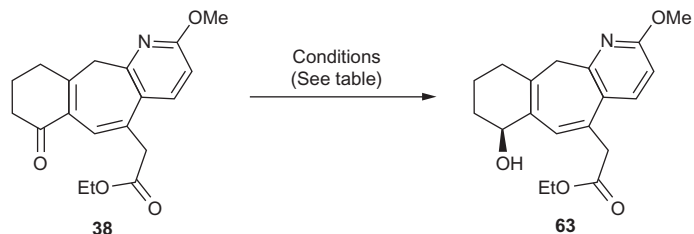
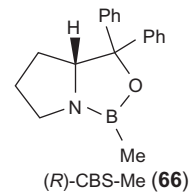
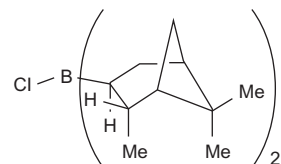
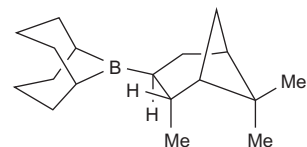
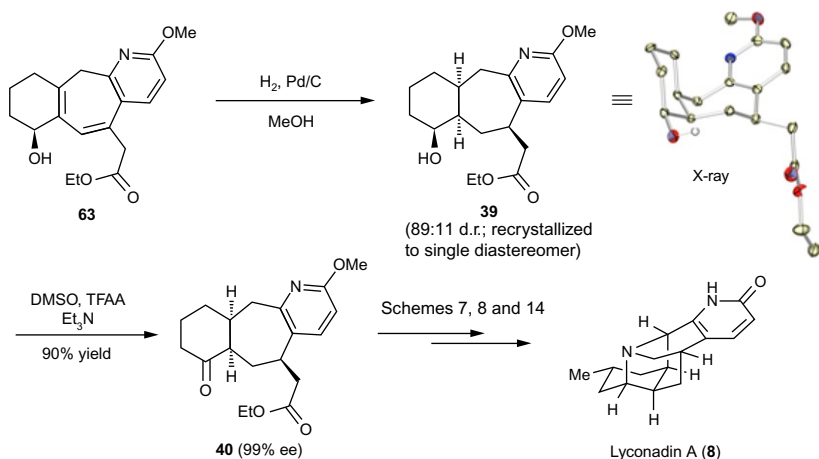


TABLE 1 Optimization of the Enantioselective Reduction of **38**.

Entry	Catalyst/Reductant	Temp (°C)	Solvent	Time (h)	Conversion	ee
1	(<i>S</i>)-Alpine Borane®	0 to rt	THF	72	Multiple products	–
2	(+)-DIP-Cl	0 to rt	THF	48	40%	–59%
3	(+)-DIP-Cl	0	THF	48	63%	–65%
4	(<i>R</i>)-CBS-Me/BH ₃ ·THF	0 to rt	THF	24	4:1 (sm:pdf)	–
5	(<i>R</i>)-CBS-Me/BH ₃ ·THF	–78	PhMe	8	1:1 (sm:pdf)	–
6	(<i>R</i>)-CBS-Me/catecholborane	–78	CH ₂ Cl ₂	8	63%	83%
7	(<i>R</i>)-CBS-Me/catecholborane	–78	THF	8	1:1 (sm:pdf)	–
8	(<i>R</i>)-CBS-Me/catecholborane	–78	PhMe	5	85%	98%



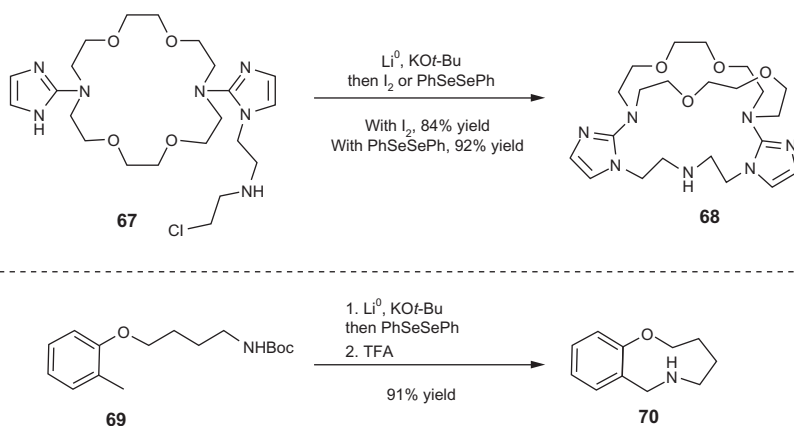
**SCHEME 15** Synthesis of enantioenriched ketone **40**.

With highly enantioenriched ketone **40** in hand, the rest of the synthesis followed closely the sequence established for the racemic series (described in [Schemes 7, 8, and 14](#)). The enantioselective synthesis of (+)-lyconadin A (**8**) was achieved in 17 steps and 6% overall yield. The development of the oxidative C—N bond-forming step was integral to the success of our strategy. However, at the time of the completion of the total synthesis, our understanding of this reaction, or the intermediates involved, was very limited. This prompted an in-depth study of this dianion oxidation process.

6. STUDIES OF THE OXIDATIVE C—N BOND FORMATION

The oxidative C—N bond formation achieved during our synthesis of lyconadin A qualifies as an umpolung reaction, which is described as an inversion in the reactivity of an atom from a donor to an acceptor or vice versa. As such, the union of two traditionally nucleophilic positions to form a bond is an umpolung reaction. Although tried umpolung favorites such as the Stetter reaction [\[18\]](#) or the use of anions generated from dithianes are well entrenched, the oxidative coupling of enolates has only recently undergone a resurgence and now provides an alternative, yet powerful, way to build complex molecules.

Ever since its discovery in 1935 [\[19\]](#), extensive research has been dedicated to the oxidative dimerization of enolates using a range of oxidants [\[20\]](#). In the area of complex molecule synthesis, perhaps the most visible contributions are the work of the Baran group in their synthetic studies of the stephacids and avrainvillamide [\[21\]](#) and Overman's synthesis of actinophyllic acid [\[22\]](#). Despite the proliferation of intramolecular oxidative C—C bond forming reactions, examples of C—N bond formation have remained relatively



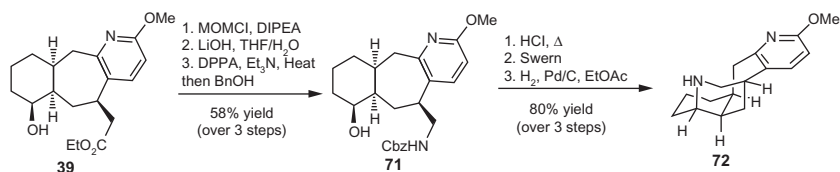
SCHEME 16 Examples of intramolecular oxidative C—N bond formation by Verkman and Carpenter.

rare [23]. The majority of the most recognized examples of oxidative C—N bond formation that have been reported (by Yamamoto/Maruoka, Dembech/Ricci and Knochel) are intermolecular and involve the use of amidocuprate intermediates [24]. The nature of preparation of the reactive intermediates has generally made it difficult to render these reactions intramolecular. An intriguing example of an intramolecular C—N bond formation was reported by Verkman and Carpenter after our initial reports on these reactions had appeared [25]. In this work, cyclic amino ethers (e.g., **67**, Scheme 16) were applied successfully to the synthesis of 6- to 15-membered rings via oxidative C—N bond formation (see **68**). A remarkable and potentially transformative variant was the reported conversion of **69** to **70**. However, to date, full details or a follow up on this work has not appeared.

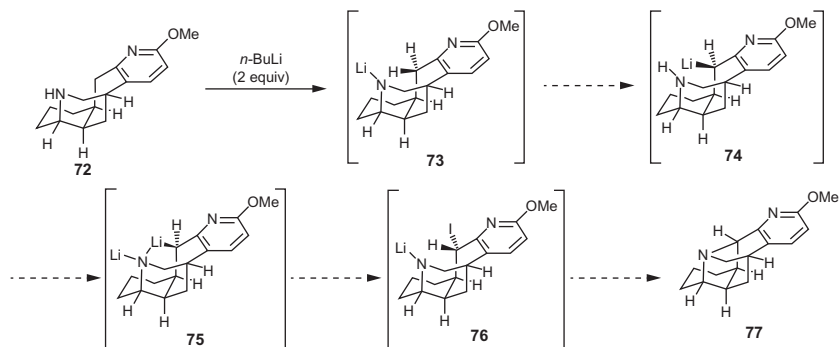
Our involvement with the oxidative C—N bond formation was a direct consequence of the simplifying disconnection it enabled (in accord with network analysis) in our synthesis of lyconadin A. However, we quickly recognized that the oxidative union of a carbanion and a nitrogen anion, should it be rendered general, would offer a powerful bond forming reaction in the synthesis of alkaloids and other complex molecules that contain nitrogens. However, prior to examining the scope of this type of C—N bond forming reaction, we decided to examine the structure and reactivity of the dianion intermediate in order to gain insight into these unique intermediates, which will inform the mechanism of the oxidative C—N bond formation.

For our structure and reactivity studies, we opted to use simplified tetracycle **72** (Scheme 17), which lacks the methyl group in the A-ring. Tetracycle **72** was synthesized from cycloheptane **39** in six steps (46% overall yield) using a sequence analogous to that already established for the synthesis of **24**.

Treatment of **72** with two equivalents of *n*-butyllithium at -78°C led to the formation of a presumed dianion (**75**, Scheme 18) via intermediates **73** and **74**.



SCHEME 17 Synthesis of the model tetracycle.

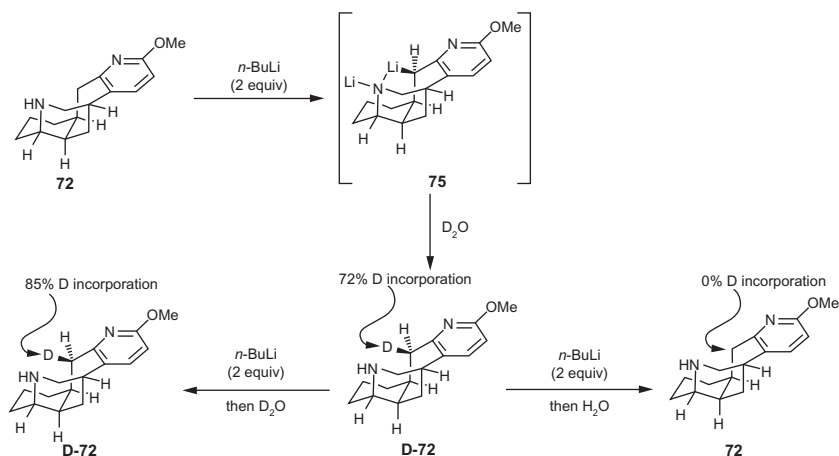


SCHEME 18 The initially proposed mechanism for C—N bond formation.

Upon the addition of iodine (1 equiv) to **75**, pentacycle **77** was observed, which could have arisen by ring closure from iodide **76**. However, no conclusive evidence was available to support the formation of either **75** or **76**. As such, we undertook a deductive analysis of each step of the proposed mechanism as well as structural and reactivity characterization and study of the intermediates.

Although the pseudo-benzylic methylene group in **72** (a.k.a, the “picolinic” position) is relatively acidic ($\text{pK}_a = 34$ in THF) [26], the initial deprotonation of the secondary amine appears to be critical to formation of the anion at C6. Presumably, the initially formed lithium amide (see **73**) serves as an intramolecular base to effect lateral deprotonation at C6 to afford carbanion **74**. A subsequent deprotonation of the resulting amine would yield dianion **75**. This dianion intermediate could exist in the form of an internal chelate, which would impart additional stability to this structure. The importance of the free secondary amine to the success of the C—N bond formation is supported by the observation that protection of the amine nitrogen (with a Boc, allyl, or Cbz group; see Scheme 13) completely thwarted lateral functionalization at C6 with a range of electrophiles including D_2O and I_2 .

As proposed in Scheme 18, dianion **75** may react with iodine through an inversion process to afford **76**, which undergoes displacement of the iodine group to afford pentacycle **77**. This is in accord with literature precedent for the reaction of polarizable, sterically demanding electrophiles with dianions. However, the reaction of dianion intermediates with small, hard electrophiles such as D_2O should proceed with retention of stereochemistry at C6 [27].



SCHEME 19 Deuteration Experiments.

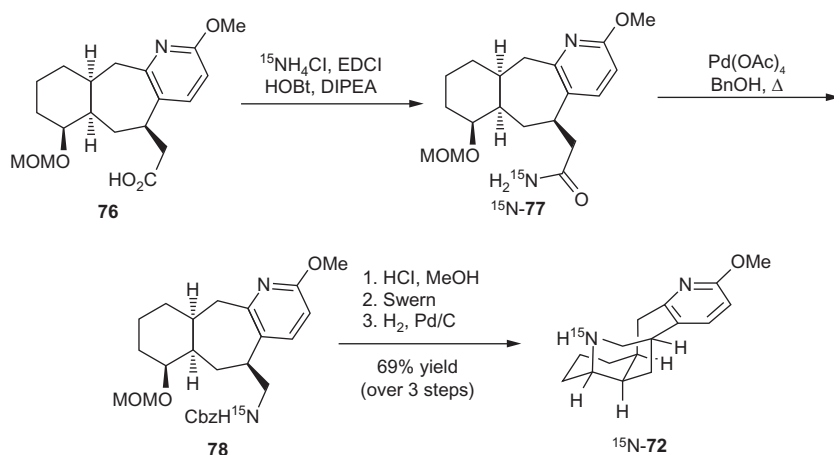
Indeed, treatment of dianion **75** (Scheme 19) with D₂O resulted in the exclusive formation of the *endo*-deuterated product **D-72** (72% D).

Examples of stereodivergence in the reaction of sterically encumbered lithium dianions based on electrophile have been previously documented by Applequist and by Glaze [28]. Furthermore, epimerization of heteroatom-stabilized carbanions in their reaction with electrophiles via a “conducted tour mechanism” has been reported by Cram [29]. In this pathway, the electrophile may interact with the minor lobe of the sp³-hybridized carbanion orbital, which would lead to an inversion in stereochemistry. Alternatively, a single electron transfer (SET) pathway could be operative involving one electron oxidation of dianion **75** by the electrophile followed by recombination to afford the inversion product (i.e., **76**).

To examine the stereoselectivity of the deprotonation of amine **72**, deuterated amine **D-72** (72% D) was treated with *n*-BuLi (2 equiv) and quenched with D₂O. Tetracycle **D-D-72** (85% D) was isolated supporting a stereospecific deprotonation at the internal (*endo*) position of **72**. Alternatively, quenching the dianion with H₂O afforded, exclusively, protio **72**. Overall, these studies support the deprotonation of the C6 *endo* proton and that quenching with D₂O or H₂O proceeds with retention.

6.1 NMR Studies of the Dianion Intermediate

In order to gain further insight into the structure of dianion **75**, we undertook a series of NMR studies in collaboration with the Collum group at Cornell University. It appeared that ¹⁵N and ⁶Li NMR studies using ¹⁵N-labeled amine ¹⁵N-**72** (Scheme 20) would provide the most insight, especially as it pertained to the direct observation of Li—N coupling. As such, the first order of business was the preparation of a ¹⁵N-labeled tetracycle. The synthesis of ¹⁵N-**72** was readily achieved using the sequence outlined in Scheme 20. This

**SCHEME 20** Synthesis of the ^{15}N -labeled tetracycle.

sequence commenced with the conversion of acid **76** to primary amide ^{15}N -**77** in 91% yield using standard amide coupling technology. A Hofmann rearrangement of ^{15}N -**77** was effected with $\text{Pb}(\text{OAc})_4$, which in the presence of benzyl alcohol provided benzyl carbamate **78** in 46% yield. Removal of the MOM protecting group, Swern oxidation and a hydrogenolysis/reductive amination afforded ^{15}N -tetracyclic amine ^{15}N -**72**.

First, treatment of ^{15}N -**72** with ^6Li -*n*-BuLi afforded a dianion intermediate (^{15}N -**75**), which was subjected to NMR spectroscopic studies. ^{15}N -decoupled ^6Li NMR of ^{15}N -**75** (Figure 3A) consists of two singlets (1:1 ratio), which corresponds to a dianion, which possesses two lithium ions in distinct environments. The ^6Li NMR of ^{15}N -**75** showed two doublets (Figure 3B). This observation nicely supports ^6Li — ^{15}N coupling for both lithium ions in the dianionic species. Consistent with this observation, the ^{15}N NMR spectrum of dianion ^{15}N -**75** (Figure 3C) shows a quintet resonance.

Further support for the proposed structure of the dianion intermediates that were observed by ^6Li - and ^{15}N -NMR was provided by DFT calculations (B3LYP/6-31G(d) with single-point MP2 correction) conducted by the Colium group, which identified tetrasolvated **81** (Figure 4) to be the most stable dianion structure of several possibilities.

6.2 Experimental Studies on the Reactivity of the Dianion Intermediate

In the successful synthesis of lyconadin A, iodine had emerged as the successful oxidant that converted the dianion intermediate to the desired pentacycle. Countless alternative oxidants such as metal salts ($\text{Pd}(\text{OAc})_2$, $\text{Cu}(\text{OTf})_2$ and FeCl_3) failed to effect the desired conversion. Upon further investigation, we discovered that other halogen electrophiles such as NCS, NBS, and NIS

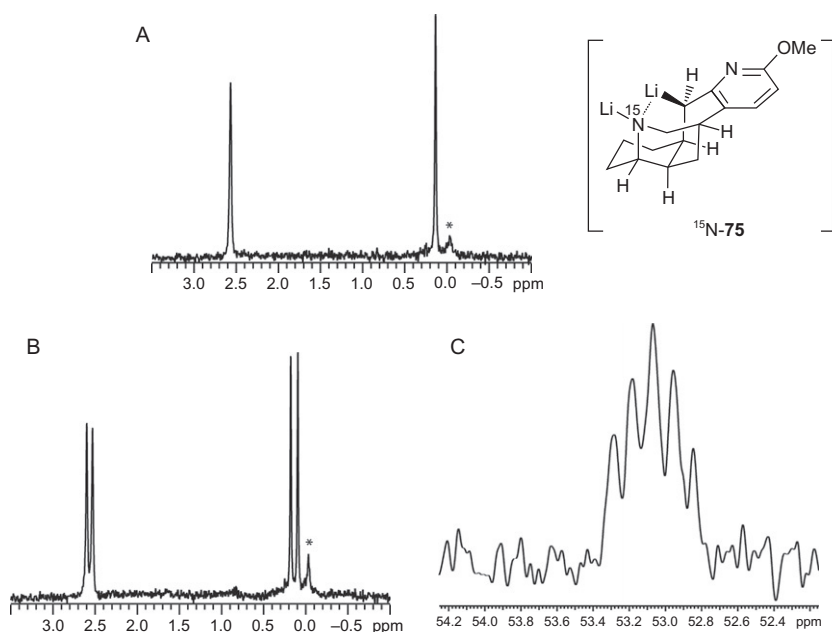


FIGURE 3 (A) ^{15}N decoupled Li NMR spectrum of 0.05 M $[^{15}\text{N}]\mathbf{75}$ and 2.0 equiv $[^6\text{Li}]n\text{-BuLi}$ in $\text{THF-}d_8$ at -90°C . *Denotes an impurity from $[^6\text{Li}]n\text{-BuLi}$. (B) ^6Li NMR spectrum of 0.05 M $[^{15}\text{N}]\mathbf{75}$ and 2.0 equiv $[^6\text{Li}]n\text{-BuLi}$ in $\text{THF-}d_8$ at -90°C . *Denotes an impurity from $[^6\text{Li}]n\text{-BuLi}$. (C) ^{15}N NMR spectrum of 0.05 M $[^{15}\text{N}]\mathbf{75}$ and 2.0 equiv $[^6\text{Li}]n\text{-BuLi}$ in $\text{THF-}d_8$ at -90°C .

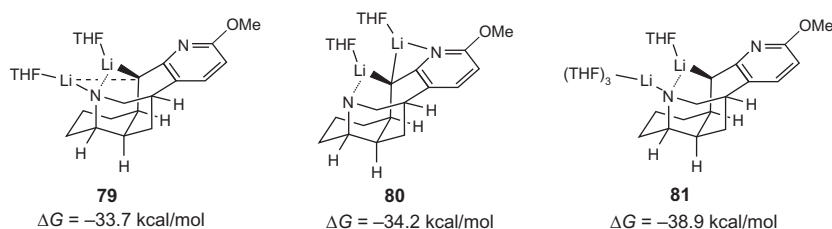
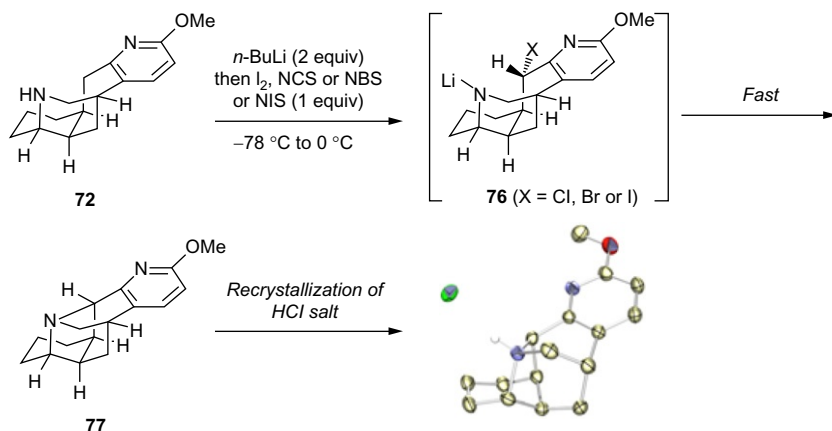
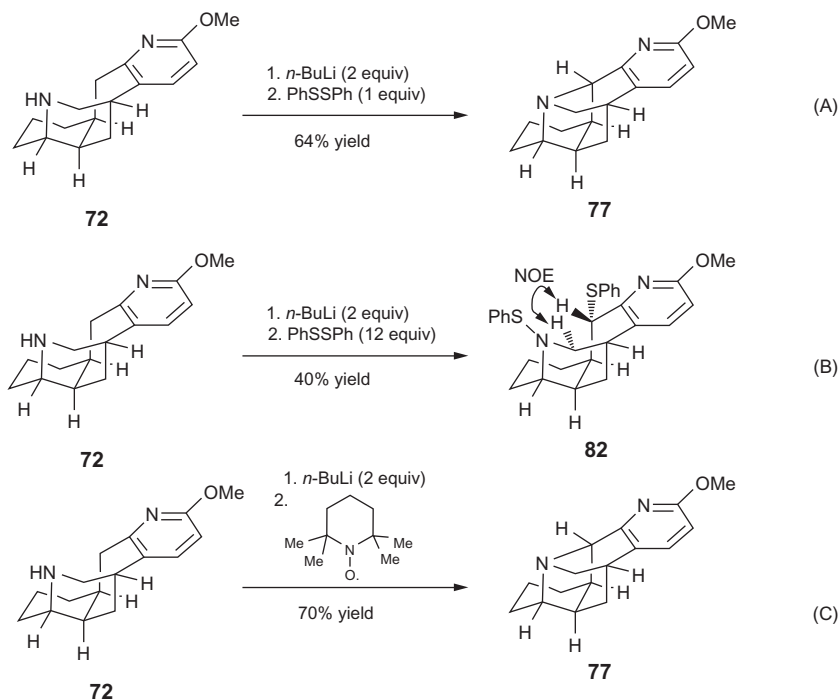


FIGURE 4 Relative energies of proposed dianion structures (calculated energies of **79** and **80** take into account two unbound THF molecules).

were also competent reagents for the formation of the pentacycle. Two mechanistic scenarios could potentially account for the success of halogen in this transformation. First, the halogen electrophile could react with the dianion to form **76** (Scheme 21) as an intermediate where the halogen group is introduced with inversion. Ensuing rapid C—N bond formation by intramolecular displacement of the halide would afford **77**. All our attempts to quench this reaction early in order to isolate the secondary amine that would correspond to **76** were futile and consistently led to the isolation of **77**, which was unambiguously identified on the basis of the X-ray diffraction studies of the



SCHEME 21 Proposed mechanism with halogen electrophiles.

SCHEME 22 Quenching studies of the dianion with PhSSPh and TEMPO.

corresponding HCl salt. This outcome strongly suggested that the C—N bond formation, if it were occurring via **76**, was rapid at $-78\text{ }^\circ\text{C}$.

In an attempt to isolate intermediates that result from quenching the dianionic intermediates with soft, polarizable electrophiles that may react similarly to the halogen electrophiles, diphenyldisulfide was identified.

Treating dianion **75** with PhSSPh (1 equiv) yielded the pentacyclic product **77** in 64% yield (Scheme 22A). Alternatively, exposure of **75** to an excess of PhSSPh (12 equiv) provided as the major product disulfide **82** (Scheme 22B) in 40% yield. These results, along with several observations that are not discussed here provided support for the possibility of inversion upon reaction of the dianionic intermediates with soft, polarizable electrophiles. However, in the case of the halogen electrophiles, the possibility of a single electron transfer process cannot be discounted given that treatment of dianion **75** with the single electron transfer oxidant TEMPO yields the pentacyclic product (**77**, Scheme 22C) in 70% yield.

7. CONCLUSION

Our synthesis of lyconadin A was our first foray into the synthesis of the *Lyco-podium* alkaloids, which has since been a rich area of investigation for our group. Although not our initial intention, this synthesis uncovered, in my mind, a remarkable direct C—N bond formation in complex systems that I believe holds a lot of promise for “stitching together complex molecules with nitrogen”.

ACKNOWLEDGMENTS

This chapter describes many of the details of our work in the area of lyconadin A. The majority of the work that is described was taken from the thesis of Scott P. West. This project would not have been possible without the dedication and tireless efforts of Scott P. West, a graduate student at the time, and Dr. Alakesh Bisai, who was a postdoc, as well as the contributions of their respective mentees, Andrew Lim and Raja Narayan. I am grateful to Professor David Collum and his student Dr. Josie Gruver for their expertise and excellent work on the collaborative study of the nature of the dianion intermediates. The intellectual contributions of many members of the Sarpong group as well as members of the Department of Chemistry at UC Berkeley are gratefully acknowledged. We thank Dr. Antonio DiPasquale for X-ray crystallographic analysis. This work was supported by the Department of Chemistry at UC Berkeley and in part by the National Institutes of Health (RO1 GM 086374). We also thank Eli Lilly, Amgen, Roche, Abbott, DuPont, Johnson and Johnson, and Astra Zeneca for support of our laboratory.

REFERENCES

- [1] For an account see: (a) <http://heathcock.org/chhgrp/Ravello/Ravello.ms.html>; (b) C.H. Heathcock, C. Chatgililoglu, V. Snieckus (Eds.), *Chemical Synthesis: Gnosis to Prognosis*, Kluwer, Dordrecht, 1996.
- [2] (a) W.A. Ayer, L.S. Trifonov, *Alkaloids*, Academic Press, 1994, vol. 45, p. 233; (b) X. Ma, D.R. Gang, *Nat. Prod. Rep.* 21 (2004) 752–772; (c) J.I. Kobayashi, H. Morita, *Alkaloids*, Academic Press, 2005, vol. 61, p. 1 ; (d) Y. Hirasawa, J. Kobayashi, H. Morita, *Heterocycles*, 77 (2009) 679–729.
- [3] (a) S.W. Grant, K. Zhu, Y. Zhang, S.L. Castle, *Org. Lett.* 8 (2006) 1867–1870; (b) M.R. Tracey, R. Hsung, *Abstracts of Papers*, 226th National Meeting of the American Chemical Society, New York, September 2003, 2003. ORGN 721 .

- [4] (a) D.C. Beshore, A.B. Smith III, *J. Am. Chem. Soc.* 129 (2007) 4148–4149.
- [5] T. Nishimura, A.K. Unni, S. Yokoshima, T. Fukuyama, *J. Am. Chem. Soc.* 133 (2010) 418–419.
- [6] For an account, see: C.H. Heathcock, *Angew. Chem. Int. Ed.* 31 (1992) 665–681.
- [7] M.A. Gray, L. Konopski, Y. Langlois, *Synth. Commun.* 24 (1994) 1367–1379.
- [8] J.W. Patterson, *Tetrahedron* 49 (1993) 4789–4798.
- [9] A. Haudrechy, C. Chassaing, C. Riche, Y. Langlois, *Tetrahedron* 56 (2000) 3181–3187.
- [10] (a) G. Majetich, *Tetrahedron* 51 (1995) 7095–7129; (b) M.E. Wolff, *Chem. Rev.* 63 (1963) 55–64.
- [11] Y. Shibnuma, T. Okamoto, *Chem. Pharm. Bull.* 33 (1985) 3187–3194.
- [12] T. Cohen, G.L. Deets, *J. Am. Chem. Soc.* 94 (1972) 932–938.
- [13] D. Grierson, *Org. React. (N.Y.)* 39 (1990) 85–295.
- [14] P. Rabe, K. Kindler, *Ber. Dtsch. Chem. Ges.* 51 (1918) 466–467.
- [15] A.C. Smith, R.M. Williams, *Angew. Chem. Int. Ed.* 47 (2008) 1736–1740.
- [16] B.L. Nilsson, L.E. Overman, J. Read de Alaniz, J.M. Rohde, *J. Am. Chem. Soc.* 130 (2008) 11297–11299.
- [17] (a) E.J. Corey, R.K. Bakshi, S. Shibata, *J. Am. Chem. Soc.* 109 (1987) 5551–5553; (b) E.J. Corey, R.K. Bakshi, S. Shibata, C.P. Chen, V.K. Singh, *J. Am. Chem. Soc.* 109 (1987) 7925–7926.
- [18] (a) For a recent review, see: J.S. Johnson, *Angew. Chem. Int. Ed.* 43 (2004) 1326–1328; (b) For an earlier account, see: H. Stetter, H. Kuhlmann, *Org. React.* 40 (1991) 407–496.
- [19] D. Ivanoff, A. Spassoff, *Bull. Soc. Chim. Fr.* 2 (1935) 76–78.
- [20] A.G. Csaky, J. Plumet, *Chem. Soc. Rev.* 30 (2001) 313–320.
- [21] (a) P.S. Baran, N.B. Ambhaikar, C.A. Guerrero, B.D. Hafensteinner, D.W. Lin, J.M. Richter, *Arkivoc* (2006) 310–325; (b) J.M. Richter, B.W. Whitefield, T.J. Maimone, D.W. Lin, M.P. Castroviejo, P.S. Baran, *J. Am. Chem. Soc.* 129 (2007) 12857–12869; (c) M.P. DeMartino, K. Chen, P.S. Baran, *J. Am. Chem. Soc.* 130 (2008) 11546–11560.
- [22] (a) C.L. Martin, L.E. Overman, J.M. Rohde, *J. Am. Chem. Soc.* 130 (2008) 7568–7569; (b) C.L. Martin, L.E. Overman, J.M. Rohde, *J. Am. Chem. Soc.* 132 (2010) 4894–4906.
- [23] C.M. Thompson, *Dianion Chemistry in Organic Synthesis*, CRC Press, Boca Raton, FL, 1994.
- [24] (a) H. Yamamoto, K.J. Maruoka, *J. Org. Chem.* 45 (1980) 2739–2740; (b) A. Alberti, F. Cane, P. Dembech, D. Lazzari, A. Ricci, G. Seconi, *J. Org. Chem.* 61 (1996) 1677–1681; (c) V. del Amo, S.R. Dubbaka, A. Krasovskiy, P. Knochel, *Angew. Chem. Int. Ed.* 45 (2006) 7838–7842.
- [25] R.D. Carpenter, A.S. Verkman, *Org. Lett.* 12 (2010) 1160–1163.
- [26] R.R. Fraser, T.S. Mansour, S. Savard, *J. Org. Chem.* 50 (1985) 3232–3234.
- [27] For a review of additions of electrophiles to dianions, see: A. Basu, S. Thayumanavan, *Angew. Chem. Int. Ed.* 41 (2002) 716–738.
- [28] (a) D.E. Applequist, G.N. Chmurny, *J. Am. Chem. Soc.* 89 (1967) 875–880; (b) W.H. Glaze, C.M. Selman, A.L. Ball Jr., L.E. Bray, *J. Org. Chem.* 34 (1969) 641–644.
- [29] D.J. Cram, L. Gosser, *J. Am. Chem. Soc.* 86 (1964) 2950–2952.

Selective Alkane C—H Bond Substitutions: Strategies for the Preparation of Functionalized Diamondoids (Nanodiamonds)*

Andrey A. Fokin[§] and Peter R. Schreiner^{||}

[§]*Department of Organic Chemistry, Kiev Polytechnic Institute, Kiev, Ukraine*

^{||}*Institute of Organic Chemistry, Justus-Liebig University, Giessen, Germany*

Chapter Outline

1. Introduction	317	3.1. Radical Reagents	322
2. Diamondoid C—H Bond Substitutions: An Exercise in Preparative Alkane Functionalization	320	3.2. Neutral Electrophiles	328
		3.3. Charged Electrophiles	330
		3.4. Single-Electron Transfer	342
3. Selectivities and Mechanisms	322	4. Concluding Remarks	345

1. INTRODUCTION

Natural diamond is the ultimate semiconductor as it displays the highest known thermal conductivity, dielectric constant, and electron saturation velocity of all materials. Hydrogen-terminated diamond surfaces are characterized by a negative electron affinity (NEA) that makes diamond potentially useful as a material for electron-emitting devices [1]. The major challenge for the practical utilization of diamond is the highly variable quality of natural, chemical vapor deposition (CVD), and detonation diamond [2]. These materials suffer from chemical non-homogeneity, surface and lattice imperfections, as well as from other growth defects such as stacking and twinning. Additionally, no natural diamond is like

* Dedicated to George A. Olah for his seminal contributions to hydrocarbon chemistry and on the occasion of his 85th birthday

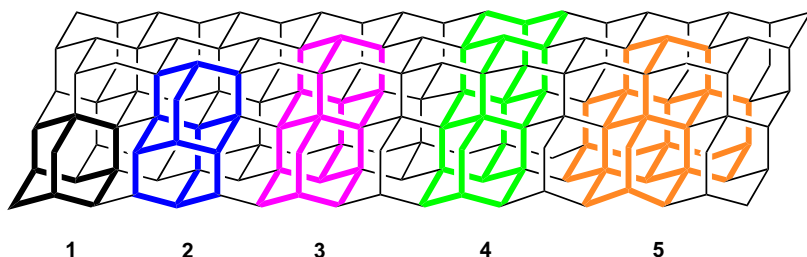


FIGURE 1 Adamantane (**1**), diamantane (**2**), triamantane (**3**), [121]tetramantane (**4**), and T_d -pentamantane (**5**) resemble parts of the diamond lattice.

another, and CVD as well as detonation diamond can also typically not be manufactured in the reproducible quality and purity required for many applications. This makes the use of diamond in nanoelectronics difficult as these require building blocks of well-defined shapes, sizes, and homogeneities.

Diamondoids represent parts of the hydrogen-terminated diamond crystal lattice (Figure 1) [3]. These nanometer-sized (starting at 0.5 nm), highly symmetric nanodiamonds (in plural form to differentiate them from nanodiamond material mixtures from CVD and detonation sources) are available as physically and chemically homogeneous materials and are currently viewed as a promising alternative to existing diamond-based electronics [4]. The nonisomeric lower diamondoids adamantane ($C_{10}H_{16}$, **1**), diamantane ($C_{14}H_{20}$, **2**), and triamantane ($C_{18}H_{24}$, **3**) are available both synthetically [5] and, as all other known diamondoids, in large amounts from petroleum [6,7]. [121] Tetramantane ($C_{22}H_{28}$, **4**), the first member of the virtually infinitely large family of higher diamondoids, can also be synthesized, but only in very small quantities by elaborate procedures [8]. Two other isomeric tetramantanes (of C_2 and C_{3v} symmetry) as well as many other higher diamondoids are available exclusively from natural sources and have been isolated and characterized up to decamantane [6,7,9]. There are six isomeric pentamantanes (T_d -pentamantane (**5**) is shown in Figure 1) and 24 hexamantanes (some of them were characterized individually) [3]. As the diamondoid order increases, the number of isomers increases as well. Beginning with the pentamantanes, they additionally are divided into different molecular weight subgroups. Nanodiamonds represent attractive hydrocarbon building blocks of various shapes (rods, disks, helices, prisms, pyramids, cubes) and sizes.

Functionalization is necessary to deliver electric charge to a material as well as to attach molecules to metal or semiconductor surfaces. Functional groups must be located at well-defined positions of the cage to keep the material chemically homogeneous. Such functionalization is more intricate than it appears as some diamondoids contain several chemically inequivalent C—H bonds (Figure 2). Even in the case of tertiary C—H bond, monosubstitution gives two isomers for **2** and **5**, four for **3** and **4**, and six for [1(2)3]tetramantane (**6**).

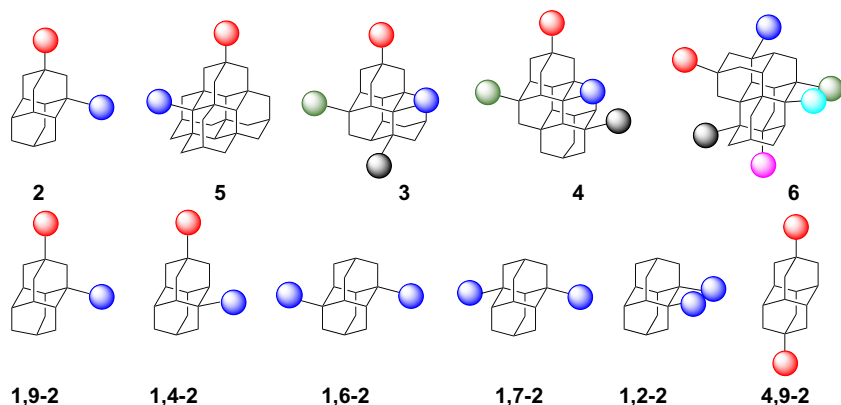


FIGURE 2 Number of the inequivalent tertiary C-H positions in monosubstituted diamondoid cages (top row) and in disubstituted diamantanes (2).

This is when our groups came into play. When Jeremy Dahl (a geochemist) and Bob Carlson (an organic chemist) isolated and purified diamondoids from petroleum sources [6] and reported this to their company's next higher administrative layer, the business units immediately saw a market for a new material that is available in very large quantities. A business unit was formed with the two chemists plus a much larger number of business people and engineers. The plans were bold and one foresaw—rightfully so—the enormous potential of these new materials. The required C—H bond functionalization for applications in polymers [10], as coatings, etc., was deemed routine and we were called on board because we had previously developed highly selective novel methods for scalable C—H bond functionalizations. Additionally, several other groups at world-renowned universities and institutes were supplied with diamondoid raw materials to produce selective OH-functionalized diamondoids in quantities beyond 100 g per batch. What a challenge! We were unsure at first whether it could be done without having to go through chromatographic separations, but eventually found the preparation of the apical and bis-apical hydroxy derivatives as the ideal entry point into this chemistry. As described in more detail below, the dinitroxylation in 100% HNO_3 (it is not as bad as it reads!) is a straightforward way for the initial functionalization [11] that is highly scalable. Water quenching delivers the dihydroxy derivatives that can be desymmetrized and converted to virtually any functional group. The alcohols themselves can readily be used for the preparation of monomers for subsequent polymerization. After a struggle for about two years, we were the only synthetic group left in the diamondoid game. However, the company's headquarters became increasingly impatient because the subcompany was not yet making a profit but supporting basic science (us!) instead. Already then we knew that the expectations were so different that this was not a long-lasting engagement. Much of the basic science had to be done first and we estimated about a good ten years of work to lay out ways to handle diamondoids properly. At the writing of this chapter, we just began year seven, so stay with us!

Double substitution results in six isomers for adamantane; for the higher diamondoids, such substitution leads to a very large number of isomers, unless the functionalization reactions are highly selective (Figure 2). Particularly attractive are the apical diamondoid derivatives (red circles), which are characterized by higher surface affinities than those that are medially substituted [12]. It has been shown that apical diamondoid thiols form highly ordered self-assembled monolayers on gold surfaces; such materials reproduce the NEA properties of surface hydrogen-terminated natural diamond, but with much higher electron-emitting efficiency [13]. These new hybrid metal/carbon materials with high H/C ratio are of great potential as key elements of cold cathodes and field emitting devices. There are many other potential applications of functionalized diamondoids, primarily as parts of ligands in catalysts for stereocontrolled organic reactions [14], as structural building blocks in organocatalysts [15], rigid building blocks for metal-organic frameworks (MOFs) [16], conformationally defined structural elements of non-natural oligopeptides for peptidomimetics [17], liquid crystal compositions [18], robust fluorescent photochromic materials [19], and as components for polymer formulations and pharmaceuticals, especially antivirals (1-(1-adamantyl)ethanamine, Rimantadine[®]) [20] and neuroprotectors [21]. The hydrochloride salt of 3,5-dimethyladamantan-1-amine (Memantine[®]) is most effective [22] for the treatment of Alzheimer's disease, and new drugs based on diamondoid derivatives are currently under study.

We attempted to make Memantine[®] available through the “petroleum route.” The common path involves reduction of acenaphthalene, Lewis-acid-catalyzed rearrangement to stabilometric 1,3-dimethyladamantane, a harsh bromination (boiling in ten-fold excess of Br₂), Ritter reaction of the resulting 1-bromo-3,5-dimethyl adamantane with acetonitrile, and finally hydrolysis to the ammonium salt (Memantine[®]). We envisioned obtaining the readily available 1,3-dimethyladamantane as a side product from diamondoid isolation directly, but negotiations never really got started because the demand for this material to produce all the Memantine[®] the world needed was around ten tons per year—much too small to start a business for an oil company! Nevertheless, we were successful in preparing 1-formamido-3,5-dimethyladamantane in one step [23]. Hydrolysis was much easier than from the acetamide so that this procedure is by far superior to the old way of preparation. We presented our results to the leading company distributing Memantine[®] and were pleased that they were interested in buying our patent, which they eventually did. Did we get rich? No.

2. DIAMONDROID C—H BOND SUBSTITUTIONS: AN EXERCISE IN PREPARATIVE ALKANE FUNCTIONALIZATION

Saturated hydrocarbons have historically been named paraffins (from *parum affinis*—lacking affinity) although Dumas showed as early as 1840 that the gas-phase chlorination of methane occurs easily [24]. In 1895, high-temperature

nitrations of paraffins with diluted nitric acid were developed by Konowalow [25]. These radical reactions are still industrially useful for lower alkanes. Enormous efforts to develop methods for practically useful alkane transformations, for example, methane to methanol or ethane to acetic acid conversions, are currently being investigated. Still, overreactions are a major problem in radical alkane chemistry that typically is characterized by low selectivities, rather than low reactivities. It was a real breakthrough for alkane chemistry when Landa showed that adamantane (**1**) reacts with neat bromine at room temperature to give the tertiary monobromo derivative almost quantitatively [26]. This discovery was followed by Schleyer's simple and convenient adamantane synthesis [27], which triggered the development of early diamondoid chemistry.¹ It was then shown that **2** [29] and **3** [30] are even more reactive toward bromine than adamantane. Such electrophilic halogenations are characteristic not only for diamondoids but also for many other cage compounds, for example, protoadamantane [31], homoadamantane [32], and dodecahedrane [33].

For a long time, alkanes were considered unreactive toward electrophiles until Olah developed a number of superacidic systems suitable for alkane isomerization and substitution in the 1960s [34]; however, such reagents are expensive and difficult to handle. Many preparatively useful transformations developed for adamantane, for example, oxidation with 96% H₂SO₄ [35], nitroxylation with 100% HNO₃ [36], selective bridgehead chlorination with ICl [37], have been elaborated for diamondoid functionalizations not involving radicals.

The suggested mechanisms for alkane C—H substitutions with electrophiles either involve hydride transfer through direct attack of E⁺ onto the C—H bond [38] or a carbon atom [39] in analogy to aromatic electrophilic substitutions. However, the term “hydride transfer” is not relevant in this case as hydrogens in alkanes carry a small positive charge, which increases *during* the H-shift reaction. The proposed electrophilic substitution mechanism should lead to the electrophile incorporated in the cage, which is, however, in contrast to experiment, where nucleophilic substitution is observed [37]. The mechanistic scenario of the attack of the electrophile onto the carbon of a C—H bond also is at variance with the high reaction orders (ca. 7.5 for adamantane bromination) [40], as well as large kinetic isotope effects (KIEs) of adamantane bromination and nitroxylation ($k_{\text{H}}/k_{\text{D}}=3.9$ and 4.4, respectively) [40,41]. These values are characteristic for linear transition structures (TSs) that are also typical for C—H activation with radical reagents. We suggested [42] that the C—H activation with charged electrophiles and conventional radicals all occur via linear or close to linear TSs (R· · · H · · · X), occupying opposite ends of the

1. A funny aside: one of the authors (PRS) received his PhD with Paul Schleyer under the condition that it must not have anything to do with adamantane or diamantane chemistry. Indeed, the PhD thesis focused on a different topic but eventually (in 2005) [28] diamondoid chemistry got a hold of the scientific escapee.

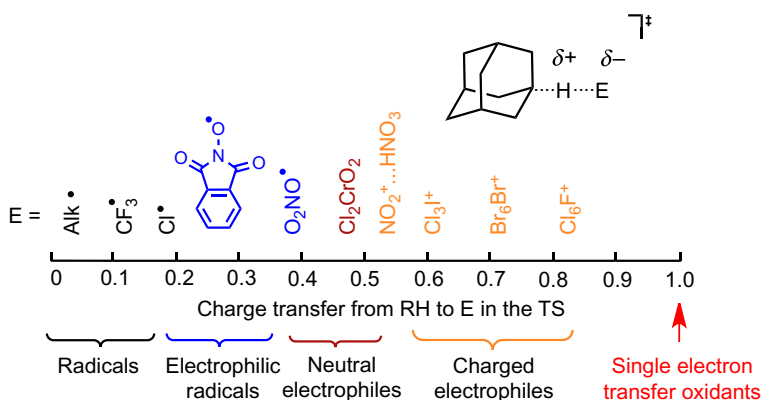


FIGURE 3 Degree of charge transfer in the transition structures for hydrogen abstraction from the tertiary C—H positions of adamantane with various electron-deficient species.

same mechanistic spectrum [43], only differing in the degree of charge transfer from the alkane to the electrophile (Figure 3). Radicals of low electrophilicity occupy the left part of the scale with charge transfer below $0.2e$. Electrophilic radicals like nitroxyl or phthalimide-*N*-oxyl (PINO) are characterized by only moderate charge transfer of 0.3 – $0.4e$.

Neutral electrophiles such as high-valent metal oxides and charged electrophiles are characterized by 0.6 – $0.8e$ charge transfer. Finally, complete removal of an electron corresponds to the reaction of an alkane with a single-electron transfer (SET) oxidant and occurs through formation of alkane radical cations. All varieties of the above reagents starting from radicals of low electrophilicity to powerful single-electron oxidants are useful for diamondoid chemistry. In the following, we will analyze the mechanisms, selectivities, and possible applications of all classes of these reagents for *preparative* diamondoid chemistry.

3. SELECTIVITIES AND MECHANISMS

3.1 Radical Reagents

The stabilities of the secondary and tertiary diamondoidyl radicals are virtually identical as the heats of formation of 1- and 2-adamantyl radicals are within 1 kcal mol^{-1} according to experimental [44,45] and computational [44] data; they are even slightly in favor of the 2-radical. As a result, the selectivities of the C—H bond substitutions in diamondoids with radicals depend almost exclusively on steric and polar effects in the TSs for hydrogen abstraction rather than on the stabilities of the resulting radicals and kinetic control prevails. The attack on the adamantane methylene groups is hindered

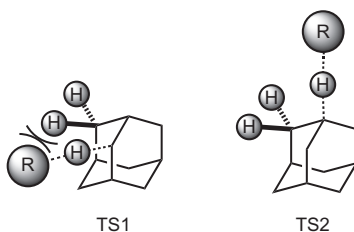
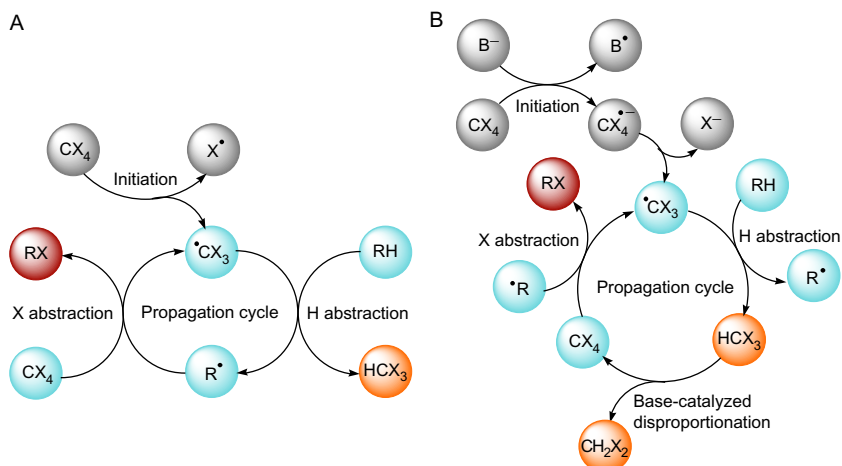


FIGURE 4 H abstraction from the secondary C—H position of adamantane is more sterically demanding (TS1) than from the tertiary position (TS2).

due to repulsive interactions between the approaching radical and the hydrogens of the neighboring methylene group (TS1, Figure 4); TS2 describes the attack on a tertiary C—H bond of adamantane, which is free of such unfavorable interactions.

Radical chlorinations [46] and brominations [47] of **1** with sterically unhindered halogen radicals, generated from photochemical or thermal decomposition of the respective *N*-halosuccinimides, are unselective (the statistically corrected tertiary to secondary ($3^\circ/2^\circ$) selectivity is less than 4). The highest selectivities were observed when bulky trihalomethyl radicals $\bullet\text{CHal}_3$ are involved in the H-activation step. Even for the relatively small CCl_3 radical, the selectivity is ($3^\circ/2^\circ$) = 21 [48] and reaches a value of 130 for the bulky triiodomethyl radical CI_3 [49]. Perfluoro-*n*-alkyl iodides for the direct radical iodination of adamantane give only $3^\circ/2^\circ$ = 27 [50] due to partial loss of steric control by less sterically hindered perfluoro-*n*-alkyl radicals in the H-abstraction step. Typically, trihalomethyl radicals are generated from homolysis of the respective tetrahalomethanes CX_4 (initiation, Scheme 1A). The trihalomethyl radical $\bullet\text{CX}_3$ thus formed abstracts a hydrogen atom from the respective hydrocarbon forming an alkyl radical, which participates in the propagation cycle with CX_4 to give the desired halogenated alkane RX . Halogen economy was achieved under phase-transfer catalytic (PTC) conditions that allow the base-induced disproportion of dihalo- and tetrahalomethanes (Scheme 1B) [51]. As happens quite often in science, our alkane PTC halogenation reaction was discovered accidentally when we found that, upon generation of dibromocarbene in the $\text{HCBBr}_3/\text{NaOH}$ system, substantial amounts of the C—H bromination products form from adamantane together with the expected carbene insertion product [52]. We were quite puzzled by these findings but realized that the observed side reaction was actually much more interesting than the mundane dibromocarbene C—H insertion. When we found that haloforms can equilibrate (disproportionate) with dihalomethanes and tetrahalomethanes [51], we realized that we had found a novel way for generating trihalomethyl radicals without radical initiators. Although many people had used CBr_2 for C—H bond insertions, the side



SCHEME 1 Conventional radical alkane C—H halogenations with tetrahalomethanes (A) and PTC halogenation in the presence of base (B).

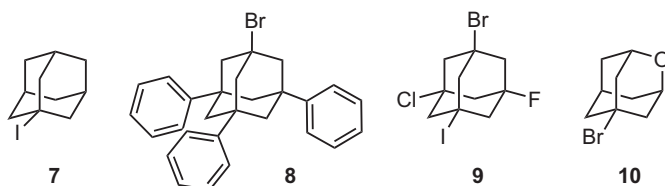


FIGURE 5 Selected adamantane derivatives obtained through the phase-transfer halogenations.

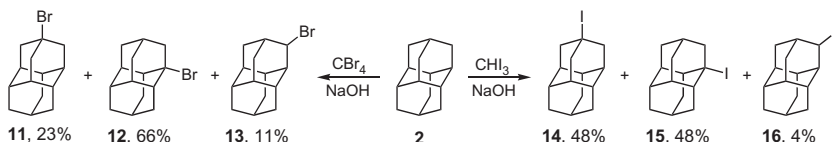
products apparently were never analyzed. This is even more surprising as the corresponding insertions with diiodocarbene historically gave extremely poor yields of insertion product, but a substantial amount of other iodo derivatives [53].

The PTC approach is highly useful when traditional halogenations with halogen radicals fail and it was successfully applied (Figure 5) to preparatively iodinate (with iodoform) **1** (53% of **7**) [51], brominate (with tetrabromomethane) [52], a large variety of alkanes even in the presence of aryl groups (89% of triphenyladamantane **8**) [54]. Halogenation can even be accomplished without halogen exchange (in the synthesis of 1-fluoro-3-chloro-5-bromo-7-iodoadamantane, **9**), and with highly deactivated compounds (39% of 5-bromo-2-oxadamantane, **10**) [55]. Compound **9** clearly is an academic “can it be made” exercise. It does, however, also prove the versatility of the method because we are unaware how to otherwise prepare this compound or an even more difficult one, 1-fluoro-3-chloro-5-bromo-7-iodocubane [56]. The context in which we placed these two compounds is that we were curious to see what happens when you geometrically perform a centrosymmetrical stretch

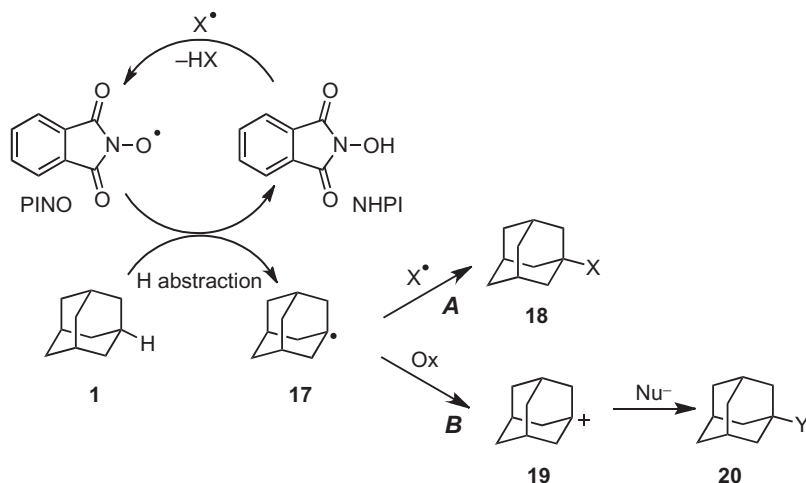
from the corresponding methane to the cubane and finally the adamantane derivative.

Steric factors also play a dominant role in the differentiation between the tertiary C—H positions of diamantane (**2**) in halogenations under the PTC conditions (Scheme 2) where tertiary (**11**, **12**, **14**, and **15**) and secondary (**13** and **16**) halogen derivatives form [28]. While the CBr_3 -radical is not able to distinguish between the medial (C^1) and apical (C^4) positions of the cage ($3^\circ(\text{C}^1)/3^\circ(\text{C}^4)=1$), the bulky CI_3 -radicals attack the less hindered apical position predominantly with $3^\circ(\text{C}^1)/3^\circ(\text{C}^4)=3$. In the latter case, high tertiary over secondary selectivity is also observed ($3^\circ/2^\circ=36$).

The selectivities for the C—H bond functionalizations substantially increase with electrophilic radicals. The phthalimide *N*-oxyl (PINO) radical was first suggested as a key intermediate in the aerobic oxidations of polycyclic compounds in the presence of *N*-hydroxyphthalimide (NHPI) [57]. The initiation requires formation of PINO via H abstraction from NHPI with a radical or another oxidant. The hydrogen abstraction with the electrophilic PINO radical is highly selective due to polar effects in the TSs for hydrogen abstraction (Scheme 3). By analogy to the ca. 12 kcal mol^{−1} higher stability of the tertiary over the secondary adamantyl cation [40], the polarization of the cage



SCHEME 2 PTC halogenations of diamantane (**2**).

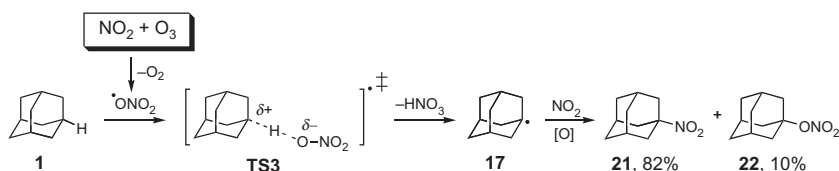


SCHEME 3 Adamantane functionalizations in the presence of *N*-hydroxyphthalimide (NHPI).

through the tertiary C—H bond is more favorable. As a result, only traces of the secondary substitution products form in NHPI oxidations of adamantane. The great advantage of this method is that NHPI can be reoxidized and may be used in catalytic amounts. The selectivities are usually much higher than in aerobic Fenton- or Gif-oxidations of adamantane [58]. There are various combinations of reagents for NHPI-assisted radical oxidations (Scheme 3, A) for the preparation of adamantane derivatives in the presence of cobalt catalysts ($X=O_2$) [59], for catalytic nitrations ($X=NO_2$) [60], and halogenations ($X=Cl, Br$) [61]. A second bromine-free method for the preparation of the neuroprotector Memantine[®] from our laboratories utilizes aerobic oxidation of 1,3-dimethyladamantane [62]. Hydroxy derivatives form as the main products in the oxidation of **2** and **3** with molecular oxygen in the presence of NHPI [62]. The NHPI-assisted oxidation with molecular oxygen is now used industrially for the preparation of 1,3-dihydroxyadamantane [63]. Strong oxidants, such as nitric acid or cerium (IV) ammonium nitrate (CAN), oxidize the radical intermediates to the respective carbocations (**19**, Scheme 3, B) and give products resulting from *nucleophilic* capture (acetamide **20**, $Y=NHC(O)CH_3$, if acetonitrile used as a solvent) [64].

High selectivities were observed in the functionalizations of **1** with the extremely electrophilic nitrate radical $\bullet ONO_2$, which can conveniently be generated through photochemical decomposition of CAN [65]. Alternatively, the nitrate radical was obtained through the oxidation of nitrogen dioxide with ozone (Kyodai nitration of aliphatic hydrocarbons) [66]. The $3^\circ/2^\circ$ selectivities in the case of Kyodai nitration of **1** exceed 50 due to polar effects in the TSs for H abstraction (TS3, Scheme 4). This is evident from the negative slope ($\rho = -2.81$) in the relationship between the nitration rates of substituted adamantanes and the electron induction parameter σ_1 [67]. This reaction displays high positional selectivity and converts **1** quantitatively to a mixture of tertiary nitrates and nitro derivatives (Scheme 4). This is due to the nature of nitrogen dioxide that gives both N- (**21**) and O- (**22**) recombination products in the adamantane radical (**17**) trapping step.

Nitrate radicals generated through photochemical decomposition of CAN [65] are quite selective ($3^\circ/2^\circ = 62$) in acetonitrile solution [68]. However, substantial amounts of O-recombination products form (1-nitroxadamantane, **22**) together with 1-acetaminoadamantane.



SCHEME 4 Kyodai nitration of adamantane involving the highly electrophilic nitrate radical $NO_3\bullet$.

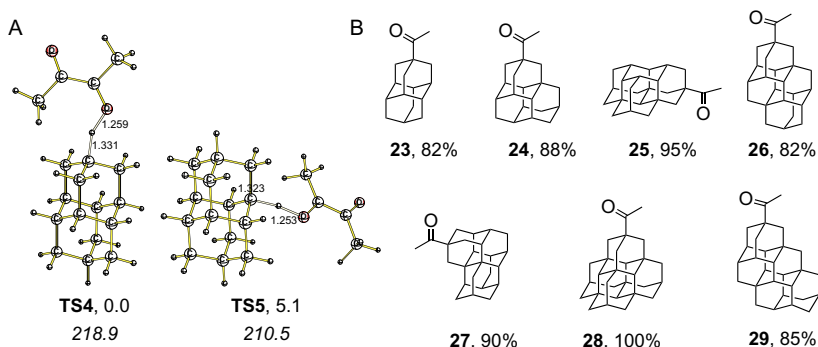
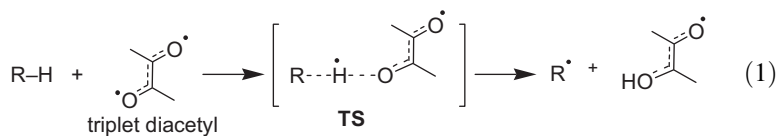


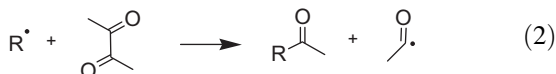
FIGURE 6 B3LYP/6-31(d) transition structures (A) for the hydrogen abstraction from the apical (TS4) and medial (TS5) positions of **2** with triplet diacetyl; selected bond lengths in Å, relative energies in kcal mol⁻¹, and the polarizabilities (B^3 , italics). The apical acetyl derivatives (**23**–**29**) obtained from the photoacetylation of the respective diamondoids and apical substitution selectivities (B).

Photoacetylation with diacetyl (CH_3CO)₂ is among the most selective radical reactions for the preparation of functionalized diamondoids [69]. Mechanistically, this reaction proceeds as an H abstraction with the triplet diacetyl diradical, generated through photoexcitation [70]. In contrast to the reaction with the PINO and nitroxy radicals, polar effects play only a minor role in determining the selectivity ($\rho^* = -0.71$ for the rates of oxidation of substituted adamantanes plotted vs. σ_1) and for a long time the reasons for the observed high tertiary selectivities were not clear [70]. It was suggested that the selectivities are governed by the higher polarizabilities of the cages in the apical direction that favors apical substitution in solution [69]. This is illustrated by the TSs for the H abstraction with triplet diacetyl from the apical and medial positions of **2** (TS4 and TS5, respectively, Figure 6), where the lowest energy structure is more stable in solution due to the higher polarizability of the cage in the apical direction (Figure 6A) [69].

This situation holds for all other diamondoids studied, for example, for the selective preparation of acetyl derivatives **23**–**29** (Figure 6B). The apical selectivities for the acetylation of diamondoids usually are high and exceed 4:1 in all cases: Even for the most difficult case, the acetylation of [123]tetramantane (**6**, Figure 2), which may give six tertiary C—H substitution products, the apical acetyl derivative **27** dominates. The photoacetylation mechanism was studied on the basis of a comparative analysis of the experimental deuterium KIEs as well as the observed C—H bond substitution selectivities [69]. The reaction proceeds as a nonchain radical process through hydrogen abstraction from the diamondoid with triplet diacetyl as the rate-limiting step (Eq. 1) followed by fast diamondoidyl radical trapping with diacetyl (Eq. 2).

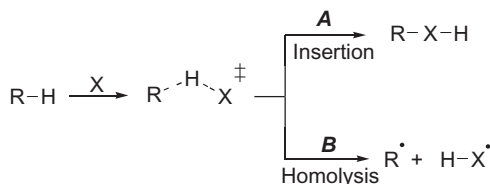


R = diamondyl



3.2 Neutral Electrophiles

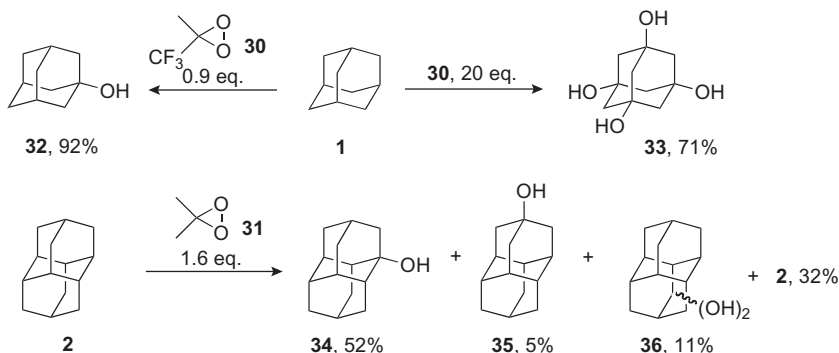
There are numerous examples for the use of neutral electrophiles for diamondoid functionalizations. Among them, dioxiranes, peracids, and metal–oxo reagents demonstrate the highest selectivities and are preparatively most useful. Mechanistically, these transformations are not well understood as these reactions may occur either through concerted insertion into the C–H bonds of an alkane or through so-called molecule-induced homolysis, where two radical species form from neutral closed-shell reactants (Scheme 5). Additionally, these reactions are quite sensitive to the presence of oxygen and radical traps.



SCHEME 5 C–H activation with neutral electrophiles occurs either through concerted insertion or molecule-induced homolysis.

Methyl(trifluoromethyl)dioxirane (**30**) and dimethyldioxirane (**31**) are effective electrophiles [71] for functionalizations of aliphatics and are very useful for selective diamondoid functionalizations. With these electrophiles, **1** forms products from tertiary C–H substitution almost exclusively. The results of the oxidations of **1** with **30** depend on the amount of the reagent employed. With close to equimolar amounts of **30**, 92% of 1-hydroxyadamantane (**32**) forms [72], while a 20-fold excess of the oxidant provides 1,3,5,7-tetrahydroxyadamantane (**33**) in 71% isolated product yield (Scheme 6) [73].

The main challenge in the oxidations of diamondoids with dioxiranes is overoxidation, as it is difficult to halt the reaction at the monosubstitution level. Diamantane (**2**) gives a mixture of monohydroxy derivatives **34** and **35** in the reaction with **31**, together with substantial amounts of isomeric dihydroxy derivatives **36** even at only 60% conversion of **2**. Remarkably, no secondary C–H insertion products form in the reactions of diamondoids with dioxiranes. A possible explanation lies again in the role that polar effects play in the TSs for oxygen insertion. The decisive influence of electronic factors



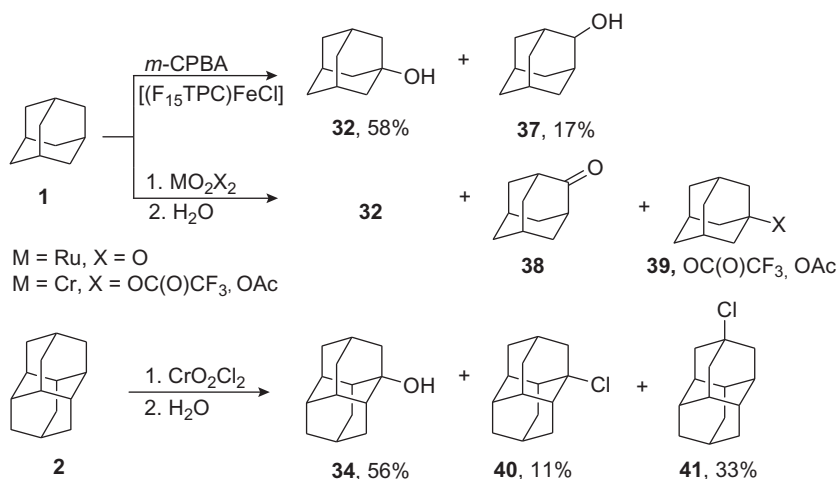
SCHEME 6 Functionalizations of diamondoids with dioxiranes **30** and **31**.

was confirmed by the excellent correlation of the Taft σ_I constants with the rates of oxidation of substituted adamantanes with **30** ($\rho_1 = -2.39$) [74].

In general, reactions with dioxiranes are recommended for polyhydroxylations of diamondoids, rather than for selective monosubstitution. The same is true for the oxidations of diamondoids with peracids as there are many mechanistic similarities between these transformations: It was shown that the reactions of peracids with tertiary C—H bonds of alkanes proceed as synchronous peroxy-oxygen insertions [75]. The combination of chromyl oxidants with H_5IO_6 gives **32** in high yield [76] due to formation of highly electrophilic Cr(VI) species that contain peroxo moieties. In contrast to dioxiranes, satisfactory conversions for the oxidations of **1** with *m*-chloroperbenzoic acid (*m*-CPBA) were achieved in the presence of either oxygen or solvents such as CCl_4 and CBrCl_3 that are prone to homolysis. However, trace amounts of secondary C—H substitution products form even in inert solvents [77]. The oxidations of **2** with *m*-CPBA in inert solvents are very similar to those of the oxidation with **31**.

Transition metal complexes are powerful catalysts in the oxidations of saturated hydrocarbons with peracids. It is believed that high-valent metal-oxo species formed *in situ* are responsible for the C—H substitution selectivities. Adamantane (**1**) is effectively oxidized by *m*-CPBA with *meso*-tris(pentafluorophenyl)corrolato iron(IV) chloride [$(\text{F}_{15}\text{TPC})\text{FeCl}$] [78], but the regioselectivity ($3^\circ/2^\circ = 10$) is reduced due to formation of 2-hydroxyadamantane (**37**) (Scheme 7). Similar selectivities were found recently in many adamantane oxidations with *m*-CPBA catalyzed by tris(2-pyridylmethyl) amine nickel(II) $\text{Ni}(\text{TPA})$ [79] and iron [80] complexes.

High-valent metal-oxo reagents are reactive species in C—H functionalizations themselves, and they represent another class of effective electrophiles for C—H bond activation. The $3^\circ/2^\circ$ selectivities for diamondoid substitutions are usually high [81], as the metal-oxo reagents involve the metal in a high oxidation state and this causes significant charge transfer from the



SCHEME 7 Oxidations of **1** and **2** with *meta*-chloroperbenzoic acid and metal–oxo reagents.

hydrocarbon moiety to the reagent in the TSs for hydrogen abstractions. The oxidations with RuO_4 give only trace amounts of the secondary C—H substitution product (adamantan-2-one, **38**, Scheme 7) [82]. This agrees well with the high negative ρ values for the Taft correlation for the oxidation of 1-substituted adamantanes with RuO_4 (-2.5 ± 0.2) and, together with the high KIEs observed experimentally ($KIE = 4.8 \pm 0.2$), provides evidence for highly polar and close to linear TSs for C—H activations with this reagent [82]. The high charge-transfer values (ca. $0.7e$) were estimated computationally for adamantane reacting with chromic acid H_2CrO_4 [83]. As a result of such strong charge-transfer control, the oxidations of diamondoids with covalent chromyl-oxo reagents demonstrate the highest positional selectivities among metal–oxo species. For instance, highly electrophilic chromyl trifluoroacetate oxidizes adamantane at room temperature forming exclusively the products of tertiary C—H substitutions [84]. The same selectivity is characteristic for chromyl acetate $CrO_2(OAc)_2$ and chromyl chloride CrO_2Cl_2 [83]. Unfortunately, a mixture of tertiary chloro-, acetoxy-, and hydroxy-derivatives forms, both for **1** [83] and **2** [28], which limits the applications of these metal–oxo reagents in the preparative diamondoid chemistry. Other metal–oxo reagents are far less effective; for instance, photooxidation of adamantane on TiO_2 gives a mixture of tertiary and secondary substitution products [85].

3.3 Charged Electrophiles

Charged electrophiles are among the most useful in diamondoid chemistry and most preparative functionalizations utilize these reagents. As H abstractions with charged electrophiles occur through highly polarized TSs (H-coupled

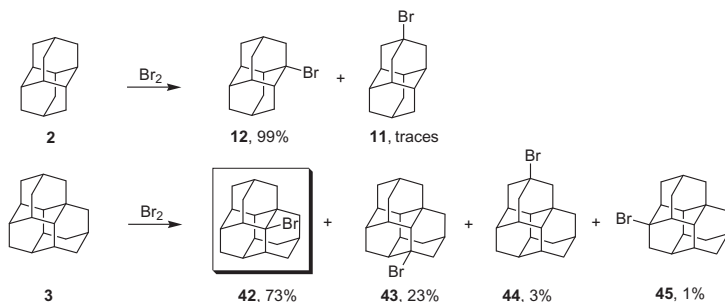
electron transfer) [40], this provides two advantages: tertiary substitution completely dominates, and due to the deactivation of the cage after incorporation of the electrophile, complete conversion of starting material gives high yields for monosubstitution products. This is in marked contrast to the chemoselectivities observed for radical reagents that are much less sensitive to polar effects. As mono- and polyfunctionalizations in electrophilic media could be performed selectively, we will analyze these approaches separately. Concentrated H_2SO_4 /oleum, neat bromine, and anhydrous (100%) nitric acid are among the most typical electrophilic media for preparative diamondoid functionalizations. Bromination with the neat bromine, which was first discovered for **1**, gives 1-bromoadamantane exclusively [26]. Mechanistically, this reaction is viewed as a hydrogen abstraction with positively charged halogen clusters, and it was modeled computationally for halogen-solvated halonium cations Hal^+Hal_n and protonated halogens H^+Hal_n [40]. The computational model agrees well with the experimental kinetics and KIEs for bromination of **1** [40]. The charge transfer in the corresponding TSs reach $0.7e$, thereby occupying the right part of the mechanistic scale in Figure 3. The electrophilic species responsible for hydrogen abstraction is the solvated nitronium cation NO_2^+ in anhydrous nitric acid and protonated sulfur trioxide HSO_3^+ in concentrated sulfuric acid or oleum.

3.3.1 Monofunctionalizations

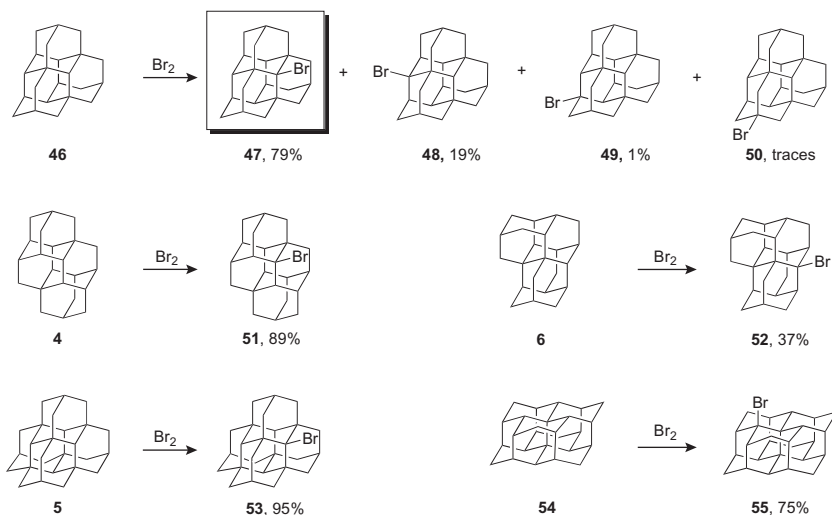
Many diamondoids can readily be brominated with neat bromine and they show much higher reactivity toward this reagent than the parent adamantane. These reactions occur at room temperature (and sometimes even require cooling and dilution with an inert solvent) and give tertiary bromo derivatives exclusively. The ratio of bromides thus obtained is determined by the relative stabilities of the corresponding tertiary diamondoid carbocations. The apical carbocations are usually less stable than the medial ones as the charge can more effectively be delocalized through the entire cage if placing the cationic carbon closer to the geometrical center of the molecule. In the case of **2**, substitution of the medial position is also favored statistically and 1-bromodiamantane (**12**) forms almost quantitatively (Scheme 8) [86]. Triamantane (**3**) gives all possible tertiary bromides, where 2-bromotriamantane (**42**) forms as a main reaction product, while the apical bromide **44** forms only in trace amounts. Bromide **42** could be separated from the isomeric bromides by crystallization from hexane in 50% yield [87].

Bromination is the most practical way to prepare the medial derivatives of higher diamondoids (Scheme 9). Bromination of [1(2)3]tetramantane (**46**) gives predominantly medial bromide **47**, which is separable from the reaction mixture by crystallization due to its high symmetry [3]. Medial bromination of **4** is even more selective and gives bromide **51** in 89% preparative yield [87].

Chiral diamondoids are likely to find applications as ligands in catalysis and as building blocks for nonlinear optical materials. [1(2)3]Tetramantane



SCHEME 8 Bromination of lower diamondoids **2** and **3**.



SCHEME 9 Brominations of higher diamondoids **5**, **6**, **46**, and **54** occurring predominantly in the medial positions of the cages.

(6) belongs to a new class of chiral molecules, namely σ -helicenes [88], and is available in optically active form [89]. Remarkably, bromination of **6**, which contains six inequivalent tertiary C—H positions, gives one dominant medial bromide (**52**), which was isolated in pure form after two recrystallizations of the reaction mixture in 37% yield [10]. The absolute configuration of bromide **52** was determined through X-ray crystal structure analysis under conditions of anomalous dispersion [89]. The assignment of the absolute configuration of **6** caused quite some dispute in the group as we all had trouble seeing the helix in **6**. Moreover, the initial configurational assignment relied on data that were initially not well converged (large *R*-factor) but agreed with the (*M*), (*P*)-assignments found Bob Carlson's book chapter on higher diamondoids [90].

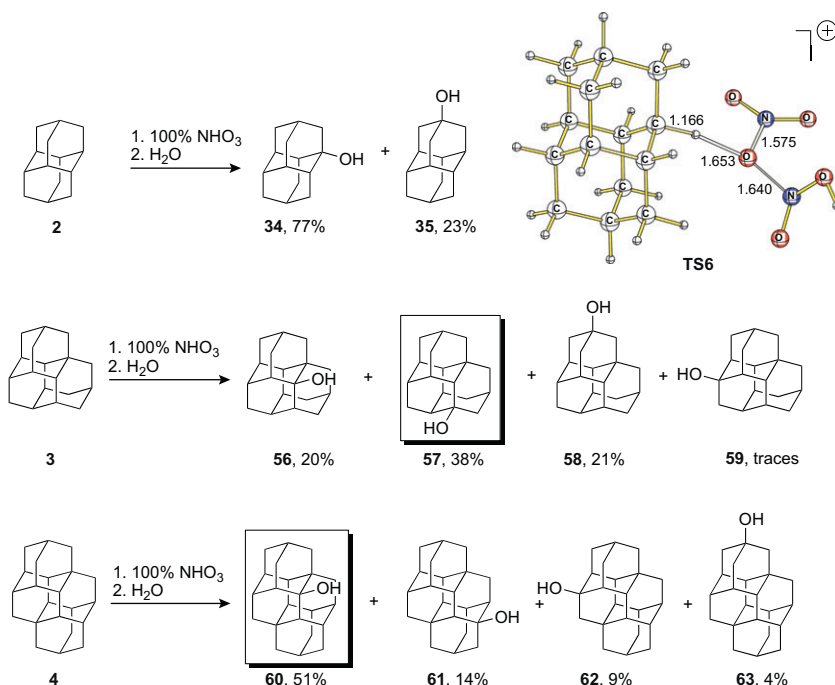
However, the computations assigned exactly the opposite configurations! What to do? Dismiss the computations as some may think these *must* be wrong if the X-ray analysis says something else? We chose to carefully look at *all* of the data again and found no flaw with the computed and measured ORD data but, there were only five data points for comparison. Additionally, we recorded and computed vibrational circular dichroism spectra that gave a very large number of lines to be compared. Again, the agreement between these two was excellent. So we requested further refinement of the X-ray data—*voilà!*—suddenly the configurational assignment had to be changed and matched that of all other experiments and computations. The only sad point we found is that the (*M*),(*P*)-assignment of **6** in Bob Carlson's book chapter was inadvertently incorrect. It is rather pleasing to see that quantum mechanical computations now have reached a maturity that even allows the assignment of absolute configurations with very high confidence.

The bromination of the next larger diamondoid representatives, tetrahedral *T_d*-pentamantane (**5**) and prism-shaped cyclohexamantane (**54**) [7], is highly selective due to the high symmetry of the cages, and a much smaller number of inequivalent C—H positions. Medial bromide **53** is the only product of the bromination of **5**. The excellent solubility of **5** in organic solvents allows its monobromination in high yields. In contrast, because of the poor solubility,² the bromination of **54** must be conducted only up to 30% conversion in order to be able isolate the monobromination product. Under these conditions, we found 2-bromocyclohexamantane (**55**) as the only reaction product (Scheme 9) [3]. This is in line with the relative stabilities of the tertiary cyclohexamantyl cations, among which the medial 2-cyclohexamantyl cation is ca. 1 kcal mol^{−1} more stable than the axial 3-cation [3].

The substitution selectivities change when anhydrous nitric acid is used as the electrophilic medium. As in classic aromatic electrophilic substitutions, the solvated nitronium cation [91] is responsible for the C—H activation. However, in contrast to reactions of aromatics, in diamondoids the *nucleophilic* part of the reagent (NO₃[−]), rather than electrophilic part (NO₂⁺) is incorporated into the substrate. As a result, **1** gives the nitroxy derivative, which forms 1-hydroxyadamantane almost quantitatively after hydrolysis [92]. The same is observed for the reactions of **1** and **2** with other nitrogen-containing electrophiles. Examples include the formation of tertiary fluorides with nitronium tetrafluoroborate NO₂⁺BF₄[−] in presence of HF [93], nucleophilic substitutions with other nitronium salts [94], and the formation of amido derivatives with nitriles in the presence of nitrosonium phosphorus pentafluoride NO⁺PF₆[−] [95].

The TSs for H-coupled electron transfer with nitronium reagents were computed at B3LYP/6-31G(d) for the nitronium cation complex with HNO₃ to model solvation effects explicitly [28]. The hydrogen abstraction with a

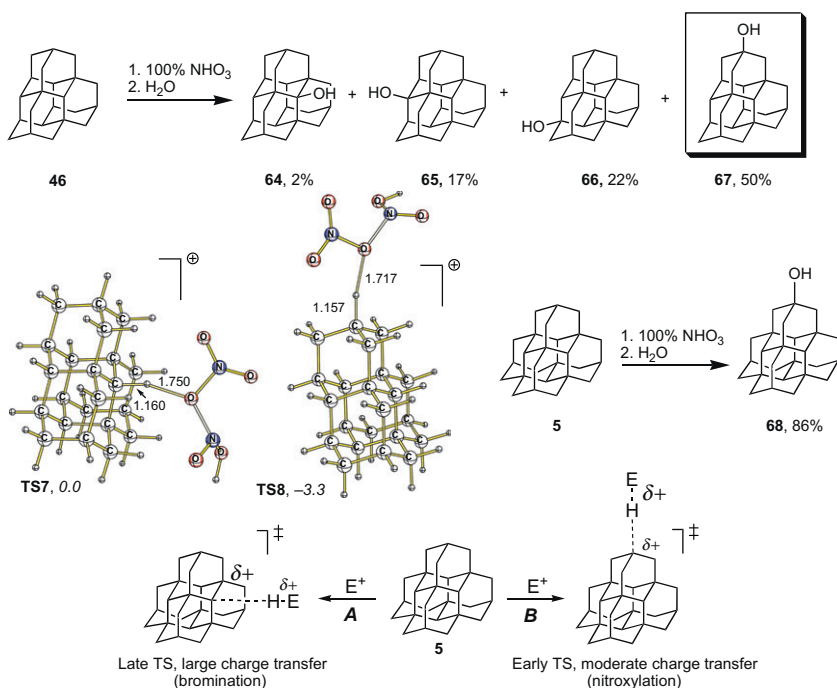
2. The solubility of cyclohexamantane (**54**) was too low to observe the signal of the quaternary carbons in its initially recorded and published ¹³C NMR spectrum [9].



SCHEME 10 Functionalizations of diamondoids **2–4** with anhydrous nitric acid and the transition structure for the hydrogen abstraction from the medial position of **2** with nitronium cation complex with nitric acid (**TS6**, B3LYP/6-31G(d)).

$\text{NO}_2^+ \cdots \text{HNO}_3$ complex is characterized by only a moderate charge transfer of ca. $0.5e$ (**TS6**, Scheme 10) [96], and steric effects play an important role in determining hydrogen abstraction selectivities with anhydrous nitric acid. In contrast to bromination, substantial amounts of the apical derivative **35** form in the case of **2** (Scheme 10) and the 3-hydroxy derivative (**57**) is a main product of the reaction of **3** with nitric acid. This is in marked contrast to the reaction of **3** with bromine, which predominantly gives the medial 2-derivative **42** (Scheme 8). The nitroxylation/hydrolysis of **4** mostly gives statistically favored medial derivatives **60** and **61**; another medial alcohol **62** forms together with small amounts of apical alcohol **63**.

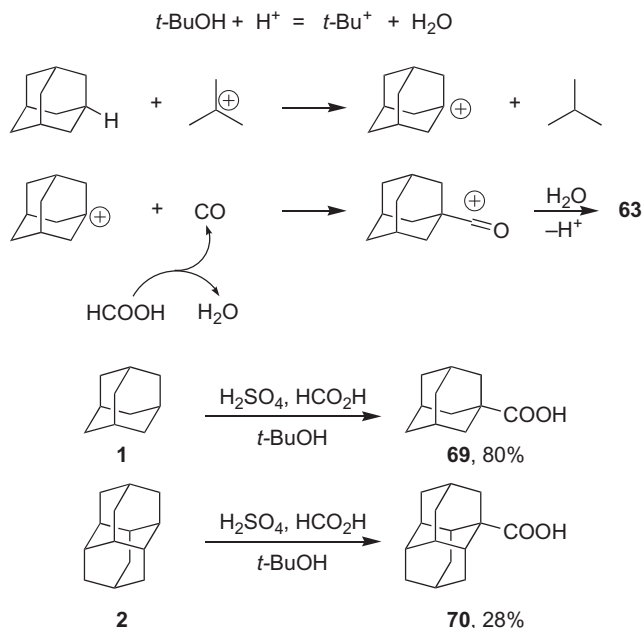
Remarkably, the apical derivative **67** dominates in the reactions of **46** with nitric acid (Scheme 11). This is due to the medial tertiary C—H bond being located on the planar C—H surface that shields it from the attack of the reagent. This could be easily verified through the comparative analysis of the critical $\text{H} \cdots \text{O}$ distances in the TSs for hydrogen abstraction with the $\text{NO}_2^+ \cdots \text{HNO}_3$ complex from the medial (**TS7**) and axial (**TS8**) position of **46** where this distance is substantially longer for medial attack (1.750 vs. 1.717 Å).



SCHEME 11 Functionalizations of diamondoids **5** and **46** with anhydrous nitric acid and the transition structures for the hydrogen abstraction from the medial (**TS7**) and axial (**TS8**) positions of **46** (B3PW91/cc-pVDZ, $\Delta\Delta H^\ddagger$ relative energies in kcal mol⁻¹, italics).

Pentamantane (**5**) shows the most pronounced differences in the regio-selectivities of halogenation versus nitroxylation: While bromination of **5** only gives the medial substitution product **53** (Scheme 9), nitroxylation exclusively proceeds with formation of the apical derivative **68** (Scheme 11). This is due to different contributions of polar effects in the H-abstraction TSs. With halogens, the high charge transfer leads to late carbocation-like TSs (Scheme 11, bottom, path **A**). Since the medial carbocation is more stable than the apical one, the bromination occurs specifically in the medial position of **5**. In contrast, the charge transfer in the reaction with nitrogen electrophiles is much lower and the substitution is controlled by the steric demand in the early TS that gives the apical substitution product (Scheme 11, bottom, path **B**).

Thus, we conclude that utilizing bromination and nitroxylation reactions, either medial or apical diamondoid derivatives can be obtained selectively. It should be mentioned that both bromine and anhydrous nitric acid are well miscible with many organic solvents, providing homogeneous conditions. This is quite important as higher diamondoids are far more reactive than **1** or **2**, requiring lower reaction temperatures and higher dilution. From this



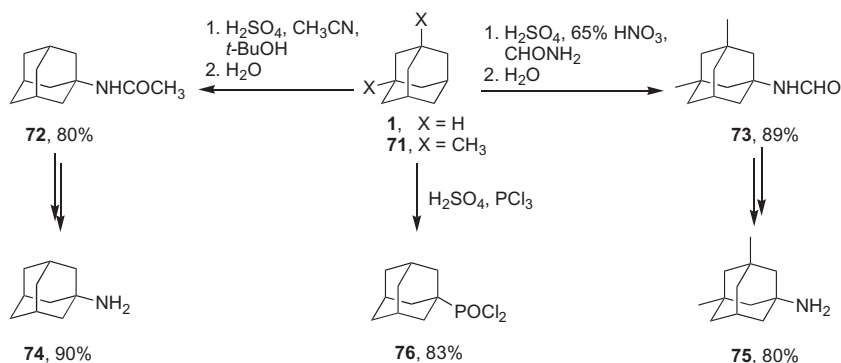
SCHEME 12 Direct carboxylation of **1** and **2** in the $\text{H}_2\text{SO}_4/\text{HCOOH}/t\text{-BuOH}$ system.

point of view, the use of concentrated sulfuric acid, which is another effective electrophilic medium, is limited because of low diamondoid solubility. The oxidation of **1** requires the presence of *t*-BuOH to generate the *t*-butyl cation, which then participates in the H-abstraction step (Scheme 12). This allows direct carboxylation of **1** [97] and **2** [29] in $\text{H}_2\text{SO}_4/\text{HCOOH}/t\text{-BuOH}$ (Koch–Haaf reaction) with formation of the corresponding carboxylic acids **69** and **70**.

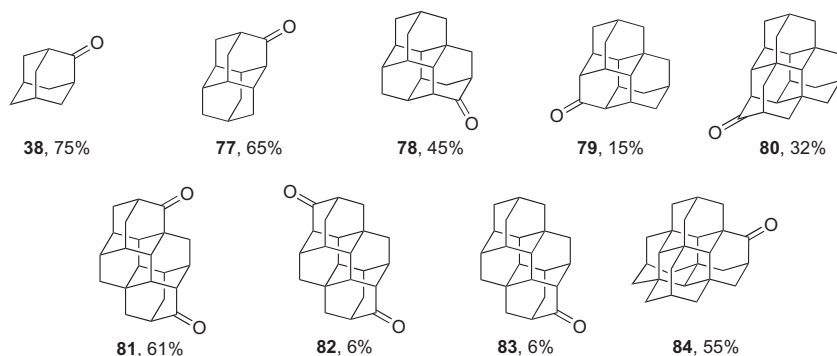
Acetamidation of **1** and formamidation of 1,3-dimethyladamantane (**71**) with $\text{H}_2\text{SO}_4/\text{CH}_3\text{CN}/t\text{-BuOH}$ [97] or $\text{H}_2\text{SO}_4/\text{HCONH}_2$ [98], respectively, provide the key precursors **72** and **73** of the commercial drugs Amantadine[®] (hydrochloric salt of 1-aminoadamantane, **74**) and Memantine[®] (*vide supra*, hydrochloride salt of 1-amino-3,5-dimethyladamantane, **75**, Scheme 13). The latter procedure is an excellent alternative to the existing technology based on the bromination of **71** (in ten-fold excess of Br_2) and is now used industrially for the preparation of bromine-free Memantine[®] [23].

Even phosphorylation of **1** with PCl_3 in concentrated sulfuric acid is possible giving (1-adamantyl)dichlorophosphonate (**76**) in 83% yield [99]. This is a viable alternative to the phosphorylation of adamantane catalyzed by Lewis acids (*vide infra*) [100].

At higher temperatures, concentrated sulfuric acid causes higher oxidation of diamondoids providing access to the corresponding ketones (Scheme 14).



SCHEME 13 Direct amidations of **1** and 1,3-dimethyladamantane (**71**) and phosphorylation of **1** in sulfuric acid.



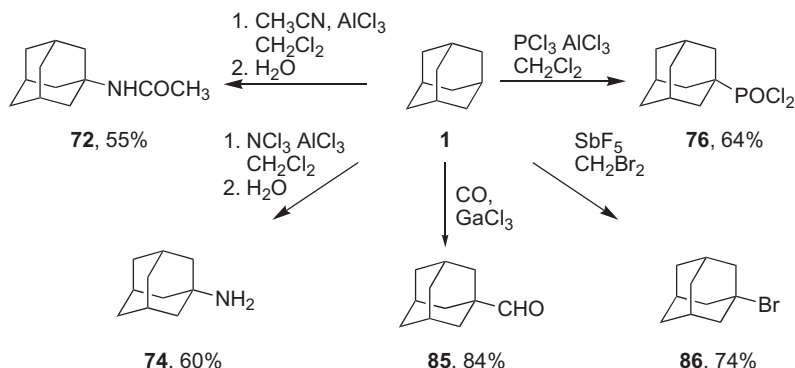
SCHEME 14 Preparative yields of ketones obtained through oxidation of the corresponding diamondoids with sulfuric acid upon heating.

Such reactions proceed through intermolecular hydrogen transfer between the intermediate tertiary cations and the secondary positions of the neutral hydrocarbons, whose methylene positions are oxidized further [101]. The oxidation of **1** in H₂SO₄ still remains the most selective method for the preparation of **38** [102], because with all other reagents, for example, oxone [103], phthalocyanine oxacomplexes [104], transition metal oxidants ([105]), and with many others [62,85,106], mixtures of oxygenated adamantanes form. The oxidation of **2** with sulfuric acid at 75 °C yields diamantan-3-one (**77**) in 65% preparative yield [107,108] together with small amounts of hydroxy derivatives [109]. Again, alternative procedures for preparation of **77**, for example, oxidation of **2** with oxygen in the presence of a Ru-catalyst [110] or NHPI [62], are much less effective. Analogous oxidation of **3** gave a mixture of ketones from which triamantan-8-one (**78**) [111] and triamantan-5-one (**79**) [108] were isolated in 45% and 15% yields, respectively. Only ketone **80** was isolated

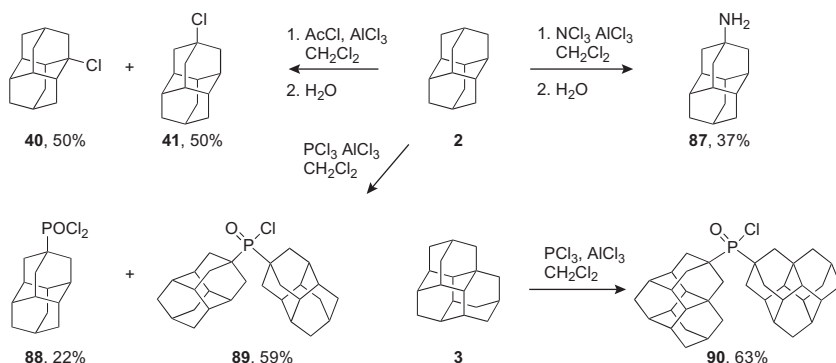
in 32% yield from a mixture of ketones formed after oxidation of **46** [108], while oxidation of **4** with sulfuric acid surprisingly gave only diketones **81** and **82** [87,108]. This was explained [87] by the low solubility of **4** in the reaction medium that leads to faster oxidation of the intermediate monoketones than of the starting material. As a result, monoketone **83** may be obtained only from alcohol **60** (Scheme 10), which is soluble in H_2SO_4 , through oxidation at a slightly higher temperature (80°C) and with shorter reaction times [87]. The oxidation of highly symmetric **5** with sulfuric acid gives ketone **84** as the sole product because only one type of CH_2 group present. We conclude that the reactions of diamondoids with sulfuric acid under heating give products of methylene group oxidation; however, the selectivities of such oxidations are low when many inequivalent CH_2 positions are present.

Many other electrophiles afford diamondoid C—H bond substitutions. Prototypical are AlCl_3 and AlBr_3 that, in the presence of halomethanes, form carbocationic species due to electrophile-assisted heterolysis of the C—Hal bond (so-called sludge). For instance, highly electrophilic $\text{AlCl}_4^-/\text{CH}_2\text{Cl}^+$ sludge forms from AlCl_3 and dichloromethane. Many useful transformations based on Lewis acid/haloalkane combinations were reported for **1**, for example, Ritter-like reactions [95], phosphorylation [112], amination [113], carbonylation [114], and ionic bromination [115] (Scheme 15).

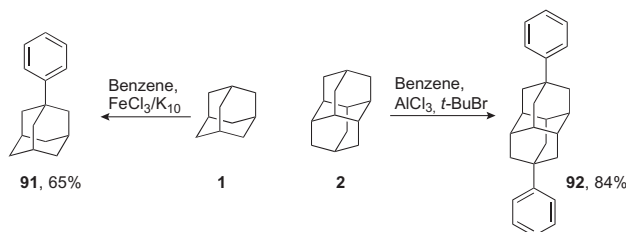
The Lewis acid/ CH_2Cl_2 -promoted monoamination [116] and monophosphorylation [117] of **2** and **3** (Scheme 16) only give apical amine (**87**) or dichlorophosphonate (**88**) owing to steric factors. Acetyl chloride as a less bulky chlorine donor gives an equimolar mixture of medial (**40**) and apical (**41**) chloro derivatives of **2** in the presence of $\text{AlCl}_3/\text{CH}_2\text{Cl}_2$ [118]. Di-9-triamantylphosphinic acid chloride (**90**) was the major product in the phosphorylation of **3** with $\text{PCl}_3/\text{AlCl}_3/\text{CH}_2\text{Cl}_2$ [117], which again agrees with the predominance of apical substitution in diamondoid phosphorylations with bulky nucleophiles.



SCHEME 15 Adamantane functionalizations promoted with Lewis acids.



SCHEME 16 Lewis acids promoted functionalizations of **2** and **3** in the presence of halomethanes.

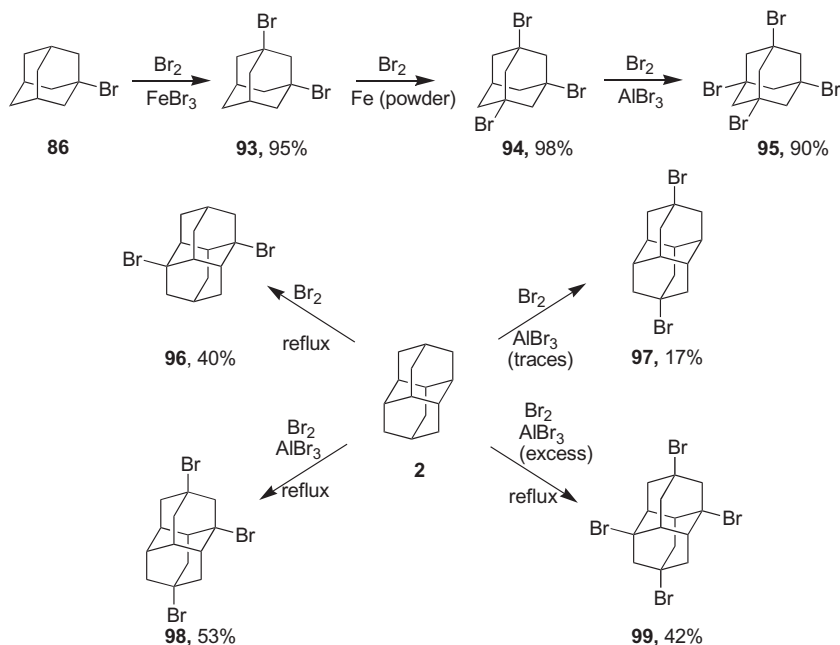


SCHEME 17 Lewis-catalyzed arylations of diamondoids.

Lewis acids also catalyze the direct arylation of diamondoids. The arylation of **1** with montmorillonite K10 clay/FeCl₃ gives 1-phenyladamantane (**91**) in good yield (Scheme 17) [119]. Diamantane (**2**) is doubly arylated in the presence of AlCl₃ in benzene [18] to give only 4,9-diphenyldiamantane (**92**) [120]. The formation of diapical derivatives of diamantane is quite typical in electrophilic media and will be discussed in more detail below.

3.3.2 Multiple Functionalizations

Polysubstituted diamondoids are widely used as building blocks for the construction of 2D and 3D rigid scaffolds, in particular for biomolecular modeling [121], MOFs [16,122], and polymers [10,123,124]. The incorporation of electron-withdrawing substituents into the diamondoid cages reduces their reactivity in subsequent substitutions, usually demanding Lewis acid catalysis [125]. While the monobromination of adamantane requires only moderate heating in neat bromine, the second substitution occurs only in the presence of Lewis acids. Selective bromination of 1-bromoadamantane (**86**) to 1,3-dibromoadamantane (**93**) [126] and to 1,3,5-tribromoadamantane (**94**)



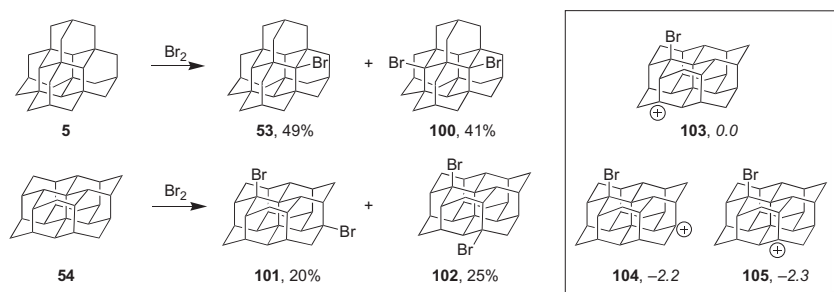
SCHEME 18 Preparation of polybromides of **1** and **2**.

[127] occurs in the presence of FeBr_3 as the catalyst. The selective tetrasubstitution to tetrabromide **95** requires excess of stronger Lewis acids an like AlCl_3 [91,128] or AlBr_3 [129] and heating.

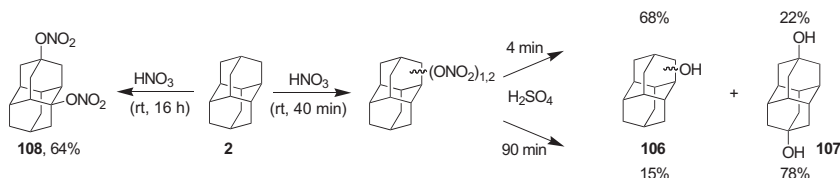
From the reaction mixture of the dibromination of **2**, the most symmetric 1,6-dibromo derivative (**96**) is separable [130] through crystallization in 40% yield (Scheme 18). In the presence of Lewis acids, the regioselectivity changes and apical derivatives dominate (as found for the arylations of **2**, Scheme 17). Bromination with traces of AlBr_3 gives diapical 4,9-dibromide (**97**), though with low yield [123]. With larger amounts of AlBr_3 , the 1,4,9-tribromo- (**98**) or 1,4,6,9-tetrabromoderivatives (**99**) form in moderate preparative yields depending on the amount of the Lewis acid.

The dibrominations of higher diamondoids also lead to mixtures of bromides. The bromination of **5** gives mono- (**53**) and dibromo- (**100**) derivatives (Scheme 19). Several dibromides form upon bromination of **54**, for which the products **101** and **102** from remote dibromine substitution were isolated and characterized. The bromination selectivities are in accord with the computed relative stabilities of the respective 2-bromocyclohexamantyl cations (**103–105**) [3].

An alternative approach utilizes the nitroxylation and further acid-catalyzed isomerization methodology (Scheme 20) eventually favoring the most thermodynamically stable [131] apical derivatives [132]. Their higher



SCHEME 19 Dibrominations of higher diamondoids **5** and **54** and relative stabilities of selected 2-bromocyclohexamantyl cations (**103**–**105**, B3PW91/cc-pVDZ).

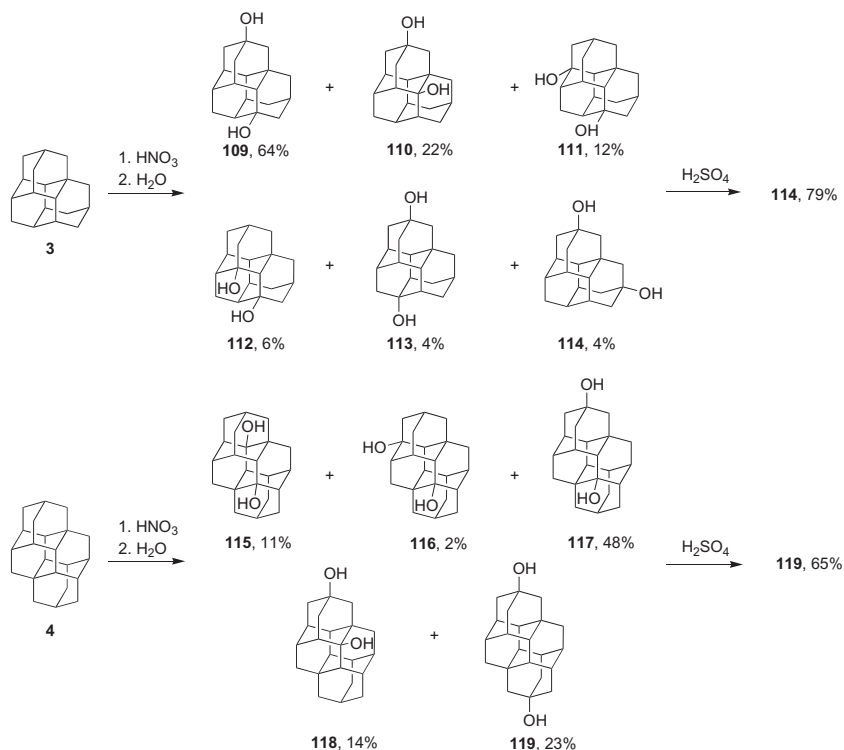


SCHEME 20 Dinitroxylation of **2** and thermodynamically controlled isomerization that provides the apical derivative.

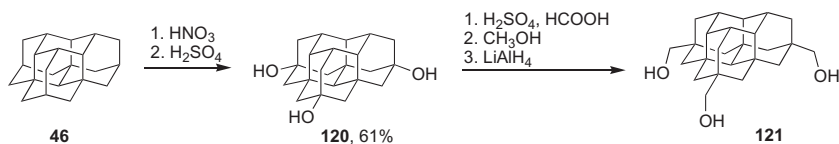
stabilities may be attributed both to differences in entropy values due to symmetry factors [118] and to unfavorable $\text{C—H}\cdots\text{Y}$ contacts that exist in the medial Y-substituted diamondoids [133]. The first step of the transformation of **2** involves the primary functionalization with 100% HNO_3 that gives a complex mixture of diamantane mono- and dinitroxy derivatives that, after treatment with concentrated sulfuric acid, leads to a thermodynamically controlled mixture of mono-alcohols (**106**) and apical dialcohol (**107**). The latter could be isolated by simple filtration of the reaction mixture after water quenching [134]. Prolonged treatment of **2** with anhydrous nitric acid [11] selectively gives 1,4-dinitrate (**108**), which was isolated and characterized [134].

This approach also provides the apical diols of **3** and **4** (Scheme 21). The initial nitroxylation of **3** gave, after hydrolysis, a rich mixture of diols **109**–**114**, which were separated and all characterized individually [134]. When treating this mixture with concentrated sulfuric acid at room temperature apical diol **114** forms in high yield (79%). The same approach was successfully used for the preparation of diapical dihydroxy derivatives of **4**: diols **115**–**119** were all characterized individually, with apical diol **119** being a minor product. This mixture gave diol **119** in 65% preparative yield (Scheme 21) upon treatment with sulfuric acid.

Remarkably, even the selective preparation of apical triols is possible utilizing the nitroxylation/isomerization approach (Scheme 22). Consecutive treatment of **46** with nitric and sulfuric acid gave triol (**120**), which was



SCHEME 21 Selective preparation of diapical derivatives of **3** and **4**.



SCHEME 22 Construction of a molecular tripod-based nitroxylation/isomerization of **46**.

subsequently used for the construction of molecular tripod (**121**) [3] for multi-dentate self-assembly of monolayers [135].

We conclude that the reactions with charged electrophiles may lead either to medial or to the apical diamondoid derivatives, depending on the reagent and reaction conditions; this provides excellent control over the diamondoid substitution patterns.

3.4 Single-Electron Transfer

As the ionization potential of **1** is rather high, its oxidations require very strong SET reagents. Computational as well as experimental data show,

however, a substantial decrease of the ionization potentials of diamondoids with increasing cage size: For instance, the computed [28] vertical ionization potential (IP_v) of **1** is 9.26 eV (the experimental value varies from 9.23 [136] to 9.25 [137,138]) and is substantially higher than that of **5** (7.87 eV [28], only the adiabatic ionization potential is available experimentally; it is 8.07 eV) [136]. The computed IP_v (9.05 eV) value for **2** agrees well with the experimental value of 8.93 eV [138]. The higher diamondoids are oxidized not only more easily than their lighter members (due to raising the energy of the HOMO level) [28,139] but also show many additional bands in the PE spectra [136]. In addition to first-order Jahn–Teller distortions that occur upon ionization [140] of structures belonging to degenerate point groups (e.g., **1**, **2**, and **5**) [126], all diamondoids undergo secondary distortions [141]. As an electron is removed from the bonding orbitals, this results in structures with elongated and partially broken σ bonds. The radical cations thus formed adopt well-defined geometries, with maximized (electron) spin and charge delocalizations through an overlapping system of elongated *syn*-periplanar C—C and C—H bonds. Because a larger number of σ bonds are involved if the distortions occur along the apical direction, all diamondoid radical cations contain elongated apical C—H bonds (Figure 7). For instance, the elongations of the apical C—H (up to 1.111 Å) and C—C (up to 1.588 Å) bonds in the diamantane radical cation (**122**) (vs. 1.09 and 1.54 Å in the neutral) are more pronounced than that in the [121]tetramantane radical cation (**123**) where these bonds are elongated only up to 1.103 and 1.579 Å, respectively. The distortions in the triamantane (**124**) and T_d -pentamantane (**125**) radical cations follow this trend.

Remarkably, the structures of the diamondoid radical cations completely determine the regioselectivity in their one-electron oxidations. With photoexcited 1,2,4,5-tetracyanobenzene (TCB), which is among the most effective one-electron acceptors [68], substitutions occur exclusively at the apical positions. Scheme 23 demonstrates the oxidation of **4** where the first step of the reaction includes SET from **4** to the excited state of TCB with formation of the radical ion pair **126**. In contrast to the gas phase, where diamondoid

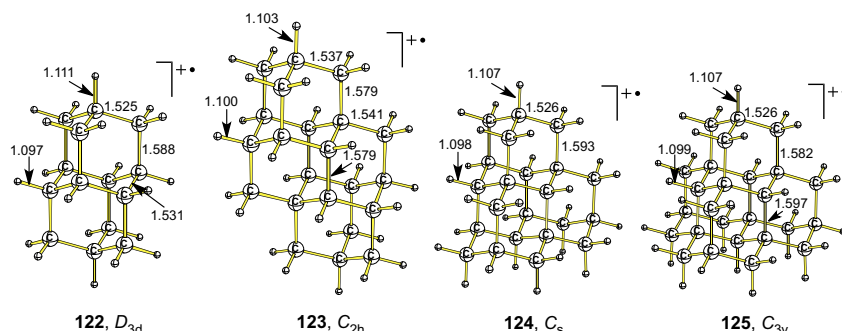
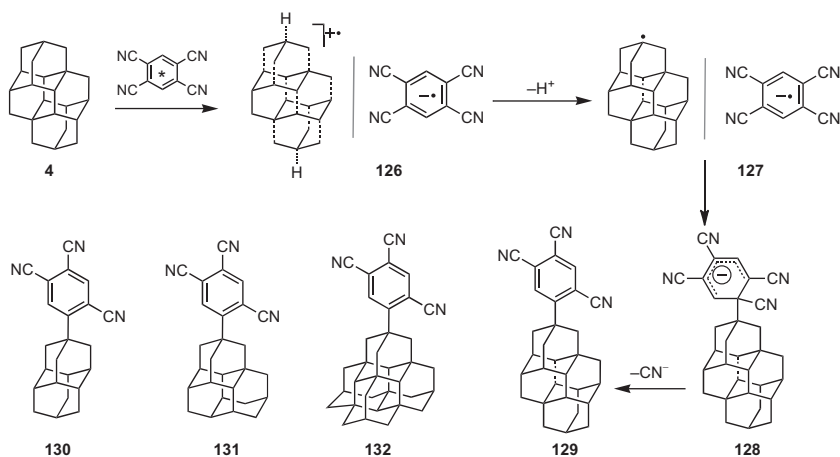


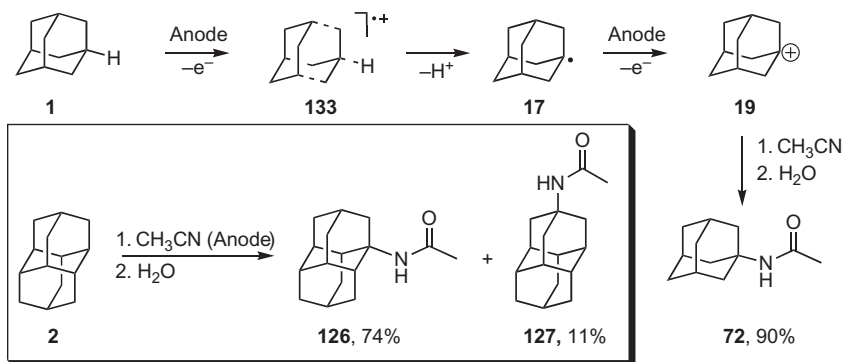
FIGURE 7 B3LYP/6-31G(d)-optimized geometries of some diamondoid radical cations (selected bond distances in Å).



SCHEME 23 SET photooxidation of **4** with photoexcited 1,2,4,5-tetracyanobenzene (TCB*) with formation of the arylation product (**129**) and the products derived from the analogous oxidations of **2** (**130**), **3** (**131**), and **5** (**132**).

radical cations are long-lived (as it was shown recently for adamantane) [142], in solution, deprotonation of the diamondoid radical cation occurs [68] readily from the apical position of the cage with formation of the diamondoid radical pair **127**. Recombination of the radical pair to intermediate **128** with concomitant elimination of the cyanide anion gives apically arylated derivative **129**. Analogous oxidations of **2**, **3**, and **5** give the corresponding apical derivatives **130–132**.

Radical cations also form upon anodic oxidation and electro-oxidation of **1** in acetonitrile on a Pt anode that gives **72** in 90% isolated yield [143]. As the passage of two electrons per adamantane molecule is required, the transformation involves the formation of the adamantane radical cation (**133**) in the first step,



SCHEME 24 Anodic oxidation of **1** and **2**.

its deprotonation to the adamantyl radical (**17**), and further oxidation to the adamantyl cation (**19**), which, after reaction with acetonitrile, gives **72** (Scheme 24).

Whereas the selectivities of the photoinduced SET and anodic oxidations are identical and lead exclusively to tertiary substitutions, the results of such oxidations differ considerably for higher diamondoids. While apical oxidation product **123** formed upon the SET oxidation of **2**, a mixture of medial (**126**) and apical (**127**) acetamides forms in a 6:1 ratio in 85% preparative yield in the corresponding anodic oxidation (Scheme 24). [144]

4. CONCLUDING REMARKS

The recent and rapidly growing field of diamondoid chemistry has been triggered by the elaboration of industrially suitable methods for their isolation from petroleum. This provides diamantane, triamantane, isomeric tetramantanes (including optically active forms after enantioseparation), as well as pentamantanes, and cyclohexamantane in sizable quantities as novel, unique building blocks for materials, ligands, catalysts, and surface coatings. As all of these applications require selective and highly scalable C—H bond functionalization, we have elaborated a large variety of approaches over the past seven years to *functionalized nanodiamonds*. Combinations of radical, electrophilic, and single-electron oxidative approaches allow the selective functionalization of diamondoids and provide apical or medial substitution patterns. We found that the C—H activation regioselectivity is primarily determined by steric and polar effects in the corresponding TSs, and these reactions are predominantly kinetically controlled. The diamondoid derivatives thus obtained usually contain —OH, —Br, —C(O)CH₃, and —COOH groups that are readily converted into other functionalities that are useful for connecting diamondoids to, for instance, metal and semiconductor surfaces (—SH [145], —CH=CH₂, —C(=CH₂)—CH=CH₂) [146] as well as to use them for polymer [10], supramolecular [16], and medicinal [21,62] applications.

REFERENCES

- [1] L. Diederich, P. Aebi, O.M. Küttel, L. Schlapbach, *Surf. Sci.* 424 (1999) L314–L320.
- [2] O.A. Shenderova, V.V. Zhirmov, D.W. Brenner, *Crit. Rev. Solid State Mater. Sci.* 27 (2002) 227–356.
- [3] A.A. Fokin, B.A. Tkachenko, N.A. Fokina, H. Hausmann, M. Serafin, J.E.P. Dahl, R.M.K. Carlson, P.R. Schreiner, *Chem. Eur. J.* 15 (2009) 3851–3862.
- [4] H. Schwertfeger, A.A. Fokin, P.R. Schreiner, *Angew. Chem. Int. Ed. Engl.* 47 (2008) 1022–1036.
- [5] (a) F.S. Hollowood, M.A. McKervey, R. Hamilton, J.J. Rooney, *J. Org. Chem.* 45 (1980) 4954–4958; (b) C. Cupas, P.v.R. Schleyer, D.J. Trecker, *J. Am. Chem. Soc.* 87 (1965) 917–918; (c) V.Z. Williams, P.v.R. Schleyer, G.J. Gleicher, L.B. Rodewald, *J. Am. Chem. Soc.* 88 (1966) 3862–3863.
- [6] J.E. Dahl, S.G. Liu, R.M.K. Carlson, *Science* 299 (2003) 96–99.

- [7] J.E.P. Dahl, J.M. Moldowan, T.M. Peakman, J.C. Clardy, E. Lobkovsky, M.M. Olmstead, P.W. May, T.J. Davis, J.W. Steeds, K.E. Peters, A. Pepper, A. Ekuan, R.M.K. Carlson, *Angew. Chem. Int. Ed. Engl.* 42 (2003) 2040–2044.
- [8] W. Burns, M.A. McKerver, T.R.B. Mitchell, J.J. Rooney, *J. Am. Chem. Soc.* 100 (1978) 906–911.
- [9] R. Lin, Z.A. Wilk, *Fuel* 74 (1995) 1512–1521.
- [10] C. Sinkel, S. Agarwal, N.A. Fokina, P.R. Schreiner, *J. Appl. Pol. Sci.* 114 (2009) 2109–2115.
- [11] P.R. Schreiner, A.A. Fokin, Preparation of Nitroxidiamantanes. WO 2007065409 A2 20070614 (2007).
- [12] T.M. Willey, J.D. Fabbri, J.R.I. Lee, P.R. Schreiner, A.A. Fokin, B.A. Tkachenko, N.A. Fokina, J.E.P. Dahl, R.M.K. Carlson, A.L. Vance, W. Yang, L.J. Terminello, T. van Buuren, N.A. Melosh, *J. Am. Chem. Soc.* 130 (2008) 10536–10544.
- [13] (a) W.L. Yang, J.D. Fabbri, T.M. Willey, J.R.I. Lee, J.E. Dahl, R.M.K. Carlson, P.R. Schreiner, A.A. Fokin, B.A. Tkachenko, N.A. Fokina, W. Meevasana, N. Mannella, K. Tanaka, X.J. Zhou, T. van Buuren, M.A. Kelly, Z. Hussain, N.A. Melosh, Z.-X. Shen, *Science* 316 (2007) 1460–1462; (b) S. Roth, D. Leuenberger, J. Osterwalder, J.E. Dahl, R.M.K. Carlson, B.A. Tkachenko, A.A. Fokin, P.R. Schreiner, M. Hengsberger, *Chem. Phys. Lett.* 495 (2010) 102–108.
- [14] H. Richter, H. Schwertfeger, P.R. Schreiner, R. Fröhlich, F. Glorius, *Synlett* (2009) 193–197.
- [15] (a) C.E. Müller, R. Hrdina, R.C. Wende, P.R. Schreiner, *Chem. Eur. J.* 17 (2011) 6309–6314; (b) R. Hrdina, C.E. Müller, P.R. Schreiner, *Chem. Commun.* (2010) 2689–2690; (c) M. Tomizawa, M. Shibuya, Y. Iwabuchi, *Org. Lett.* 11 (2009) 1829–1831; (d) C.E. Müller, D. Zell, P.R. Schreiner, *Chem. Eur. J.* 15 (2009) 9647–9650.
- [16] A.B. Lysenko, G.A. Senchyk, J. Lincke, D. Lassig, A.A. Fokin, E.D. Butova, P.R. Schreiner, H. Krautscheid, K.V. Domasevitch, *Dalton Trans.* 39 (2010) 4223–4231.
- [17] (a) I.L. Karle, D. Ranganathan, M.G. Kumar, R. Nagaraj, *Biopolymers* 89 (2008) 471–478; (b) N. Basaric, K. Molcanov, M. Matkovic, B. Kojic-Prodic, K. Mlinaric-Majerski, *Tetrahedron* 63 (2007) 7985–7996.
- [18] T. Gushiken, S. Ujiie, T. Ubukata, Y. Yokoyama, *Bull. Chem. Soc. Jpn.* 84 (2011) 269–282.
- [19] T. Fukaminato, T. Umemoto, Y. Iwata, S. Yokojima, M. Yoneyama, S. Nakamura, M. Irie, *J. Am. Chem. Soc.* 129 (2007) 5932–5938.
- [20] J. Wang, C. Ma, V. Balannik, L.H. Pinto, R.A. Lamb, W.F. DeGrado, *ACS Med. Chem. Lett.* 2 (2011) 307–312.
- [21] A.A. Fokin, A. Merz, N.A. Fokina, H. Schwertfeger, S.G.L. Liu, J.E.P. Dahl, R.K.M. Carlson, P.R. Schreiner, *Synthesis* (2009) 909–912.
- [22] S.K. Sonkusare, C.L. Kaul, P. Ramarao, *Pharmacol. Res.* 51 (2005) 1–17.
- [23] P.R. Schreiner, A.A. Fokin, L. Wanka, D.M. Wolfe, Method for Producing 1-Formamido-3,5-Dimethyladamantane. US 2009/0299097 A1.
- [24] J.B. Dumas, *Liebig's Ann.* 33 (1840) 187–191.
- [25] M. Konowalow, *Chem. Ber.* 28 (1895) 1852–1865.
- [26] S. Landa, S. Kriebel, E. Knobloch, *Chem. Listy* 48 (1954) 61–64.
- [27] P.v.R. Schleyer, *J. Am. Chem. Soc.* 79 (1957) 3292.
- [28] A.A. Fokin, B.A. Tkachenko, P.A. Gunchenko, D.V. Gusev, P.R. Schreiner, *Chem. Eur. J.* 11 (2005) 7091–7101.
- [29] T.M. Gund, M. Nomura, P.v.R. Schleyer, *J. Org. Chem.* 39 (1974) 2987–2994.
- [30] F. Hollowood, A. Karim, M.A. McKerver, P. McSweeney, H. Duddeck, *J. Chem. Soc. Chem. Commun.* (1978) 306–308.
- [31] A. Karim, M.A. McKerver, *J. Chem. Soc. Perkin Trans. 1* (1974) 2475–2479.

- [32] (a) F.N. Stepanov, S.S. Isaeva, *Vestn. Kiev. Politekhn. In-ta. Ser. Khim. Mashinostr. i Tekhnol.* 12 (1975) 15–16; (b) R.J. Israel, R.K.J. Murray, *J. Org. Chem.* 48 (1983) 4701–4705.
- [33] L.A. Paquette, J.C. Weber, T. Kobayashi, Y. Miyahara, *J. Am. Chem. Soc.* 110 (1988) 8591–8599.
- [34] G.A. Olah, *Angew. Chem. Int. Ed. Engl.* 34 (1995) 1393–1405.
- [35] H.W. Geluk, J.L.M.A. Schlattmann, *Chem. Commun.* (1967) 426.
- [36] I.K. Moiseev, P.G. Belyaev, N.V. Barabanov, O.P. Bardyug, E.H. Vishnevskii, N.I. Novatskaya, E.L. Golod, B.V. Gidasov, *Zh. Org. Khim.* 11 (1975) 214–215.
- [37] A.G. Yurchenko, N.I. Kulik, V.P. Kuchar, V.M. Djakovskaya, V.F. Baklan, *Tetrahedron Lett.* (1986) 1399–1402.
- [38] G.A. Olah, *Angew. Chem. Int. Ed. Engl.* 12 (1973) 173–254.
- [39] (a) P.R. Schreiner, P.v.R. Schleyer, H.F. Schaefer III, *J. Am. Chem. Soc.* 117 (1995) 453–461; (b) P.R. Schreiner, P.v.R. Schleyer, H.F. Schaefer III, *J. Am. Chem. Soc.* 115 (1993) 9659–9666.
- [40] A.A. Fokin, T.E. Shubina, P.A. Gunchenko, S.D. Isaev, A.G. Yurchenko, P.R. Schreiner, *J. Am. Chem. Soc.* 124 (2002) 10718–10727.
- [41] Y.N. Klimochkin, O.V. Abramov, I.I. Moiseev, M.F. Vologin, M.V. Leonova, E.I. Bagrii, *Pet. Chem.* 40 (2000) 415–418.
- [42] A.A. Fokin, P.R. Schreiner, P.A. Gunchenko, S.A. Peleshanko, T.E. Shubina, S.D. Isaev, P.V. Tarasenko, N.I. Kulik, H.-M. Schiebel, A.G. Yurchenko, *J. Am. Chem. Soc.* 122 (2000) 7317–7326.
- [43] A.A. Fokin, P.R. Schreiner, *Chem. Rev.* 102 (2002) 1551–1593.
- [44] G.H. Kruppa, J.L. Beauchamp, *J. Am. Chem. Soc.* 108 (1986) 2162–2169.
- [45] C. Aubry, J.L. Holmes, J.C. Walton, *J. Phys. Chem. A* 102 (1998) 1389–1393.
- [46] G.W. Smith, H.D. Williams, *J. Org. Chem.* 26 (1961) 2207–2212.
- [47] F. Minisci, F. Fontana, L. Zhao, S. Banfi, S. Quici, *Tetrahedron Lett.* 35 (1994) 8033–8036.
- [48] I. Tabushi, J. Hamuro, R. Oda, *J. Am. Chem. Soc.* 89 (1967) 7127–7129.
- [49] P.R. Schreiner, O. Lauenstein, E.D. Butova, P.A. Gunchenko, I.V. Kolomitsin, A. Wittkopp, G. Feder, A.A. Fokin, *Chem. Eur. J.* 7 (2001) 4996–5003.
- [50] L. Liguori, H.R. Bjørsvik, A. Bravo, F. Fontana, F. Minisci, *Chem. Commun.* (1997) 1501–1502.
- [51] P.R. Schreiner, O. Lauenstein, E.D. Butova, A.A. Fokin, *Angew. Chem. Int. Ed. Engl.* 38 (1999) 2786–2788.
- [52] P.R. Schreiner, O. Lauenstein, I.V. Kolomitsyn, S. Nadi, A.A. Fokin, *Angew. Chem. Int. Ed. Engl.* 37 (1998) 1895–1897.
- [53] E.V. Dehmlo, S.S. Dehmlo, *Phase-Transfer Catalysis*, VCH, Weinheim, 1993.
- [54] K. Nasr, N. Pannier, J.V. Frangioni, W. Maison, *J. Org. Chem.* 73 (2008) 1056–1060.
- [55] R.W. Alder, F. Carta, C.A. Reed, I. Stoyanova, C.L. Willis, *Org. Biomol. Chem.* 8 (2010) 1551–1559.
- [56] A.A. Fokin, O. Lauenstein, P.A. Gunchenko, P.R. Schreiner, *J. Am. Chem. Soc.* 123 (2001) 1842–1847.
- [57] Y. Ishii, S. Kato, T. Iwahama, S. Sakaguchi, *Tetrahedron Lett.* 37 (1996) 4993–4996.
- [58] A.A. Fokin, P.R. Schreiner, *Adv. Synth. Catal.* 345 (2003) 1035–1052, and refs. therein.
- [59] Y. Ishii, T. Iwahama, S. Sakaguchi, K. Nakayama, Y.J. Nishiyama, *J. Org. Chem.* 61 (1996) 4520–4526.
- [60] S. Sakaguchi, Y. Nishiwaki, T. Kitamura, Y. Ishii, *Angew. Chem. Int. Ed. Engl.* 40 (2001) 222–224.

- [61] T.S. Zhuk, P.A. Gunchenko, Y.Y. Korovai, P.R. Schreiner, A.A. Fokin, *Theor. Exp. Khim.* 44 (2008) 46–51.
- [62] T.S. Zhuk, E.Y. Bratko, A.E. Pashenko, G.P. A., A.G. Yurchenko, P.R. Schreiner, A.A. Fokin, *J. Org. Pharm. Chem.* 8 (2010) 62–66.
- [63] F. Recupero, C. Punta, *Chem. Rev.* 107 (2007) 3800–3842.
- [64] S. Sakaguchi, T. Hirabayashi, Y. Ishii, *Chem. Commun.* (2002) 516–517.
- [65] R.W. Glass, T.W. Martin, *J. Am. Chem. Soc.* 92 (1970) 5084–5093.
- [66] H. Suzuki, N. Nonoyama, *Chem. Commun.* (1996) 1783–1784.
- [67] H. Suzuki, N. Nonoyama, *J. Chem. Soc. Perkin Trans. 1* (1997) 2965–2971.
- [68] M. Mella, M. Freccero, T. Soldi, E. Fasani, A. Albini, *J. Org. Chem.* 61 (1996) 1413–1422.
- [69] A.A. Fokin, P.A. Gunchenko, A.A. Novikovskiy, T.E. Shubina, B.V. Chernyaev, J.E.P. Dahl, R.M.K. Carlson, A.G. Yurchenko, P.R. Schreiner, *Eur. J. Org. Chem.* (2009) 5153–5161.
- [70] I. Tabushi, S. Kojo, K. Fukunishi, *J. Org. Chem.* 43 (1978) 2370–2374.
- [71] R. Curci, L. D'Accolti, C. Fusco, *Acc. Chem. Res.* 39 (2006) 1–9.
- [72] R. Mello, M. Fiorentino, C. Fusco, R. Curci, *J. Am. Chem. Soc.* 111 (1989) 6749–6757.
- [73] R. Mello, L. Cassidei, M. Fiorentino, C. Fusco, R. Curci, *Tetrahedron Lett.* 31 (1990) 3067–3070.
- [74] R.W. Murray, H. Gu, *J. Org. Chem.* 60 (1995) 5673–5677.
- [75] A.R. Groenhof, A.W. Ehlers, K. Lammertsma, *J. Phys. Chem. A* 112 (2008) 12855–12861.
- [76] S. Lee, P.L. Fuchs, *J. Am. Chem. Soc.* 124 (2002) 13978–13979.
- [77] A. Bravo, H.-R. Bjorsvik, F. Fontana, F. Minisci, A. Serri, *J. Org. Chem.* 61 (1996) 9409–9416.
- [78] A.N. Biswas, P. Das, A. Agarwala, D. Bandyopadhyay, P. Bandyopadhyay, *J. Mol. Catal. A* 326 (2010) 94–98.
- [79] T. Nagataki, Y. Tachi, S. Itoh, *Chem. Commun.* (2006) 4016–4018.
- [80] R. Mayilmurugan, H. Stoeckli-Evans, E. Suresh, M. Palaniandavar, *Dalton Trans.* 26 (2009) 5101–5114.
- [81] R.C. Bingham, P.v.R. Schleyer, *J. Org. Chem.* 36 (1971) 1198–1202.
- [82] J.M. Bakke, A.E. Frohaug, *J. Phys. Org. Chem.* 9 (1996) 507–513.
- [83] B.A. Tkachenko, T.E. Shubina, D.V. Gusev, P.A. Gunchenko, A.G. Yurchenko, P.R. Schreiner, A.A. Fokin, *Theor. Exp. Chem.* 39 (2003) 90–95.
- [84] J.W. Suggs, L. Ytuarte, *Tetrahedron Lett.* 27 (1986) 437–440.
- [85] L. Cermenati, D. Dondi, M. Fagnoni, A. Albini, *Tetrahedron* 59 (2003) 6409–6414.
- [86] T.M. Gund, M. Nomura, J.V.Z. Williams, P.v.R. Schleyer, *Tetrahedron Lett.* (1970) 4875–4878.
- [87] P.R. Schreiner, N.A. Fokina, B.A. Tkachenko, H. Hausmann, M. Serafin, J.E.P. Dahl, S. Liu, R.M.K. Carlson, A.A. Fokin, *J. Org. Chem.* 71 (2006) 6709–6720.
- [88] (a) A. de Meijere, A.F. Khlebnikov, R.R. Kostikov, S.I. Kozhushkov, P.R. Schreiner, A. Wittkopp, D.S. Yufit, *Angew. Chem. Int. Ed. Engl.* 38 (1999) 3474–3477; (b) A. de Meijere, A.F. Khlebnikov, S.I. Kozhushkov, D.S. Yufit, O.V. Chetina, J.A.K. Howard, T. Kurahashi, K. Miyazawa, D. Frank, P.R. Schreiner, C. Rinderspacher, M. Fujisawa, C. Yamamoto, H. Okamoto, *Chem. Eur. J.* 12 (2006) 5697–5721.
- [89] P.R. Schreiner, A.A. Fokin, H.P. Reisenauer, B.A. Tkachenko, E. Vass, M.M. Olmstead, D. Bläser, R. Boese, J.E.P. Dahl, R.M.K. Carlson, *J. Am. Chem. Soc.* 131 (2009) 11292–11293.
- [90] R.M.K. Carlson, J.E.P. Dahl, S.G. Liu, M.M. Olmstead, P.K. Buerki, R. Gat, *Diamondoid molecules found in petroleum. New Members of the H-terminated diamond series*, in:

- D.M. Gruen (Ed.), *Synthesis, Properties, and Applications of Ultrananocrystalline Diamond*, Springer, Berlin, 2005, pp. 63–78.
- [91] I.K. Moiseev, N.V. Makarova, M.N. Zemtsova, *Russ. Chem. Rev.* 68 (1999) 1001–1020.
- [92] I.K. Moiseev, Y.N. Klimochkin, M.N. Zemtsova, P.L. Trakhtenberg, *Zh. Org. Khim.* 20 (1984) 1435–1438.
- [93] G.A. Olah, J.G. Shih, B.P. Singh, B.G.B. Gupta, *J. Org. Chem.* 48 (1983) 3356–3358.
- [94] (b) D. Rajagopal, D. Reddy, *Synth. Commun.* 26 (1996) 3495–3501; (b) G.A. Olah, P. Ramaiah, C.B. Rao, G. Sandford, R. Golam, N.J. Trivedi, J.A. Olah, *J. Am. Chem. Soc.* 115 (1993) 7246–7249.
- [95] G.A. Olah, B.G.B. Gupta, *J. Org. Chem.* 45 (1980) 3532–3533.
- [96] A.A. Fokin, P.R. Schreiner, N.A. Fokina, B.A. Tkachenko, H. Hausmann, M. Serafin, J.E.P. Dahl, S. Liu, R.M.K. Carlson, *J. Org. Chem.* 71 (2006) 8532–8540.
- [97] H. Koch, W. Haaf, *Angew. Chem.* 17 (1960) 628.
- [98] (a) P.R. Schreiner, A.A. Fokin, L. Wanka, D. Wolfe, preparation of Amidoadamantanes. (Justus-Liebig-Universitaet Giessen, Germany). PCT Int. Appl. (2007), 18pp. CODEN: PIXXD2 WO 2007101535 A1 20070913 Patent written in German. Application: WO 2007-EP1431 20070220. Priority: DE 2006-102006009278 20060301. CAN 147:365191; AN 2007:1030086. Patent issued June 20, 2010. (b) L. Wanka, C. Cabrele, M. Vanejews, P.R. Schreiner, *Eur. J. Org. Chem.* (2007) 1474–1490
- [99] R.I. Yurchenko, L.P. Peresypkina, *Zh. Obshch. Khim.* 64 (1994) 1564.
- [100] H. Stetter, W.D. Last, *Chem. Ber.* 102 (1969) 3364–3366.
- [101] D.R. Adams, P.D. Bailey, I.D. Collier, S.A.H. Leah, C. Ridyard, *Chem. Commun.* (1996) 333–334.
- [102] H.W. Geluk, V.G. Keizer, *Org. Synth.* 53 (1973) 8.
- [103] B. De Poorter, M. Ricci, B. Meunier, *Tetrahedron Lett.* 26 (1985) 4459–4462.
- [104] H.M. Neu, V.V. Zhdankin, V.N. Nemykin, *Tetrahedron Lett.* 51 (2010) 6545–6548.
- [105] I. Yamanaka, T. Furukawa, K. Otsuka, *Chem. Commun.* (2000) 2209–2210.
- [106] (a) S.J. Song, K.S. Kim, K.H. Kim, J.B. Kim, J.H. Kim, K.S. Kim, H. Shin, D.L. Cho, *Chem. Lett.* 37 (2008) 1052–1053; (b) G. Balavoine, D.H.R. Barton, J. Boivin, A. Gref, *Tetrahedron Lett.* 31 (1990) 659–662.
- [107] J. Janku, J. Burkhard, L. Vodicka, *Zeit. Chem.* 21 (1981) 67–68.
- [108] A.A. Fokin, T.S. Zhuk, A.E. Pashenko, P.O. Dral, P.A. Gunchenko, J.E.P. Dahl, R.M.K. Carlson, T.V. Koso, M. Serafin, P.R. Schreiner, *Org. Lett.* 11 (2009) 3068–3071.
- [109] T. Courtney, D.E. Johnston, J.J. Rooney, M.A. McKervey, *J. Chem. Soc. Perkin Trans. 1* (1972) 2691–2696.
- [110] R. Neumann, A.M. Khenkin, M. Dahan, *Angew. Chem. Int. Ed. Engl.* 34 (1995) 1587–1589.
- [111] Z. Kafka, L. Vodicka, M. Hajek, *Sbor. Vys. Sk. Chem. Technol. D50* (1984) 245–250.
- [112] G.A. Olah, O. Farooq, Q. Wang, A. Wu, *J. Org. Chem.* 55 (1990) 1224–1227.
- [113] P. Kovacic, P.D. Roskos, *Tetrahedron Lett.* (1968) 5833–5835.
- [114] M. Oshita, N. Chatani, *Org. Lett.* 6 (2004) 4323–4325.
- [115] G.A. Olah, A. Wu, O. Farooq, *J. Org. Chem.* 54 (1989) 1463–1465.
- [116] P.A. Cahill, *Tetrahedron Lett.* 31 (1990) 5417–5420.
- [117] H. Schwertfeger, M.M. Machuy, C. Wurtele, J.E.P. Dahl, R.M.K. Carlson, P.R. Schreiner, *Adv. Synth. Catal.* 352 (2010) 609–615.
- [118] D.E. Johnston, J.J. Rooney, M.A. McKervey, *J. Chem. Soc. Chem. Comm.* (1972) 29–30.
- [119] S. Chalais, A. Cornelis, A. Gerstmann, W. Kolodziejski, P. Laszlo, A. Mathy, P. Metra, *Helv. Chim. Acta* 68 (1985) 1196–1203.

- [120] S.D. Karlen, R. Ortiz, O.L. Chapman, M.A. Garcia-Garibay, *J. Am. Chem. Soc.* 127 (2005) 6554–6555.
- [121] (a) D. Ranganathan, S. Kurur, *Tetrahedron Lett.* 38 (1997) 1265–1268; (b) R. Pathak, A. Marx, *Chem. Asian J.* 6 (2011) 1450–1455; (c) W. Maison, J.W. Frangioni, N. Pannier, *Org. Lett.* 6 (2004) 4567–4569.
- [122] J. Kim, B.L. Chen, T.M. Reineke, H. Li, M. Eddaoudi, D.B. Moler, M. O’Keeffe, O.M. Yaghi, *J. Am. Chem. Soc.* 123 (2001) 8239–8247.
- [123] A.A. Malik, T.G. Archibald, K. Baum, M.R. Unroe, *Macromolecules* (1991) 5266–5268.
- [124] (a) Y.T. Chern, C.M. Huang, *Polymer* 39 (1998) 6643–6648; (b) Y.T. Chern, *Macromolecules* 31 (1998) 1898–1905; (c) T.D. Dang, M.J. Dalton, N. Venkatasubramanian, J.A. Johnson, C.A. Cerbus, W.A. Feld, *J. Polym. Sci. A* 42 (2004) 6134–6142.
- [125] H. Stetter, C. Wulff, *Chem. Ber.* 93 (1960) 1366–1371.
- [126] I.R. Likhovtsov, N.L. Dovgan, G.I. Danilenko, *Zh. Org. Khim.* 13 (1977) 897.
- [127] R.E. Delimarsky, V.N. Rodionov, A.G. Yurchenko, *Ukr. Khim. Zh.* 54 (1988) 437–438.
- [128] A.P. Khardin, I.A. Novakov, S.S. Radchenko, *Zh. Org. Khim.* 9 (1973) 429.
- [129] G.S. Lee, J.N. Bashara, G. Sabih, A. Oganessian, G. Godjoian, H.M. Duong, E.R. Martinez, C.G. Gutierrez, *Org. Lett.* 6 (2004) 1705–1707.
- [130] T.M. Gund, P.v.R. Schleyer, G.D. Unruh, G.J. Gleicher, *J. Org. Chem.* 39 (1974) 2995–3003.
- [131] T. Clark, T.M. Knox, M.A. McKerver, H. Mackle, *J. Chem. Soc. Perkin Trans. 2* (1980) 1686–1689.
- [132] J. Burkhard, J. Janku, L. Vodicka, *Sbor. Vys. Sk. Chem. -Technol. D50* (1984) 231–243.
- [133] A. Kolocouris, N. Zervos, F. De Proft, A. Koch, *J. Org. Chem.* 76 (2011) 4432–4443.
- [134] N.A. Fokina, B.A. Tkachenko, A. Merz, M. Serafin, J.E.P. Dahl, R.M.K. Carlson, A.A. Fokin, P.R. Schreiner, *Eur. J. Org. Chem.* (2007) 4738–4745.
- [135] P. Chinwangso, A.C. Jamison, T.R. Lee, *Acc. Chem. Res.* 44 (2011) 511–519.
- [136] K. Lenzke, L. Landt, M. Hoener, H. Thomas, J.E. Dahl, S.G. Liu, R.M.K. Carlson, T. Möller, C. Bostedt, *J. Chem. Phys.* 127 (2007) 084320 (084324p).
- [137] G.D. Mateescu, S.D. Worley, *Tetrahedron Lett.* 52 (1972) 5285–5289.
- [138] M.J.S. Dewar, S.D. Worley, *J. Chem. Phys.* 50 (1969) 654–667.
- [139] (a) G.C. McIntosh, M. Yoon, S. Berber, D. Tománek, *Phys. Rev. B* 70 (2004) 045401; (b) A.A. Fokin, P.R. Schreiner, *Mol. Phys.* 107 (2009) 823–830.
- [140] (a) H.A. Jahn, E. Teller, *Phys. Rev.* 49 (1936) 874; (b) I.B. Bersuker, *Chem. Rev.* 101 (2001) 1067–1114.
- [141] T.E. Shubina, A.A. Fokin, *WIREs Comput. Mol. Sci.* 1 (2011) 661–679.
- [142] A. Guerrero, R. Herrero, E. Quintanilla, J.Z. Davalos, J.M. Abboud, P.B. Coto, D. Lenoir, *ChemPhysChem* 11 (2010) 713–721.
- [143] L.L. Miller, V.R. Koch, *Tetrahedron Lett.* (1973) 693–696; (b) V.R. Koch, L.L. Miller, *J. Am. Chem. Soc.* 95 (1973) 8631–8637; (c) A.A. Novikovskiy, P.A. Gunchenko, P.G. Prihodchenko, Y.A. Serguchev, P.R. Schreiner, A.A. Fokin, *Russ. J. Org. Chem.* 47 (2011) 1293–1299.
- [144] F. Vincent, R. Tardivel, P. Mison, P.v.R. Schleyer, *Tetrahedron* 33 (1977) 325–330.
- [145] B.A. Tkachenko, N.A. Fokina, L.V. Chernish, J.E. Dahl, S. Liu, R.M.K. Carlson, A.A. Fokin, P.R. Schreiner, *Org. Lett.* 8 (2006) 1767–1770.
- [146] A.A. Fokin, E.D. Butova, L.V. Chernish, N.A. Fokina, J.E.P. Dahl, R.M.K. Carlson, P.R. Schreiner, *Org. Lett.* 9 (2007) 2541–2544.

A Dipolar Cycloaddition Strategy for the Synthesis of 3,8-Diazabicyclo[3.2.1]Octane Tetrahydroisoquinoline Antitumor Antibiotics: The Total Synthesis of (–)-Lemonomycin

Eric Ashley* and Brian Stoltz†

*Global Process Chemistry, Merck Research Laboratories, Rahway, USA

†Division of Chemistry and Chemical Engineering, California Institute of Technology, Pasadena, California, USA

Chapter Outline

1. Introduction	351	5. The Total Synthesis of (–)-Lemonomycin	360
2. Lemonomycin and the Tetrahydroisoquinoline Antitumor Antibiotics	352	5.1. Pictet–Spengler Cyclization Alternatives	364
3. Strategic Considerations for the Synthesis of (–)-Lemonomycin	354	5.2. Synthesis of Lemonomycin Aminoglycoside	366
4. Retrosynthetic Analysis of Lemonomycin	358	5.3. Completion of (–)-Lemonomycin	367
		6. Concluding Remarks	371

1. INTRODUCTION

The Stoltz research group began its operations in the summer of 2000. Crowned with newly renovated labs and a nine-strong contingent of ambitious, freshly minted graduate students, we set out to apply our best efforts toward solving problems in chemical synthesis, catalysis, and asymmetric methods. Several of these

projects arose from the lab's early research proposals, including palladium-catalyzed dehydrogenation methods, dinucleophile–dielectrophile approaches to phloroglucinol natural products, and synthesis of the dragmacidin family of natural products. Others grew organically from our broad interest in the interplay between novel routes to complex molecules and novel mechanisms for complex reactions, as well as our goal to synthesize molecules that could positively impact human medicine. It was within this context that our interest was sparked by the antitumor antibiotic (–)-lemonomycin. We envisioned many interesting approaches to the stereochemically dense, polycyclic framework that would require fundamental advancement of existing reaction technologies, and we thought further toward the long-term application of the reactions we might develop to a broad array of related compounds. One approach sketched out in our very first planning session was the asymmetric dipolar cycloaddition of a cyclic azomethine ylide with an acrolein equivalent. Implementation of this idea consumed 3 years of concentrated effort by the two of us and our coconspirators, Ernest Cruz and Tammy Lam, leading eventually to completion of the natural product on October 5, 2003. Due to the etiology of “lemonomycin,” our final success was marked by placing a lemon outside the door of Brian's office. We and Eric's baymate, Jennifer Stockdill, have fondly remembered “lemonomycin day” each October since.

We have ultimately found success parlaying our new reactions into the synthesis of other important structures. Kevin Allan joined the project in 2004, aiding in the partial synthesis of cyanocycline A and eventually utilizing the asymmetric dipolar cycloaddition as a key step in the synthesis of (–)-quinocarcin. Further application to other members of the tetrahydroisoquinoline antitumor antibiotics is ongoing as of this writing.

2. LEMONOMYCIN AND THE TETRAHYDROISOQUINOLINE ANTITUMOR ANTIBIOTICS

The tetrahydroisoquinoline antitumor antibiotics are a broad class of natural products and synthetic molecules characterized by bridged diazabicyclic core structures fused to a tetrahydroisoquinoline ring system [1]. This ring system, in combination with the common toxicity of these structures toward bacterial and mammalian cells, provides the class with its name. Members of the family can be categorized by the nature of their diazabicyclic cores, specifically separating compounds that contain a 3,8-diazabicyclo[3.2.1]octane core (e.g., quinocarcin, cyanocycline A, tetrazomine, and lemonomycin, [Figure 1](#)) from those that contain a 3,9-diazabicyclo[3.3.1]nonane core, which is itself part of a second tetrahydroisoquinoline subunit (e.g., saframycin A, renieramycin C, and ecteinascidin 743). Additional bridging elements, side-chain substituents, and oxidation patterns distinguish individual members of the family.

Lemonomycin was isolated in 1964 by Whaley *et al.* from a fermentation broth of the soil bacterium *Streptomyces candidus* [2]. The compound proved to be a potent, broad-spectrum antibiotic with activity comparable to penicillin G and erythromycin. Both gram-positive and gram-negative bacteria were

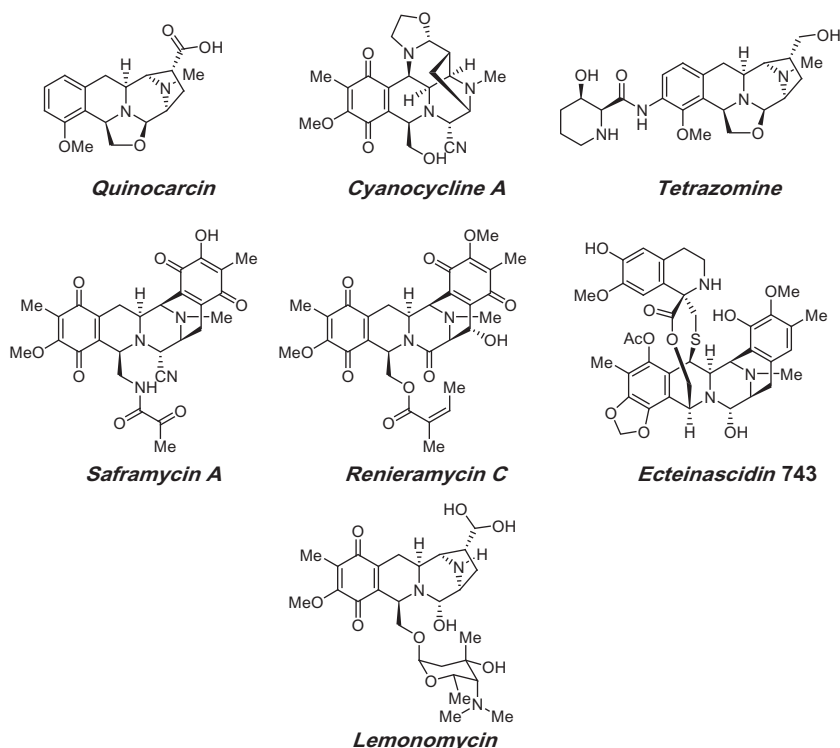


FIGURE 1 Representative tetrahydroisoquinoline antitumor antibiotics.

susceptible to lemonomycin *in vitro*. The authors further note that lemonomycin, administered either orally or subcutaneously, protected mice from staphylococcal and streptococcal infections, but unfortunately the antibiotic was found to be lethal at levels only slightly higher than the therapeutic dose.

A total of 4 g of lemonomycin hydrochloride was purified from 2000 L of fermentation broth. Lemonomycin free base was prepared by dissolution of the hydrochloride salt with aqueous sodium hydroxide and extraction into chloroform, followed by precipitation from aqueous acetone. This precipitation provided “lemon-yellow spheres” of the antibiotic, leading to the name lemonomycin. Whaley *et al.* were not able to fully determine the structure of lemonomycin, but IR and ^1H NMR studies established the presence of quinone, *N*-methyl, and *O*-methyl functionality, while potentiometric titration indicated the presence of two basic sites. Degradation studies were found to liberate dimethylamine.

The study of lemonomycin became reinvigorated in the late 1990s as part of a Wyeth-Aherst effort toward investigating the activity of older antibiotics against newly evolved, highly antibiotic-resistant bacterial strains [3]. These researchers found that lemonomycin is active against methicillin-resistant *Staphylococcus aureus* and vancomycin-resistant *Enterococcus faecium* with minimal inhibitory concentrations of 0.4 and 0.2 $\mu\text{g/mL}$, respectively.

The natural product also exhibited activity against the human colon tumor cell line HCT116 with an IC_{50} of 0.36 $\mu\text{g/mL}$.

The Wyeth-Aherst team also determined the connectivity and relative stereochemistry of the natural product by NMR spectroscopic methods. The complex alkaloid exhibits an oxidized tetrahydroisoquinoline portion reminiscent of the saframycin subfamily and a 3,8-diazabicyclo[3.2.1]octane core similar to quinocarcin. Contrastingly, lemonomycin is unique among the nearly 60 natural products and hundreds of synthetic analogues in this family in that it bears glycosylation at C(18). The 2,6-dideoxy-4-aminoglycoside is rare in nature, having been isolated only as a substituent of glycothiohexide α [4], nocathiacin I [5], and MJ347-81F4 A [6,7]. All of these natural products are potent antibiotics, indicating that the aminoglycoside may be important to lemonomycin's biological activity.

In addition to the unique nature of lemonomycin's glycosylation, the compound bears an aldehyde hydrate at C(16) that is unprecedented in the tetrahydroisoquinoline antitumor antibiotics. One OH group of the hydrate is poised to form an intramolecular hydrogen bond to N(12). This hydrogen bond stabilizes the acetal and modulates the basicity of the secondary amine. Additionally, the acetal hydrogen atoms may be involved in DNA binding *in vivo*, which could contribute to lemonomycin's effectiveness as a DNA-damaging agent [8].

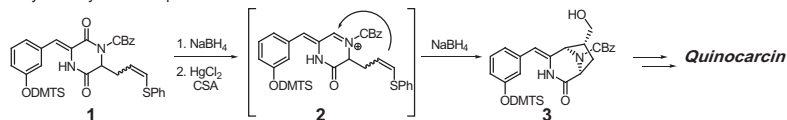
3. STRATEGIC CONSIDERATIONS FOR THE SYNTHESIS OF (–)-LEMONOMYCIN

Lemonomycin presents numerous challenges to the synthetic chemist. Most prominent is the diazabicyclooctane core, which contains five of the molecule's ten stereocenters, two of its three basic nitrogen atoms, and the sensitive acetal and carbinolamine functionalities. The aminoglycoside provides a second major source of complexity, both through the stereochemical array of the hexose and via the requirement for an anomerically pure attachment to the aglycone. Finally, the oxidized tetrahydroisoquinoline contains the unsymmetrical, fully substituted quinone and the C(1)–C(3)-skipped stereodiad.

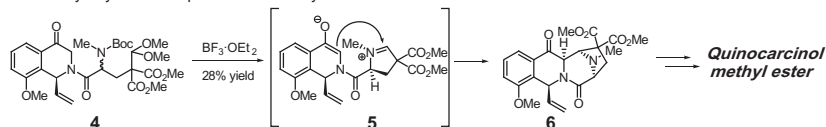
Three general routes have been disclosed for approaching the diazabicyclic core of compounds structurally related to lemonomycin, specifically iminium ion cyclizations of piperazinium and pyrrolidinium derivatives, cyclization of pyrrolidine aldehydes or amides, and cycloadditions of acrylate derivatives with alkylated pyrazine dipoles.

Two general classes of iminium ion cyclizations have been disclosed for the synthesis of the diazabicyclic core of quinocarcin (Scheme 1). The first method involves formation of the pyrrolidine portion of the bicycle by cyclization of a piperazine-derived iminium ion with an attached nucleophile. This bond connection is displayed in Fukuyama's synthesis of quinocarcin [9], in which diketopiperazine derivative **1** is treated with sodium borohydride followed by mercuric chloride to form iminium ion **2**. This iminium ion undergoes cyclization of the pendant vinyl sulfide to form the bicyclic core. Further reduction provides bicyclic enamide **3** [10,11].

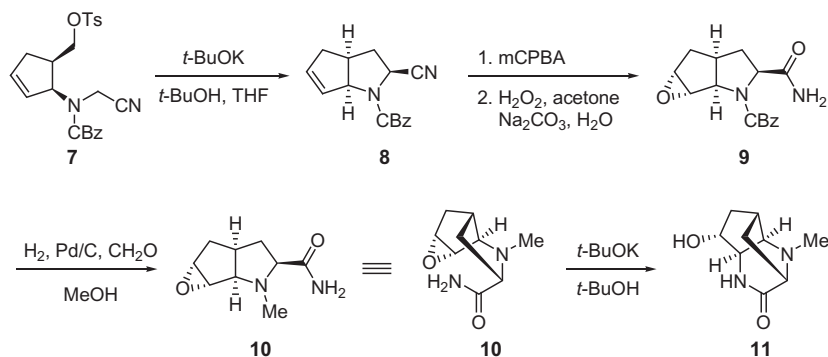
Fukuyama's synthesis of quinocarcin



Danishefsky's synthesis of quinocarcinol methyl ester

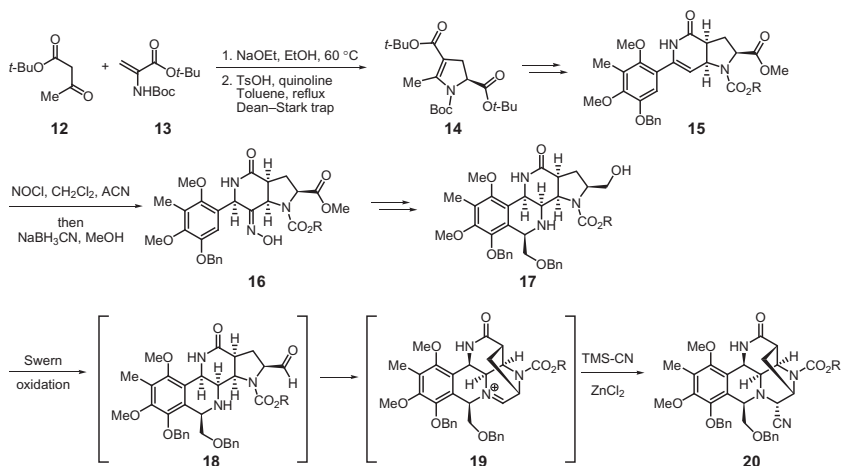
**SCHEME 1** Iminium ion cyclization routes to diazabicyclo[3.2.1]octanes.

Evans' synthesis of cyanocycline A

**SCHEME 2** Evans' cyanocycline A route.

The second iminium ion cyclization method involves formation of a piperazine ring by cyclization of a nucleophilic component onto a pyrrolidine-derived iminium ion. In Danishefsky's synthesis of quinocarcinol methyl ester, a pyrrolidine iminium ion (**5**) is formed from carbamate **4** by the action of boron trifluoride diethyl etherate [12]. This iminium ion then undergoes Mannich-type closure, allowing the construction of both rings of the diazabicyclo in a single operation (i.e., **4** to **6**, Scheme 1) [13]. The rather modest yield is due, in part, to the formation of compounds arising from the undesired diastereomer of the starting material. Notably, both iminium ion cyclization routes provide high levels of diastereoselectivity for the formation of both the bridgehead and a neighboring stereocenter.

Cyclizations of preformed pyrrolidines potentiated both the Evans and Fukuyama's syntheses of cyanocycline A (Scheme 2). In the Evans' work, pyrrolidine amide **9** was synthesized from nitrile **7** by nucleophilic displacement of the tosylate, epoxidation with *m*-CPBA, and partial nitrile hydrolysis [14]. Conversion of the carbamate to the *N*-methyl derivative **10** allowed formation of the diazabicyclic core by highly regioselective anionic opening of the



SCHEME 3 Fukuyama's route to cyanocycline A.

epoxide.¹ The carbon atoms of the additional ring were eventually incorporated into the tetrahydroisoquinoline and piperidine rings of the natural product.

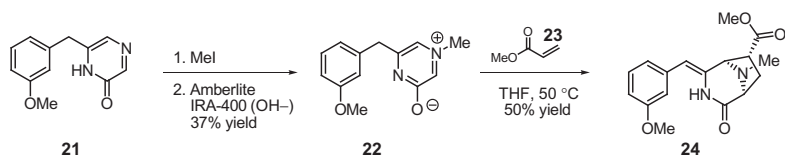
Fukuyama accessed the pyrrolidine core of cyanocycline A by a two-step cyclization of dehydroalanine derivative **13** with ketoester **12** to form pyrroline **14**, which contains all of the carbon atoms and one of the nitrogen atoms of the eventual diazabicyclooctane (Scheme 3) [15]. This pyrroline was advanced to cyclic enamide **15**, from which the final nitrogen atom was installed via treatment with nitrosyl chloride followed by sodium cyanoborohydride. Oxidation state adjustment and Pictet–Spengler cyclization provided alcohol **17**, which was cyclized to the diazabicycle by oxidation and treatment with trimethylsilyl cyanide.

Dipolar cycloadditions of pyrazinium ions comprise perhaps the most direct approach to the diazabicyclo[3.2.1]octane core structures of the tetrahydroisoquinoline antitumor antibiotics. Such cycloadditions have been studied by Joule [16], Garner [17], and Williams [18] (Scheme 4). Joule investigated the cycloaddition reactions of isolated oxidopyrazinium salts such as **22**, which reacted in a diastereoselective manner with acrylate derivatives to provide the racemic core of quinocarcin in a single step. Garner approached a pyrazinium dipole with a much different method. Photolysis of aziridinium **25** generates a transient dipolar species **26**,² which can be trapped with the acrylamide of Oppolzer's sultam. The chiral auxiliary imparts high diastereocontrol in the cycloaddition, which potentiated Garner's synthesis of (+)-quinocarcin with

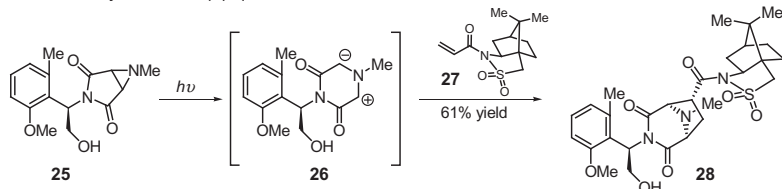
1. Cyclization of the carbamate derivative proceeded with poor regioselectivity.

2. Compound **26** may be more appropriately described as a diradical rather than a dipole due to the homolytic nature of the aziridine opening.

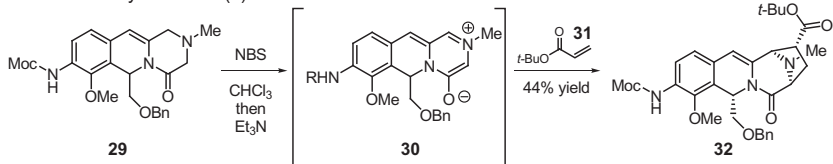
Joule's approach to quinocarcin



Garner's total synthesis of (–)-quinocarcin



Williams' total synthesis of (–)-tetrazomine



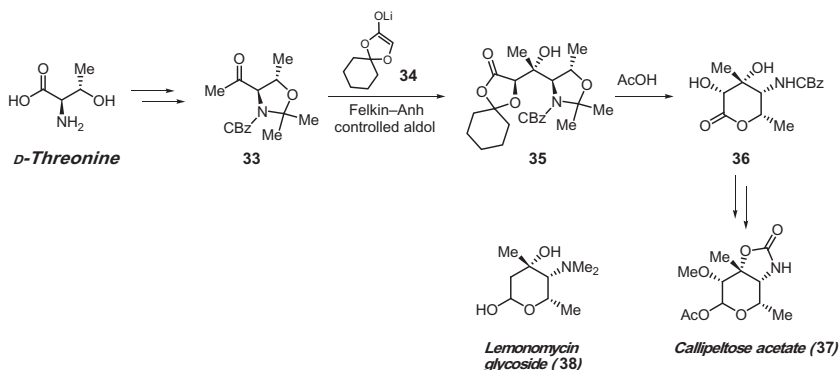
SCHEME 4 Dipolar cycloaddition approaches to the diazabicyclooctane core.

high enantiomeric purity. Williams has reported a third method for generating pyrazine dipoles. Oxidation of enamide **29** with *N*-bromosuccinimide followed by deprotonation with triethylamine provides dipole **30**. Cycloaddition with *tert*-butyl acrylate leads to the core of tetrazomine, although the resident benzylic stereocenter directs cycloaddition to the undesired face of the dipole.

The lemonomycin glycoside bears a striking resemblance to callipeltose, the glycoside of callipeltoside A. The Evans Synthesis of callipeltose contains a highly useful Felkin–Anh aldol addition of lithium enolate **34** to D-threonine-derived ketone **33** [19]. Lactone **36** is readily accessed from the aldol adduct by treatment with acetic acid. Reduction of the lactone and functional group manipulation then leads to callipeltose acetate (Scheme 5).

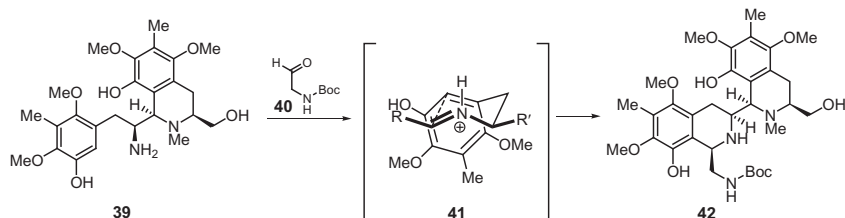
The 1,3-*cis*-disubstituted tetrahydroisoquinoline motif common to this family of molecules is most commonly accessed by Pictet–Spengler cyclization of a β -aminoethyl arene [20]. Chirality transfer from C(3) to C(1) through a chair-like transition state provides the *cis* orientation around the tetrahydroisoquinoline. The power of this reaction is displayed in a highly complex context in Fukuyama's synthesis of saframycin A (Scheme 6) [21]. Condensation of primary amine **39** with α -carbamoyl aldehyde **40** followed by cyclization through transition state **41** provides tetrahydroisoquinoline **42**.

Pictet–Spengler cyclizations typically require primary or secondary amine nucleophiles. However, in rare cases, amides have proven sufficiently reactive for similar reactions. The Evans' synthesis of cyanocycline A contains such a

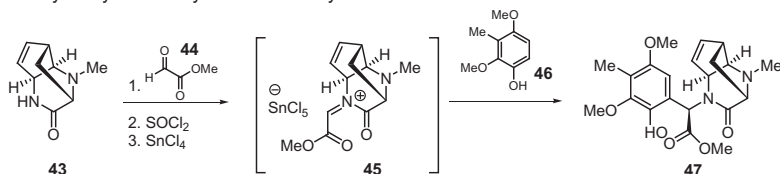


SCHEME 5 Evans synthesis of callipeltose.

Fukuyama's saframycin A Pictet–Spengler cyclization



Evans' cyanocycline A acyl iminium ion arylation



SCHEME 6 Pictet–Spengler cyclization and acyl iminium ion arylation.

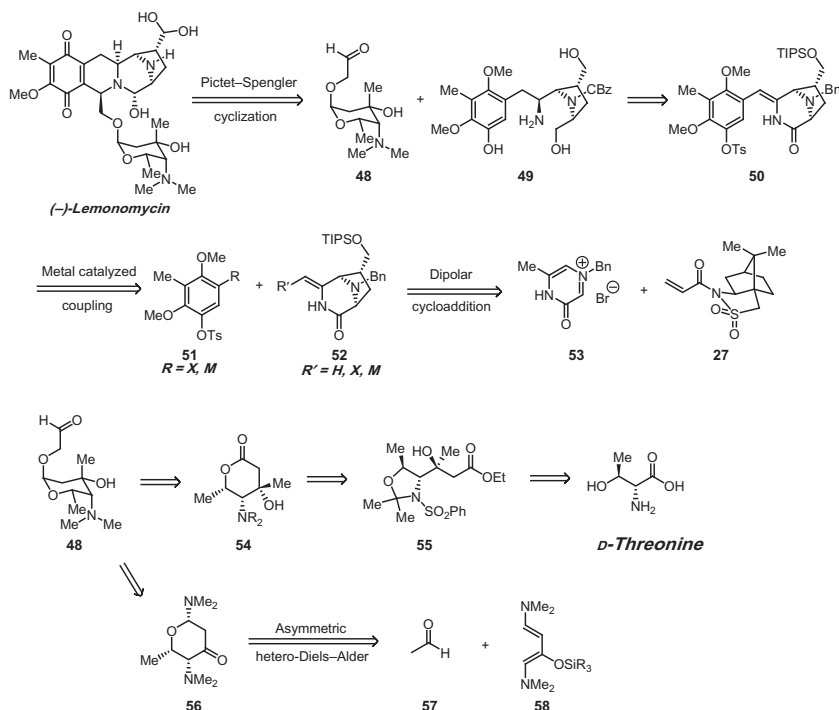
reaction, wherein amide **43** is converted to acyl iminium **45** by sequential treatment with methyl glyoxylate (**44**), thionyl chloride, and tin(IV)chloride. Subsequent addition of phenol **46** leads to amide **47** via Friedel–Crafts arylation.

4. RETROSYNTHETIC ANALYSIS OF LEMONOMYCIN

In light of the precedents described above, we planned to disconnect the tetrahydroisoquinoline ring of lemonomycin with a late stage Pictet–Spengler transform, revealing aminotriol **49** and glycosyloxy acetaldehyde **48**. The choice to incorporate the aminoglycoside carries important strategic implications, in that it maximizes the convergence of the synthetic route and provides the opportunity to control the anomeric stereochemistry in the absence of the sensitive aglycone. We expected that aminotriol **49** could be derived from

diazabicyclooctane **50** by oxidation state and functional group manipulation. Application of a metal-catalyzed coupling transform leads to arene **51** and enamide **52**. For the construction of **52**, we planned to utilize the oxopyrazinium bromide **53** in conjunction with the Oppolzer's sultam acrylamide (**27**), essentially combining the best aspects of the Joule and Garner's strategies.

Glycosyloxy acetaldehyde **48** was expected to arise from lactone **54**. Retro-synthetic opening of the lactone reveals acetate aldol adduct **55**, which could in turn arise from D-threonine in a manner similar to the Evans' synthesis of calipeltose [19]. Use of D-threonine in this manner greatly simplifies the stereochemical challenges of the glycoside synthesis, since two of the four stereocenters are drawn from the chiral pool and a third is generated by the highly predictable aldol addition. However, the route is somewhat lengthy, involving both protecting group manipulations and linear fragment additions. We therefore also considered routes based on chiral catalysis that might be more efficient. The most promising alternative route to the aminoglycoside would involve an asymmetric hetero-Diels–Alder cycloaddition. Specifically, **48** could be derived from ketone **56** by diastereoselective methyl anion addition and incorporation of the oxo-ethoxy unit. Ketone **56** might be available in a single step by cycloaddition of diene **58** with acetaldehyde (**57**) (Scheme 7) [22].

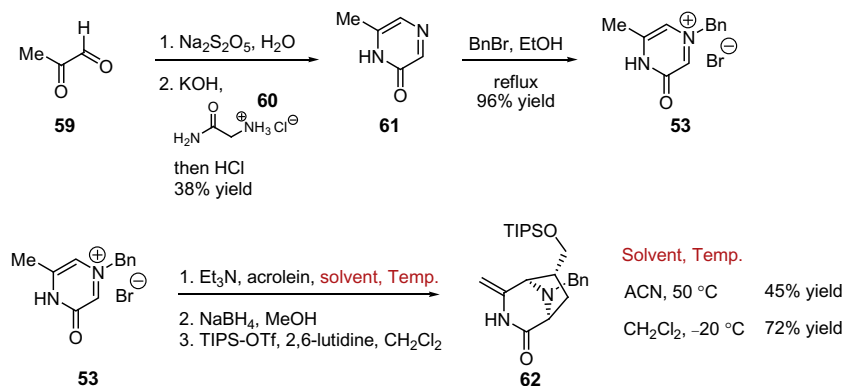


SCHEME 7 Retrosynthetic analysis of lemonomycin.

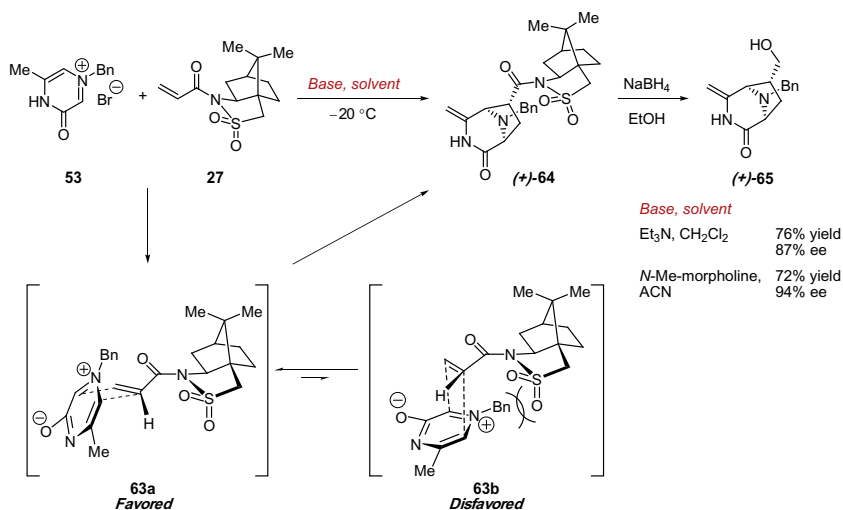
5. THE TOTAL SYNTHESIS OF (–)-LEMONOMYCIN

We began our synthetic studies with an investigation of the Joule dipolar cycloaddition, which suffered from moderate yields under the originally reported conditions [16]. Oxopyrazinium bromide **53** was readily synthesized by known procedures, beginning with cyclocondensation of glycinamide hydrochloride (**60**) with pyruvaldehyde (**59**) to form pyrazinone **61**. *N*-alkylation with benzyl bromide provided bromide salt **53** as a bench-stable powder (Scheme 8) [23]. When this compound was treated with triethylamine and acrolein in acetonitrile at 50 °C, a mixture of inseparable cycloadducts resulted, with a single isomer (**62**) available in 45% yield after reduction, silylation, and silica gel chromatographic purification. Gratifyingly, the yield of silyl ether **42** could be increased to 72% simply by performing the cycloaddition reaction in dichloromethane under cryogenic conditions. The increased yield is primarily due to regio- and diastereoselectivity, which minimizes the formation of other cycloadduct isomers.

Having developed optimized conditions for the dipolar cycloaddition of **53** with acrolein, we investigated the use of chiral auxiliaries for the production of enantioenriched diazabicyclic compounds. The acrylamide of Oppolzer's sultam (**27**) [24] was tested due to its well-precedented use in dipolar cycloadditions of nitrile oxides, silyl nitronates, and azomethine ylides, particularly the direct precedent from Garner's synthesis of (–)-quinocarcin [17,25]. To our delight, under the conditions utilized for our racemic cycloaddition, this acrylamide provided good diastereocontrol in the production of enamide (+)-**64**, such that alcohol (+)-**65** could be isolated in 87% ee after reductive cleavage of the auxiliary (Scheme 9). After a screen of conditions, it was found that (+)-**65** could be produced with 94% ee if *N*-methyl morpholine



SCHEME 8 Optimization of the Joule dipolar cycloaddition.



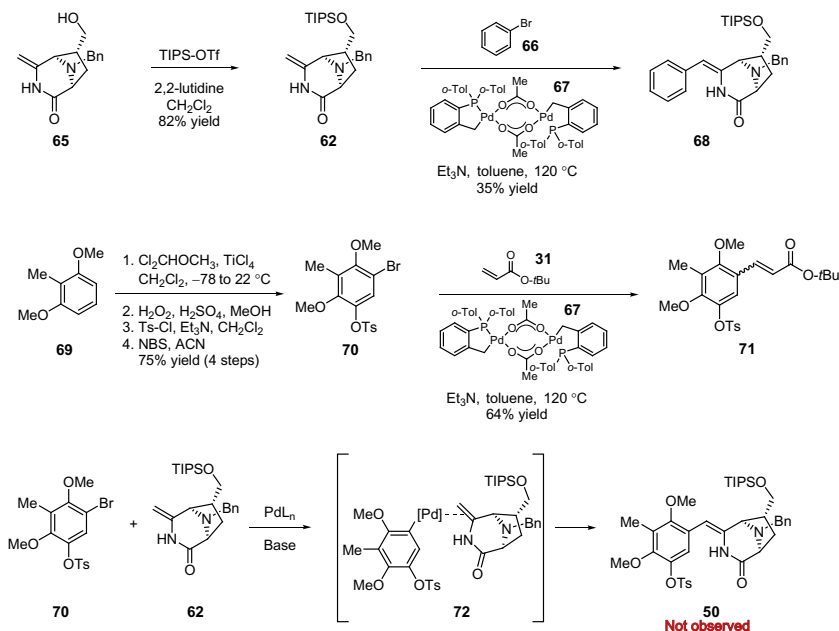
SCHEME 9 Asymmetric dipolar cycloaddition.

was utilized as the base and acetonitrile as the solvent.³ The major factor in the improved selectivity was the choice of the milder base, while solvent effects were comparably minor.

In analogy to proposed models, the cycloaddition of **53** with **27** is expected to occur through transition states **63a** and **63b**. The conformation of the acrylamide is controlled by lone pair repulsion, which causes the carbonyl oxygen to rotate away from the sulfonamide oxygen atoms, and the steric influence of the sulfonamide, which enforces an *s-cis* geometry around the acrylamide. In this conformation, the pseudoaxial sulfonamide oxygen blocks the lower face of the alkene (**63b**), while unencumbered cycloaddition across the top face of the alkene (**63a**) leads to the major observed product **(+)-64**. The marked effect of *N*-methyl morpholine on the reaction's diastereoselectivity may result from a hydrogen bonding complex between either the dipole or the sulfonamide and the ammonium salt. The greater acidity of the morpholinium cation, in comparison to triethylammonium, could lead to closer contact through the hydrogen bond and consequently greater effective size of the reacting partners.

With an effective synthesis of enantioenriched enamide **(+)-65** in hand, we turned to the challenge of appending an appropriate arene precursor to the eventual quinone. In this regard, **65** was silylated with triisopropylsilyl tri-flate to produce silyl ether **62** (Scheme 10). The enamide of **62** was readily

3. The ee of **65** could be raised to >98% by chromatographic purification of **64** prior to the cleavage of the auxiliary.



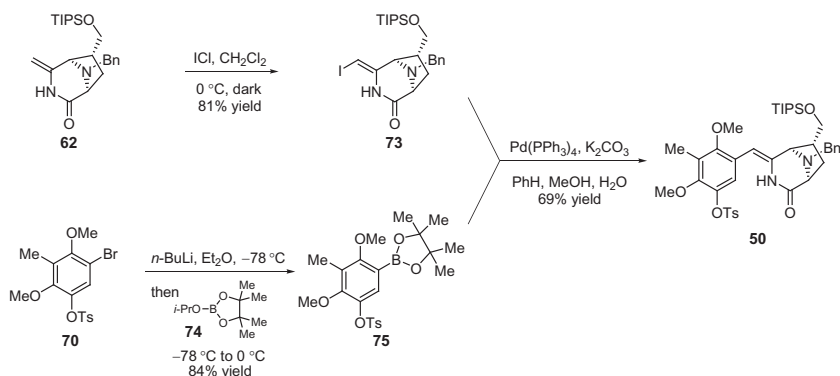
SCHEME 10 Attempted Heck coupling of the diazabicyclic enamide.

arylated by a Heck reaction with bromobenzene (**66**) catalyzed by palladium acetate/*triorthotolyl*phosphine dimer **67**.

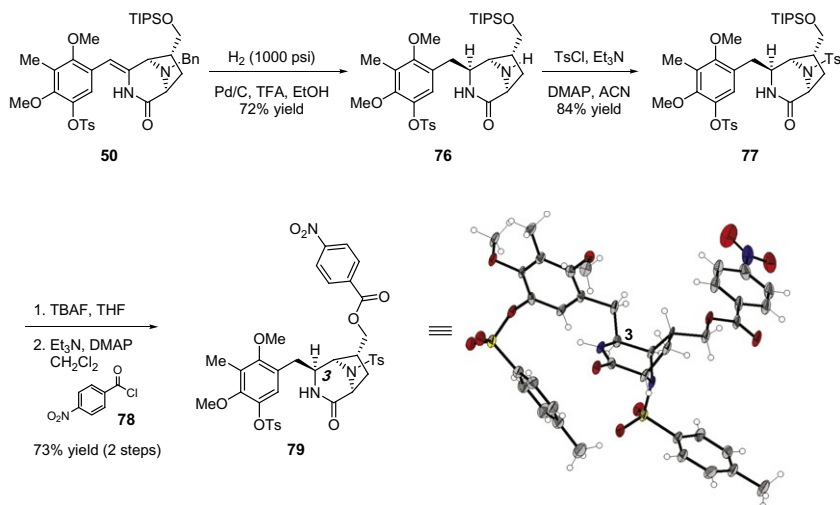
Encouraged by this result, we prepared coupling partner **70** from dimethylresorcinol **69** by the sequence of formylation, hydrolytic Baeyer–Villiger oxidation, tosylation, and bromination. This aryl bromide also participated in Heck coupling catalyzed by **67**, specifically providing enoate **71** by reaction with *tert*-butyl acrylate. Unfortunately, despite an extensive screen of known catalysts and conditions, the Heck union of **62** with **70** could not be realized. This failure likely results from the steric congestion provided by the *ortho*-methoxy group of **70**, which prevents the formation of enamide–palladium complex **72**.

In response to the failure of the Heck coupling, we turned to metal-catalyzed cross-coupling reactions as an alternative. Thus, enamide **62** was smoothly iodinated with iodine monochloride. To generate a coupling partner, we turned to a procedure suggested by Grubbs group mentor Arnab Chatterjee, wherein aryl bromide **70** was subjected to lithium–bromide exchange followed by trapping with borate **74** to generate arylboronic ester **75** (Scheme 11). Standard Suzuki coupling conditions then provided styrene **50** in good yield.

The next challenge was hydrogenation of styrene **50** with necessary control of stereochemistry (Scheme 12). After substantial experimentation, it was discovered that carbon-supported palladium(0) in acidic ethanol was uniquely effective for the hydrogenation and hydrogenolysis of



SCHEME 11 Suzuki coupling.



SCHEME 12 Diastereoselective reduction of the enamide.

50.⁴ Employment of trifluoroacetic acid as the acidic cosolvent provided lactam **76** as single diastereomer, which arose by hydrogenation of the enamide from the convex face of the diazabicyclic. Interestingly, the use of acetic acid as cosolvent led to a mixture of **76** and an apparently diastereomeric compound,⁵ indicating a potential changeover in the mechanism of hydrogenation between fully and partially protonated substrates.

4. Hydrogenolysis of the benzyl amine proceeded at a rate that was competitive with the rate of olefin hydrogenation. Under conditions with lower hydrogen pressures, a debenzylated compound with the styrene intact could be isolated.

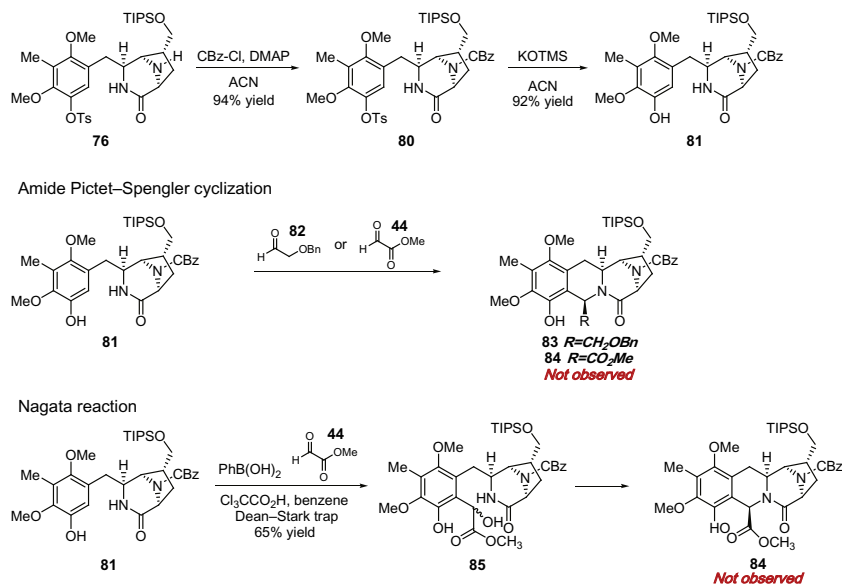
5. The second product from the hydrogenation in the presence of acetic acid reaction was not fully characterized.

To prove the stereochemistry of **76**, a crystalline substance was required.⁶ Toward this end, treatment of amine **76** with tosyl chloride produced tosylamide **77**. Silyl ether cleavage followed by acylation with 4-nitrobenzoyl chloride (**78**) then provided ester **79** as a highly crystalline solid. X-ray diffraction analysis of a single crystal of **79** proved that the stereocenter at C(3) matched the stereochemistry reported for the natural product.

5.1 Pictet–Spengler Cyclization Alternatives

Amide **76** was advanced synthetically by conversion of the amine to a urethane with CBz-Cl and DMAP in acetonitrile (Scheme 13). Cleavage of the tosylate was accomplished with potassium trimethylsilanolate to provide phenol **81**. While we had originally planned to convert the amide of **81** to a primary amine substrate for a traditional Pictet–Spengler cyclization, we investigated alternative cyclization modes beginning directly from the amide. Unfortunately, treatment of **81** with benzyloxyacetaldehyde under a variety of conditions failed to provide any cyclized product. In analogy to the protocol utilized by Evans for the synthesis of cyanocycline A [14], we attempted to condense **81** with monomeric methyl glyoxylate. Unfortunately, these conditions also failed to cause any conversion of the starting material.

The proposed Pictet–Spengler cyclization would mechanistically form a carbon–nitrogen bond followed by a carbon–carbon bond. Due to the failure

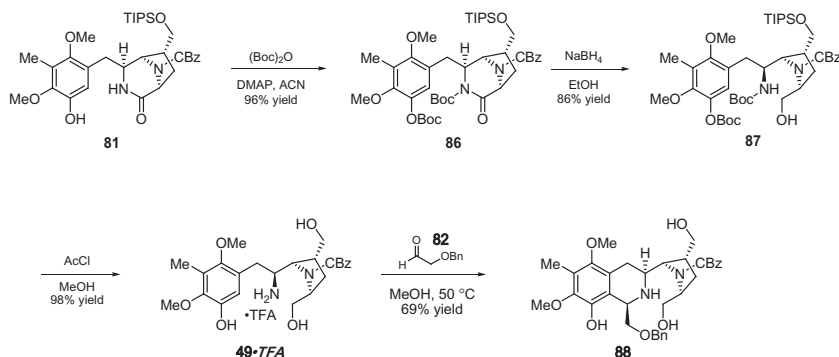


SCHEME 13 Amide Pictet–Spengler and Nagata cyclization attempts.

6. Due to the overlap of key signals in the 1H NMR spectrum, the stereochemistry of **76** was recalcitrant to NOE analysis.

of the amide Pictet–Spengler protocols, we searched for a reaction that would allow for direct synthesis of the carbon–carbon bond. In a previous research project, we had investigated an asymmetric version of the Nagata reaction [26], wherein a phenol, an aldehyde, and an arylboronic acid are condensed to yield a dioxaborolane, forming the key carbon–carbon bond in the process. With this precedent in mind, phenol **81** was treated with methyl glyoxylate, phenylboronic acid, and catalytic trichloroacetic acid according to Nagata’s procedure. The reaction indeed made the desired carbon–carbon bond connection, providing an inseparable mixture of diastereomeric alcohols **85** (dr=4:3), the structures of which were assigned by ^1H NMR and mass spectral data.⁷ Unfortunately, cyclization of this compound to tetrahydroisoquinoline **84** could not be induced under protic or Lewis acidic conditions, nor by conversion of the alcohol to a better leaving group.⁸

Undeterred by the failure of reaction at the weakly nucleophilic amide, we returned to our original plan of synthesizing aminotriol **49**. Due to the difficulty of direct reduction of amides to amino alcohols, lactam **81** was activated by conversion to imide **86** (Scheme 14). Reduction of **86** with excess sodium borohydride in ethanol then cleaved the lactam to protected amino alcohol **87**. Treatment of this compound with *in situ*-generated methanolic hydrochloric acid effected cleavage of the silyl ether, the *tert*-butyl carbamate, and the phenolic carbonate to provide aminotriol **49**, which was isolated as the trifluoroacetate salt after preparative HPLC purification. In model Pictet–Spengler reactions with a variety of α -hydroxyacetaldehyde derivatives, **49** typically generated diastereomerically pure tetrahydroisoquinoline products, for example, in the conversion to **88** with benzyloxyacetaldehyde.



SCHEME 14 Aminotriol synthesis and Pictet–Spengler cyclization.

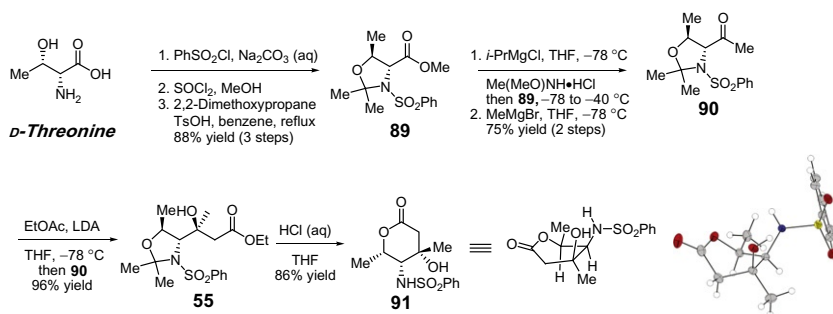
7. To our surprise, no intermediate dioxaborolane was observed in the conversion of **81** to **85**, as the reaction provided the phenol–alcohol directly. It is not known whether this indicates a mechanistic distinction from the traditional Nagata reaction, or whether the intermediate dioxaborolane is merely cleaved during workup and purification of **85**.

8. Treatment of **85** with trifluoroacetic acid, trimethylsilyl iodide, palladium(0) catalysts, or triphenylphosphine and carbon tetrabromide failed to yield any cyclized product.

5.2 Synthesis of Lemonomycin Aminoglycoside

With an effective amine substrate for the Pictet–Spengler reaction in hand, we began the synthesis of an aldehyde-appended aminoglycoside fragment (i.e., **48**, Scheme 7) as the Pictet–Spengler coupling partner. D-Threonine was advanced to methyl ester **89** following known procedures (Scheme 15) [27].⁹ The methyl ester was converted via the Weinreb amide [28] to methyl ketone **90**, which was expected to be an excellent substrate for Felkin–Anh-controlled diastereoselective addition of nucleophiles [29]. Thus, addition of the lithium ketene acetal of ethyl acetate to ketone **90** generated tertiary alcohol **55** as a single observable diastereomer. Cleavage of the oxazolidine ring under acidic conditions proceeded with concomitant lactonization to provide lactone **91**, the relative stereochemistry of which was proven by X-ray diffraction analysis of a single crystal.

Lactone **91** was converted to oxazolidine **92** with dimethoxymethane and trimethylsilyl triflate (Scheme 16). This oxazolidine ring served two important functions. First, the oxazolidine methylene acts as a latent methyl group for eventual conversion to the dimethylamine substituent. Second, the *cis*-fused bicyclic structure of oxazolidine **92** allowed for the highly diastereoselective introduction of an allyloxy group. This allylation was conducted by reduction of **92** with DIBAL followed by treatment with methanesulfonic acid and allyl alcohol. Diastereoselectivity arose from the cup-shaped structure of intermediate oxocarbenium ion **94**.¹⁰ Attack from the convex face of **94** provided allyl glycoside **95** with trace amounts of the easily separable anomer.¹¹ Subsequent Red-Al reduction removed the benzenesulfonyl group and cleaved the oxazoli-

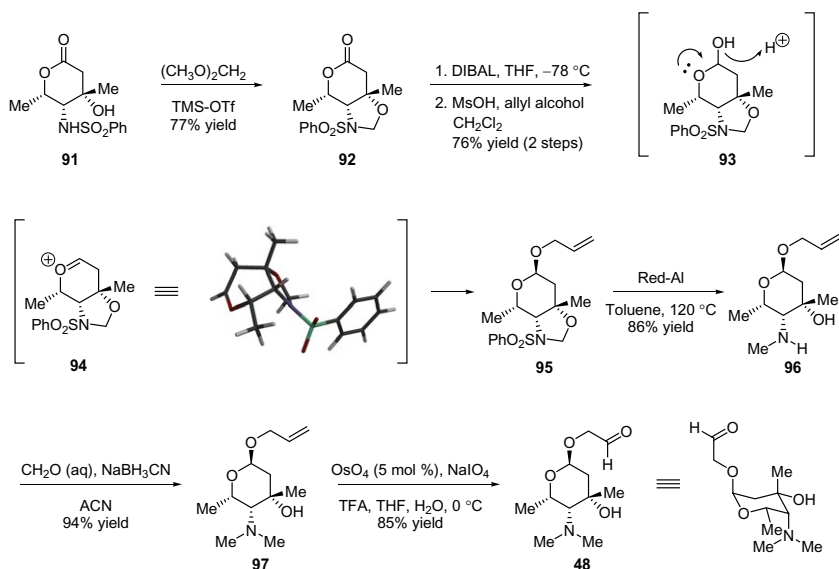


SCHEME 15 δ -Lactone synthesis for the aminoglycoside.

9. This synthetic route was also performed with L-threonine as the starting material, such that both enantiomers of each compound in aminoglycoside synthesis have been prepared.

10. The conformation of **94** was minimized by AM1 semiempirical calculations utilizing Spartan '02 v1.0.8 (Wavefunction, Inc.).

11. An analogous reduction and allyloxy group installation with a methylamino group in place of the oxazolidine ring provided an approximately 1:1 mixture of anomers, pointing to the importance of the *cis*-fused bicycle in controlling diastereoselective addition to the oxocarbenium ion.



SCHEME 16 Oxoethyl aminoglycoside synthesis.

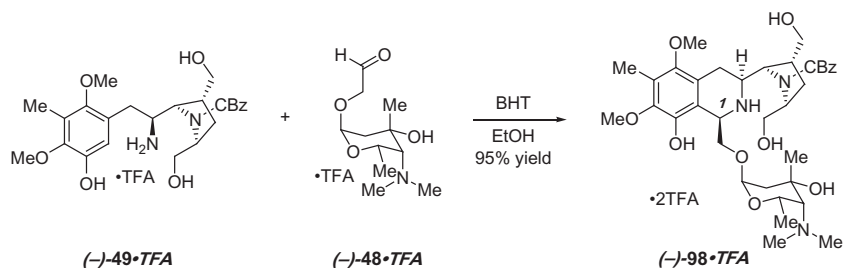
dine ring to yield secondary amine **96**, which was readily converted to the tertiary amine by reductive methylation. Oxidative cleavage of the allyl group was then effected by catalytic dihydroxylation in the presence of sodium periodate, leading directly to glycosyloxy acetaldehyde **48** [30].

5.3 Completion of (–)-Lemonomycin

With the Pictet–Spengler substrates **48** and **49** in hand, we began the final campaign toward lemonomycin. To our delight, we discovered that simply mixing the trifluoroacetate salts of (–)-**48** and (–)-**49** in ethanol at room temperature provided 95% yield of tetrahydroisoquinoline (–)-**98** as a single diastereomer at C(1) (Scheme 17).¹² This reaction marked the first example of a Pictet–Spengler cyclization employing a complex α -glycosyloxy aldehyde as a substrate. The high yielding and completely diastereoselective reaction also accomplished a highly convergent strategy for the synthesis of the lemonomycin core structure.

The remaining challenges for converting tetrahydroisoquinoline (–)-**98** to (–)-lemonomycin were threefold and deceptively simple (Figure 2). The two primary alcohols were to be oxidized to the carbinolamine and aldehyde hydrate, respectively, ideally in a single reaction. The oxidation of the

12. Tetrahydroisoquinoline **98** was the only compound recovered from the Pictet–Spengler cyclization. Any traces (<3%) of diastereomeric compound arising from the minor enantiomer of **49** (94% ee) are most likely removed during HPLC purification of **98**.



SCHEME 17 Pictet–Spengler cyclization.

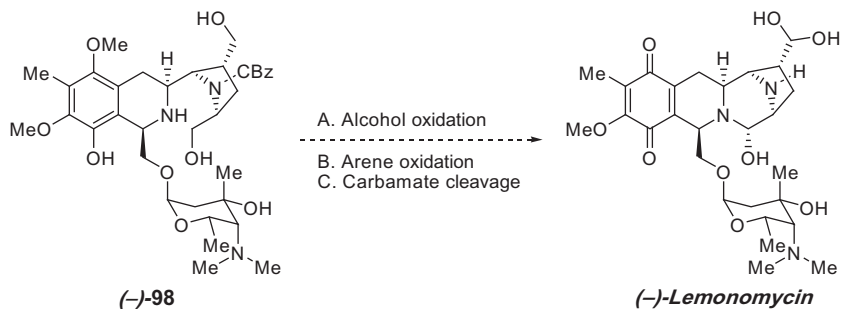
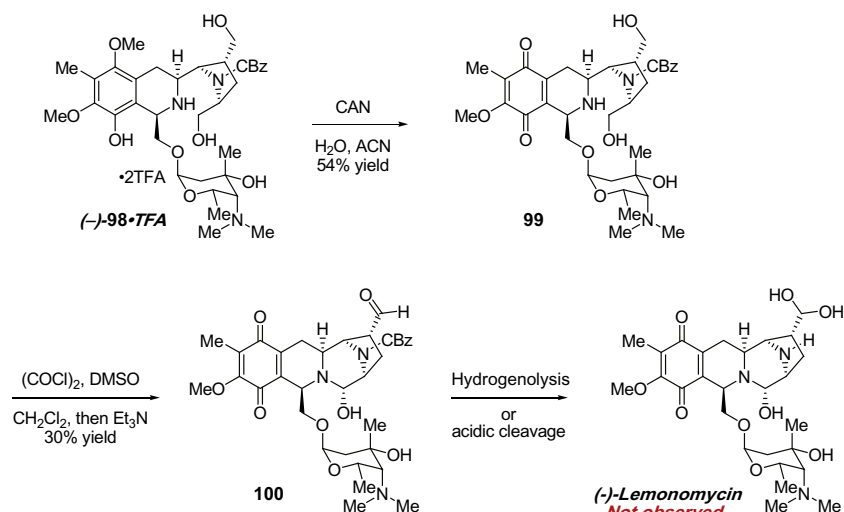


FIGURE 2 Endgame challenges.

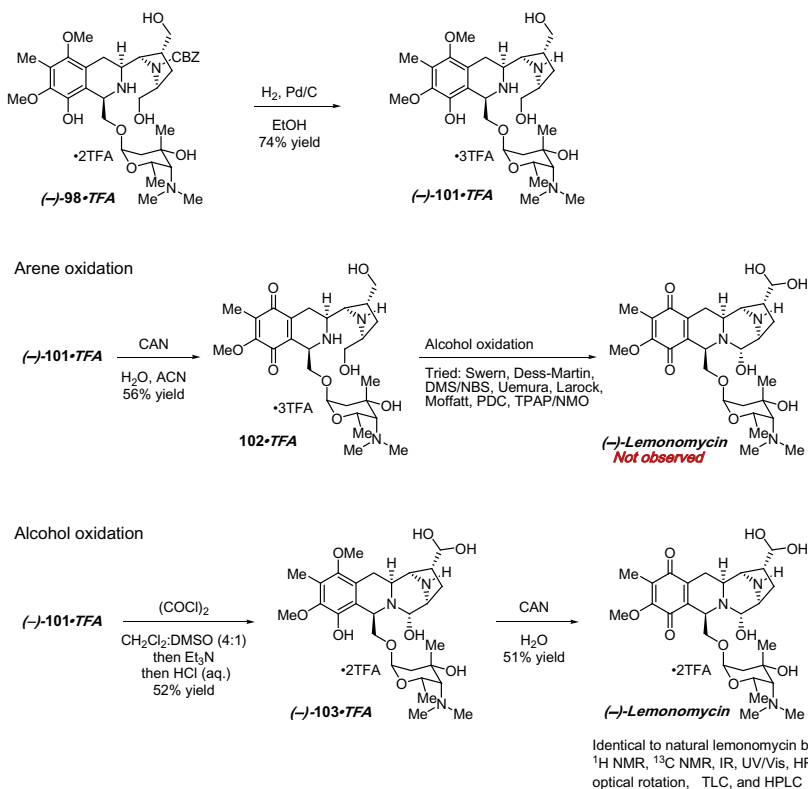
dimethoxyphenol to a *para*-quinone was required and, the carbamate protecting group had to be removed.

We first attempted to advance $(-)\text{-}98$ by alcohol oxidation to forge the full ring structure of lemonomycin, but standard conditions for conversion to the aldehyde–carbinolamine (Swern oxidation, Dess–Martin periodinane, TPAP/NMO) failed with this compound, and only complex mixtures of unidentifiable compounds were obtained. The aromatic oxidation was then tried as the first of the three steps. This oxidation was achieved with ammonium cerium(IV) nitrate, generating quinone **99** in moderate yield (Scheme 18). Alcohol oxidation then was accomplished under Swern conditions, giving our first access to the full tetrahydroisoquinoline core ring structure as aldehyde–carbinolamine **100**. Our enthusiasm was diminished by the relative instability of **100**, which led to low yields in the oxidation. Moreover, attempts to remove the CBz group under hydrogenolytic or acidic conditions generated an array of unidentifiable decomposition products without even a trace of the natural product.

Faced with the difficulties of routes beginning with either of the oxidations, we decided to first remove the benzyl carbamate (Scheme 19), which we considered a markedly risky strategy considering that the eventual oxidation state adjustments would need to be carried out in the presence of a free secondary amine. Nonetheless, we proceeded with hydrogenolysis of $(-)\text{-}98$, which provided triaminotetraol $(-)\text{-}101$ in good yield. Ammonium



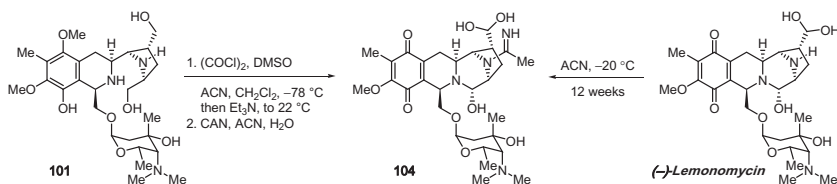
SCHEME 18 Arene oxidation endgame.



SCHEME 19 Completion of (–)-lemonomycin.

cerium(IV) nitrate oxidation then yielded quinone (–)-**102** with no sign of *N*-oxidation, again bringing us within a single step of the natural product. Unfortunately, alcohol oxidation utilizing the Dess–Martin periodinane [31], Swern conditions, DMS/NBS [32], Uemura conditions [33], Larock conditions [34], pyridinium dichromate, or TPAP/NMO [35] failed to provide any amount of lemonomycin. Even the venerable Moffatt [36] oxidation, which had proven uniquely effective in a previous synthesis by one of us [37], provided no solution in this case.

We therefore turned to the only path still available, which would require alcohol oxidation of triaminotetraol (–)-**101**. Despite the presence of confounding functionality in the form of the phenol, tertiary alcohol, and two secondary amines, we discovered that carefully controlled Swern oxidation conditions with DMSO cosolvent effected the oxidation of both primary alcohols. The oxidation was complicated by the formation of intermediate methylthiomethyl ether or amine groups,¹³ but this problem was mitigated by treatment of the crude reaction mixture with aqueous hydrochloric acid, yielding clean phenol (–)-**103** in 52% yield along with two monooxidized compounds in 33% and 13% yield, respectively.¹⁴ The completion of the synthesis was then accomplished by cerium(IV) oxidation of the phenol to provide (–)-lemonomycin. Our synthetic sample was identical to a natural sample by all spectroscopic and chromatographic methods, including ¹H NMR, ¹³C NMR, IR, UV/Vis, HRMS, optical rotation, TLC, and HPLC coinjection.¹⁵



13. Mass spectrometry analysis of the crude reaction mixtures showed $\text{M}+61$ and $\text{M}+121$ in addition to $\text{M}+\text{H}$, indicating the presence of one or two methylthiomethyl groups.

14. In principle, these monooxidized compounds could be resubmitted to the Swern oxidation to yield additional **103**. However, these reactions were not conducted.

15. In addition to the spectroscopic matching of natural and synthetic (–)-lemonomycin, our synthetic intermediates were chemically correlated with the natural product through a serendipitous discovery. Specifically, Swern oxidation of **101** with acetonitrile as the cosolvent followed by CAN oxidation yielded amidine **104**, wherein the secondary amine had attacked an equivalent of acetonitrile. Amidine **104** was also produced when natural (–)-lemonomycin was stored as a solution in acetonitrile for a period of several weeks.

6. CONCLUDING REMARKS

The first total synthesis of (–)-lemonomycin was accomplished in an efficient and highly convergent manner. Important strategic choices facilitated the synthesis, particularly the use of the chiral auxiliary-controlled dipolar cycloaddition for the construction of the diazabicyclo[3.2.1]octane core, the employment of transition metal-catalyzed fragment coupling, and the incorporation of the aminoglycoside within the highly stereoselective Pictet–Spengler coupling. Numerous tactical challenges were encountered and conquered along the way, including three cases of chirality transfer. The concavity of the diazabicyclooctane was utilized to set C(3) stereochemistry during olefin hydrogenation, and the concavity of the *cis*-fused oxazolidine was utilized to set the anomeric stereocenter during the glycoside synthesis. Navigation of the minefield of compound instability during the endgame led to the non-obvious choice of early protecting group cleavage. In retrospect, the requirement for early removal of the benzyl carbamate is not entirely surprising; protecting group removal necessarily involved cleavage of strong bonds, which became more challenging as each sensitive functional group was added to the molecular core.

Completion of the total synthesis of (–)-lemonomycin accomplished a major goal of our work on this compound. Two areas of research, however, could warrant further attention. First, the synthesis of the lemonomycin aminoglycoside from D-threonine, though effective, is somewhat lengthy. A much shorter synthesis might be achieved if efficient and enantioselective conditions could be developed for the hetero-Diels–Alder reaction proposed in [Scheme 7](#). Second, our synthesis of lemonomycin aminoglycoside was applied to both enantiomeric series, thus providing the (+)-*O*-oxoethyl aminoglycoside in addition to the (–)-*O*-oxoethyl aminoglycoside utilized for the synthesis (–)-lemonomycin. Use of the (+)-*O*-oxoethyl aminoglycoside in an analogous Pictet–Spengler cyclization would lead to a diastereomer of lemonomycin that might have altered biological activity. In a broader investigation, this strategy could be used for the incorporation of many different glycosyl units into the lemonomycin structure, leading to a library of antineoplastic agents and antibiotics with potentially improved efficacy against highly resistant bacterial and cancer strains.

REFERENCES

- [1] For a comprehensive review of the tetrahydroisoquinoline family of antitumor antibiotics, see: J.D. Scott, R.M. Williams, *Chem. Rev.* 102 (2002) 1669–1730.
- [2] H.A. Whaley, E.L. Patterson, M. Dann, A.J. Shay, J.N. Porter, *Antimicrob. Agents Chemother.* 8 (1964) 83–86.
- [3] H. He, B. Shen, G.T. Carter, *Tetrahedron Lett.* 41 (2000) 2067–2071.
- [4] (a) D.A. Steinberg, V.S. Bernan, D.A. Montenegro, D.R. Abbanat, C.J. Pearce, J.D. Korshalla, N.V. Jacobus, P.J. Petersen, M.J. Mroczenski-Wildey, W.M. Maiese, M. Greenstein, *J. Antibiot.* 47 (1994) 887–893; (b) P.T. Northcote, D. Williams, J.K. Manning, D.B. Borders, W.

- M. Maiese, M.D. Lee, *J. Antibiot.* 47 (1994) 894–900; (c) P.T. Northcote, M. Siegel, D. B. Borders, M.D. Lee, *J. Antibiot.* 47 (1994) 901–908.
- [5] K.L. Constantine, L. Meuller, S. Huang, S. Abid, K.S. Lam, W. Li, J.E. Leet, *J. Am. Chem. Soc.* 124 (2002) 7284–7285.
- [6] MJ347-81F4 A has identical connectivity to nocathiacin I, but the relative stereochemistry was not disclosed. MJ347-81F4 B contains the lemomycin aminoglycoside wherein one of the *N*-methyl groups is replaced by hydrogen, see: T. Sasaki, T. Otani, H. Matsumoto, N. Unemi, M. Hamada, T. Takeuchi, M. Hori, *J. Antibiot.* 51 (1998) 715–721.
- [7] An oxidized form of the sugar is also present as a substituent of the saccharocarbons, see: V.R. Hegde, M.G. Patel, P.R. Das, B. Pramanik, M.S. Puar, *J. Antibiot.* 50 (1997) 126–134.
- [8] (a) DNA binding has been implied as part of the biological mode of action for many of the tetrahydroisoquinoline antitumor antibiotics. For binding studies with saframycin A, see: J.W. Lown, A.V. Joshua, J.S. Lee, *Biochemistry* 21 (1982) 419–428; (b) Interactions leading to the DNA binding, including hydrogen bonding to the bridging ammonium, have been implicated in a computational study based on crystal structures of DNA and the antibiotics, see: G.C. Hill, W.A. Remers, *J. Med. Chem.* 34 (1991) 1990–1998; (c) A covalent complex of cyanocycline A with DNA has also been reported, see: M.J. Zmijewski, K. Miller-Hatch, M. Goebel, *Antimicrob. Agents Chemother.* 21 (1982) 787–793.
- [9] T. Fukuyama, J.J. Nunes, *J. Am. Chem. Soc.* 110 (1988) 5196–5198.
- [10] For a similar cyclization utilizing a 1,3-diester as the nucleophile, see: H. Saito, T. Hirata, *Tetrahedron Lett.* 28 (1987) 4065–4068.
- [11] Similar disconnections have been used in progress toward the lemomycin framework, see: (a) K. Rikimaru, K. Mori, T. Kan, T. Fukuyama, *Chem. Commun.* 3 (2005) 394–396; (b) P. Magnus, K.S. Matthews, *J. Am. Chem. Soc.* 127 (2005) 12476–12477.
- [12] S.J. Danishefsky, P.J. Harrison, R.R. Webb II, B.T. O’Neil, *J. Am. Chem. Soc.* 107 (1985) 1421.
- [13] A similar disconnection was utilized in Weinreb’s synthesis of quinocarcin, see: T. A. Lessen, D.M. Demko, S.M. Weinreb, *Tetrahedron Lett.* 31 (1990) 2105.
- [14] (a) D.A. Evans, S.A. Biller, *Tetrahedron Lett.* 26 (1985) 1907–1910; (b) D.A. Evans, S. A. Biller, *Tetrahedron Lett.* 26 (1985) 1911–1914; (c) D.A. Evans, C.R. Illig, J.C. Sandler, *J. Am. Chem. Soc.* 108 (1986) 2478–2479; (d) S.A. Biller, *An Approach to the Total Synthesis of (±)-Naphthyridinomycin A*, (1982) Ph.D. Thesis, California Institute of Technology, Pasadena, CA; (e) C.R. Illig, *The Total Synthesis of (±)-Cyanocycline A and (+)-Cyanocycline A*, (1987) Ph.D. Thesis, Harvard University, Cambridge, MA.
- [15] (a) T. Fukuyama, A.A. Laird, *Tetrahedron Lett.* 27 (1986) 6173–6176; (b) T. Fukuyama, L. Li, A.A. Laird, R.K. Frank, *J. Am. Chem. Soc.* 109 (1987) 1587–1589.
- [16] (a) M. Kiss, J. Russell-Maynard, J.A. Joule, *Tetrahedron Lett.* 28 (1987) 2187–2190; (b) P. A. Allway, J.K. Sutherland, J.A. Joule, *Tetrahedron Lett.* 31 (1990) 4781–4782; (c) N. D. Yates, D.A. Peters, P.A. Allway, R.L. Beddoes, D.I.C. Scopes, J.A. Joule, *Heterocycles* 40 (1995) 331–347.
- [17] P. Garner, W.B. Ho, H. Shin, *J. Am. Chem. Soc.* 115 (1993) 10742–10753.
- [18] (a) M.E. Flanagan, R.M. Williams, *J. Org. Chem.* 60 (1995) 6791–6797; (b) J.D. Scott, R. M. Williams, *Angew. Chem. Int. Ed. Engl.* 40 (2001) 1463–1465; (c) J.D. Scott, R.M. Williams, *J. Am. Chem. Soc.* 124 (2002) 2951–2956.
- [19] D.A. Evans, E. Hu, J.S. Tedrow, *Org. Lett.* 3 (2001) 3133–3136.
- [20] (a) The Pictet–Spengler cyclization was originally reported in 1911, see: A. Pictet, T. Spengler, *Ber. Dtsch. Chem. Ges.* 44 (1911) 2030–2036; (b) For a recent review of the Pictet–Spengler cyclization, see: E.D. Cox, J.M. Cook, *Chem. Rev.* 95 (1995) 1797–1842.

- [21] T. Fukuyama, L. Yang, K.L. Ajeck, R.A. Sachleben, *J. Am. Chem. Soc.* 112 (1990) 3712–3714.
- [22] (a) For recent examples of catalytic asymmetric hetero-Diels–Alder reactions, see: Y. Huang, A.K. Unni, A.N. Thadani, V.H. Rawal, *Nature* 424 (2003) 146; (b) A.N. Thadani, A.R. Stankovic, V.H. Rawal, *Proc. Natl. Acad. Sci. USA* 101 (2004) 5846–5850; (c) A.G. Dossetter, T.F. Jamison, E.N. Jacobsen, *Angew. Chem. Int. Ed. Engl.* 38 (1999) 2398–2400; (d) S.E. Schaus, J. Brnalt, E.N. Jacobsen, *J. Org. Chem.* 63 (1998) 403–405.
- [23] W.B. Lutz, S. Lazarus, S. Klutchko, R.I. Meltzer, *J. Org. Chem.* 29 (1964) 415–418.
- [24] C. Thom, P. Kocienski, *Synthesis* (1992) 582–586.
- [25] For a review of thermal reactions utilizing Oppolzer's sultam, see: B.H. Kim, D.P. Curran, *Tetrahedron* 49 (1993) 293–318.
- [26] W. Nagata, K. Okada, T. Aoki, *Synthesis* (1979) 365–368.
- [27] (a) R.C. Roemmele, H. Rapoport, *J. Org. Chem.* 53 (1988) 2367–2371; (b) B. Szechner, O. Achmatowicz, Z. Galdecki, A. Fruzinski, *Tetrahedron* 50 (1994) 7611–7624.
- [28] For the synthesis of Weinreb amides from esters with *N,O*-dimethylhydroxylamine hydrochloride and isopropylmagnesium chloride, see: J.M. Williams, R.B. Jobson, N. Yasuda, G. Marchesini, U.-H. Dolling, E.J.J. Grabowski, *Tetrahedron Lett.* 36 (1995) 5461–5464.
- [29] (a) M. Chérest, H. Felkin, *Tetrahedron Lett.* 9 (1968) 2205–2208; (b) N.T. Anh, *Top. Curr. Chem.* 88 (1980) 145–162; (c) T.M. Reetz, *Chem. Rev.* 99 (1999) 1121–1162.
- [30] For the use of periodate and catalytic osmium tetroxide for the production of carbonyls from alkenes, see: R. Pappo, D.S. Allen Jr., R.U. Lemieux, W.S. Johnson, *J. Org. Chem.* 21 (1956) 478–479.
- [31] For a review of hypervalent iodine reagents for alcohol oxidation, including the Dess–Martin periodinane, see: H. Tohma, Y. Kita, *Adv. Synth. Catal.* 346 (2004) 111–124.
- [32] (a) For reviews of alcohol oxidation with activated DMSO reagents, including the Swern, Moffatt, and DMS/NBS oxidations, see: T.T. Tidwell, *Synthesis* (1990) 857–870; (b) T.T. Tidwell, *Org. React.* 39 (1990) 297–572.
- [33] T. Nishimura, T. Onoue, K. Ohe, S. Uemura, *J. Org. Chem.* 64 (1999) 6750–6755.
- [34] K.P. Peterson, R.C. Larock, *J. Org. Chem.* 63 (1998) 3185–3189.
- [35] For a review of tetrapropylammonium perruthenate-catalyzed alcohol oxidation, see: S.V. Ley, J.N. Norman, W.P. Griffith, S.P. Marsden, *Synthesis* (1994) 639–666.
- [36] K.E. Pfizner, J.G. Moffatt, *J. Am. Chem. Soc.* 87 (1965) 5670–5678.
- [37] (a) J.L. Wood, B.M. Stoltz, S.N. Goodman, *J. Am. Chem. Soc.* 118 (1996) 10656–10657; (b) J.L. Wood, B.M. Stoltz, S.N. Goodman, K. Onwueme, *J. Am. Chem. Soc.* 119 (1997) 9652–9661.

Studies on the Synthesis of the Apoptolidins

Stephen T. Chau^{*}, Gary A. Sulikowski^{*} and Bin Wu^{†1}

^{*}Department of Chemistry, Vanderbilt University, Nashville, Tennessee, USA, [†]Department of Chemistry, Texas A&M University, College Station, Texas, USA

Chapter Outline

1. Introduction and Background	375	4.1. First-Generation Approach to Apoptolidinone	380
2. Biosynthesis	377	4.2. Approach to Pseudoapoptolidin A	383
3. Total Syntheses of Apoptolidin A	378	4.3. Total Synthesis of Apoptolidinone A	386
3.1. Nicolaou Synthesis	378	5. Precursor-Directed Glycosylation	390
3.2. Koert Synthesis	379	6. Conclusion and Epilogue	392
3.3. Crimmins Synthesis	379		
4. Total Syntheses of Apoptolidinone A and D	380		

1. INTRODUCTION AND BACKGROUND

A series of reviews by Newman and coworkers estimated over 60% of new anticancer agents approved by regulatory agencies since 1981 are of natural product origin [1]. In the interest of identifying natural products with selective cytotoxicity against tumor cells, Hayakawa and Seto established pRb-inactivated glia cells by transformation with the adenovirus E1A oncogene [2]. When screened against this cell line, an actinomycete identified as *Nocardopsis* sp. was found to produce an active metabolite designated as apoptolidin [3]. The natural product was determined to induce apoptosis in the E1A-transformed cells but not in normal cells or 3Y1 rat fibroblasts transformed with other oncogenes including *H-ras* or *V-src*. In the initial publication, only the two-dimensional structure of apoptolidin was reported with the complete stereochemical

1. Current Address: Amgen Inc., One Amgen Center Drive, Thousand Oaks, California, USA

assignment released in 1998 [4]. Expectedly, apoptolidin drew attention as a synthetic target and potential tool molecule for defining new targets for the development of anticancer agents [5].

Studies aimed at target identification and therapeutic development of apoptolidin were augmented by fermentation, as the yield of apoptolidin by fermentation was 109 mg/l (Figure 1) [6]. Salomon and coworkers studied the mode of action of apoptolidin using a combination of molecular and cell-based pharmacological assays and concluded the cellular target resides within the mitochondria [7]. The correlation of cell cytotoxicity using the NCI 60 cell line panel with known cytotoxic macrolides led to the conclusion that F_0F_1 -ATPase was the likely mitochondrial target. In a biochemical assay, apoptolidin inhibited F_0F_1 -ATPase activity in intact yeast mitochondria and solubilized enzyme preparations with IC_{50} of 4–5 μ M.

Production of apoptolidin by fermentation has resulted in the identification of minor metabolites apoptolidins B–G and designation of apoptolidin as apoptolidin A [8]. Aside from apoptolidins C and G, the macrolactone demonstrates a propensity to equilibrate with a ring-expanded isomer by acyl migration from the C19 to C20 hydroxyl group, these 20-membered macrolides were named isoapoptolidins [6a,b]. In general, a significant loss of

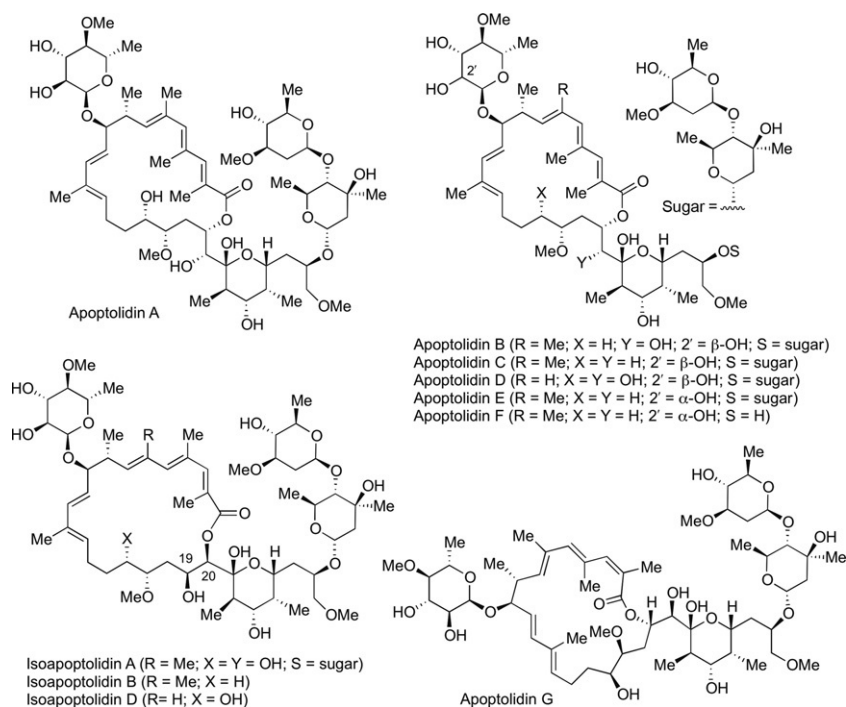


FIGURE 1 Structures of apoptolidins and isoapoptolidins.

cytotoxicity has only been observed in apoptolidins lacking the C27 disaccharide, a pattern of activity mirrored with the isoapoptolidin series as well [9].

2. BIOSYNTHESIS

Recently, in collaboration with the Bachmann group at Vanderbilt University, we have identified and expressed the apoptolidin gene cluster from the microbial producer *Nocardiopsis* sp. FU40 [10]. The gene cluster comprises a type I polyketide synthase consisting of 13 homologating modules. Polyketide assembly is proposed to be followed by C16/C21 oxidation, C9 glycosylation, and C27 glycosylation. A representation of the apoptolidin assembly is shown in Figure 2. The noniterative type I polyketide synthase incorporates the typical varying open-reading frame repeat of ketosynthase, acyl transferase, ketoreductase, dehydratase, and acyl carrier protein. Macrocyclization by way of a

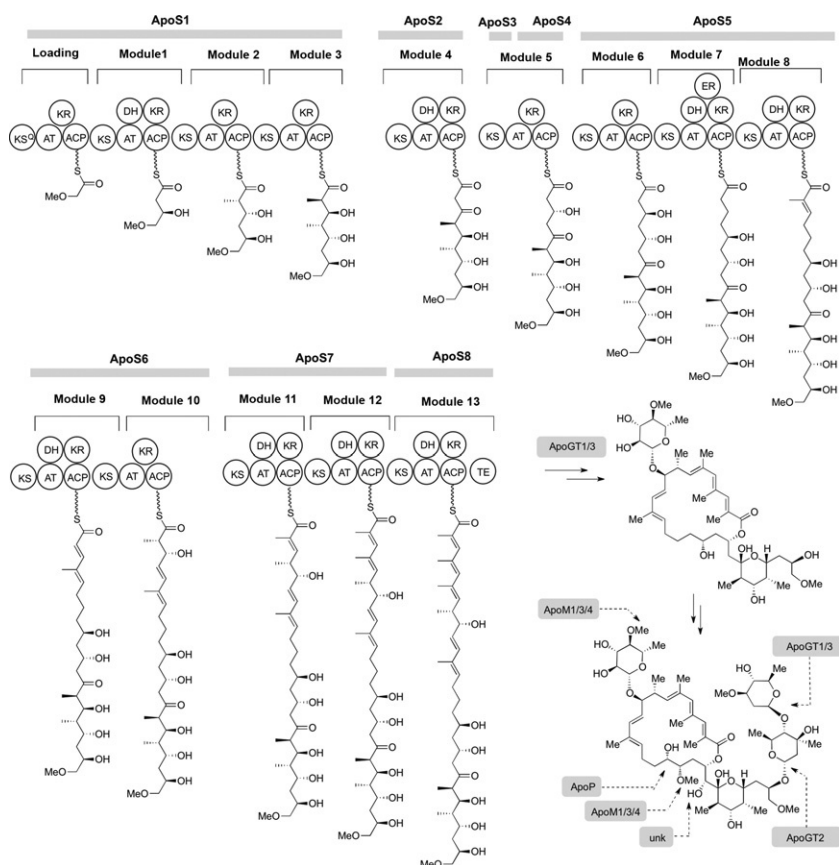


FIGURE 2 Generalized biosynthetic pathway leading to apoptolidins.

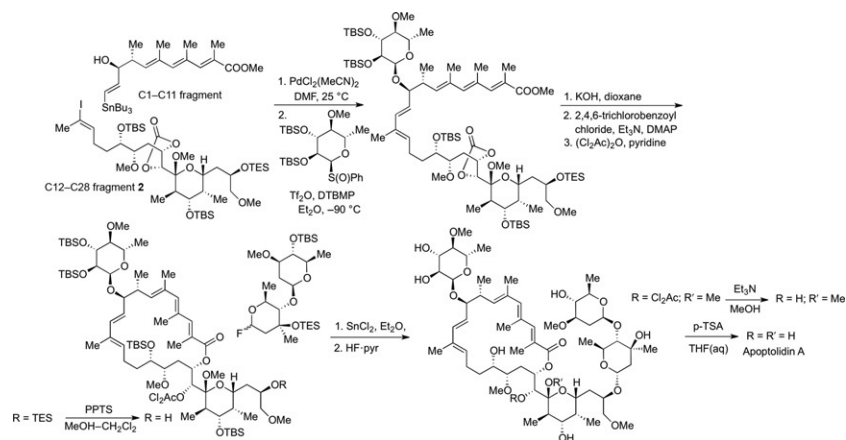
thioesterase is then followed by post-PKS transformations of oxidation and glycosylation. Manipulation of the gene cluster will provide an opportunity for analog production aimed at developing the apoptolidins as biological probes and therapeutic leads.

3. TOTAL SYNTHESIS OF APOPTOLIDIN A

Apoptolidin A has attracted attention from the synthetic community as a target for total synthesis due to its reported cell-selective cytotoxicity and challenging molecular structure [5,11,12]. A particularly difficult hurdle in the total synthesis of apoptolidin A is the incorporation of deoxy sugars located at C9 and C27. In general, the complete assembly of the aglycone and carbohydrate components of natural products remains a difficult task due to the necessity to effect stereo- and chemoselective glycosylation of an often poly-oxygenated aglycone. In this section, we narrow the scope of our discussion primarily to the order of assembly of the fragments with particular attention to the timing of deoxy sugar incorporation.

3.1 Nicolaou Synthesis

In 2001, Nicolaou and coworkers described the first total synthesis of apoptolidin A (Scheme 1) [13]. The core aglycone was assembled by formation of the C11—C12 carbon—carbon bond by employing a Stille cross-coupling between C1—C11 and C12—C28 fragments. The coupling reaction was immediately followed by C9 glycosylation using a glycosyl sulfoxide donor under Kahne glycosylation conditions [14]. Treatment of the intermediate methyl ester with aqueous KOH in dioxane resulted in the ester saponification accompanied by loss of the C19—C20 carbonate. The intermediate seco acid



SCHEME 1 Nicolaou strategy.

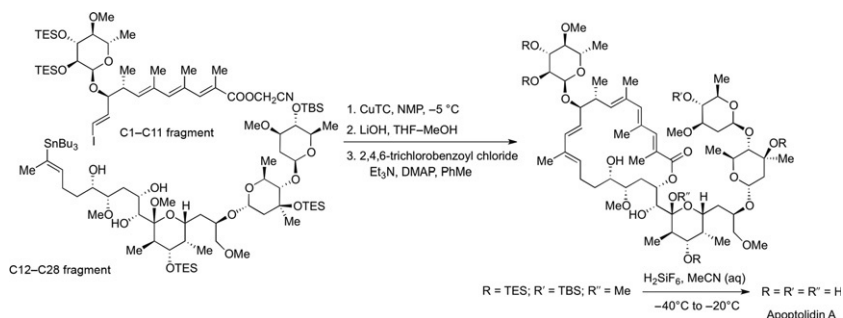
was cyclized under Yamaguchi macrocyclization conditions, resulting in selective closure on the C19 hydroxyl group. Following protection of the C20 hydroxyl group as a dichloroacetate, the C27 triethylsilyl group was removed (PPTS, MeOH, CH_2Cl_2) and the newly revealed secondary alcohol was glycosylated with a glycosyl fluoride donor. Finally, HF-pyridine treatment removed all silyl protecting groups, while triethylamine-methanol served to remove the dichloroacetate group and acidic methanol released the C21 hemiacetal to complete apoptolidin A.

3.2 Koert Synthesis

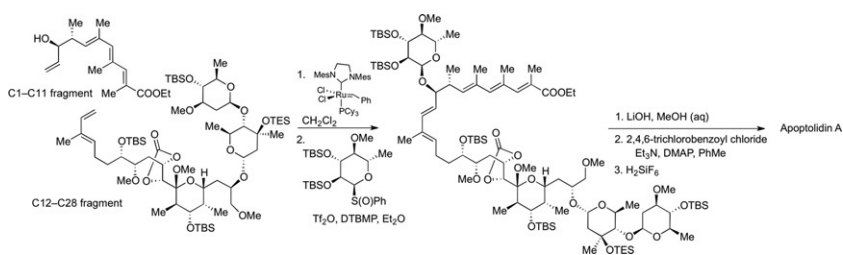
Koert described the first synthesis of the apoptolidin aglycone, apoptolidinone [12a], in 2001 followed by the total synthesis of apoptolidin in 2004 (Scheme 2) [15]. Koert's synthetic route was distinct from Nicolaou's reported synthesis as the C1—C11 and C12—C28 fragments were coupled as C9 and C27 glycosylated units, respectively. The strategy led to a convergent approach whereby Stille coupling using Liebeskind's reagent (CuTC in NMP) [16] served to form the C11—C12 bond and, following hydrolysis, the C1 cyanomethyl ester afforded the corresponding seco acid, poised for a Yamaguchi cyclization. Another notable feature in Koert's synthesis was the use of 25% aqueous H_2SiF_6 in acetonitrile to globally remove silyl ethers and the C21 methyl acetal in the final step of the total synthesis to afford apoptolidin A.

3.3 Crimmins Synthesis

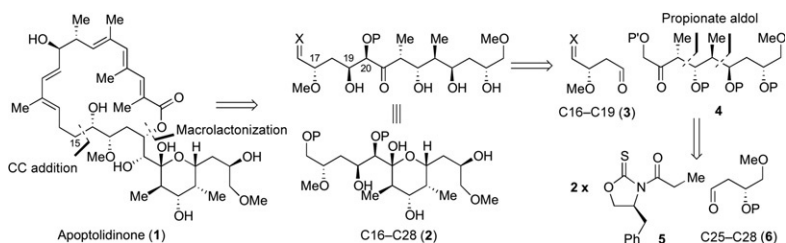
From a strategic perspective, the Crimmins total synthesis of apoptolidin A followed the Nicolaou strategy, whereby the C9 and C27 sugars were introduced at the seco acid stage of assembly (Scheme 3) [17]. Unique to Crimmins' synthesis was the use of a cross-metathesis reaction to form the C10—C11 carbon-carbon double bond. Also noteworthy was the use of thioxazolidinones in key stereoselective aldol reactions employed in the fragment assembly [18] (Scheme 4).



SCHEME 2 Koert strategy.



SCHEME 3 Crimmins strategy.



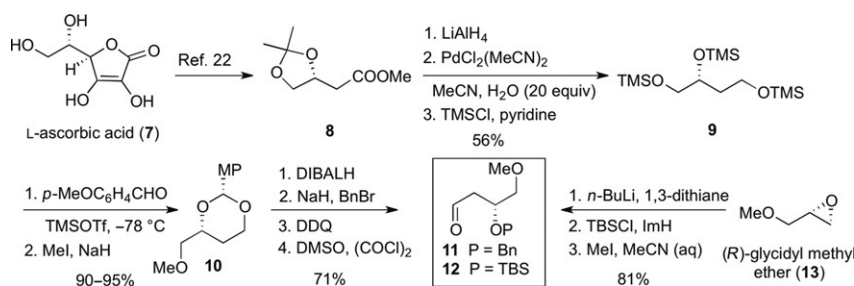
SCHEME 4 First-generation synthetic strategy.

4. TOTAL SYNTHESIS OF APOPTOLIDINONE A AND D

4.1 First-Generation Approach to Apoptolidinone

In 1998, apoptolidin attracted our attention as a synthetic target due to its reported cell selective cytotoxicity and complex molecular structure. Our initial synthetic analysis focused on the aglycone, apoptolidinone (**1**), with disconnections at C15—C16 and the macrolactone to reveal the C16—C28 fragment (**2**) as a primary synthetic target [19]. When analyzed in the extended zig-zag conformation, the *anti-syn* stereochemical relationship spanning the C17, C19, and C20 stereocenters in conjunction with the location of the C20 keto group suggested a Mukaiyama aldol reaction between the silyl enol ether derived from α -alkoxy ketone **4** and β -methoxy aldehyde **3** to deliver adduct **2**. The predicted stereoselectivity of the proposed aldol reaction was based on studies reported by Evans and coworkers [20], who described the closely related double diastereoselective Mukaiyama aldol additions. Harbored within the C20—C28 ketone (**4**) intermediate were two contiguous *syn*-propionate aldol retrons of opposite relative stereochemistry. At the time of our analysis, a report by Crimmins *et al.* [21] provided a direct solution to the installation of these two propionate units using a common thioxazolidinone (**5**) twice starting from aldehyde **6**.

Over the course of our 6-year study culminating in the total synthesis of apoptolidinones A and D, we developed several routes to key fragments including protected C25—C28 aldehydes **11** and **12** (Scheme 5). The first route leading to benzyl ether **11** began with a known six-step conversion of L-ascorbic acid (**7**) to methyl ester **8** [22]. Reduction of **8** followed by

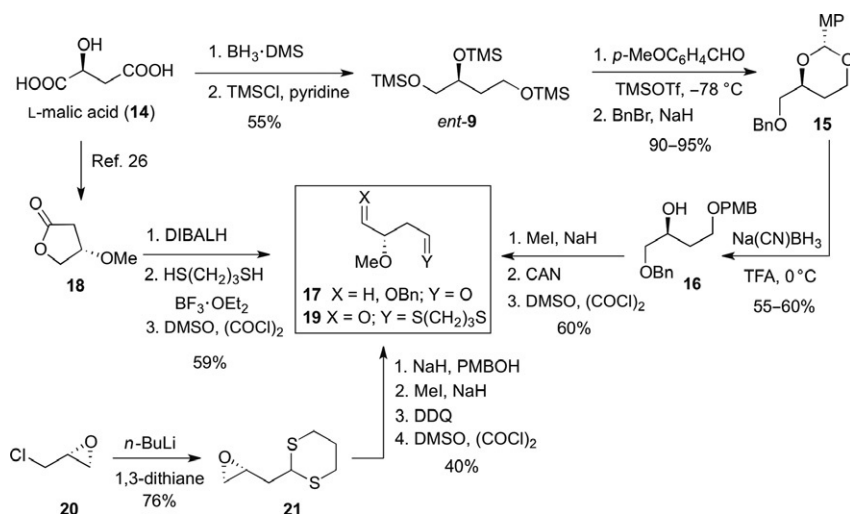


SCHEME 5 Two synthetic routes leading to C25—C28 fragment.

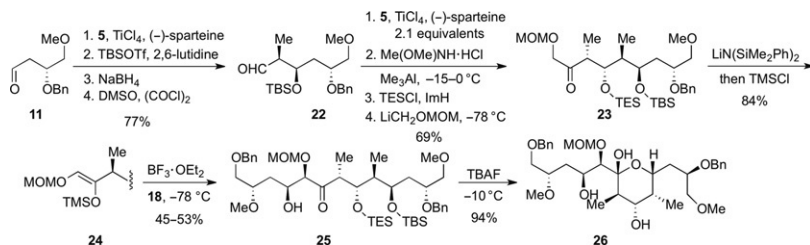
palladium(II)-mediated acetonide removal using a nonaqueous work-up [23] and persilylation provided tris-trimethylsilyl ether **9**. The latter was protected as a 1,3-anisylidene under aprotic conditions [24] and the remaining primary alcohol methylated to afford **10**. Chelation-directed reductive fragmentation of **10** was followed by benzylation, PMB removal, and Swern oxidation to give aldehyde **11**. A more expedient route to TBS-protected aldehyde **12** was later developed starting with dithiane opening of commercially available (*R*)-glycidyl methyl ether **13** followed by TBS protection of the resulting secondary alcohol. Hydrolysis of the protected thioacetal using Fetizon conditions afforded **12** in high overall yield [25].

Synthesis of the C16—C19 fragment posed an interesting problem as a differentiated chiral 1,4-dialdehyde (**17** and **19**, Scheme 6). Two routes starting from L-malic acid (**14**) were developed, the first proceeding by way of ent-**9** derived from malic acid in two steps [26]. Once again, 1,3-diol protection under aprotic conditions revealed a primary alcohol, in this case protected as a benzyl ether (**15**). As we required selective release of the secondary alcohol, nonchelating (TFA, Na(CN)BH₃) reductive cleavage conditions were employed to afford alcohol **16** [27]. Methylation of **16** was followed by oxidative removal of the PMB group to release a primary alcohol subsequently oxidized to aldehyde **17**. Thioacetal **19** was derived from malic acid by way of lactone **18** (Scheme 6). Reduction of **18** with DIBAL afforded an intermediate lactol that was condensed with 1,3-propanediol with concomitant release of a primary alcohol. Oxidation of the latter intermediate using Swern conditions completed aldehyde **19**. A less efficient route to thioacetal **19** started from (*S*)-epichlorohydrin **20** and proceeded by way of epoxide **21** [28]. A four-step reaction sequence then transformed **21** to **19**.

Our first-generation synthesis of the C16—C28 fragment of apoptolidin started with addition of the titanium(IV) enolate of thioxazolidinone **5** to aldehyde **11** to afford an intermediate Evans aldol adduct in accord with a nonchelate Zimmer–Traxler model (Scheme 7). Alcohol protection as a TBS ether followed by reduction and oxidation then gave aldehyde **22** in 77% overall yield. The second aldol reaction was conducted using a second equivalent of titanium(IV) chloride leading to the non-Evans aldol adduct by way of a closed-chelate transition state model in accord with earlier reports by



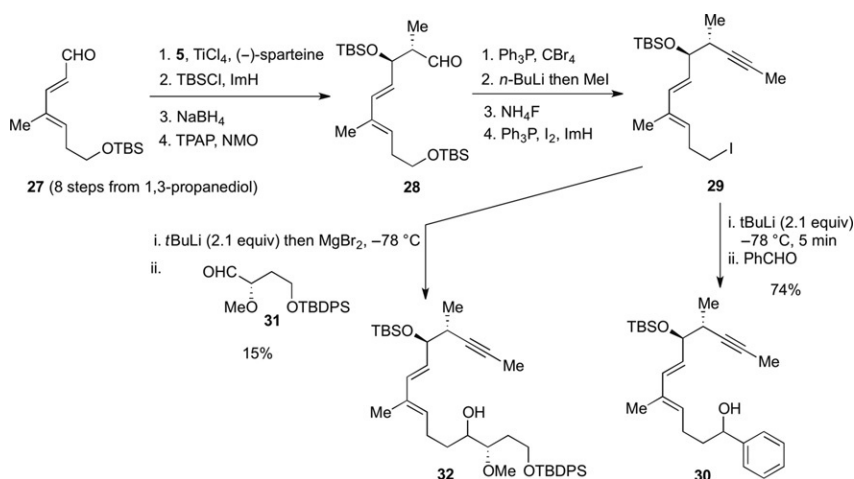
SCHEME 6 Three synthetic routes leading to C16–C19 fragment.



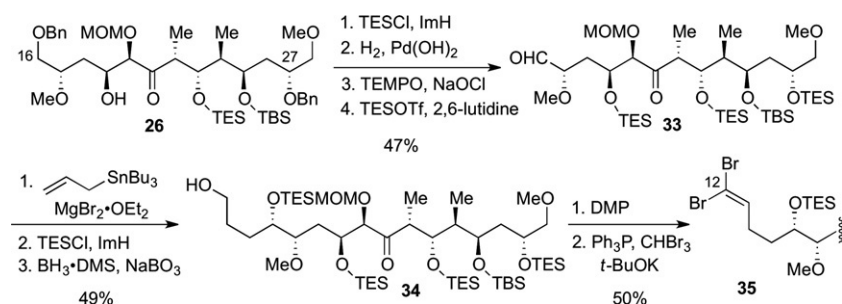
SCHEME 7 First-generation route to C16–C28 fragment.

the Crimmins group [21]. Exchange of the thiooxazolidinone auxiliary for a Weinreb amide was then followed by alcohol protection (TESCl, ImH) and addition of the MOM-protected methyl alcohol anion to give ketone **23**. Treatment of ketone **23** with the Masamune base [29] and TMSCl provided Z-silyl enol ether **24**. Addition of **24** to aldehyde **19** was promoted by $\text{BF}_3 \cdot \text{OEt}_2$ and completed assembly of the C16–C28 fragment (**25**). We further verified the stereochemistry of **25** via pyran acetal **26**.

As shown in Scheme 4, we planned to merge apoptolidinone fragments by the addition of an appropriate organometallic reagent to a C16 aldehyde with reliance on a chelation-controlled addition to deliver the desired secondary alcohol product stereochemistry. An early model study aimed at evaluating the feasibility of coupling a C6–C15 fragment by way of an organolithium reagent derived from iodide **29** is shown in Scheme 8 [30]. Alkyl iodide **29** was prepared in eight steps starting from dienal **27** commencing with a Crimmins aldol reaction, TES protection, reduction, and oxidation to afford aldehyde **28**. A Corey–Fuchs alkynylation [31] followed by selective TBS removal and iodination then completed **29**. Using conditions described by



SCHEME 8 Model studies directed toward C15—C16 bond formation.

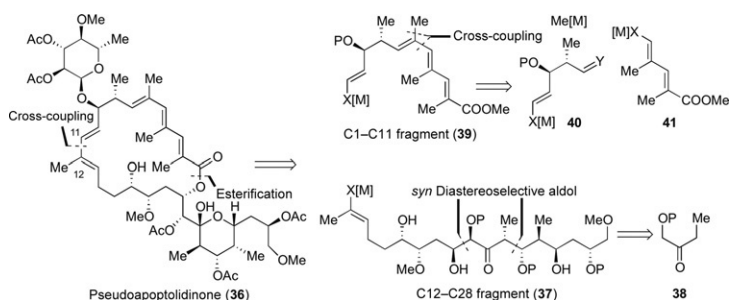


SCHEME 9 Linear extension of C16—C28 to C12—C28 fragment.

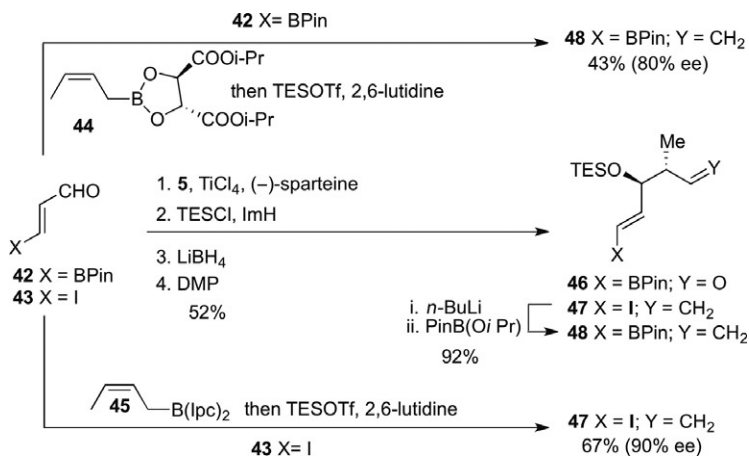
Bailey (2.1 equivalents of *t*-butyllithium) [32], an alkylolithium reagent was derived from **29** and upon addition of benzaldehyde gave secondary alcohol **30**. Unfortunately, addition of the organometallic reagent derived from **29** to α -methoxy aldehyde (**31**) provided **32** as a mixture of isomers in low yield. With this discouraging result, we reevaluated our approach to fragment coupling and examined the addition of allyltributylstannane to aldehyde **33** promoted by a Lewis acid (Scheme 9). The conversion of previously described ketone **26** to aldehyde **33** required four steps including a selective primary alcohol oxidation [33]. Allylation of **33** proceeded with excellent stereoselectivity [34] and led to alcohol **34** following TES protection and hydroboration. Finally, alcohol **34** was oxidized and the aldehyde product was converted to dibromide **35** following an olefination using the Ramirez method [35].

4.2 Approach to Pseudoapoptolidin A

The linearity of the synthetic route leading to **35** and poor performance of the Grignard reagent derived from C6—C15 iodide (**29**) in the model aldehyde



SCHEME 10 Second-generation synthetic strategy.



SCHEME 11 Synthetic routes leading to C7—C11 fragment (46–48).

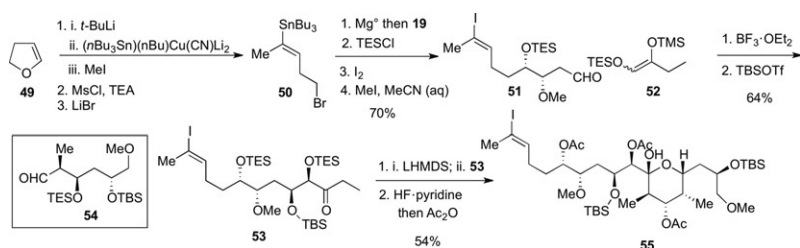
addition (Scheme 8) prompted us to propose a second-generation synthetic strategy toward apoptolidinone (Scheme 10). At this time, we also developed a degradation of apoptolidin A leading to the removal of the C27 disaccharide which, following peracetylation, provided pseudoapoptolidinone (36, Scheme 10) [6a]. Since at this time the total synthesis of apoptolidin had not been reported, we anticipated that the corroboration of the structural assignment of apoptolidin could be achieved by comparison of synthetic pseudoapoptolidinone 36 with material obtained by degradation (pseudoapoptolidinone). In our approach to 36, a key change in fragment coupling was proposed employing a cross-coupling reaction between C12—C28 fragment (37) and C1—C11 fragment (39). We further proposed to simplify assembly of the C12—C28 fragment (37) by using ketone 38 as a “linchpin” element in two substrate-controlled aldol reactions. Finally, the planned assembly of the C1—C11 fragment (39) featured two cross-coupling reactions starting from optically active secondary alcohol 40, dienoate 41, and a methyl metal reagent.

Approaches to synthetic equivalents of secondary alcohol 40 (46–48, Scheme 11) required consideration of enantio- and diastereoselectivity in

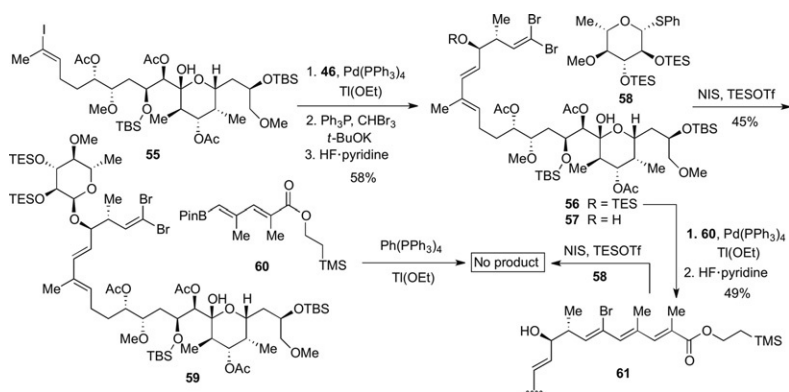
the introduction of the C8 and C9 stereocenters as well as functional group identity at the fragment termini (C7). In earlier studies, we showed that addition of thioxazolidinone **5** to 3-borylacrolein (**42**) [36] proceeded smoothly to provide a crystalline aldol adduct leading to aldehyde **46** following a standard three-step reaction sequence [28]. We subsequently observed asymmetric crotylation of aldehyde **42** afforded *syn*-crotyl alcohol **48** with good diastereoselectivity (>95:5, *syn:anti*) but modest enantioselectivity (80% ee) when employing Roush's *Z*-allyl boronate (**44**) [37]. Surprisingly, the addition of the same crotylating reagent to 3-iodoacrolein (**43**) [38] resulted in significant loss of enantioselectivity (26% ee). Fortunately, addition of Brown's reagent (**45**) [39] to 3-iodoacrolein (**43**) gave the corresponding *syn*-crotyl alcohol in 90% ee and TES ether **47** following alcohol protection (TESOTf, 2,6-lutidine). Lithium–halogen exchange followed by a pinacol boronate quench provided **48** in 95% yield. Overall, the latter sequence proved most efficient in terms of yield and stereoselectivity.

As illustrated in Scheme 10, we proposed to develop a convergent assembly of the C12–C28 fragment using ketone **38** as a “linchpin” fragment as the corner substrate in two substrate-controlled diastereoselective aldol reactions. To this end, aldehyde **51** was prepared starting with the addition of the Grignard reagent derived from bromide **50** to aldehyde **51** (Scheme 12). Koert was the first to employ **50**, prepared from dihydrofuran (**49**), in the total synthesis of apoptolidinone [12a,40]. Following the chelation-controlled addition of the derived Grignard reagent to **19**, alcohol protection, tin–iodine exchange, and thioacetal hydrolysis gave aldehyde **51**. Kinetic deprotonation of ketone **38** (P=TES) followed by a TMSCl quench gave silylenol ether **52** as the major regioisomer (ca. 8:1). Aldol addition of **52** to aldehyde **51** was promoted by $\text{BF}_3 \cdot \text{OEt}_2$ and, following TBS protection, provided ketone **53** diastereoselectively [20]. Gratifyingly, the lithium enolate derived from **53** added to aldehyde **54** providing exceptional diastereoselectivity to complete assembly of the C16–C28 fragment [29]. Selective removal of TES protecting groups followed by peracetylation afforded pyran acetal **55**, poised for advancement to peracetyl apoptolidinone (**36**).

We now turned our attention to the completion of the apoptolidin seco acid with incorporation of the C9 deoxy sugar (Scheme 13). Suzuki cross-coupling between vinyl iodide **55** and vinyl boronate **46** proceeded smoothly, as did



SCHEME 12 Synthesis of C12–C28 fragment.



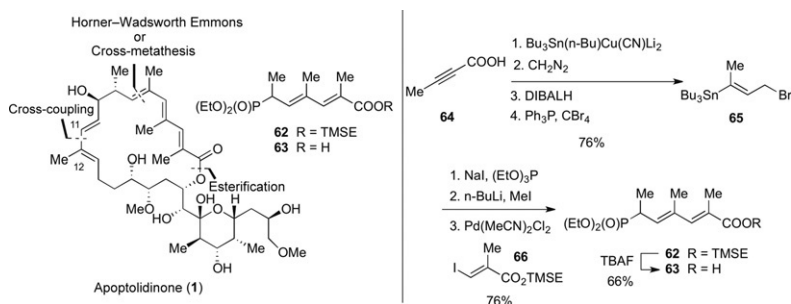
SCHEME 13 Glycosylation and seco acid assembly studies.

the olefination of the intermediate enal to provide dibromide **56** [41]. Next, the C9 hydroxyl group was revealed by selective HF-pyridine-mediated removal of the TES ether (**56**), thus setting the stage for the C9 α -selective glycosylation. Following extensive screening of various α -selective glycosylation reactions, optimal conditions were identified using thioglycoside **58** as a glycosyl donor activated with NIS–TESOTf as described by Frasier-Reid [42]. The glycosylation product (**59**) was obtained in 40–45% yield and 4:1 (α/β) ratio. Unfortunately, all attempts to extend **59** to the complete apoptolidin seco acid by cross-coupling with vinyl boronate **60** failed. Attempts to reverse the glycosylation cross-coupling sequence stalled at seco acid **61** as glycosylation of **61** also failed. At this time, the total synthesis of apoptolidin was reported by the Nicolaou *et al.* [13] diminishing our appetite to intersect with our apoptolidin degradation product **36**. We therefore returned our attention to the synthesis of apoptolidinone itself.

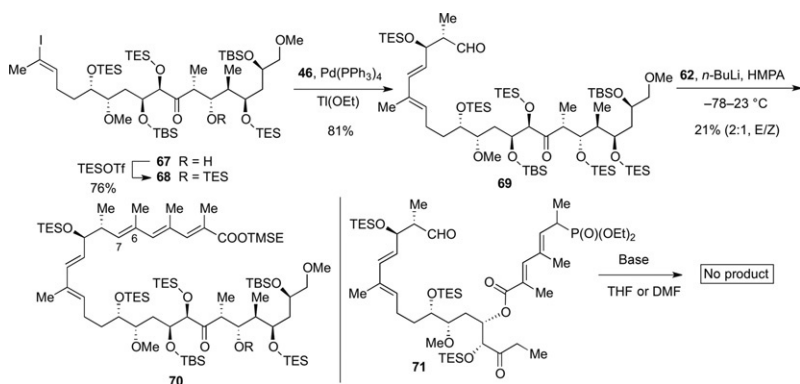
4.3 Total Synthesis of Apoptolidinone A

Our synthetic studies directed toward pseudoapoptolidin A (**36**) established C11–C12 carbon–carbon bond formation as a favorable approach to fragment coupling. Our failure to concurrently orchestrate Me–C5 and C4–C5 bond formations led us to examine the C5–C6 double bond formation as an approach to complete apoptolidinone. As shown in Scheme 14, we considered either a Horner–Wadsworth–Emmons (HWE) olefination or a cross-metathesis reaction as method of C5–C6 bond construction. The former required access to unsaturated phosphonate ester **62** or acid **63**. Ester **62** would be employed in an intermolecular HWE reaction, while carboxylic acid **63** could be employed in an intramolecular reaction following intermolecular esterification.

Phosphonate ester **62** was prepared starting with the addition of a higher-order stannyl cuprate to 2-butyric acid (**64**), according to the method of Duchêne and Parrain (Scheme 14) [43]. Following esterification with



SCHEME 14 Third-generation synthetic analysis and synthesis of C1—C6 fragment.

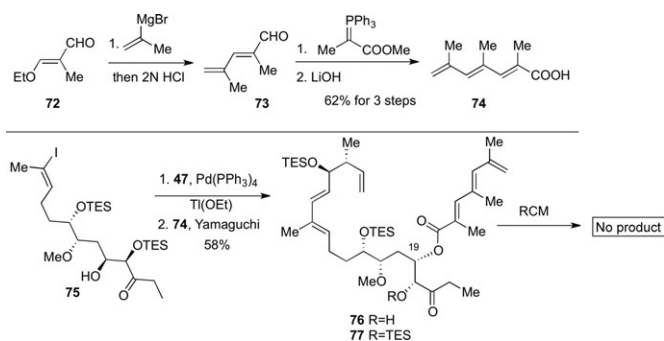


SCHEME 15 Horner–Wadsworth–Emmons approaches to C5—C6 bond formation.

diazomethane, DIBAL reduction to the allylic alcohol and dehydrative bromination provided allyl bromide **65** in good overall yield. Heating a solution of **65** with triethyl phosphite yielded the corresponding diethyl phosphonate. Deprotonation of the latter with *n*-butyllithium followed by a methyl iodide quench was followed by a Stille cross-coupling reaction with vinyl iodide **66** to complete ester **62**. Removal of the trimethylsilylethyl group provided carboxylic acid **63**.

Aldol adduct **67**, an intermediate [Scheme 12](#) in (conversion of **53** to **55**), was protected as TES ether **68**, and cross-coupled with vinyl boronate **46** to afford aldehyde **69** ([Scheme 15](#)). A variety of bases and additives were examined in an effort to effect a HWE reaction between **69** and phosphonate **62** with the combination of *n*-BuLi and HMPA leading to trienoate **70** in 21% yield. In addition to an unacceptably low chemical yield, the stereoselectivity of the olefination was poor (*E/Z*, 2:1). Unfortunately, an intramolecular variant of the HWE reaction failed to improve the yield or stereoselectivity of the process as treatment of **71** with a variety of bases failed to provide any product ([Scheme 15](#)).

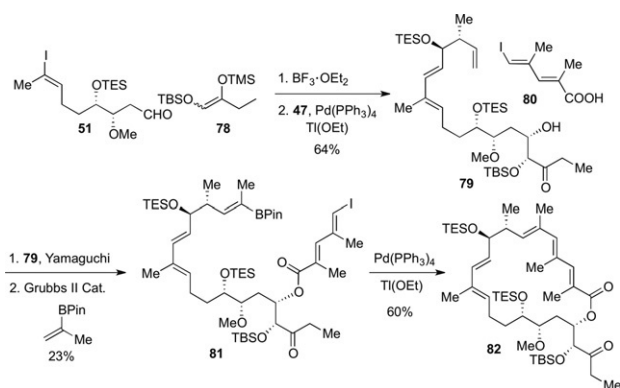
Since the early 1990s, application of the metathesis reaction in organic synthesis has grown as a method of alkene construction. The difficulty in



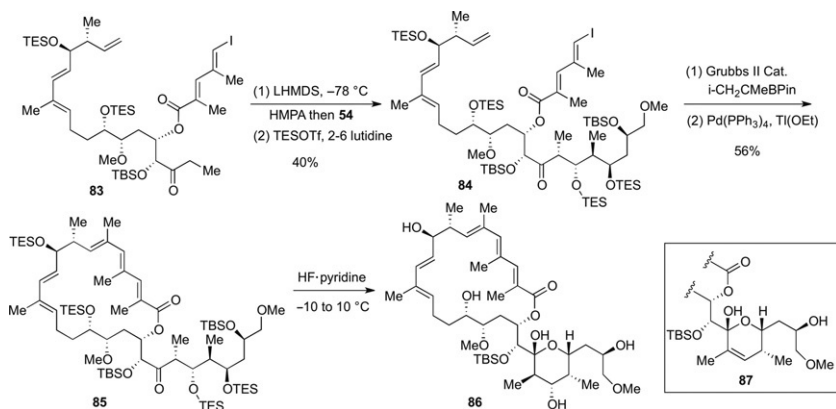
SCHEME 16 Ring-closing metathesis approaches to the 20-membered macrolide.

forming the C5—C6 double bond of apoptolidinone by way of the HWE reaction prompted us to consider a ring-closing metathesis reaction to effect bond formation. At the time, we recognized this reaction would be testing the limits of the RCM process, which further justified the examination of this proposal [44]. We first required access to trienoic acid **74** in order to effect esterification of the C19 alcohol to examine the intramolecular metathesis reaction. To this end, addition of propenyl Grignard to aldehyde **72** followed by an acidic work-up provided dienal **73** [45]. Olefination of **73** with a stabilized ylide followed by ester hydrolysis furnished the requisite carboxylic acid **74**. Prior to C19 esterification, vinyl iodide **75** was coupled with vinyl boronate **47** under standard Suzuki reaction conditions. While the yield of the reaction was very good (80–86%), we observed considerable base-catalyzed migration of the TES protecting group from C19 to C20, resulting in a 1:1 mixture of desired C19 alcohol **15** and C20 alcohol **76**, an unforeseen problem we would address later. Yamaguchi esterification of the desired isomer with carboxylic acid **74** provided the RCM substrate **77**. Unfortunately, neither Grubbs first- nor second-generation catalysts yielded the desired cyclized product.

At the time of our struggles in forming the C5—C6 double bond by way of a metathesis reaction, two publications describing the use of a cross-metathesis reaction between an alkene and vinyl boronate came to our attention [46]. We then conceived the synthetic route summarized in Scheme 17 that led to the long sought after macrolactone formation. As expected based on previous results, the aldol reaction between aldehyde **51** and TBS enol ether **78** proceeded with high stereoselectivity. Suzuki coupling between the aldol product and vinyl boronate **47** proceeded smoothly with silyl migration from C20 to C19 (cf. Scheme 16), suppressed by replacement of the labile TES protecting group by a TBS group. Yamaguchi esterification between **79** and carboxylic acid **80** was followed by the key cross-metathesis reaction between propenyl boronate and the terminal alkene to give vinyl boronate **81** with high stereoselectivity, albeit in 34% yield. To our delight, intramolecular Suzuki cross-coupling proceeded in 60% yield to provide macrolactone **82** [47]. Attempts to



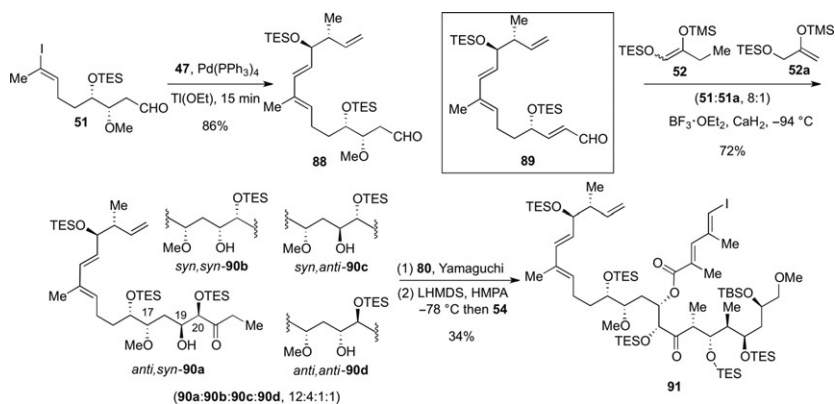
SCHEME 17 Intramolecular Suzuki assembly of 20-membered macrolide.



SCHEME 18 Completion of apoptolidinone core structure.

effect aldol reaction between the enolate derived from ketone **82** and aldehyde **54** failed. Effecting the aldol reaction prior to macrolactone construction as summarized in [Scheme 18](#) easily circumvented this problem.

Conveniently, esterification of the C19 alcohol with trienoic acid **80** eliminated the need for the use of a protecting group as kinetic deprotonation of **83** [LHMDS (2 equiv) – HMPA (3 equiv)] followed by the addition of aldehyde **54** proceeded with excellent stereoselectivity ([Scheme 18](#)). While the yield of the aldol reaction was only 33–39%, we could recover up to 45% starting ketone **83**. The TES-protected aldol product (**84**) was then subjected to the cross-metathesis/cross-coupling reaction sequence to give macrolactone **85**. In the final deprotection step, we encountered a problem due to our use of a C20 TBS protecting group in order to suppress C20 to C19 silyl migration. Removal of silicon protecting groups with HF·pyridine at a temperature of -10°C resulted in isolation of TBS-protected apoptolidinone **86**. While



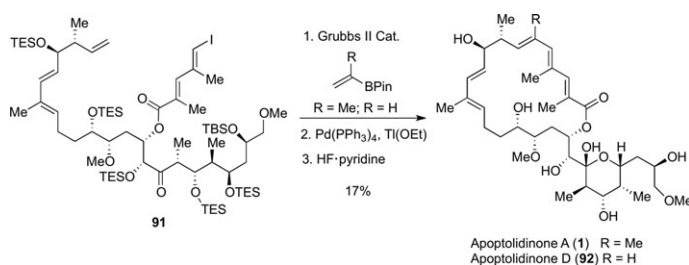
SCHEME 19 Total synthesis of apoptolidinone.

warming the reaction to 10°C did result in removal of the C20 TBS group, the reaction was accompanied by dehydration to **87**, a degradation reaction reported earlier by Khosla and Salomon [7c].

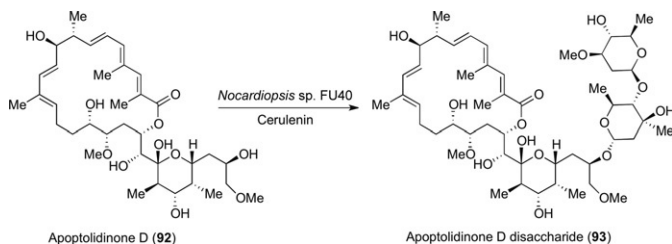
The observed dehydration of the pyran acetal occurring prior to removal of the C20 TBS protecting required us to reconsider the use of a TES protecting group. As the C20 TES group of aldol adduct **75** had the tendency to migrate from C20 to C19 under the Suzuki cross-coupling conditions (Scheme 16), leading us to employ a TBS group, we considered the order of aldol and Suzuki reactions as an alternative to resolving this problem. In other words, Suzuki cross-coupling of vinyl boronate **47** and aldehyde **51** would avoid the protecting group migration altogether. Notably, while the cross-coupling was determined to proceed in 86% yield (15 min), extended reaction times produced significant amounts of enal **89** (Scheme 19). The key Mukaiyama aldol between **52** and aldehyde **88** proceeded to afford **90a** in 71% yield. When the reaction was conducted on larger scale, minor aldol adducts **90b–90d** were isolated and characterized [48]. However, analysis by NMR could not distinguish *syn,anti*-**90c** and *anti,anti*-**90d** isomers. Following Yamaguchi esterification with trienoic acid **80**, aldol reaction with aldehyde **54** afforded adduct **91** in 48% yield. From intermediate **91**, we were able to prepare apoptolidinone A and D by simply changing the cross-metathesis partner from propenyl boronate to vinyl boronate. Suzuki cyclization of the intermediate boronate followed by global desilylation completed apoptolidinones A and D (Scheme 20).

5. PRECURSOR-DIRECTED GLYCOSYLATION

Apoptolidin A and derivatives had been evaluated for cytotoxicity by the Wender group against H292 lung carcinoma cells [8a–c]. We also determined apoptolidin A to be cytotoxic against H292 cells with an EC_{50} of approximately 20 nM [48]. In contrast, neither apoptolidinone A nor D, prepared by



SCHEME 20 Total synthesis of apoptolidinone A (1) and D (92).



SCHEME 21 Whole cell glycosylation of apoptolidinone D assisted by a chemical ketosynthase knockdown.

total synthesis, displayed any cytotoxic or cytostatic effects, illustrating the importance of the deoxy sugars in maintaining activity. As our goal was to prepare fluorescent and/or affinity probes of apoptolidins, we required an approach to incorporate the three deoxy sugars to deliver an “active” probe. We judged the incorporation of deoxy sugars into the apoptolidin synthesis by chemical means to be a significant challenge and decided to examine a precursor-directed glycosylation method. We were particularly interested in the possibility of incorporating unnatural aglycones with appropriately positioned functional groups (such as an azido group) for ready conjugation to either a fluorescent or affinity tag. Our first “unnatural” aglycone was 6-normethyl apoptolidinone, later identified as apoptolidinone D by Wender. Nonetheless, we chose to examine 6-normethylapoptolidinone as a substrate in a precursor-directed glycosylation.

In precursor-directed biosynthesis, an unnatural substrate (in this case 6-normethylapoptolidinone) necessarily competes with the endogenous or natural substrate (Scheme 21). Without any alteration of the producing microorganism, the best we could hope for would be a mixture of glycosylation products (natural and unnatural). One method to suppress production of the natural aglycone is to construct a PKS knockout, but this would require knowledge of the expressing gene cluster [49]. At the time of these experiments, we had limited information on the gene cluster, let alone the ability to construct a PKS knockout. Instead, we elected to take advantage of a report of Omura in which he reported cerulenin to effect a “chemical” KS knockdown [50].

In the event, when a growing culture of the apoptolidin producer (*Nocardiopsis* sp. FU40) was inoculated with apoptolidinone D and cerulenin, a unique apoptolidin was produced, apoptolidinone D disaccharide (**93**) [9]. When evaluated for cytotoxicity against H292 cells, **93** showed significant return of activity (EC_{50} 200 nM). Interestingly, the C9 sugar was not incorporated into **93**, an observation that could have implications regarding the order of glycosylation.

6. CONCLUSION AND EPILOGUE

The apoptolidins are structurally representative of polyketide natural products, composed of an aglycone conjugated to a series of deoxy sugars. As has been demonstrated in many cases, sugar units play a critical role in maintaining bioactivity and the apoptolidins are no exception. Also, the comprehensive assembly of the central aglycone and associated sugars remains a significant obstacle in chemical synthesis. The ability to engineer microorganisms combined with synthetic fragments opens avenues to the ready production of natural product analogs by means of chemobiosynthesis. We believe this approach will allow for the expansion of natural product-derived probes for biology and therapeutic leads in drug discovery.

ACKNOWLEDGMENTS

This research was supported by the National Institutes of Health (CA 059515) and the Vanderbilt Institute of Chemical Biology.

REFERENCES

- [1] D.J. Newman, *J. Med. Chem.* 51 (2008) 2589–2599.
- [2] Y. Hayakawa, K. Sohda, K. Furihata, T. Kuzuyama, K. ShinYa, H. Seto, *J. Antibiot.* 49 (1996) 974–979.
- [3] J. Kim, H. Adachi, K. ShinYa, Y. Hayakawa, H. Seto, *J. Antibiot.* 50 (1997) 628–630.
- [4] Y. Hayakawa, J. Kim, H. Adachi, K. Shin-ya, K. Fujita, H. Seto, *J. Am. Chem. Soc.* 120 (1998) 3524–3525.
- [5] For a review of work on the apoptolidins up to 2006, see: P.T. Daniel, U. Koert, J. Schuppan, *Angew. Chem. Int. Ed. Engl.* 45 (2006) 872–893.
- [6] Degradation studies and semisyntheses: (a) J. Pennington, H. Williams, A. Salomon, G. Sulikowski, *Org. Lett.* 4 (2002) 3823–3825; (b) P. Wender, A. Gullledge, O. Jankowski, H. Seto, *Org. Lett.* 4 (2002) 3819–3822; (c) P.A. Wender, O.D. Jankowski, E.A. Tabet, H. Seto, *Org. Lett.* 5 (2003) 2299–2302; (d) P.A. Wender, O.D. Jankowski, E.A. Tabet, H. Seto, *Org. Lett.* 5 (2003) 487–490; (e) C.A. Lewis, K.E. Longcore, S.J. Miller, P. A. Wender, *J. Nat. Prod.* 72 (2009) 1864–1869.
- [7] (a) A. Salomon, D. Voehringer, L. Herzenberg, C. Khosla, *Proc. Natl. Acad. Sci. USA* 97 (2000) 14766–14771; (b) A. Salomon, D. Voehringer, L. Herzenberg, C. Khosla, *Chem. Biol.* 8 (2001) 71–80; (c) A. Salomon, Y. Zhang, H. Seto, C. Khosla, *Org. Lett.* 3 (2001) 57–59.

- [8] (a) P.A. Wender, M. Sukopp, K. Longcore, *Org. Lett.* 7 (2005) 3025–3028; (b) P.A. Wender, K.E. Longcore, *Org. Lett.* 9 (2007) 691–694; (c) P.A. Wender, K.E. Longcore, *Org. Lett.* 11 (2009) 5474–5477; (d) B.O. Bachmann, R. McNees, B.J. Melancon, V.P. Ghidu, R. Clark, B. C. Crews, S.M. DeGuire, L.J. Marnett, G.A. Sulikowski, *Org. Lett.* 12 (2010) 2944–2947.
- [9] V.P. Ghidu, I. Ntai, J. Wang, A.T. Jacobs, L.J. Marnett, B.O. Bachmann, G.A. Sulikowski, *Org. Lett.* 11 (2009) 3032–3034.
- [10] Y. Du, D.K. Derewacz, S.M. DeGuire, J. Teske, J. Ravel, G.A. Sulikowski, B.O. Bachmann, *Tetrahedron* 67 (2011) 6568–6575.
- [11] Work directed toward the synthesis of apoptolidins: (a) K. Nicolaou, Y. Li, B. Weyershausen, H. Wei, *J. Chem. Soc. Chem. Commun.* (2000) 307–308; (b) J. Schuppan, B. Ziemer, U. Koert, *Tetrahedron Lett.* 41 (2000) 621–624; (c) K. Toshima, T. Arita, K. Kato, D. Tanaka, S. Matsumura, *Tetrahedron Lett.* 42 (2001) 8873–8876; (d) K. Abe, K. Kato, T. Arai, M. Rahim, I. Sultana, S. Matsumura, K. Toshima, *Tetrahedron Lett.* 45 (2004) 8849–8853; (e) W. Paquette, R. Taylor, *Org. Lett.* 6 (2004) 103–106; (f) L. Bouchez, P. Vogel, *Chem. Eur. J.* 11 (2005) 4609–4620; (g) L. Bouchez, P. Vogel, *Chem. Eur. J.* 12 (2006) 349; (h) C. Craita, C. Didier, P. Vogel, *Chem. Commun.* (2007) 2411–2413; (i) Y. Kim, P.L. Fuchs, *Org. Lett.* 9 (2007) 2445–2448; (j) M. Handa, K.A. Scheidt, M. Bossart, N. Zheng, W.R. Roush, *J. Org. Chem.* 73 (2008) 1031–1035; (k) M. Srinivasarao, Y. Kim, X.H. Li, D.W. Robbins, P.L. Fuchs, *J. Org. Chem.* 76 (2011) 7834–7841; (l) M. Srinivasarao, T. Park, Y. Chen, P.L. Fuchs, *Chem. Commun.* 47 (2011) 5858–5860.
- [12] Total syntheses of apoptolidinones: (a) J. Schuppan, H. Wehlan, S. Keiper, U. Koert, *Angew. Chem. Int. Ed. Engl.* 40 (2001) 2063–2066; (b) M. Crimmins, H. Christie, K. Chaudhary, A. Long, *J. Am. Chem. Soc.* 127 (2005) 13810–13812; (c) J. Schuppan, H. Wehlan, S. Keiper, U. Koert, *Chem. Eur. J.* 12 (2006) 7364–7377; (d) T.R. Vargo, J.S. Hale, S. G. Nelson, *Angew. Chem. Int. Ed. Engl.* 49 (2010) 8678–8681.
- [13] (a) K. Nicolaou, Y. Li, K. Sugita, H. Monenschein, P. Guntupalli, H. Mitchell, K. Fylaktakidou, D. Vourloumis, P. Giannakakou, A. O’Brate, *J. Am. Chem. Soc.* 125 (2003) 15443–15454; (b) K. Nicolaou, K. Fylaktakidou, H. Monenschein, Y. Li, B. Weyershausen, H. Mitchell, H. Wei, P. Guntupalli, D. Hepworth, K. Sugita, *J. Am. Chem. Soc.* 125 (2003) 15433–15442; (c) K. Nicolaou, Y. Li, K. Fylaktakidou, H. Mitchell, H. Wei, B. Weyershausen, *Angew. Chem. Int. Ed. Engl.* 40 (2001) 3849–3854; (d) K. Nicolaou, Y. Li, K. Fylaktakidou, H. Mitchell, K. Sugita, *Angew. Chem. Int. Ed. Engl.* 40 (2001) 3854–3857.
- [14] (a) D. Kahne, S. Walker, Y. Cheng, D. Vanengen, *J. Am. Chem. Soc.* 111 (1989) 6881–6882; (b) J. Gildersleeve, R. Pascal, D. Kahne, *J. Am. Chem. Soc.* 120 (1998) 5961–5969.
- [15] H. Wehlan, M. Dauber, M.-T. Mujica Fernaud, J. Schuppan, R. Mahrwald, B. Ziemer, M.-E. Juarez Garcia, U. Koert, *Angew. Chem. Int. Ed. Engl.* 43 (2004) 4597–4601.
- [16] G. Allred, L. Liebeskind, *J. Am. Chem. Soc.* 118 (1996) 2748–2749.
- [17] M.T. Crimmins, H.S. Christie, A. Long, K. Chaudhary, *Org. Lett.* 11 (2009) 831–834.
- [18] M. Crimmins, B. King, E. Tabet, *J. Am. Chem. Soc.* 119 (1997) 7883–7884.
- [19] G. Sulikowski, W. Lee, B. Jin, B. Wu, *Org. Lett.* 2 (2000) 1439–1442.
- [20] (a) D. Evans, M. Dart, J. Duffy, M. Yang, *J. Am. Chem. Soc.* 118 (1996) 4322–4343; (b) D. Evans, M. Yang, M. Dart, J. Duffy, A. Kim, *J. Am. Chem. Soc.* 117 (1995) 9598–9599.
- [21] (a) M. Crimmins, B. King, E. Tabet, *J. Am. Chem. Soc.* 119 (1997) 7883–7884; (b) M. Crimmins, B. King, E. Tabet, K. Chaudhary, *J. Org. Chem.* 66 (2001) 894–902.
- [22] (a) A. Tanaka, K. Yamashita, *Synthesis* (1987) 570–573; (b) C. Wei, S. Debernardo, J. Tengi, J. Borgese, M. Weigele, *J. Org. Chem.* 50 (1985) 3462–3467.

- [23] B. Lipshutz, D. Pollart, J. Monforte, H. Kotsuki, *Tetrahedron Lett.* 26 (1985) 705–708.
- [24] (a) P. Breuilles, G. Oddon, D. Uguen, *Tetrahedron Lett.* 38 (1997) 6607–6610; (b) T. Tsunoda, M. Suzuki, R. Noyori, *Tetrahedron Lett.* 21 (1980) 1357–1358.
- [25] M. Fetizon, M. Jurion, *J. Chem. Soc. Chem. Commun.* (1972) 382–383.
- [26] P. Kocienski, C. Yeates, S. Street, S. Campbell, *J. Chem. Soc. Perkin Trans. 1* 1 (1987) 2183–2187.
- [27] R. Johansson, B. Samuelsson, *J. Chem. Soc. Perkin Trans. 1* 1 (1984) 2371–2374.
- [28] B. Wu, Q. Liu, B. Jin, T. Qu, G. Sulikowski, *Eur. J. Org. Chem.* (2006) 277–284.
- [29] S. Masamune, J. Ellingboe, W. Choy, *J. Am. Chem. Soc.* 104 (1982) 5526–5528.
- [30] Jin, B. Ph.D. Thesis, Texas A&M University, 2002.
- [31] E. Corey, P. Fuchs, *Tetrahedron Lett.* 13 (1972) 3769–3772.
- [32] W. Bailey, E. Punzalan, *J. Org. Chem.* 55 (1990) 5404–5406.
- [33] A. DeMico, R. Margarita, L. Parlanti, A. Vescovi, G. Piancatelli, *J. Org. Chem.* 62 (1997) 6974–6977.
- [34] G. Keck, E. Boden, *Tetrahedron Lett.* 25 (1984) 265–268.
- [35] P. Michel, D. Gennet, A. Rassat, *Tetrahedron Lett.* 40 (1999) 8575–8578.
- [36] B. Jin, Q. Liu, G. Sulikowski, *Tetrahedron* 61 (2005) 401–408.
- [37] W. Roush, K. Ando, D. Powers, A. Palkowitz, R. Halterman, *J. Am. Chem. Soc.* 112 (1990) 6339–6348.
- [38] C. Meyer, I. Marek, J. Normant, *Synlett* (1993) 386–388.
- [39] H. Brown, K.J. Bhat, *J. Am. Chem. Soc.* 108 (1986) 5919–5923.
- [40] V. Fargeas, P. LeMenez, I. Berque, J. Ardisson, A. Pancrazi, *Tetrahedron* 52 (1996) 6613–6634.
- [41] (a) N. Miyaaura, A. Suzuki, *Chem. Rev.* 95 (1995) 2457–2483; (b) S. Frank, H. Chen, R. Kunz, M. Schnaderbeck, W. Roush, *Org. Lett.* 2 (2000) 2691–2694.
- [42] P. Konradasson, U. Udodong, B. Fraser-Reid, *Tetrahedron Lett.* 31 (1990) 4313–4316.
- [43] J. Thibonnet, V. Launay, M. Abarbri, A. Duchene, J. Parrain, *Tetrahedron Lett.* 39 (1998) 4277–4280.
- [44] For a review on RCM in natural product total synthesis, see: A. Gradillas, J. Perez-Castells, *Angew. Chem. Int. Ed. Engl.* 45 (2006) 6086–6101.
- [45] C. Spangler, R. McCoy, A. Karavakis, *J. Chem. Soc. Perkin Trans. 1* (1986) 1203–1207.
- [46] (a) A. Chatterjee, R. Grubbs, *Angew. Chem. Int. Ed. Engl.* 41 (2002) 3171–3173; (b) J. Njardarson, K. Biswas, S. Danishefsky, *J. Chem. Soc. Chem. Commun.* (2002) 2759–2761.
- [47] For a review on the combined use of metathesis and cross-coupling reactions, see: S. Kotha, K. Mandal, *Chem. Asian J.* 4 (2009) 354–362.
- [48] V.P. Ghidu, J. Wang, B. Wu, Q. Liu, A. Jacobs, L.J. Marnett, G.A. Sulikowski, *J. Org. Chem.* 73 (2008) 4949–4955.
- [49] J. Kennedy, *Nat. Prod. Rep.* 25 (2008) 25–34.
- [50] (a) A. Nakagawa, S. Omura, *J. Antibiot.* 49 (1996) 717–741; (b) S. Omura, N. Sadakane, Y. Tanaka, H. Matsubara, *J. Antibiot.* 36 (1983) 927–930.

The Story Behind the Total Synthesis of Vibsanin E and 5-*epi*-Vibsanin E

Craig M. Williams

School of Chemistry and Molecular Biosciences, University of Queensland, Brisbane, Queensland, Australia

In April 2002, I visited the library to perform the weekly literature update, and on this occasion I picked up the latest issue of *Chemical and Pharmaceutical Bulletin* (2002, No. 3). Contained within this issue was an article by Prof. Yoshiyasu Fukuyama describing his recent work at the time on the chemical composition of the piscicidal active (fish poison) plant *Viburnum awabuki* (Caprifoliaceae) [1]. I was immediately captivated by the elegance of the complex caged bicyclic structures and seven-membered ring compounds being described, not to mention the discussion surrounding their postulated biosynthesis via possible Cope rearrangement [1]. On returning to my office, I performed a complete literature search on the most interesting compound to me at the time, vibsanin E (**1**) (Figure 1). I discovered that vibsanin E (**1**) was first reported in 1980 [2] and that through the use of X-ray crystal analysis, its structure had been fully elucidated, including its absolute stereochemistry [3]. Even more surprising was that there were no reported total syntheses or studies toward the total synthesis on what seemed to be a structurally very interesting natural product, in spite of its being known for over 20 years. This was simply too enticing to lay rest as a junior academic who had recently

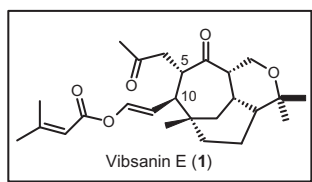


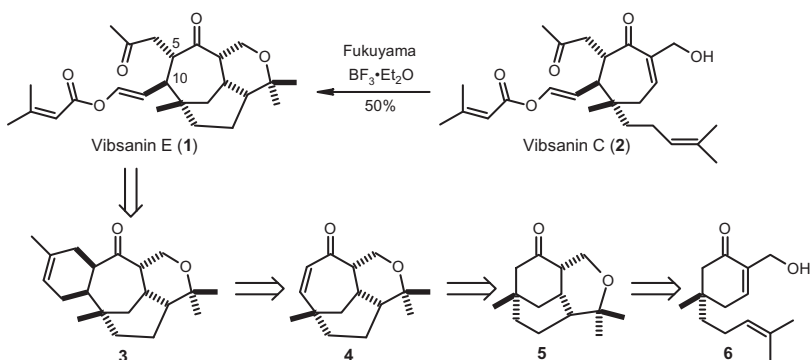
FIGURE 1 Absolute stereochemistry of Vibsanin E.

graduated from the Lewis Mander (Prof. Australian National University) school of natural product total synthesis.

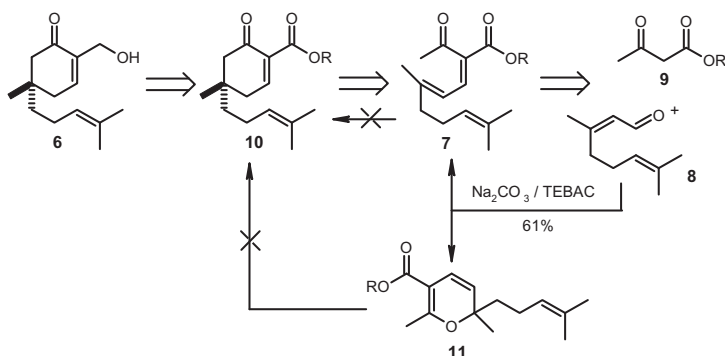
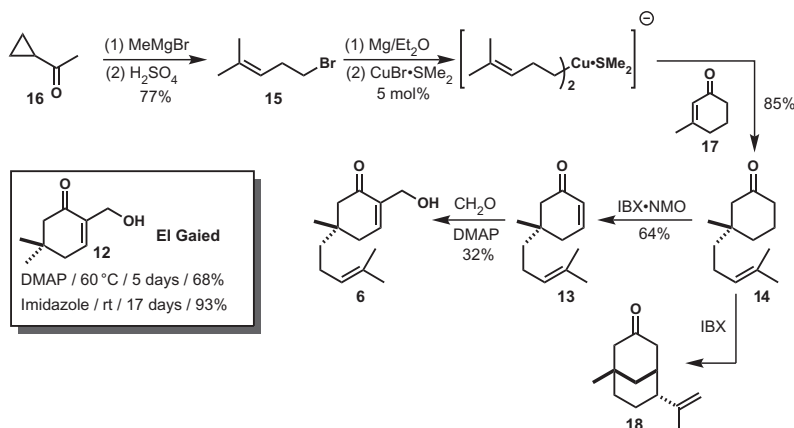
On the same day as the library visit, I contemplated a retrosynthesis (racemic) based on the biosynthesis proposed by Fukuyama starting from vibsanin C (**2**) [4] (Scheme 1) and presented it to my then postdoc, Stefan Wiedemann (Ph.D, Prof. Armin de Meijere, University of Göttingen), who was working on a medicinal chemistry project and took this on as an “after-hours” hobby project. The initial strategy was to introduce the enol acetate and keto side chains (positions 10 and 5, respectively) concomitantly from a Diels–Alder annulation involving isoprene (i.e., **3**), which would be derived from enone **4**. It was considered best that enone **4** be accessed from the all six-membered ring system **5** via ring expansion. The key step, however, was the conversion of cyclohexenone **6** into **5**, which emulated the conditions disclosed by Fukuyama from the conversion of vibsanin C (**2**) into vibsanin E (**1**) [4] (i.e., boron trifluoride etherate) (Scheme 1).

The question now arose, “How can cyclohexenone **6** be obtained?” In the first instance, I thought that the condensation product **7** derived from citral (**8**) and ethyl acetoacetate (**9**) [5] could be forced to undergo an intramolecular conjugate addition giving the ethyl ester **10**. Unfortunately, this was far too ambitious in terms of its simplicity, as any forward manipulation of the product **7** (an equilibrium mixture of **7** and **11**) resulted mostly in a bright red solution that met its destiny as an intractable tar (Scheme 2).

Noticing that the desired methylene hydroxy system contained within cyclohexenone **6** resembled Mortia–Baylis–Hillman (MBH) functionality [6], a search of the literature revealed the work of El Gaid [7], who detailed the first MBH reactions involving cyclohexenones (e.g., **12**) and formaldehyde using *N,N*-4-dimethylaminopyridine (DMAP) or imidazole. To investigate this route, cyclohexenone **13** was required. This was best obtained by dehydrogenation of cyclohexane **14** using iodoxybenzoic acid *N*-methylmorpholine *N*-oxide complex (IBX.NMO) [8]. Fortuitously, when using IBX

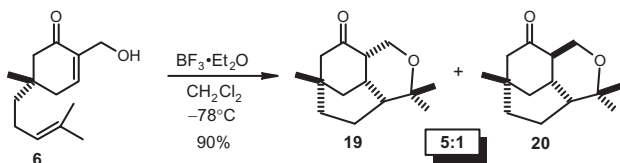


SCHEME 1 Retrosynthetic analysis of vibsanin E (**1**) based on the proven biosynthesis postulate made by Fukuyama by conversion from vibsanin C (**2**).

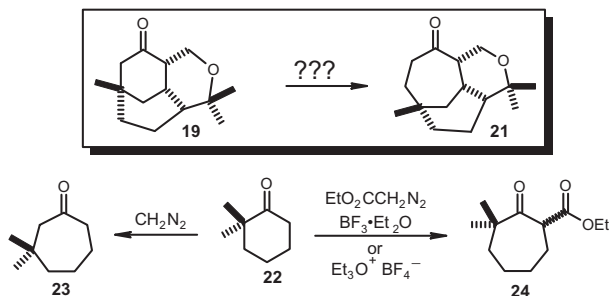
SCHEME 2 First attempt to access the key starting material cyclohexenone **6**.SCHEME 3 A viable synthesis of cyclohexenone **6**.

alone, bicyclo[3.2.1]nonane **18** was obtained, via acid-catalyzed intramolecular cyclization of **13** [9]. This opened up synthetic options toward spirovibsanin A [10]. Cyclohexanone **14** could be sourced from the cuprate addition of the homoprenyl Grignard reagent (via the bromide **15** synthesized by a Julia reaction starting with cyclopropyl methyl ketone **16**) to 3-methylcyclohexenone **17** (Scheme 3). After substantial optimization, it was discovered that treating **13** with formaldehyde and DMAP in aqueous tetrahydrofuran gave the MBH product **6** in 32% yield (43% brsm).

With cyclohexenone **6** in hand, all the required functionality seen in vibsanin C (**2**) except for the substitution of a six-membered ring in place of a seven-membered ring was in hand, and the system was poised for evaluating the key step. It should be pointed out that it was not possible to start with a seven-membered ring because a seven-membered ring does not allow introduction of the homoprenyl unit via conjugate addition. When we first started the domino cyclization cascade study, we only had small quantities of **6** so when we treated **6** with $\text{BF}_3 \cdot \text{Et}_2\text{O}$, following exactly the conditions of



SCHEME 4 Cascade reaction leading to the desired tricycle **19**.



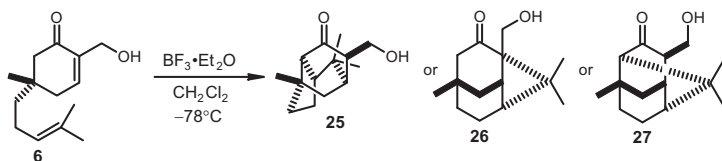
SCHEME 5 Carbene-derived ring expansion understanding.

Fukuyama, we obtained the desired material **19** (X-ray confirmed) and what we believed at the time to be **20**, but is now best considered an unidentified product (Scheme 4).

Accessing the tricycle **19** was a great result and allowed investigations into ring expansion (i.e., **21**) to begin. What a nightmare! Ring expansion (i.e., one step) alone stalled the project by at least 18 months. In terms of classical ring expansion methodology, and associated understanding, nonstabilized carbenes insert into the carbon–carbon bond that joins the carbonyl and the most substituted alpha carbon (e.g., **22** gives **23**) [11]. Stabilized carbenes on the other hand tend to insert into the carbon–carbon bond that joins the carbonyl and the least substituted alpha carbon (e.g., **22** gives **24**) [12] (Scheme 5).

The only issue with these protocols was that neither worked on our system (i.e., **19**). This was the beginning of a stressful journey. We then turned to alternate ring expansion procedures as those skilled in the art often do. The first procedure attempted was that reported by Nagao using lithiated ethyl diazoacetate, but that failed [13], as did Yamamoto's procedure using TMS-diazomethane [14].

It was at this time I received my first invitation to speak at an international conference. Dr. Paul Clarke (then at Nottingham now at York, UK), whom I knew well from when we both interviewed at Newcastle Upon Tyne in 1998, invited me to present at the Gregynog Organic Synthesis Workshop (Wales, UK) in the coveted Saturday night slot. Unbeknownst to me, this was a very dangerous slot, as the audience was full of beer and as such unforgiving. I decided to present the vihsanin E project as it stood. Dr. Richard Grainger



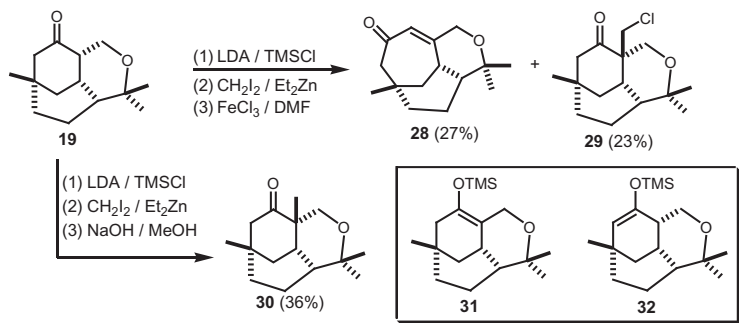
SCHEME 6 Mystery product (either **25**–**27**) obtained when treating **6** on large scale with boron trifluoride etherate.

introduced me and opened with the line “Craig tells me that he has read one of my papers.” A question was shouted from the drunken audience: “Did you reject it!” That set the tone of the night during which I now needed to deliver an acceptable lecture. Luckily, it was well received and good suggestions regarding Baylis–Hilman reaction were made.

On my return from the UK, Dr. Ralf Heim (Ph.D, Prof. Elz, Regensburg) took over the project as Stefan was leaving. Ralf was tasked with the job of solving the ring expansion maneuver, but before this could happen, he needed to repeat the synthesis of tricycle **19** on a larger scale. All went well and, as most postdocs do, he was even able to substantially improve the cuprate addition reaction (i.e., **14**, Scheme 3). When attempting the cyclization, however, he was unable to obtain tricycle **19**. Although we were never able to prove the structure beyond doubt, the same compound was obtained each time, which had characteristics matching either **25**, **26**, or **27** (Scheme 6).

After much investigation, we discovered that because Stefan and Prof. Fukuyama had worked on small scale, the reaction was driven by hydrofluoric acid and not $\text{BF}_3 \cdot \text{Et}_2\text{O}$. Therefore, when Ralf, who was extremely meticulous and working on larger scale, was able to completely remove water from the system, he failed to repeat the result. The key experiment that supported this hypothesis was adding four equivalents of water to the reaction containing $\text{BF}_3 \cdot \text{Et}_2\text{O}$, which afforded the long-lost tricycle **19** (47%, -78°C). A subsequent reaction variation using dry hydrochloric acid also afforded **19** (60%, -78°C). This result was a great relief.

With access to tricycle **19** now reestablished, focus could again be trained on regioselective expansion to the seven-membered ring. Because the required ring expansion was based on a one-carbon unit insertion, most reported procedures attempted were underpinned by cyclopropane formation and subsequent cleavage. The first of these procedures was the well-known method reported by Saegusa [15], which would not only provide ring expansion but also afford an enone as the ring-expanded product. However, when applied to tricycle **19**, two products were obtained: the first was the ring-expanded enone (**28**), which possessed the incorrect regiochemistry, and the second was the chloride **29** (Scheme 7). Using a variation of Saegusa’s method reported by Patel [16] gave the methylated material **30**, confirming that using the kinetic, hindered base lithium diisopropylamide (LDA) gave



SCHEME 7 Ring expansion by enolate cyclopropanation methodology.

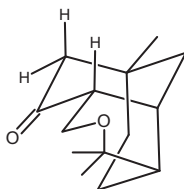


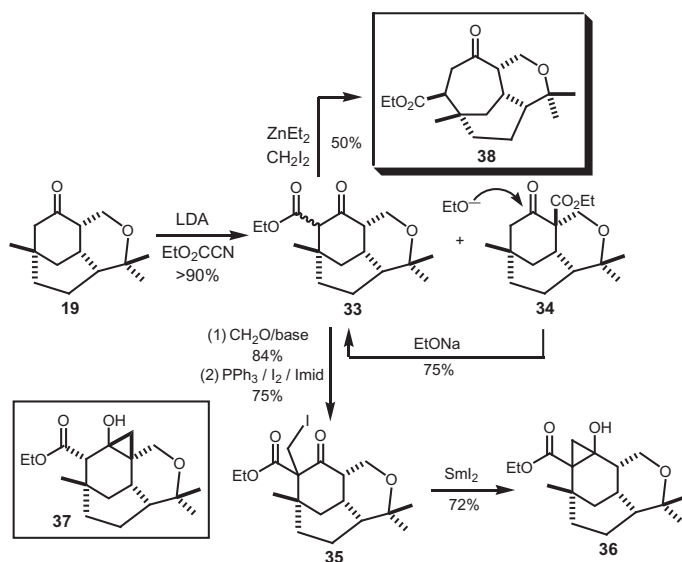
FIGURE 2 Three-dimensional representation of tricyclic **19**.

the thermodynamic enolate [i.e., as the trimethylsilyl ether (**31**)] rather than the kinetic enolate (i.e., not **32**) (Scheme 7).

This dichotomy over kinetic and thermodynamic product was to plague this project from this point through to completion. There were a number of factors that could contribute to this unusual phenomena either individually or in combination, namely: (1) the kinetic position is inherently hindered as neopentyl, (2) the thermodynamic position is tertiary meaning the hydrogen bond is longer than secondary hydrogens and kinetically favored, and (3) the first-formed “thermodynamic” enolate could be stabilized by π orbital overlap with the $\sigma^*\text{C}=\text{O}$ orbital [17] (Figure 2).

Ralf had left the group by now and I had no funding for this project, so I worked on it myself spending up to 18 h a week at the bench while teaching and running a sizable group. Normally, the return of a supervisor to the laboratory would scare most students and postdocs (it certainly shocked my academic colleagues); in this case, the group and I became closer in that we had more laughs and talked more chemistry. It is a pity that academia is such that the most experienced chemist is stuck in the office buried under pointless administrative tasks rather than teaching Ph.D. students and postdocs “old school” laboratory techniques and tricks.

About this time when I was running out of ring expansion ideas, I presented at the Royal Australian Chemical Institute’s Organic division meeting in Cairns (Queensland, 2004). After my talk, Lew Mander suggested that the six- to seven-membered ring expansion should be attempted using a

**SCHEME 8** Beckwith–Dowd and Zercher ring expansion results.

Beckwith–Dowd rearrangement [18]. A Beckwith–Dowd ring expansion requires a 1,3-dicarbonyl system, which was why it was off our radar. The best way to install a suitable 1,3-dicarbonyl unit into our system was to utilize Mander's reagent (NCCO_2Et) [19] (Scheme 8). Hence, treating tricycle **19** with Mander's reagent gave a mixture of the desired 1,3-dicarbonyl compound **33** and the regioisomer **34**. Conveniently, a retro-Dieckmann/Dieckmann cascade smoothly converted the unwanted regioisomer **34** into desired **33** (thermodynamic product). The second functionality requirement for a Beckwith–Dowd ring expansion is the alpha substitution of the 1,3-dicarbonyl with a methylene halide unit, usually using diiodo- or dibromomethane. However, **33** failed to react. To circumvent this problem, **33** was first reacted with formalin giving the hydroxymethylene derivative (84%), which was converted into the iodide **35** (75%), using triphenylphosphane, iodine and imidazole. Unfortunately, all attempts to force the Beckwith–Dowd ring expansion failed to deliver the desired transformation. Surprisingly, when using samarium diiodide [20], only cyclopropanol **36** (72%) was obtained. This compound (**36**) generated much interest first from Prof. Hans-Ulrich Reissig (Freie Universität, Berlin) who informed me that **36** represented the first donor–acceptor (push–pull) cyclopropane [21] ever isolated. When I mentioned this at a lecture at the University of Melbourne, Prof. Jonathan White asked if we could send him some crystals for X-ray analysis for further insight into this unusual structure. Repeating the synthesis to generate more material proceeded as described, but it was not possible to grow suitable crystals. In-depth NMR analysis, however, suggested that the structure was misassigned and matched

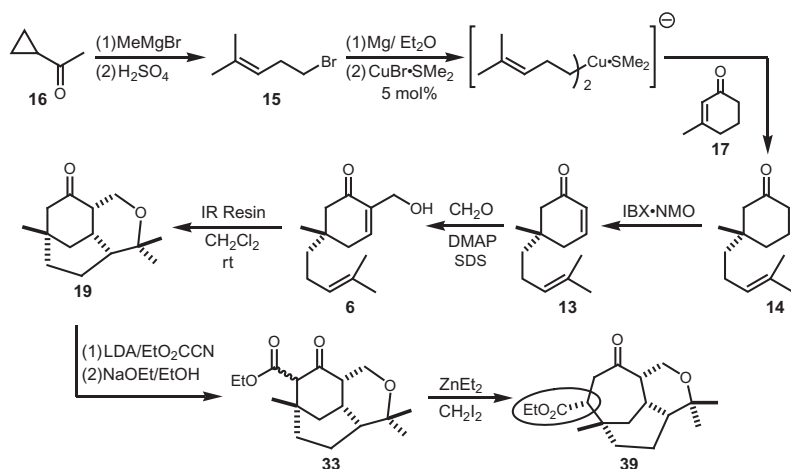
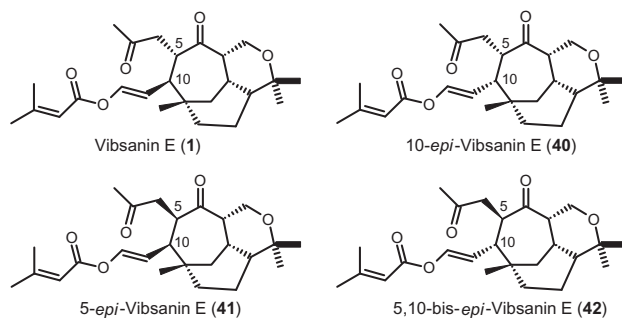
more closely cyclopropanol **37**, which explains why we could never understand why **36** could not be encouraged to ring expand (Scheme 8). When all seemed to be lost, I saw the Zercher reaction in an organometallics textbook, which I was reading at home in front of the television.

The Zercher reaction [22] is a one-pot, one-carbon unit homologation protocol for the conversion of 1,3-dicarbonyls into 1,4-dicarbonyls using the Furukawa reagent [23] (EtZnCH_2I from $\text{ZnEt}_2/\text{CH}_2\text{I}_2$), which is applicable to both acyclic and cyclic systems. The Furukawa reagent acts initially as a base to deprotonate the 1,3-dicarbonyl acidic hydrogen generating an enolate, which is then cyclopropanated, giving rise to a donor–acceptor cyclopropane that undergoes cyclopropane cleavage, affording the homologated product. Recent calculations by my group in collaboration with Prof. Zercher (Chuck Zercher, University of New Hampshire) have revealed two possible mechanistic pathways, which consist of a classical donor–acceptor cyclopropane *intermediate* (never observed spectroscopically) and a cyclopropane *transition state* pathway [24].

Applying the Zercher reaction to our system (i.e., **33**) afforded with much jubilation the desired ring-expanded material **38** in 50% yield (dr 95:5). The yield could not be increased using any variation (e.g., Xue's modified Zercher conditions [25]), but after such a long journey, 50% was indeed heavenly and meant that the work could now be disclosed (Scheme 9) [26,27].

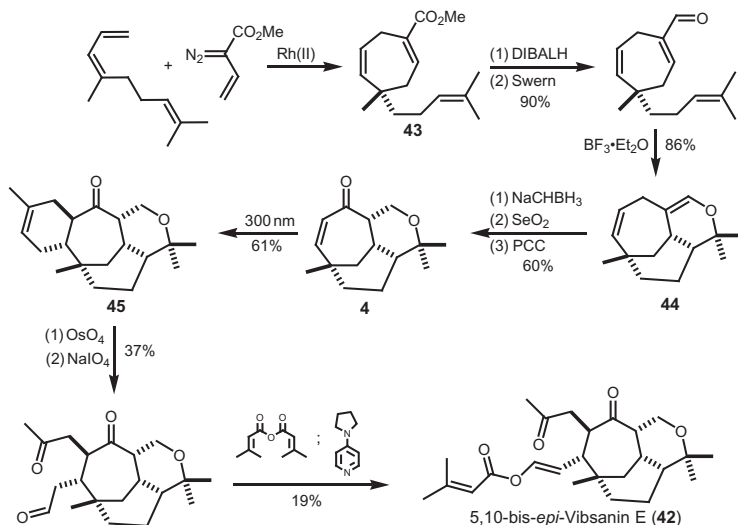
In 2006, I was funded by the Australian Research Council to work on the vibsanine family of natural products and as such was able to employ Dr. Brett Schwartz (Ph.D, Prof. James DeVoss, Queensland), among other things, to hopefully complete the synthesis of vibsanin E (**1**). The first task was to scale up the synthesis of the seven-membered ring **38**, which meant further optimization of the route outlined in Schemes 3, 4, and 8. Brett made immediate impact performing the cuprate addition on large scale giving **14** in batches of 100 g (Scheme 9). The real problematic scale-up step in this process was the Baylis–Hillman reaction and in collaboration with another postdoc in the group at the time, Dr. Achim Porzelle (Ph.D, Prof. W.-D. (Woody) Fessner, Darmstadt), Brett, and Achim discovered that completely removing THF as solvent and using only water and the surfactant sodium dodecyl sulfate dramatically improved the yield of **6** up to 85% on small scale and 48% on a 12-g scale [28,29]. Through another borderline divine intervention, Brett was also able to further improve the reaction sequence by treating **6** with Amberlyst resin in undistilled dichloromethane at room temperature giving tricycle **19** in 68% yield, avoiding the prior need for low temperature and anhydrous conditions (Scheme 9). Large-scale Zercher reactions were capricious with most reactions affording between 10% and 90% yield. Considerable time was spent trying to understand why this was the case (i.e., using different sources of diethylzinc), but nothing conclusive could be drawn.

Unfortunately, we discovered at this point via an X-ray crystal structure of a derivative [30] that the stereochemistry of the ester substituent on **38** was in fact alpha (i.e., **39**) and not beta (i.e., **38**, Schemes 8 and 9). This came as a

SCHEME 9 Optimized route to the ring-expanded material **39**.FIGURE 3 The structures of vibsanin E (**1**), 10-*epi*-vibsanin E (**40**), 5-*epi*-vibsanin E (**41**), and 5,10-bis-*epi*-vibsanin E (**42**).

particular surprise as molecular mechanics calculations suggested the lowest energy arrangement was one in which the ester function occupied the β position, albeit NOE studies were not able to sufficiently decipher between the two. This was a major blow to the project as all attempts to epimerize this position completely failed, meaning only a 10-*epi* synthesis of vibsanin E (**1**) would be possible (i.e., **40**), which unlike 5-*epi* (**41**) was not a natural product (Figure 3).

It was about this time that I opened the door of my office one morning to find a copy of an *Organic Letters* ASAP article describing the synthesis of 5,10-bis-*epi*-vibsanin E (**42**) reported by Prof. Huw Davies (then Buffalo, now Emory) [31] at which point my heart skipped a beat. In fact, this news had spread very quickly through my group, but as in the game “Chinese Whispers”, the group had thought that it was the natural product (i.e., **1**) and not the non-natural diastereoisomer (**42**) that had been synthesized (Figure 3).



SCHEME 10 Davies' synthesis of 5,10-bis-*epi*-vibsanin E (**42**); only isomers and yields leading to **42** are shown.

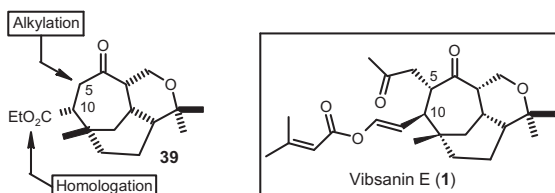


FIGURE 4 Appending the 5- and 10-position functionality.

The beauty of the Davies approach was fourfold: (1) the elegant formation of the substituted seven-membered ring (**43**) using the rhodium-catalyzed formal [4+3] cycloaddition chemistry for which Davies is very well known, (2) the ensuing hetero-[4+2] cycloaddition giving tricycle **44**, (3) the photochemical-mediated Diels-Alder with isoprene [32] giving **45**, and (4) the scale of the process (i.e., 0.2 mol) (Scheme 10).

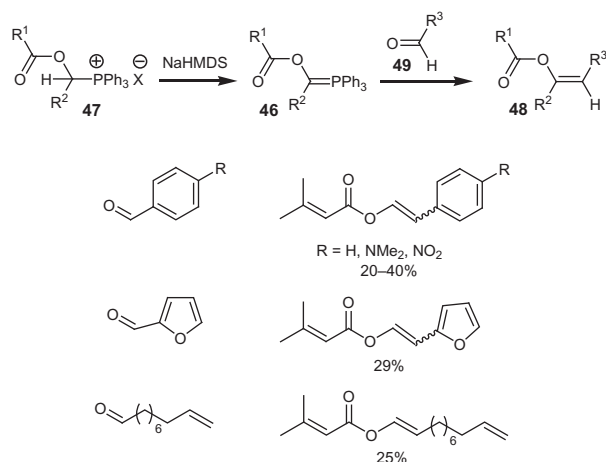
At the end of the day, our perseverance with the project was based on the fact that (1) we were the first group to enter the field of synthetic studies toward vibsanin E (**1**), (2) Huw's group had made 5,10-bis-*epi*-(**42**) (i.e., not the natural product), and (3) we (at best) were headed for 10-*epi*- synthesis (i.e., **40**), which would be an improvement on a bis-*epi* synthesis. It is amazing what excuses one can come up with when your gut says "keep going," but your mind is saying cut your losses and get out.

The next phase of our studies involved both the introduction of the masked acetone unit at position 5 and homologation of the ester, which was required to insert the enol ester side chain (Figure 4). The alkylation at C5 was of slight

concern because of the issues associated with overcoming the thermodynamic and kinetic enolate dilemma seen with the tricycle **19** (see [Scheme 7](#)). However, the real challenge was to homologate the ester at C10 by one-carbon unit and introduce an aldehyde function (required to construct the enol ester functionality). A traditional approach to this problem would require possible protection, reduction, one-step oxidation, homologation (i.e., Wittig; Ph_3PCHOMe), hydrolysis, and possibly deprotection, totaling a potential seven steps, which was clearly not viable for the end-game synthesis.

I guess this is the wonder of natural product total synthesis in that a point in the synthesis is reached, forcing the practitioner to find, or invent, a solution to a seemingly immovable problem. Of course, this practice of forced methodological invention, and/or pushing known literature to its limits, benefits not only the synthesis of the target molecule but also those operating in fields of applied organic chemistry such as nanotechnology, medicinal, and agricultural chemistry.

Tackling this ever-welcomed challenge usually starts by spending a number of hours interrogating SciFinder and Reaxys, and on this occasion, there was one reoccurring hit: a series of *Angewandte Chemie* papers [33] published by Prof. Ernst Anders (University of Jena) [34] describing an unusually substituted Wittig reagent (i.e., ylid **46**), derived from acyl phosphonium salt **47**, giving benzoyl enol esters **48** from benzaldehydes **49** in one step ([Scheme 11](#)). Before our work, these papers had received only limited citations of which most were legitimate self-citation. Publication metrics would suggest that these papers were of little scientific value, but we were about to prove otherwise, establishing the limited value of publication metrics, save, perhaps, for button pushers and bean counters.

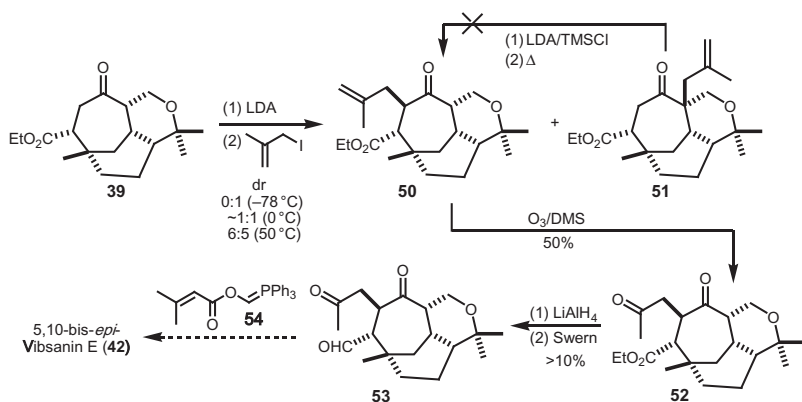
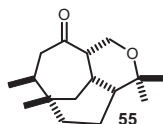


SCHEME 11 Anders–Gaßner reaction and Anders–Williams variation.

The major drawback to the Anders methodology was applicability to our system, as only aryl systems had been reported, which suited the conditions of using strong base to perform selective deprotonation of the Wittig salt (i.e., **47**). Although our system (3,3-dimethylacroyl) was susceptible to γ -deprotonation, we argued that the acidity difference of the protons under consideration favored ylid formation over γ -deprotonation. Synthesis of the 3,3-dimethylacroyl phosphonium salt (i.e., **47**) proceeded smoothly, and to our surprise, so did the formation, and trapping with various aldehydes, of the 3,3-dimethylacroyloxyalkylidenephosphorane (i.e., **46**) (Scheme 11). The yields, however, were on the low side, ranging from 21% to 41%. To put these one-step yields into perspective, when the aliphatic aldehyde shown in Scheme 11 was prepared using the classical conditions (see Scheme 10), the isolated yield was only 8%, in comparison to our significantly improved yield of 25%.

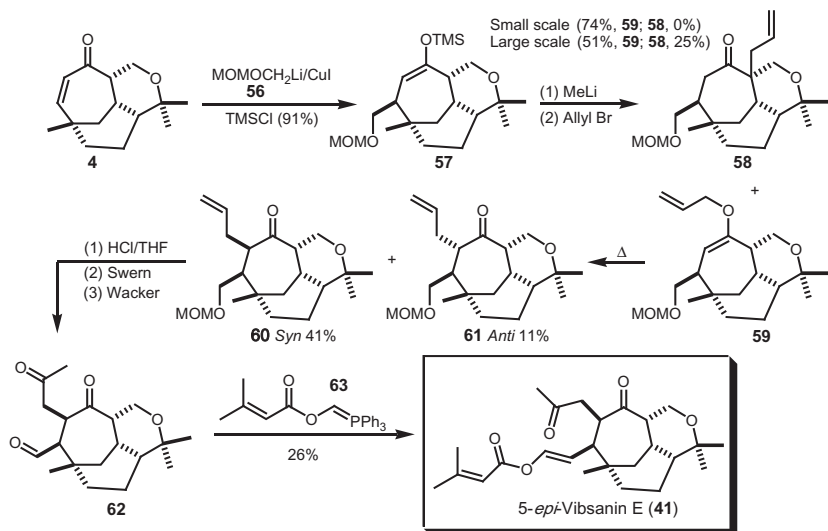
With the methodology in place for construction of the enol ester functionality, attention was now directed toward implementation of the acetone side chain at position 5. Installation of this functional group instinctively called for enolate chemistry, but with the thermodynamic versus kinetic enolate issues experienced above (see Scheme 7), we knew the job ahead was unlikely to be straightforward. To this end, two electrophiles were considered. Initially, the lithium enolate of **39**, derived from LDA, was reacted with bromoacetone, but this afforded the desired product in only trace amounts. Increasing the reactivity of the electrophile using methallyl bromide gave the desired material **50** in 37% optimized yield, in addition to the regioisomer **51**. Regulating the temperature of the reaction was key to the outcome. Holding the temperature at -78°C gave only undesired regioisomer **51** in 11% yield. When the enolate was quenched at 0°C , however, the desired **50** was accessed in 15% yield. Unfortunately, the undesired isomer **51** occurred in equal amount (17%) (Scheme 12). Further improvement in ratio and yield [**50** (37%):**51** (25%)] could be obtained if the enolate solution was heated to 50°C before addition of methallyl bromide. To complicate matters, transformation of **51** into the required isomer (i.e., **50**) by a Cope rearrangement, via the silyl enol ether, produced many side products. Even though ozonolysis of **50** afforded the acetone side chain (**52**), the best yield was only 50%. Unfortunately, dihydroxylation followed by oxidative cleavage also failed. Overall, the acetone side chain was introduced in $\sim 20\%$ yield. Global reduction proceeded smoothly but global oxidation was very problematic, giving aldehyde **53** in very low yield. The issue was that in reality we had only 1 mg of **53** and no reserves of material to bring through, meaning a Hail Mary pass in the hope that the final Wittig would deliver a 5,10-bis-*epi*-vibsanin **42** synthesis. On this scale, this was a considerable challenge and I guess it was no surprise that no product could be obtained for characterization. This was the end, or was it?

Again faced with final defeat, in a bold move, I decided to approach our competitor at the time, Prof. Huw Davies, to probe the possibility of

SCHEME 12 Attempt to access the 5,10-bis-*epi*-vibsanin **42**.FIGURE 5 Product **55** showing the stereochemical outcome of the addition of methyl cuprate.

collaboration. I wrote to Huw explaining that we could not complete the synthesis but had a lot of experience with the end-game functionalities. I also hinted very diplomatically that I surmised his group might also be experiencing problems as no total synthesis had appeared in the literature. I suggested that we should join forces, in that he would supply the material containing the vibsanin E core and we would decorate the core, thus completing the synthesis. I waited a very anxious 6 days and on the seventh Huw replied. Before I opened the e-mail, the thought went through my mind that he would simply graciously decline the offer as his group had completed the synthesis and were writing up the manuscript. Thankfully, Huw simply stated that he thought it was a great idea and would send us 1 g of racemic **4** (Scheme 10), and if we were successful, he would then send the enantiopure material. His delay in replying arose from the fact that he was in Ireland reviewing grants.

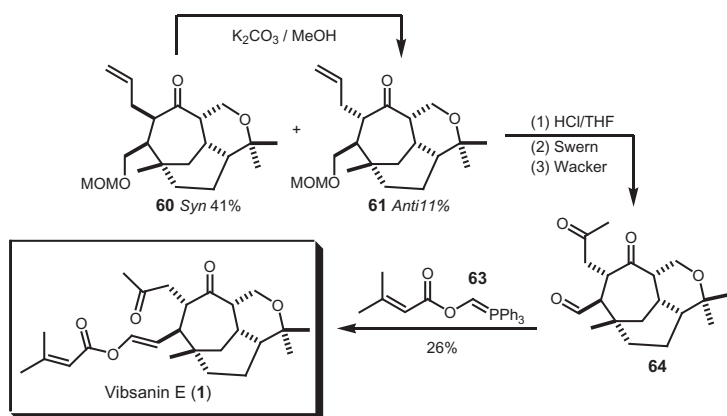
I naively proposed in the new approach that the key maneuver would be based on a diastereoselective cuprate addition to **4**. Huw warned that his group had investigated a range of cuprate carbanions and had only observed reaction with methyl cuprate, so they abandoned that approach. However, even though methyl was of little value for further manipulation, it gave only the desired diastereomer (**55**) (Figure 5), suggesting that if a suitable cuprate could be found, stereochemistry should not be an issue. I had seen anion **56** (i.e., MOMOCH₂Li derived from MOMOCH₂SnBu₃) utilized in the Mander group for the total synthesis of sordaricin [35] completed by Regan Thomson

SCHEME 13 Racemic synthesis of 5-*epi*-vibsanin E.

(now a professor at Northwestern), so we started on the synthetic plan shown in Scheme 13. Within a month of Huw's sending racemic **4**, Brett had synthesized 5-*epi*-vibsanin E (**41**).

An overview of the successful transformations detailed in Scheme 13 is given above. Fortunately, TMSCl was required to drive the 1,4-addition, which at the same time regioselectively trapped the desired enolate as silyl enol ether **57** in 91% yield. Transmetalation of **57** with methyllithium regenerated the desired enolate, which quenched with allyl bromide afforded the *O*-allylated material **59**. The sole product of the reaction on small scale was **59**; however, significant amounts of the undesired *C*-allylated material **58** (25%) were obtained when the scale was increased. A Claisen rearrangement of **59**, promoted by microwave irradiation, afforded *syn*-**60** (41%) and *anti*-**61** (11%) diastereoisomers. Deprotection of the acetal followed using hydrochloric acid in methanol, which caused slight epimerization. Sequential oxidations, Swern and then Wacker, gave aldehyde **62** in 20% yield over three steps. Utilization of ylid **63** afforded racemic 5-*epi*-vibsanin E (**41**) in 26% yield. Later, using the same sequence, Brett converted **61** into racemic vibsanin E (**1**) [36]. This was only possible because Brett found that **60** could be epimerized into **61** using potassium carbonate in methanol (Scheme 14).

We submitted this work to *Angewandte Chemie* and then to the *Journal of the American Chemical Society*, both as communications. Sadly, they were rejected. Clearly, an asymmetric synthesis was required, so Huw's group started on the enantioselective synthesis of **4**. This was not a trivial exercise as previous work in Huw's laboratory had shown that the asymmetric version of the reaction leading to **43** (Scheme 10) using either the Rh₂(*S*-DOSP)₄ (**65**)

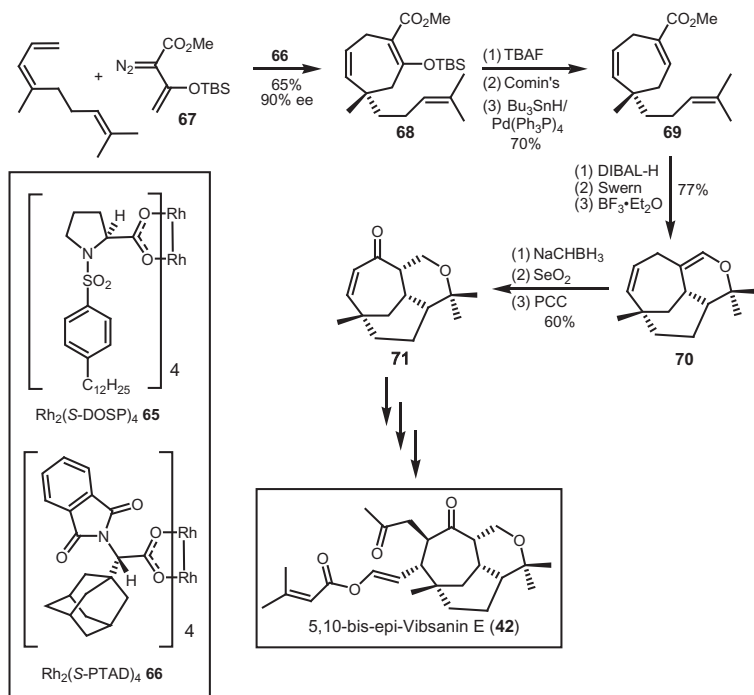


SCHEME 14 Racemic synthesis of vibsanin E (1).

or $Rh_2(S-PTAD)_4$ (**66**) ligand systems did not proceed with high asymmetric induction. Only after considerable effort was a desirable outcome achieved, but it required the use of the siloxyvinyldiazoacetate **67**, in conjunction with the $Rh_2(S-PTAD)_4$ (**66**) system, giving **68** in 67% yield and 90% ee. The use of **67** meant that the initial synthesis en route to the enantiomer of **4** (i.e., first part, Scheme 10) required reworking to remove the oxygen functionality (Scheme 15). TBS deprotection and trapping the resulting enol as the triflate facilitated reduction under palladium-catalyzed conditions to give **69** (70% yield over three steps), the enantiomer of **43** (Scheme 10). With **69** in hand, the same sequence that had been previously used in the racemic series could be applied. Conversion of the ester **69** to the corresponding aldehyde using DIBAL-H and Swern oxidation followed by a Lewis acid-catalyzed hetero-Diels–Alder reaction provided tricycle **70** in 77% overall yield. Enol ether reduction followed by sequential two-stage allylic oxidation generated the key tricyclic enone **71**. This material could be further enriched by a single recrystallization, but we chose to remove the minor isomer completely by preparative enantioselective HPLC, which was available at the University of Queensland. With >99% ee material now available, the same sequence to that described in Scheme 13 was applied and (–)-5-*epi*-vibsanin E (**41**) was prepared (Scheme 15).

We submitted this work as a full paper to the *Journal of the American Chemical Society* (JACS), which was accepted [37], and very pleasingly, it was among the top 10 most downloaded articles in JACS in the second quarter of 2009. It is at this point I want to sincerely thank Prof. Huw Davies and his team for a wonderful collaboration and to my group for their persistence and belief in their supervisor.

In conclusion, long-term challenging synthetic projects are hard to complete and even harder to get funded. Was it worth it? I would not have it



SCHEME 15 Asymmetric total synthesis of (-)-5-*epi*-vibsanin E (41).

any other way! The scholarship, friendships, and chemistry that developed in the course of this international collaboration were the epitome of the concept of a “chemistry community.” To me, these are worth more than gold.

ACKNOWLEDGMENTS

I thank Professors Huw M.L. Davies (Emory University) and Yoshiyasu Fukuyama (Tokushima Bunri University) for a fruitful collaboration and copies of Vibsanin E NMR spectra, respectively. Doctors Schwartz, Denton, Wiedemann, Heim, and Lian for dedication to laboratory work and the project. With gratitude I acknowledge the University of Queensland, the Australian Research Council (DP0666855) and the University of Buffalo for financial support.

REFERENCES

- [1] Y. Fukuyama, H. Minami, A. Matsuo, K. Kitamura, M. Akizuki, M. Kubo, M. Kodama, *Chem. Pharm. Bull.* 50 (2002) 368–371.
- [2] K. Kawazu, *Agric. Biol. Chem.* 44 (1980) 1367–1372.
- [3] K. Fukuyama, Y. Katsube, K. Kawazu, *J. Chem. Soc. Perkin 1* 2 (1980) 1701–1703.
- [4] Y. Fukuyama, H. Minami, M. Kagawa, M. Kodama, K. Kawazu, *J. Nat. Prod.* 62 (1999) 337–339.

- [5] G.V. Kryshnal, V.V. Kulganek, V.F. Kuchеров, L.A. Yanoskaya, *Synthesis* (1979) 107–109.
- [6] D. Basavaiah, A.J. Rao, T. Satyanarayana, *Chem. Rev.* 103 (2003) 811–891.
- [7] (a) F. Rezgui, M.M. El Gaied, *Tetrahedron Lett.* 39 (1998) 5965–5966; (b) R. Gatri, M.M. El Gaied, *Tetrahedron Lett.* 43 (2002) 7835–7836.
- [8] (a) K.C. Nicolaou, T. Montagnon, P.S. Baran, *Angew. Chem. Int. Ed. Engl.* 41 (2002) 993–996; (b) K.C. Nicolaou, D.L.F. Gray, T. Montagnon, S.T. Harrison, *Angew. Chem. Int. Ed. Engl.* 41 (2002) 996–1000.
- [9] M.J. Gallen, R. Goumont, T. Clark, F. Terrier, C.M. Williams, *Angew. Chem. Int. Ed. Engl.* 45 (2006) 2929.
- [10] M.J. Gallen, C.M. Williams, *Eur. J. Org. Chem.* (2008) 4697–4705.
- [11] R.A. Barnes, W.J. Houlihan, *J. Org. Chem.* 26 (1961) 1609–1611.
- [12] (a) H.-J. Liu, W.-L. Yeh, E.N.C. Browne, *Can. J. Chem.* 73 (1995) 1135–1147; (b) Z. Ahmad, P. Goswami, R.V. Vendateswaran, *Tetrahedron* 45 (1989) 6833–6840.
- [13] K. Nagao, M. Chiba, S.W. Kim, *Synthesis* (1983) 197–199.
- [14] K. Maruoka, A.B. Concepcion, H. Yamamoto, *Synthesis* (1994) 1283–1290.
- [15] Y. Ito, S. Fujii, T. Saegusa, *J. Org. Chem.* 41 (1976) 2073–2074.
- [16] H.A. Patel, J.B. Stothers, S.E. Thomas, *Can. J. Chem.* 72 (1994) 56–68.
- [17] L.M. Murray, P. O'Brien, R.J.K. Taylor, S. Wünnemann, *Tetrahedron Lett.* 45 (2004) 2597–2601.
- [18] (a) A.L.J. Beckwith, D.M. O'Shea, S. Gerba, S.W. Westwood, *J. Chem. Soc. Chem. Commun.* (1987) 666–667; (b) A.L.J. Beckwith, D.M. O'Shea, S.W. Westwood, *J. Am. Chem. Soc.* 110 (1988) 2565–2575; (c) P. Dowd, W. Zhang, *Chem. Rev.* 93 (1993) 2091–2115.
- [19] L.N. Mander, S.P. Sethi, *Tetrahedron Lett.* 24 (1983) 5425–5428.
- [20] (a) M. Takano, A. Umino, M. Nakada, *Org. Lett.* 6 (2004) 4897–4900; (b) S.H. Chung, M. S. Cho, J.Y. Choi, D.W. Kwon, Y.H. Kim, *Synlett* (2001) 1266–1268; (c) E. Hasegawa, T. Kitazume, K. Suzuki, E. Tosaka, *Tetrahedron Lett.* 39 (1998) 4059–4062.
- [21] H.-U. Reissig, R. Zimmer, *Chem. Rev.* 103 (2003) 1151–1196.
- [22] (a) J.B. Brogan, C.K. Zercher, *J. Org. Chem.* 62 (1997) 6444–6446; (b) C.A. Verbicky, C. K. Zercher, *J. Org. Chem.* 65 (2000) 5615–5622; (c) R. Hilgenkamp, C.K. Zercher, *Tetrahedron* 57 (2001) 8793–8800; (d) S. Lai, C.K. Zercher, J.P. Jasinski, S.N. Reid, R.J. Staples, *Org. Lett.* 3 (2001) 4169–4171; (e) Q. Pu, E. Wilson, C.K. Zercher, *Tetrahedron* 64 (2008) 8045–8051; (f) W. Lin, R.J. McGinness, E.C. Wilson, C.K. Zercher, *Synthesis* (2007) 2404–2408; (g) M.D. Ronsheim, C.K. Zercher, *J. Org. Chem.* 68 (2003) 1878–1885.
- [23] (a) J. Furukawa, N. Kawabata, J. Nishimura, *Tetrahedron Lett.* 7 (1966) 3353–3354; (b) J. Furukawa, N. Kawabata, J. Nishimura, *Tetrahedron* 24 (1968) 53–58; (c) J. Furukawa, N. Kawabata, J. Nishimura, *Tetrahedron Lett.* 9 (1968) 3495–3498.
- [24] W.A. Eger, C.K. Zercher, C.M. Williams, *J. Org. Chem.* 75 (2010) 7322–7331.
- [25] S. Xue, Y.-K. Liu, L.-Z. Li, Q.-X. Guo, *J. Org. Chem.* 70 (2005) 8245–8247.
- [26] R. Heim, S. Wiedemann, C.M. Williams, P.V. Bernhardt, *Org. Lett.* 7 (2005) 1327–1329.
- [27] B.D. Schwartz, D.P. Tilly, R. Heim, S. Wiedemann, C.M. Williams, P.V. Bernhardt, *Eur. J. Org. Chem.* (2006) 3181–3192.
- [28] A. Porzelle, C.M. Williams, B.D. Schwartz, I.R. Gentle, *Synlett* (2005) 2923–2926.
- [29] B.D. Schwartz, A. Porzelle, K.S. Jack, J.M. Faber, C.M. Williams, I.R. Gentle, *Adv. Synth. Catal.* 351 (2009) 1148–1154.
- [30] B.D. Schwartz, C.M. Williams, P.V. Bernhardt, *Beilstein J. Org. Chem.* 4 (2008) 34.
- [31] H.M.L. Davies, Ø. Loe, D.G. Stafford, *Org. Lett.* 7 (2005) 5561–5563.

- [32] J. Nikolai, Ø. Loe, P.M. Dominiak, O.O. Gerlitz, J. Autschbach, H.M.L. Davies, *J. Am. Chem. Soc.* 129 (2007) 10763–10772.
- [33] (a) E. Anders, T. Gassner, *Angew. Chem. Int. Ed. Engl.* 21 (1982) 289–290; (b) E. Anders, T. Gaßner, *Angew. Chem. Suppl.* (1982) 675–685; (c) E. Anders, T. Gassner, *Angew. Chem. Int. Ed. Engl.* 22 (1983) 619–620.
- [34] (a) See also E. Anders, T. Gaßner, *Chem. Ber.* 117 (1984) 1034–1038; (b) E. Anders, T. Gaßner, A. Stankowiak, *Chem. Ber.* 118 (1985) 124–131; (c) E. Anders, T. Clark, T. Gaßner, *Chem. Ber.* 119 (1986) 1350–1360.
- [35] L.N. Mander, R.J. Thomson, *J. Org. Chem.* 70 (2005) 1654–1670.
- [36] B.D. Schwartz, J.R. Denton, H.M.L. Davies, C.M. Williams, *Aust. J. Chem.* 62 (2009) 980–982.
- [37] B.D. Schwartz, J.R. Denton, Y. Lian, H.M.L. Davies, C.M. Williams, *J. Am. Chem. Soc.* 131 (2009) 8329–8332.

Note: Page numbers followed by “f” indicate figures, and “t” indicate tables.

A

- Abudinol, 225–260
- Abudinol B, first-generation synthesis, 233–242
- Abudinol B, second-generation synthesis, 242–249
- Abudinols A and B, 229–233
- Abudinols A and B, biosynthetic schemes for, 230–231
- A549 cell line, 172
- 1-Acetaminoadamantane, 326
- Acetic anhydride, 114–115, 272–273
- Acetonide deprotection, 264–265
- Acetyl chloride, 338
- Acetylcholinesterase inhibition, 292
- “Achiral” enolization, 148, 149
- Achmatowicz rearrangement, 82–83
- Acid-catalyzed condensation, 176–177, 282–283
- Acid-catalyzed elimination, 4, 5–6, 18, 19–20
- Acid-catalyzed hetero-Diels–Alder reaction, 408–409
- Ac₂O, 36, 39–40, 71, 82, 89, 136, 181–182, 252f
- Acrylamide of Oppolzer’s sultam, 356–357, 358–359, 360–361
- Acrylonitrile, 43, 44
- Acryloyl chloride, 175
- Actinophyllic acid, 307–308
- Acyl carrier protein, 377–378
- Acyl spirocyclic aryl glycopyranoside, 111, 113
- Acylstannanes, 15–16, 16t
- Acyl transferase, 377–378
- Adamantane, 318, 318f, 320–326, 321np, 322f, 323f, 324f, 327, 328–330, 331, 336–338, 339–340, 343–345
- Adamantane functionalizations, NHPI, 325–326
- Adamantane, monobromination of, 339–340
- Adamantane radical cation, 344–345
- Adamantane, radical chlorinations and brominations of, 323–324
- Adamantane synthesis, 320–321
- Adamantan-2-one, 329–330
- Adamantine, Kyodai nitration, 326
- (1-Adamantyl)dichlorophosphonate, 336
- 1-(1-Adamantyl)ethanamine, 320
- Adamantyl radicals, 322–323, 344–345
- Adenovirus E1A oncogene, 375–376
- Adiabatic ionization potential, 342–343
- Affinity probes, 390–391
- Aglycone, 378–379, 380, 391–392
- Ag₂O, 87–88
- AgOTf, 99–100, 101t
- AIDS, 80
- Aigialomycin C and D, 153–169
- Aigialomycin D, 153–169
- Aigialomycin D, retrosynthetic analysis of, 154–162, 163–167
- Aigialus parvus* BCC 5311, 153–154
- AlBr₃, 338, 339–340
- AlCl₃, 338, 339–340
- AlCl₃/CH₂Cl₂, 338
- AlCl₄[−]/CH₂Cl⁺, 338
- Alder-ene reaction, 184–185, 188–191
- Aldol addition, 102–105
- Aldol cyclization, 58–59, 60–63, 137–138
- Aldol reaction, 58, 59, 60, 62–64, 65, 66–67, 85–86, 102–105, 104t, 133, 141–143, 176–177, 252–253, 379, 380, 381–384, 385, 388–390
- Aldol reactions, asymmetric vinylogous Mukaiyama, 176
- Aldol reactions, copper hydride-induced, 60
- Aldol reactions, diastereoselective substrate-controlled, 385
- Aldol reactions, Evans catalytic asymmetric, 65
- Aldol reactions, intramolecular, 58, 60
- Aldol reactions, Lewis-base-catalyzed, 105
- Aldol reactions, Mukaiyama, 176–177, 380, 390
- Aldol reactions, stereoselective, 379
- Aldol reactions, vinylogous, 102–105, 104t

- Aliphatic hydrocarbons, Kyodai nitration of, 326
- Aliphatic side chain, 267–268, 268*f*, 269*f*
- Alkane halogenation reaction, 323–324
- Alkanes, 317–350
- Alkene, 6, 9, 36, 100–101, 155–156, 157, 163, 175, 178–179, 183–186, 186*r*, 187, 228, 229–231, 233–234, 235, 235*f*, 241–242, 246, 251–252, 253*f*, 264, 265*f*, 267–268, 274, 387–388
- Alkylation, Brook rearrangement, 245, 245*f*, 249, 250*f*
- Alkyndiones, 62–63
- Allyl alcohol, 45, 100–101, 137, 144, 158–160, 164–165, 174–175, 176–177, 180, 187, 190–191, 280–282, 285, 305, 366–367, 386–387
- Allylation, 47, 85–86, 106–109, 173–174, 175, 177–179, 366–367, 382–383, 408
- Allylation, Brown asymmetric, 173–174
- Allylation, Brown, 175
- Allylation, Brown-type, 106
- Allyl(Ipc)₂B, 106
- Allylboration, 4, 5–6
- Allylboronate, 4
- π -Allyl etherification, 194–195
- Allylic boronic ester, 6
- Allylic carbocation, 191, 192
- Allylic oxidation, 408–409
- Allylic stannane, 178–179
- Allylic transposition, 3–4, 184, 189–191, 192–193, 194–195
- Allylic transposition, allylic alcohols, 190–191
- Allylic transposition, Rhenium-catalyzed, 194–195
- Allyl indium species, 8
- Allylmagnesium bromide, 106, 175, 267
- [allylPdCl]₂, 87–88, 91*t*
- π -Allyl-Pd complexes, 187–188
- π -Allyl-Pd-mediated cyclization, 185–186
- π -Allyl ruthenium hydride, 190
- Allyltributylstannane, 382–383
- Allyltributyltin, 106
- Allyltrichlorosilane, 106–108
- Alpha-selective glycosylation, 385–386
- S-Alpine-Borane[®], 305
- Alternative structure for muzitone, 256*f*
- Altmann and Gertsch synthesis of (–)-dactylolide, 181–182
- Alzheimer's disease, 292, 320
- Amberlyst-15 H⁺ resin, 134
- Amberlyst resin, 402
- Amidations, 280–282, 336, 337
- Amidocuprate intermediates, 307–308
- Amination, 211–213, 217, 297, 328–329, 338, 340
- Aminoglycoside, 354, 358–359, 366–367
- Ammonium cerium(IV) nitrate, 325–326, 368–370
- Amphipathic molecules, 80
- Anders, E., 405
- Anders–Gaßner reaction, 405
- Anders methodology, Vibsanin E synthesis, 406
- Anders–Williams variation of Anders–Gabner reaction, 405
- Anhydrous nitric acid, 330–331, 333–334, 335–336, 340–341
- Anisaldehyde, 205, 218
- Annulated cycloheptadienes, 294–295
- Anodic oxidation, 344–345
- Anomalous dispersion, 331–333
- Anomer isomerisation, 98
- ansa*-carbon natural products, 261–262
- ansa*-fragments and chain, 263
- ansa*-skeleton, 263–264
- Antiangiogenic effects, 57
- anti*-E-2-ene-1,4-diols, 4, 5
- Antifungal activity, 80
- Antifungal agents, 80, 82–83
- Antimalarial, 153–154
- Anti-Markovnikov alkene additions, 230–231
- anti*-1,3 reduction, 282
- 1,3-*anti*-selective reduction, 264–265, 267, 270
- Antitumor, 57, 127–152, 153–154, 351–373
- Antitumor action, mechanism of, 138
- Apoptolidin A, Crimmins synthesis, 379
- Apoptolidin A, Koert synthesis, 379
- Apoptolidin A, Nicolaou synthesis, 378–379
- Apoptolidin gene cluster, 377–378
- Apoptolidinone A and D, 380–390, 391
- Apoptolidinone D, 380–392
- Apoptolidinone, first-generation approach, 380–383
- Apoptolidinone, synthetic routes to C25–C28 fragment, 380–381
- Apoptolidins, synthesis of, 375–394
- Arene oxidation, 368, 369
- Aromatic iodide, optimization, 95–97
- Aryl- β -D-C-glycopyranoside, 82–83
- Arylboronic acid, 364–365
- Aryl bromide, 264, 265*f*, 267, 268–269, 274, 282–283, 362
- Aryl-C-glycoside atropisomerism, 265–267

- 1-Aryl glucal, 98–99
Aryl-tetrahydropyranyl moiety, 267, 267f
Asymmetric alkylation, 32–33, 38, 99–100, 138–139, 148, 187–188, 202, 245, 245f, 250f
Asymmetric allylation reaction, 32–33, 105–109, 107t, 138–139, 148
Asymmetric dipolar cycloaddition, 352, 360–361
Asymmetric hetero-Diels–Alder cycloaddition, 359
Asymmetric hetero-Diels–Alder reaction, 179–180
Asymmetric hydrogenation of geraniol, 85–86, 100–101
Asymmetric synthesis, lucinone, 60, 62
Asymmetric vinylogous Mukaiyama aldol reaction, 176
Atropisomerism, 265–267, 284–285
Avrainvillamide, 307–308
Axinellidae sponges, 229–230
2-Azido imidazolium species, 213–214
(+)-Azinothricin, 130
Azo-abudinol, 239–240
Azobisisobutyronitrile (AIBN), 30–31, 35, 36, 129, 135, 276f
Azodicarboxydipiperidine (ADDP), 15, 16np
Azomethine ylides, 351–352, 360–361
- B**
Ba(OH)₂, 178, 181–182
Baeyer–Villiger oxidation, 264–265, 362
Baldwin, Jack, 50–52
Barrett's approach, papulacandin synthesis, 83–84
Barton–Kellogg reaction, 239–240
Barton McCombie xanthate reduction, 274–276
Barton nitrite ester oxidation, 302
Barton nitrite oxidation, 302
Base-catalyzed migration, 387–388
Baylis–Hillman reaction, 39–41, 42, 43, 50–52, 396–397, 402
(+)-B-chlorodiisopino-campheylborane, 305
Bcl-xl inhibition, 261–262
Beckwith–Dowd and Zercher ring expansion, 400–402
Beckwith–Dowd rearrangement, 400–402
Benzaldehyde, 14, 15t, 218–219, 382–383, 405
Benzonitrile, 95, 134–137
Benzoquinone, 193–194, 263, 266f
Benzoyl chloride, 142–143
Benzoyl enol esters, 405
Benzylation, 380–381
Benzylic alcohol, 90–91, 95, 96–97, 96t, 271, 272–273, 272f
Benzyloxyacetaldehyde, 364, 365
(1,3)-Beta-D-glucan synthase, 80, 81–82
BF₃·etherate, 234
BF₃·Et₂O, 133, 397–398, 399
BF₃·OEt₂, 89, 133, 145, 146, 181, 189, 228f, 229f, 268f, 355, 381–382, 385, 397–398, 399, 404, 410
Bicyclization approach, abudinol B, 235, 235f
Bicyclization cascade, 231, 233–235, 251–252
Bidirectional cyclizations, 230–231
BINAL-H, 15
BINOL/Ti(Oi-Pr)₄, 106
BINOL–titanium tetraisopropoxide (BITIP), 178–179
Biomimetic tricyclization, 250
Biotinylated probe molecules, 138
N,O-bis(trimethylsilyl)acetamide, 203
Bis[chloro(*p*-cymene)-ruthenium(II)], 89–90, 93–95
5,10-Bis-*epi*-vibsanin E, 403–404, 403f, 406, 407, 410
[Bis(acetoxy)iodo]benzene (BAIB), 143–144
bis-olefin, 9
bis-oxidation, 67, 176–177
bis-para-nitrobenzoate, 254–255, 255f
Bisphosphoramidate catalyst, 102–104, 106–108
BITIP-catalyzed allylation, 178–179
Boeckman's synthesis, (+)-eremantholide A, 132
Boron trifluoride diethyl etherate, 355
Boronic esters, synthesis of, 192t
Brevetoxins, 81f, 226–228, 227f
Breynolide, 128–129
Brigl's intermediates, oxidative spiroketalization, 98–99
Bromide, 30–31, 34–36, 82–84, 176–177, 244, 244f, 245, 267–268, 331–333, 385
Bromination and nitroxylation, 321–322, 335–336
Bromination of functionalized diamondoids, 320, 321, 323, 331–333, 335, 339–340, 341
Bromination of [1(2)3]tetramantane, 331
Brominations, 134, 265–267, 270–271, 272–273, 320, 321–322, 323–324, 330–334, 335–336, 338, 339–340, 362
Bromination with NBS, 272–273
Bromine, 34–36, 265–267, 320–321, 325–326, 330–331, 333–334, 335–336, 339–340
Bromoacetone, 406

1-Bromoadamantane, 330–331, 339–340
 2-Bromocyclohexamantane, 333
 2-Bromocyclohexamantyl cations, 340, 341
 1-Bromodiamantane, 331
 5-Bromo-2-oxaadamantane, 324–325
 3-Bromopropan-1-ol, 13
 2-Bromotriamantane, 331
 1-Bromo-4-trimethylsilyl-2-butyne, 236–237, 237f
 Brønsted base activation, 90
 Brook, A., 56
 Brook rearrangement–alkylation, 245, 245f, 249, 250f
 Brown allylation, 175
 Brown asymmetric allylation, 173–174
 Brown-type allylation, 106
 Brussonol, 294–295
 Bryostatins, 130
 Bu₃P, 27–29, 36, 44–45, 176–177
 Bu₃SnCl, 13–14, 19
 Bu₃Sn(Bu)CuCNLi₂, 181–182
 Bu₃SnH, 30–31, 35, 36, 129, 135, 241–242, 410
 Bu₃SnLi, 16np, 44–45
N-butyllithium, 308–309, 386–387
 Butyl vinyl ether, 38, 48–49
 2-Butynoic acid, 181–182, 386–387
 2-Butyn-1-ol, 236–237

C

Calcaridine A, 199–200, 200f, 201, 217–221
 Calcaridine A, first-generation total synthesis of, 218, 219
 Callipeltose, Evans synthesis of, 357–358
 CAN, photochemical decomposition of, 326
 Carbamate, 4–5, 13–16, 17, 38, 355–356
 Carbene cyclization cycloaddition cascade (CCCC) reaction, 64, 65, 67, 68, 75
 Carbene-derived ring expansion, 398
 Carbocation-like TSs, 335
 Carbomethoxymethylene triphenylphosphorane, 143–144
 Carbon-ICD reaction, 42, 43
 Carbonyl addition reaction, 85–86, 105
 Carbonylation, 68–70, 338
 Carbonylation, palladium-catalyzed, 69–70, 82, 85, 122, 184–185, 187, 188–189, 240–241, 240f, 248–249, 351–352, 408–409
 Carbonyl lone pair, hydrogen bond, 161–162
 Carbonyl reduction via tosylhydrazones, 264–265
 Carboxylation, 335–336

Carboxylic acid, 26, 109, 110, 111
 Carlson, R.M.K., 319
 C-aryl glycoside, 82, 85, 265–267, 287
 C-aryl-2-H-pyrans, synthesis of, 86–87
 Cascade carbacyclization, 245
 Cascade cyclization, 59, 226–227, 226f, 228, 230–233, 236, 238–239, 242, 245–248, 250–252, 256, 397–398
 Cascade oxacyclization, 233–239
 Catalytic hydrogenation, 203, 204–205, 218, 219–221
 Catalytic nitrations, 325–326
 Cation, 56, 115–117, 175, 231, 325–326, 330–331, 333–334, 335–336, 342–345, 360, 361
 CBrCl₃, 329
 CBr₃-radical, 325
 CBz-Cl, 364
 C9/C10 disconnection approach (RCM), kendomycin synthesis, 278–280
 C10/C11 disconnection approach (RCM), kendomycin synthesis, 282–285
 C13/C14 disconnection approach (RCM), kendomycin synthesis, 264–277
 C19/C20 disconnection approach (RCM), kendomycin synthesis, 280–282
 C16–C28 fragment synthesis, apoptolidin, 381–382
 CCl₄, 253f, 254f, 329
 C4,C5-substituted derivatives, Leucetta-derived alkaloids, 205–209
 C16–C28 to C12–C28 fragment synthesis, apoptolidinone, 382–383
 CDK1/cyclin, selective kinase inhibitor for, 153–154
 CeCl₃, 36, 49, 176–177, 178, 179, 183
 Cerium (IV) ammonium nitrate (CAN), 325–326, 341, 368, 369
 Cerulenin, 391–392
 CF₃Ph, 67–68
 C-Glycosidation, 263–264, 270–271
 C–H activation, 190, 321–322, 328, 329–330, 333, 345
 Chain elongation, spiro system, 33–34
 Chair conformation, 98, 175
 Charged electrophiles, 330–342
 C–H bond functionalization, 319, 325–326, 345
 Chelation-controlled addition, 154–155, 158, 382–383, 385
 Chelation-controlled reduction, ketone, 158–160, 164–165

- Chelation-directed reductive fragmentation, 380–381
- Chelation–hydroalumination, 158–160, 164–165
- Chemical genetics, 153–154
- Chemical vapor deposition (CVD), 317–318
- Chemobiosynthesis, 392
- Chemoselective hydrolysis, 236–237
- Chemoselective macrocyclization vs. triene, 157–158
- Chemoselectivity, 17–18, 19–20, 59, 144, 155, 183–184
- Cheng, K.F., 56
- Chiral α -hydroxy aldehyde, 158, 163–164
- Chiral aldehyde, 163–164, 165
- Chiral auxiliaries, 29, 142–143, 356–357, 360–361
- Chiral auxiliary-controlled dipolar cycloaddition, 371
- Chiral bisphosphoramidate, 106–108, 122
- Chiral chromium(III) catalyst, Jacobsen's, 179–180
- Chiral diamondoids, 331–333
- Chirality transfer, 190–191, 357, 371
- “Chiral” lithium, 147–148
- Chiral oxazolidinone, 150
- Chiral pool, 359
- Chloramine-T, 217
- Chlorination, selective bridgehead, 321
- 2-Chlorobenzimidazole, 214–216
- Chlorocarbonyl-pyridinium cation, 115–117
- Chlorodimethylsilane, 89–90, 92–93
- N*-chlorosuccinimide, 300–301
- Chromyl chloride, 329–330
- C(3)-hydroxyl group protection, 85, 89–93, 93*t*
- Cl₃-radicals, 323–324, 325
- Circular dichroism, 229–230, 242, 331–333
- cis*- and *trans*-2,6-disubstituted tetrahydropyrans, 186–187
- cis*-2,6-disubstituted-4-methylene tetrahydropyran, 172–173, 174–175, 176
- cis*-non-3-enal, 14, 15–16, 15*r*, 16*r*
- cis*-vinyl boronates, 190
- (*S*)-Citronellol, 100–101, 270, 280–283
- Claissen rearrangement, 7–8, 38, 47, 48–50, 51*f*, 134–137, 179–180, 263–264, 264*f*, 281*f*, 285, 286*f*, 287, 408
- Clark, Robin J. H., 129–130
- Clarke, P., 398–399
- C6, lateral deprotonation, 303–304, 309
- Clathridine A, 203
- Closed-chelate transition state, 381–382
- C(17) methyl group, 37
- C–N bond formation, oxidative, 300–304, 307–314
- Colvin's methodology, 282–283
- Colvin's one carbon chain elongation, 278
- Commercial bleach solution, 214
- Cl–O–MOM deprotection, 270–271, 271*f*
- Concentrated sulfuric acid, 330–331, 335–338, 340–341
- Conducted tour mechanism, 310
- (*E,Z*)-conjugated ester, 175
- Conjugate displacement, intramolecular, 39–41, 42, 42*f*, 43, 44
- Conjugate reduction-aldol cyclization, 59
- Constanolactone A, 2*f*
- Constanolactones, 1
- Constanolactones A–D, 4
- Constructing trisubstituted olefins, 129–130
- Cope rearrangement, 395–396, 406
- Copper-catalyzed opening of epoxide, 181–182
- Copper hydride, 59, 60–63, 76
- Copper hydride-catalyzed hydrostannation, 62–63
- Copper hydride-induced aldol reaction, 60
- Copper hydride-induced reductive aldol cyclization, 60–63
- Corey–Bakshi–Shibata (CBS) reduction, 305
- Corey, E.J., 245, 296
- Corey–Fuchs alkynylation, 382–383
- Cotton effects, 229–230, 242
- Coupling, two segments, 239–242
- cPLA₂, 27
- Crimmins synthesis of apoptoludin A, 379
- CrO₂(OAc)₂, 329–330
- CrO₂Cl₂, 329–330
- Cross-coupling reaction, 85–88, 90–92, 93*r*, 95, 96–97, 121, 155, 362, 383–384, 386–387, 389–390
- Cross-coupling sequence, 84, 97, 385–386
- Cross-metathesis (CM) reaction, 105–106, 139–140, 149, 154–156, 157–158, 161–162, 167–168, 179–180, 183–184, 185–186, 297, 357–358, 379, 386, 388–390
- Crown ethers, 69–70
- Cs₂CO₃, 48, 181
- C4-substituted derivatives, Leucetta-derived alkaloids, 203–205
- Cu(OTf)₂, 311–313
- CuCl, 60–62
- CuCN·2LiCl, 206–209
- Cu–Pybox complex, 176, 177

Curtius rearrangement, 300
 Cu(OTf)₂, 65
 CuTC, 379
 Cyanocycline A, 352, 353*f*, 355–356, 357–358, 364
 Cyanocycline A, Fukuyama's route, 356
 Cyanocycline A, Fukuyama's synthesis, 355–356
 Cyclic boronic acid half ester, 184–185, 189, 190–191
 Cyclic boronic esters, synthesis of, 192*t*
 Cyclic sulfates, 227
 Cyclization, Prins-type stereoselective, 181–182
 Cyclizations, polyene, 236–237
 Cycloetherification, 188–189
 1,4-Cyclohexadiene, 34
 Cyclohexamantane, 333*np*, 333, 345
 Cyclohexenone, 396–398
O-cyclohexylidenation, 142–143
 Cyclopropanation, 8, 9, 12, 399–400
 Cyclopropanes, 2*f*, 7–8, 9, 399–402
 Cyclopropyl lactones, 1, 3–4, 8, 12, 13
 Cyclopropyl methyl ketone, 396–397

D

DABCO, 39–40, 44
 (–)-Dactylolide, 171–197
 (–)-Dactylolide, Altmann and Gertsch synthesis of, 181–182
 (+)-Dactylolide, Floreancig synthesis of, 176–177
 (–)-Dactylolide, Ghosh synthesis of, 182–184
 (–)-Dactylolide, Hoyer synthesis of, 174–175
 (–)-Dactylolide, Jennings synthesis of, 175–176
 (+)-Dactylolide, Keck synthesis of, 177–179
 (–)-Dactylolide, McLeod synthesis of, 179–180
 (+)-Dactylolide, Smith synthesis of, 173–174
 (–)-Dactylolide, Uenishi and Tanaka synthesis of, 180–181
Dactylosporgia, 172
 Dahl, J., 319
 Danishefsky, S., 32, 38–39, 46, 56, 58–59, 157–158, 355
 Danishefsky's synthesis of quinocarcinol methyl ester, 355
 Davies, H., 403–404, 406–407, 409
 Davis oxaziridine, 218
 Davis reagent, 219–221
 DCC, 9
 Dehydratase, 58, 60, 63–64, 68, 134, 137–138, 205–206, 377–378, 389–390, 396–397
 (–)-Delobanone, 8
 de Meijere, A., 396
 Denmark's bisphosphoramidate ligand, 176–177
Deoxy-aigialomycin C, 162, 163, 167–168
 Dess–Martin oxidation, 133, 274–276
 Dess–Martin periodinane (DMP), 29, 30, 133, 193, 194, 211–213, 276*f*, 368–370
 Desulfonylation, 32, 129–130, 238*f*, 248–249
 Desulfonylation, palladium-catalyzed, 248–249
 Desulfurization, 31–32
 Detonation diamond, 317–318
 DFT calculations, 311
 Diacetone D-glucose, 134–137
 Diacetyl (CH₃CO)₂, 327
 Diamantane, 318, 318*f*, 319*f*, 320, 321*np*, 325, 328–329, 339, 340–341, 342–343, 345
 Diamantane radical cation, 342–343
 Diamantan-3-one, 336–338
 Diamond crystal, hydrogen-terminated, 318, 318*f*
 Diamond surfaces, hydrogen-terminated, 317–318
 Diamondoid phosphorylations, 338
 Diamondoids, 317–350
 Diamondoids, bromination of functionalized, 320, 321–322, 323–324, 330–331, 332, 333, 335–336, 339–340, 341
 Diamondoids, selective functionalization of, 345
 Diamondoids with dioxiranes, oxidations of, 328–329
 Diastereomer, 63, 67–68, 108–109, 180, 219–221, 234, 242, 245–246, 247–248, 248*f*, 250, 255–256, 272–273, 298–300, 407–408
 Diastereomeric π -allyl-Pd complexes, equilibration of, 188
 Diastereomeric ratio, 3–4, 158–160
 Diastereoselective reduction, enamide, 158–160, 164–165, 175, 362–363
 Diastereoselectivity, 4, 6, 16, 60, 64, 67–68, 85–86, 98–99, 153–169, 175, 218–219, 233–234, 245–246, 247, 267, 269–270, 280–282, 297, 298–300, 304–305, 355, 356–357, 359, 360, 361, 363, 366*np*, 366–367, 380, 384–385, 407–408
 Diastereoselectivity, substrate-controlled, 98–99, 385

- 3,9-Diazabicyclo[3.3.1]nonane core, 352
Diazabicyclooctane, 354, 356, 357, 371
3,8-Diazabicyclo[3.2.1]octane, 351–373
Diazabicyclooctane core, 354, 357
1,8-Diaza-bicyclo-[5.4.0]-undec-7-ene (DBU), 34, 35, 36, 37, 43, 51, 69, 133, 135, 136, 137–138, 148–149, 212, 216, 217, 267, 267*f*, 270*f*, 297–298, 299, 303
Diazoketone, 64, 65–66, 67
Diazomethane, 386–387
Dibrominations, diamondoids, 340, 341
1,3-Dibromoadamantane, 339–340
Dibromocarbene, 323–324
2,3-Dichloro-5,6-dicyanobenzoquinone (DDQ), 50, 71, 74, 173, 177, 178, 179, 181, 182–183, 266*f*, 279*f*, 286–287, 287*f*
Dictyota indica, 75
2,6-Dideoxy-4-aminoglycoside, 354
Dieckmann cyclization, 132
Diels–Alder annulation, 396
Diels–Alder chemistry of 4-vinylimidazoles, 211–213
Diels–Alder reaction, 154, 179–180, 211–213, 371, 408–409
Dienylaldehyde 28, 100–101
Diepoxides, 242, 247, 248–249, 250–251
Diethyl ethyl phosphonate, 274–276, 276*f*
Diethyl ketal, 74–75
Diethylzinc, 14, 402
Dihydrocinnamaldehyde, 14, 15*r*
Dihydrolycolucine, 293*f*
Dihydropyridinones, 47, 47*f*, 48, 49
5,7-Dihydroxy-2,2-dimethyl-4H-1,3-benzodioxan-4-one, 154–155, 158
Dihydroxylation, 12, 183, 227, 253–254, 274–276, 366–367
Diimide, 284–285
Diiodocarbene, 323–324
Diiodoethane, 89–90
4,5-Diiodoimidazole, 202, 203, 204–205
Dimedone, 29, 30
3,4-Dimethoxybenzaldehyde, 204–205
Dimethoxymethane, 366–367
3,3-Dimethoxypentane, 66–67
2,2-Dimethoxypropane, 158–160, 164–165
3,3-Dimethylacroyloxyalkylidenephosphorane, 406
3,3-Dimethylacryl phosphonium salt, 406
3,5-Dimethyladamantan-1-amine, 320
1,3-Dimethyladamantane, 320, 325–326, 336, 337
N,N-4-Dimethylaminopyridine (DMAP), 9, 13, 33, 46, 49, 65, 71, 72, 74, 110, 111, 115–117, 116*t*, 116*np*, 119, 120, 136, 147, 155–156, 173, 177, 178, 181, 182, 189, 228*f*, 251*f*, 252*f*, 255*f*, 281*f*, 283*f*, 286*f*, 298, 356, 361, 363, 364, 365, 396–397
Dimethylaminosulfonyl (DMAS) group, 206–209
2,2-Dimethyl-1,3-benzodioxan-4-one, 154–155, 157
Dimethyldioxirane (DMDO), 97–98, 277, 278*f*, 282–283, 328
Dinitroxylolation, 319, 341
Dioxo-bicyclo[3.3.0]octanone, 131–132
Dioxaborolane, 364–365, 365*np*
Dioxirane, 97–98, 233–234, 247, 328–329
(+)-DIP-Cl, 305, 306*t*
4,9-Diphenyldiamantane, 339
Diphenyldisulfide, 313–314
Diphenylphosphinobenzoic acid (DPPBA) ligands, 187–188
Dipolar cycloadditions, 351–373
Dipolar cycloadditions, asymmetric, 352, 360–361
Dipolarophile, 64
Di(*t*-butyl)silylene acetal, 92–93, 109–110, 117–119
Disobutylaluminium (DIBAL), 7–8, 9, 12, 27–29, 33–34, 43–44, 95, 96–97, 100–101, 102, 103, 134–137, 144, 174–175, 176, 179, 180, 181–182, 189–190, 211–213, 216, 269*f*, 271*f*, 279*f*, 366–367, 381, 386–387, 404, 408–409, 410
Disobutylaluminium hydride (DIBAL-H), 27–29, 33–34, 43–44, 95, 96–97, 100–101, 102, 103, 144, 174–175, 180, 181–182, 189–190, 211–213, 216, 269*f*, 271*f*, 408–409, 410
Disproportion of dihalo- and tetrahalomethanes, 323–324
1,1-Disubstituted alkene, 141, 235, 235*f*, 247, 250–251
2,6-Di-*tert*-butyl-4-methylpyridine (DTBMP), 234, 234*f*, 235, 235*f*, 238–239, 238*f*, 245–246, 246*f*, 247–248, 248*f*, 249, 251*f*, 252*f*, 299
Di-9-triamantylphosphinic acid chloride, 338
DME, 134
DMF, 40–41, 100, 101*r*, 110, 142–143, 160, 165, 188–189
DMS/NBS, 368–370

DMSO, 50, 117–119, 118*t*, 119*f*, 120, 121, 136, 179, 189, 211–213, 233*f*, 266*f*, 282*f*, 284–285, 299, 307, 369, 370–371
 DNA binding, 138, 139*f*, 354
 DNA-damaging agent, 354
 D₂O, 270–271, 309–310
 Dodecahedrane, 320–321
 Dötz benzannulation, 264*f*
 Doubly vinyllogous aldol addition, 102–104
 (*R,R*)-DPPBA ligand, 187
 (*S,S*)-DPPBA ligand, 187–189
 Dragmacidin D, Stoltz approach, 294, 295
 Durgamone, 229–230, 229*f*, 235–236, 236*f*, 242

E

E-allylsilane, 19–21
 E1A-transformed cells, 375–376
 E1_{cb} elimination, 69–70
 (–)-Echinospirin, 128–129
 Ecteinascidin 743, 352, 353*f*
 Eight-membered lactone, 7–8, 10*r*, 11, 11*f*
 Eight-membered ring formation by RCM, 11
 Electron-emitting efficiency, 320
 Electro-oxidation, 344–345
 Electrophiles, 309–310, 322, 328–342
 Electrophilic chromyl trifluoroacetate, 329–330
 Enantio- and diastereoselectivity, 4, 384–385
 Enantioenriched cyclopropanes, 7–8
 Enantioenriched stannane, 4, 14
 Enantioselective hydrogenation, 304–305
 Enantioselective method, 106–108
 Enantioselective reduction, 304–305, 306*t*
 Enantioselective synthesis, lyconadin A, 304–307
endo-mode oxacyclization, 226–227, 227*f*
endo-selective *cascade* cyclization, 227
 6-*endo-trig* cyclization, 30–31
 2-ene-1,4-diols, 1–2, 4–7, 19, 21
 2-ene-1,4-diols, synthesis of, 4–6, 21
 Enolate cyclopropanation methodology, 399–400
 Enolates, oxidative dimerization of, 307–308
 Enol ether, 406
 Enolization-enol triflate cross-coupling method, 129–130
 Enolsilane, 233–235, 233*f*, 234*f*, 242–243, 245–246, 249
 Enolsilane-diepoxide, bicyclization, 234, 234*f*
 Enol triflate, 129–130, 240–241
 Enol triflation, 69–70
 Enone system, 36–37
N-enoyl sultam, 269–270
ent-abudinol B, 236, 237*f*, 241–243, 241*f*, 243*f*, 247–248, 248*f*
ent-durgamone synthesis of, 235–236, 236*f*
 Enterococcus faecium, vancomycin-resistant, 353–354
ent-muzitone, 249, 250*f*, 253–254, 253*f*
ent-nakorone, conversion, 239, 239*f*
ent-nakorone, synthesis of, 236, 238–239
epi-aigialomycin D, 162, 167–168
 Epibatidine, 26
epi-C6 aigialomycin D, 161, 162
 (*S*)-epichlorohydrin, 381
 5-*epi*-vibsanin E, 395–412
 10-*epi*-vibsanin E, 403*f*
 Epoxidation, 4, 6, 7–8, 17–18, 19–20, 21, 84, 98–99, 141–142, 144, 174–175, 226–228, 228*f*, 229*f*, 233–234, 233*f*, 236–238, 238*f*, 242, 243–244, 244*t*, 246, 247, 247*f*, 248–249, 250–251, 251*f*, 297–298, 299, 355–356
 Epoxidation-olefination reaction, 17–18
 Epoxidations, stereoselective, 226
 Epoxide-opening reactions, 264, 268–269, 268*f*, 282–283
o-epoxone, 228*f*, 244*t*, 250–251
 Epoxonium ion, 235–236, 238–239
 Epoxy alcohol, 8
 EPR spectrum, 277
 (+)-Eremantholide A, 127–152
 (+)-Eremantholide A, Boeckman's synthesis, 132
 (+)-Eremantholide A, Hale-Li retrosynthetic analysis, 138–142
 (+)-Eremantholide A (17), Hale-Li total synthesis, 142–150
 (+)-Eremantholide A, retrosynthetic analysis, 138–142
 (+)-Eremantholide A, Tadano's synthesis of, 134–137
Eremanthus elaeagnus, 131–132
 Eritrea, 229–230
 Erythromycin, 352–353
Escherichia coli, 138
E-selective Horner–Wadsworth–Emmons (HWE) olefination, 274
 Ester linkage, 85
 Ester reduction (NaBH₄, CaCl₂), 27–29
 Et₃COK, 134

1-Ethyl-3-(3-dimethylaminopropyl)
carbodiimide (EDCI), 71, 72, 283f
Ethyl sorbate, 102–104
Ethyl(tri-*n*-butylstannyl)zinc, 14
EtMgBr, 203, 204–209, 218, 221
Et₃N, 9, 17, 35, 37, 48–49, 50, 51, 71,
106–108, 107f, 110, 111–112, 113, 119, 120,
121, 133, 135, 136, 148–149, 155–156, 189,
211–213, 228f, 233f, 244f, 301, 357, 360,
361, 362, 363, 369
Et₃SiH, 65, 175, 176, 203, 205–206, 207,
218–219, 221, 267, 267f
Et₃SiH/TFA, 205–206, 218–219
EtZnCH₂I, 402
Evans aldol addition, 142–143, 280, 282, 284,
285, 287, 381–382
Evans aldol methodology, 270, 282, 287
Evans aldol reaction, 142–143
Evans asymmetric alkylation, 29
Evans catalytic asymmetric aldol
reaction, 65
Evans cyanocycline A route, 355–356
Evans oxazolidinone, 280–282
Evans synthesis of callipeltose, 357–358
5-*exo-trig* cyclization, 30–31

F

Farnesyl benzoate, 228, 228f, 229f, 237, 238f,
243–244, 244f, 248–249
Farnesyl bromide, 237
Farnesyl *p*-tolyl sulfone, 243–244
Farnesyl *tert*-butyl carbonate, 243–244
Fasciospongia rimosa, 172
Fawcettimine, 292f
FeBr₃, 339–340
FeCl₃, 311–313
Felkin–Anh aldol addition, 357
Felkin–Anh-controlled diastereoselective
addition, 358, 366
Fenton-or Gif-oxidations, 325–326
Fetizon conditions, 380–381
F₀F₁-ATPase, 376
Finkelstein reaction, 280–282
First-generation approach to apoptolidinone,
380–383
First-generation synthesis of abudinol B,
233–242
First-generation total synthesis, calcaridine A,
218, 219
Fischer glycosidation, 141, 145–146
(–)-FK506 structure, 128–130

Floreancig synthesis of (+)-dactylolide,
176–177
Fluorescent photochromic materials, 320
Fluoride-free cross-coupling, 88
1-Fluoro-3-chloro-5-bromo-7-iodoadamantane,
324–325
1-Fluoro-3-chloro-5-bromo-7-iodocubane,
324–325
Formaldehyde, 148–149, 396–397
Free secondary amine, 303–304, 309, 368–370
Friedel–Crafts acylation, 264–265, 357–358
Friedel–Crafts arylation, 357–358
Friedel–Crafts cyclization, 205–209
Friedel–Crafts reaction, intramolecular, 201
Fries rearrangement, 264–265
D-fructose, 236
L-fructose, 236
Fukuyama reduction, 65–66
Fukuyama, Yoshiyasu, 395–396
Fukuyama's route, cyanocycline A, 356
Fukuyama's synthesis of cyanocycline A,
355–356
Fukuyama's synthesis of quinocarcin, 354, 355
Functionalized diamondoids, 317–350
3(2H)-Furanones, 133, 138–139, 141, 148
Furukawa reagent, 402

G

Gal4-transactivation domain, 138, 139f
Garegg iodination procedure, 146–147
Garg, N., 294
Garners synthesis of (+)-quinocarcin, 356–357
Garners synthesis of (–)-quinocarcin, 357,
360–361
gem-dichloride, 239–240
Geminal diol, 253–254
Geraniol, 100*np*, 122
Geraniol, asymmetric hydrogenation of,
85–86, 100–101
Geranyl bromide, 245, 245f, 249, 250f
Ghosh synthesis of (–)-dactylolide and
(–)-zampanolide, 182–184
Gilman reagent, 298–300
Global silyl deprotection (or global
deprotection), 84, 90–91, 92–93, 95, 99,
111–114, 119–121
Glucal silanol, 89–95
D-glucolactone, 82–83
Glucose, 80, 82–83, 98
α-D-glucose, 89
D-glutamic acid, 27–29

(*R*)-Glycidyl methyl ether, 380–381
 Glycopyranoside, 82–83, 85, 90–91, 93–95, 97–99, 100, 109–110, 111, 119–120, 121
 Glycosylation, alpha-selective, 385–386
 Glycosylation, precursor-directed, 354, 377–379, 385–386, 390–392
 Glycosylation, stereo and chemoselective, 378
 Glycosyl fluoride, 378–379
 α -Glycosyloxy aldehyde, 367
 Glycosyl sulfoxide donor, 378–379
 Glycithiohexide α , 354
 Gold surfaces, 320
 Grainger, R., 398–399
 Grignard-halogen exchange, 222
 Grignard reagent, 65–66, 67, 202–203, 204–206, 218, 221, 245, 268–269, 383–384, 385, 396–397
 Grubbs' catalyst, 161, 163, 165–167
 Grubbs' cross metathesis, 297
 Grubbs–Hoveyda second-generation catalyst, 193–194
 Grubbs' II catalyst, 10*r*, 10, 11*f*, 81–82, 106, 109, 129, 149, 154–155, 157, 165–167, 174, 176, 179, 183, 192–194, 274*f*, 279–280, 280*f*, 284*f*, 387–388

H

H-abstraction TSs, 323–324, 323*f*, 325–326, 327, 330–331, 335–336
 Hail Mary pass, 406
 Hale–Li retrosynthetic analysis, (+)-eremantholide A, 138–142
 Hale–Li total synthesis, (+)-eremantholide A (17), 142–150
 Halichlorine, 25–54
 Halicholactone, 1, 2*f*, 4, 9
Halichondria okadai Kadota, 27
 Halogen clusters, 330–331
N-halosuccinimides, 323–324
 η^1 - and η^3 -allyl interconversion, 187–188
 Harpp–Ando double thioalkylation, 134
 Hashimoto's catalyst, 67–68
 HCB r_3 /NaOH, 323–324
 HCl, 98, 99, 137–138, 141, 145–146, 150, 158–160, 162, 164–165, 209, 214–216, 272–273, 277, 284–285, 297, 302, 311–313
 H $_2$ CrO $_4$, 329–330
 Heathcock, C., 40–41, 291–292, 296
 Heck coupling, 362
 Heck cyclization, intramolecular, 297
 Heck reaction, 264, 267–268, 361–362
 HeLa cells, 205–206
 σ -Helicenes, 331–333
 Hetero-Diels–Alder cycloaddition, asymmetric, 359
 Hetero-Diels–Alder reaction, 82–83, 179–180, 371, 408–409
 Hetero-Diels–Alder reaction, acid-catalyzed, 408–409
 Hetero-Diels–Alder reaction, asymmetric, 179–180
 Hetero-Michael addition, 264
 1,1,1,2,2,2-Hexachloroethane, 134
 Hexamethylphosphoramide (HMPA), 29, 30, 69–70, 103, 112*t*, 133, 134, 281*f*, 387, 389–390
 Hexanal, 13, 15*r*
 HF, 46, 111–114, 112*t*, 117–119, 118*np*, 120, 121, 173, 176, 177, 178, 182, 183, 286–287, 287*f*, 333, 378–379, 385–386, 389–390
 HF·NEt $_3$, 111–114, 112*t*, 117–120, 118*np*
 HF-pyridine, 46, 112–114, 378–379, 385–386, 389–390
 Hg (OAc) $_2$, 38, 48–49, 50
 HI, 146–147, 251–252, 252*f*
 Himastatin, 131
 HIO $_3$, 298–300
 H $_5$ IO $_6$, 329
 Hitachimycin, 128–129
 Hiyama–Denmark coupling, 87–88
 Hiyama–Kishi reaction, 280–282
 H292 lung carcinoma cells, 390–392
 HMBC studies, 255
 HMDS, 173–174
 HNO $_3$, 319, 321, 322*f*, 333–334, 337, 340–341, 342
 H $_2$ O $_2$, 16–17, 18*r*, 42, 43, 87, 173–174, 176, 177, 181, 270, 298–300, 355, 362
 Hoffman–Löffler–Freitag (HLF) reaction, 297, 300–301, 302
 Hole-transfer promoted hydrogenation, 241–242
 Homoadamantane, 320–321
 Homoallylic carbonates, 188–189
 Homologated aldehyde, 38–39
 Homologation, 29, 66, 74–75, 104–106, 142–143, 178–179, 187, 377–378, 402, 404–405
 Homoprenyl Grignard reagent, 396–397
 Homopropargylic alcohols, 186–187, 188–189, 194–195
 Horner–Wadsworth–Emmons (HWE) cyclizations, 263–264, 276–277, 276*f*, 277*f*

- Horner–Wadsworth–Emmons (HWE)
 macrocyclization, 274–277
- Horner–Wadsworth–Emmons (HWE)
 olefination, 82–83, 85–86, 100–101,
 173–174, 175, 176–179, 180, 181, 264, 264*f*,
 269–270, 274, 386
- Horner–Wadsworth–Emmons (HWE) reaction,
 72, 74–75, 85–86, 173–174, 175, 177–179,
 180, 181–182, 264–265, 269–270, 274–277,
 275*f*, 386, 387–388
- Hoveyda–Grubbs type II catalyst 85, 149
- Hoye synthesis, (–)-dactylolide and (–)-
 zampanolide, 174–175
- HPLC, 32–33, 50, 102–104, 104*np*, 280–282,
 365, 367*np*, 369, 370–371, 408–409
- H₂SiF₆, 379
- H₂SO₄, 321, 330–333, 335–338, 341, 342, 362,
 403
- H₂SO₄/HCOOH/*t*-BuOH (Koch–Haaf
 reaction), 335–336
- H₂SO₄/oleum, 330–331
- HSP90, 153–154
- HT29 cell line, 172
- Human colon tumor cell line HCT116,
 353–354
- Hünig’s base, 29
- Hybridolactone, 2*f*
- Hydridoruthenation, 190
- Hydroboration, 33–34, 382–383
- Hydrofluoric acid, 112–114, 399
- Hydrogen abstraction, 322–323, 322*f*,
 325–326, 327–328, 327*f*, 329–331, 333–334,
 335
- Hydrogenation, 21, 32–33, 60–62, 73, 85–86,
 100–101, 134, 158–160, 161–162, 165–167,
 203, 204–205, 218, 219–221, 236, 241–242,
 241*f*, 255–256, 264*f*, 265–267, 297–301,
 304–305, 321–322, 336–338, 351–352, 354,
 361, 362–363, 371, 400, 402
- Hydrogenation, catalytic, 203, 204–205, 218,
 219–221
- Hydrogenation, enantioselective, 304–305
- Hydrogenation, hole-transfer promoted,
 241–242
- Hydrogenation, Noyori asymmetric, 100–101
- 1,5-Hydrogen atom abstraction, 302
- Hydrogenolysis, 29, 30–31, 90–91, 117, 121,
 216, 297, 300, 310–311, 362–363, 363*np*,
 368–370
- Hydrogenolytic debenzilation, 99, 100
- Hydrogen-terminated diamond crystal, 318,
 318*f*
- Hydrogen-terminated diamond surfaces, 317–318
- Hydrolysis, chemoselective, 236–237
- Hydrolysis, oxidative, 89–90, 93–95, 94*t*
- 1-Hydroxyadamantane, 328, 333
- 2-Hydroxyadamantane, formation of, 329
- β-Hydroxy-*E*-allylsilane, 5–6, 19–20
- (4*S*)-(+)–4-(2-hydroxyethyl)-2,2-dimethyl-1,3-
 dioxolane, 188–189
- Hydroxy selenides, 42, 45
- Hydroxystannane, 14, 15–16, 15*t*
- Hydroxystannes, synthesis of, 14, 15*t*, 16
- Hydrozirconation, 84, 278, 282–283
- Hydrozirconation/iodination, 278, 282–283
- Hypochlorite ion, 214–216
- I**
- I₂, 304, 309
- IBX oxidation, 278, 282
- ICD process, 40–41
- ICD reactions, 42, 50–52
- Icetexane diterpenoid family, 294–295
- ICI, 321, 363
- ImH, 381–382
- Imidazole, 144, 200–201, 202–203, 204–205,
 206–209, 211–214, 218, 219–221, 222,
 396–397, 400–402
- Imidazolium salt, 202–203, 213–216, 217, 218
- Iminium ion cyclizations, 354, 355
- Iminium ion cyclizations of piperazinium and
 pyrrolidinium derivatives, 354
- (–)-Indicol, 75
- Inhibition of cytosolic phospholipase, 27
- Internal ketalization, 137–138
- Intramolecular aldol reaction, 58, 60
- Intramolecular conjugate displacement (ICD),
 39–41, 42, 42*f*, 43, 44
- Intramolecular Friedel–Crafts reaction, 201
- Intramolecular Heck cyclization, 297
- Iodine, 29, 308–310, 311–313, 362, 400–402
- 3-Iodoacrolein, 384–385
- 2-Iodoacrylic acid, 192
- 4-Iodoani-sole, 88
- o*-Iodobenzoic acid (IBX), 189–190, 211–213,
 279*f*, 286–287, 298–300, 396–397
- Iodoimidazole, 202, 203
- Iodoxybenzoic acid *N*-methylmorpholine
 N-oxide complex (IBX–NMO), 396–397
- Ionic reduction, 202–203, 204–205
- Ionization potential, adiabatic, 342–343
- i*-Pr₂NEt, 101*t*, 104*np*, 106–108, 107*t*, 114,
 115–117, 116*np*, 121

[IrCl(C₈H₁₂)]₂, 93–95
 Ireland–Claisen rearrangements, 179–180, 280–283, 281*f*, 285, 286*f*, 287
 IR spectroscopy, 71–73
 Isobutyryl chloride, 144–145
 Isobutyryl imidazolidine, 145–146
 Isolated ketone, 59
 Isonaamidine E, 204–205
 Isonaamidines, 199–200
 Isonaamine A, 199–200, 200*f*
 Isonaamine C, 204–205
 Isonaamine C and isonaamidine E, 204–205
 Isonaamines, 199–200
 Isoprene, 396, 403–404
 Isopropenylmagnesium bromide, 269–270
 Isopropylidene triphenylphosphorane, 163–164

J

Jacobsen's chiral chromium(III) catalyst, 179–180
 Jahn–Teller distortions, 342–343
 Jennings synthesis of (–)-dactylolide, 175, 176
 Johnson orthoester Claisen rearrangement, 134–137
 Joule dipolar cycloaddition, 360
 Julia–Kocienski olefination, 154, 173–174

K

Kahne glycosylation, 378–379
 KAPA, 241–242
 KB and vero cancer cell lines, 153–154
 KB nasopharyngeal carcinoma cells, 132
 K₂CO₃/MeOH, 72, 142–143
 Kealiinine C, 208, 209–211, 213–217
 Kealiiquinone, 200*f*, 201, 210*f*, 211–213
 Keck allylation, 106, 400
 Keck macrolactonization, 46
 Keck synthesis of (+)-dactylolide, 177–179
 Kendomycin, 261–289
 Kendomycin, biosynthesis of, 262–263, 262*f*
 Kendomycin synthesis, macrocyclization strategies, 264*f*
 Ketal formation, 158–160, 164–165
 Ketalization, internal, 137–138
 β-Keto-phenylsulfones, 129
 β-Ketophosphonate, 180–181
 Ketoreductase, 377–378
 Ketosynthase (KS), 377–378, 391
 KF, 142–143
 Kinetic deprotonation, 385, 389–390

Kinetic enzymatic resolution, 7–8
 Kinetic isotope effects (KIEs), 321–322, 327–328, 329–331
 Kobusine, 300–301
 Koert synthesis, apoptolidin aglycone, 379
 KOH, 302–303, 378–379
 KOSiMe₃, 90, 91*r*
 KOtBu, 60–62, 302–303
 KOTMS, 109
 Kumada coupling, 180–181
 Kyodai nitration of adamantane, 326
 Kyodai nitration of aliphatic hydrocarbons, 326

L

Lactones and lactams, RCM, 11, 11*f*
 LAH, 66–67, 158–160
 Larock conditions, 368–370
 Lateral deprotonation, 297, 302–303, 304, 309
 Lateral functionalization approaches, 302, 303, 309
 Laumalide, 172
 Lautens, M., 56, 68–69
 LDBB, 68–70
 Lead tetraacetate, 253–254
 Lemonomycin, retrosynthetic analysis of, 358–359
 (–)-Lemonomycin, total synthesis of, 351–373
 Le Quesne–Brennan biosynthetic proposal, 138, 141
Leucetta and *Clathrina* sponges, 199–200
Leucetta chagosensis, 205–206
Leucetta-derived alkaloids, 199–224
 Lewis acid/CH₂Cl₂-promoted monoamination, 338
 Lewis acid-catalyzed arylations, diamondoids, 339
 Lewis acid-promoted cyclizations, 228
 Lewis acid-promoted polycyclizations, 242–243
 Lewis acids, 5, 6, 44–45, 82, 104–105, 167, 168, 190–191, 228, 233–235, 242–243, 270–271, 286, 320, 336, 338, 339–340, 364–365, 382–383, 408–409
 Lewis-base catalyst, 104–105, 106–108
 Lewis-base-catalyzed aldol reaction, 105
 Lewis-base-catalyzed asymmetric aldol addition reactions, 102–105
 Lewis-base-catalyzed asymmetric aldol reaction, 102–105
 Ley, Steve, 144
 LHMDs, 389–390

- LiAlH₄, 280–282
LiBH₄, 29, 32–33, 142–143, 158–160
Liebeskind's reagent, 379
Li⁺Et₃BH[−], 237–238, 238f, 249f
Ligands in catalysis, 331
LiHBEt₃, 100–101
LiHMDS, 134, 148–149, 266f
LiOH, 89, 264–265, 270, 274–276
LiOH/H₂O₂, 270
Lithiated acetonitrile, 8
α-Lithiated carbamate, 6–7
Lithiated carbamates, 4, 13–17, 21
Lithiated dibromomethane, 269–270
Lithiation, 12, 13, 89, 204–205, 222, 284
Lithiation–borylation–allylation, 12, 16–17, 18r, 19, 21
Lithiation–deuteration experiments, 14
Lithium and sodium borohydrides, 158–160
Lithium bis[(*R*)-α-methylbenzylamide], 147–148
Lithium–bromide exchange, 362
Lithium diisopropylamide (LDA), 68–69, 144–145, 298–300, 302–303, 399–400, 406
Lithium divinyl cuprate, 48
Lithium–halogen exchange, 384–385
Lithium–iodine exchange, 89–90
Lithium ketene acetal of ethyl acetate, 366
Lithium naphthalenide, 89
LiTMP, 302–303
Lone pair repulsion, 361
Luche conditions, 36–37, 274–276
Luche reduction, 48–49, 82–83, 137
Luciduline, 293f
Lucinone, asymmetric synthesis, 60, 62
2,6-Lutidine, 13, 31, 35, 46, 50, 65, 99, 100, 110, 182, 236f, 360, 384–385
Lycodine, 292f
Lyconadin A, 291–315
Lyconadin C, 293f
Lyconadins A and B, biosynthesis of, 293–294
Lycopodine, 292f
Lycopodium alkaloid lyconadin A, 291–315
Lycopodium alkaloids, 292–294
Lymphatic leukemia, 172
- M**
Macrocyclic precursor, 160, 163, 165–167
Macrocyclic ring-closing metathesis, 192–193
Macrocyclization, 153–169, 173–175, 177–179, 181–182, 184–185, 263–264, 264f, 265–267, 273–277, 287, 377–379
Macrocyclization strategies, kendomycin synthesis, 264f
Macrocyclization via RCM, 273–274
Macrolactonization, 12, 154, 286, 286f
Macrolide ester, 154–155
Macrolides, 154–155, 376–377, 388, 389
L-malic acid, 381
Mander, L., 395–396, 400–402
Mander's reagent (NCCO₂Et), 400–402
Marine natural products, 25–26, 229f
Marine polyether terpenes, 226–233
Masamune base, 381–382
m-chloroperbenzoic acid (*m*-CPBA), 5, 6, 17–18, 19–20, 21, 82, 97–99, 266f, 299, 302, 303, 329, 330, 355–356
McLeod synthesis of (–)-dactylolide, 179–180
McMurry coupling, 239–240
Mechanism(s) of antitumor action, 138
Meerwein's reagent, 38
Meerwein's salt, 39–40
MeI, 89–90, 137, 144–146, 214–216, 278, 280–282
MEL28 tumor cell line, 172
Memantine®, 320, 325–326, 336
Me₄NBH(OAc)₃, 267
(MeO)₃CH/PPTS, 145–146
Mercuric chloride, 354
Me₃SiBr, 38–39
Me₃SiOCOCF₃, 46
Me₃SiONa, 38
Me₃SiOTf, 43–44, 46
meso-tris(pentafluorophenyl)corrolato iron(IV) chloride [(F₁₅TPC)FeCl], 329
Mesylation, 37, 137–138, 146–147
O-mesylation, 137–138, 146–147
O-mesylation and DBU-promoted elimination, 137–138
Metalation, 90–91, 202–203, 204–205, 206–209, 211–213, 218, 219–221, 222, 267–269
Metalation, selective, 89–90
Metal-catalyzed cross-coupling, 180, 362
1,2-Metallate rearrangement, 4, 5
Metal-organic frameworks (MOFs), 320, 339–340
Metathesis, 11, 60–62, 161–162, 184–185, 193–194, 387–388
Methallyl bromide, 406
Methanesulfonic acid, 366–367
Methicillin-resistant *Staphylococcus aureus*, 261–262, 353–354

- 1-Methoxy-1-trifluoromethyl-phenylacetyl (MTPA) chloride, 108–109
- Methyl acrylate, 39–40, 43, 106
- α -Methylbenzylamide, 147–148
- Methyl (*E*)-bromoacrylate, 84
- 3-Methylcyclohexenone, 396–397
- Methyl 3,5-dihydroxybenzoate, 111, 114
- Methyl(trifluoromethyl)dioxirane, 328
- Methyldorimidazole, 200*f*
- N*-methyl formanilide, 205–206
- Methyl glycoside, 137–138, 141, 145–146, 150
- Methyl glyoxylate, 357–358, 364–365
- Methyl iodide, 386–387
- Methylmagnesium bromide, 175, 180–181
- N*-methyl morpholine, 27–29, 276*f*, 360–361
- Methyl parabanic acid, 199–200, 203, 204–205
- Methyl propionate, 33–34
- Methyl pyruvate, 65
- Methyltriphenylphosphonium bromide, 246
- MgBr₂, 111–112, 112*r*
- O*-Michael reaction, 180
- Microtubules, 57, 172
- Mitsunobu inversion, 279–280
- Mitsunobu reaction, 173–174, 180
- MJ347-81F4, 354
- MnO₂, 102, 211–213
- Modification of the norté hypothesis, 256
- Moffatt oxidation, 368–370
- Molecular tripod, 341–342
- Molecular tripod-based nitroxylation/isomerization, 341–342
- MOM acetal, 154–155
- MOM ether, 155–156, 272–273, 297–298, 300
- MOM methoxymethyl, 272–273, 273*f*
- MOMOCH₂Li, 407–408
- MOMOCH₂SnBu₃, 407–408
- MOM protecting group, 38–39, 158–160, 164–165, 268–269, 272–273, 285, 310–311
- MOM-protection, 134, 158–160, 163–164, 274, 381–382
- Monobromination of adamantane, 339–340
- Monofunctionalizations, 331–339
- Monophosphorylation, 338
- Montmorillonite K10 clay/FeCl₃, 339
- Mortia–Baylis–Hillman (MBH), 396–397
- Mosher's ester analysis, 108–109, 109*f*, 261–262
- Mukaiyama aldol reactions, 176–177, 380, 390
- Mukaiyama conditions, 216
- Multiple functionalizations, 339–342
- Muzitone, 225–260
- Muzitone, alternative structure for, 256*f*
- Muzitone, biosynthesis of, 231, 231*f*, 232*f*
- Muzitone, purported structure of, 249–255
- Muzitone, retrosynthetic analysis of, 250*f*
- ## N
- Na(Hg), 31, 32
- Naamidine A, 199–200, 200*f*
- Naamidine G, 205, 206
- Naamidine H, 205–209
- Naamidines, 200–201, 204–205, 217
- Naamine, 201, 204–205
- Naamine A, 199–200, 200*f*
- Naamine G, 206–209
- NaBH₄, 27–29, 36, 49, 50, 133, 135, 136, 142–143, 150, 176, 177, 178, 204–205, 233*f*, 253*f*, 286, 300, 301, 355, 360, 361, 365
- Na(CN)BH₃, 381
- NaBH₄–NiCl₂, 29
- NADPH-mediated 1,4-reduction and internal Dieckmann cyclization, 132
- Nagata reaction, 364–365, 365*np*
- NaH, 89–90, 137, 145–146, 160, 165, 213–214, 302–303
- NaHCO₃, 16–17, 18*r*, 97–98, 99
- NaHMDS, 9, 13, 17, 18, 20, 173, 176–177, 178, 235*f*, 302–303, 405
- NaH/ MeI, 137, 145–146
- NaI/butanone, 146–147
- NaIO₄, 17, 20, 45, 133, 135, 183, 253*f*, 254*f*, 274, 277*f*, 367, 404
- Nakanishi hypothesis, 227–228
- Nakanishi, K., 226–227
- Nakorone, 229–230, 229*f*, 236, 237*f*, 238–239, 239*f*, 242
- Nakorone and durgamone, 229–230, 242
- NaNH₂, 302–303
- Nankakurine, 293*f*
- Nanodiamonds, 317–350
- NaOAc, 89
- NaOCl, 214
- NaOH, 16–17, 18*r*, 214, 272–273
- NaO*t*-Bu, 90, 91*r*, 93*r*, 97
- Naphthimidazole derivatives, *Leucetta*-derived alkaloids, 209–217
- NaSet, 304
- Natural product total synthesis, 395–396, 405
- N*-bromosuccinimide (NBS), 267*f*, 311–313, 356–357
- n*-BuCN, 93–95, 94*r*

- n*-BuLi, 4, 8, 158, 164–165, 202, 203, 209, 218, 303–304, 310, 311, 312*f*, 387
*n*BuLi/TMEDA, 270–271, 282
n-Bu₄NF, 142–143, 144
n-BuSH, 111–112, 112*r*
NCI 60 cell line panel, 376
NCS, 214, 215, 301, 311–313
¹⁵N-decoupled ⁶Li NMR, 311, 312*f*
Negative electron affinity (NEA), 317–318, 320
Negishi coupling, 278, 280, 281*f*
Negishi cross-coupling, 278, 282–283
Neohalicholactone, 2*f*
Neutral electrophiles, 322, 328–330
NH₄F, 46
NHPI oxidations of adamantane, 325–326, 336–338
N-hydroxyphthalimide (NHPI), 325–326
Nicolaou synthesis, Apoptolidin A, 378–379
NIS, 181–182, 311–313, 385–386
NIS-TESOTf, 385–386
Nitrate radical, 326
Nitrations, catalytic, 325–326
Nitric acid, 320–321, 325–326, 330–331, 333–334, 335–336, 340–341
Nitric acid, anhydrous, 330–331, 333–334, 335–336, 340–341
Nitrile oxides, 360–361
Nitrobenzoate protection, 14, 15*r*
Nitrogen-containing rings, 40–41
Nitrogen heterocycles reaction, 41, 42
Nitronium cation, 330–331, 333–334
Nitronium tetrafluoroborate, 333
Nitrosonium phosphorus pentafluoride NO⁺PF₆[−], 333
1-Nitroxadamantane, 326
Nitroxyl, 321–322
Nitroxylation, 321–322, 333–334, 335–336, 340–342
Nitroxylation/hydrolysis, 333–334
Nitroxylation/isomerization, 341–342
N-methylmorpholine-*N*-oxide (NMO), 27–29, 276*f*
NO₂⁺BF₄[−], 333
Nocardiosis sp. FU40, 377–378, 391–392
Nocathiacin, 354
NOCl, 302, 356
NOE, 104*np*, 158–160, 265–267, 266*f*, 364*np*, 402–403
(*Z*)-nona-1,3-diene, 13–14
Nonchain radical process, 327–328
Non-Evans aldol adduct, 381–382
Nonlinear optical materials, 331–333
Nonoxidative spirocyclization, 95, 96–97
Normant's Grignard reagent, 65–66, 67
6-Normethylapoptolidinone, 390–392
Norte's hypothesis, 231–233, 232*f*
Norte's hypothesis, modification of, 256
Noyori asymmetric hydrogenation, 100–101
Nozaki–Hiyama–Kishi (NHK) reaction, 3–4
Nucleophiles, 40–41, 42, 187–188
Nucleophilic and electrophilic oxidants, 141–142
- ## O
- Olefin metathesis, 109
Olefin metathesis catalysts, 273–274
Oppolzer's 1,4-addition/enolate-trapping protocol, 269–270
Oppolzer's sultam acrylamide, 356–357, 358–359, 360–361
Organocatalysts, 320
Organocatalytic reaction, stereoselective, 182–183
ORTEP, 72, 73*f*
ortho-benzoquinone, 263
ortho-directed lithiation, 272–273, 278, 284, 287
ortho-Fries rearrangement, 264–265, 285, 286
ortho-lithiation, 272–273, 279, 280, 282
ortho-metalation, 270–271
Orthoquinone, 277, 286–287
Osmate ester, 253–254
Osmium tetraoxide, 134, 253–254
OsO₄, 27–29, 133, 253*f*, 274, 277*f*, 367, 404
OsO₄/NMO, 274
Ovarian carcinoma (SK-OV-3), 172
Oxacyclization, 226–227, 227*f*, 228, 229–230, 233–239
Oxalic acid-induced cleavage, 133
Oxatricyclic, 64
Oxazolidine, 281*f*, 366*np*, 366–367, 371
Oxazolidinone, 29, 48, 150, 280–282
Oxidation, 15–16, 27–29, 38–39, 42, 44, 45, 46, 48, 49–50, 67, 74–75, 81–83, 90–91, 98–99, 100–101, 133, 134–137, 142–144, 157–160, 164–165, 173–174, 175, 176–177, 178–180, 181–182, 183–184, 189–190, 194, 200–201, 201*f*, 211–217, 222, 230–231, 233–234, 261–263, 264–265, 264*f*, 269–271, 272–273, 274–276, 277, 278, 279, 280–283, 285, 286–287, 293–294, 298–300, 302, 304–305, 307, 310–311, 321, 325–326, 327,

- 328–330, 335–338, 343–345, 352, 356–357, 358–359, 362, 367–371, 368*f*, 370*np*, 377–378, 380–383, 387–388, 390–391, 408–409
- Oxidations of diamondoids with dioxiranes, 328–329
- Oxidation with MnO_2 , 48
- Oxidative cleavage, 12, 19, 174–175, 233–234, 252–254, 253*f*, 256, 366–367, 406
- Oxidative C–N bond formation, 300–304, 307–314
- Oxidative dimerization of enolates, 307–308
- Oxidative hydrolysis, 89–90, 93–95, 94*t*
- Oxidative rearrangement, 218–221
- Oxidative spiroketalization, 85, 90–91, 97–99
- Oxidized derivatives, Leucetta-derived alkaloids, 217–221
- Oxidopyrazinium salts, 356–357
- Oxocarbenium ion, 98–99, 366*np*, 366–367
- Oxone®, 133, 134, 228*f*, 244*t*, 250–251, 336–338
- Oxonene rings, 139–140, 141
- Oxonium ion intermediate, 234–235
- Oxygen bridge cleavage, 69–71
- Oxylipins, 4
- Ozonides, 142–143
- Ozonolysis, 34–36, 47, 48, 100–101, 137, 163–164, 173–174, 229–230, 239–240, 252–253, 254, 406
- P**
- Palladium-catalyzed carbonylation, 69–70, 82, 85, 122, 184–185, 187, 188–189, 240–241, 240*f*, 248–249, 351–352, 408–409
- Palladium-catalyzed cross-coupling, diene, 240–241, 240*f*
- Palladium(0)-catalyzed cross-coupling reaction, 82–83
- Palladium-catalyzed dehydrogenation methods, 351–352
- Palladium-catalyzed desulfonylation, 248–249
- Palladium-catalyzed organosilanolate-based, cross-coupling, 122
- Palladium-catalyzed reaction, 90, 91*t*
- Palladium(II)-mediated acetonide removal, 380–381
- Palladium-mediated rearrangement, 282–283
- Papulacandin A, 80, 80*f*
- Papulacandin B, 80, 80*f*
- Papulacandin C, 80, 80*f*
- Papulacandin D synthesis, 79–126
- Papulacandins, 80, 80*f*, 81–82, 83–84
- Papulacandin synthesis, Barrett's approach, 83–84
- Papularia sphaerosperma*, 80
- Parikh–Doering oxidation, 233–234
- $\text{Pb}(\text{OAc})_4$, 174, 253*f*, 310–311
- $[\text{p-BrPh}]_3\text{N}^+ \cdot \text{SbCl}_6^-$, 241–242
- PCC, 134–137, 211–213
- P388 cell line, 172
- PCl_3 , 336, 337, 338, 339
- $\text{PCl}_3/\text{AlCl}_3/\text{CH}_2\text{Cl}_2$, 338
- $\text{Pd}(\text{OAc})_2$, 69, 298–300, 311–313
- $(\text{Ph}_3\text{P})_4\text{Pd}$, 29, 30
- 10% Pd/C, 34, 134–137
- Pd-catalyzed allylic alkylation mechanism, 187–188
- Pd–C/ H_2 , 205, 209, 211–213
- $\text{Pd}_2(\text{dba})_3 \cdot \text{CHCl}_3$, 91*t*, 96*t*, 97
- Pelorusides, 172
- Penicillin G, 352–353
- Penitrem D, 128–129, 128*f*
- Pentacycle N–Cl compound, 302–303
- Pentamantanes, 318, 333, 335, 345
- Pentynylcopper, 132
- Peptidomimetics, 320
- Perfluoro-*n*-alkyl iodides, 323–324
- Perhydroazulene, 58, 70–71
- Periodate cleavage, 253–254, 274–276
- Petasis–Ferrier rearrangement, 173–174
- Peterson olefination, 176–177
- P-gp efflux pump, 57
- Phacidins, 307–308
- Ph_3As , 87–88
- Phase-transfer catalytic (PTC) conditions, 323–325
- 1-Phenyladamantane, 339
- 2-Phenylsulfonylimidazolet, 213–214
- Phlegmarine, 292–294, 292*f*
- Phospholipase, inhibition of, 27
- Phosphorylation, 336, 337, 338
- Photoacetylation, diacetyl, 327–328, 327*f*
- Photoacetylation mechanism, 327–328
- Photochemical decomposition of CAN, 326
- Photochemical-mediated Diels–Alder, 403–404
- Photo-Fries reaction, 263–264, 285–286
- Photo-Fries rearrangement, 286*f*, 287
- Photoinduced SET, 345
- Photolysis, 300–301, 302, 356–357

- Ph₃P/CBr₄, 34
Ph₃P=CH(OMe), 38–39, 49–50
Ph₃PCHOMe, 404–405
[Ph₃PCuH]₆, 59, 60–62
Ph₃P/I₂/imidazole, 144, 146–147
PhSeCl, 135, 137, 298–300
PhSeCN, 36, 44–45, 176–177
PhSeCN and Bu₃P, 36, 44–45, 177
PhSeH, 175
PhSSPh, 313–314
PhSSPh and TEMPO, 313–314
Phthalimide *N*-oxyl (PINO), 321–322, 325–326
Phyllanthostatin natural products, 127
Pictet–Spengler cyclization, 356, 357–358, 359, 364–365, 367, 367*np*, 368, 371
Pictet–Spengler reactions, 365, 366
Pinacol-type rearrangement, 218–219
Pinnaic acid, 27*f*, 32
Pinnick, 46, 280–282
Pinnick oxidation, 46, 280–282, 281*f*
Piperazic acid, 130
Piperazinium and pyrrolidinium derivatives, omium ion cyclizations of, 354
Piperidines, substituted, 50, 51*f*
Pivaloyl chloride, 32–33
Plasmodium falciparum K1, 153–154
PMB-protected (*R*)-glycidol, 180
PMB removal, 380–381
p-Methoxybenzyl bromide, 206–209
Pochonin J, 161–162
Polonovski rearrangement, 302
Polyene cyclizations, termination of, 236–237
Polyepoxide cyclizations, 226–228, 229–230, 233, 256
Polyketide synthase (PKS) knockout, 262–263, 377–378, 391–392
Polymer bound DCC, 178–179
Polymers, 178–179, 319, 320, 339–340, 345
Polysubstituted diamondoids, 339–340
Potassium carbonate in methanol, 252–253, 408
Potassium hexamethyldisilazane (KHMDS), 144–145, 148, 275*f*
Potassium *tert*-butoxide, 246
Potassium trimethylsilanolate, 364
Potassium vinyl trifluoroborate, 155
PPTS, 13, 100, 101, 117, 119, 136, 145–146, 158–160, 164–165, 166, 178, 181, 183, 299, 378–379
*p*Rb-inactivated glia cells, 375–376
Preclathridine, 203
Precursor-directed glycosylation, 390–392
Premuzitone, 231, 251–252
Premuzitone, biosynthesis, 231–233, 232*f*
Prins reaction, 263–264
Prins-type reaction, 181, 182
Prins-type reaction, stereoselective, 181
L-proline, 41, 42
1,3-Propanedithiol, 144–145, 146
Propargylic alcohol, 158, 164–165
Propargylic silanes, 236–237
2-Propenylmagnesium bromide, 192, 269–270
Propionaldehyde, 133
Proposed biosynthesis of lyconadins A and B, 294
2-Propyn-1-ol, 8
Proteasome inhibition, 261–262
Protecting groups, 12, 38–39, 47, 83–84, 85, 88, 90–97, 99–100, 109–110, 111–119, 120, 121, 137–138, 142–143, 158–160, 164–165, 176–177, 178–180, 190–191, 206–209, 216, 218–219, 264–265, 265*f*, 269*f*, 271, 272–273, 279, 283*f*, 285, 286–287, 310–311, 359, 371, 378–379, 385, 387–390
Protecting group strategy, 85, 90–91, 92*f*, 114–119, 121
Protiodesilylation, 86–87, 88, 90, 93–95, 96–97
Protoadamantane, 320–321
Protonated sulfur trioxide HSO₃⁺, 330–331
PrSLi, 29, 30
Pseudoapoptolidin A, 383–386
Pseudoapoptolidin A, synthetic routes to C7–C11 fragment, 384–385
Pseudoapoptolidin A, synthetic routes to C15–C18 fragment, 381, 382
Pseudolaric acid A, 55–78
Pseudolarix amabilis, 56–58
PTC halogenation reaction, 323–324
PTC halogenations, diamantane, 325
p-TsOH, 142–143, 271
Pyran subunit preparation, 185–189
Pyrazine dipoles, 354, 356–357
Pyridine, 114–115, 142–143, 155, 282*f*, 302, 378–379, 389–390, 396–397
Pyridinium dichromate, 368–370
- ## Q
- Quinine, Rabe synthesis of, 302–303
Quinocarcin, 352, 353*f*, 354, 355, 356–357
Quinocarcin, Fukuyama's synthesis, 354, 355

(+)-Quinocarcin, Garner synthesis of, 356–357
 (–)-Quinocarcin, Garner synthesis of, 357, 360–361
 Quinocarcinol methyl ester, Danishefsky's synthesis of, 355
 Quinine, Rabe's synthesis of, 302–303
 Quinone methide, 261–262, 263, 277, 287

R

Rabe synthesis of quinine, 302–303
 Racemic synthesis, 297, 304–305, 407–408, 409
 Racemization, 29
 Radical cations, 322, 342–345, 343f
 Radical cyclization, 27–29, 30–32, 34–37, 137
 Radical reagents, 322–328
 Ramberg–Backlund rearrangement, 132, 134
 Ramirez method, 382–383
 Raney nickel, 12, 58–59
 RCM macrocyclization, 161–162, 167–168
 RCM reactions, 11, 141, 154, 157, 160, 161, 162, 163, 165–168, 182–183, 263–264, 273–274, 273f, 279–280, 280f, 284–285
 Reagent control, 67–68, 147–148
 Rearrangement, Claisen, 34–36, 38, 47, 48–49, 408
 Rearrangement, oxidative, 201, 218–221
 Red-Al, 158–160, 164–165, 166, 177, 366–367
 1,4-Reduction, 132
 Reduction, stereocontrolled, 48, 49
 Reductive aldol cyclizations, 59, 60–63
 Reductive amination, 297, 300, 310–311
 Reductive elimination, 70–71, 140, 144, 180–181, 190
 Reformatsky sequence, 182–183
 Regioselective epoxidation, 236–238
 Regioselective hydrostannation, 62–63
 Reich–Kuwajima methodology, 249
 Reich protocol, 298–300
 Reissig, H.-U., 400–402
 Relay metathesis, 184–185, 193–194
 Renieramycin C, 263, 353f
 Re₂O₇, 189, 190–191
 Resorcinol moiety, 95
 Resorcinyl compounds, 153–154
retro-aldol, 12, 66–67
retro-Dieckmann/Dieckmann cascade, 400–402
retro-ozonolysis, 239–240
 Retrosynthesis of abudinol B, first generation, 236
 Retrosynthesis of solandelactone E and F, 7
 Retrosynthetic analysis, 6–7, 85–86, 138–142, 154–162, 163–167, 184–185, 250f, 296, 358–359, 396
 Retrosynthetic analysis of aigialomycin D, 154–162, 163–167
 Retrosynthetic analysis of (+)-eremantholide A, 138–142
 Retrosynthetic analysis of lemonomycin, 358–359
 Retrosynthetic analysis of muzitone, 250f
 Rh₂(OAc)₄, 67
 Rh₂(S-BPTV)₄, 67–68
 Rh₂(S-DOSP)₄, 408–409
 Rh₂(S-PTAD)₄, 408–409
 Rhenium-catalyzed allylic transposition, 194–195
 Rhenium-promoted process, 227
 Rhodium, 64, 67–68
 Rhodium-catalyzed CCCC reactions, 67
 Rimantadine[®], 320
 Ring-closing metathesis (RCM), 7–8, 9, 10r, 10, 11, 11f, 12, 138–140, 141, 149, 154, 157–158, 160, 161–162, 163, 164, 165–168, 172, 174–175, 179, 180, 182–185, 192–195, 263–264, 264f, 265f, 272f, 273–274, 273f, 274f, 276–277, 278–285, 279f, 280f, 283f, 284f, 287, 387–388
 Ring expansion, 231–233, 235–236, 376–377, 396, 398, 399–402, 403
 Ritter-like reactions, 338
 Ritter reaction, 320
 Roush's Z-allyl boronate, 384–385
 R₃SnH/AIBN, 129
 RuO₄, 329–330
 Ru(OAc)₂[(S)-BINAP], 100–101
 Ruthenacyclopentene intermediate, 190
 Ruthenium alkylidene-catalyzed cross metathesis, 185–186
 Ruthenium-catalyzed Alder-ene reaction (RCAER), 184–187, 190, 194–195
 Ruthenium-catalyzed oxidative cleavage, 252–253, 254
 Ruthenium olefin metathesis catalysts, 11

S

Saegusa–Ito oxidation, 298–300
 Saframycin A, 352, 353f, 357, 358
 Sakurai reaction, 180
 Saponification, 89, 92–93, 109, 175, 180, 285, 300, 378–379

- s*-BuLi, 4, 16
Schleyer, P., 320–321, 321*np*
Schlosser-Fouquet conditions, 269–270
Second-generation synthesis of abudinol B, 242–249
Selective bridgehead chlorination, 321
Selective functionalization of diamondoids, 345
Selective kinase inhibitor for CDK1/cyclin, 153–154
Selective metalation, 89–90
Selectivities for the C—H bond functionalizations, 325–326
Selenide, 36, 42
Selenium, 34–37, 42, 43
Selenium-stabilized carbanion, 44–45
Selenoxide, 36, 42, 137, 176–177
Selenoxide elimination, 42, 137
SEM ether deprotection, 111, 112*t*
Semiquinone radical, 277
L-serine methyl ester hydrochloride, 48
Shapiro reaction, 239–240
Sharpless asymmetric epoxidation (SAE), 84, 141–142, 144, 174–175
Sharpless enantioselective epoxidation, 228
Sharpless epoxidation, 7–8, 12, 21
Shi epoxidation, 227–228, 228*f*, 229*f*, 233–234, 233*f*, 236, 237–238, 238*f*, 242, 243–244, 244*t*, 246, 247, 247*f*, 248–249, 250–251, 251*f*
1,2-Shift, acetoxo group, 36–37
Sigmatropic rearrangement, 192, 274–276
[2,3]-Sigmatropic rearrangement, 177
[3,3]-Sigmatropic rearrangement, 180, 191, 192
Silane, 89–90, 92–95
Silanol, 85–87, 88, 89–95, 97, 122
Silanolate, 90, 96–97
Silanolate-based cross-coupling, 96–97
Silanols, 85–87, 88, 89–95, 96–97, 122
Silicon-based, cross-coupling reactions, 85–86
Silicon tetrachloride, 102–104
Siloxynyldiazoacetate, 408–409
Silyl nitronates, 360–361
 β -Silyl vinyl borane, 4–5
Simpkins–Marshall–Whitesell chiral bases, 148
Simpkins–Marshall–Whitesell chiral lithium amide base, 138–139
Single electron transfer (SET), 310, 313–314, 322, 322*f*, 339–340, 342–345, 380–381, 383–386
Siphenol A, 228, 229*f*, 230
Six-membered transition state, 4, 300–301
Sludge, 338
SmI₂–Barbier reaction, 263–264
Smith III, A.B., 127, 128*f*, 129, 296
Smith Synthesis of (+)-dactylolide, 173–174
SnCl₄, 267
S_N2 closure, 300–301
S_N1 substitution, 72
S_N1 tetrahydropyran formation, 284–285
S_N1-type cyclizations, 271, 272–273, 287
Sodium borohydride, 134, 137–138, 158–160, 253–254, 354, 365
Sodium in liquid ammonia, 69–70
Sodium methoxide, 134
Sodium periodate, 134, 253–254, 277, 366–367
Solandelactone A, 3*f*
Solandelactone B, 3*f*
Solandelactone C, 3*f*
Solandelactone D, 3*f*
Solandelactone E, 2–5, 3*f*, 6–19, 20–21
Solandelactone F, 2–3, 3*f*, 5–7, 19–21
Solandelactone G, 3*f*
Solandelactone H, 3*f*
Solandelactones, 1–23
Solanderia secunda, 1
Sonogashira coupling, 180–181
Sorbic acid, 109–110
Sordarin, 407–408
Spirocalcaridine, 200–201, 217, 222
(–)-Spirocalcaridine A, 200*f*
(–)-Spirocalcaridine B, 200*f*
Spirocyclic, 31–32
Spirocyclic amine, 26–27
Spirocyclic aryl glycopyranoside, 86–100, 111, 119–120
Spirocyclic aryl glycoside, 86–100
Spirocyclic *C*-aryl glycopyranoside, 93–95
Spiroketalization, oxidative, 85, 90–91, 97–99
Spiroleucettadine, 199–201, 200*f*, 222
Spirolucidine, 293*f*
Squalene 2,3-diol, 231
Squalene epoxides, 242–243
Squalene tetraepoxide synthesis, 248–249
Squalene tetraol, biosynthesis, 231, 231*f*
Stannane carbamate, 16, 17
Stannyl cupration, 181–182, 386–387
Stephacidins, 307–308
Stereo and chemoselective glycosylation, 378
Stereochemical integrity, 48, 192
Stereocontrolled reduction, 48, 49

- Stereoselective aldol reactions, 379
- Stereoselective 1,4-conjugate addition of cuprate, 132
- Stereoselective epoxidations, 226
- Stereoselective organocatalytic reaction, 182–183
- Stereoselective Prins-type cyclization, 181–182
- Stereoselective Prins-type reaction, 181
- Stereoselective synthesis, 227–228
- Stereospecific ring contraction, 235–236, 236f
- Stetter reaction, 307
- Stille coupling, 379
- Stille cross-coupling reaction, 378–379, 386–387
- Still–Gennari approach, 274, 275f
- Still–Gennari variant, Z-selective, 274
- Stoltz approach, dragmacidin D, 294, 295
- Stoltz, B., 294
- Stork–Danheiser protocol, 297
- Streptavidin–gal4 DNA-binding domain, 138
- Streptomyces candidus*, 352–353
- Streptomyces* metabolite, 261–262
- Streptomyces violaceoruber*, 261–262
- Stryker's reagent, 59, 60–63, 61t
- Substrate controlled synthesis of functionalized tetrahydropyrans, 186f
- Substrate-directed lithiation, 19
- Sulfuric acid, 241–242, 330–331, 335–338, 340–342
- Sulfuric acid, concentrated, 330–331, 335–338, 340–341
- Super-Hydride®, 237–238
- Suzuki coupling, 184–185, 190–191, 192, 193, 362, 363, 388–389
- Suzuki cross-coupling, 155, 385–386, 388–389, 390
- Suzuki–Miyaura cross-coupling, 240–241
- Suzuki reaction, 192, 387–388, 390
- Swern conditions, 211–213, 300, 368–370, 381
- Swern oxidation, 38–39, 143–144, 211–213, 269–271, 269f, 270f, 271f, 273f, 279, 279f, 305, 310–311, 356, 368–371, 370np, 380–381, 408–409
- Swern-type protocols, 211–213
- syn-E*-1,4-diol, 3–4
- syn-E*-2-ene-1,4-diols, 5–6, 19
- syn-* or *anti*-2-ene-1,4-diols, 1–2
- syn*-selective aldol addition, 264–265
- Synthesis of apoptolidins, 375–394
- Synthesis of *C*-aryl-2-*H*-pyrans, 86–87
- Synthesis of cyclic boronic esters, 192t
- Synthesis of 2-ene-1,4-diols, 4–6, 21
- Synthesis of *ent*-durgamone, 235–236, 236f
- Synthesis of *ent*-nakorone, 236, 238–239
- Synthesis of hydroxystannanes, 14, 15t, 16
- Synthesis of purported structure of muzitone, 249–255
- Synthesis of squalene tetraepoxide, 248–249
- Synthetic routes to C25–C28 fragment, apoptolidinone, 380–381
- Synthetic routes to C7–C11 fragment, pseudoapoptolidin A, 384–385
- Synthetic routes to C15–C18 fragment, pseudoapoptolidin A, 381, 382
- ## T
- Taber cyclopropanation reaction, 7–8, 12, 21
- Tadano's synthesis of (+)-eremantholide A, 134–137
- Taft correlation, 329–330
- Tandem asymmetric electrophilic hydrazination–nucleophilic cyclization, 130
- Tandem Brook rearrangement–alkylation, 245f, 250f
- Tandem hydrozirconation/cross-coupling sequence, 84
- TaniaPhos, 62–63
- Tautomeric equilibrium, 209–210
- Tautomeric isomers, 209–210, 210f
- Taxol, 57, 172
- TBAOH, 90
- TBS deprotection, 180, 408–409
- TBSOTf, 65, 179, 234, 234f
- t*-BuLi, 92np, 92–93, 268–269
- t*-Butyl cation, 335–336
- t*-Butyllithium, 382–383
- TEMPO, 143–144, 313–314
- TEMPO/BAIB, 144
- TEOC–Cl, 114–115, 117–119, 121
- TEOC deprotection, 118t
- Termination of polyene cyclizations, 236–237
- tert*-butanol (*t*-BuOH), 34, 58–59, 63, 246, 335–336, 337, 355
- tert*-butyl acrylate, 356–357, 362, 365
- tert*-butylcinnamyl carbonate, 183
- tert*-butyldimethylsilyl chloride (TBSCl) provided, 233–234

- tert*-butyldiphenylsilyl (TBDPS)/TIPS ethers, 86–87, 89–90, 95, 99, 176–177
- Tertiary cations, 336–338
- Tertiary diamondoid carbocations, 331
- TES-Cl, 92–93, 104*t*, 109, 381–382
- Tetrabutylammonium fluoride (TBAF), 89–90, 111, 112*t*, 137, 158, 163–164, 245–246, 269*f*, 274
- Tetrabutylammonium hydroxide (*n*-Bu₄N⁺OH⁻), 88
- Tetrabutylammonium iodide (TBAI), 99–100, 101*t*
- 1,2,4,5-Tetracyanobenzene (TCB), 343–344
- Tetracyclic intermediate synthesis, 297–298, 301
- Tetrahalomethanes, 323–324
- Tetrahydroisoquinoline antitumor antibiotics, 351–373
- Tetrahydropyran, 187, 269, 284–285
- Tetrahydropyrans, substrate controlled synthesis of, 186*t*
- 1,3,5,7-Tetrahydroxyadamantane, 328
- Tetramantane radical cation, 342–343
- Tetramantanes, 318, 318*f*, 327–328, 331–333, 345
- Tetramethylethylenediamine (TMEDA), 13–14, 16–17, 18*t*, 271*f*
- Tetrazomine, 352, 353*f*, 356–357
- TFA, 43, 135, 175, 176, 203, 204, 205–206, 207, 209–210, 218–219, 220, 221, 308, 363, 365, 367, 368, 369, 381
- Thionyl chloride, 357–358
- Thiooxazolidinones, 379, 380, 381–382, 384–385
- Third-generation total synthesis, calcaridine A, 221
- Thorpe–Ingold effect, 141
- D-threonine, 358, 359, 366, 371
- Ti(O*i*Pr)₄, 9, 11, 167
- Ti(O^{*t*}Bu)₄, 174–175
- TiCl₃(O*i*Pr-*i*), 29
- Tin(IV)chloride, 357–358
- TiO₂, 329–330
- TIPSOTf, 99
- Titanium carbene, 239–240
- Titanium chelate, 174–175
- Titanium(IV) chloride, 381–382
- Titanium(IV) enolate, 381–382
- Titanocene chloride, 144
- Ti(O*i*Pr)₄/tBuOOH, 17–18, 19–20, 21
- TMSCH₂MgCl, 176–177, 183, 235*f*
- TMSCl, 297–298, 381–382, 385, 408
- TMSCl/DBU, 133
- TMS-diazomethane, 211–213, 216, 398
- TMSI, 181–182
- TMSOTf, 173–174, 177, 178, 235, 235*f*, 238–239, 238*f*, 245–246, 246*f*, 247–248, 248*f*, 249, 251*f*, 252*f*
- TMS₂S, 134
- Tol₂S₂/Bu₃P, 27–29
- Tosylation, 100–101, 274, 355–356, 362, 364
- Total synthesis of (–)-lemonomycin, 351–373
- Total synthesis of vibsanin E, 395–412
- TPAP/NMO, 143–144, 158–160, 163–165, 166, 178, 368–370
- TPAP oxidation, 38–39, 44
- TPSCI, 267
- Transannular aldol, 252–253, 253*f*
- Transannular hydroamination, 293–294
- Transannular interactions, 67
- trans*-dioxolane diastereomer, 162
- trans*-fused perhydroazulene, 63–64
- Transition metal-catalyzed fragment coupling, 371
- Transition metal complexes, 329
- Transition structures (TSs), 321–323, 322*f*, 327, 327*f*, 328–330, 335
- Transmetalation, 14, 87–88, 132, 180–181, 202–203, 206–209, 408
- trans-syn-trans*-fused polycyclic ethers, 226–227, 227*f*, 228
- Triacetoxylglucal, 122
- Triamantane and T_d-pentamantane radical cations, 343
- Triamantan-5-one, 336–338
- Triamantan-8-one, 336–338
- Triaminotetraol, alcohol oxidation, 370–371
- 1,3,5-Tribromoadamantane, 339–340
- Tributyltin hydride, 14
- Tributyltin magnesium chloride, 15
- 2,4,6-Trichlorobenzoyl chloride, 110, 119–120
- Tricyclic lactams, 34
- Trienes, Shi epoxidations, 247, 247*f*
- Trienyl-propargylsilane, 237–238, 238*f*
- Trienyl silyl ketene acetal, 102–104
- Triepoxide, 226, 228, 228*f*, 243–244, 244*t*, 247, 250–251
- Triethylamine, 106–108, 356–357, 360, 378–379
- Triethyl phosphite, 386–387
- Triflic acid, 216
- Trifluoroacetic acid, 137, 203, 300–301, 362–363, 365*np*, 389–390
- Trihalomethyl radicals, 323–324

Triisopropylsilyl triflate, 361–362
 Trimethylsilyl cyanide, 356
 2-(Trimethylsilyl)ethanol, 114–117, 121
 Trimethylsilylethoxycarbonyl (TEOC),
 114–119, 116*t*, 118*np*, 118*t*, 120*np*, 121
 2-(trimethylsilyl)ethoxymethyl (SEM)
 deprotection, 111–114
 2-(trimethylsilyl)ethoxymethyl (SEM) ether,
 99–100, 111
 1-Trimethylsilyl-2-propyne, 137, 236–237
 Trimethylsilyl triflate (TMSOTf), 235, 366–367
 Triphenylphosphane, 400–402
 Triphosgene, 114–117
 Triplet diacetyl, 327–330, 327*f*
 Tris(2-pyridylmethyl) amine nickel(II) Ni
 (TPA), 329
 Tris(dimethylamino)sulfonium
 difluorotrimethylsilicate (TASF), 87–88,
 111, 112–114, 112*t*
 Trisubstituted alkene, 178–179, 241–242,
 251–252
 Trisubstituted olefins, 129–130, 165–167
 Trisyl azide, 204–205, 206–209
 TROESY NMR measurements, 31–32
 Trost–Kita macrocyclization, 181
 Trost's diphenylphosphinobenzoic acid
 (DPPBA)-based chiral ligands, 187
 TsN₃ or TrisN₃, 202, 203, 205, 213–214, 218
 TSs for hydrogen abstraction, 322–323,
 325–326, 329–330, 334
Tujingpi, 56–57
 Type I polyketide synthase, 377–378
 Type III polyketide synthase (PKS), 262–263

U

Uemura conditions, 368–370
 Uenishi and Tanaka synthesis of (–)-
 Dactylolide, 180–181
 Umpolung, 307
 Undecenal, 102
 α,β -Unsaturated isomer, 178–179

V

Vancomycin-resistant *Enterococcus faecium*,
 353–354
 Vascular cell adhesion molecule-1 (VCAM-1),
 27
 Vertical ionization potential, 342–343
 Vibans natural products, 402
 Vibsanin E and 5-*epi*-vibsanin E, 395–412
 Vibsanin E, total synthesis of, 395–412
Viburnum awabuki (Caprifoliaceae), 395–396

Vicinal coupling constants, 98
 Vinyl boronate, 189–192, 240–241, 240*f*,
 385–386, 387–389, 390
 Vinyl boronate, Z-trisubstituted, 189–192
 Vinylic boronate, 240–241
 Vinylmagnesium bromide, 48, 175, 181–182
 Vinylmagnesium chloride, 245
 Vinylogous aldol addition, 104–105
 Vinylogous aldol reactions, 102–105, 104*t*
 Vinylogous Horner–Wadsworth–Emmons
 (HWE) olefination reaction, 85–86, 100–101
 Vinylogous Mukaiyama aldol reaction,
 asymmetric, 176
 Vinyl silyl boronic ester, 19–20

W

Wacker oxidation, 408
 Weinreb amide, 26–27, 366, 381–382
 White, J., 3–4, 7–8, 11, 20–21, 400–402
 Williams, R., 302–303
 Wittig homologation, 29, 142–143
 Wittig methylenation, 137–138, 175, 181–182,
 237, 246, 247*f*, 250–251, 251*f*, 278
 Wittig olefination, 19, 21, 49–50, 84, 109,
 134–137, 140, 141–142, 163–164, 173–174,
 183
 Wittig reactions, 12, 13, 16, 38–39, 179–180,
 182–183, 194–195, 250–251
 Wittig reagent, 246, 405

X

Xanthate reduction, 137, 274–276
 X-ray crystal analysis, 131–132, 209–210,
 219–221, 297–298, 331–333, 395–396,
 400–402
 X-ray crystallographic analysis, 63, 72, 203,
 209, 216, 229–230, 239, 241, 248, 251–252,
 254–255, 305, 314
 X-ray crystal structures, 209–210, 222, 234,
 256, 297, 331–333
 X-ray diffraction analysis, 38, 261–262,
 311–313, 364, 366

Y

Yamaguchi acylation, 84
 Yamaguchi conditions, 175, 183–184
 Yamaguchi cyclization, 379
 Yamaguchi esterification, 181–182, 387–389,
 390
 Yamaguchi lactonization, 12, 21
 Yamaguchi macrocyclization, 154, 378–379

Yamaguchi macrolactonization, [154–155](#)

3Y1 rat fibroblasts, [375–376](#)

Z

(+)-Zampanolide, [172](#), [174](#)

(–)-Zampanolide, [172–173](#), [172f](#), [174–175](#),
[182–184](#)

Zercher, C., [402](#)

Zercher reaction, [400–402](#)

Zimmerman-Traxler model, [381–382](#)

Zn dust, [144](#)

ZnEt₂/CH₂I₂, [402](#)

Z-selective RCM, [273–274](#), [274f](#)

Z-selective Still–Gennari variant, [274](#)

Z-trisubstituted vinyl boronate, [189–192](#)